Characterisation of stromal gene expression in soft tissue sarcoma

Nada AL-Shaaili

A thesis submitted in partial fulfilment of the requirements for the degree of
Doctor of Philosophy

The University of Sheffield
Faculty of Medicine, Dentistry & Health
The Medical School

November 2022

Acknowledgment

This thesis represents the work of the best, most challenging four years of my life. First and foremost, I would like to express my sincere gratitude to my supervisor Dr. William English for his continuous support, advice, motivation, encouragement and guidance especially during the pandemic. Thanks for making this work possible! I would like also to thank Dr. Karen Sisley and her group for their constant help and support. A big thank to Dr. Mark J Dunning and Dr. Emily V chambers from the bioinformatics core facility, for helping me in the dry lab part of this thesis.

A special thanks to Dr. English group for being the best group ever during this four year, but a special thank is devoted to my friend Claudia Madrigel, for being always there with or without asking, for sharing all the moments with me and for making the journey easier and shorter. Thankful for the laughs and tears we shared during this memorable journey.

Arwa ALhulwa, I am sure this journey would not be possible without you, thanks a lot for being part of it. Thanks for always being there for me and keeping me sane, I am so lucky to have you in my life.

My mother, words can't express my appreciation and love for you, thanks for supporting, encouraging and teaching me the importance of education. Thanks for calling me every day to make sure my kids and me are doing well. I owe this work to you and my father. My late father, thanks for being my first teacher in life, I wish you were here today. Alaa, thanks for bringing joy, happiness and contentment for us from Glasgow to Sheffield.

Finally, my family, my husband Said thanks for supporting me and endure the difficulties of long distance relationship, and my kids Renad, Rana & Issa, thanks for accepting this journey with me, thanks for all the memories we made together. You really impressed me on how strong you were. Sami, my little one, thanks for joining the journey in 2020 and helping me with analysing and writing the thesis with your little fingers.

Lastly, I would like to thank everyone who had an impact on this work by encouraging and supporting from family and friends. Love you all.

Abstract

Background: Soft Tissue Sarcomas (STS) are a biologically rare, heterogeneous and complex population of solid tumours of mesenchymal origin. Recent studies have emphasised the important role of mesenchymal cells like fibroblasts in cancer biology. Very little is known about the role of Sarcoma Associated Fibroblasts (SAF) as most studies have focused on Carcinoma Associated Fibroblasts (CAF). The study of SAF is challenging for two reasons; firstly, there are few STS cell lines available that are matched to their original histotype. Secondly, as STS cells and SAF are both mesenchymal, no selective markers have been identified to facilitate their study. This study will focus on characterising SAF in the poorly differentiated, genomically complex and mesenchymal-like STS including Undifferentiated Pleomorphic Sarcoma (UPS) and Myxofibrosarcoma (MFS).

Objectives: To identify STS and SAF specific gene expression profiles to improve our fundamental understanding of STS biology.

Methodology: Eight STS cell lines (UPS, MFS, and LMS), recently described by Salawu *et al* (Salawu et al., 2016) or donated by Professor Heymann (Nantes, France) were used in this project. Expression of mesenchymal proteins (transgelin, αSMA, vimentin, fibronectin, N-cadherin, FSP-1, FAPα and SOX2) was compared between the STS cell lines and normal human mesenchymal cells (dermal, lung, uterine fibroblasts and mesenchymal stem cells) using western blot and Immunocytochemistry. Tumours were then grown from the UPS cell lines in NSG mice and immunohistochemistry and immunofluorescence staining were applied to tumour sections to further characterise mesenchymal protein expression. Finally, RNAseq was used to characterise differences in stromal gene expression between the STS cells and the mouse stroma by aligning reads against the human and mouse reference genomes (Bradford et al. 2013).

Findings: *In vitro,* expression of Transgelin/ SM22α and αSMA was significantly decreased in UPS and MFS cells compared to normal fibroblasts. All the other proteins (vimentin, N-cadherin, fibronectin, FSP-1, FAPα and SOX2) were expressed equally in all cells (UPS, MFS and normal mesenchymal cells). Three of four UPS cell lines were

successfully grown as xenografts in NSG mice. Although expression of mesenchymal proteins was confirmed by immunostaining, we were unable to segment UPS cells from stromal cells to confirm the differences in expression levels detected by western blot. 12 samples were selected for RNAseq analysis based on RNA quality, average mean vascular density and necrosis. For each sample there were an average of 39 million human reads and 40 million mouse reads. All samples showed high quality sequence data on quality control and comparison of the xenograft's transcriptomes with human STS showed a high degree of similarity with clinical UPS and MFS. RNAseq analysis confirmed that transgelin and αSMA expression was reduced in STS cells when compared with the stroma, which make these very likely to be SAF markers. Although typical CAF markers FSP-1 and FAPα were also increased in the stroma compared to the UPS cells, our earlier immunofluorescence studies showed a high percentage of cells positive for these were also positive for the mouse macrophage marker F4/80 and so are not exclusively SAF markers. Additional genes normally considered mesenchymal were found to be highly expressed in the stroma when compared with STS cell lines, allowing the identification of a possible "SAF gene panel" signature for STS including: transgelin, αSMA, vimentin and MFAP5. Although there was a trend for decreased overall survival in STS patients with low expression levels of our SAF gene panel, this was not statistically significant.

Conclusions: Of all the mesenchymal proteins examined so far, Transgelin showed the most promise for the identification of SAF versus STS cells. Analysis of the RNAseq data shows it was possible to identify mouse stromal genes from UPS xenografts. Differential gene expression between the three UPS tumours was used to identify a novel stromal gene signature and subsequently led to the identification of a possible "SAF gene panel" for use in future STS studies.

Table of Contents

List of Figures

Chapter 1

Chapter 2

Chapter 3

Chapter 4

Chapter 5

Appendix

List of Tables

Chapter 5

Appendix

Chapter 1

Introduction

1.1 Cancer

Cancer is a leading cause of mortality worldwide and caused approximately 9.6 million deaths in 2018 (Cancer Research UK, 2020). It is characterised by uncontrolled cell growth, which can occur anywhere in the body. Hanahan and Weinberg originally proposed cancer hallmarks in 2000. These have since expanded from the original six to eight hallmarks leading to cancer development and progression (Hanahan & Weinberg, 2011). Additionally, healthy stromal cells only differentiate into a neoplastic state when they exhibit all of these hallmarks (Fig. 1.1). If one cancer development stage is disturbed, then cancer will stop at the primary site (Joyce & Pollard, 2009). Two enabling characteristics were added to the core eight cancer traits: genome instability and mutation and tumour-promoting inflammation (Hanahan & Weinberg, 2011). Moreover, Hanahan and Weinberg (2022) recently added another four traits to the core cancer hallmarks: unlocking phenotypic plasticity, non-mutational epigenetic reprogramming, polymorphic microbiomes, and senescent cells (Hanahan, 2022).

1.2 The molecular basis of cancer

Cancer is a complicated and multi-step process caused by genetic mutations affecting important cellular development pathways. Oncogenes and tumour suppressor genes directly affect cancer development and progression when mutated. Oncogenes are involved in the transition of normal cells to cancerous cells, and their higher expression is associated with cancer development. Oncogenic Kirsten rat sarcoma viral oncogene homolog (*KRAS*) is one of the most common oncogenes that plays a vital role in cancer development in different carcinomas, including pancreatic (Kisiel et al., 2012) breast (Hwang et al., 2019), and colorectal (Dinu et al., 2014). *KRAS* is a member of RAS gene family which known to play an important role in cell development, cell proliferation and cell signalling (Miller & Miller, 2011). Evidences illustrated that the variety of RAS mutations will results in different outcome, some studies found that *KRAS* mutation was linked with poorer overall and progression free survival (Liu et al., 2011; Miller & Miller, 2011). Liu *et al.* (2011) showed that mutated *KRAS* played an important role in sustaining cancer proliferation, one of the cancer hallmarks (Fig. 1.1). Mutant tumour protein p53 (*TP53*) is a common tumour suppressor gene in various carcinomas, including colorectal

(Li, 2015) and breast (Duffy et al., 2018).*TP53* mutations are present in most sarcomas, including Ewing sarcoma, rhabdomyosarcoma (RMS), undifferentiated pleomorphic sarcoma (UPS), and leiomyosarcoma (LMS), indicating that the p53 pathway is commonly altered in sarcomas (Thoenen et al., 2019). P53 is a transcription factor that regulates G2/M checkpoint and activates apoptosis (Fischer et al., 2016). Oncogenes induce DNA replication stress through uncontrolled proliferation, resulting in DNA damage and, eventually, genomic instability (Yao & Dai, 2014).
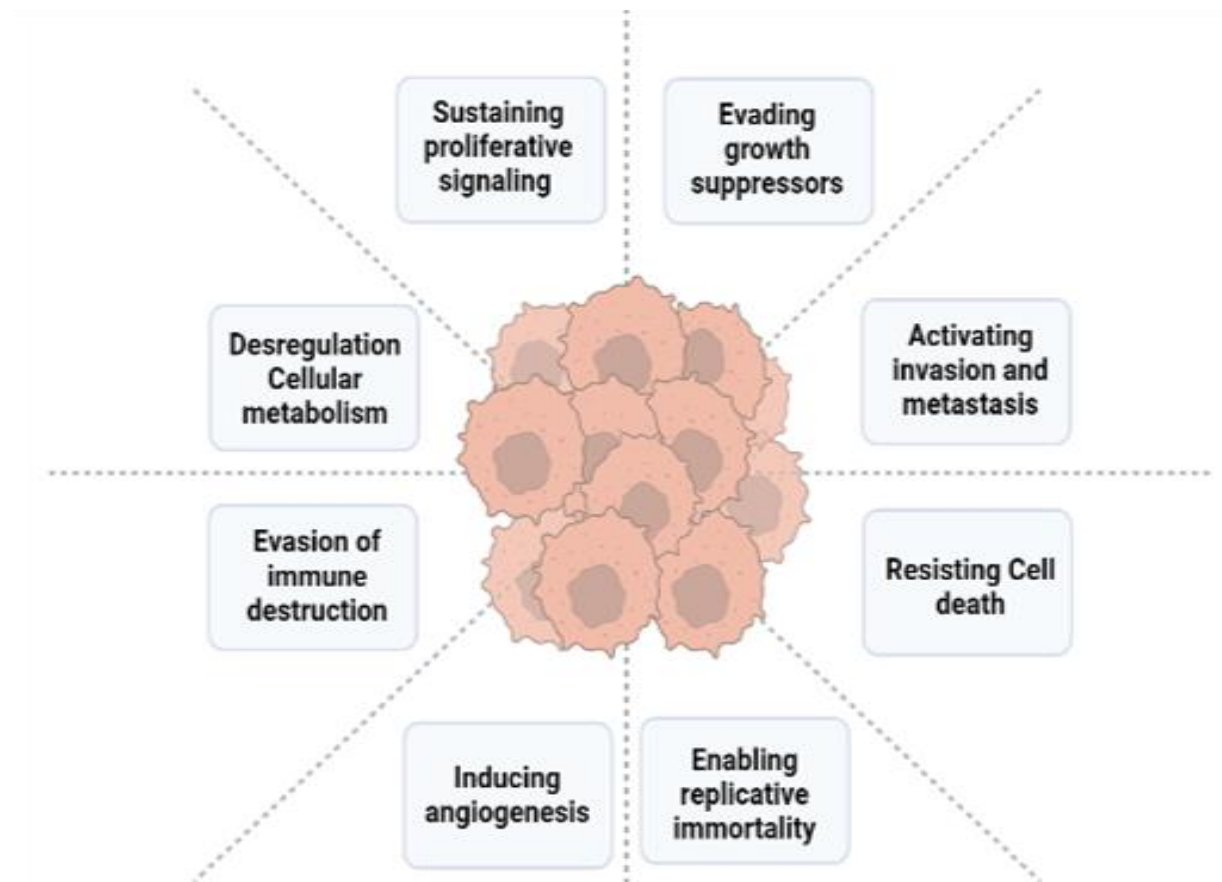
Figure 1. 1: Cancer hallmarks: the eight cancer cell traits.

This figure was adapted from Hanahan and Weinberg (2011) and created using Biorender.com.

1.3 Sarcoma

Carcinomas are malignant tumours derived from epithelial cells. However, sarcomas are malignant tumours arising from connective tissues (mesenchymal cells) (Saggioro et al., 2020). Sarcomas are biologically rare, heterogeneous, and complex solid tumours of mesenchymal origin. About 80% originate from soft tissues, while the remaining 20% originate from bone (Bulbul et al., 2017). They can occur at all ages, with some sarcoma types more common in children than adults (Monika & Olle, 2015). The incidence rate of sarcomas in the UK is ~4,295 new cases annually (Cancer Research UK, 2019). They account for 1%–2% of all human malignancies (Morozov et al., 2010). It is a heterogeneous disease comprising >70 subtypes classified based on their histological appearance, tumour location, similarity to their origin tissue, genetics, and age at onset (Abeshouse et al., 2017; Fletcher, 2014; Jo & Fletcher, 2014). Sarcomas can be categorised based on the tumour location as bone and soft tissue (STS) sarcomas. Moreover, sarcomas may be classified based on genetic mutations into simple and complex karyotypes (Xiao et al., 2013). Sarcoma histotype heterogeneity is considered a consequence of transformation from highly heterogeneous normal mesenchymal cell populations (Fig. 1.2).
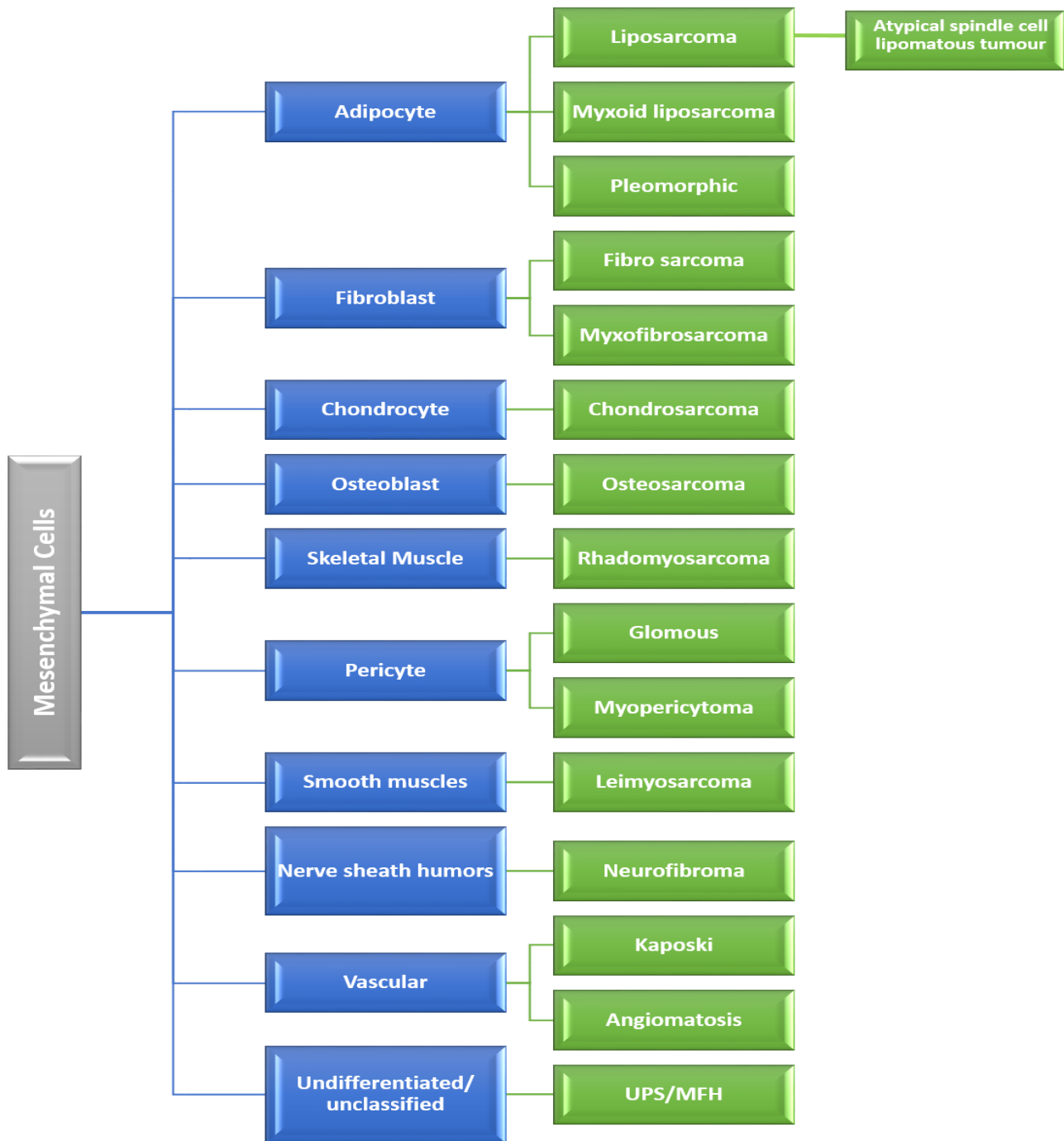
Figure 1. 2: The predominant sarcoma histotypes.

Based on the current WHO classifications of tumours: soft tissue and bone tumours 2020. This diagram shows the common sarcoma histotype and the normal mesenchymal cells they are hypothesised to originate from. Some sarcomas are well differentiated like liposarcomas whereas others are less differentiated like fibrosarcoma and myxofibrosarcoma. Furthermore, UPS/MFH have an uncertain origin with most likely origin of mesenchymal stem cells (Robles-Tenorio & Solis-Ledesma, 2022).

Since my PhD studies will be focused on adult STSs, the remainder of this review will focus on this sarcoma subset. For bone sarcomas, please see the recent reviews by (Bleloch et al., 2017; Savvidou et al., 2021; Z. Xin et al., 2021).

1.4 Soft Tissue Sarcomas (STS)

STS comprises approximately 70 subtypes categorised based on histological and molecular pathology (Sbaraglia et al., 2021). As mentioned in the previous section, they show characteristics suggesting they arise from different normal mesenchymal cell populations (e.g. muscle, cartilage, blood vessels, nerve, and fat) (Vodanovich & M Choong, 2018).

1.4.1 STS classifications

Only ~20% of STSs have previously identified diagnostic markers such as gene mutations or chromosomal aberrations (Abeshouse et al., 2017; Jo & Fletcher, 2014). The genotype classifications broadly divide STSs with genetic aberrations into recurrent translocation-driven, non-translocation-driven STSs (Genadry et al., 2018), and complex karyotypes with no definite pattern (Jain et al., 2010) groups. The World Health Organisation STS classification scheme, updated and released in 2020, is based on the histological (Fig 1.2) and genetic (Doyle, 2014) findings. STS's rarity, heterogeneity, and genetic complexity make identifying targeted therapies difficult.

1.4.1.1 Most common STSs

1- **Undifferentiated Pleomorphic Sarcoma (UPS)**, previously called malignant fibrous histiocytoma, as it has a "histiocytes-like" appearance and is rich in histiocytes (Genadry et al., 2018). It is the most common type of STS in adults, accounting for ~50% of all STSs (Sbaraglia et al., 2021). Its origins are uncertain, possibly mesenchymal stem cells (MSCs) (Fig. 1.2). It is classified into four subtypes (Table 1.1) (Matushansky et al., 2009).

Name	Percentage	Where in the body	Prognosis	References
Storiform-pleomorphic	70%	Extremities	Poor	(Matushansky et al., 2009)
Giant-cell	10%	Extremities & trunk	Poor	(Matushansky et al., 2009)
Inflammatory	5%	Retroperitoneum	Poor	(Matushansky et al., 2009)
Angiomatoid fibrous histiocytoma (AFH)	0.3%	Extremities(children and young adult)	Good	(Saito et al., 2017)

Table 1. 1: Four UPS subtypes classified based on their histological appearances.

2- **Myxofibrosarcoma (MFS)**

- It is one of the most common STSs.
- It accounts for 10%–20% of STSs.
- It was previously called myxoid fibrous histiocytoma and was a UPS subtype until 2002 when it became an independent entity.
- It commonly occurs in the extremities (Widemann & Italiano, 2018).

3- Liposarcoma (LPS)

- It is hypothesized to arise from adipocytes (Fig. 1.2).
- It accounts for 12.8% of all STSs.
- LPS classified into four subtypes (Table 1.2).

Subtype	Name	Percentage	Where in the body	Metastases	References
WD-LPS	Well-differentiated (Atypical spindle cell lipomatous)	40-45%	Extremities & retroperitoneum	Rarely metastasis and show low recurrence rate	(Arvinius et al., 2017)
MR-LPS	Myxoid/Round cells	30-35%	Extremities	1/3 of patients will develop metastasis	(Genadry et al., 2018)
DD-LPS	Dedifferentiated	15-20%	retroperitoneum	Metastasize by 15-20%	(Genadry et al., 2018)
P-LPS	Atypical Pleomorphic lipomatous	5%	Limbs	Associated with pulmonary metastasis	(Wang et al., 2018)

Table 1. 2: Four LPS subtypes classified based on their histology and prognosis.

4- Leiomyosarcoma (LMS)

- It is hypothesized to arise from smooth muscle (Fig.1.2).

- It accounts for 10-20% of all STS (Anderson et al., 2021).

- Characterized by genomic instability and non-chromosomal translocation (Genadry et al., 2018).

- It is classified into three subtypes (Table 1.3) (Guo et al., 2015).

Subtype	Name	Where in the body	Prognosis
I	Subtype I	Smooth muscle cells	Good
II	Subtype II	Smooth muscle cells	Poor
III	Subtype III	Uterus/scrotum	Poor

Table 1. 3: The three subtypes of LMS, where it occurs and the prognosis.

Data extracted from (Guo et al., 2015).

1.4.2 STS Aetiology prognosis and treatment:

The exact cause of STS remains unknown. Like other cancers, environment and genetics are important risk factors. Environmental factors include chemical exposure and ionising radiation. Genetic factors, including DNA mutations, were defined as STS causes based on genetic predisposition and iatrogenic factors (Benna et al., 2018).

The 5-year survival rate of STS patients is 50%–60%, depending on the tumour type, age at onset, and stage (Genadry et al., 2018). The 2-year survival rate of patients with metastatic disease at diagnosis is currently <20%.

1.4.3 Current standard care and newer target therapies:

The current standard care for these tumours is surgical intervention, chemotherapy, and radiotherapy or their combinations. STS's heterogeneity has made identifying a single effective therapy challenging. Therapy choice depends on clinical interpretation, tumour sites, types, and grades (Vodanovich & M Choong, 2018). Chemoresistance is very common in STS, and new therapies must depend on tumour-specific biology (Ehnman & Larsson, 2015). While radiotherapy is commonly used with tumour removal, not all STS are radiosensitive, depending on tumour type and origin (Hoefkens et al., 2016). Prof Catharine West's group, Manchester, worked with peripheral limb STSs collected from the phase III (Randomized Trial of **Vo**lume of Post-operative **R**adiotherapy given to adult patients with **eX**tremity Soft Tissue Sarcoma) VorteX trial (NCT00423618) to identify a biomarker panel for radiotherapy response (Forker et al., 2017).

Moreover, present standard care for patients, such as carotuximab (TRC105) with pazopanib, did not improve progression-free survival (PFS) compared to pazopanib alone to treat angiosarcoma (Forker et al., 2017). Pazopanib is a tyrosine kinase inhibitor that inhibits angiogenesis (Jones et al., 2022). TRC105 targets CD105 (endoglin), endoglin is an endothelial marker which known as an angiogenesis marker (Ehlerding et al., 2018). In addition, olaratumab, a monoclonal antibody targeting platelet-derived growth factor receptor-alpha (PDGFRα), used in combination with doxorubicin did not improve overall survival (OS) compared to doxorubicin alone in advanced STS (Tap et al., 2016).

A newer targeted treatment focusing on cancer stem cells (CSCs), also called tumour-initiating cells, has been developed for all cancers. CSCs can recreate the original tumour heterogeneity from a very small number of cells and act as a small reservoir of drug-resistant cells that can overcome chemotherapy (Genadry et al., 2018). A new goal is to identify unique CSCs for all STS subtypes so that CSCs can be used as a better prognostic indicator for therapy response (Genadry et al., 2018). Moreover, immune checkpoint inhibitors have been emerging for many cancers. In STS, a higher expression of PD-L1 as an immune checkpoint protein was associated with poor OS (Orth et al., 2020). Another study was done on STS patients revealed that better response to anti-PD-L1 therapy was linked to higher immune cell infiltration (Keung et al., 2020).

However, since STSs are highly diverse and have few common genetic abnormalities, new investigation avenues are needed to identify novel therapeutic options. The tumour microenvironment (TME) is not as well characterised in STS as in carcinomas. Since STS is mesenchymal rather than epithelial in origin, its cellular communication with the stroma may be significantly different and present novel opportunities for therapy.

Therefore, the role of non-transformed mesenchymal cells is particularly poorly understood in STS compared to carcinomas. This review will now introduce key aspects of TME and discuss the role of mesenchymal cells in cancer and STS in particular in the following sections.

1.5 The Tumour Microenvironment (TME):

Recent studies have shown that the cancer pathogenicity does not only come from the genetically transformed cancer cell, but also from the surrounding stroma.

The local environment encompassing the stroma and cancer cells is referred to as the Tumour Microenvironment (Balkwill et al., 2012). The TME comprises the extracellular matrix (ECM) and a diverse mixture of cells, including cancer cell itself and stromal cells such as fibroblasts, endothelial cells, pericytes, adipocytes, myeloid cells (e.g. macrophages), and lymphocytes (e.g. T-Cells) (Li et al., 2007; Noma et al., 2008). These surrounding cells enhance tumour growth, differentiation, invasion, and metastasis (Kidd et al., 2012). Paget was the first to propose the TME's importance, postulating his 'seed and soil' theory (Ribatti et al., 2006). Paget showed that whenever the 'soil' (the surrounding environment) provides a suitable environment, the 'seed' (cancer cells) will grow and spread into the secondary site (Ribatti et al., 2006). Moreover, he believed that metastasis never occurs unless 'the seed and soil' were well-matched (Joyce & Pollard2008).
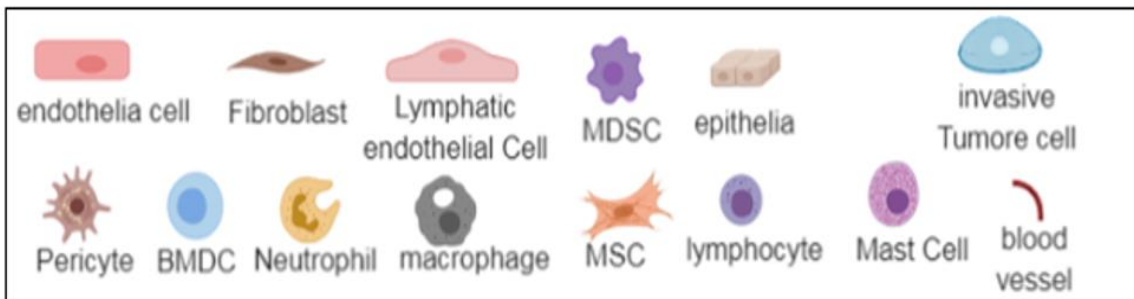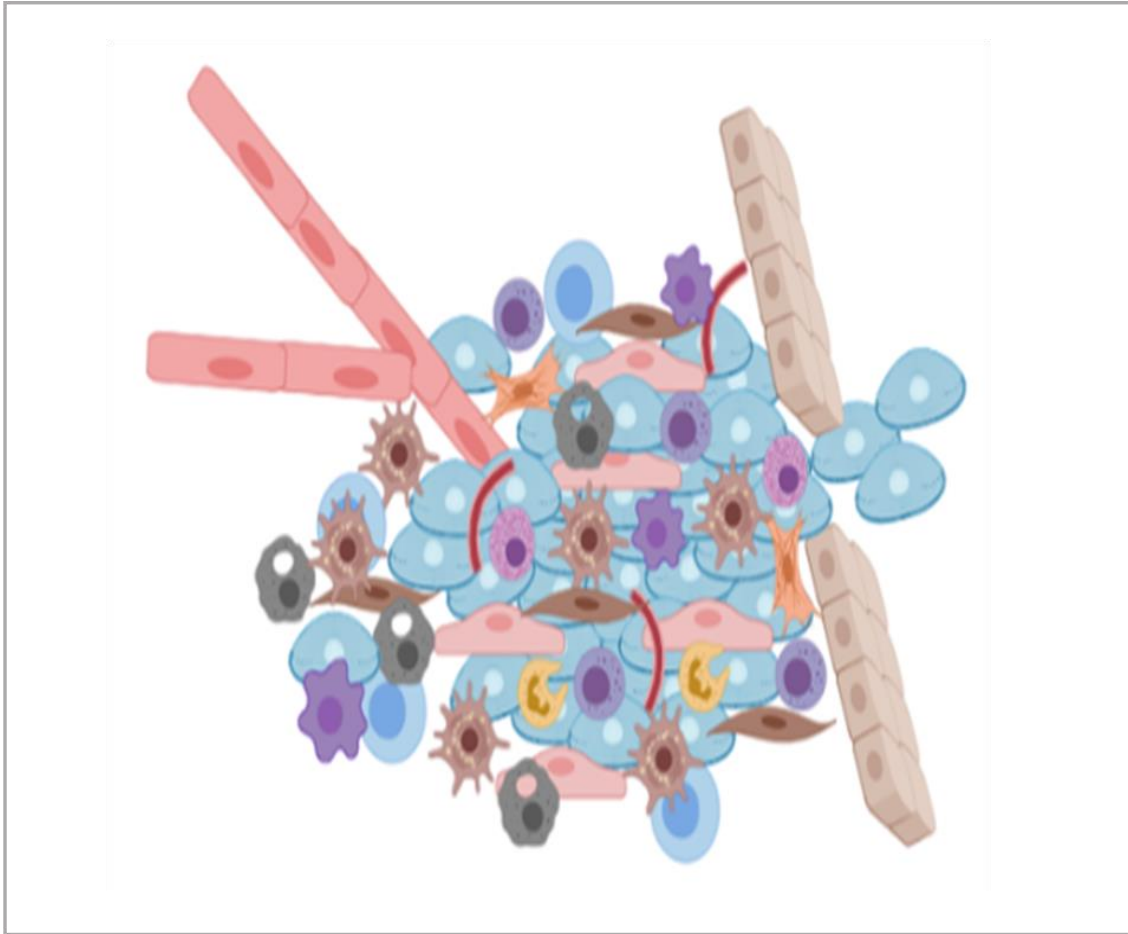
Figure 1. 3: Tumour Microenvironment.

The cellular environment where cancer cells exist along with the stromal cells including MSC, pericytes, fibroblasts, immune cells, blood vessels all embedded in the Extracellular Matrix (ECM). Created using Biorender.com.

1.5.1 The Extracellular Matrix (ECM):

The ECM is a significant TME component. It comprises a complex network of macromolecules such as collagen, fibronectin, elastin, proteoglycans and non-collagenous glycoproteins (Järveläinen et al., 2009), which constructs a three-dimensional matrix with distinctive biochemical and biomechanical functions (Pickup et al., 2014). It regulates organ hemostasis and cellular mechanisms including cell growth, movement, survival, and differentiation. It also provides a supportive matrix for tissue function and cell adhesion. It maintains the TME by regulating growth factor and cytokines bioavailability and diffusion, and maintains hydration and PH (Pickup et al., 2014). However, normal ECM functions are disturbed in cancer (Lu et al., 2012). Dynamic changes in ECM turnover are crucial during development, controlled by specific enzymes such as Matrix Metalloproteinase (MMPs). The cell mainly responsible for ECM production is the fibroblasts and myofibroblasts as these produce a number of ECM molecules and also the proteinases like MMPs that control the turnover. These cells are also responsible for fibrosis and proteinase production in cancer (L. E. Tracy et al., 2016). However, fibrosis and angiogenesis are promoted when the ECM dynamics are deregulated after normal development is completed (Lu et al., 2012). This chapter, will focus on mesenchymal cells as they predominantly contribute to ECM remodelling including how they affect other stromal components within the TME (Bhowmick et al., 2004). In sarcoma, many ECM molecules expression was detected in different STS subtype, but the functional role of ECM in STS is still poorly understood (Pankova et al., 2021).

1.5.2 Important cells in the TME:

1.5.2.1 Immune cells.

The immune cells are an important TME component. It is divided into tumour-inhibiting groups and tumour-promoting group. The tumour provoking group composed of effector Tcells, Natural killer (NK) cells, Dendritic cells (DC), M1 polarized macrophages and N1 polarized neutrophils. This group aim to destroy cancer cells by secreting chemokines (Habif et al., 2019), but some cancer cells will escape the immune function and will block

the tumour provoking immune cells via specific mechanism, resulting in evasion immune destruction (one of hallmark of cancer (Fig.1.1).The tumour promoting group composed of Regulatory T cells (Treg), and M2 polarized macrophages, which enhance tumourgenesis by enhancing angiogenesis, cell migration and metastasis (Lei et al., 2020). In sarcoma, the common immune cell type was M2 macrophages followed by lymphocytes (D'Angelo et al., 2015; Stahl et al., 2019). Understanding immune cells is a good predictor for disease outcome and progression and therapy response.

1.5.2.2. Mesenchymal cells.

Several different terminologies used for fibroblasts in tumours, however as in non-neoplastic tissue mesenchymal cells they can broadly be put into three groups: Mesenchymal Stem Cells (MSCs)/ pericytes, "resident fibroblasts" and activated fibroblasts/ myofibroblasts. MSCs don't express activated fibroblast markers and when isolated, should be able to transdifferentiate into adipocytes, osteoblasts and myofibroblasts. Pericytes have been described as having MSC- characteristics, and are associated with the vasculature. Resident fibroblasts are not stem cells nor pericytes as they cannot tri-differentiate, and do not express activated fibroblast markers. Activated fibroblasts (myofibroblasts) and CAFs: show elevated expression of alpha smooth muscle actin (αSMA), collagen-I, III, XI, fibronectin (FN), MMPs, Tissue Inhibitors of Metalloproteinase (TIMP-1, TIMP-3), connective tissue growth factor (CTGF/CCN2) and have evidence of SMAD activation. These characteristics are the classical definition of an activated fibroblast contributing to fibrosis and repair. One key feature they have in common is they typically can contract collagen or fibrin gels in culture. They also express cytokines and growth factors that act on the immune system and activate EMT in cancer cells (Cushing et al., 2008). Transforming growth factor (TGF-β) is a prominent regulator of MSCs differentiation into activated fibroblasts and can also activate EMT. TGFβ is released from the ECM through proteolysis, often secreted by fibroblasts during activation to myofibroblasts and immune cells.

This chapter will explain the role of these three types mesenchymal cell in normal tissue and their role in cancer.

Cells	Features	Alternative names	Markers
MSC	• Tri-Differentiation • Multi-potent • Self-renewable		Vimentin N-cadherin PDGFRβ** FSP-1*
Pericytes	MSCs associated with the vasculature		Desmin NG2 PDGFRα/β αSMA
Resident Fibroblasts	• Lost tri-differentiation capability. • Able to respond to factors to be activated into myofibroblasts.	Resting mesenchymal cells	FSP-1
Activated fibroblast	• Contractile. • Migratory and invasive. • ECM synthesis and remodelling.	• Myofibroblasts. • Cancer Associated fibroblasts (CAFs).	αSMA

Table 1. 4: Most common cells in the TME.

*Fibroblast Specific Protein-1 (FSP-1). ** Beta-type platelet-Derived Growth Factor Receptor (PDGFRβ).Vimentin, PDGFRβ.FSP-1 and αSMA were known as CAF marker (Han et al., 2020).

1.5.2.2.1 Mesenchymal stem cells (MSCs) in normal tissue:

The mesenchyme is derived from the mesoderm that forms during embryonic development. Mesenchymal cells can differentiate into hematopoietic and connective tissue cells including smooth muscle cells, endothelial, connective tissue cells, and blood cells (Adolfo, 2009). MSCs are a heterogeneous group of fibroblast-like, self-renewable, multipotent stem cells originating from the bone marrow and adipose tissue and can differentiate into different cell types including: osteocytes, adipocytes, chondrocytes, muscle cells and fibroblasts (Gazdic et al., 2015) (Fig 1.4).
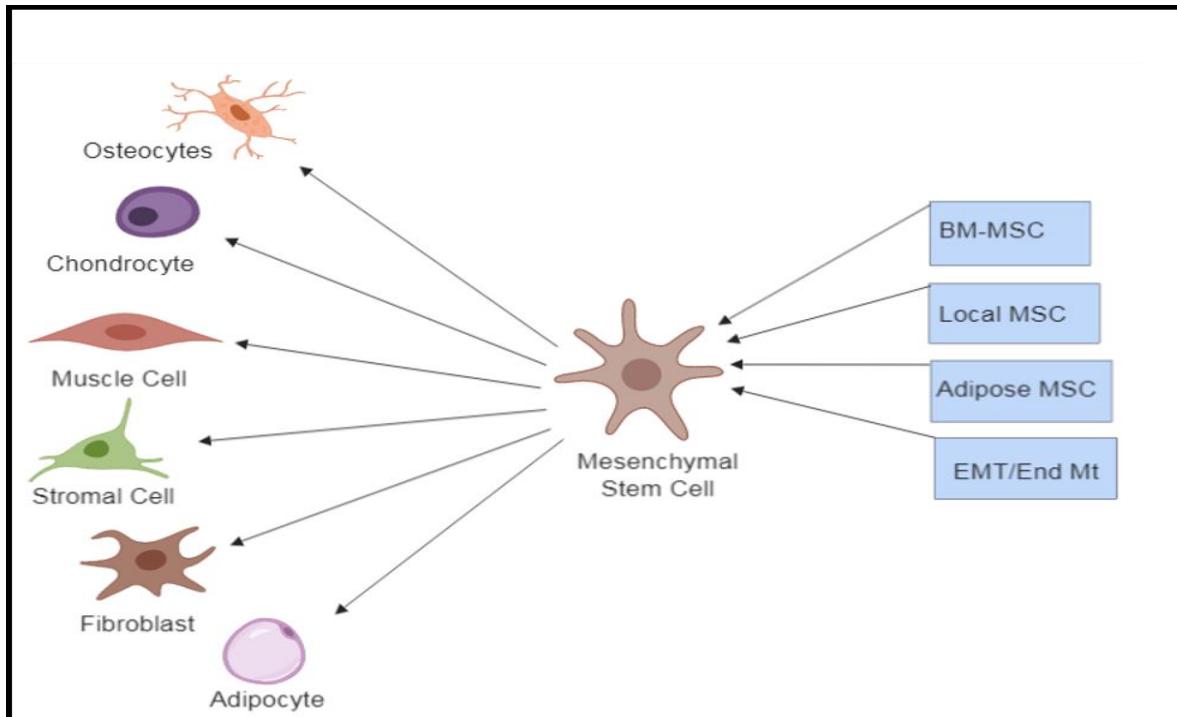
Figure 1. 4: Mesenchymal heterogeneity.

This figure shows the different origins of the MSC, and how MSCs can differentiate to osteocytes, chondrocytes, muscle cells, stromal cells, fibroblasts and, adipocytes. Created using biorender.

MSCs play a crucial role in immune regulation since they can change the immune response by altering the cross talk between cells or by secreting different factors (Gazdic et al., 2015). Recent studies have shown that MSCs can adopt an immunosuppressive phenotype when exposed to high levels of pro-inflammatory cytokines such as Interferon gamma and tumour necrosis factor alpha (TNFα). Therefore, MSCs have been widely studied in preclinical and clinical studies of autoimmune disease such as rheumatoid arthritis and multiple sclerosis (Gazdic et al., 2015). Moreover, mesenchymal cells derived from epithelial-mesenchymal transition (EMT) can play an important role in maintaining connective tissue and organ structure (Tennakoon et al., 2015). The site-directed delivery features of MSCs to the injury site mean they can play a crucial role in tissue repair (Marion & Mao, 2006; Tanabe, 2014). One example is the role of MSCs in the wound-healing mechanism includes secretion of specific factors or "inflammatory mediators", including growth factors such as vascular endothelial growth factor A (VEGFA) and Angiopoietin-1, can activate wound-repair mechanisms including cell recruitment, angiogenesis and differentiation (Isakson et al., 2015).

Fibroblasts are a major connective tissue component of mesenchymal origin in the tissue matrix known by their spindle-shape morphology surrounded by collagen (type I and III). (Kalluri & Zeisberg, 2006).

Fibroblast functions in normal tissues include:

- **Wound healing**

  Platelets are released in the injury site. In contact with the collagen produced by fibroblast, they will adhere to the injured area and release growth factors such as (TGF-β), platelet derived growth factor (PDGF), interleukin 1-beta and MMPs to activate fibroblasts which migrate to the wound site (Paraiso & Smalley, 2013). The activated fibroblasts secrete growth factors such as TGF-β, and express αSMA facilitating their migration towards the wound and wound contraction(Kalluri & Zeisberg, 2006). The activated fibroblast become larger, contractile and secrete ECM (Collagen-I, FN and growth factors fibroblast growth factor 2 (FGF2), PDGF, epidermal growth factor (EGF), and TGF-β) that regulate and recruit immune cell

(macrophage, neutrophil, and lymphocyte) and other – (endothelial cells, nerve cells and skin keratinocytes) cells to repair the wound.

- **Tissue repair/remodelling/fibrosis**

  Fibroblasts release specific signals to respond to the damage. They can differentiate into myofibroblasts, which are responsible for wound closure and scarring through their specialised contractile feature. Two factors are essential for normal tissue repair: fibroblast activation and ECM remodelling. Fibrosis will occur when one of these factors is disrupted (Krieg, 2008) . When wounding or acute or chronic inflammation causes fibrosis, fibroblasts will be activated and secrete growth factors such as TGF-β, and express αSMA which will facilitate migration towards the wound and wound contraction(Kalluri & Zeisberg, 2006). The activated fibroblast will acquire the same phenotype as in wound healing section.

1.5.2.2.2 Mesenchymal Stem Cells in cancer:

MSCs migrate towards tumour sites in cancer using similar mechanisms to migration towards inflammation sites in the wound-healing process (Ridge et al., 2017). Bone marrow MSCs (BM-MSCs) have a dual role in tumorigenesis since they can inhibit or stimulate tumour growth depending on different factors, including cancer type and MSCs heterogeneity (Barcellos-de-Souza et al., 2013; Ridge et al., 2017). MSCs are known for enhancing apoptosis and cell cycle arrest in the G0/G1 phase, which results in inhibition of tumour progression (Rastegar et al., 2010). Tumour suppression by MSCs has been found in melanoma, Kaposi sarcoma, breast cancer and hepatoma (Ridge et al., 2017). However, MSCs can stimulate tumour progression when found in the primary tumour. Karnoub *et al.* have postulated that MSCs could be considered a "cellular vehicle" that direct anti-cancer substances to the tumour site (Antoine et al., 2007). They also suggested that MSC could change the behaviour of the cells surrounding the tumour and promote the metastasis of breast cancer cells to the lung. Moreover, they found that MSCs effect on metastasis was only evident at the primary site for a short period, concluding that MSCs do not contribute to metastasis alone and that other stromal cells may also be involved (Antoine et al., 2007).

They enhance metastasis due to their ability to migrate to the tumour site and secrete pro-angiogenic paracrine factors such as fibroblast growth factor-basic (bFGF), VEGF, and TGF-β (Rastegar et al., 2010) (Table 1.4). The interaction between the MSCs and the tumour cells via paracrine secretions induces EMT, contributing to tumour invasion and metastasis (Ridge et al., 2017).

Resident fibroblasts in cancer

Resident fibroblasts are usually resting mesenchymal cells that have lost their differentiation capability. In cancer, resident fibroblasts are considered precursors of activated fibroblasts or CAFs. However, little is known about their role in cancer (Butti et al., 2021).

Activated fibroblasts/ myofibroblasts in cancer

TGF-β can activate fibroblasts in cancer. These activated fibroblasts express high levels of αSMA and vimentin. When fibroblasts are activated, they cause ECM remodelling and induce fibrosis and desmoplasia. Desmoplasia is the formation of fibrous connective tissue and is a TME feature; it has been shown to cause tumour invasion, proliferation, and chemoresistance in pancreatic ductal adenocarcinoma (PDAC) (Cannon et al., 2018). Excessive production of ECM proteins and collagen type I in particular induce desmoplasia. Desmoplasia or fibrosis is associated with poor prognosis in breast, pancreatic and liver cancer (Declerck, 2012). In addition, excessive production of ECM proteins by CAFs will increase the ECM stiffness which will lead to activating EMT independently of other factors (Piersma et al., 2020). MSCs functions in normal and cancerous tissues are similar. However, the main difference is that activated MSCs in normal tissue undergo apoptosis after the wound has healed but remain active and are resistant to apoptosis in cancer tissue (Kalluri, 2016a, 2016b). Unlike MSCs, CAFs secrete high levels of VEGFA, TGF-β, HGF, interleukins 4 and 10, and TNFα that promote tumourgenesis. (Ridge et al., 2017).

While activated fibroblasts have different names in the literature (Table 1.4), I will be using CAFs to refer to activated fibroblasts in the remainder of the thesis introduction.

1.6 Cancer-Associated Fibroblasts (CAFs)

Kalluri *et al.* (2016) postulated that resident tumour fibroblasts are resting MSCs and when exposed to specific stimuli will be activated and form Cancer-Associated Fibroblasts or CAFs (Table 1.4). While the mechanism behind this transition is poorly understood, many studies suggest that CAFs are activated fibroblasts.

1.6.1 CAFs and Myofibroblasts:

CAFs share some characteristics with myofibroblasts, including:

1. Their "spindyloid appearance": Large spindle-shaped cells (Xing et al., 2010) .
2. High *αSMA* expression level (Li et al., 2007).
3. High fibroblast-specific protein-1 (FSP1; (Cirri & Chiarugi, 2011) and vimentin production (Quante et al., 2011).
4. Both exhibit contractility phenotype due to high expression of αSMA (Nurmik et al., 2020).

1.6.2 Origin of CAFs:

CAFs origin varies between different cancer types (Cirri & Chiarugi, 2011).

1.6.2.1 Resident fibroblast derived:

CAFs form from fibroblast activation by different tumour stimulation factors, including TGF-β, PDGF, and bFGF, and express *αSMA*, *MMP1*, *MMP3*, and collagen (Quante et al., 2011). Kojima *et al.* (2010) confirmed this origin using a breast xenograft model, showing that human fibroblasts co-injected with breast cancer cells became CAFs through signalling pathways regulated by TGF-β and stromal-derived factor-1 (*SDF1*) cytokine expression (Kojima et al., 2010).

1.6.2.2 Mesenchymal stem cell derived:

During cancer initiation, growth factors VEGF, bFGF, and EGF secreted by cancer cells recruit MSCs (Cirri & Chiarugi, 2011). Spaeth *et al.* (2009) used an animal model to show that MSCs present in the tumour mass can differentiate into CAFs and pericytes (Spaeth et al., 2009). Moreover, Miyazaki *et al.* (2020) postulated that CAFs differentiated from adipose-derived MSCs (AD-MSCs). They co-cultured AD-MSCs and Capan-1 cells and then used transcriptome analysis to show that co-cultured cells expressed many CAF markers, indicating that MSCs may be CAF progenitors (Miyazaki et al., 2020).

1.6.2.3 Endothelial to mesenchymal transition (EndMT):

This transition occurs in response to TGF-β secretion, when endothelial cells delaminate from an organized cell layer lose their endothelial phenotype, and acquire a mesenchymal phenotype and migratory ability (Potenta et al., 2008).In brain endothelial cancer, EndMT can lead to metastasis, as the transition of endothelial cells into myofibroblast will acquire all the myofibroblasts phenotype including plasticity and migratory ability which key factor in metastasis event (Krizbai et al., 2015).

1.6.2.4 Epithelial-mesenchymal transition (EMT):

EMT occurs when epithelial cells lose their epithelial characteristics (e.g. cell-cell contact, columnar shape, basal-apical polarity, basement membrane attachment-dependent survival, and cytokeratin and E-cadherin expression) and acquire mesenchymal characteristics (e.g. cell-cell contact loss, spindle shape, polarised migration direction, and increased ECM, MMP, N-cadherin, and vimentin levels; (Xing et al., 2010). One hypothesis is that a mutation in genes regulating the EMT pathway enables epithelial cells to differentiate into CAFs. Tuhkanen *et al.* (2004) showed that a mutation in TP53 and phosphatase and tensin homolog (*PTEN*) leads to EMT-promoting cancer growth (Cirri & Chiarugi, 2011; Tuhkanen et al., 2004). Another study using prostate carcinoma cells showed that CAFs are responsible for the EMT (Togo et al., 2013). The TGF-β signalling pathway can augment CAF activity and tumorigenesis. However, CAFs phenotype is generally considered more stable in comparison with myofibroblasts, although the mechanism that controls this is not clear (Kalluri & Zeisberg, 2006). For example, is the

origin of CAFs and their phenotype cancer type-dependent? While many studies have studied CAFs, many questions remain to be answered.

1.6.3 CAFs functions

1.6.3.1   CAFs in tumour initiation

CAFs play an important role in tumour initiation, where they form 'gap junctions' between the activated fibroblasts to enhance cancer growth (Cirri & Chiarugi, 2011).Co-injection study of cancer cells with CAFs revealed an important role in tumour initiation, development and tumourgenesis (Anderberg et al., 2009).

1.6.3.2   CAFs in angiogenesis

Tumours require a vascular network to grow and spread (Li et al., 2007). Vascular Endothelial Growth Factor A (VEGFA) is the primary growth factor responsible for vasculature formation. As mentioned above CAFs produce VEGFA promoting tumour angiogenesis (Li et al., 2007). However, these new vessels are abnormal and have an irregular phenotype leading to hypoxia and enhanced VEGFA production (Li et al., 2007). CAFs also secrete many MMP family members that play an essential role in tumour angiogenesis (Kalluri, 2016).

1.6.3.3   CAFs in cancer metastasis:

CAF's role in tumour progression correlates with their MMP13 production since MMP13 is known to enhance tumorigenesis by destroying the ECM and basement membrane (Xing et al., 2010). Cell-cell interactions between CAFs and cancer cell induce adjacent ECM remodelling increasing cancer cell metastasis (Simian et al., 2001). Other studies have shown that CAFs accompany cancer cells travelling to secondary sites during metastasis (Xing et al., 2010). CAFs are considered as a guidance structure that aid cancer cell migration and invasion through the ECM (Cedric et al., 2007; Xing, 2011). Elevated MMP expression by CAFs will increase cancer metastasis through increased ECM degradation, facilitating invasion, the release of sequestered growth factors, and

chemokine activation. ECM secretion by CAFs increases stiffness that can also drive EMT in cancer cells (Cedric et al, 2007).

1.6.3.4   CAFs in immune regulation:

Cancer growth and proliferation are triggered by factors produced through inflammation (Balkwill & Mantovani, 2001). In a normal wound-healing process, infiltrating immune cells such as neutrophils and macrophages secrete growth factors and cytokines that increase fibroblast migration into the injury site becoming activated and transforming into myofibroblasts that remodel the ECM and contract the wound. After the injury is repaired the activated-fibroblast will undergo apoptosis to restore the normal tissue phenotype (Xing et al., 2010). However, pro-inflammatory cytokines produced by immune cells, CAFs, and cancer cells during cancer trigger increased immune cell migration towards the tumour (Xing et al., 2010). Macrophage, neutrophil, and lymphocyte levels are elevated in the tumour region. For example, macrophages differentiate into tumour-associated macrophages (TAMs) due to VEGF, hepatocyte growth factor (HGF), MMPs, and interleukin-8 secretion, triggering angiogenesis and cancer proliferation and metastasis. TAMs are classified as type 1 (classical-M1), which inhibit tumour growth, and type 2 (alternative-M2), which promote tumour growth (De Palma & Lewis, 2013). However, TAMs do not appear to undergo apoptosis. A strong relationship has been found between the tumour and inflammation, in which, inflammatory immune cells recruited to neoplasia, leading to tumour invasion and proliferation (Erez et al., 2010).

Fibroblast activation protein-α (FAPα)-CAFs are immune regulatory cells. In animal models, they exhibited an antitumor impact through blocking CD8+ T cell mediated killing of the cancer cell (Kalluri, 2016). In addition, a transgenic mouse study found that *αSMA* expressing CAFs led to an invasive tumour with elevated regulatory T cells, indicating an immunosuppressive TME phenotype (Kalluri, 2016).

Ligand-receptor interactions between programmed cell death protein 1/programmed cell death ligand 1 (PD-1/PDL-1) and cytotoxic T-lymphocyte associated protein 4/cluster of differentiation 80 (CTLA-4/CD80) regulate the two main immune checkpoints. . A PDAC study found that T cell functions were suppressed by immune regulatory FAPα+ cells controlling these two cell checkpoint antagonists (Christine et al., 2013). CAFs appear to suppress T cell function since T cells were absent in regions with high C-X-C motif

chemokine ligand 12 levels, which can be produced by CAFs (Christine et al., 2013). The blockading of these immune checkpoints may be a promising therapy. Since CAFs produce pro-inflammatory mediators, they can trigger an immunosuppressive response

These all may contribute to immune resistance, which is discussed later in this chapter.

1.6.3.5   CAFs in therapy:

According to their crucial role in all stages of tumour initiation, angiogenesis, metastasis and immune regulation, CAFs are considered promising therapeutic target (Tables 1.5 and 1.6).

	Features	Advantage	Reference
CAFs	"Genetically stable."	Retain drug sensitivity.	(Loeffler et al., 2006)
	Constructing the TME	Facilitate the anti-drug agent circulation in a solid tumour.	(Loeffler et al., 2006)
	Paracrine signalling between CAFs & cancer cell promote tumour invasion and ECM remodelling	Target these signalling may be a focus for pharmaceutical	(Loeffler et al., 2006)

Table 1. 5: CAFs features making them a potential therapeutic target.

Function	Targeted drug	Clinical trial phase	Type of cancer	Reference
Responsible for constructing the blood vessels	VEGF inhibitors	Phase II	Metastatic colon cancers	(Tang & Moore, 2013)
Secreted by CAFs and it enhances cancer proliferation	anti-Tenascin-C	Phase II	brain cancer	(Reardon et al., 2006)
EMT	anti-FAP (Sibrotuzumab)	phase I	colorectal cancer	(Scott, 2003)

Table 1. 6: Examples of Therapeutic targets targeting growth factors and/or CAFs markers.

1.6.3.6   CAFs and drug resistance:

CAFs can regulate resistance to antiangiogenic therapy, the mechanism behind the resistance is still unclear (Crawford et al., 2009). Tao *et al*. (2016) found that CAFs treated with cisplatin increased chemoresistance in lung adenocarcinoma cells. Interleukin 11 (IL-11) is a cytokine expressed by CAFs. High *IL-11* expression correlates with poor prognosis in many carcinomas. *IL-11* was found to be highly expressed in CAFs treated by cisplatin under co-culture conditions, promoting anti-apoptosis signalling and facilitating lung adenocarcinoma cell colonisation (Tao et al., 2016). Moreover, CAFs increase radiotherapy resistance in rectal cancer cells through cytokine secretion, which enhances cancer cell proliferation and migration (Liska et al., 2017).

As can be seen from the literature cited in previous sections, the majority of research into the role of mesenchymal cells in the TME has been primarily into their role in carcinoma. Sarcomas are a rare cancer that arises from genetic mutations in mesenchymal populations of cells, rather than epithelial cell populations that give rise to carcinomas. The next sections contrast the known roles of Sarcoma Associated Fibroblasts (SAF) with CAFs.

1.7 Common mesenchymal proteins

Common mesenchymal proteins expressed by CAFs will be discussed in the next section of this chapter and their usefulness in identifying SAFs.

Protein	MSC/pericytes	Fibroblast/ Myofibroblasts	CAF	Reference
Transgelin	√	√	√	(Elsafadi et al., 2020; Nurmik et al., 2020)
αSMA	√	√√√	√√√	(Nurmik et al., 2020)
Vimentin	√	√	√	(Nurmik et al., 2020)
N-cadherin	√	√	√	(Hinz et al., 2004)
Fibronectin	√	√√√	√√√	(Erdogan et al., 2017)
FSP-1	√	√	√	(Nurmik et al., 2020)
FAPα	√	√√√	√√√	(L. Xin et al., 2021; Yuan et al., 2021)
SOX2	√	√	√	(Chen et al., 2008)
PDGFRα/β	√	√√	√√√	(Nurmik et al., 2020)
NG2/CSPG4	√	√	√	(Davidson et al., 2020)
Desmin	√	√	√	(Xing et al., 2010)
Tenascin N	√	√	√	(Hashimoto et al., 2021)
MFAP5	√	√	√	(Chen et al., 2020)

Table 1. 7: Common mesenchymal proteins and transcription factors expressed by the most common cells in the TME.

√= expressed, **√√√**= highly expressed.

Protein	LMS	UPS	MFS	Other STS	References
Transgelin	√√√ (Uterine LMS)	?	?	√ ESS	(Tawfik et al., 2014).
αSMA	√√	√	√	?	(Miettinen, 2014)
vimentin	√ ASPS	√	√	√ RMS	(Andrade et al., 2010; Folpe & Deyrup, 2006)
N-cadherin	√	√	√	√ SS	(Niimi et al., 2013)
Fibronectin	√	√	√	√ Ewing sarcoma	(Hawkins et al., 2018)
FSP-1	?	√	√	?	(Zhang et al., 2012)
FAPα	?	√√√	√√√	√ fibrosarcoma	(Baird et al., 2015)
SOX2	?	√	?	√ SS	(Genadry et al., 2018; Zayed & Petersen, 2018)
PDGFRα/β	√	√	√	√ SS, LPS	(Brahmi et al., 2021)
NG2/CSPG4	√	√	?	√ LPS	(Boudin et al., 2022)
Desmin	√ ASPS	?	?	√ RMS	(Andrade et al., 2010; Folpe & Deyrup, 2006)
Tenascin N	√	?	?	√ Ewing sarcoma	(Hawkins et al., 2019)
MFAP5	√	?	?	?	(Ke et al., 2022)

Table 1. 8: Common mesenchymal proteins and transcription factors expressed by different soft tissue sarcoma subtypes.

√= expressed, √√√= highly expressed, ? = not known. LMS= leiomyosarcoma, UPS=undifferentiated pleomorphic sarcoma, MFS=myxofibrosarcoma, ESS= Endometrial stromal sarcoma, ASPS= Alveolar soft part sarcoma, RMS=Rhabdomyosarcoma, SS=synovial sarcoma, LPS= Liposarcoma.

Protein	Protein Family	Normal function	Role in cancer	Marker	References
Transgelin	Calponin	• Maintain cell motility • Regulate the structure of actin cytoskeleton	A correlation between transgelin and poor prognosis in cancer.	Smooth muscle cells marker	(Liu et al., 2017; Zhou et al., 2016)
αSMA	Actin	• Crucial in fibrotic response. • Fibroblasts contractility • Fibrogenesis	Enhance metastasis, angiogenesis and chemoresistance	CAF- specific marker	(Kalluri, 2016b; Wintzell et al., 2012)
Vimentin	intermediate filament (IF)	• maintain cellular integrity • provide resistance against stress	Cancer invasion, tumour growth and Poor prognosis.	Marker of EMT	(Nieminen et al., 2006; Satelli & Li, 2011)
N-Cadherin or Cadherin-2	Transmembrane protein	• Facilitate cell-cell adhesion.	A strong correlation between N-cadherin and cancer progression.	Marker of EMT	(Mrozik,2018)

Fibronectin	Glycoprotein	• Cell adhesion • Cell migration • Cell differentiation	Enhance tumour growth and associated with chemoresistance	Prognostic cancer marker.	(Han et al., 2006; Kim et al., 2020; Kujawa et al., 2020)
FSP-1	S100	Regulating cell cycle and cell differentiation	Enhance tumour growth	Fibroblasts. Macrophages. Monocytes.	(Xing,2011;Oster reicher,2011)
FAPα	Serine protease	Function as: dipeptidyl peptidase collagenase activity.	Play a role in tumourgenesis and angiogenesis	CAFs. Macrophages. Monocytes.	(Lai et al., 2012)
SOX2	Transcription factor	1-maintanance in embryonic development. 2-Cabability of Self-renewable.	Elevated expression of SOX2 correlates with poor prognosis in various cancer.	Undifferentiated cell marker	(Chen et al., 2008; Sholl et al., 2010; Zhang et al., 2012)
PDGFRα/ β	Receptor tyrosine kinase	1-Maintanace of embryonic development. 2-Regulating Cell proliferation	1- Tumour angiogenesis. 2- Tumorigenesis , drug resistance and poor survival.	Mesenchymal progenitors	(Ding et al., 2010; Homsi & Daud, 2007; Kitadai et al., 2006; Song et al., 2005)
NG2/CSP G4	Proteoglycan	Play a crucial role in cell proliferation and migration	Protein expression was linked with poor outcome in STS and glioblastoma.	Prognostic cancer marker	(Benassi et al., 2009; Svendsen et al., 2011)

Desmin	intermediate filament (IF)	• Mechanical support for the muscles • Regulating gene expression	High expression correlates with poor prognosis in colorectal cancer.	Muscle-Specific	(Costa et al., 2004)
Tenascin C	Glycoprotein of the Extracellular matrix	Cell adhesion Cell proliferation	High expression was linked with poor outcome in various cancer.	ECM marker	(Lowy & Oskarsson, 2015; Raitz et al., 2003; Wang et al., 2010)
MFAP5	Glycoprotein	Integration of elastic microfibers, maintain cell behaviour and survival.	Overexpression was associated with poor outcome in breast cancer. Enhance tumour progression and metastasis in bladder cancer.	Prognostic cancer marker	(Wu et al., 2019; Zhou et al., 2020)

Table 1. 9: Common marker proteins and their functions in normal cells and in cancer cells.

Transgelin or Smooth Muscle 22 actin (sm22α) , is a marker of smooth muscle cell differentiation that enhances cell motility and contractility (Robin et al., 2013). One study on sarcoma showed that transgelin was more highly expressed in LMS than in UPS and MFS (Robin et al., 2013). Desmin and αSMA were used as markers for myofibroblast differentiation in muscle derived STS tumour (i.e. LMS) (Povýšil et al., 1997). αSMA has been widely used to identify CAFs and myofibroblast transformation since CAFs show higher αSMA expression than myofibroblasts (Chaurasia et al., 2009; Shen et al., 2017). Vimentin is used as a mesenchymal marker that is induced during EMT and produced by all mesenchymal cells. It plays a vital role in cell motility, adhesion, and migration (Nieminen et al., 2006). N-cadherin is an EMT marker whose expression is associated with various cancers, such as prostate (Jennbacken et al., 2010; Wang et al., 2016). A melanoma study showed that N-Cadherin expression is a positive sign of tumour growth. Fibronectin regulates mesenchymal cell migration. One study using 13 LMS samples showed that all highly expressed vimentin, 62% expressed desmin, and 38% expressed αSMA (Schürch et al., 1987). Both FSP-1 and FAPα are expressed in MSCs, myofibroblasts, and CAFs. FSP1 expression was detected in UPS and LPS tissues using immunohistochemistry (IHC) staining (Hashimoto et al., 1984). SRY-box transcription factor 2 (SOX2) is a transcriptional factor that plays an important role in regulating pluripotency and stem cell self-renewal. In cancer SOX2 plays a vital role in cancer stem cell (CSC) maintanace. Takeda *et al.* (2018) suggested that SOX2 may be a biomarker for colorectal cancer (CRC) since high SOX2 levels were associated with poor PFS in patients (Takeda,2018). CAFs express high levels of mesenchyme-specific proteins (See table 1.7). Most of these markers have been used to identify CAFs in the TME of different cancers (Augsten, 2014).

These markers are not consistently expressed in all CAFs, giving this population its heterogeneity. This heterogeneity has been associated with differences in phenotype and origin, resulting in different CAF subtypes. Sugimoto *et al.* (2006) postulated that there was more than one CAFs type in his *in vivo* study. While one CAF subtype expressed αSMA, PDGFRβ, and NG2, other subtypes predominantly express FSP-1. CAF marker proteins can be used to determine the prognosis of different tumour types (Cirri & Chiarugi, 2011). Cirri *et al.* (2011) postulated that carbonic anhydrase IX expression in

CAFs results in poor lung adenocarcinoma prognoses. However, another study showed that high caveolin-1 and *PTEN* expression lead to a better prognosis (Cirri & Chiarugi, 2011). CAFs secrete TGF-β and HGF in colon cancer, inducing primary tumour growth (Charlotte et al., 2004). Moreover, FSP-1 is also known to enhance tumour proliferation by a study conducted by Grum-Schwensen *et al.*(2005) in FSP-1 knockout mice, the tumour didn't grow. However in another study, an overexpression of FSP-1, triggered the tumour growth (Xing et al., 2010), confirming that the expression of FSP-1 can change the tumour fate. Another study showed that Stromal Cell-derived factor 1 (SDF-1) secreted by CAFs can enhance tumor metastasis (Goh et al., 2007).

However, in sarcoma, many of these studies are only looking at the markers in tumours and not distinguishing between tumour and stromal cells. Are these markers expressed by SAFs in the same manner as CAFs? The origin of SAFs is poorly understood. Like CAFs, do they have different origins? Are SAFs phenotypes STS histotype-dependent? Does SAFs exist? The following section will review the current literature on SAFs to determine if there are currently answers to these questions.

1.8 Previous studies on SAFs:

This section will describe the evidence for the existence of SAFs in previous literature. Cells in tumour microenvironment have been studied in different types of sarcomas and these are summarized in (Table 1.9). Since fibroblasts are the most abundant cells in the TME, fibroblasts markers were studied in the tumours but no study could distinguish between the marker expression between the tumour and the stroma making identification of SAF very difficult. In (Table 1.9), activated fibroblasts which might be SAF, were compared with MSC and myofibroblast, and their role was determined in each study.

Paper	Model/techniques	Activated fibroblats like MSC?	Activated fibroblasts like Myofibroblast?	Activated fibroblasts role	Sarcoma histotypes	Key Findings
(Lagacé et al., 1980)	histopathology		√	SAF= Contractile properties	MFH(UPS)	SAF found in Desmoplasia area.
				Responsible for fibromatoses in STS.	Liposarcoma	High number of SAF correlate with high amount of collagen in the neoplasm.
				Role in pathogenicity	fibrosarcoma	
(Xiao et al., 2013)	in vitro and in vivo culture	√		Initiate sarcoma. Enhance tumour progression	Fibrosarcoma. LMS	SAF differentiate into sarcoma is histotypes-dependent? / emphasized on the importance of the TME to determine the SAF fate.

Reference	Method			Description	Cancer type	Findings
(Yu et al., 2011)	co-culture mouse SAF+OS cells		√	Produce high amount of αSMA	Osteosarcoma	Expression of αSMA. Fused cells result in a multi-nucleated giant cells
(Bonuccelli et al., 2014)	Co culture OS cell line with normal MSC	√		Mitochondrial dysfunction. Tumour feeder (activate aerobic glycolytic pathway). Produce lactate	Osteosarcoma	SAF enhance pathogenicity and it enhance cancer cell migrations. SAF manipulate the OS cellular mechanism in the tumour site
(Genin et al., 2008)	xenografts model contain the reciprocal ASPL-TFE3 fusion		√	Produce high amount of α-SMA, exhibit SRF, enhance tumour growth & invasion	ASPS	inhibition of SRF by inhibiting TGF-β/SRF-Smad3 results in decrease the tumour growth and development
(Libura et al., 2002)	Immunostaining and fluorescence-activated cell sorter (FACS) analysis				Rhabdomyosarcoma	CXCR4-SDF-1 axis play an important role in metastasis. Expression of CXCR4 correlate with more aggressive form of RMS. SDF-1 alone shows indirect effect on tumour progression.

(Morozov et al., 2010)	Co culture sarcoma cell line with normal MSC. Xenograft	√		SAF differentiate to sarcoma	Osteosarcoma. Liposarcoma. Synovial, UPS	sarcoma cell lines exhibit MSC properties
(Salvatore et al., 2015)	Co culture OS cell line with normal human fibroblast		√	SAF produce MMP	Osteosarcoma	high MMP result in high YKL-40 protein, which is the main marker affect tumour growth
(Strahm et al., 2008)	Reverse transcription polymerase chain reaction (RT-PCR) and ELIZA		√		Rhabdomyosarcoma	Block the CXCR4-SDF-1 will decrease the migration of the tumour cells. SDF-1 influence the tumour migration in all RMS subtypes
(Dohi et al., 2009)	Reverse transcription polymerase chain reaction (RT-PCR) and immunohisto chemistry		√	SAF produce FAP &DPP-IV	Osteosarcoma. Ewing. UPS. RMS and others	Expression of FAP & DPP-IV is independent of malignancies potential in tumour.
(Koga et al., 2007)	Co culture ES with NHDF		√	SAF produce emmprin, which stimulate MMP-2	ES= Epithelioid Sarcoma	investigate the role of emmprin in SAF to upregulate MMP-2 production, resulting in tumour invasion

			productio n		
(Salvatore et al., 2014)	Co culture OS cell line with normal human fibroblast		√	SAF produce YKL-40	Osteosarc oma	The co cultured cells produce YKL-40 protein which known to promote tumour angiogenesis

Table 1. 10: A Summary of previous Studies on activated fibroblasts in STS microenvironment.

The limited numbers of studies of activated fibroblasts in STS also raise a number of questions regarding the existence of "SAFs". Does "SAF" functions vary in different STS subtypes? It also highlights the gaps in knowledge between CAFs and "SAFs". Which factors activate "SAFs"? Can "SAFs" transform to STS? Addressing these questions may be pivotal for developing newer targeted therapies for STS. However, before these can be answered identification of markers to differentiate "SAF" from STS cells are needed for improved characterisation of "SAF" function.

1.9 Project hypothesis and aim:

As the TME is considered to play a crucial role in tumorigenesis, and since mesenchymal cells contribute to the majority of the TME, their role should be more widely studied in STS. The overall aim of this PhD is to increase our knowledge in this area. The project hypothesis is to find a way to distinguish between fibroblast in sarcoma's stroma and STS cells. Since both fibroblast and STS are of mesenchymal origin, both must express common mesenchymal markers (e.g. table 1.7 in this chapter) which highlight the difficulty in using these markers to distinguish between tumours and the stromal cells in STS.

Objectives:

- To compare expression of mesenchymal proteins between human STS cell lines and normal human mesenchymal cells.

- To grow STS cell lines as xenografts in mice to allow identification of stromal gene expression of mouse transcripts by aligning RNAseq reads against the human and mouse reference genomes.

- To identify STS and "SAF" specific gene expression profiles to improve our fundamental understanding of STS biology.

- To determine if expression of mesenchymal genes influence prognosis in UPS and MFS STS subtypes.

Chapter 2

Materials & Methods

2.1 Cell lines

In this project nine tumour cell lines were studied. Seven of these cell lines were isolated from soft tissue sarcoma patients at the Sheffield Teaching Hospital Trust and collected between 2010 and 2012 (Salawu et al., 2016; Salawu et al., 2018). National research ethical approval was obtained for the tumour isolation and testing (Reference number 09/H1313/52). These cell lines were given an STS laboratory designation according to the order and year they were obtained. For example: STS 06/11 is a cell line derived from the sixth tumour isolated in 2011. The STS cell lines used in this project in Table 2.1.

Cell line	Naming	Subtype	Source	University
STS14/10	UPS1	UPS	Dr Karen Sisley	University of Sheffield
STS06/11	UPS2	UPS	Dr Karen Sisley	University of Sheffield
STS09/11	UPS3	UPS	Dr Karen Sisley	University of Sheffield
STS13/12	UPS4	UPS	Dr Karen Sisley	University of Sheffield
MUG2A	MUG2A	NA	Prof. Dominique Heymann	University of Nantes*
STS21/11w1	MFS1	MFS	Dr Karen Sisley	University of Sheffield
STS21/11W2	MFS2	MFS	Dr Karen Sisley	University of Sheffield
OH931	MFS3	MFS	Prof. Dominique Heymann	University of Nantes*
STS02/11	LMS	LMS	Dr Karen Sisley	University of Sheffield

Table 2. 1: STS cell lines used in this project.

 * From the European Sarcoma Network (EuSARC).

Four primary mesenchymal cell lines used as controls were purchased from PromoCell GmbH. These were isolated from pooled donors and used between passage 2 and 9 (Table 2.2).

Cell line	Naming	Company	Catalogue number
Normal Human Dermal Fibroblasts	NHDF	PromoCell	C-12302
Human Uterine Fibroblasts	HUF	PromoCell	C-12385
Human Pulmonary Fibroblasts	HPF	PromoCell	C-12360
Human mesenchymal stem cells from Adipose tissue	AD-MSCs	PromoCell	C-12977

Table 2. 2: Primary mesenchymal cell lines used in this project.

Two mouse cell lines were used in this project. (Table2.3)

Cell line	Naming	Source
T241-GFP	T241	professor Yihai Cao*
FS188	FS188	Dr William English **

Table 2. 3: Mouse cell lines used in this project.

*The T241 cell line is a spontaneously occurring fibrosarcoma from C57BL/6J mice.

** The Fs188 is a mouse fibrosarcoma cell line, expressing only the VEGFA-188 isoform, isolated from $vegfa^{188/188}$ E13.5 embryonic fibroblasts transformed with SV40 and hRAS (English et al., 2017).

2.1.1 Cell Culture.

Soft tissue sarcoma cells (all UPS, LMS ,STS21/11, OH931) were maintained in Roswell Park Memorial Institute 1640 Medium (RPMI) (LONZA) supplemented as outlined in (Table 2.4).MUG2A, Normal human dermal fibroblasts (NHDF), Human uterine fibroblasts (HUF), human pulmonary fibroblasts (HPF), T241 & FS188 were maintained in Dulbecco's Modified Eagle's Medium (DMEM) (Gibco) medium supplemented as outlined in (Table 2.4) .Human mesenchymal stem cells were cultured in MSC growth medium 2 (PromoCell) supplemented with 10% v/v of medium supplements (PromoCell). All cells were maintained in T75 cm² flasks (Nunc) and incubated at 37°C in 5% CO_2 incubator. Media were stored at 4°C and pre warmed at 37°C in a water bath prior to use.

Cell line	Media	Supplement	%(v/v)	Company
STS06/11	RPMI			
STS09/11		Foetal Bovine Serum (FBS)	10%	Gibco
STS13/12		Penicillin/Streptomycin (100 units/100ug/ml)	1%	Sigma
STS14/10		D+glucose (2.25mM)	0.40%	Sigma
STS21/11w1		L-Glutamine (200mM)	1%	Sigma
STS21/11W2		Amphotericin B	1%	Sigma
STS02/11				
MUG2A	DMEM	Heat inactivated Foetal Bovine Serum (FBS)	10%	Sigma
		Penicillin/Streptomycin(100 units/100ug/ml)	1%	Sigma
		L-Glutamine (200mM)	1%	Sigma
		Insulin Transferase Selenium (ITS)	1%	Gibco
OH931	RPMI	Heat inactivated Foetal Bovine Serum (FBS)	20%	Sigma
		L-Glutamine (200mM)	1%	Sigma
NHDF	DMEM	Heat inactivated Foetal Bovine Serum (FBS)	10%	Sigma
HUF		Penicillin/Streptomycin (100 units/100ug/ml)	1%	Sigma
HPF		L-Glutamine (200mM)	1%	Sigma
hMSC	MSC growth medium 2	Supplement Mix	10% v/v	PromoCell
T241	DMEM	Heat inactivated Foetal Bovine Serum (FBS)	10%	Sigma
		Penicillin/Streptomycin (100 units/100ug/ml)	1%	Sigma
		L-Glutamine (200mM)	1%	Sigma
FS188	DMEM	Heat inactivated Foetal Bovine Serum (FBS)	10%	Sigma
		Penicillin/Streptomycin (100 units/100ug/ml)	1%	Sigma
		L-Glutamine (200mM)	1%	Sigma
		Puromycin (2ug/ml)	1%	Sigma
		G418 (600ug/ml)	1%	Sigma

Table 2. 4: Media used in this project with the specific supplements for each cell line.

2.1.2 Cell thawing:

Cells in cryotubes were removed from -80°C and placed in a 37°C water bath for 1 to 1.5 minutes until 80% of the cells had defrosted, then cells were transferred into 15 ml centrifuge tubes containing 4 ml of pre-warmed cell culture medium. Cells were centrifuged at 400 xg for 5 minutes. Then the supernatant was discarded, and cells were re-suspended in 5 ml medium, transferred to a T25 culture flask and incubated in a humidified incubator at 37°C with 5% CO_2.

2.1.3 Cell passage:

Cell passaging (sub-culture) was done when the cells had reached 70-80% confluence. Spent medium was removed and cells were washed twice using sterile Phosphate Buffered Saline (PBS) (Lonza). Then Trypsin-EDTA (Sigma) (3-4 ml per T75 cm² flask) was added and cells incubated in a humidified incubator at 37°C with 5% CO_2 for 1-2 minutes. Cell detachment was observed under the microscope. An equal amount of media was added to the flasks to inactivate the Trypsin. Cells were collected by centrifugation at 400 xg for 5 min. After centrifugation, the supernatant was discarded, and the cell pellet was re-suspended with fresh media and split into an appropriate number of flasks. Flasks then incubated at 37°C with 5% CO_2 in a humidified incubator. Cells were checked daily until they reached 80% confluence, and media were changed every other day.

2.1.4 Automated cell counting

The viability of cells was checked using the TC20^{TM} automated cell counter (Bio-Rad). After following all the steps in sections 2.1.3 and when cells are resuspended with fresh media a 10 µl of the cell suspension was gently mixed with 10 µl of trypan blue (Bio-Rad) and 10 µl of the cell resuspension was loaded in the half circle chamber of the counting slide (Bio-Rad), then the slide was inserted into the slide slot of the cell counter and viability and cell number was recorded.

2.2 Western Blotting

2.2.1 Protein Extraction

Cells were seeded in T75 cm² flasks until reach 80% confluence. The flask was kept on ice while spent media was removed, then cells were washed with ice-cold PBS (Lonza).

Cells were scrapped using 1 ml of iced-cold lysis buffer composed of EDTA (5mM), Phosphatase and protease inhibitors (2x) (Roche).Then cells were passed through needles starting from 25G to 30G to lyse the cells. Cells were then transferred to a pre-cooled 1.5 ml microcentrifuge tube and centrifuged at 4°C for 10 min at 10,000 x g. The supernatants (protein lysates) were collected and dispensed into a new 1.5 ml pre-cooled microcentrifuge tube in aliquots and stored at -80 until needed.

2.2.2 Protein quantification using the Bicinchoninic Acid (BCA) assay kit

Pierce ™ BCA protein assay kit was used to quantify total protein in the cell lysates (ThermoFisher Scientific):

- BCA Reagent A: containing sodium carbonate, sodium bicarbonate, bicinchoninic acid and sodium tartrate in 0.1M sodium hydroxide.
- BCA Reagent B: containing 4% cupric sulfate.
- Albumin Standard Ampules: containing bovine serum albumin (BSA) at 2mg/mL in 0.9% saline and 0.05% sodium azide.

Standards were prepared using BSA with serial dilutions to obtain different concentrations for the standard curve (Table 2.5):

Standards	BSA (µl)	PBS (µl)	Final concentration (µg/ml)
A	100	900	200
B	75	925	100
C	50	950	50
D	37.5	962.5	25
E	25	975	12.5
F	12.5	978.5	6.25
BLANK		1000	0

Table 2. 5: Preparation of diluted Albumin (BSA) standards.

BSA reagent was prepared according to the manufacturer instruction, and Working Reagent (WR) was prepared using the following formula:

 (no. of standards +no. of samples) X (no. of replicates) X (Volume of WR per sample) = Total volume of WR required. (50 part of reagent A: 1 part of reagent B)

Protein samples were diluted as (1:100) in PBS.150 µl of standards or protein samples were added in triplicates into a 96 well plate, subsequently (1:1) BCA assay reagent was added to each well, then the plate was incubated for 30 minutes in 37°C/ CO_2 incubator. The absorbance was measured at 560 nm using a spectraMax M5e plate reader.

A standard curve was developed using this BSA standards assuming a linear relationship between the protein concentration and absorbance. The equation (y=ax+b) generated by the plotted line was used to determine the protein concentration of each sample, where X is the protein concentration.

2.2.3 Casting gels for polyacrylamide gel electrophoresis (PAGE)

Sodium dodecyl sulphate (SDS)-PAGE gel was performed according to the manufacturer's instructions using the following reagents:

- o ProtoGel 30% (acrylamide with bis-acrylamide) (National Diagnostics).
- o Resolving buffer (x 4 concentrate, National Diagnostics).
- o Stacking gel buffer (x 4 concentrate, National Diagnostics).
- o N, N, N', N'-Tetramethyl ethylenediamine (TEMED) (Sigma).
- o Isopropanol (Sigma).

8%, 12% or 15% v/v gel was prepared according to the desired antibody's Molecular Weight (MW).

2.2.4 Protein sample preparation and gel loading

The loading samples were prepared by mixing 40 µl of the sample with 10 µl of the 4x Laemmli sample buffer (Bio-Rad). The loading mixture were heated at 95°C for 5 minutes in a heating block to denature the proteins. 30 µg of protein samples were loaded in each well of an SDS-PAGE gel (8-15%). A protein ladder was used as a reference to estimate the molecular weight of the protein of interest (10-250 KDa, Bio-Rad). The gel was run for 120 minutes at 120 V in a running buffer (Tris Glycine SDS PAGE Running buffer, 10 x, National Diagnostics).

2.2.5 Protein Transfer

A semi-dry technique using Trans blot SD was used for Electrophoretic transfer of proteins to nitrocellulose membrane (Bio-Rad). When the SDS-PAGE gel had run, the gel and membrane were sandwiched between thick blotting sheets (Bio-Rad), all were soaked in 10% v/v transfer buffer (NuPAGE™ (20x, invitrogen) and 10% methanol (Fisher scientific). The transferred sandwich was placed in the transfer chamber (Bio-Rad) and run for 30 minutes at 15 V.

2.2.6 Antibody staining and detection

When the transfer is completed, membrane was blocked with 5% w/v milk powder (Non-fat dried powdered milk) in tris-buffered solution (TBS) containing 0.1%v/v of Tween 20 (TBS-T) for 30 min on the shaker at Room Temperature (RT). Then the membrane was incubated with the primary antibody (made in TBS-T with milk) at the appropriate dilutions (Table 2.6) overnight at 4°C with gentle agitation. Afterwards, the membrane was washed three times with (TBS-T) for 15 minutes each. Then the membrane was incubated with the appropriate secondary HRP-coupled antibody diluted in TBS-T with 2.5%w/v milk (1:1000) (Table 2.5) for one hour on the shaker at RT and the membrane was washed three times with (TBS-T) for 15 minutes. The Amersham ECL™ Western blotting detection kit (VWR) was used for protein detection. Equivalent volumes of Reagent A (luminol solution) and Reagent B (peroxide solution) were mixed, 1 ml of the detection reagent was added to the membrane and incubated for 1-2 min at RT. The membrane was visualized using the ChemiDoc™ MP imaging system (Bio-Rad).

Antibody	Host	manufacturer	Catalogue no.	Working dilution	Molecular Weight (MW)	% Acrylamide used
Vimentin	Mouse	Abcam	Ab8978	1:1000	~57KDa	12%
Transgelin	Rabbit	Abcam	Ab14106	1:1000	~23KDa	12%
N-Cadherin	Rabbit	Abcam	Ab18203	1:1000	~100KDa	8%
FSP-1/S100A4	Rabbit	Millipore	07-2274	1:1000	~17KDa	15%
α- sma	Rabbit	Abcam	Ab5694	1:1000	~42KDa	12%
FAPα	Rabbit	Abcam	Ab28246	1:1000	~88KDa	8%
GAPDH	Mouse	Abcam	Ab8245	1:10000	~36KDa	
Sox2	Rabbit	Abcam	Ab	1:1000	~34KDa	12%
Fibronectin	Rabbit	Abcam	Ab8245	1:500	~220KDa	8%

Table 2. 6: Primary Antibodies used for WB in this project.

2.2.7 Stripping and re-probing of membranes:

The membrane was re-probed for antibodies against the housekeeping gene GAPDH after detection of the primary antibody as follows; the membrane was rinsed in TBS-T buffer and then incubated in the stripping buffer (Restore™ Plus Western Blot Stripping Buffer (Thermo Scientific™) for the complete removal of the 1st and 2nd antibodies for 15 min with gentle agitation at RT. After that, the membrane was washed with TBS-T for three times at 5 min intervals. The membrane was then blocked with 5% w/v milk and incubated for one hour on the shaker at RT. The membrane then was incubated with the antibody to GAPDH as described in section 2.2.6.

2.3 DNA Extraction

For DNA extraction a DNeasy® blood and tissue kit (QIAGEN®) was used. When the cultured cells were 80% confluent, they were harvested for DNA extraction. All steps were as in 2.1.3 until the cells were dissociated and neutralized by complete medium. After centrifugation, the pellet was re-suspended in 1 ml of media in a 1.5 ml centrifuge tube. Cells were then centrifuged at 300 x g for 5 min. The supernatant was discarded, and the pellet re-suspended in 200 µl of PBS. 20µl of Proteinase K (provided by the kit) and 200µl of lysis buffer (AL Buffer, provided by the kit) were added, mixed by vortexing and incubated at 56°C for 10 min. 200 µl of ethanol (96-100%) was added to the sample and mixed gently by vortexing. The mixture was then transferred into the DNeasy Mini spin column placed in a 2 ml collection tube, centrifuged at 6,000 xg for 1 min. Then the DNeasy Mini spin column (provided by the kit) was placed in a new 2 ml collection tube, 500µl of buffer AW1 was added and centrifuged at 6,000 xg for 1 min. The collection tube was discarded and the DNeasy Mini spin column placed in a new collection tube before 500µl of buffer AW2 was added and centrifuged at 10,000 xg for 3 min. The collection tube was discarded and the DNeasy Mini spin column placed in a new 1.5 ml centrifuge tube. 200µl of AE buffer was added and incubated at room temperature for 1 min, then centrifuged at 10,000 xg for 1 min.

2.4 RNA extraction

2.4.1 Sample preparation

Frozen tissue sections were used for RNA extraction. Frozen sections from tumours embedded in OCT embedding matrix (Cell Path) were cut and stored at -80°C. A cryostat (Leica Microsystem) was used to cut 10µm of the sections and place it on either laboratories slides (ThermoScientific) or in 1.5 ml Eppendorf tubes and stored at -80°C until further use.

2.4.2 RNA extraction protocol

RNeasy mini kit (QIAGEN®) was used to extract RNA from frozen sections as mentioned in 2.4.1. The samples were homogenized using QIA shredder homogenizer (QIAGEN®). 10µl of β-mercaptoethanol (B-ME) was mixed with 1 ml of buffer RLT then 600µl of the mix was added to the sample and centrifuged at maximum speed for 2 min. Then the lysates were centrifuged at full speed for 3 min. The supernatant was carefully removed by pipetting and transferred into a new microcentrifuge tube (provided by the kit). 600µl of 70% v/v ethanol was added to the lysates and mixed by pipetting. The sample was transferred to an RNeasy spin column (provided by the kit) placed in a 2 ml collection tube, centrifuged at 8,000 x g for 15 sec. The flow-through was discarded.

700µl of buffer AW1 (provided by the kit) was added and centrifuged at 8,000 x g for 15 sec. Then 500µl of RPE was added to the spin column and centrifuged at 10,000 x g for 15 sec. The flow-through was discarded. 500 µl of RPE was added and centrifuged at 10,000 x g for 2 min and flow through was discarded. The RNeasy spin column was placed in a new 1.5 ml and 35µl of RNAse -free water was added and centrifuged at full speed for 1 min.

2.4.2.1 Nanodrop to measure DNA & RNA concentrations:

DNA and RNA concentrations were measured using nanodrop spectrophotometer 1000 UV-Vis system at a wavelength of 260 nm. Concentrations and 260/280 absorbance were recorded.

2.5 Short Tandem Repeat (STR)

Sort Tandem Repeat profiling (STR) was performed using the service provided by the Genomic core facility in the University of Sheffield on all cell lines to confirm the genomic identity of each cell lines and exclude any cross-contamination. Alleles for 10 human loci (THO1, D21S11, D5S818, D13S317, D7S820, D16S539, CSFIPO, AMEL, vWA and TPOX) were examined

2.6 Immunocytochemistry (ICC)

Cells were prepared according to section 2.1.3 then seeded at 20,000 cells/ml in a 12 well plate containing a round cover glass (size 10mm, thickness 1.5) (Agar Scientific), the cells were incubated in a humidified incubator at 37°C with 5% CO2 for overnight.

When the cells reached the desired confluencey, immunocytochemistry was performed on the cells while attached to the cover glass. Cells were washed with Hank's Balanced Salt Solution) HBSS (-Cacl$_2$, -Mgcl$_2$) (Gibco) twice for 5 min. Then the cells were fixed using formalin fixative (10% formalin, 4% formaldehyde) (sigma) for 20 min at room temperature (RT). Cells were rinsed again with HBSS twice for 5 min. Then the cells were incubated with 0.1% v/v Triton X-100 (Sigma) for 5 min at RT. Cells were washed with PBS (Lonza) twice for 5 min. Subsequently cells were incubated with the primary antibody diluted in PBS (1:100) for 1 hour at RT. After the antibody incubation, cells were washed with PBS three times for 15 min each. Then cells were incubated with the secondary antibody diluted in PBS (1:500) for 1 hour at RT in a dark container. After the secondary antibody incubation, cells were washed with PBS three times for 15 min each. Cells were then washed twice with water before adding 3 µl of DAPI (Vector lab,UK) and mounted on a slide cell facing down. Cells were incubated over night at RT in a dark chamber to

dry before the cover glass was sealed with nail varnish. Slides were imaged using an Evos microscope at 20X (EVOS® FL AUTO Imaging system)

2.6.1 ICC analysis

JACoP (Just Another Co-localizaiton plugin) is a plugin for Image J and was used to measure Pearson's correlation coffecient (PCC) in the cells. ICC was used to compare expression of common mesenchymal genes between STS cell lines and the fibroblasts cells. It was used to co localize the proteins within cells. A statistical analysis was performed using GraphPad Prism software 7.0 (GraphPad Prism Software Inc) Parametric analysis for the data was done by applying one-way ANOVA, followed by Dunnett comparison test. The differences were considered significant at $P<0.05$. *,$P<0.05$ **,$P <0.01$; ***,$P < 0.001$, ns, not significant. A complete list of primary and secondary antibodies used for ICC is listed in Table 2.7.

Antibody	Host	manufacturer	Catalogue no.	Working dilution
Vimentin	Mouse	Abcam	Ab8978	1:100
Transgelin	Rabbit	Abcam	Ab14106	1:100
N-Cadherin	Rabbit	Abcam	Ab18203	1:100
FSP-1/S100A4	Rabbit	Millipore	07-2274	1:100
αSMA	Rabbit	Abcam	Ab5694	1:100
FAPα	Rabbit	Abcam	Ab28246	1:100
Sox2	Rabbit	Abcam	Ab97959	1:100
Fibronectin	Rabbit	Abcam	Ab2413	1:100
Mouse anti-Human Mitochondria Primary Antibody (mt-AB)	Mouse	Novus	NBP2-32980	1:100
F4/80	Mouse	Abcam	Ab28246	1:100
Alexa Fluor™ 488, Goat anti-Mouse IgG (H+L) Highly Cross-Adsorbed Secondary Antibody	Mouse	Invitrogen	A-11029	1:500
Alexa Fluor™ 488, Goat anti-Rabbit IgG (H+L) Highly Cross-Adsorbed Secondary Antibody,	Rabbit	Invitrogen	A-11034	1:500
Alexa Fluor™ 633 Phalloidin		Invitrogen	A-22284	1:400

Table 2. 7: Primary and secondary Antibodies used for ICC in this project.

2.7 Immunofluorescence of frozen tissue sections (IF)

Slides mounted with frozen tumour sections were prepared according to section 2.4.1. Slides were defrosted at room temperature for 10 min. Then slides were fixed with ice-cold fixative acetone - methanol (1:1, Fisher Chemical) at -20°C for 20 min. Slides were allowed to air dry before being washed twice with PBS (Lonza) for 10 min each. After that, the sections were encircled using a hydrophobic Immedge pen (Vector). Sections then were blocked in PBS containing 5% v/v goat serum (Vector) for 2 hours at RT. After that, sections were incubated with the primary antibody diluted to a suitable concentration (Table 2.8) in PBS containing 1% v/v goat serum, in a humidified dark container at 4°C for overnight.

The following day, sections were washed three times with PBS for 15 min each. Subsequently, sections were incubated with the secondary antibody diluted 1:500 in PBS containing 1% v/v goat serum for one hour in a dark container at RT. Sections were washed three times with PBS for 30 min each. Then, slides were rinsed with distilled water twice before mounting them with ProLong® Gold antifade reagent with DAPI (Invitrogen) and covered with a cover glass (Menzel-GLASER, 24 x 50mm). Slides were kept at RT for overnight in a dark container. Fluorescent stained slides were imaged using an EVOS® FL Auto Imaging System (objective 20X). A complete list of all primary and secondary antibody in (table 2.8).

2.7.1 IF analysis

Cell fluorescence was measured using imagej 1.53S software. Corrected total cell fluorescence (CTCF) was calculated using the following formula: CTCF=Integrated density- (Area of selected cell X Mean fluorescence of background readings), Results were plotted using GraphPad Prism 9.4.1. Cell counting was calculated manually using imagej 1.53S software.

Antibody	Host	manufacturer	Catalogue no.	Working dilution
Vimentin	Mouse	Abcam	Ab8978	1:200
Transgelin	Rabbit	Abcam	Ab14106	1:200
N-Cadherin	Rabbit	Abcam	Ab18203	1:200
FSP-1/S100A4	Rabbit	Millipore	07-2274	1:200
α- SMA	Rabbit	Abcam	Ab5694	1:200
FAPα	Rabbit	Abcam	Ab28246	1:200
Sox2	Rabbit	Abcam	Ab97959	1:200
Fibronectin	Rabbit	Abcam	Ab2413	1:200
Mouse anti-Human Mitochondria Primary Antibody(mt-AB)	Mouse	Novus	NBP2-32980	1:100
F4/80	Mouse	Abcam	Ab28246	1:200
Purified Rat Anti-Mouse CD31 RUO	Mouse	BD p	550274	1:500
Alexa Fluor™ 488, Goat anti-Mouse IgG (H+L) Highly Cross-Adsorbed Secondary Antibody	Mouse	Invitrogen	A-11029	1:500
Alexa Fluor™ 488, Goat anti-Rabbit IgG (H+L) Highly Cross-Adsorbed Secondary Antibody,	Rabbit	Invitrogen	A-11034	1:500
Alexa Fluor™ 555, Goat anti-Mouse IgG (H+L) Highly Cross-Adsorbed Secondary Antibody	Mouse	Invitrogen	A-21424	1:500

Table 2. 8: Primary and secondary antibodies used for IF in this project.

2.8 Immunohistochemistry (IHC)

Immunohistochemistry was carried out on formalin fixed, paraffin wax embedded (FFPE) slides. These were prepared by Mrs. Maggie Clover in the histology core facility, Department of Oncology and Metabolism, University of Sheffield. Slides were dewaxed twice in xylene for 5 min each. Slides then were rehydrated using reduced gradient alcohol of 100%, 95% and 70% v/v ethanol in dH_2O, for 3 min each. Endogenous peroxidase activity was blocked by incubating the sections in 10% (v/v) hydrogen peroxide (H_2O_2) diluted in Methanol (life chemicals) for 30 min. To wash off the hydrogen peroxide, slides were kept under running water for 5 minutes. Antigen retrieval method was performed on the slides by incubating the slides in 10% DAKO (DAKO® Target Retrieval Solution, 10X concentrate) diluted with dH_2O in a pressure cooker (2100 Retriver) at 121°C for 2 hours. After that, slides were washed twice with PBST (PBS+0.1%Tween 20) for 3 min. The sections were encircled using a hydrophobic Immedge pen (Vector Labs). Slides were then blocked with 10% v/v goat serum (Vector Labs) diluted in BSA/PBS (50ml PBS+0.5g BSA+50µl triton) for one hour at RT. Then slides were incubated with the primary antibody diluted with the desired dilution (Table2.9) in 2% v/v BSA/PBS in a dark and humidified container at 4 °C overnight. The next day slides were washed twice with PBST for 5 min. Then slides were incubated with a secondary antibody diluted 1:200 in PBS for one hour at RT. Subsequently, slides were washed twice with PBST for 5 min. ABC solution (Vector Labs) was prepared by mixing 2 drops of reagent A with 2 drops of reagent B and mixed well by vortexing. Then the ABC solution was added to the slides and incubated for 30 min at RT. Following this, slides were washed with PBST twice for 5 min. Then DAB (Vector Lab) was prepared by mixing 2 drops of buffer with 4 drops of DAB and 2 drops of H_2O_2 and mixed by vortexing. Then DAB was added to the slides for 4-9 min and meanwhile slides were observed under a light microscope. To remove the excess DAB, slides were kept under running water for 5 min. Slides were subsequently counterstained with hematoxylin for 40 sec. Then slides were kept again under running water for 2 min. Slides were dehydrated in 70%, 90%, 95%, then 100% ethanol twice and then xylene respectively for 3 min in each. Finally, slides were mounted in DPX mounting medium and covered by a cover glass (Menzel-GLASER,

24 x 50mm), then the sections were allowed to dry for overnight at RT. Slides were scanned using slide scanner (3D Histech Pannoramic 250 Flash III,Objective 20X). A complete list of all primary and secondary antibody are shown in Table 2.9.

Antibody	Host	manufacturer	Catalogue no.	Working dilution
Vimentin	Mouse	Abcam	Ab8978	1:400
Transgelin	Rabbit	Abcam	Ab14106	1:200
N-Cadherin	Rabbit	Abcam	Ab18203	1:200
FSP-1/S100A4	Rabbit	Millipore	07-2274	1:400
α- sma	Rabbit	Abcam	Ab5694	1:100
FAPα	Rabbit	Abcam	Ab28246	1:400
Sox2	Rabbit	Abcam	Ab97959	1:200
Fibronectin	Rabbit	Abcam	Ab2413	1:200
Purified Rat Anti-Mouse CD31 RUO	Mouse	BD	550274	1:200

Table 2. 9: Primary and secondary antibodies used for IHC.

2.8.1 IHC analysis

2.8.1.1 Necrosis scoring criteria

Haematoxylin and Eosin (H&E) staining was used to score necrosis in the tumours using the bioimage analysis platform QuPath (https://qupath.github.io).

2.8.1.2. Mean vascular density scoring criteria

Mean vascular density (MVD) scoring was assess by two independent people (myself and SSC student) an average of both results was taken. It was done using a light

microscope with a 9X9 50X50 µm^2 grid in the eye piece, then counts how many squares have CD31 positive vessels in them and divided by the area to get a percentage. An average percentage was recorded for each tumour.

2.8.1.3 Protein intensity scoring criteria

Antibody intensity of proteins listed in table 2.9, were scored using the bioimage analysis platform QuPath (https://qupath.github.io).

Positive cell detection tool was used, the full tumour section was selected and DAB staining intensity threshold was set to 0.1 based on the recommended settings, cells classified as positive or negative if the threshold is above or below 0.1, respectively.

2.9 Statistical analysis

Data were plotted and analysed using GraphPad Prism software 9.4.1 (GraphPad Prism Software Inc). To compare between two groups, unpaired two-tailed t test were used. While parametric analysis for grouped data was done by applying one-way ANOVA, followed by Fisher's LSD comparison test, Dennett's comparison test or Tukey comparison test. The differences were considered significant at $P<0.05$. *, $P<0.05$ **,$P<0.01$; ***,$P < 0.001$, NS, not significant.

2.10 In silico methods

2.10.1 The Cancer Genome Atlas (TCGA)

The Cancer Genomic Atlas (TCGA) is a landmark collection of cancer genomic data. TCGA SARC is comprised of soft tissue sarcoma including: Leiomyosarcoma (LMS), Undifferentiated Pleomorphic Sarcoma (UPS), Dedifferentiated Liposarcomas (DDLP), Myxofibrosarcoma (MFS), Malignant Peripheral Nerve Sheath Tumour (MPNST) and Synovial Sarcoma (SS). TCGA SARC project has 77 samples of poorly differentiated

'Fibroblastic' group including MFS and UPS that were available in UCSC Xena platform (http://xena.ucsc.edu).

2.10.2 Randomised trial of Volume of post-operative radiotherapy given to adult patients with Extremity soft tissue sarcoma (Vortex)

VorteX (trial number is NCT00423618/REC Number is 21/NW/0237) is a randomised phase III trial of adjuvant radiotherapy given to adult extremity STS patients to evaluate if lime function can be increased by reduce the amount of adjuvant radiotherapy compared with giving adjuvant therapy to a wider area of tissue surrounding the tumour (standard care) (Forker et al, 2016). Tissue samples were collected from the Vortex biobank (VBB, Manchester) at the initial stage before treatment including: 68 UPS, 52 MFS, 37 Liposarcomas, 9 LMS and 37 from other STS subtypes (Forker et al, 2016). RNAseq data was accessible to us as part of a collaboration with Professor Catharine West and Dr Laura Forker of the VBB. The associated clinical data was obtained from the VorteX Clinical Trial Management Centre (Birmingham), after a favourable opinion was given by the Research Ethics Committee (REC Number: 21/NW/0237, Protocol Number: Research Project 170751, IRAS Project ID: 266902). RNAseq and clinical data associated with 70 samples were used in this study (40 UPS and 30 MFS).

2.11 Survival analysis

Survival analysis was estimated using Kaplan-Meier (KM) analysis and the computed hazard ratio for each group using IBM® SPSS Statistics (version 27). Clinically relevant phenotypic attributes such as Age, gender, histological type, Overall Survival (OS), Progression-Free survival (PFS), vital status, primary disease and the gene expression of (TAGLN, ACTA2, VIM, CDH2, FN1, SOX2, S1A400, & FAP) was obtained for each sample.

The association between high and low gene expression was examined using a linear regression model to examine if high gene expression affecting overall and progression free survival (Delgado et al., 2014). Hazard ratios at 95% confidence intervals were

obtained using Cox's regression model. Survival rates were performed using Kaplan Meier analysis and the comparisons between the low and high groups were done using the log rank test. Univariate analysis was done to assess if low or high gene expression impact survivals OS and PFS analysis was performed in 2 years, 5 years and 10 years. P- Values <0.05 were considered statistically significant.

2.12 RNAseq of UPS Xenografts

A representative diagram of the in silico pipeline used in this project is shown in (Fig.2.1)
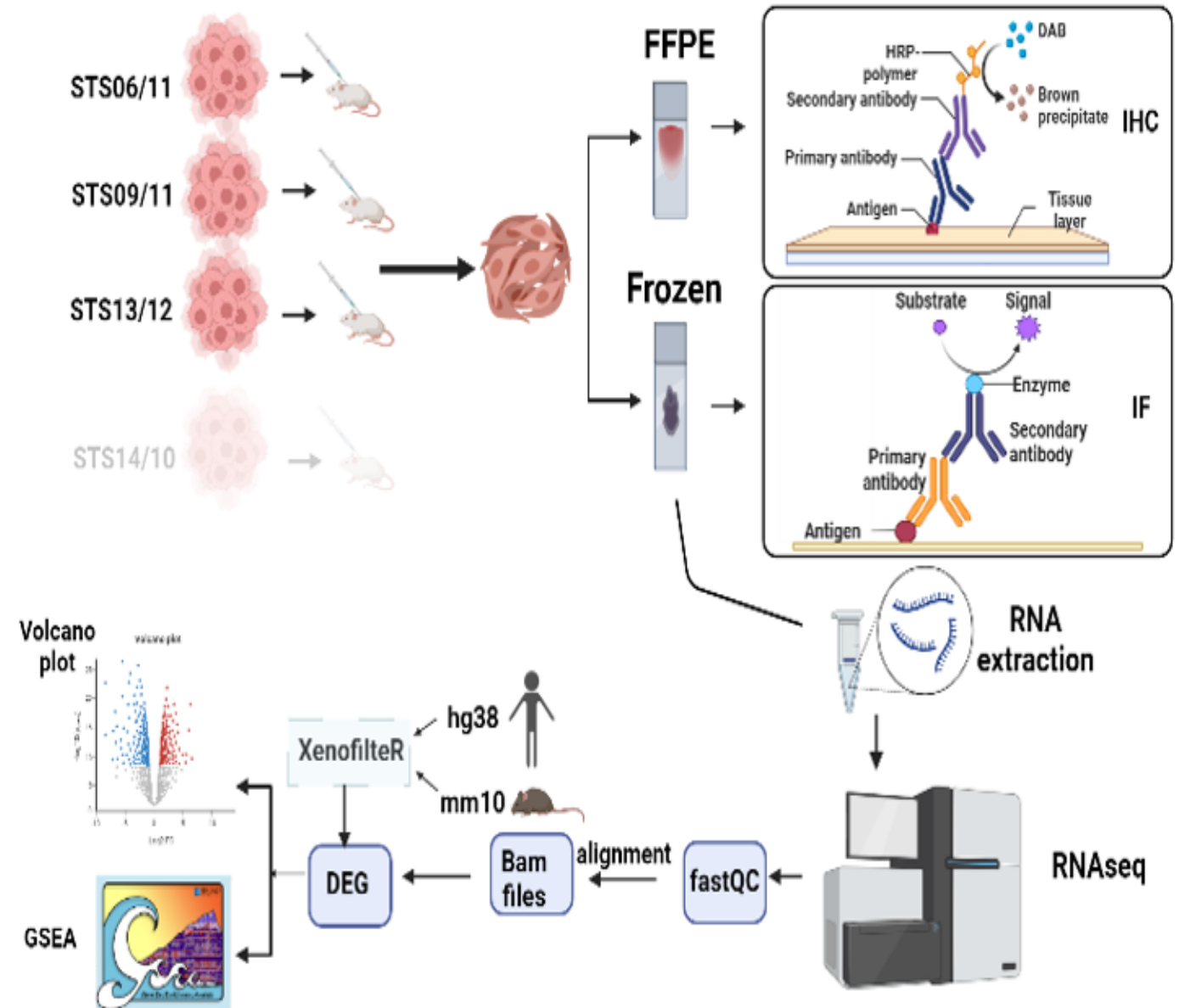
Figure 2. 1: A chart illustrating the methods used in this project.

Tumour cells were subcutaneously injected in mice, three out of four cell lines make tumour in mice. Subsequently, tumours were removed and split into frozen and FFPE. The FFPE sections were used for IHC, while frozen were used for IF and RNA extraction. RNAseq raw data were processed to FASTQC, then bam files were processed for DEG. Created with BioRender.com

2.12.1 Quality control of RNAseq data

RNA quality was checked using Nanodrop as discussed in section (2.3.1), for RNA Integrity Number (RIN) samples were sent to Sheffield Institute for Translational Neuroscience (SITRAN) and RIN was obtained using bioanalyzer. Samples were chosen based on the quality (RIN ≥9.1, 260/280 ≥1.97, 260/230 ≥2.0). Out of 16 samples, 12 RNA samples (four from each of 3 different UPS xenograft) were sent to the Genetics department at Children hospital (Sheffield) for RNAseq. Results were provided as Fastq files with paired reads. The Fastq files were pre-processed using the online data analysis webserver Galaxy (http://usegalaxy.org) (Blankenberg et al., 2010). Quality checks were performed using the FASTQC tool from the Galaxy platform. FASTQC is an open-tool which provide a set of analysis to assess the quality of the samples. Different Parameters were checked for instance: quality scores across all bases, sequence content per base and GC distribution per sequence. A Representative diagram of the FASTQC report is provided in the Appendix (Figure S1).

2.12.2 Alignment against reference genomes

Fastq files were mapped and aligned against reference genomes. An average of 35 million reads of each sample were aligned to the human (GRCh38/hg38) and mouse reference genomes (GRCm38/mm10) separately using the Bowtie2 tool. Bowtie2 was used as it is faster and can align more reads when compared with other alignment tools (Langmead & Salzberg, 2012). The outputs of the alignment tools are Binary Alignment Map (BAM) files, which are sorted, processed and converted to Sequence Alignment Map (SAM) files using SAMtools index (Li et al., 2009).Bam files were also aligned against the global reference genome (hg38/mm10). The number of read counts for each sample is shown in Figure S2.

2.12.3 Data processing using XenofilteR

BAM files were also filtered using the XenofilteR tool in RStudio (version 4.1.2) for deconvolution of human and mouse sequence reads from xenograft sequence reads. XenofilteR is an open tool and available: https://github.com/PeeperLab/XenofilteR. The output was two BAM files classified as human and mouse (Kluin et al., 2018).

2.12.4 Identification of Differentially Expressed Genes (DEGs)

Deferentially expressed Genes (DEGs) were identified using the edgeR package in RStudio (version 4.1.2). A raw count matrix was used to perform the DEG analysis. Four comparisons were made: the first one was between the three xenografts transcripts, the second one was between the human (STS) vs the mouse (stroma), the third comparison was between human transcripts and the fourth was between the mouse transcripts. Read counts were filtered with a threshold of CPM > 0.5. Raw counts were normalised using the default normalisation tool from the edgeR package. A false-discovery rate (FDR) was ≤ 0.5 used as a cut-off to identify DEGs.

2.12.5 Gene Set Enrichment Analysis (GSEA)

Gene set enrichment analysis was performed using GSEA software (version 4.2.2). Pre-ranked analysis was perforemed using the default setting (GSEAPreranked) with the exception" No_collapse" since our data set contained gene symbols which match the current MsigDB version. Prior to analysis, gene expression rank (.rnk) files were generated from the edgeR result by calculating the rank metric using the formula (Rank= sign(logFC) X -log10 (p value)). Pre-ranked lists of 15,906 genes were uploaded to the software. The Hallmark gene set (h.all. v7.5.1 MsigDB) was applied to examine if genes were linked to specific biological processes (Liberzon et al., 2015). FDR q-values < 0.05 was set as cut off to determine the significance of gene sets.

2.12.6 Cell content prediction

Cell subset analysis was performed using the xCell software, which is a gene expression matrix allowing the identification of 64 cell types (Aran et al., 2017).

The abundance of (Pericytes, Skeletal muscles, Smooth muscles, Lymphatic endothelial, Microvascular endothelial, Hematopoietic Stem Cells (HSC), Mesenchymal Stem Cells (MSC), endothelial, Fibroblasts, Macrophages and Macrophages M1/M2) were studied and two comparison were made : the first one between the cell lines, the second: between the human and mouse transcriptomes. Comparisons were analysed using one-way ANOVA, and the multiple comparisons were made using Tukey's method, while the comparisons between the human and mouse transcriptomes were performed using Wilcoxon's t-test. P values < 0.05 are considered statistically significant.

Chapter 3

Differential expression of common mesenchymal markers between normal fibroblasts, mesenchymal stem cells and soft tissue sarcoma cell lines.

3.1. Introduction

Soft Tissue Sarcomas (STS) are a biologically rare, heterogeneous and complex population of solid tumours of mesenchymal origin. The tumour microenvironment (TME) is a crucial component of solid tumours, and an improved understanding of its role in STS biology is needed to make further improve patient survival. Many recent studies have emphasised on the importance of mesenchymal cells within the TME, often called CAFs, in controlling cancer biology. However, most have investigated their role in carcinomas and very little is known about the role of Sarcoma Associated Fibroblasts (SAFs) in STS biology. This has been challenging for two reasons; firstly, few validated STS cell lines are available that are closely matched to their original histotype. Secondly, since STS cells and SAFs are both mesenchymal, no selective markers have yet been identified that would facilitate their study. Similarly, no contemporary studies have investigated the expression of the most commonly expressed mesenchymal genes used to identify CAFs in STS cell lines with a correctly assigned histotype. In order to characterise this further, Western blot and immunocytochemistry were performed to quantify and characterise the most commonly expressed mesenchymal proteins in STS cell lines recently isolated and characterised by Salawu *et al* (2016) in comparison with normal human mesenchymal cells. This study examined eight common mesenchymal proteins (transgelin, αSMA, vimentin, fibronectin, N-cadherin, SOX2, FAPα, and FSP1), discussed in more detail below.

Transgelin, or Sm22α, is a protein with a molecular weight (MW) of 23 KDa. It is a calponin family smooth muscle actin-binding protein expressed in all human tissues containing large or small smooth muscles. Transgelin is highly expressed during vascular and visceral smooth muscle cell differentiation (Assinder et al., 2009).It regulates smooth muscle cell development, contractile function, and migration. Moreover, it functions as a tumour suppressor since it suppresses *MMP9* expression, making it an important mesenchymal protein to study (Assinder et al., 2009). High transgelin levels are considered bad prognositic for overall survival (OS) and progression- free survival (PFS) in colorectal cancer (CRC). It has been associated with the stimulation of cell migration, invasion and activation of epithelial to mesenchymal transition (EMT), and has been

identified as a regulator of metastasis and chemotherapy resistance (Elsafadi et al., 2020). Alabiad *et al* (2020) showed that transgelin could be used as a biomarker to distguish between Leiomyosarcoma (LMS) and Endometrial Stromal Sarcoma (ESS), where transgelin was positive in LMS but not ESS samples (Alabiad et al., 2020).

Alpha smooth muscle actin (αSMA) is a protein with a MW of 42 KDa. It is a smooth muscle actin protein expressed in vascular smooth muscle and non-muscle cells. It plays an important role in cell contractility during wound-healing processes (Hinz et al., 2001). It is known for it's role in EMT, which manifests in cancer progression (Anggorowati et al., 2017). It has also been associated with cell motility integrity (Nurmik et al., 2020).

αSMA is known as a myofibroblast/CAFs marker, making it an interesting mesenchymal protein to be included in this study. Different studies have considered αSMA as a CAFs marker. Since myofibroblasts are abundant in the ECM, αSMA is known to play a vital role in ECM remodeling (Ruiz-Zapata et al., 2020). Several studies reported that elevated αSMA levels result in poor prognosis in breast cancer (Muchlińska et al., 2022), CRC (Tsujino et al., 2007) and oral squamous cell carcinoma (OSCC) (Marsh et al., 2011).

Moreover, αSMA expression was higher in the metastatic invasive breast cancer group than in the non-metastatic group, with higher αSMA expression negatively correlated with OS and PFS (Yamashita et al., 2012).

Vimentin is a protein with a MW of 57 KDa. It is a type III intermediate filament protein highly and widely expressed in mesenchymal cells. It regulates cell integrity, has been used as an EMT marker hence, it plays an important role in cancer metastasis (Mendez et al., 2010).

N-cadherin or cadherin 2, is a protein with a MW of 125-135 KDa. It is a member of the calcium-dependent transmembrane adhesion protein family. It plays a vital role in development processes by mediating cell-cell adhesion and cell migration. However, in cancer, it plays a vital role in EMT and tumour invasion and metastasis, since increased N-cadherin expression has been associated with tumour progression in breast cancer, making it an important marker to be studied (Hazan et al., 2004).

Fibronectin is a protein with a high MW of 220 KDa. It is an ECM glycoprotein with adhesive and ealstic features that plays a cruical role in tissue repair, hemostasis and fibrosis (To & Midwood, 2011). Fibronectin mediates between the ECM and cancer cells, enabling their survival, proliferation, and invasion. It is also well-known EMT marker. High fibronectin expression has been associated with poor prognosis in many carcinomas, including breast cencer, bladder cancer,head and neck squamous cell carcinoma and CRC (Arnold et al., 2016; Bae et al., 2013; Mhawech et al., 2005; Wang et al., 2021).

It was selected for study in this thesis because of its ability to promote cell growth, movement, and contractility. Moreover, it has been described as a promising cancer therapy target (Lauren E. Tracy et al., 2016).

Fibroblast-specific protein1 (FSP-1) or S100A4, is a protein with a MW of ~12 KDa. It is a member of the S100 superfamily of cytoplasmic calcium-binding proteins. FSP-1 has cruical roles in enhancing cell motility, migration and regulating apoptosis. Moreover, FSP-1 is known to enhance and regulate the secretion of different cytokines and matrix metalloproteinases (MMPs), which play important roles in pro-inflammatory processes (Li et al., 2020). FSP-1 is expressed in normal cells, including fibroblasts, macrophages, nuetrophiles, monocytes, lymphocytes and bone-marrow derived cells (Li et al., 2010). FSP-1 is a fibroblast marker used widely to identify fibroblasts in different organs (Nishitani et al., 2005). FSP-1 plays an important role in EMT and fibrosis, leading to cancer progression and metastasis (Nishitani et al., 2005). Increased FAP-1 levels correlate with poor prognosis in many carcinomas, including breast, colorectal and pancreatic. While it is an important and commonly used marker for fibroblasts and myofibroblasts, its expression is known not to be restricted to these cells. Therefore, we selected it for this study.

FAPα or fibroblast activation protein is a protein with a MW of ~97 KDa. It is a type II transmembrane glycoprotein and a serine protease family member. It is highly expressed by myofibroblasts during wound-healing, inflammation, fibrosis and cancer and is involved in tissue remodelling (Puré & Blomberg, 2018). FAPα is also expressed by fibroblasts, macrophages, tumour cells and tumour associated macrophages (TAMs) (Muliaditan et al., 2018). It plays a potential role in cancer metastasis by enhancing cell

proliferation, migration and invasion (Busek et al., 2018). CAFs overexpress FAPα in many carcinomas, which was associated with poor (J. Shi et al., 2020). It was included in this study due to its selective expression in CAFs.

SOX2 (SRY-Box Transcription factor 2) is a protein with a MW of 34 KDa. It is a member of the SOX transcription factor family. It is important in embryogenesis, organogenesis, and stem cell regulation. It is cosidered as a Cancer Stem Cell (CSC) marker. CSCs are a group of tumour cells capable of self-renewal and initiating tumours. SOX2's pluripotency property correlated with cancer stemness in osteosarcoma (Basu-Roy et al., 2012). Osteosarcoma and Rhabdomyosarcoma tumourigenicity was enhanced by SOX2 expression (Skoda et al., 2016). In addition, (Schaefer & Lengerke, 2020) found that in breast cancer, increased SOX2 expression was correlated with chemotherapy resistance. It was selected for this study because of its crucial role in embryonic stem cell and human MSC pluripotency, proliferation, and differentiation (Park et al., 2012).

3.1.1. Aim

To compare expression of mesenchymal proteins between human STS cell lines and normal human mesenchymal cells.

3.1.2 Experimental approach and statistical analysis

- Eight soft tissue sarcoma cell lines were used in this project (seven cell lines including four UPS, two MFS and one LMS were established and isolated from patients at Royal hallamshire hospital, Sheffield by Dr Karen Sisley's group and one MFS cell line was donated by Prof Dominique Heyman, France).
- Four fibroblast cell lines (dermal, uterine, pulmonary and adipose human mesenchymal stem cell) were used in this project.
- The expression of seven mesenchymal proteins (Transgelin, α SMA, vimentin, N-cadherin, fibronectin, FSP-1 and FAPα) and one transcription

factor (SOX2) was compared between STS cell lines and fibroblasts using western blot method.

- Protein localisation was determined in all cell lines using immunocytochemistry method.

3.2. Results

3.2.1 STS cell line verification

Cell authentication is important to confirm cell identity and exclude cross-contaminated cells Cell line verification was performed to confirm the cell lines used in this project and ensure that we used non-contaminated cell lines to produce robust results. This verification was performed by comparing the cells' morphology with their original description by Salawu *et al.* (2016; 2018) and screening for gross genomic changes that have occurred using short tandem repeats (STRs). This process is described in more detail in the following sections.

3.2.1.1 STS cell line morphology

One simple and direct method is to check cell morphology using microscopy. Cell morphology is a crucial 'macroscopic manifestation' of cell physiology (Juneau, 2017). Phase-contrast microscopy is a useful tool for studying cell morphology and determining whether it remains stable over different passages. STS cell lines were passaged and maintained as described in Section 2.2. The cells were examined daily using a phase-contrast microscope to record their morphology and compare it with the morphology observed when first described by Salawu *et al* (2016). All STS cell lines showed a spindle-shaped morphology similar to the normal human dermal fibroblasts (NHDF), human MSCs (hMSC), human uterine fibroblasts (HUF) and human pulmonary fibroblasts (HPF) (Fig.3.1, 3.2, 3.3, 3.4 & Table 3.1). All UPS, MFS and the LMS cell lines showed morphology consistent with those previously reported by Salawu *et al* (2016; 2018).

Cell line	Passage	Morphology	Growth in distinct colonies	Figure
UPS1 (STS14/10)	72	spindle-shaped		Figure 3.1
UPS2 (STS06/11)	76	spindle-shape	√	Figure 3.1
UPS3 (STS09/11)	26	spindle-shaped		Figure 3.1
UPS4 (STS13/12)	70	spindle-shaped	√	Figure 3.1
MUG2A	2	elongated cells	√	Figure 3.2
MFS1 (STS21/11 W1)	21	spindle-shaped		Figure 3.2
MFS2 (STS21/11 W2)	21	spindle-shaped	√	Figure 3.2
MFS3 (OH931)	3	spindle-shaped		Figure 3.2
LMS	36	spindle-shaped	√	Figure 3.3

Table 3. 1: Morphology and growth characteristics of the STS cell lines used in this thesis.

This table shows the nomenclature for the STS cell lines used in this thesis and the nomenclature used by Salawu et al (2014). The number of passage (since October 2018) is shown along with their morphology and grown characteristics. The figure which shows representative images of the cells is indicated in the right-hand column.
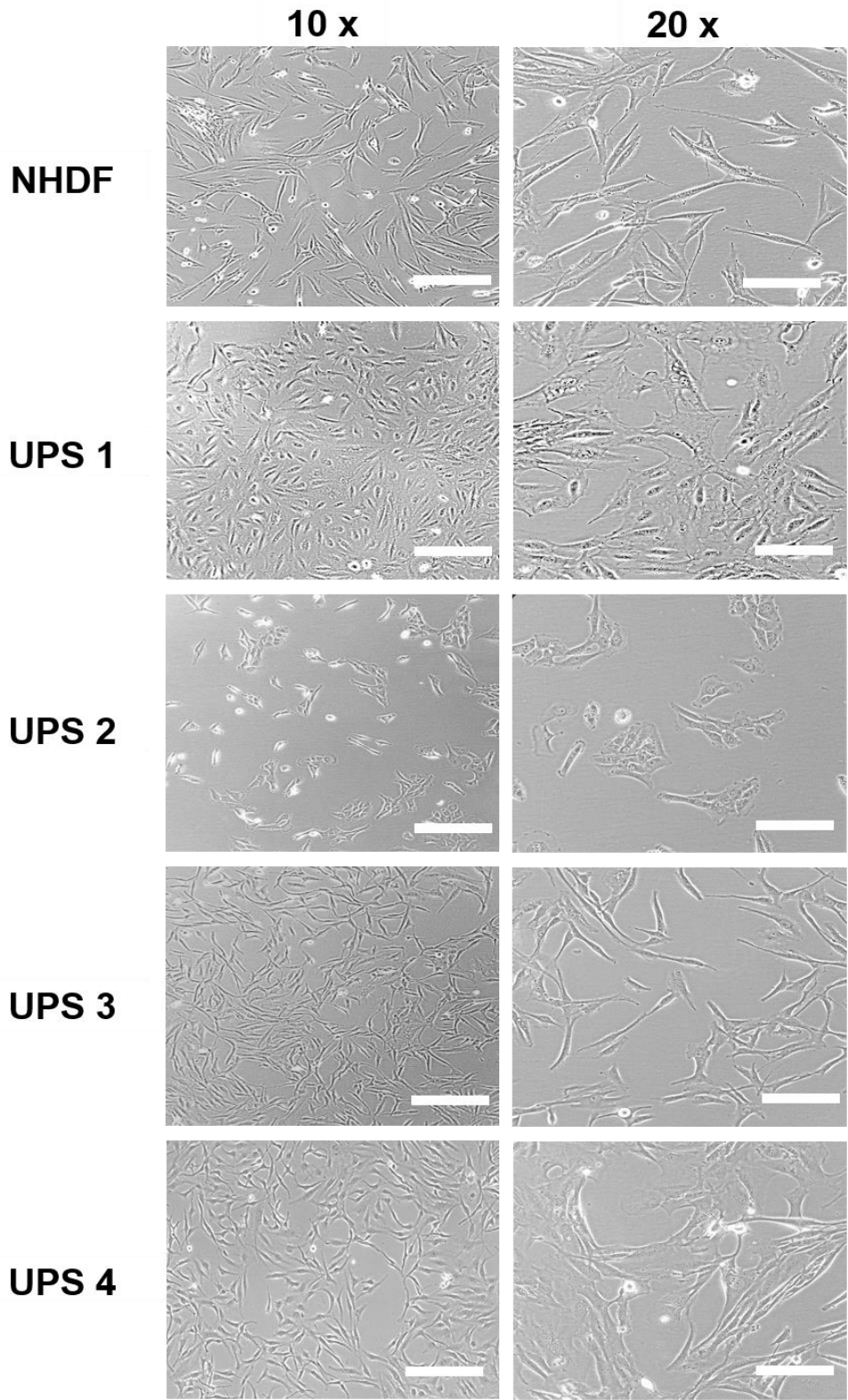
Figure 3. 1 Illustrative phase-contrast micrographs of NHDF and UPS cell lines.

Scale bar for 10 X and 20 X magnification are 100 μm and 50 μm respectively.
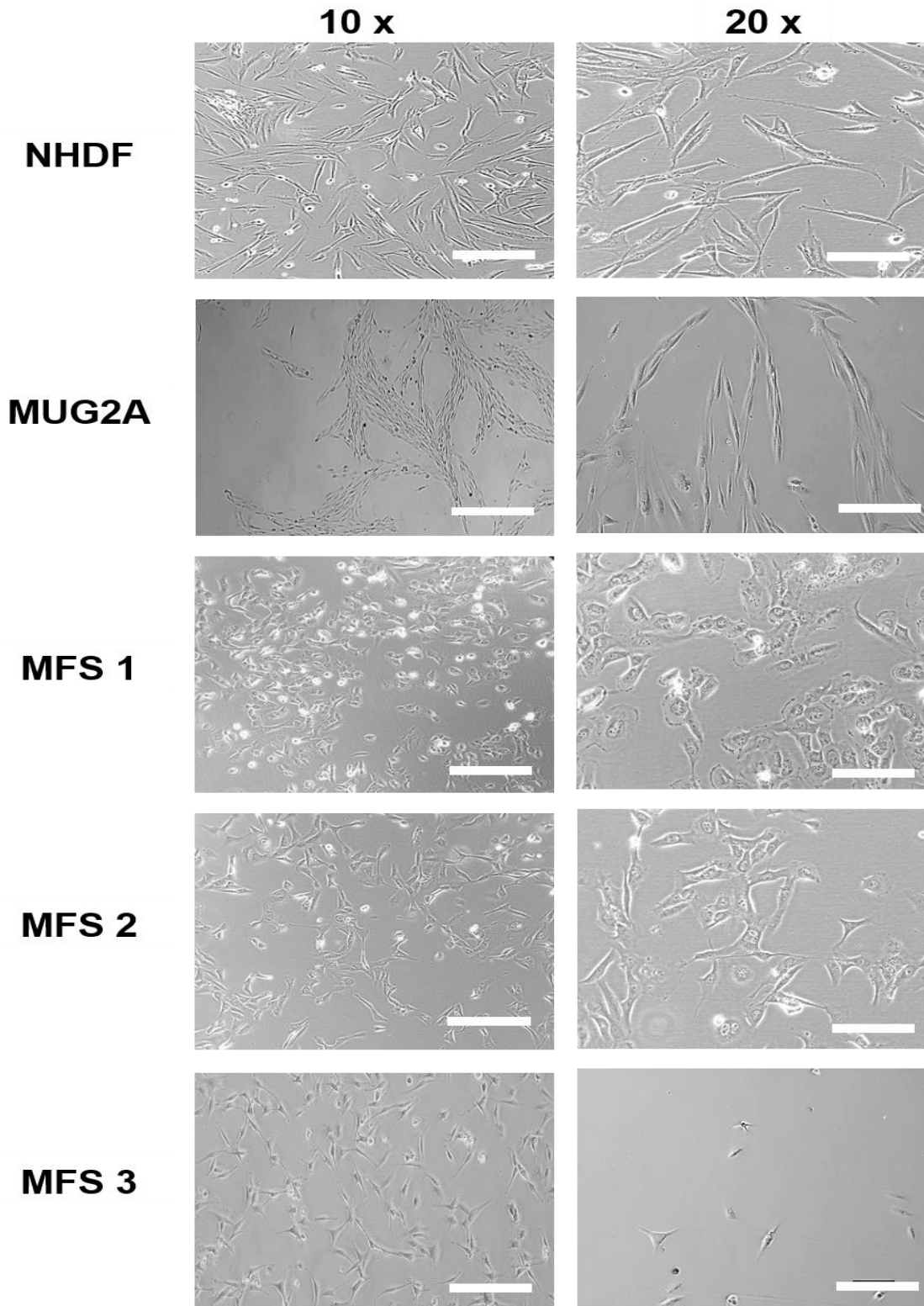
Figure 3. 2: Illustrative Phase-contrast micrographs of NHDF and MFS cell lines.

Scale bar for 10 X and 20 X magnification are 100 μm and 50 μm respectively.
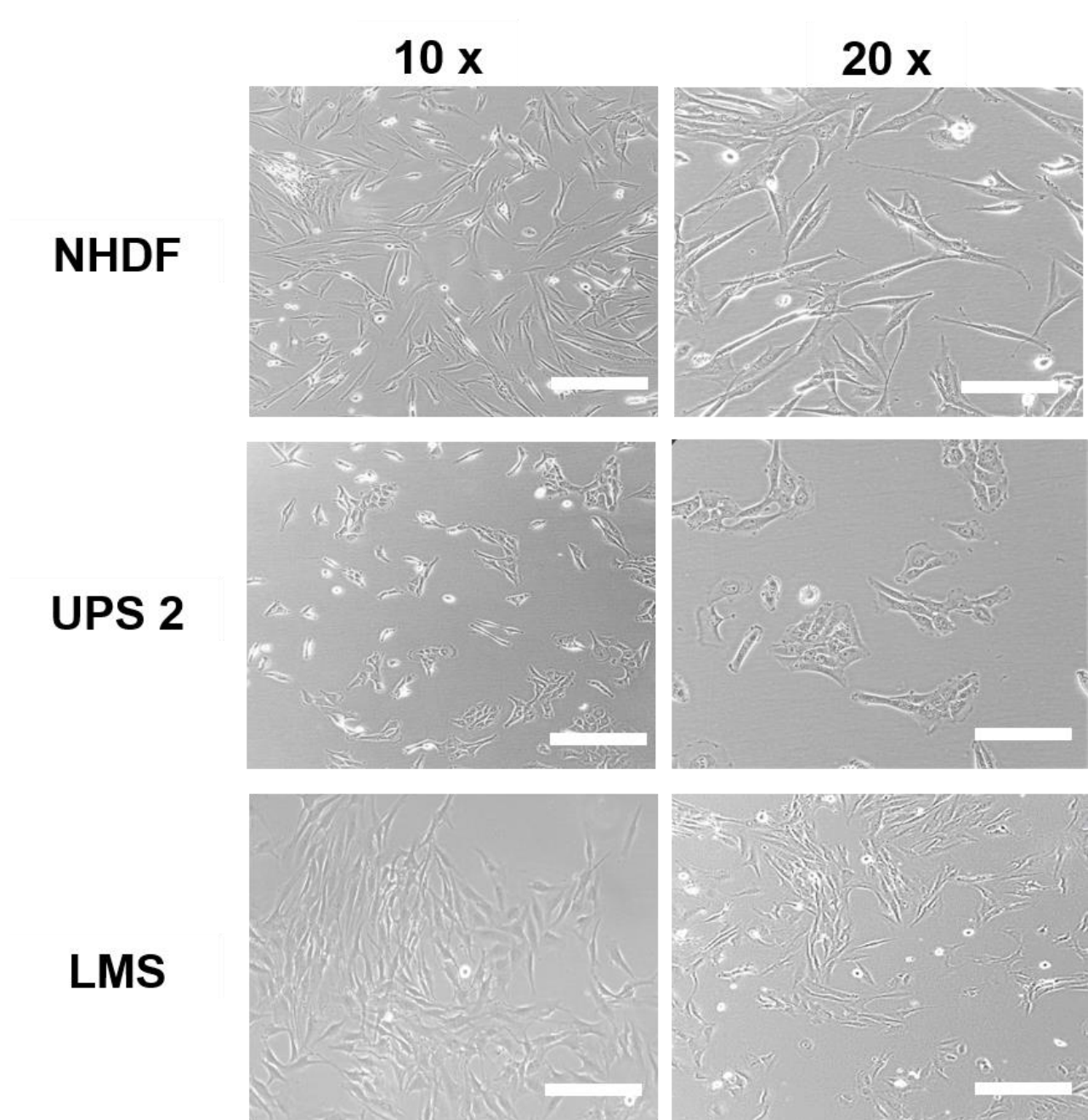
Figure 3. 3: Illustrative Phase-contrast micrographs of NHDF, UPS1 and LMS cell lines.
Scale bar for 10 X and 20 X magnification are 100 μm and 50 μm respectively.
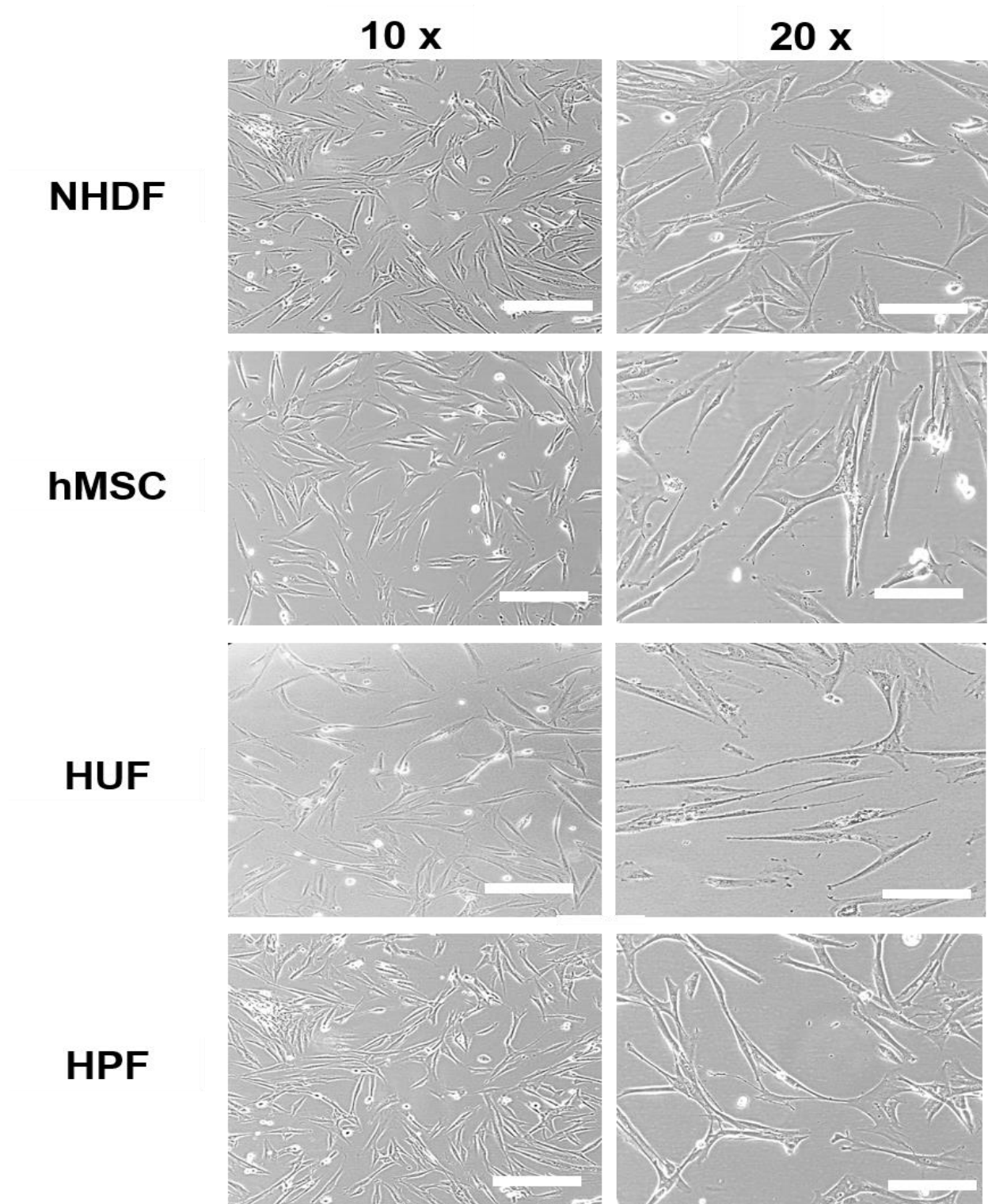
Figure 3. 4: Illustrative Phase-contrast micrographs of NHDF hMSC, HUF and HPF cell lines.

Scale bar for 10 X and 20 X magnification are 100 μm and 50 μm respectively.

3.2.1.2 Short Tandem Repeat (STR) analysis

STR or DNA fingerprinting is a DNA profiling method used for cell line authentication (Fan & Chu, 2007). STRs are short (2-5 base pair) DNA repeat sequences that are valuable for determining cell identity since these repeats vary among individuals. STRs are used to characterise and confirm cell line identity, exclude cross-contamination, and detect genomic drift since their genotyping is rapid, cost-effective, and automated. STRs are genotyped using polymerase chain reactions (PCRs) to amplify their encompassing regions in genomic DNA samples. PCR amplicons are then separated using a genetic analyser, and the result is analysed using software to compare the newly generated data with the previous data from Salawu *et al.* (2016) (Nims, 2010).

STR genotyping was performed for all STS cell lines to confirm their identity and exclude cross-contamination (Nims et al., 2010). Alleles for 10 human STR loci (THO1, D21S11, D5S818, D13S31, D7S82, D16S53, CSF1P0, AMEL, vWA and TPOX) were examined in nine cell lines (UPS1, UPS2,UPS3, UPS4, MUG2A,MFS1, MFS2, MFS3 and LMS). In six cell lines (UPS1, UPS2, UPS4, MFS2, MFS3 and LMS), no alleles matched > 70%, and were very similar to the results obtained from the results of Salawu *et al* (2016) (Table 3.2). MFS1 cell lines showed no allelic match (Table 3.2). However, UPS3 showed a partial match indicating genetic drift but not contamination (Table 3.2). Genetic drift is a change in cell allelic frequencies in cells due to chance and is not a contamination. Drift naturally occurs with increasing passages. Therefore, STR profiling must be performed regularly. However, MUG2A showed a 100% match with human Calu-6 anaplastic carcinoma cell line, an 80% match with human hTERT RPE-1 retinal epithelium cell line and an 80% match with the human NCI-H720 lung carcinoma cell line indicating possible contamination. Therefore, MUG2A was excluded from subsequent experiments (Table 3.2).

Cell line	Passage number	THO1	D21S11	D5S818	D13S317	D7S820	D16S539	CSF1P0	AMEL	vWA	TPOX	Allele match
STS 14/19 (UPS 1)	P72	6, 7	27, 30	12, 13	8, 11	8	14	12	X	16	8	No match found
STS06/11 (UPS 2)	P79		31,33	9,13	14	8	11	10,11	X,Y	17,18	8	No match found
STS09/11 (UPS 3)	P26	6, 9.3	28, 31.2	9	11	10	9	10	X	17	8	No match found
STS13/12 (UPS 4)	P64	6	31.2, 33.2	11	12	10, 12	11	11	X, Y	18	8	Partial match
MUG2A	P3	6,9	29	10,11	11	10,11	13,14,15	12,14	X	17,18	8	3 matches found
STS21/11w2 (MFS 2)	P21	8	30,31.2	13	13	8,9	12	10	X,Y	14,16	11	No match found
STS21/11w1 (MFS 1)	P22	8	30,31.2	13	13	8,9	12	10	X,Y	14,16	11	No match found
OH931 (MFS 3)	P3	9	29,31.2	11	10	9,12	11,13	12	X	16,17	8,11	No match found
LMS	p39	9	27,30	11	14	10,11	11	10,12	X	16		No match found

Table 3. 2: Short tandem repeat (STR) of STS cell lines.

DNA fingerprinting for STS cell lines .THO1, D21S11, D5S818, D13S317, D7S820, D16S539, CSFIPO, AMEL, vWA & TPOX are markers (locus names) and the numbers in the boxes are the allele call (number of repeats).

3.3 Comparison of mesenchymal gene expression between STS cell lines and normal human mesenchymal cells

As discussed in this chapter's introduction, STSs and SAFs are both mesenchymal lineage cells, and no selective markers have yet been identified that might facilitate their study. Western blots were used to examine whether different STS subtypes express common mesenchymal markers found in normal fibroblasts and CAFs and to confirm whether these were unsuitable for SAF identification in STSs.

Chemiluminescent western blotting is a semi-quantitative method used for protein detection and quantification (Mahmood & Yang, 2012). All STS cell lines were compared to three human primary fibroblasts from three different tissue sources and human MSCs from adipose tissue (AD-MSCs.). All primary fibroblasts were used below passage ten, and hMSC below passage seven. Cells were cultured to 60%-80% confluence for three independent biological repeates, and lysates were harvested and analysed by western blot as described in Section 2.2. Glyceraldehyde-3-phosphate dehydrogenase (GAPDH), with a MW of 36 KDa, and is ubiquitously expressed in all human tissues, was used to normalise the protein measurements between repeats, primary cells and STS cell lines. Protein levels were quantified by chemiluminescent western blotting followed by densitometric analysis using the Chemi Doc software. This software measures the signal density of a specific protein band and compares it with the background area to provide a reproducible measurement (Section 2.2.6). This value was normalised with repsect to the densiotemtric value obtained for the housekeeping GAPDH protein to correct protein loading differences. The value was then normalised to the NHDF value, which then equalled one, allowing for comparisons among independent repeats. Transgelin, αSMA, vimentin, N-cadherin, fibronectin, FSP-1, FAPα and SOX2 expression were measured between STS cell lines with respect to NHDF.Three biological repeats of each cell line was used in the western blots showed in (Fig. S3 & Fig. S4), while the representative blot just showing single lane of each cell to make it easier to visualise the result in (Fig.3.5 &Fig.3.8). All proteins showed positive expression in all celll lines, with transgelin and αSMA showing faint bands in the UPS and MFS cell lines relative to NHDF (Fig. 3.5,Fig.S3 &Fig.S4). FAPα blots detected two bands, one at the expected MW of 88 kDa

and a smaller band. This smaller band possibly represents cleaved or digested FAPα protein or the detection of another protein by the antibody (Fig.3.5, Fig.3.8 & Fig.S5).
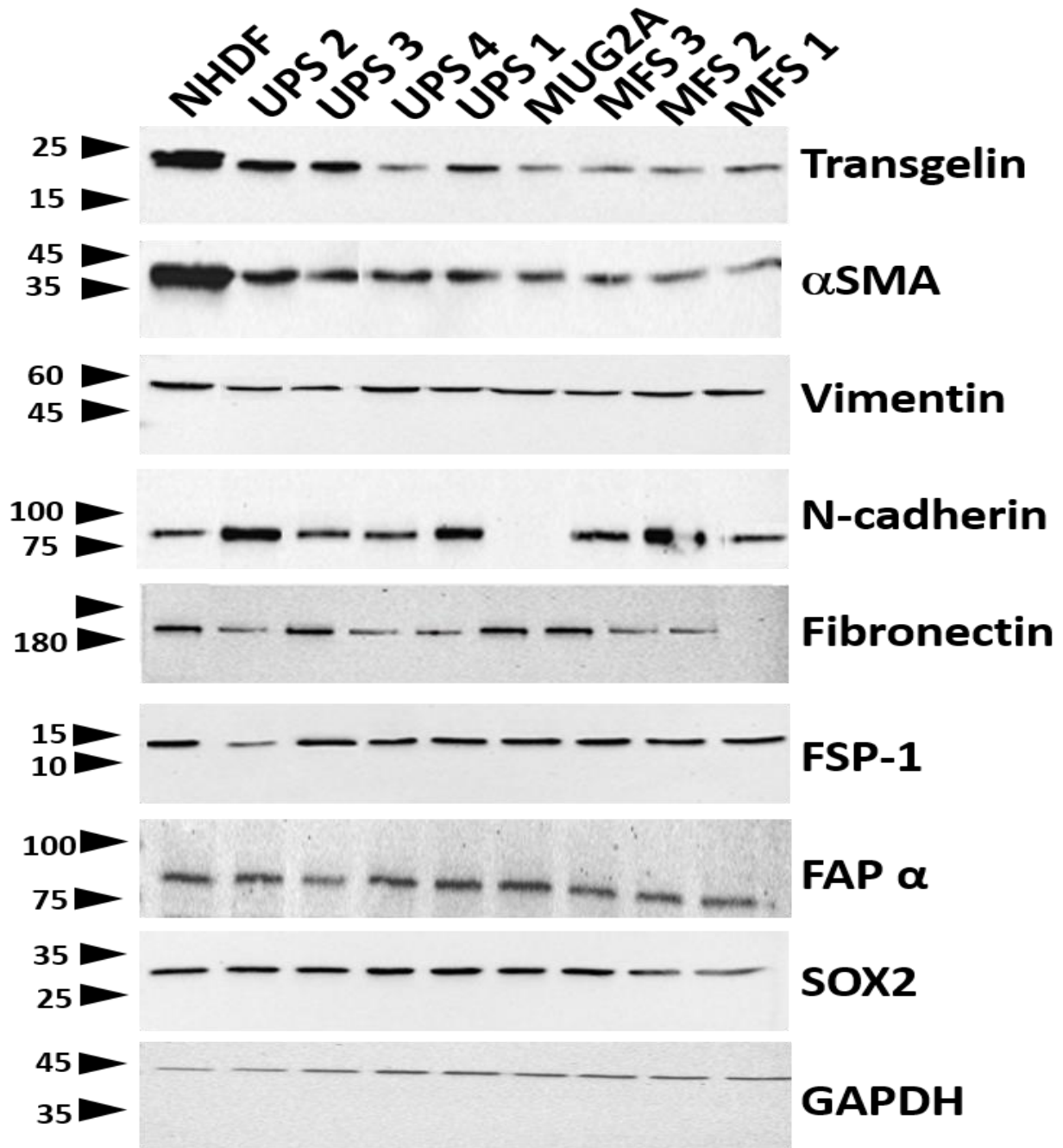
Figure 3. 5: Representative Western blots of expression of mesenchymal proteins in NHDF, UPS and MFS cells.

The labels at the top are the cell lines loaded into the gel. The numbers at the left are the molecular weight of the ladder to show the approximate band size.

3.3.1 Densitometry analyses show an increase of some mesenchymal protein expressions in primary mesenchymal cells compared to STS cells.

After normalisation against GAPDH, transgelin and αSMA showed lower levels of expression in UPS and MFS cell lines when compared with the NHDF (Fig. 3.6 & 3.7). All the other proteins (vimentin, N-cadherin, fibronectin, FSP-1, FAPα and SOX2) showed a similar level of expression across all UPS and MFS cell lines when compared with NHDF, although levels of N-Cadherin were more variable in the UPS lines (Fig. 3.6 & 3.7).
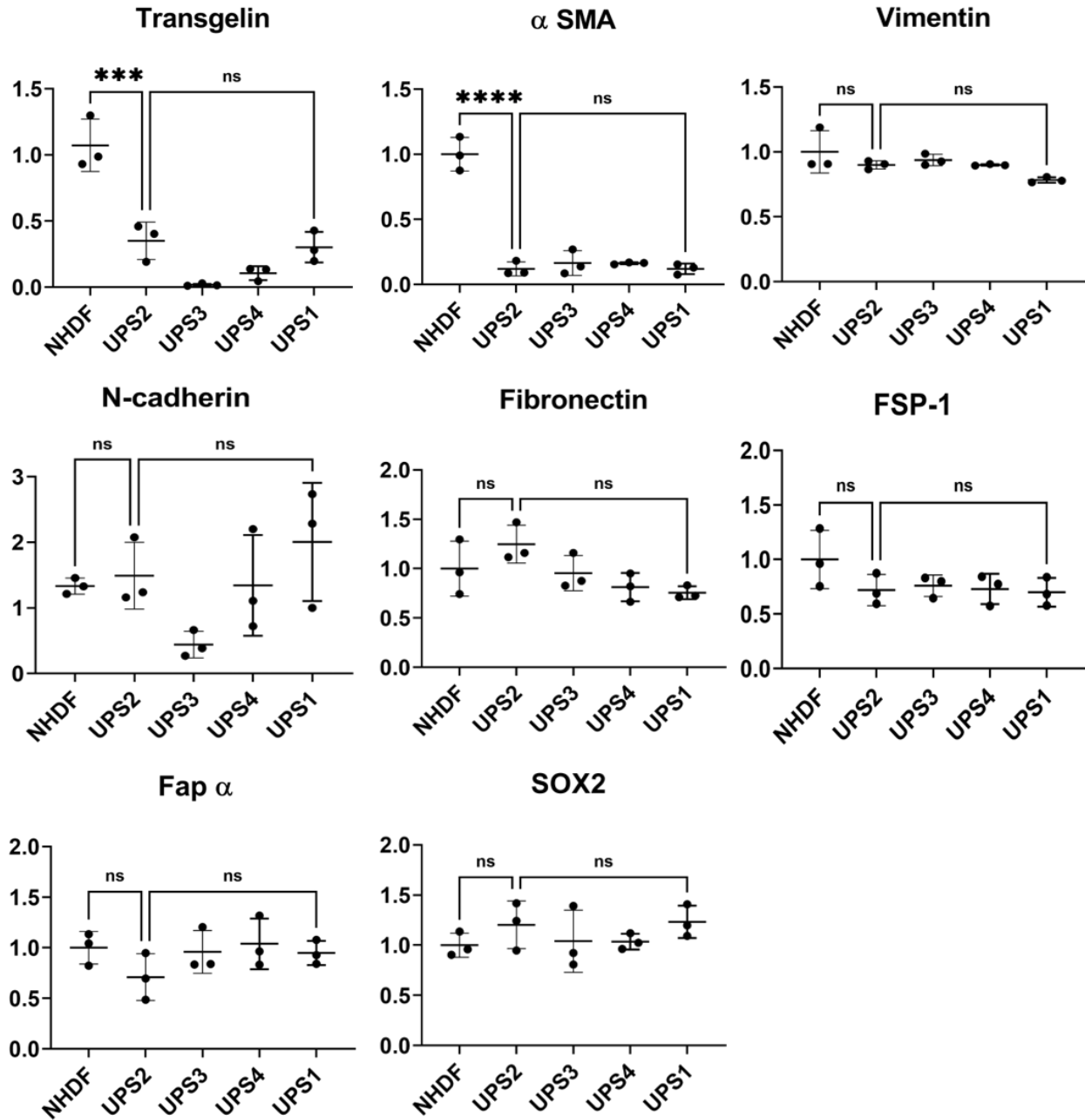
Figure 3. 6: Semi-quantitative Western blot analysis of mesenchymal protein in UPS cell lines compared to NHDF.

For each cell line including the NHDF three independent replicates were used, dots showing each replicate and the error bar demonstrating Standard Error of the mean (SEM). Individual values were adjusted with respect to GAPDH levels to control for protein loading differences and then normalised with respect to the mean intensity for the three NHDF samples. X-axis are the cell lines and y-axis is the normalised intensity. Error bars are ± SEM. *, P<0.05, **, P <0.01; ***, P < 0.001; NS, not significant.
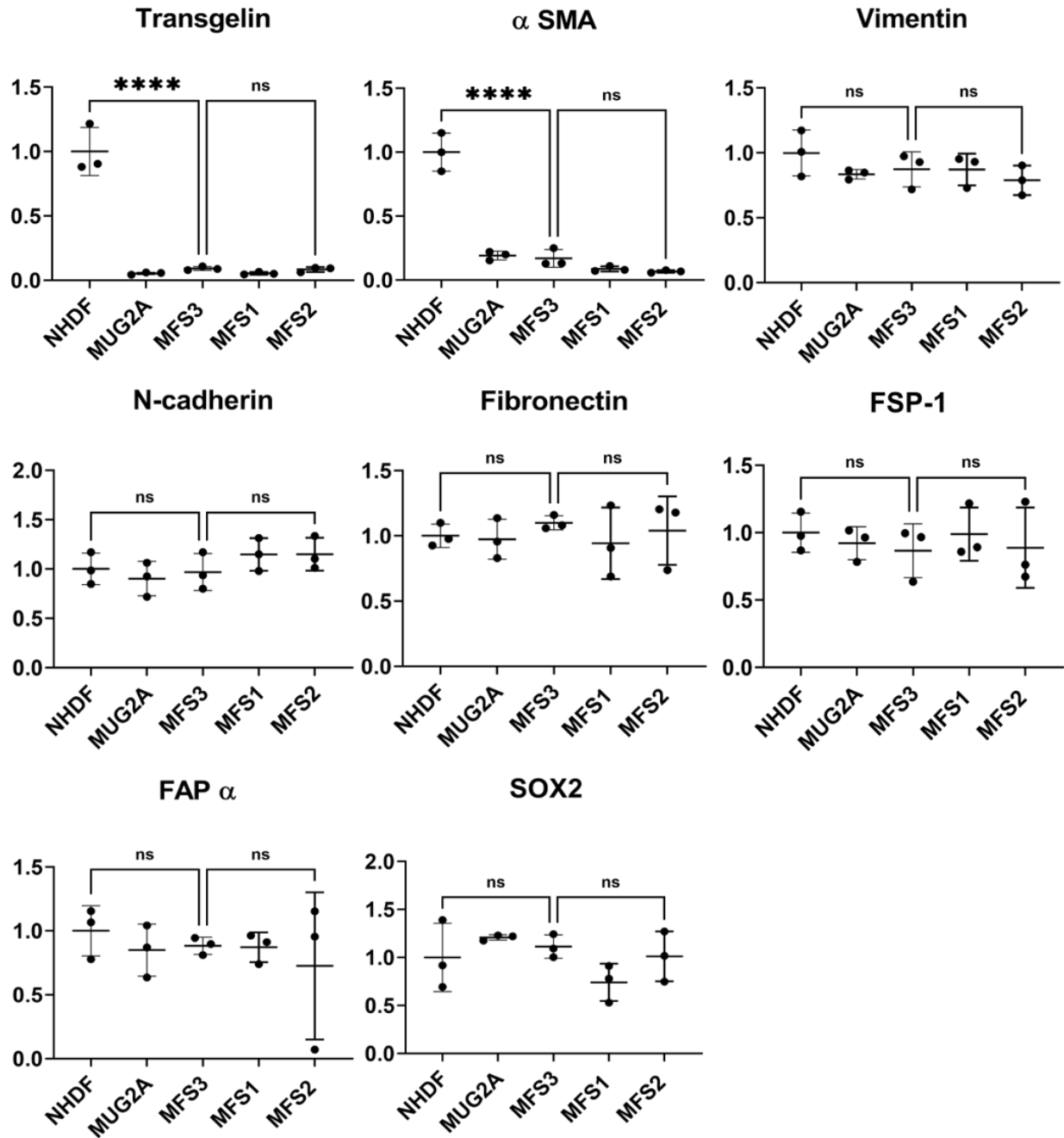
Figure 3. 7: Semi-quantitative Western blot analysis of mesenchymal protein in MFS cell lines compared to NHDF.

For each cell line including the NHDF three independent replicates were used, dots showing each replicate and the error bar demonstrating Standard Error of the mean (SEM). Individual values were adjusted with respect to GAPDH levels to control for protein loading differences and then normalised with respect to the mean intensity for the three NHDF samples. X-axis are the cell lines and y-axis is the normalised intensity. Error bars are ± SEM. *, P<0.05, **, P <0.01; ***, P < 0.001; NS, not significant

3.4. Comparison of mesenchymal gene expression between UPS, LMS and normal human mesenchymal cells.

Differences in relative protein levels between LMS and UPS were examined by western blot to determine whether there were any significant differences in common mesenchymal protein levels between less differentiated (UPS) and more differentiated (LMS) sarcoma subtypes. Guled *et al.* (2014) noted that LMS showed higher αSMA and desmin levels than UPS using immunohistochemistry (IHC) (Guled et al., 2014). While LMS is a well-differentiated sarcoma, its genomic profile greatly resembles that of UPS (Guled et al., 2014). Moreover, since LMS and UPS overlapped in unsupervised hierarchical clustering of genome copy number profiles, identifying specific markers to help distinguish them is important (Carneiro et al., 2009). Relative transgelin, αSMA, vimentin, N-cadherin, fibronectin, FSP1, FAPα, and SOX2 levels were compared between the LMS and UPS1 cell lines as (a representative cell line) with respect to NHDF. All proteins showed positive expression in all celll lines, with transgelin and αSMA showing lower expression in the UPS cell line than in the LMS and NHDF (Fig. 3.8 & Fig. S8).

Figure 3. 8: Representative Western blots of expression of mesenchymal proteins in NHDF, UPS and LMS cells.

The labels at the top are the cell lines loaded into the gel. The numbers at the left are the molecular weight of the ladder to show the approximate band size.

3.4.1 Densitometry analyses show an increase of some mesenchymal protein expressions in LMS compared to UPS cells

After normalisation against GAPDH, transgelin and αSMA showed similar levels of expression in the LMS cell line when compared with the NHDF, which were higher than expression in UPS (Fig. 3.9). All the other proteins (vimentin, N-cadherin, fibronectin, FSP-1, FAPα and SOX2) showed a similar level of expression across UPS and LMS cell lines when compared with NHDF (Fig. 3.9).
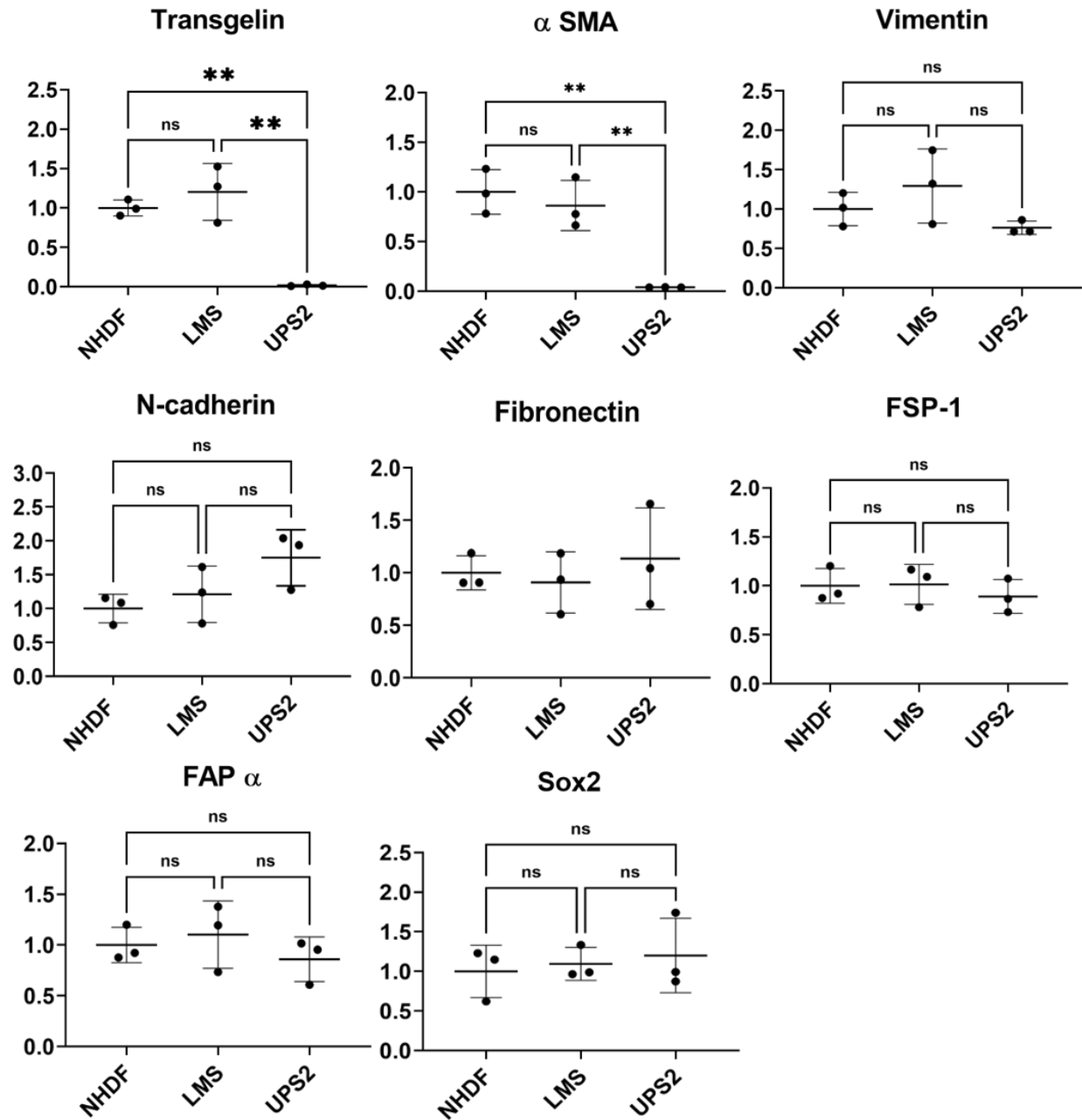
Figure 3. 9: Semi-quantitative Western blot analysis of mesenchymal protein in UPS2 and LMS cell lines compared to NHDF.

For each cell line including the NHDF three independent replicates were used, dots showing each replicate and the error bar demonstrating (SEM). Individual values were adjusted with respect to GAPDH levels to control for protein loading differences and then normalised with respect to the mean intensity for the three NHDF samples. X-axis are the cell lines and y-axis is the normalized intensity. Error bars are ± SEM. *, $P<0.05$, **, $P <0.01$; ***, $P < 0.001$; NS, not significant.

3.5. Comparison of mesenchymal gene expression between primary human fibroblasts from different tissues

Differences in relative protein levels between HUFs, HPFs, and hMSC were explored to determine whether there were significant differences in common mesenchymal proteins between the different tissue fibroblast sources and hMSC. NHDF were initially chosen because they originate from the embryonic mesoderm, similar to the STS cell lines (Thulabandu et al., 2018). hMSC were chosen since they are fibroblast precursors and express similar cell surface markers to fibroblasts (Denu et al., 2016). However, they are a less differentiated cell type that may reflect changes in STS cells upon transformation. Relative transgelin, αSMA, vimentin, N-cadherin, fibronectin, FSP1, FAPα, and SOX2 levels were compared between fibroblasts (HUFs and HPFs) and hMSC with respect to NHDF. All proteins showed positive expression in all celll lines (Fig.3.10 and Fig.3.11, respectively). SOX2 blots showed two bands, one at the expected MW and a smaller band. The smaller band possibly represents cleaved, digested, or phosphorylated SOX2 protein or the detection of another protein by the antibody (Fig. S6).
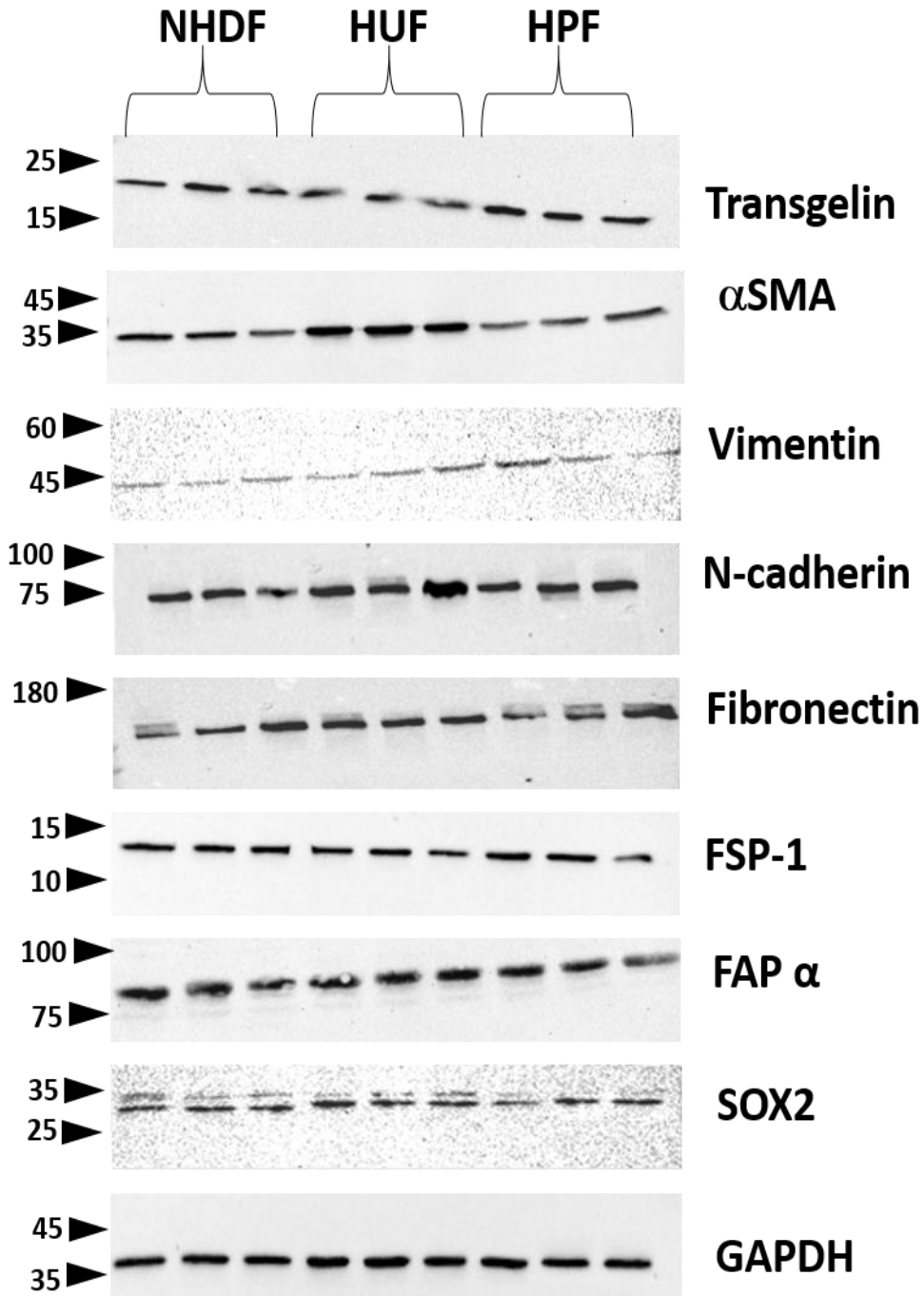
Figure 3. 10: Representative Western blots of expression of mesenchymal proteins in NHDF, HUF and HPF cells.

The labels at the top are the cell lines loaded into the gel. The numbers at the left are the molecular weight of the ladder to show the approximate band size.
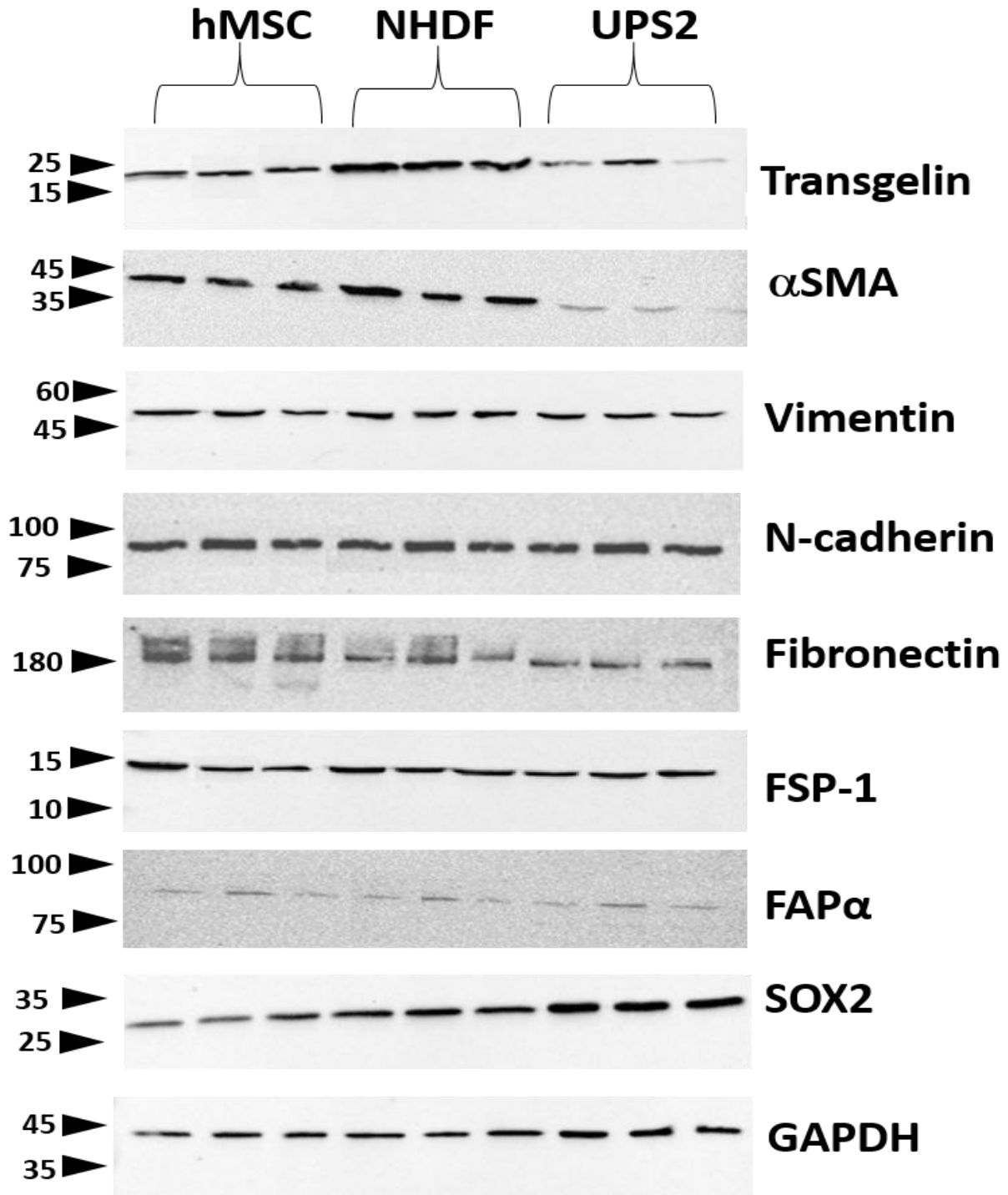
Figure 3. 11: Representative Western blots of expression of mesenchymal proteins in hMSC, NHDF and UPS2 cells.

The labels at the top are the cell lines loaded into the gel. The numbers at the left are the molecular weight of the ladder to show the approximate band size.

3.5.1 Densitometric analyses of western blots show similar mesenchymal protein expressions in fibroblasts and human mesenchymal stem cells compared to NHDF cells

After normalisation against GAPDH, all examined proteins (transgelin, α SMA, vimentin, N-cadherin, fibronectin,SOX2, FSP-1 & FAPα) showed similar levels in two additional tissue derived fibroblats (HUF and HPF) and hMSCs compared to NHDF (Fig.3.12 and Fig.3.13,respectively).
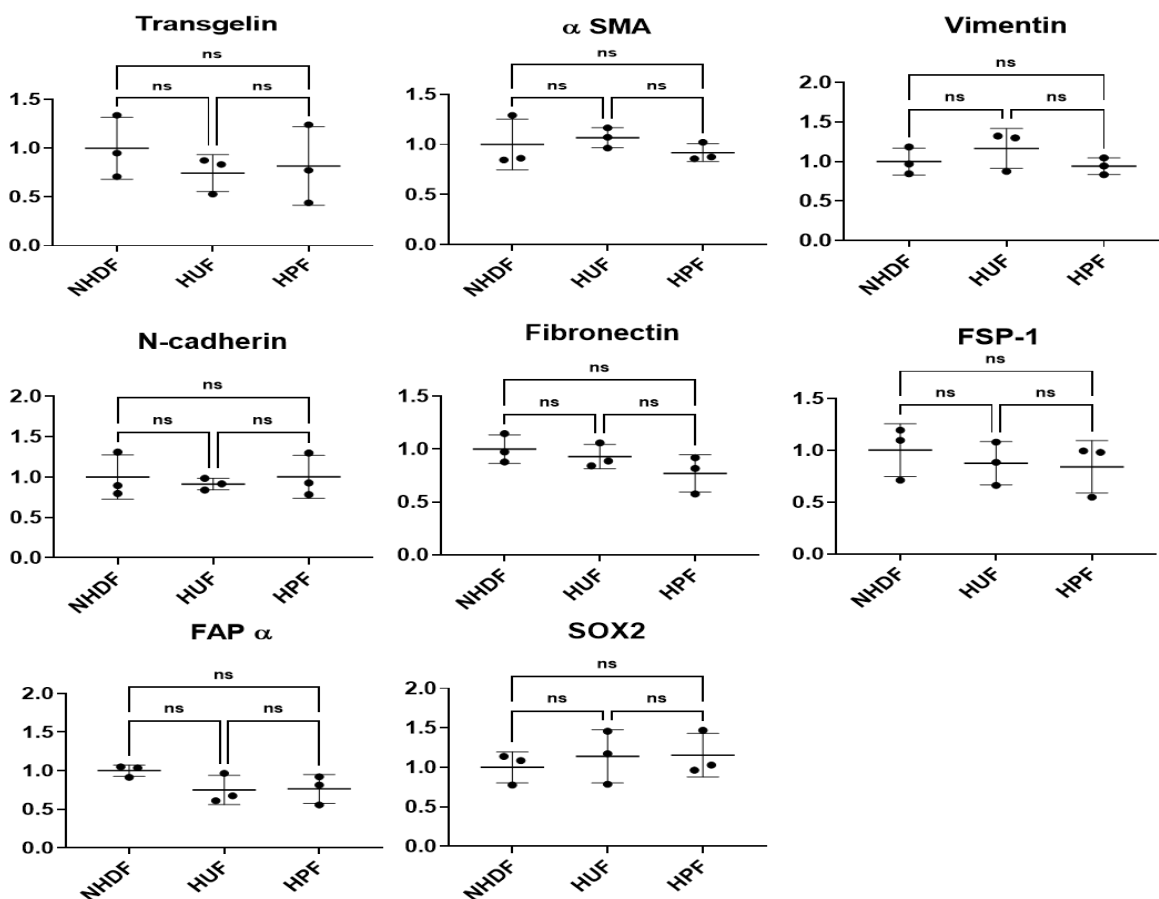
Figure 3. 12: Semi-quantitative Western blot analysis of mesenchymal protein in HUF and HPF cell lines compared to NHDF.

For each cell line including the NHDF three independent replicates were used, dots showing each replicate and the error bar demonstrating (SEM). Individual values were adjusted with respect to GAPDH levels to control for protein loading differences and then normalised with respect to the mean intensity for the three NHDF samples. X-axis are the cell lines and y-axis is the normalized intensity. Error bars are ± SEM. *, P<0.05, **, P <0.01; ***, P < 0.001; NS, not significant.
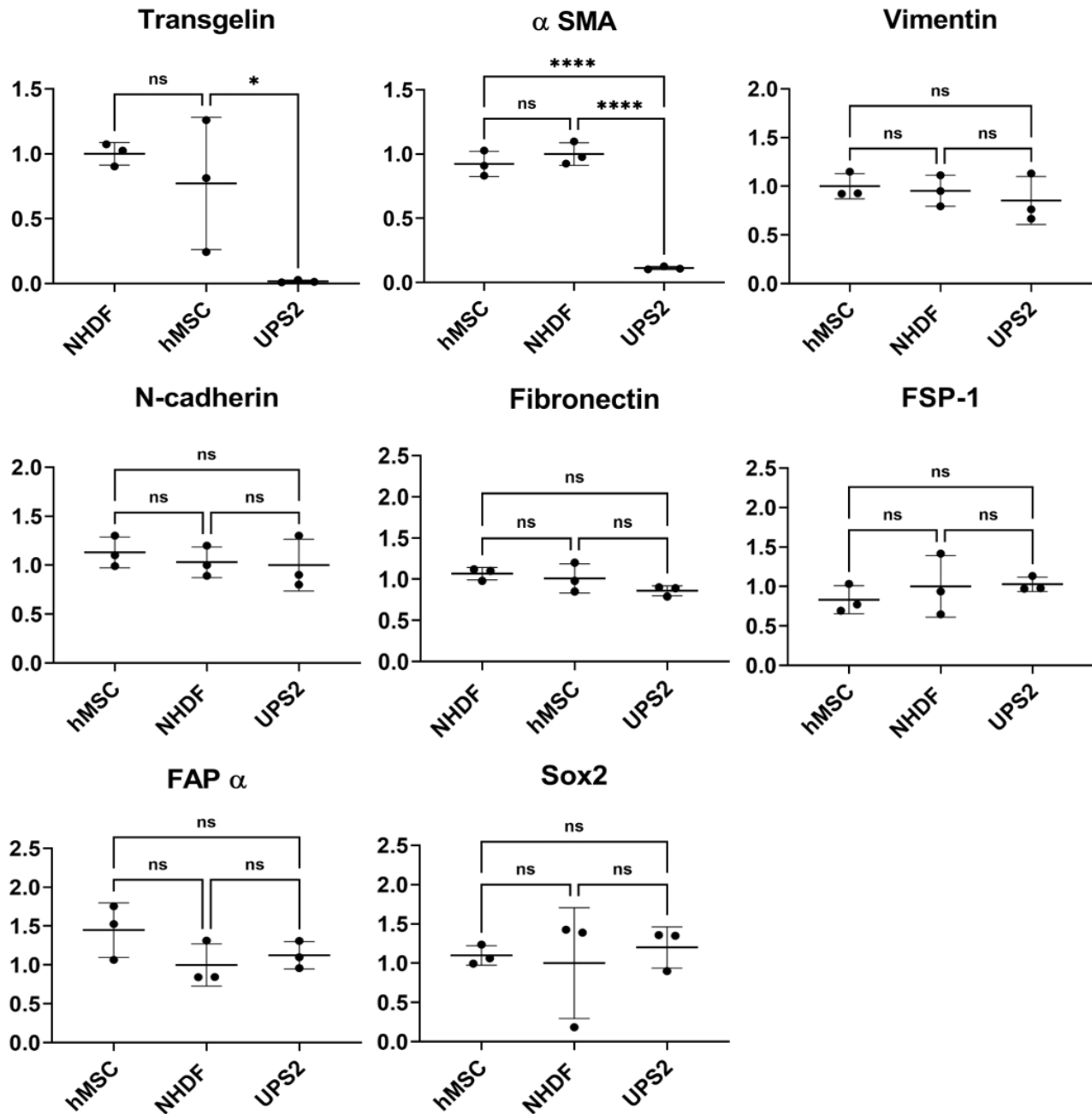
Figure 3. 13: Semi-quantitative Western blot analysis of mesenchymal protein in hMSC and UPS2 compared to NHDF.

For each cell line including the NHDF three independent replicates were used, dots showing each replicate and the error bar demonstrating Standard Error of the Mean (SEM). Individual values were adjusted with respect to GAPDH levels to control for protein loading differences and then normalised with respect to the mean intensity for the three NHDF samples. X-axis are the cell lines and y-axis is the normalized intensity. Error bars are ± SEM. *, P<0.05, **, P <0.01; ***, P < 0.001; NS, not significant.

3.6 Comparison of mesenchymal protein cellular localisations between STS cell lines and NHDF

The subcellular localisations of transgelin, αSMA, vimentin, N-cadherin, fibronectin, ,FSP-1, FAPα and SOX2 were determined to explore whether they differ significantly among STS cell lines relative to NHDF. Protein localisation is important for understanding its cell-specific role (Paciorek et al., 2006). Phalloidin was used to visualise cellular filamentous actin (F-actin) in the cells. Subcellular localisation was performed using immunocyto-chemistry (ICC). ICC is a semi-quantitative method used for fluorescence-based protein detection and visualisation and is very useful for protein localisation within cells. Cells were prepared for ICC as described in Section 2.5. All antibodies were stained with a green fluorescent conjugate (transgelin, αSMA, vimentin, N-cadherin, fibronectin, FSP1, FAPα, and SOX2), and 4′, 6-diamidino-2-phenylindole (DAPI) was used to stain nuclei. DAPI nuclear staining is shown in blue, and phalloidin F-actin staining is shown in red. Pearson's Correlation Coefficient (PCC) (r) was used to quantify the colocalisation between F-Actin (phalloidin) and the studied protein. The r coefficient ranges from +1 (perfect positive correlation) and −1 (perfect negative), with 0 representing no correlation (Zinchuk & Zinchuk, 2008).

Transgelin localised to the cytoplasm in most cell lines (Fig. 3.14,Fig.S9, Fig.S10 & Fig.S11). However, it was localised to both the cytoplasm and nucleus in the UPS2 and UPS3 cell lines (Fig.3.14 & Table 3.3). Transgelin and F-actin localisations were highly correlated ($r \geq 0.751$; Table S1) and did not differ significantly from NHDFs (Fig. S33). While transgelin did not localise to the nucleus in UPS, the colocalisation coefficient (r) was the same.
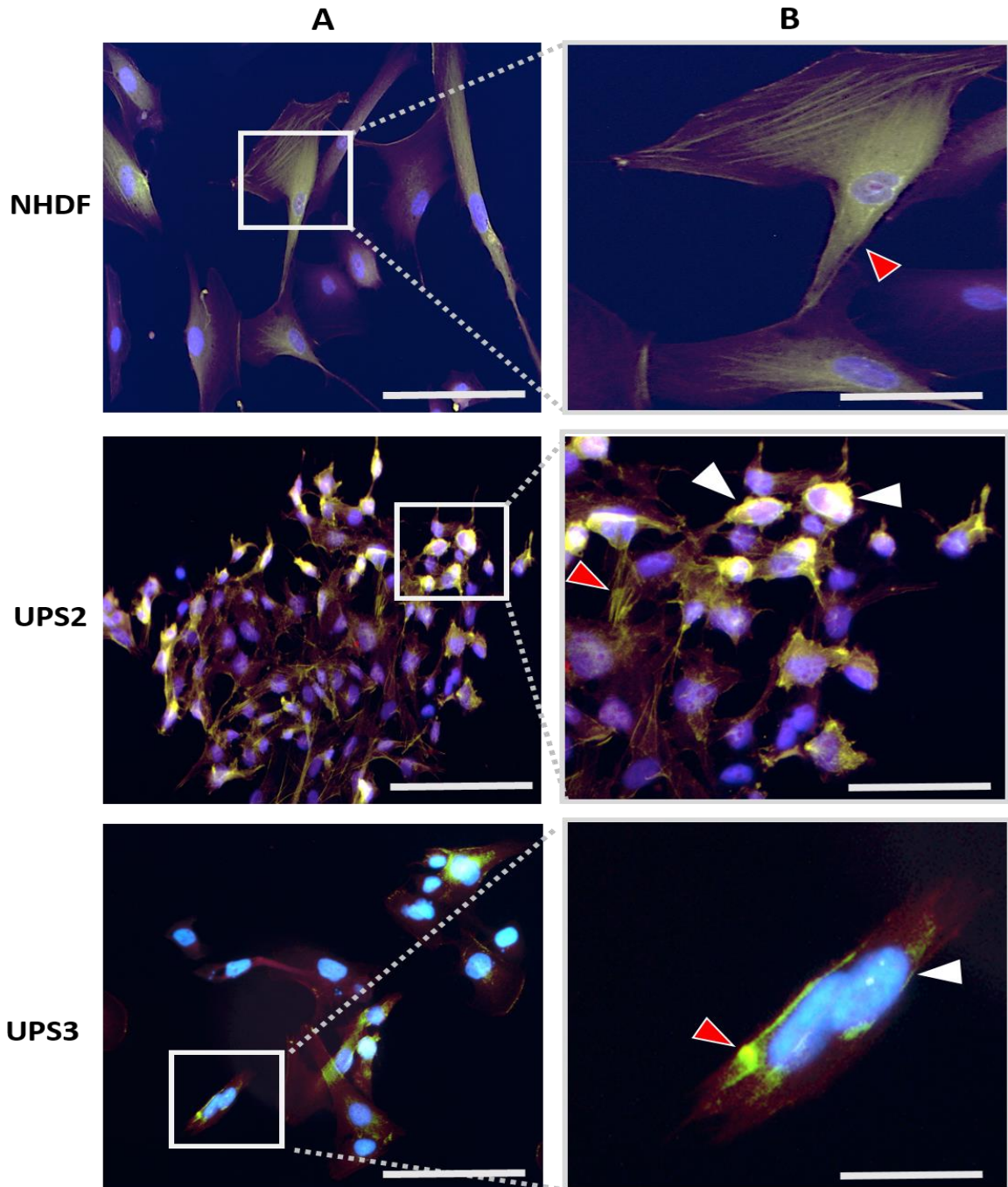
Figure 3. 14: Representative Immunocytochemistry images of transgelin.

Transgelin localised to the cytoplasm in NHDF (red arrow). In UPS2 and UPS3, It localised to the nucleus (white arrows) and to the cytoplasm (red arrow). The nuclei are stained blue with DAPI, transgelin is stained green, and F-actin is stained red with phalloidin. **(A)** Scale bar is 100µm. **(B)** scale bar is 50µm. All images were taken at 20X Magnification.

αSMA localised mainly to the cytoplasm in most cell lines (Fig. 3.15,Fig.S12,Fig.S13 & Fig.S14), However, it was localised to both the cytoplasm and the nuclues in UPS3 cell line (Fig. 3.15 &Table 3.3). αSMA and phalloidin were highly correlated (r ≥ 0.844 ;Table S1), and did not differe singnificanlty from NHDF (Fig. S33).
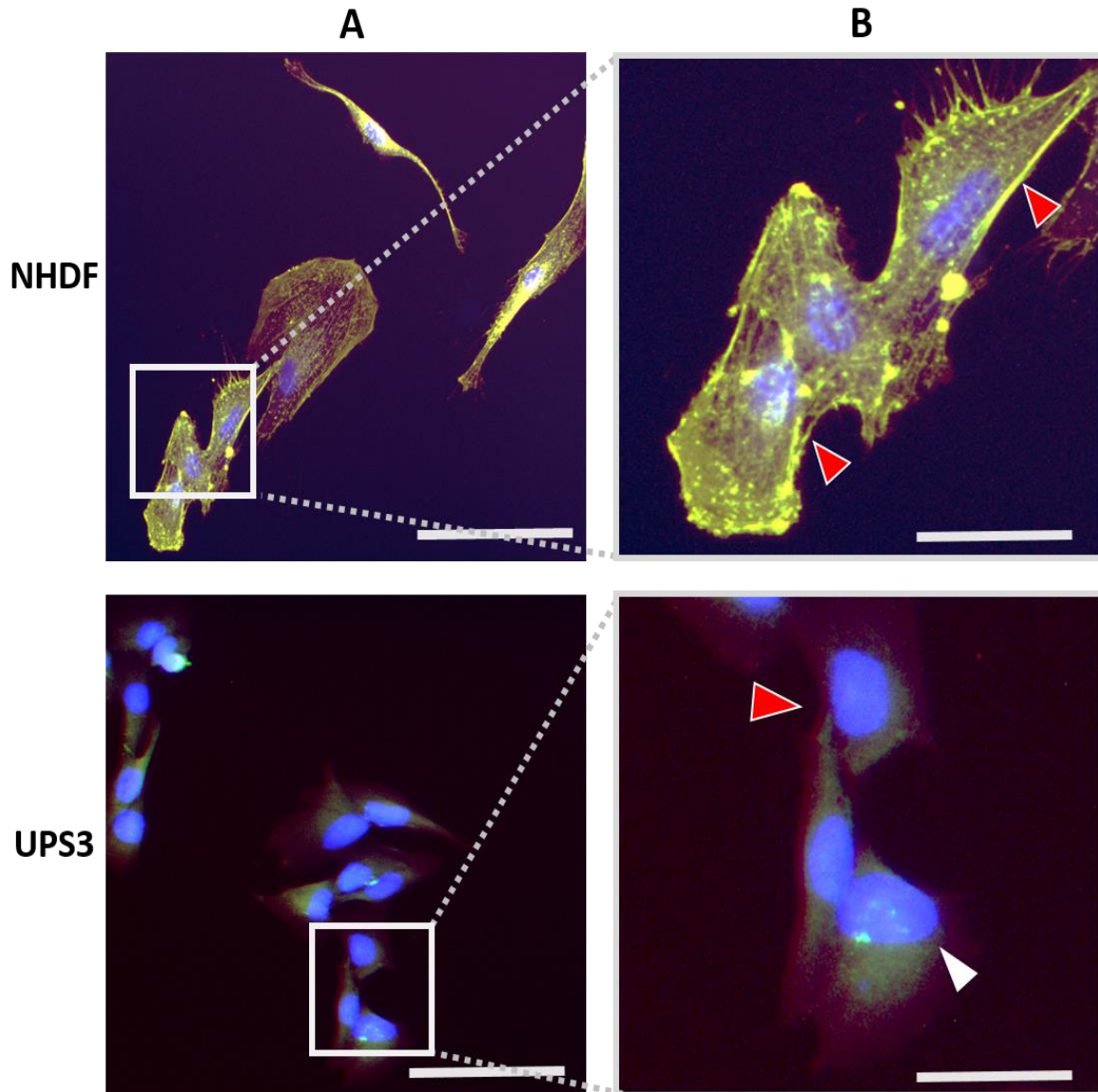
Figure 3. 15: Representative Immunocytochemistry images of αSMA.

αSMA localised to the cytoplasm in NHDF (red arrows). In UPS3, it localised to the cytoplasm (red arrow) and to the nucleus (white arrows).The nuclei are stained blue with DAPI, αSMA is stained green, and F-actin is stained red with phalloidin. **(A)** Scale bar is 100μm. **(B)** Scale bar is 50μm. All images were taken at 20X Magnification.

Vimentin localised mainly to the cytoplasm in most cell lines (Fig. 3.16,Fig.S15,Fig.S16 &Fig.S17). However it was localised to both the nuclues and the cytoplasm in UPS3 and MFS1 cell lines (Fig. 3.16 & Table 3.3). Vimentin and phalloidin localisations were highly correlated (r ≥ 0.761 ;Table S1) and did not differ significantly from NHDF (Fig. S33).
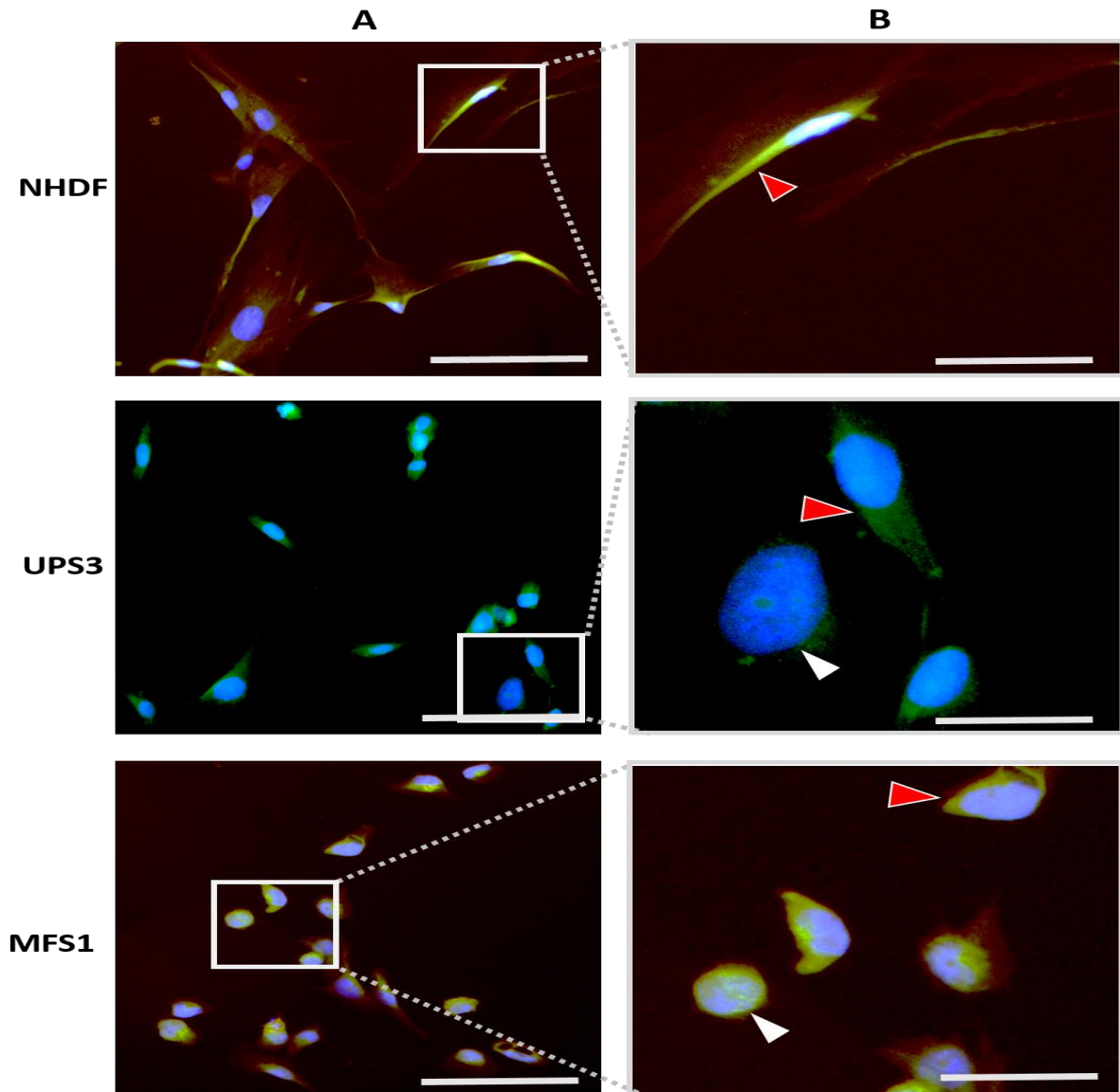
Figure 3. 16: Representative Immunocytochemistry images of Vimentin.

Vimentin localised to the cytoplasm in NHDF (red arrows) .In UPS3 and MFS1, it localised to both the cytoplasm (red arrows) and the nucleus (white arrows). The nuclei are stained blue with DAPI, Vimentin is stained green and F-actin is stained red with phalloidin. **(A)** Scale bar is 100µm. **(B)** Scale bar is 50µm. All images were taken at 20X Magnification

N-cadherin localised mainly to the cytoplasm in most STS cell lines (Fig. 3.17,Fig.S18,Fig.S19 &Fig.S20), However, it was localised to both the nuclues and the cytoplasm in MFS2 cell lines (Fig. 3.17 & Table 3.3). N-cadherin and phalloidin localisations were highly correlated (r ≥ 0.843 ;Table S1), and did not differ significantly from NHDF (Fig. S33).
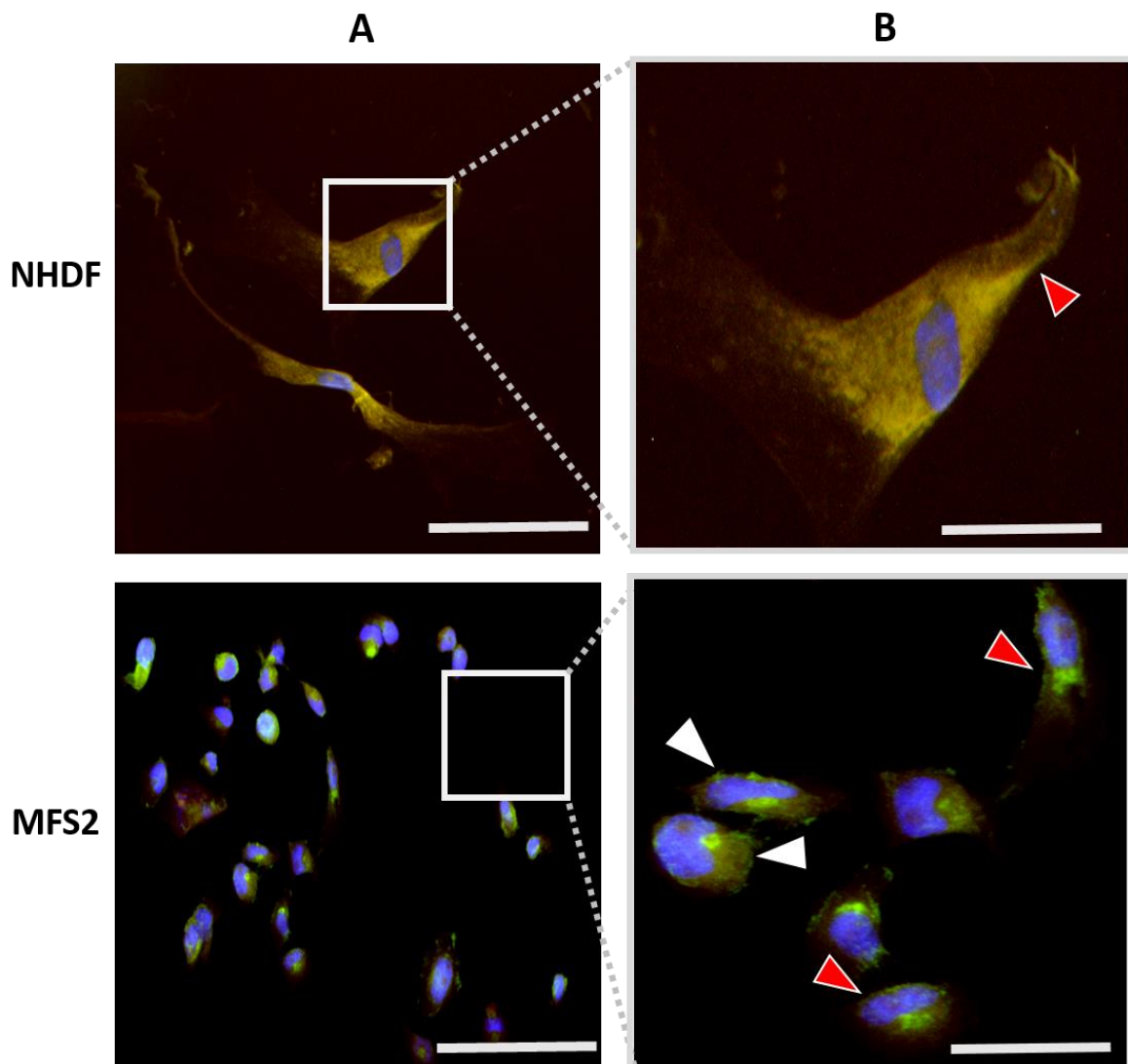
Figure 3. 17: Representative Immunocytochemistry images of N-cadherin.

N-cadherin localised to the cytoplasm in NHDF (red arrows) .In MFS2, it localised to the nucleus (white arrows) and to the cytoplasm (red arrow). The nuclei are stained blue with DAPI, N-cadherin is stained green and F-actin is stained red with phalloidin. **(A)** Scale bar is 100µm. **(B)** Scale bar is 50µm. All images were taken at 20X Magnification.

Fibronectin localised mainly to the cytoplasm in most cell lines (Fig. 3.18,FigS21,Fig.S22 & Fig.S23). However, it was localise to both the cytoplasm and the nucleus in MFS1 cell lines (Fig. 3.18 & Table 3.3). Fibronectin and phalloidin localisations were highly correlated (r ≥ 0.804 ;Table S1), and did not differ significantly from NHDF (Fig. S33).
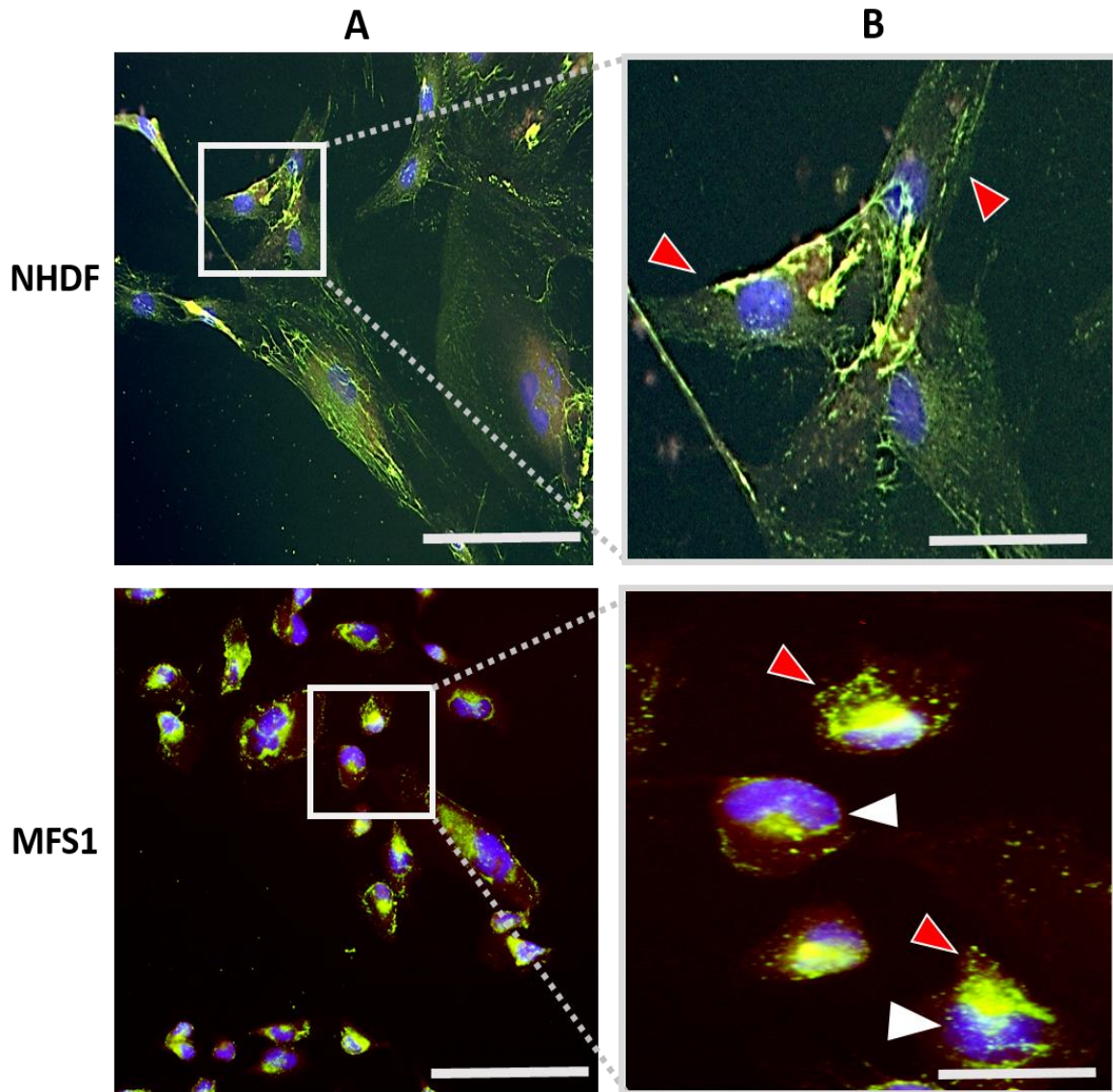
Figure 3. 18: Representative Immunocytochemistry images of Fibronectin.

Fibronectin localised to the cytoplasm in NHDF (red arrows). In MFS1, it localised to the nucleus (white arrows) and to the cytoplasm (red arrow). The nuclei are stained blue with DAPI, Fibronectin is stained green and F-actin is stained red with phalloidin. **(A)** Scale bar is 100µm. **(B)** Scale bar is 50µm. All images were taken at 20X Magnification.

FSP-1 localised mainly to the cytoplasm in most cell lines (Fig.3.19,Fig.S24,Fig.S25 &Fig.S26). However, it was localised to both the cytoplasm and the nuclues in MFS1 cell lines (Fig. 3.19 & Table 3.3). FSP-1 and phalloidin localisation were highly correlated (r ≥ 0.854 ;Table S1), and did not differ significantly from NHDF (Fig.S33).
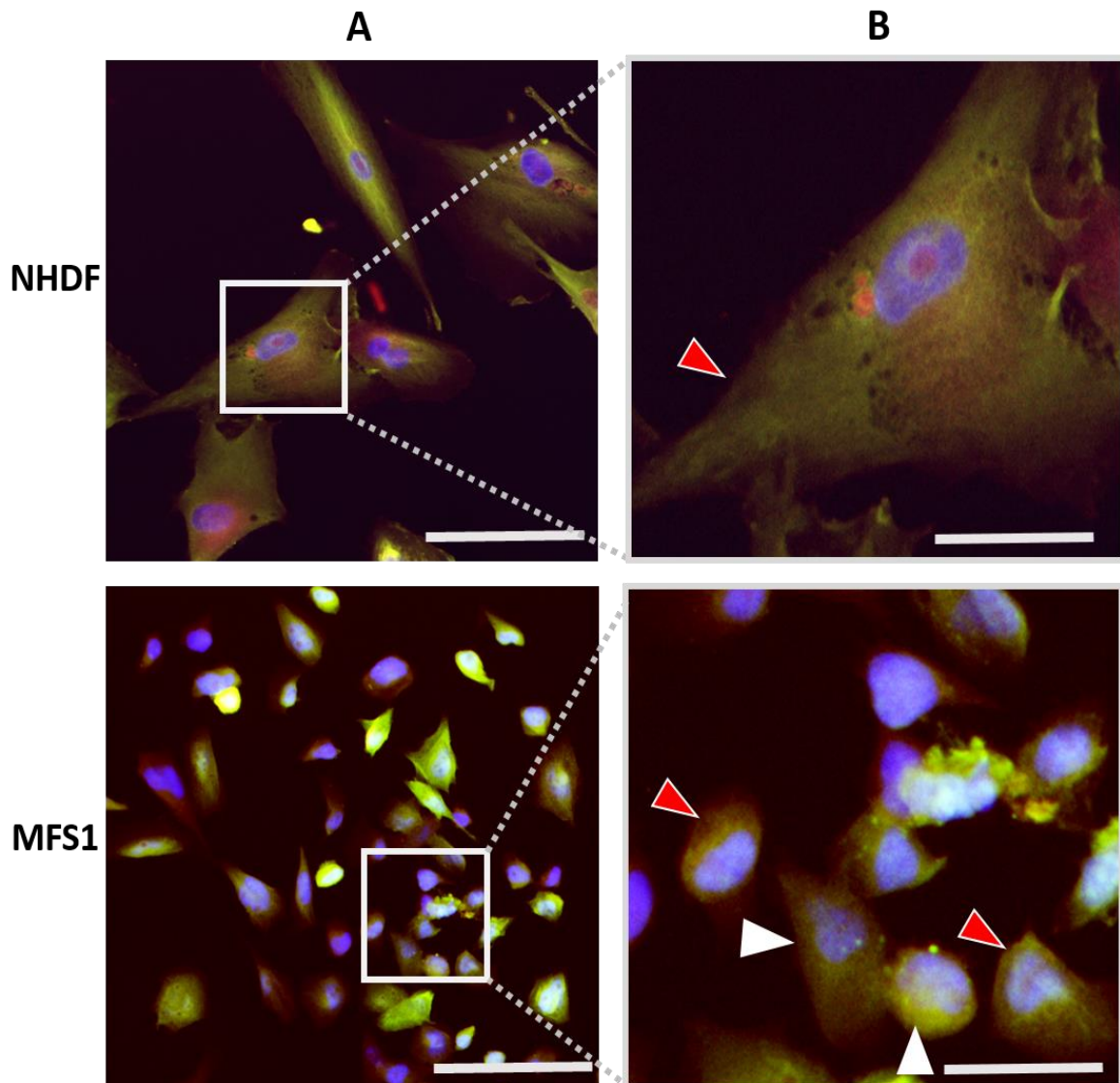
Figure 3. 19: Representative Immunocytochemistry images of FSP-1.

 FSP-1 localised to the cytoplasm in NHDF (red arrows). In MFS1, it localised to the nucleus (white arrows) and to the cytoplasm (red arrow). The nuclei are stained blue with DAPI, FSP-1 is stained green and F-actin is stained red with phalloidin. **(A)** Scale bar is 100µm. **(B)** Scale bar is 50µm. All images were taken at 20X Magnification.

FAPα localised mainly to the cytoplasm in most cell lines (Fig. 3.20,Fig.S27,Fig.S28 &Fig.S29). However, it was more diffuesd in UPS1 and diffused and localised to the nucleus in MFS2 cell lines (Fig.3.20 & Table 3.3). FAPα and phalloidin localisation were higlhy correlated (r ≥ 0.864 ;Table S1), and did not differ significantly from NHDF (Fig.S33).
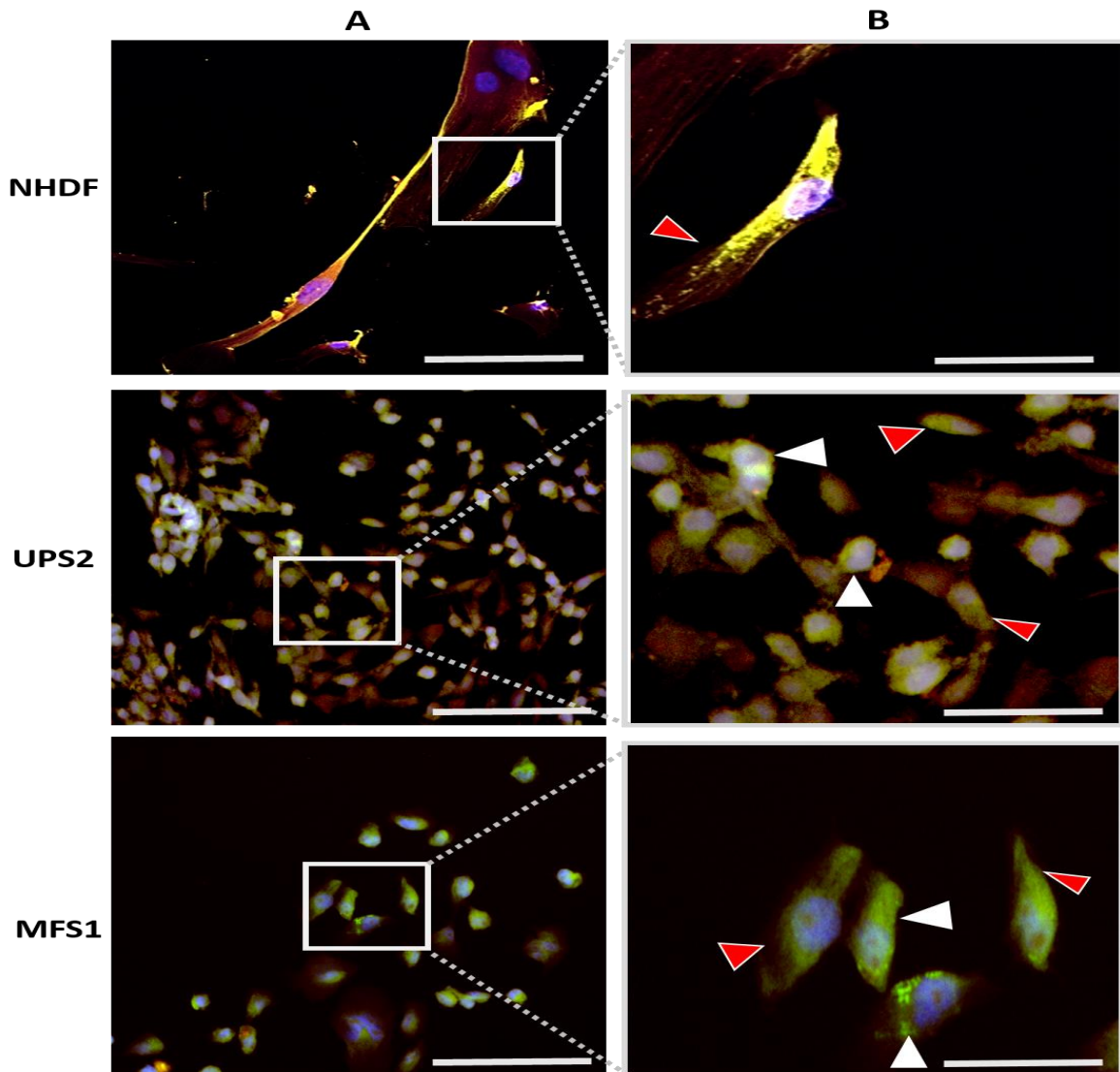
Figure 3. 20: Representative Immunocytochemistry images of FAPα.

FAPα localised to the cytoplasm in NHDF (red arrows). In UPSS2 and MFS1, it localised to the nucleus (white arrows) and to the cytoplasm (red arrow). The nuclei are stained blue with DAPI, FAPα is stained green and F-actin is stained red with phalloidin. **(A)** Scale bar is 100µm. **(B)** Scale bar is 50µm. All images were taken at 20X Magnification.

SOX2 localised mainly to the cytoplasm in most cell lines (Fig.3.21,Fig.S30,Fig.S31 & Fig.S32). However, it was localsed to both the nuclear and the cytoplasm in UPS3 and MFS1 cell lines (Fig.3.21, & Table 3.3). SOX2 and phalloidin localisation were highly correlated (r ≥ 0.80 ;Table S1), and did not differ significantly from NHDF (Fig.S33).
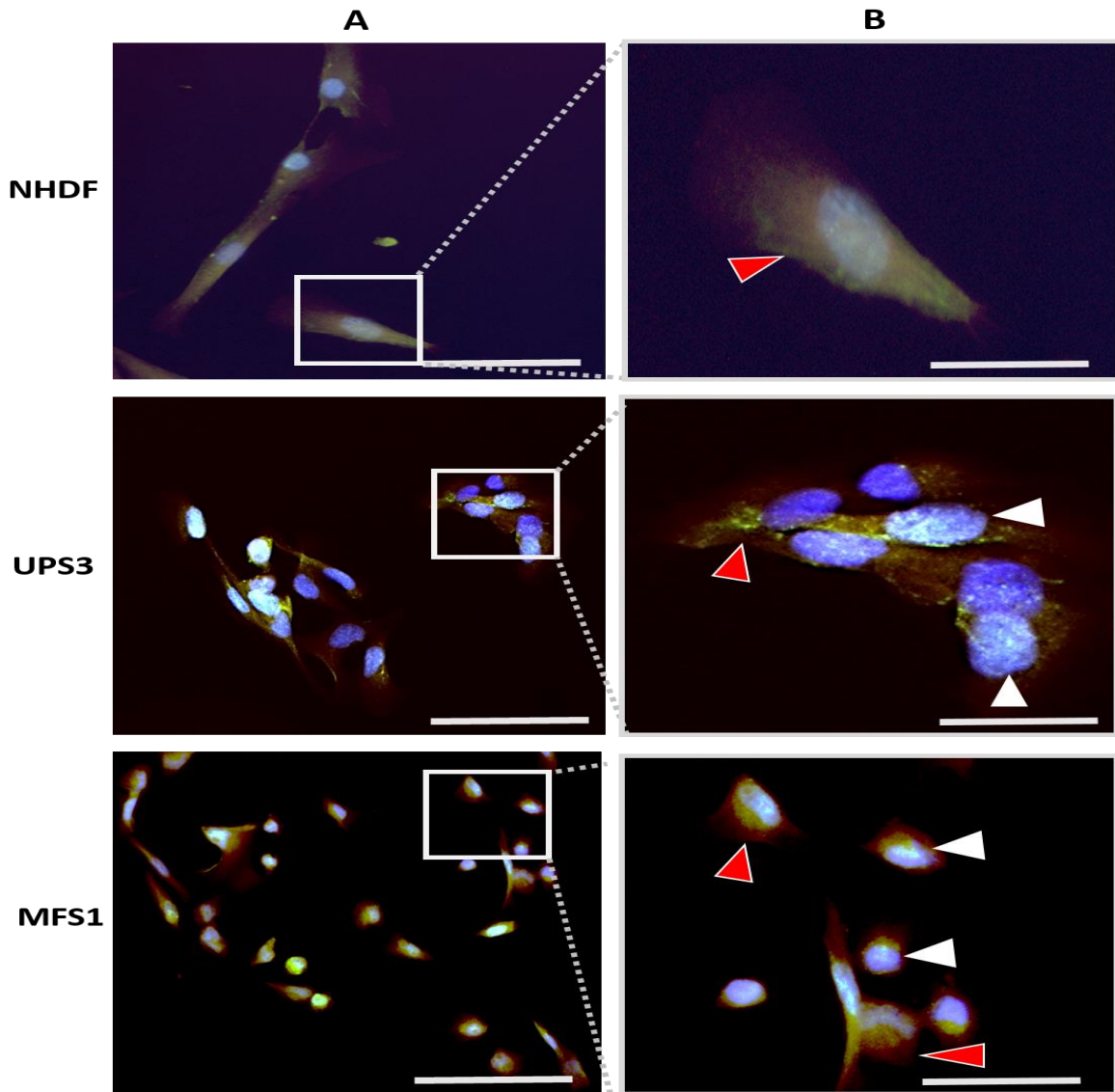
Figure 3. 21: Representative Immunocytochemistry images of SOX2.

SOX2 localised to the cytoplasm in NHDF (red arrows). In UPS3 and MFS1, it localised to the nucleus (white arrows) and to the cytoplasm (red arrow). The nuclei are stained blue with DAPI, FAPα is stained green and F-actin is stained red with phalloidin. **(A)** Scale bar is 100µm**. (B)** Scale bar is 50µm. All images were taken at 20X Magnification

		NHDF	UPS2	UPS3	UPS4	UPS1	MFS3	MFS1	MFS2	LMS	HUF	HPF	hMSC
Transgelin	Cytoplasmic	√	√	√	√	√	√	√	√	√	√	√	√
	Nucleus		√	√					√				
α SMA	Cytoplasmic	√	√	√	√	√	√	√	√	√	√	√	√
	Nucleus			√									
Vimentin	Cytoplasmic	√	√		√	√	√		√	√	√	√	√
	Nucleus			√				√					
N-cadherin	Cytoplasmic	√	√	√	√	√	√	√	√	√	√	√	√
	Nucleus								√				
Fibronectin	Cytoplasmic	√	√	√	√	√	√		√	√	√	√	√
	Nucleus							√					
FSP-1	Cytoplasmic	√	√	√	√	√	√	√	√	√	√	√	√
	Nucleus												
FAP α	Cytoplasmic	√		√	√	√			√	√	√	√	√
	Nucleus						√	√					
SOX2	Cytoplasmic	√	√	√	√	√	√	√	√	√	√	√	√
	Nucleus												

Table 3. 3: Subcellular localisation of common proteins in our cell lines.

This table showing the subcellular localisation of the common proteins tested in this project (√) indicate the cellular localisation of the certain protein in the cell line either cytoplasmic or nucleus. Each protein coloured in a different colour to make it easier for visualisation. Coloured boxes indicates if protein localised nucleus rather than cytoplasm in specific cell line.

3.6 Summary:

Early studies using light and transmission electron microscopy characterised SAFs as myofibroblast-like cells surrounding STS cells based on their histological appearance (e.g. nuclear morphology, size, shape in the connective tissue, and fibronexus presence). These findings suggested that they may share similar functions with myofibroblasts and CAFs (Lagacé et al., 1980; Weitz et al., 2003). In this project, a combination of STS cell lines recently isolated from STS tumours by Salawu *et al.* (2016) were studied along with two STS cell lines donated by collaborator Prof Dominique Heyman at the Universite de Nantes. Commercially available cell lines do not show the same level of heterogeneity as tumours, and few are available that closely match their original histotype. However, cell lines from a STS tumour itself would be the best alternative for a better understanding of cancer, and these are the type of cell line used in this project (Salawu et al., 2016). All UPS, MFS1, MFS2 and LMS cell lines resembled their original morphology described by Salawu *et al.* (2016).

STR or microsatellite analyses were used for cell authentication. UPS4 showed a partial mismatch that was concluded to be due to genomic drift.

MUG2A showed a 100% match with human Calu-6 Anaplastic Carcinoma cells, 80% match with human hTERT RPE-1 retinal epithelium cell line and 80% match of human NCI-H720 lung carcinoma cells. Therefore, it was concluded to be contaminated and was excluded from this project. The UPS2, UPS3, UPS1, MFS1, MFS2, and LMS cell lines showed the same STR profile described by Salawu *et al.* (2016), confirming their identity and excluding any misidentification. The MFS3 cell line showed a unique STR profile, excluding any contamination

Limited studies indicate a significant overlap in mesenchymal marker gene expression (e.g., vimentin, αSMA, FSP-1, FAPα) between STS cells, SAFs and other mesenchymal cell populations (Fisher, 2004; Heim-Hall & Yohe, 2008). This chapter investigated whether there are significant differences in protein levels between fibroblasts (NHDF, hMSC, HUF and HPF) and STS cells and whether these vary between histotypes. Results presented in this chapter indicate that some stromal protein levels were lower in UPS and

MFS cell lines than in LMS cell lines and primary fibroblasts. Western blot analyses were performed in all UPS and MFS cell lines and one LMS cell line using different antibodies to compare their levels of mesenchymal protein with normal human dermal fibroblasts. It also compared hMSC and two other primary fibroblasts (HUF and HPF) with NHDF and UPS cell lines. This project's results show positive vimentin, N-cadherin, fibronectin, SOX2, FSP1, and FAPα expression in all STS cell lines. Transgelin and αSMA expression tended to be lower in all UPS and MFS cell lines than in NHDF. However, LMS, HUF, and HPF cell lines showed similar transgelin and αSMA expression to NHDF.

Lower transgelin and αSMA expression was noted in the UPS and MFS cell lines, which are poorly differentiated sarcoma, than in the more differentiated STS (LMS) cell lines, whose expression was similar to NHDFs.

Transgelin plays an important role in carcinoma tumour migration, invasion, progression, and metastasis. Higher transgelin expression in carcinomas was associated with poor patient survival (Zhou et al., 2016). In this project, transgelin expression was higher in LMS cell lines and NHDF than in the less differentiated STS (UPS and MFS) cell lines.

αSMA is a widely known CAF marker. Yu *et al.* (2011) found that SAFs share some functions with CAFs since both produce high αSMA amounts in osteosarcoma. αSMA plays an important role in cancer progression and drug resistance. Higher αSMA levels correlate with poor prognosis in many carcinoma types (Ha et al., 2014). In this project, αSMA expression was higher in NHDF and LMS cell lines than in the less differentiated STS (UPS and MFS) cell lines. Could that make both Transgelin and/or αSMA potential stromal mesenchymal marker for STS?

Vimentin expression levels in all STS cell lines were very close to NHDF. In carcinoma, vimentin overexpression was associated with tumour progression (Satelli & Li, 2011). Most STS cell lines show similar N-Cadherin expression to NHDFs. However, the UPS2, UPS1, and MFS1 cell lines showed non-significantly higher N-cadherin expression than NHDF. N-cadherin is an EMT marker, and its high expression was correlated with decreased OS in STS and bone cancer patients (Niimi *et al.*, 2013).

All STS cell lines showed positive fibronectin expression levels similar to NHDF. Fibronectin is one of the potential ECM proteins secreted by CAFs. It is responsible for adhesion, proliferation, and differentiation. In carcinomas, lower fibronectin expression was associated with poor prognosis (Erdogan *et al.*, 2017).

SOX2 expression levels in all STS cell lines were similar to NHDFs. SOX2 is vital in cancer progression since it enhances proliferation, survival, stemness, invasion, and drug resistance (Zhang et al., 2020). SOX2 overexpression was associated with low survival rates in some carcinomas (Wuebben & Rizzino, 2017), and high SOX2 expression was associated with poor outcomes in sarcoma (Menendez et al., 2020; Sannino et al., 2019). FSP-1 expression levels in all STS cell lines were similar to NHDFs. FSP1 has been used as a CAF marker in many carcinoma studies. It plays a dual role in cancer since it can regulate invasion and metastasis via VEGFA and tenascin-C secretion and enhance the anti-tumour immune response by activating CD8^{+} T cells (Han et al., 2020). Higher FSP-1 expression in carcinoma has been associated with low survival rates (Ha et al., 2014). FAPα expression levels in all STS cell lines were similar to NHDFs. FAPα is a known CAF marker. It facilitates cancer progression through ECM remodelling (Han et al., 2020). Elevated FAPα levels are associated with poorer survival in many carcinomas (Ha et al., 2014).

This result addressed our aim that since both STS and SAF share a common origin, few selective makers can be used to distinguish them, with the possible exception of transgelin and αSMA. Consequently, transgelin and αSMA could be selective UPS and MFS markers to distinguish them from normal mesenchymal cells in the STS stroma.

Lower transgelin and αSMA expression in STS cell lines might affect cell contractility. Zeidan *et al.* (2004) found that while transgelin knockout mice were fertile and developed normally, they had reduced contractility in their arteries and veins due to changes in actin filaments structure. Another transgelin knockout mouse study showed similar normal mice viability and reduced contractility (Zhang et al., 2001). αSMA was considered a myofibroblast differentiation marker. Higher αSMA expression was associated with higher contractility (Hinz et al., 2001).

ICC was used to visualise the proteins in STS and fibroblast cells at the cellular level. It confirmed that transgelin, αSMA, vimentin, N-cadherin, fibronectin, FSP1, FAPα, and SOX2 were positively expressed in all STS and fibroblasts cell lines and mainly localised to the cytoplasm with some exceptions where it was either diffused or to the nucleus. Transgelin localised to the cytoplasm in most cell lines. However, it localised to both the cytoplasm and nucleus in UPS2 and MFS2 cells and was more diffuse in UPS3 cells. αSMA localised to the cytoplasm in all cell lines, except in UPS3 where it was instead diffused. Vimentin was localised to the cytoplasm in most cell lines, except UPS3 and MFS1, where it was diffused and in the nucleus. Several studies reported that vimentin was localised to the nucleus in glioblastoma multiforme (Wang et al., 2010), neuroblastoma (Mergui et al., 2010) and Gastric cancer (Zhao et al., 2013). N-cadherin was localised to the cytoplasm in most cell lines but was found in the nucleus in the MFS2 cell line. Nuclear N-cadherin was associated with poor OS in nasopharyngeal carcinoma patients (Luo et al., 2012). Fibronectin localised to the cytoplasm in all cell lines, but was also found in the nucleus in MFS1 cell line. FSP-1 localised to the cytoplasm in all cell lines but was also diffuse in MFS1 cells. FAPα localised to the cytoplasm of most cell lines but was diffuse in UPS3 and MFS1 cells and was in the nucleus in MFS3 and MFS1 cells. SOX2 localised to the cytoplasm in most cell lines but was also diffuse in UPS3 and MFS2cells. SOX2 diffuse staining pattern was strongly correlate with OSCC lymph node metastasis (Michifuri et al., 2012).

Colocalisation coefficients of all eight proteins with F-actin indicated relatively similar localisations.

In this chapter, eight common mesenchymal proteins were characterised and compared between STS and fibroblasts using cell lines western blots and ICC methods. The results support the possibility of transgelin as a potential SAF marker. To further study its potential, UPS cell lines were grown in mice as xenografts to identify the stromal expression of mouse mesenchymal gene by aligning RNAseq reads against the human and mouse reference genomes as previously described (Bradford *et al.*, 2013).

Chapter 4

Tumour growth and charactrisation of patient derived UPS cell lines in NSG mice.

4.1 Introduction

Xenografts have been widely used in translational cancer research. Xenografting is the process of growing one species's cells in another species, such as grafting human patient cells into immunodeficient mice to obtain a tumour microenvironment model (J. Shi et al., 2020). The advantage of xenografts over cell culturing is that they retain the tumour's heterogeneity, genetic and histological characteristics, and original phenotype (J. Shi et al., 2020). This project used xenografts from patient-derived cell lines. Xenografts were generated by injecting three undifferentiated pleomorphic sarcoma (UPS) cell lines into mice. Initial, limited characterisation by Drs English and Salawu showed they were more likely to form tumours than myxofibrosarcoma cell lines, provided they were injected into highly immunocompromised mouse strains.

Formalin fixed and paraffin embedded (FFPE) sections were analysed using immunohistochemistry (IHC) to characterise the UPS tumours. IHC is an immunostaining method widely used in tumour diagnosis and pathology (Painter et al., 2010). IHC has been used to identify tumour cells, study tumour morphology, and compare it with the original tumour histology. IHC is a semi-quantitative method used to quantify protein expression in xenograft tissues. IHC was used to characterise the tumour microenvironment based on necrosis and mean vascular density (MVD) scores of FFPE sections stained with haematoxylin and eosin (H&E) and antibodies against platelet and endothelial cell adhesion molecule 1 (PECAM1/CD31). IHC was also used to characterise the protein expressions characterised by western blots in chapter 3, including transgelin, αSMA, vimentin, N-cadherin, fibronectin, FSP-1, FAPα and SOX2.

Indirect immunofluorescence (IF) methods were used to quantify and visualise proteins in our xenografts. IF uses a fluorescence labelled antibody to identify and locate the protein of interest in the tissue (Betterle & Zanchetta, 2012). Indirect IF was used to quantify and locate common proteins of interest (vimentin, N-cadherin, fibronectin and SOX2).Double IF was used to detect transgelin and the human mitochondrial antibody (MT-AB) to attempt to distinguish human cancer and mouse stroma cells. Similarly, αSMA was co-stained with CD31 to identify and quantify pericytes associated blood vessels in

the xenografts, a vascular function indicator. Moreover, FSP-1 and FAPα were co-stained with F4/80 antigen, a macrophage marker, to distinguish these cells from mesenchymal cells. The four most representative tumours were selected for next-generation RNA sequencing (RNAseq) according to the following criteria: closest to the mean tumour volume, necrosis, and MVD and high Nanodrop- and Bioanalyser-based RNA quality. This chapter addresses our aim to grow UPS cell lines as xenografts and to characterise them before choosing the most representative tumours for RNAseq.

4.1.1 Aim

To grow STS cell lines as xenografts in mice to allow identification of stromal gene expression of mouse transcripts by aligning RNAseq reads against the human and mouse reference genomes.

4.1.2 Experimental approach and statistical analysis

- Four UPS cell lines were injected subcutaneously into NSG mice (each cell lines were injected into six NSG mice), only three cell lines made tumours.
- Sixteen tumour sections were removed and were cut into half, one half was frozen and the other half was fixed with paraffin.
- RNA quality was checked in the tumour sections and only 12 sections were chosen (four sections from each cell line) for RNA-seq analysis.
- The eight common mesenchymal proteins that was characterised in STS cell lines in chapter 3 were used to try to compare their expression between UPS cell lines and the stroma using Immunohistochemistry (IHC)and immunofluorescence (IF) methods.

4.2 Selection of UPS tumours for RNAseq analysis

4.2.1 Growth of UPS cell lines in NSG mice

Four UPS cell lines (5×10^6 cells) were injected subcutaneously by Dr English into six male (8–10 week-old) highly immunodeficient NOD SCID gamma (NSG) mice in a 1:1 phosphate-buffered saline to Matrigel solution since pilot studies showed this improved tumour uptake consistency. Tumours were removed when they reached 600–800 mm^3. Half of the tumour was frozen in optimal cutting temperature compound and stored at −80°C, while the other half was FFPE. UPS4 tumours were removed after 70 days, UPS2 tumours after ~100 days, and UPS3 tumours after >100 days. UPS1 cells did not form tumours (Fig. 4.1). Sixteen tumours were resected: six UPS2, four UPS3, and six UPS4.

Figure 4. 1: UPS subcutaneous growth curve.

The curve shows the growth of the three UPS cell lines in NSG mice. X- axis is the day post injection. STS13/12 was the most consistnent tumour to start growing after 35 days, STS06/11 started to grow 50 days post injection, while STS09/11 started to grow much slower after 70 days and UPS1 didn't grow. UPS2 is STS06/11,UPS3 is STS09/11, UPS4 is STS13/12 and UPS1 is STS14/10.

4.3 Characterisation of the tumour microenvironment through immunohistochemical and immunofluorescence staining

4.3.1 Necrosis scoring by Haematoxylin and Eosin (H&E) staining

Necrosis is a post-inflammatory form of cell death characterised by organelle swelling in the cytoplasm and mitochondria, nuclei rupture, and plasma membrane breakdown (Festjens et al., 2006). Necrosis levels were quantified by cutting three FFPE tumour sections and staining them with H&E. H&E is a valuable staining method used to observe tissue histology. H&E staining is a combination of two dyes: haematoxylin (a natural basic dye extracted from the logwood tree), which stains basophilic structures such as the nucleus and rough endoplasmic reticulum in a purplish blue colour, and eosin (an acidic dye), which stains eosinophilic structures such as the extracellular matrix and cytoplasm a bright pink colour (Painter et al., 2010). Necrosis scoring was performed as described in Section 2.8.1. UPS3 had higher necrosis scores (mean = 38.5%), followed by UPS4 (mean = 34.7%), and UPS2 (mean = 28.9%). A statistical analysis was performed according to Section 2.9 (Fig. 4.2).

UPS2

UPS3

UPS4

Necrosis
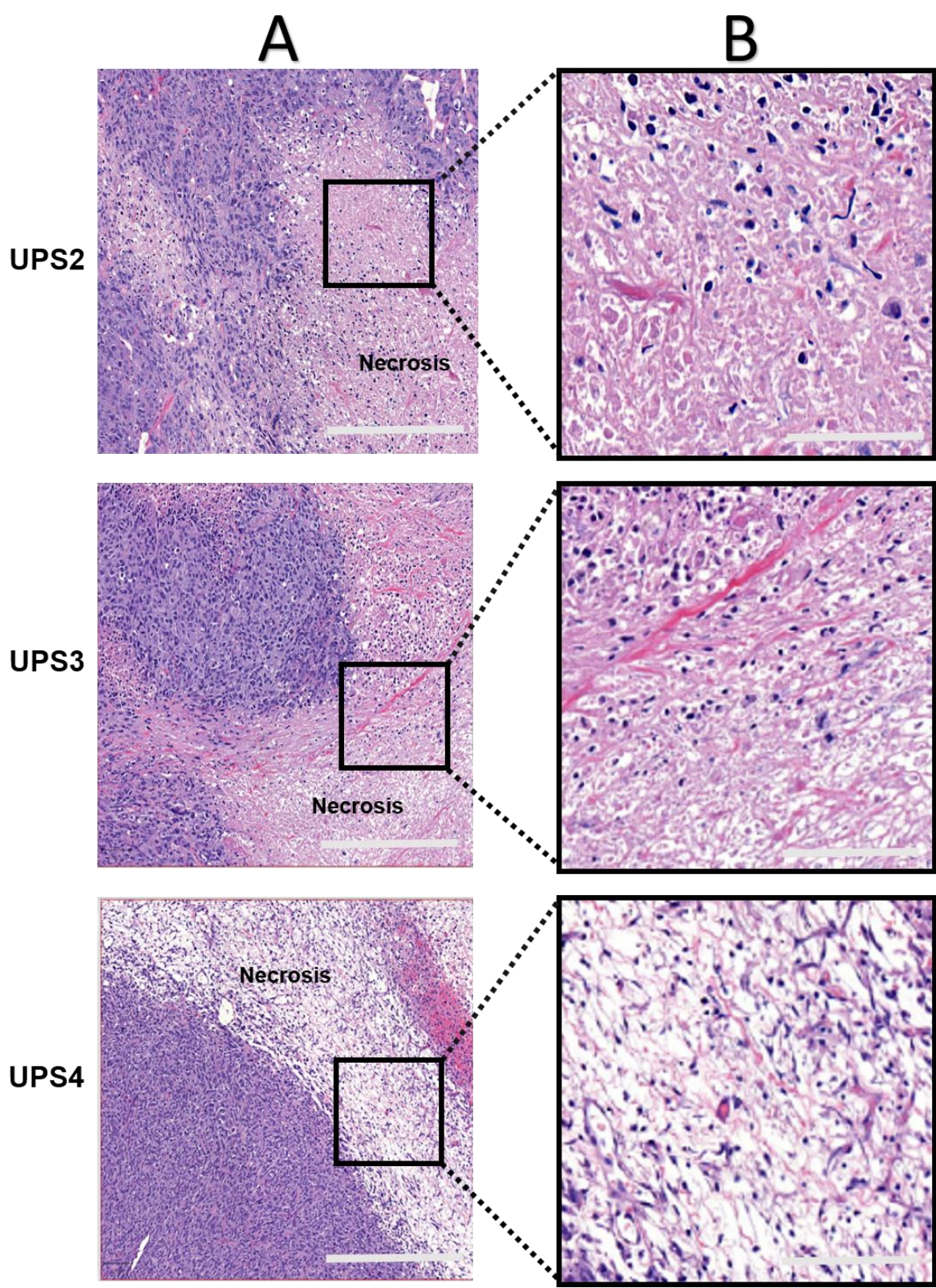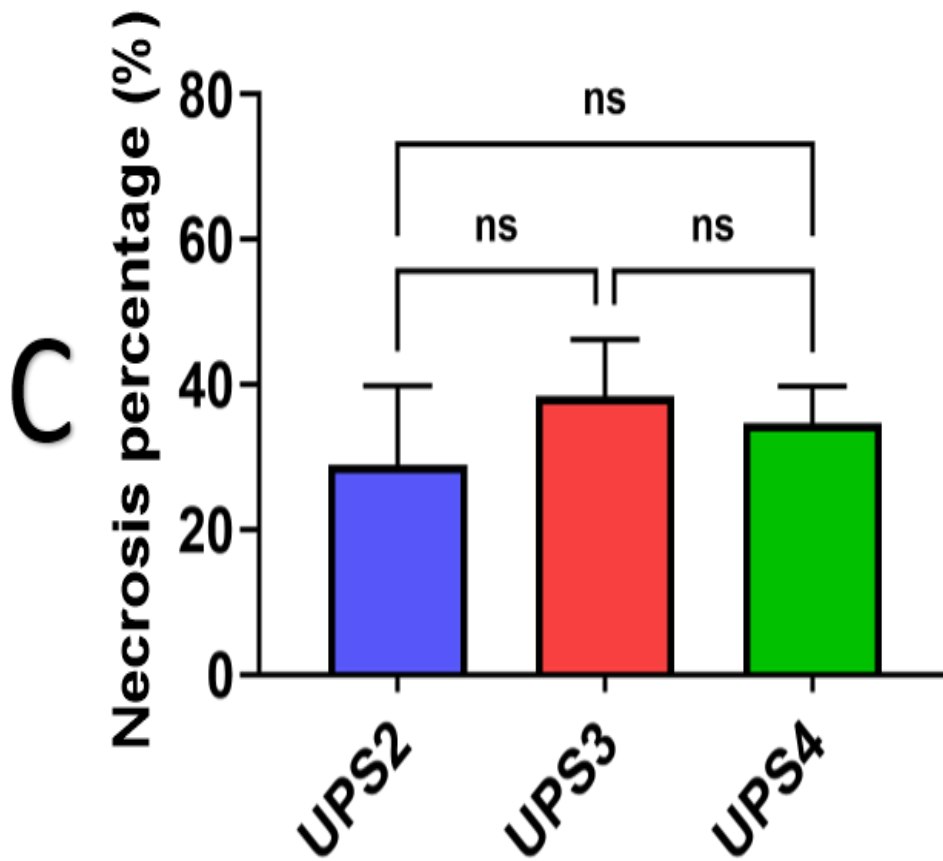
Necrosis

Necrosis

Figure 4. 2: Necrosis in H&E stained xenografts.

(A) H&E stained xenografts at 20X magnification (scale bar = 100 μm). (B) Magnified images (scale bar = 50 μm). (C) Bar chart of mean necrosis scores in xenografts. Key: *, $P < 0.05$; **, $P < 0.01$; ***, $P < 0.001$; ns, not significant. Error bars denote ± standard error of the mean (SEM).

4.3.2 Quantification of mean vascular density (MVD) after staining for CD31

Angiogenesis, or neovascularisation, is the formation of new blood vessels to supply the tumour with oxygen and nutrients, leading to tumour progression and metastases (Lugano et al., 2020). We measured MVD to assess the tumour vascularisation level of our xenografts (Sie et al., 2010).

MVD was quantified after IHC staining for CD31. Platelet endothelial cell adhesion molecule-1 (PECAM-1) or CD31 is an endothelial marker used to quantify vascularisation (Lugano et al, 2020). It is an integral membrane protein expressed on the endothelial cell's surface and is crucial for cell-cell adhesion, cell migration, and angiogenesis (Wang et al., 2008).

A semi-quantitative analysis was performed on CD31-stained tumours, calculating the number of CD31-positive vessels per square millimetre (Section 2.7.1). All three xenograft tissues showed a uniform vasculature distribution, with some collapsed vessels and open lumen vessels characteristic of tumours vessels (Fig. 4.3A-B). Analysis showed that the MVD did not differ significantly among the three xenograft tissues (Fig.4.3D). Negative control was done without the primary antibody (Fig. 4.3C).

UPS2

UPS3

UPS4

NC

C

D
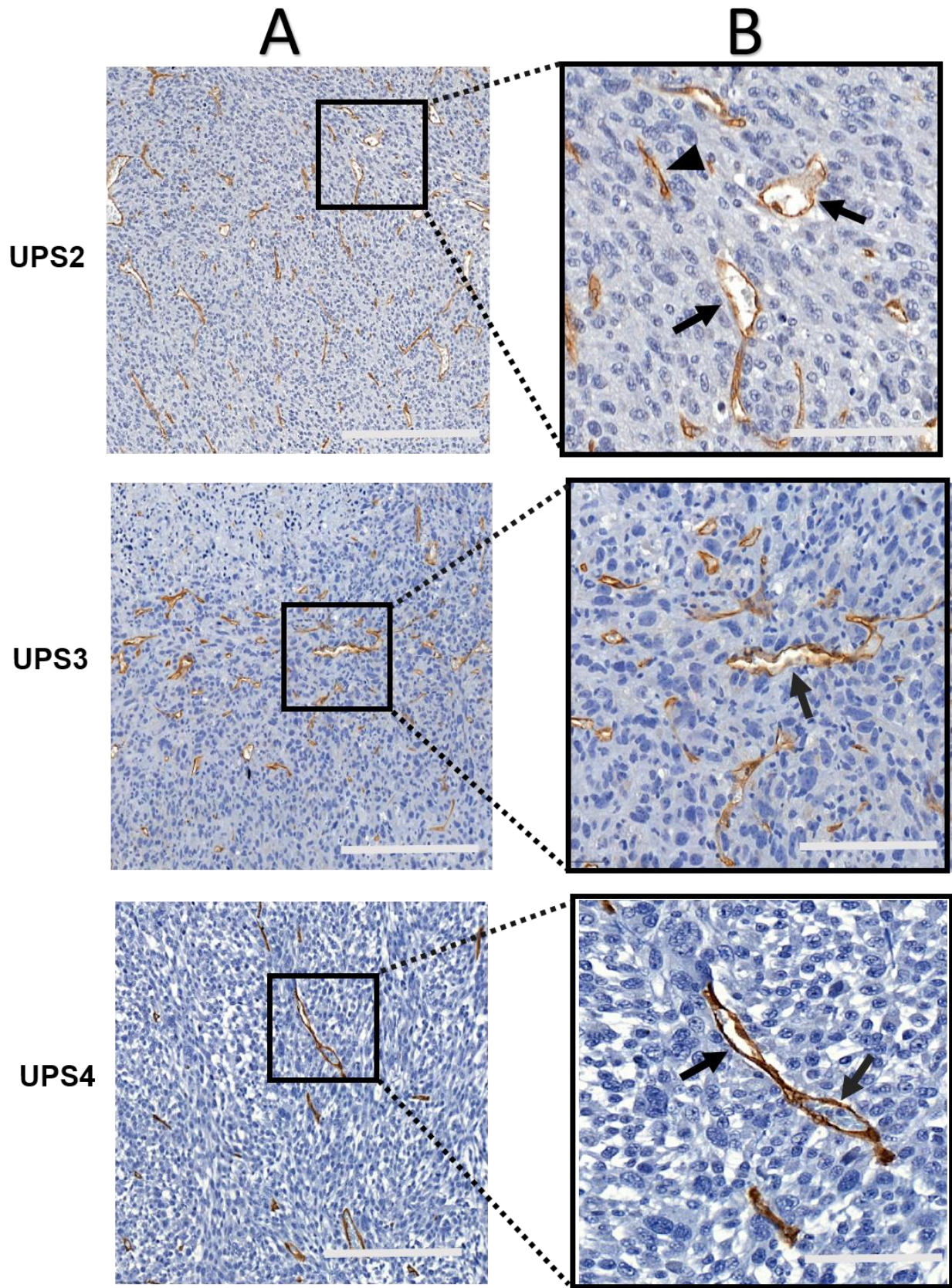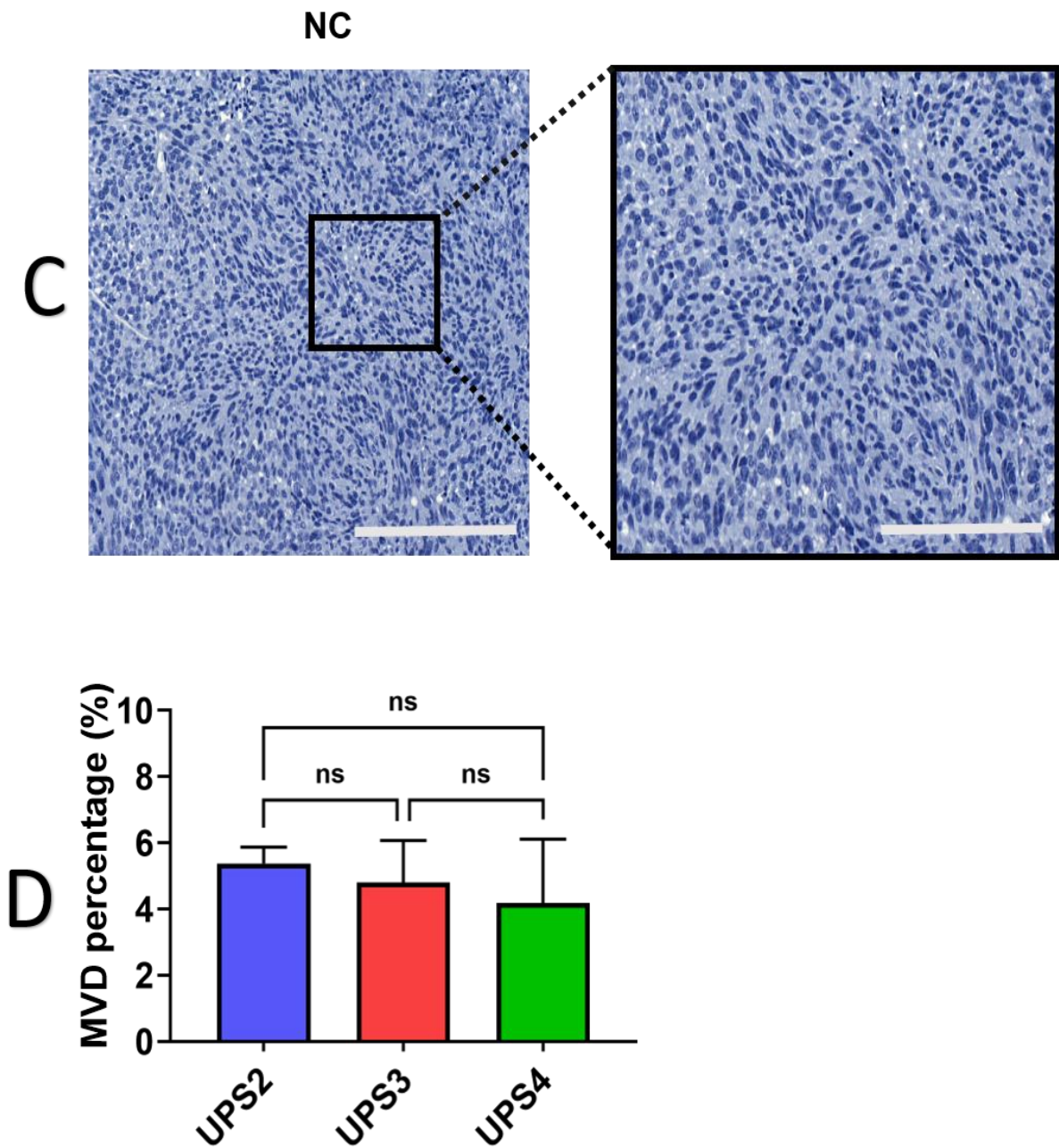
Figure 4. 3: IHC CD31 staining-based microvascular density.

(A) CD31 stained xenografts at 20× magnification (scale bar = 100 μm). (B) Magnified images (scale bar = 50 μm). (C) Negative control for CD31. (D) Bar chart of MVD percentages in xenografts. Arrows show open lumen vessels. Key: *, $P < 0.05$; **, $P < 0.01$; ***, $P < 0.001$; ns, not significant. Error bars denote ± SEM.

4.3.3 Quantification of the expression of mesenchymal genes in xenografts by IHC and IF

Transgelin, αSMA, vimentin, N-cadherin, fibronectin, FSP-1, FAP α and SOX2, previously characterised by western blot and immunocytochemistry (ICC) in cultured cells in Chapter 3, were examined and quantified in xenografts by IHC of FFPE tissues and IF of frozen tissues.

4.3.3.1 Transgelin

Transgelin is a calponin family actin-binding protein and a specific marker for smooth muscle differentiation (Tawfik et al., 2014). It plays a crucial role in cell migration and contractile functions. Xenograft sections were stained with an anti-transgelin antibody (Sections 2.7 and 2.8). Positive transgelin staining was defined as dark brown cytoplasmic staining. The cellular staining pattern did not differ among the three xenograft sections (Fig. 4.4A-B). Transgelin staining intensity was evaluated using the Qupath software. Transgelin intensity (%) means the percentage of transgelin positively stained cells in region of interest (in this case the whole tumour section. Quantification of staining of transgelin using IHC showed no significant differences in expression among the three xenografts (Fig.4.4D). The negative control was processed without adding the primary antibody (Fig. 4.4C). Xenograft sections were also stained for transgelin using IF method. All xenograft sections showed positive green cytoplasmic staining. Fluorescence intensity was measured using ImageJ software and calculated using corrected total cell fluorescence (CTCF) according to Section 2.6.1. Statistical analysis showed that transgelin levels did not differ significantly among the three xenografts (Fig.4.5).
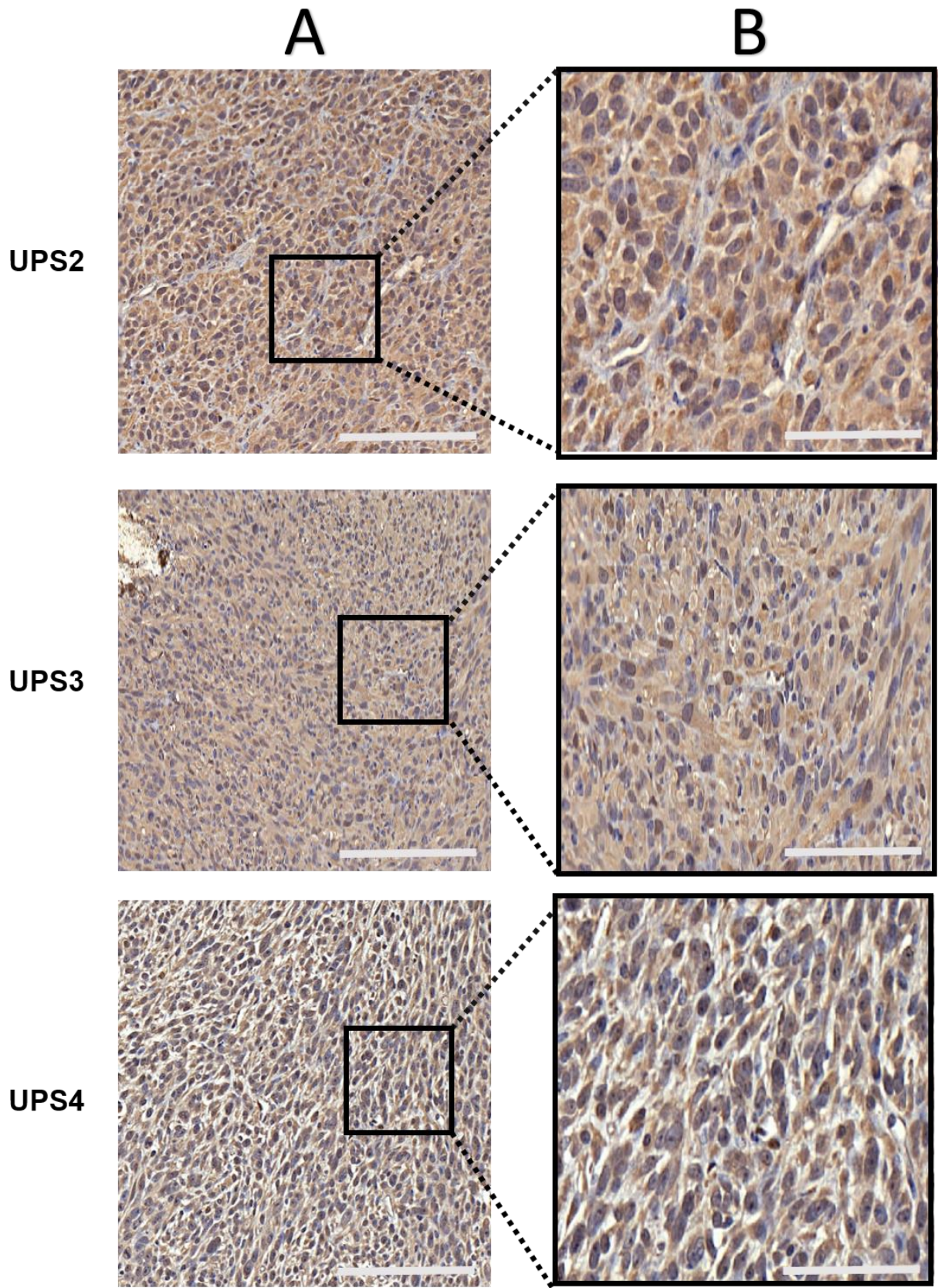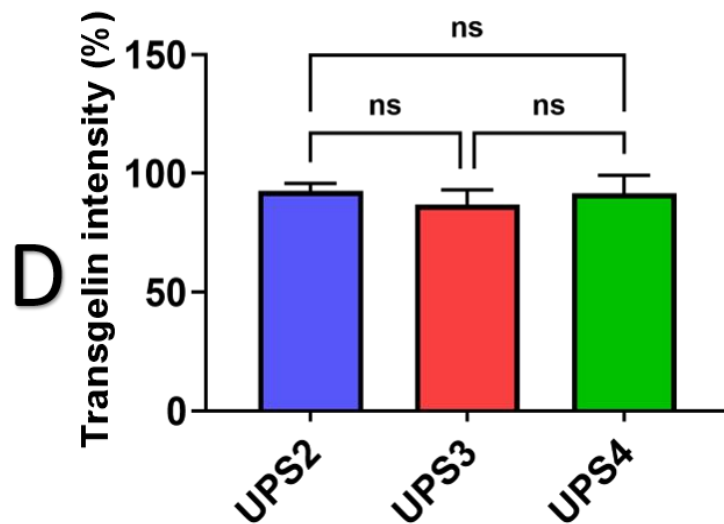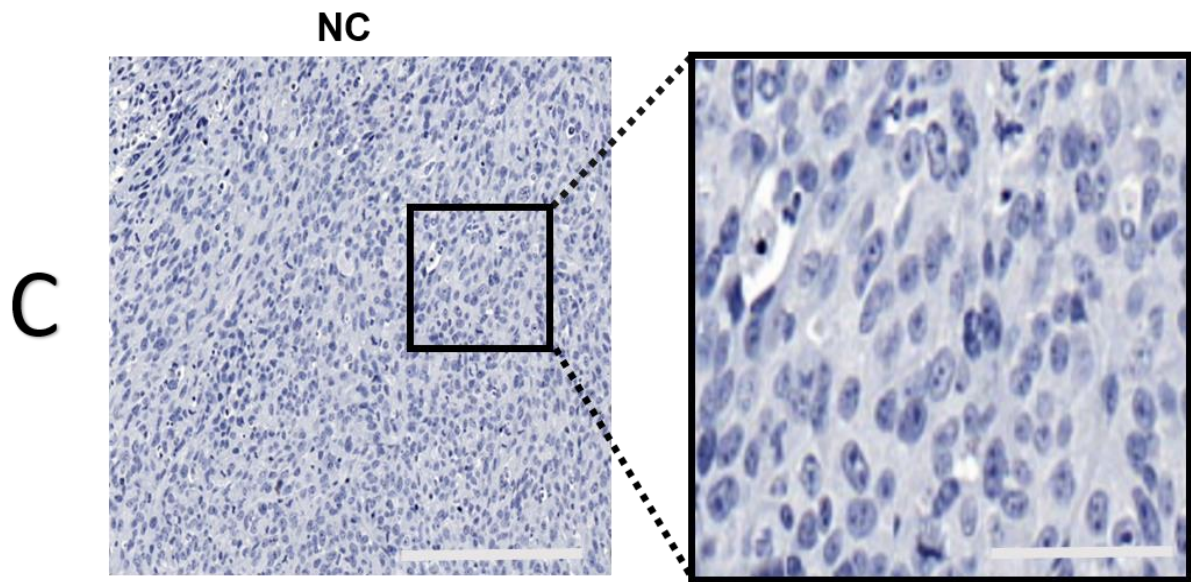
Figure 4. 4: IHC staining for transgelin in xenografts.

(A) Transgelin-stained xenografts at 20X magnification (scale bar = 100 μm). The nuclei are stained blue with haematoxylin, and transgelin is stained brown. (B) Magnified images for respective xenografts (scale bar = 20 μm). (C) Negative control for transgelin. (D) Bar chart of transgelin intensity in xenografts. Key: *, $P < 0.05$; **, $P < 0.01$; ***, $P < 0.001$; ns, not significant. Error bars denote ± SEM.

Merged+DAPI	**Transgelin**
UPS2	
UPS3	
UPS4	

Merged+DAPI

DAPI

NC
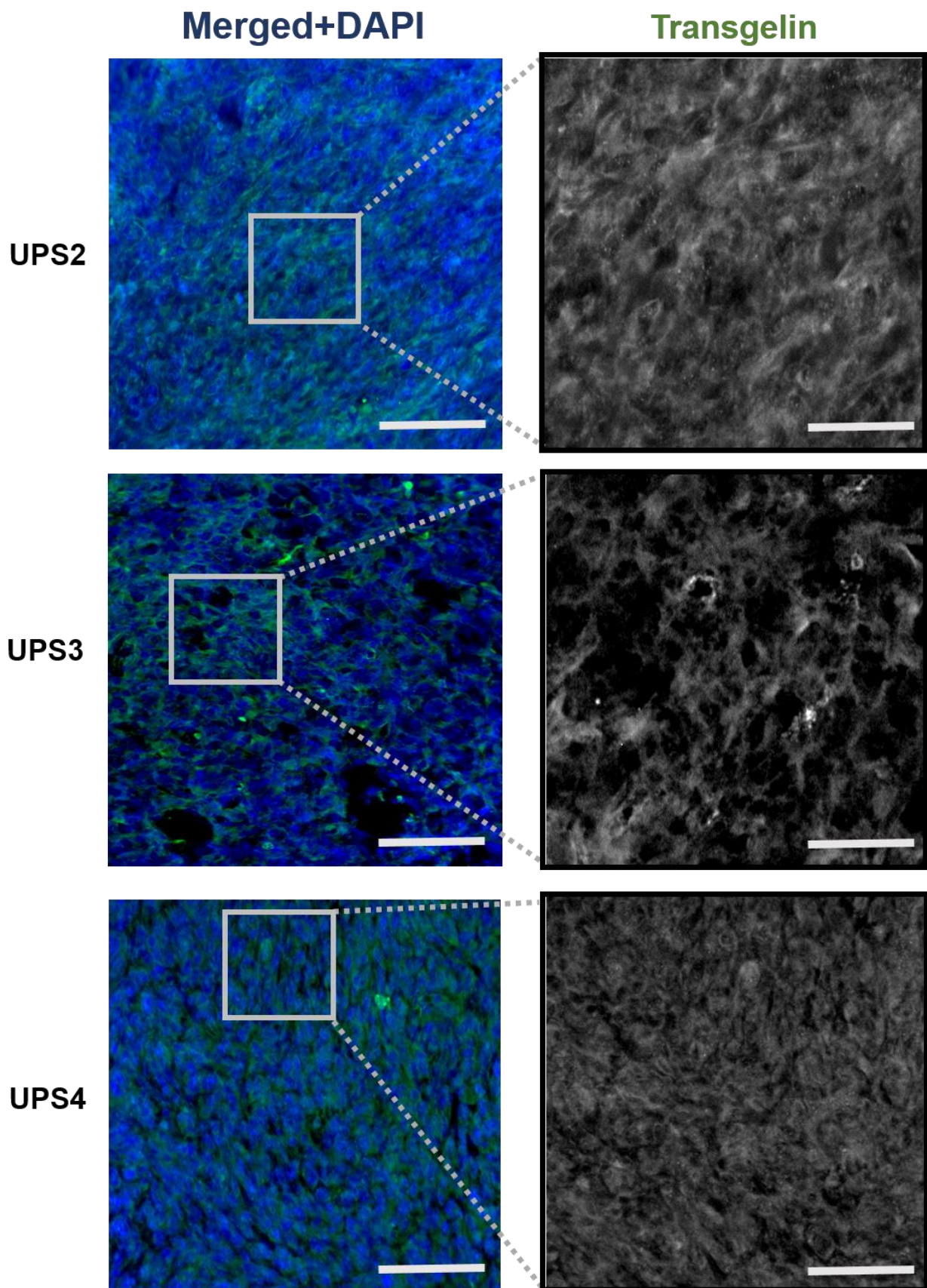
Transgelin

Figure 4. 5: IF staining for transgelin in xenografts.

Transgelin-stained xenografts at 20X magnification (scale bar = 100 μm) and magnified images (scale bar = 20 μm). The nuclei are stained blue with DAPI, and transgelin is stained green. NC= Negative control for transgelin. Bar chart of transgelin CTCF in xenografts. Key: *, $P < 0.05$; **, $P < 0.01$; ***, $P < 0.001$; ns, not significant. Error bars denote ± SEM.

4.3.3.2 αSMA

αSMA is an actin isoform that plays an important role in fibrogenesis. It is an intracellular protein located in actin filaments and microtubules. It is also frequently used as a marker for cancer-associated fibroblasts (CAFs) but is also found in myofibroblasts and smooth muscle cells. Positive αSMA staining appear as a dark brown cytoplasmic staining in IHC, which was positive in all xenograft sections and showed no difference in cellular staining patterns (Fig. 4.6A&B). αSMA staining intensity was evaluated using the Qupath software.αSMA intensity (%) means the percentage of transgelin positively stained cells in region of interest (in this case the whole tumour section. Quantification of staining of αSMA using IHC showed no significant differences in expression among the three xenografts (Fig.4.6D). The negative control was processed without adding the primary antibody (Fig.4.6C). Xenograft sections were also stained for αSMA using an IF method. All xenograft sections showed positive green cytoplasmic staining, with more intense staining in UPS3 reminiscent of vascular staining, possibly indicating pericytes. Fluorescence intensity was measured using the ImageJ software and calculated using as CTCF according to Section 2.6.1. Statistical analysis showed αSMA levels did not differ significantly among the three xenografts (Fig. 4.7).

NC
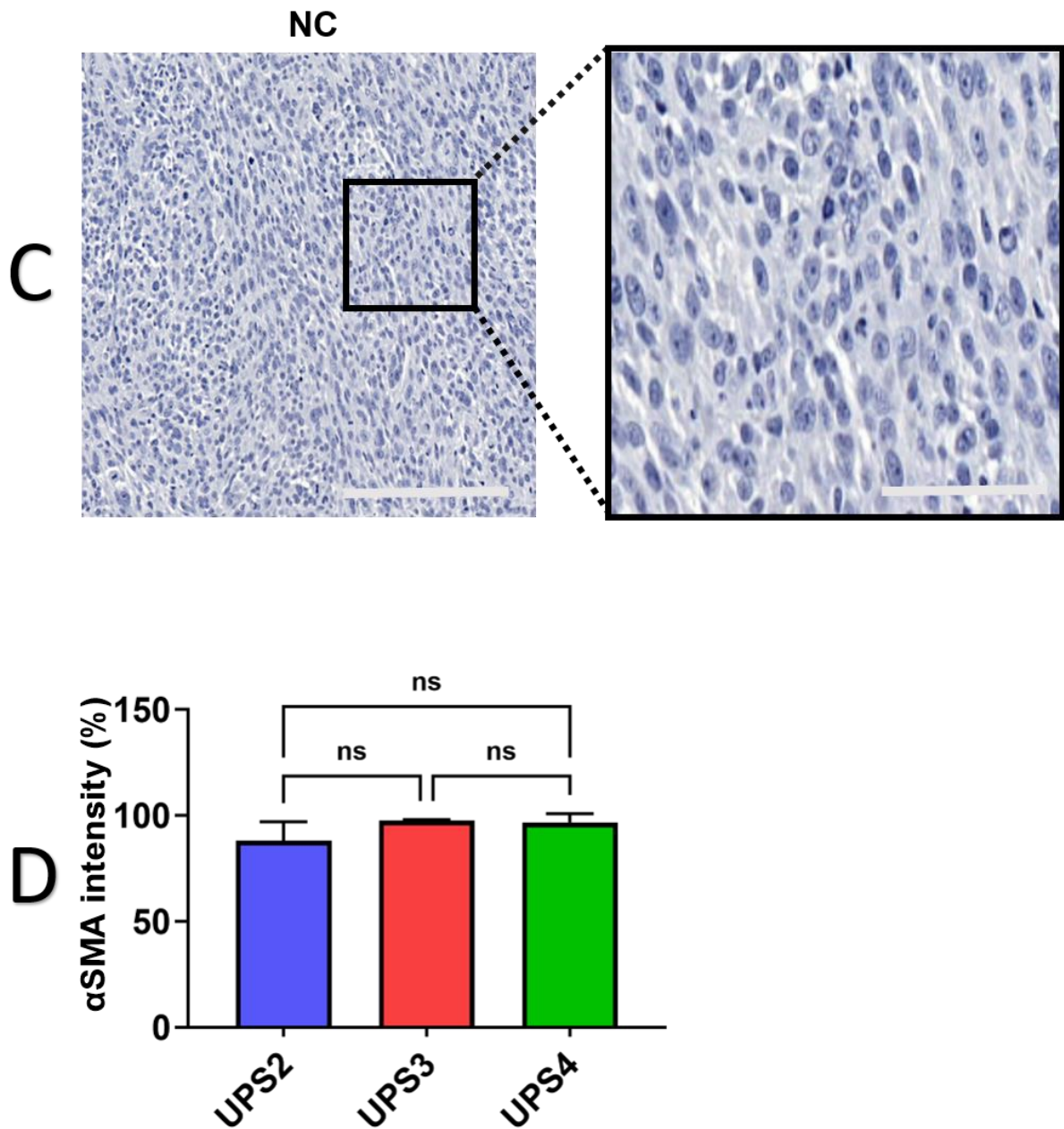
Figure 4. 6: IHC staining for αSMA in xenografts.

(A) αSMA-stained xenografts at 20X magnification (scale bar = 100 μm). The nuclei are stained blue with haematoxylin and αSMA is stained brown. (B) Magnified images for respective xenografts. (scale bar =20μm). (C) Negative control for αSMA. (D) Bar chart for αSMA intensity in xenografts. Key: *, $P < 0.05$; **, $P < 0.01$; ***, $P < 0.001$; ns, not significant. Error bars denote ± SEM.

	Merged+DAPI	**αSMA**
UPS2		
UPS3		
UPS4		
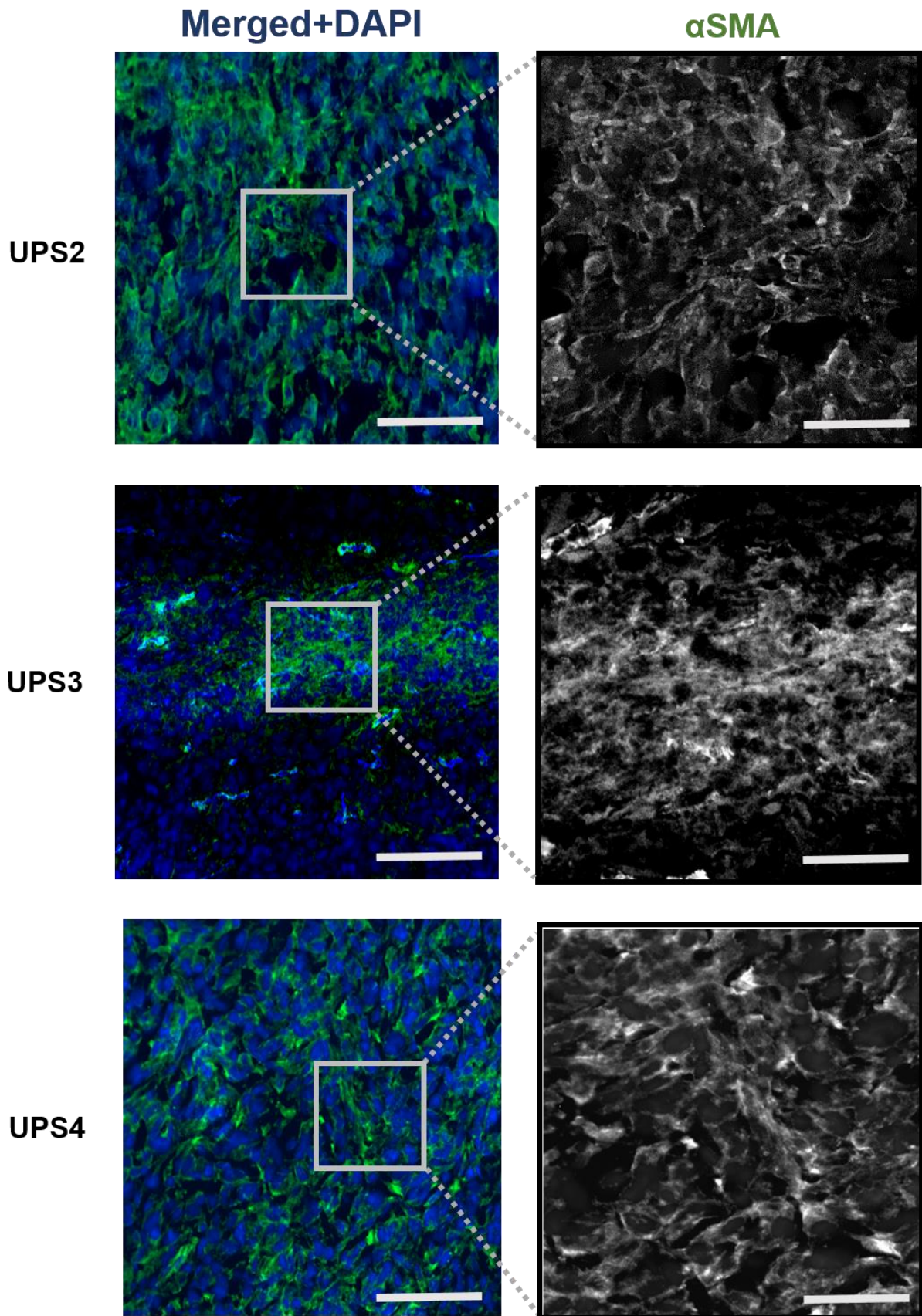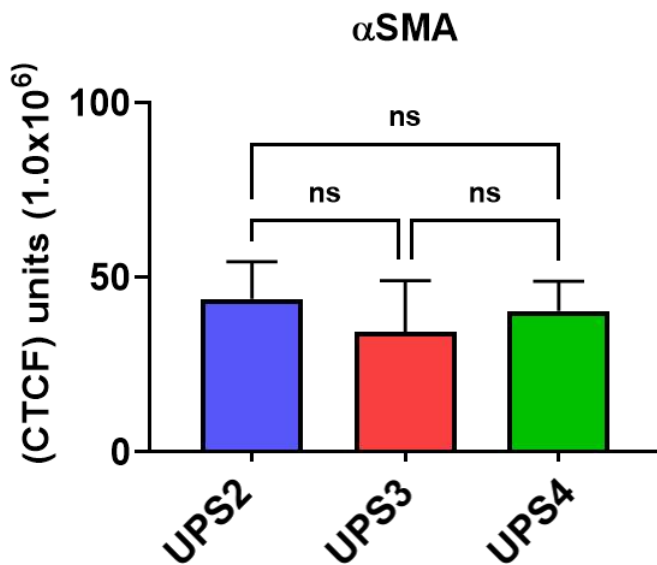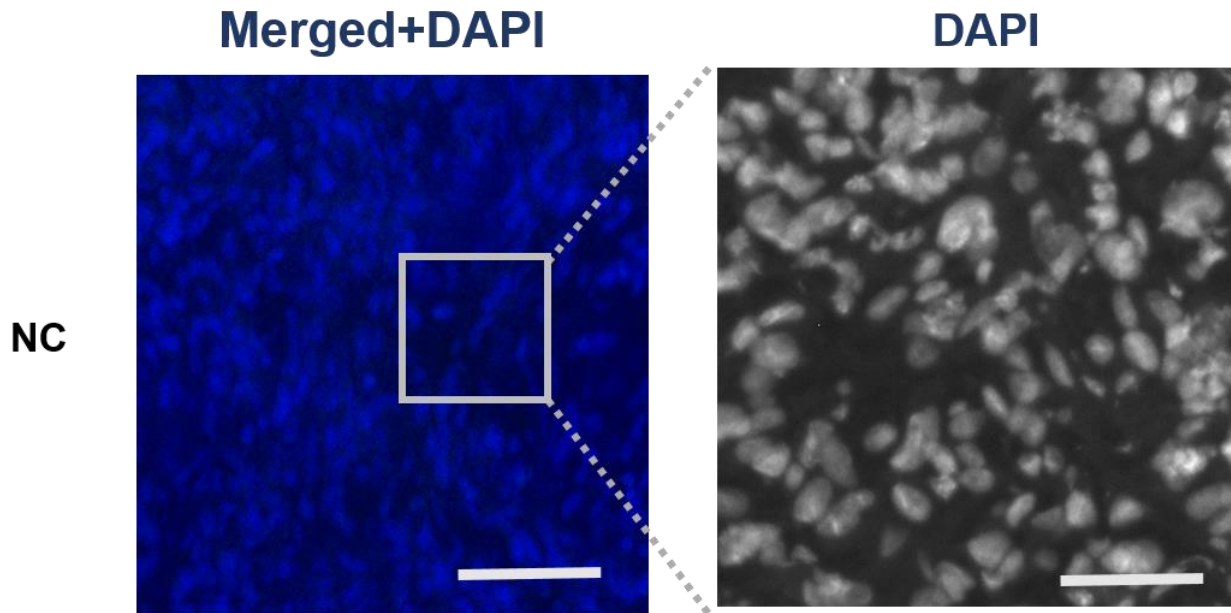
Figure 4. 7: IF staining for αSMA in xenografts.

αSMA-stained xenografts at 20X magnification (scale bar=100 μm) and magnified images (scale bar = 20 μm).. The nuclei are stained blue with DAPI and αSMA is stained green. The nuclei are Negative control for αSMA. Barchart of αSMA CTCF in xenografts. Key: *, $P < 0.05$; **, $P < 0.01$; ***, $P < 0.001$; ns, not significant. Error bars denote ± SEM.

4.3.3.3 Vimentin

Vimentin is an intermediate filaments protein. It is one of the most common mesenchymal proteins that maintain cell growth, adhesion, and migration. It is an intracellular protein located in intermediate filaments. Vimentin has been associated with various diseases, such as cataracts (Matsuyama et al., 2013). Vimentin is also an EMT marker, emphasising its role in tumour progression and metastasis (Ivaska et al., 2007). Positive vimentin staining identified as a dark brown cytoplasmic staining, in all xenograft sections in which had similar cellular staining patterns (Fig. 4.8A&B). Vimentin intensity was evaluated using Qupath software. Vimentin intensity (%) means the percentage of transgelin positively stained cells in region of interest (in this case the whole tumour section. Quantification of staining of vimentin using IHC showed no significant differences in expression among the three xenografts (Fig.4.8D). The negative control was processed without adding the primary antibody (Fig.4.8C). Xenograft sections were also stained for vimentin using an IF method. All xenograft sections showed positive green cytoplasmic staining. Fluorescence intensity was measured using ImageJ software and calculated as CTCF according to Section 2.6.1. Statistical analysis showed that vimentin levels did not differ significantly between UPS1 and UPS2 cells. However, IF staining showed higher vimentin levels in UPS3 cells than UPS2 cells (Fig. 4.9). Vimentin staining confirms the mesenchymal origin of our UPS tumours (Thway et al., 2011).

NC

C

D
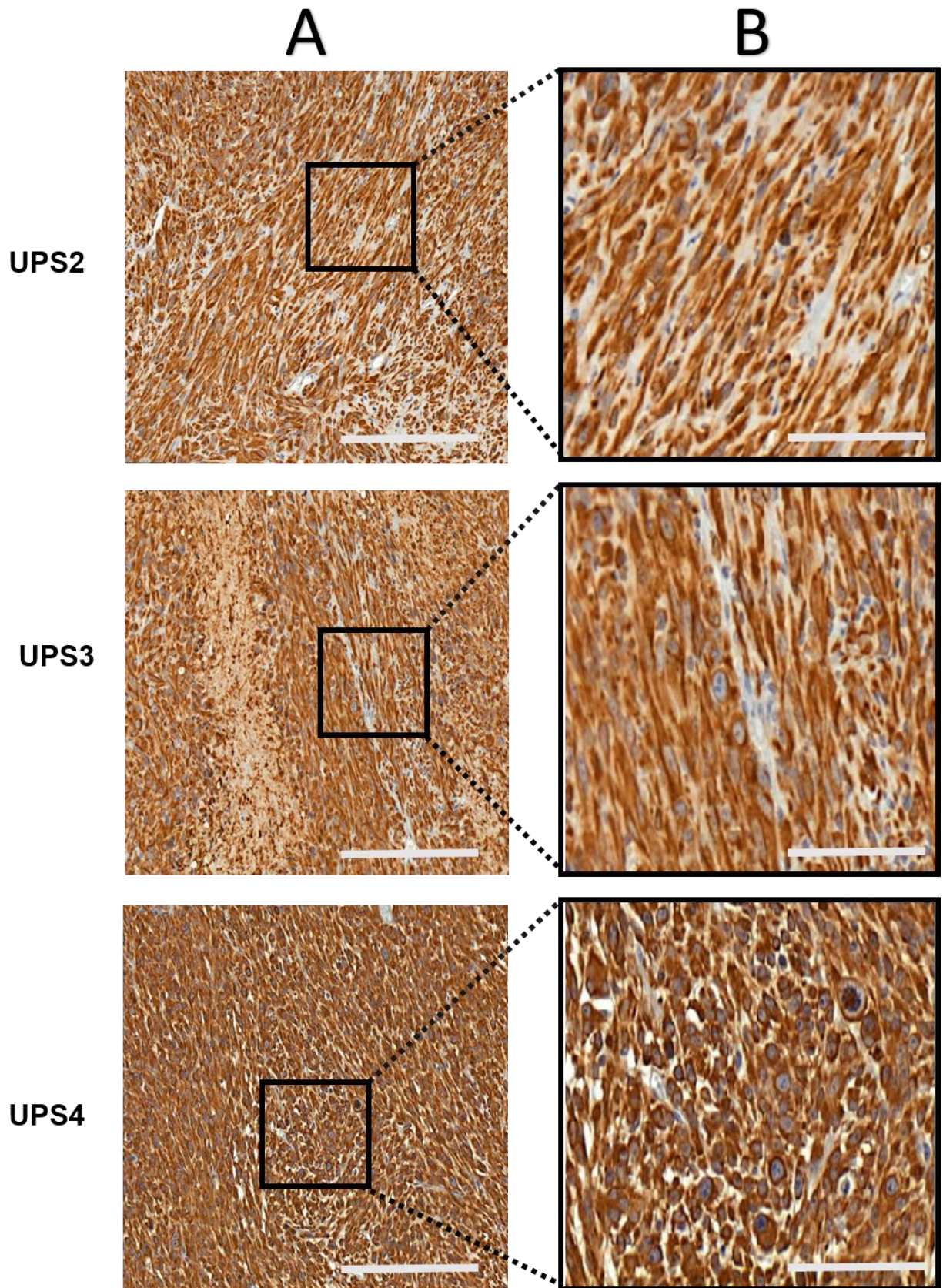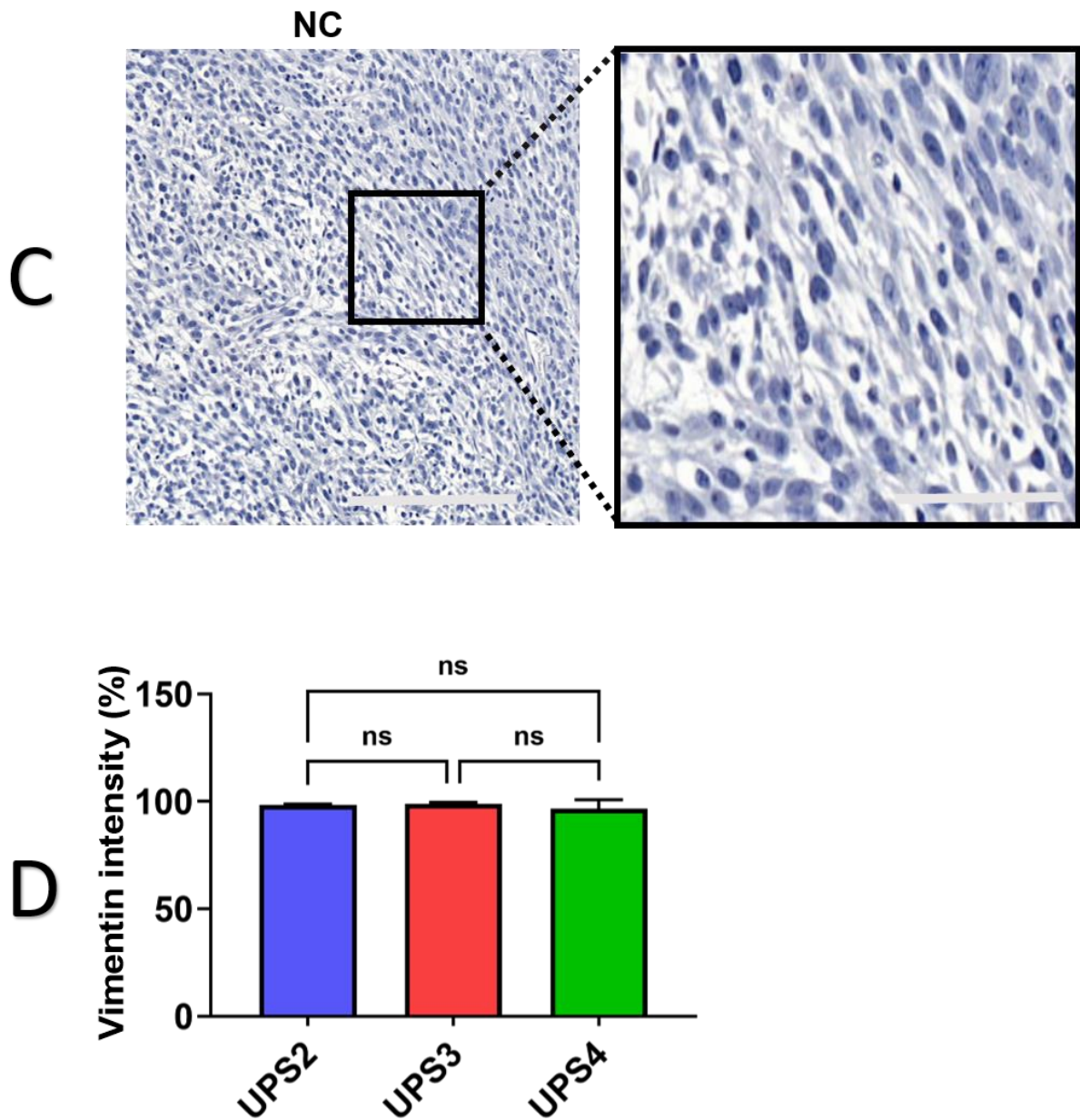
Figure 4. 8: IHC staining for vimentin in xenografts.

(A) Vimentin-stained xenografts at 20X magnification (scale bar = 100 µm). The nuclei are stained blue with haematoxylin and vimentin is stained brown. (B) Magnified images for respective xenografts (scale bar =20µm). (C) Negative control for vimentin. (D) Bar chart for vimentin intensity in xenografts. Key: *, $P < 0.05$; **, $P < 0.01$; ***, $P < 0.001$; ns, not significant. Error bars denote ± SEM.

Merged+DAPI   **Vimentin**

UPS2

UPS3

UPS4
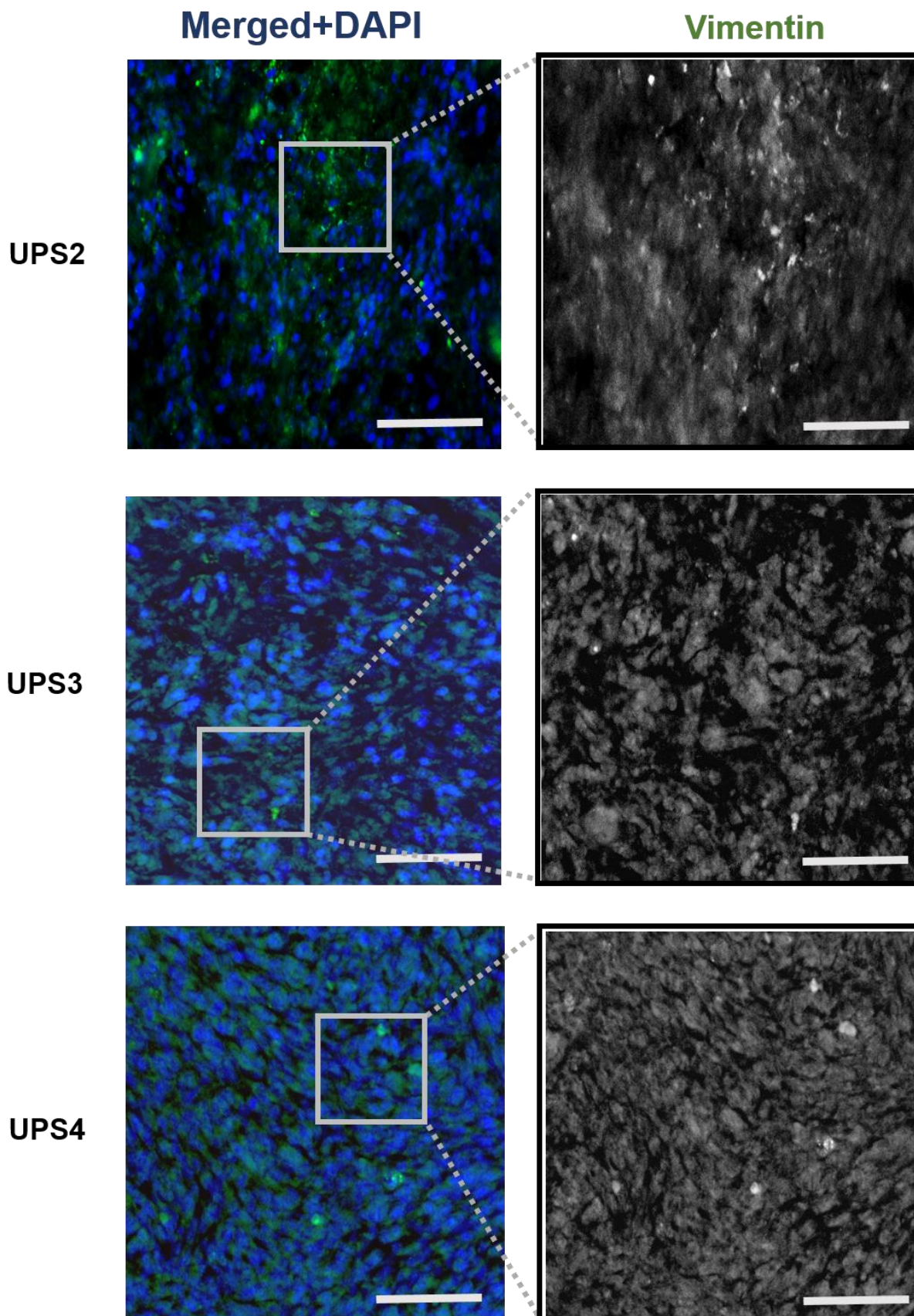
Figure 4. 9: IF staining for vimentin in xenografts.

Vimentin-stained xenografts at 20X magnification (scale bar=100 μm) and magnified images (scale bar = 20 μm). The nuclei are stained blue with DAPI and vimentin is stained green. The nuclei are Negative control for vimentin. Bar chart of vimentin CTCF in xenografts. Key: *, $P <$ 0.05; **, $P < 0.01$; ***, $P < 0.001$; ns, not significant. Error bars denote ± SEM.

4.3.3.4 N-cadherin

N-cadherin is a calcium calponin protein of the classical cadherin family that plays an important role in embryogenesis, cell adhesion, and integrity. It is an intracellular protein located in plasma membranes and cell junctions. N-cadherin is expressed ubiquitously in many cells, including fibroblasts, skeletal muscle, and endothelial cells. It plays an important role in the EMT process, which enhances cancer metastasis (Mrozik et al., 2018). Positive N-cadherin staining was identified as a dark brown cytoplasmic staining in all xenograft sections, which showed similar cellular staining pattern (Fig. 4.10A&B). N-cadherin staining intensity was evaluated using the Qupath software. N-cadherin intensity (%) means the percentage of transgelin positively stained cells in region of interest (in this case the whole tumour section. Quantification of staining of N-cadherin using IHC showed no significant differences in expression among the three xenografts (Fig.4.10D). The negative control was processed without adding the primary antibody (Fig.4.10C). Xenograft sections were also stained for N-cadherin using an IF method. All xenograft sections showed positive green cytoplasmic N-cadherin staining. Fluorescence intensity was measured using ImageJ software and calculated as CTCF according to Section 2.6.1. Statistical analysis showed that N-cadherin levels did not differ significantly among the three xenografts (Fig. 4.11).
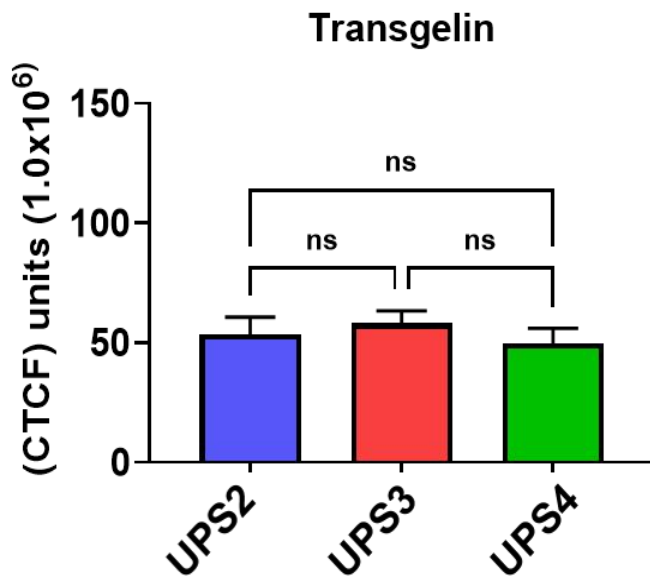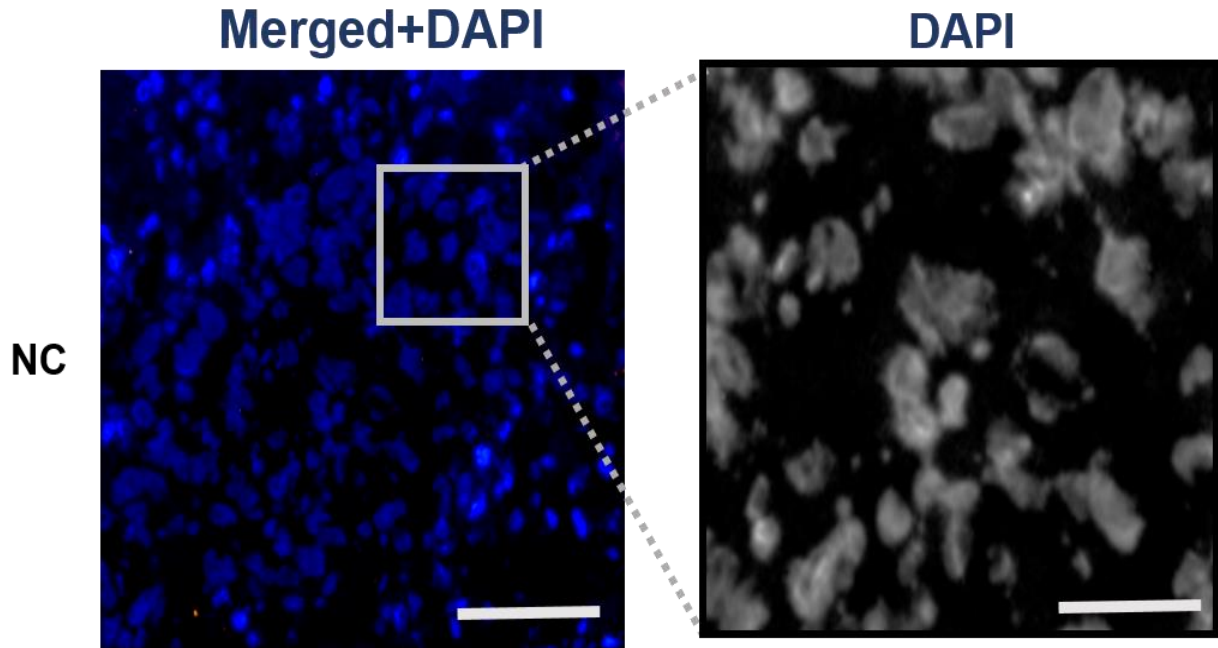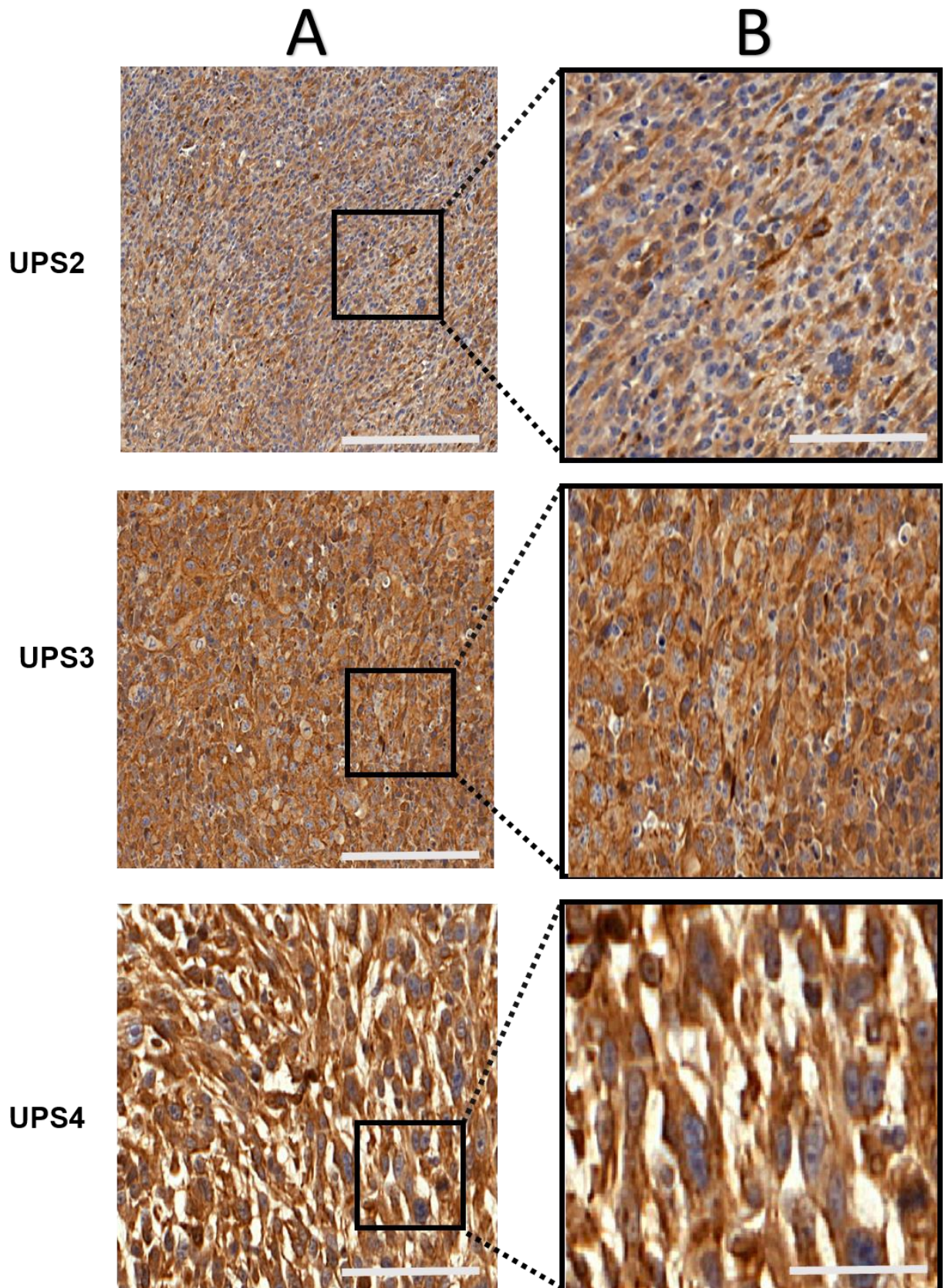
UPS2

UPS3

UPS4

A

B

NC

C

D
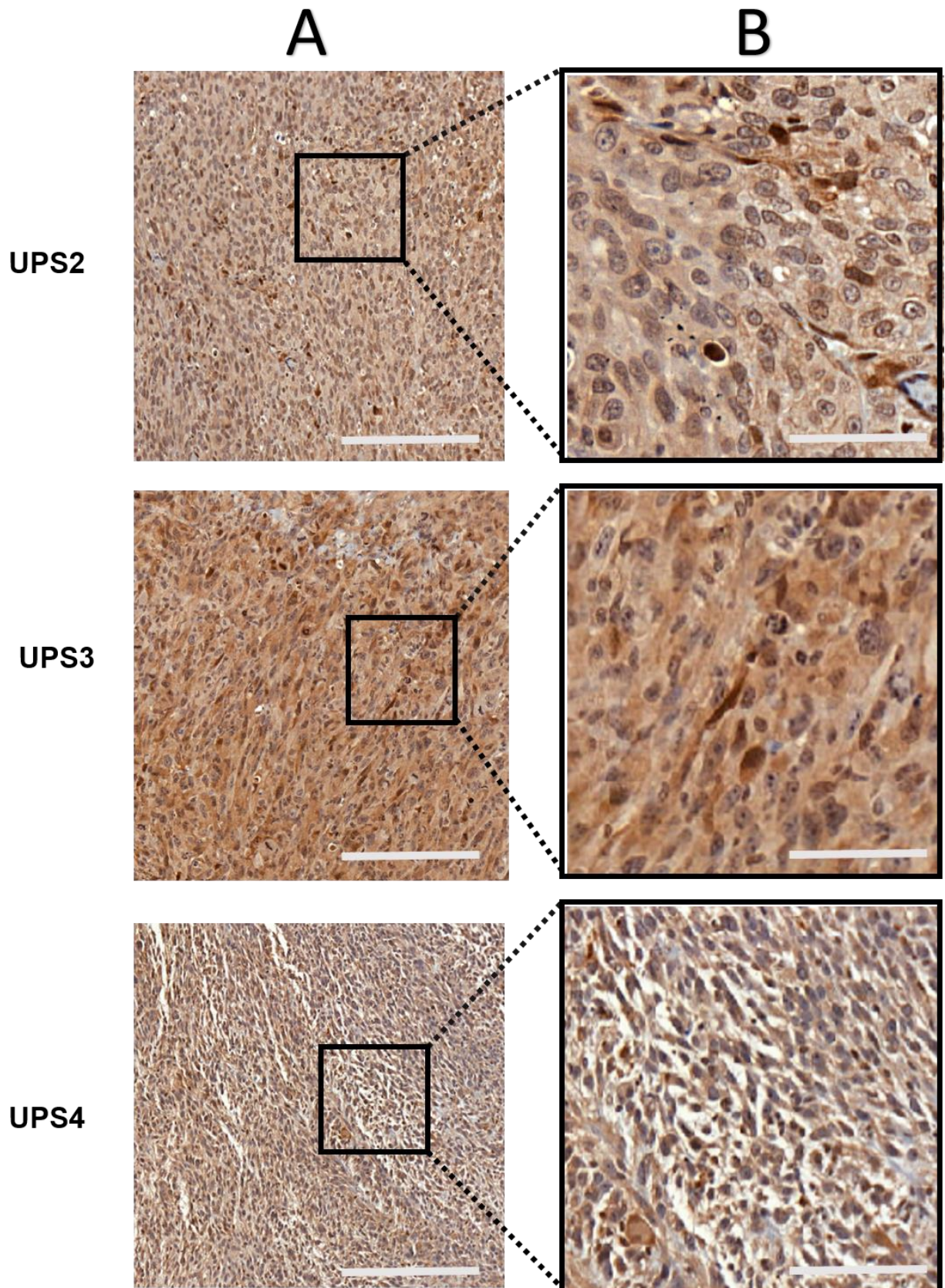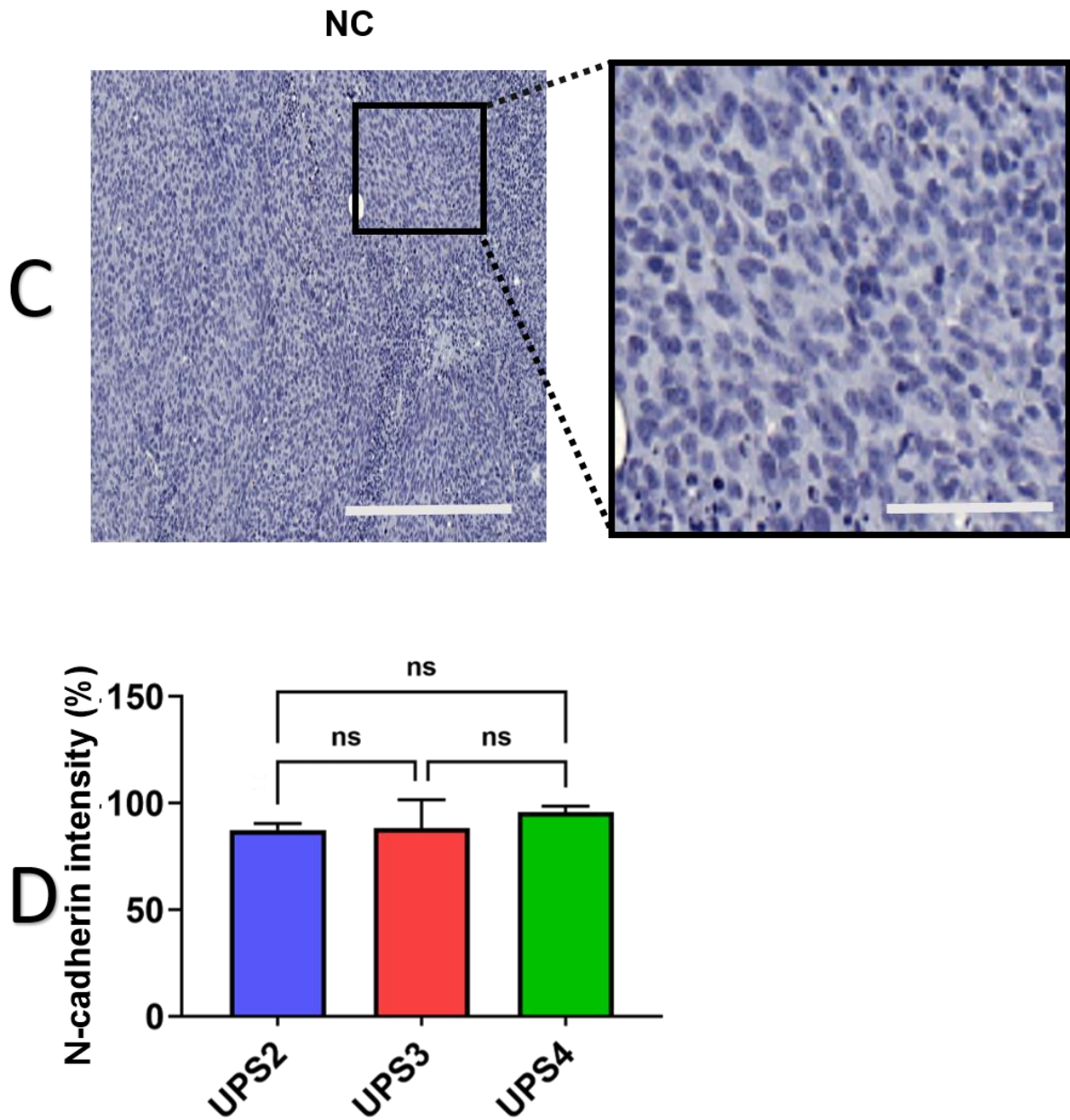
Figure 4. 10: IHC staining for N-cadherin in xenografts.

(A) N-cadherin-stained xenografts at 20X magnification (scale bar = 100 µm). The nuclei are stained blue with haematoxylin and N-cadherin is stained brown. (B) Magnified images for respective xenografts (scale bar =20µm). (C) Negative control for N-cadherin. (D) Bar chart for N-cadherin intensity in xenografts. Key: *, $P < 0.05$; **, $P < 0.01$; ***, $P < 0.001$; ns, not significant. Error bars denote ± SEM.

Merged+DAPI **N-cadherin**

UPS2

UPS3

UPS4

Merged+DAPI **DAPI**

NC
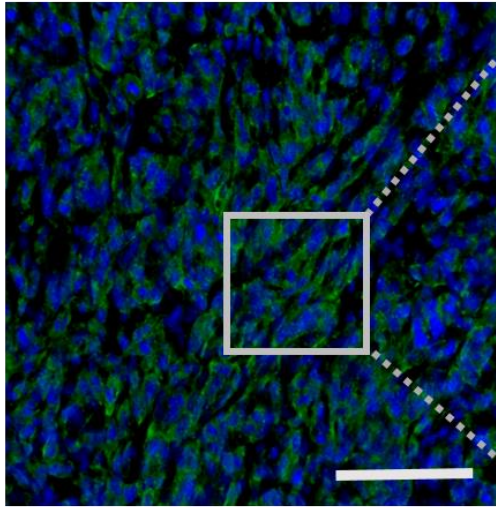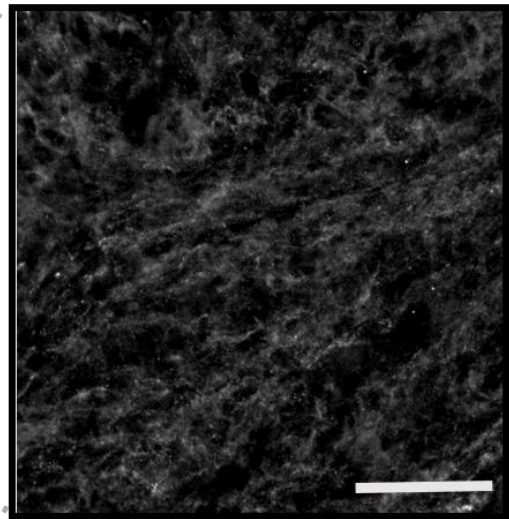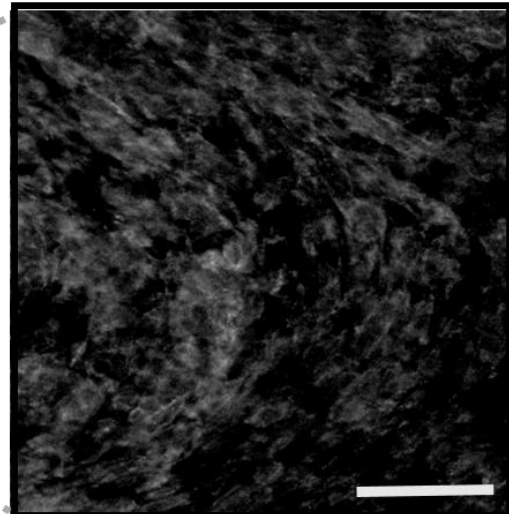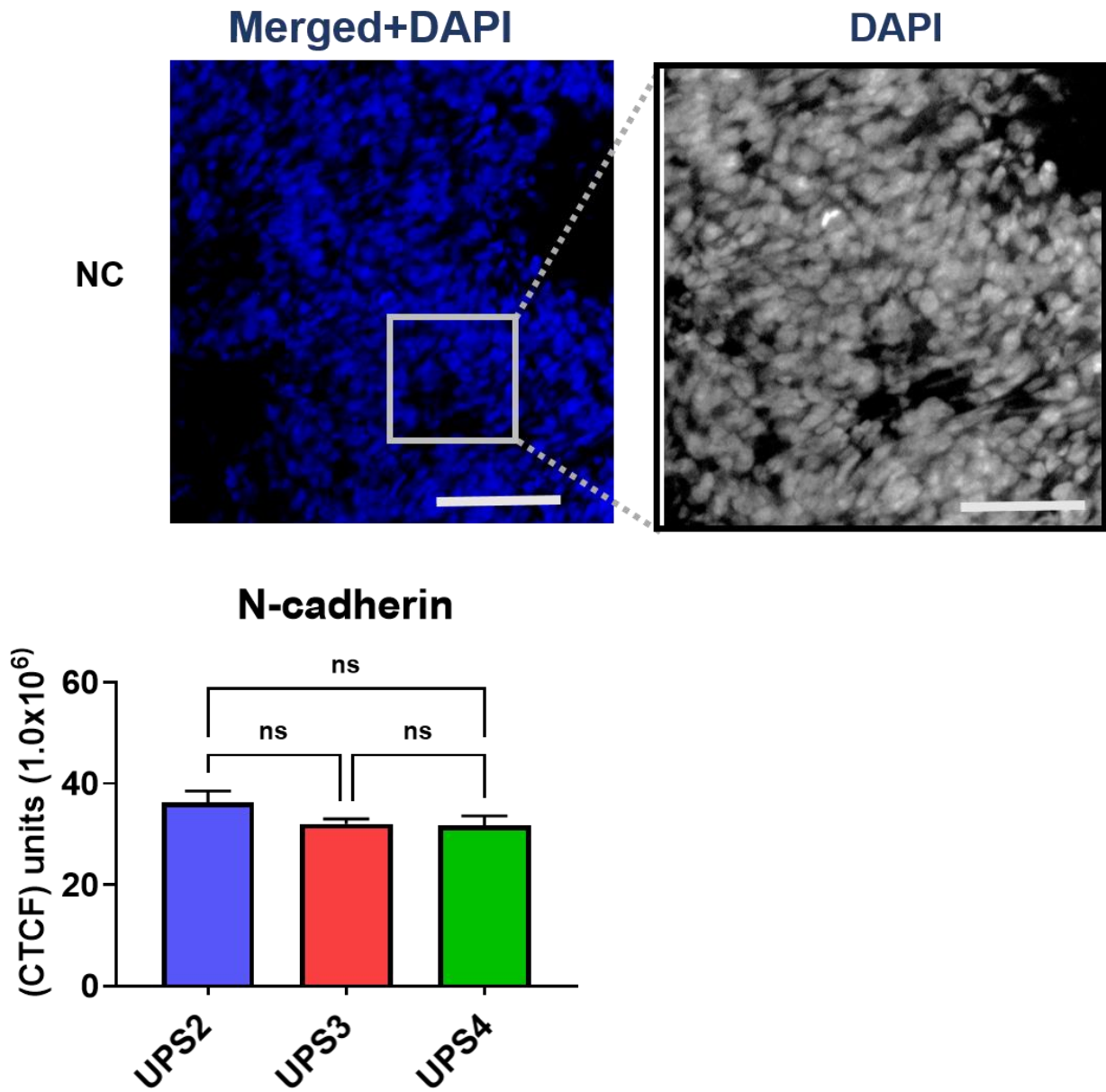
N-cadherin

Figure 4. 11: IF staining for N-cadherin in xenografts.

N-cadherin-stained xenografts at 20X magnification (scale bar=100 μm) and magnified images (scale bar = 20 μm). The nuclei are stained blue with DAPI and N-cadherin is stained green. The nuclei are Negative control for N-cadherin. Bar chart of N-cadherin CTCF in xenografts. Key: *, $P < 0.05$; **, $P < 0.01$; ***, $P < 0.001$; ns, not significant. Error bars denote ± SEM.

4.3.3.5 Fibronectin

Fibronectin is a large glycoprotein that exists in a soluble form found in plasma membranes and an insoluble intracellular form. It plays an important role in cell-cell adhesion, migration, differentiation, and embryogenesis. It was associated with cancer progression and has been identified as an EMT marker (Bae et al., 2013). IHC-based fibronectin staining did not differ significantly among the three xenografts (Fig. 4.12). Positive fibronectin staining identified as a dark brown cytoplasmic and diffuse nuclear staining in all xenograft sections, which showed similar cellular staining patterns (Fig. 4.12A&B). Fibronectin staining intensity was evaluated using the Qupath software. Fibronectin intensity (%) means the percentage of transgelin positively stained cells in region of interest (in this case the whole tumour section. Quantification of the staining of fibronectin using IHC showed no significant differences among the three xenografts (Fig.4.12D). The negative control was processed without adding the primary antibody (Fig.4.12C). Xenograft sections were also stained for fibronectin using an IF method. All xenograft sections showed positive patchy green cytoplasmic staining. Fluorescence intensity was measured using the ImageJ software and calculated as CTCF according to Section 2.6.1. Statistical analysis showed that fibronectin levels did not differ significantly between UPS2 and UPS3 cells and between UPS1 and UPS3 cells. However, fibronectin levels were significantly higher in UPS1 than in UPS2 cells (Fig. 4.13).

NC

C

D
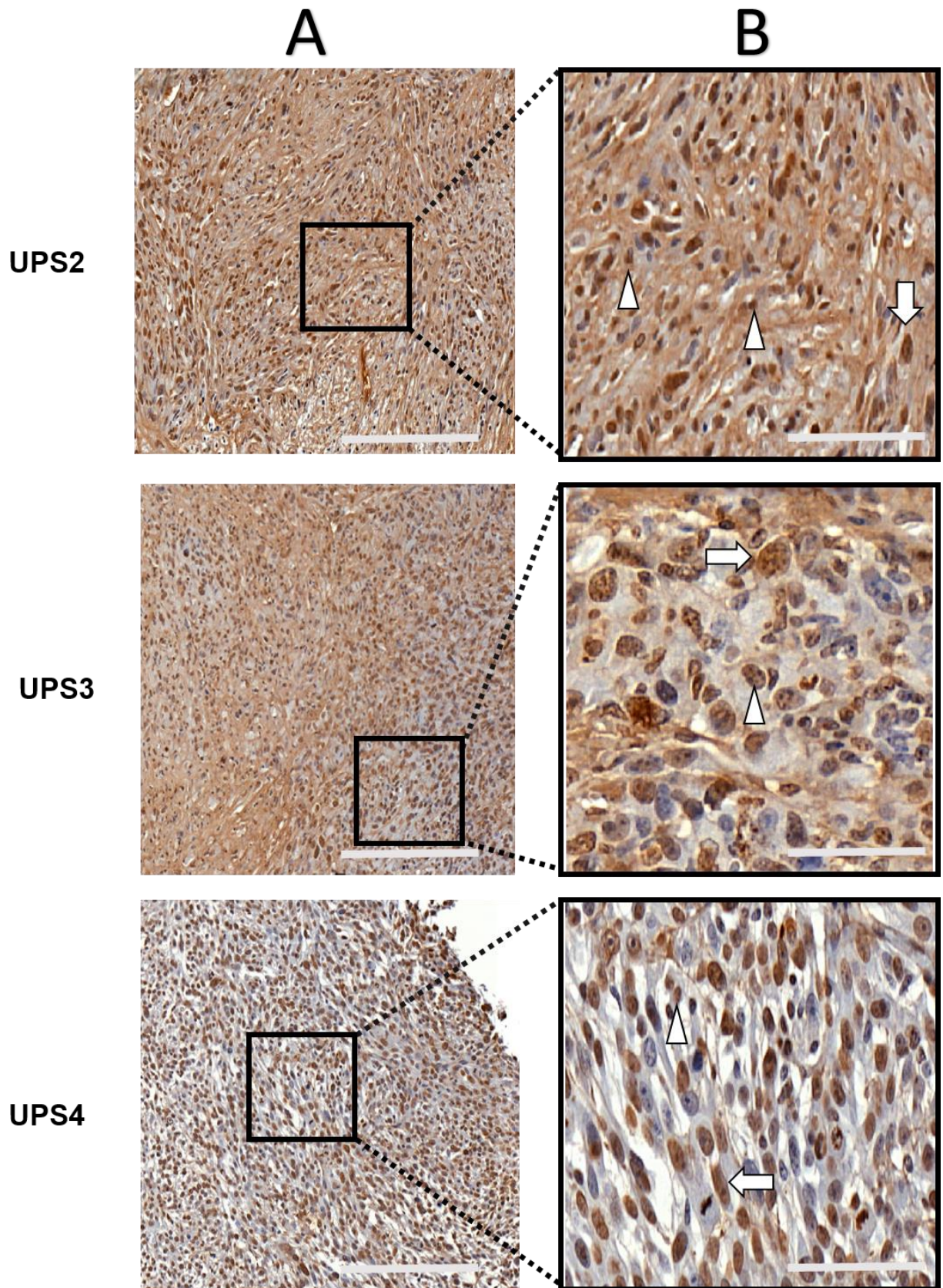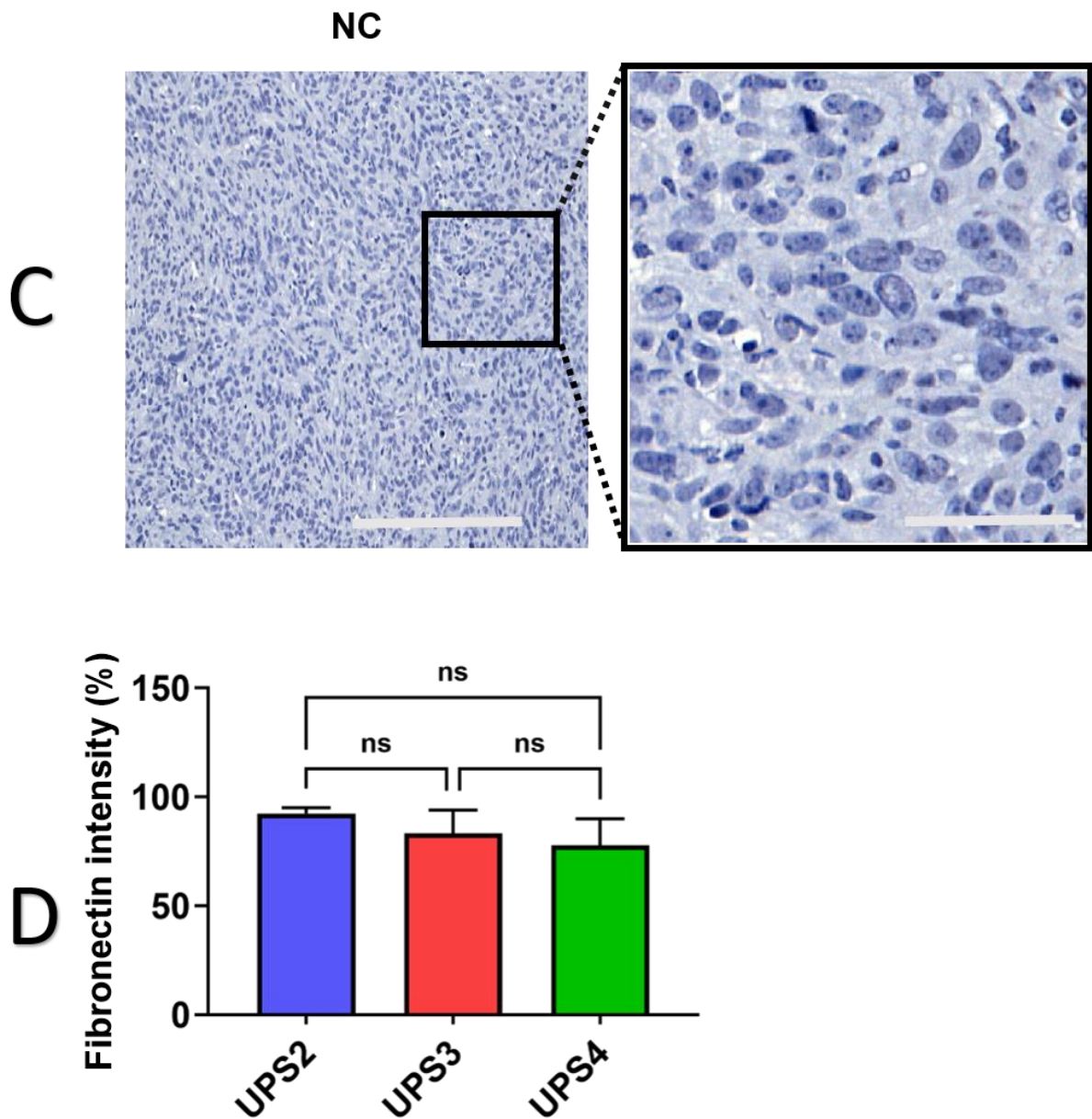
Figure 4. 12: IHC staining for fibronectin in xenografts.

(A) Fibronectin-stained xenografts at 20X magnification (scale bar = 100 µm). The nuclei are stained blue with haematoxylin and fibronectin is stained brown. (B) Magnified images for respective xenografts (scale bar =20µm). Arrows indicate cytoplasmic staining and arrowheads indicate nuclear staining. (C) Negative control for fibronectin. (D) Bar chart for fibronectin intensity in xenografts. Key: *, $P < 0.05$; **, $P < 0.01$; ***, $P < 0.001$; ns, not significant. Error bars denote ± SEM.

Merged+DAPI	Fibronectin

UPS2
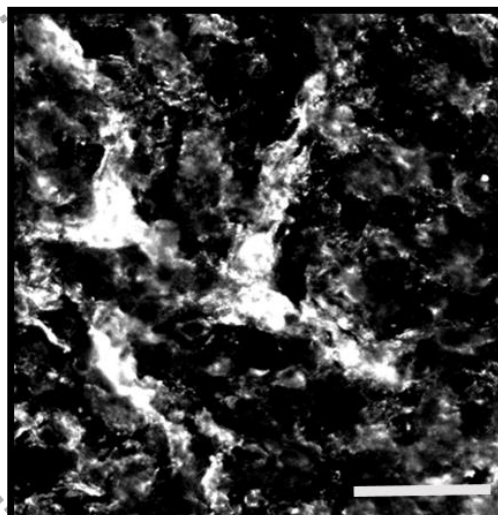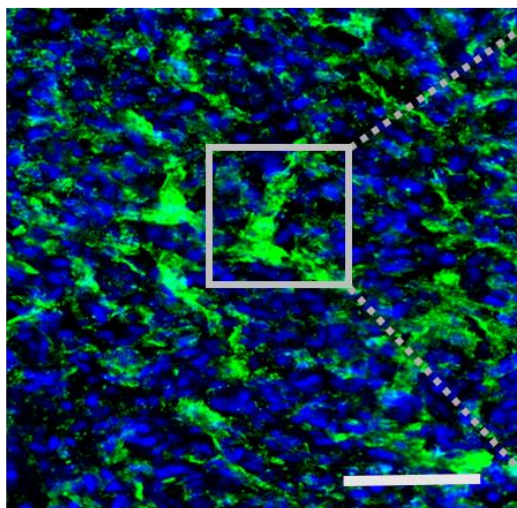
UPS3
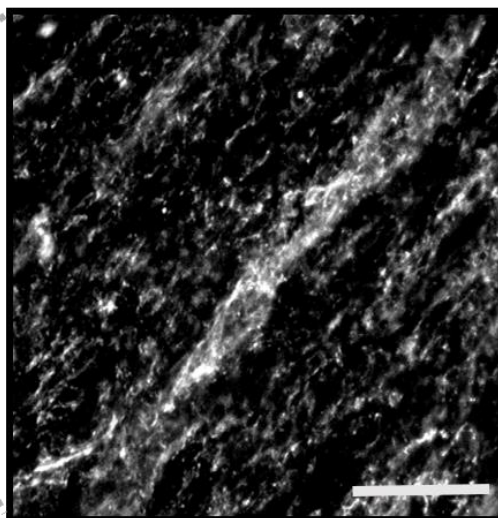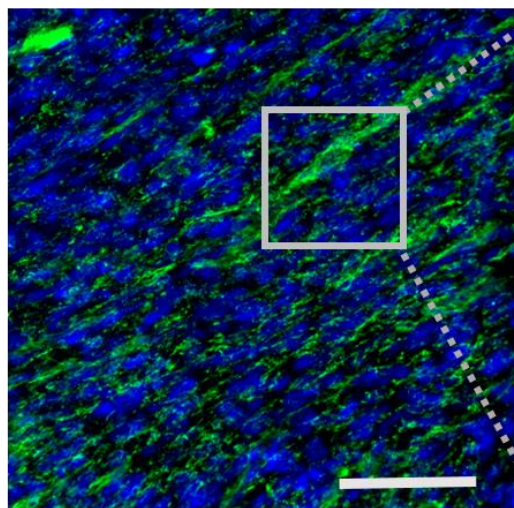
UPS4
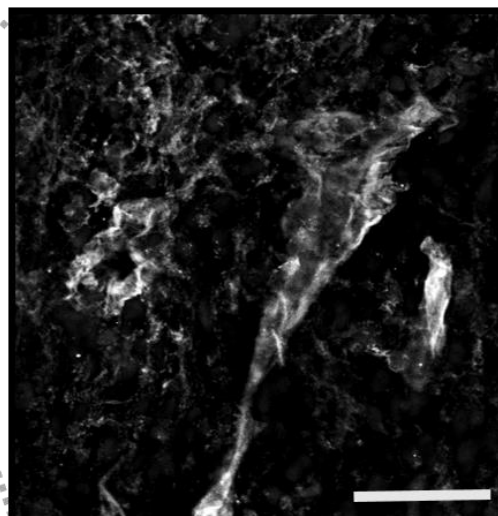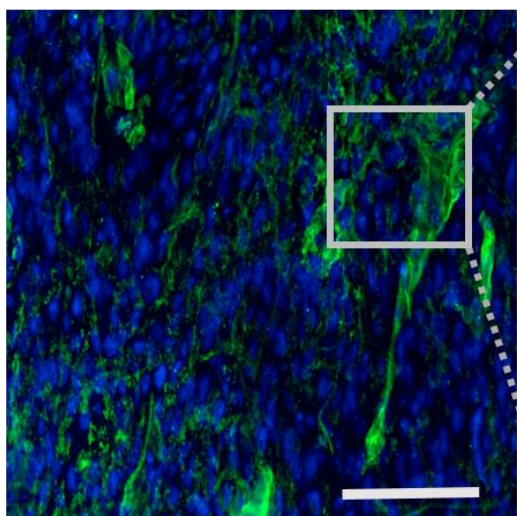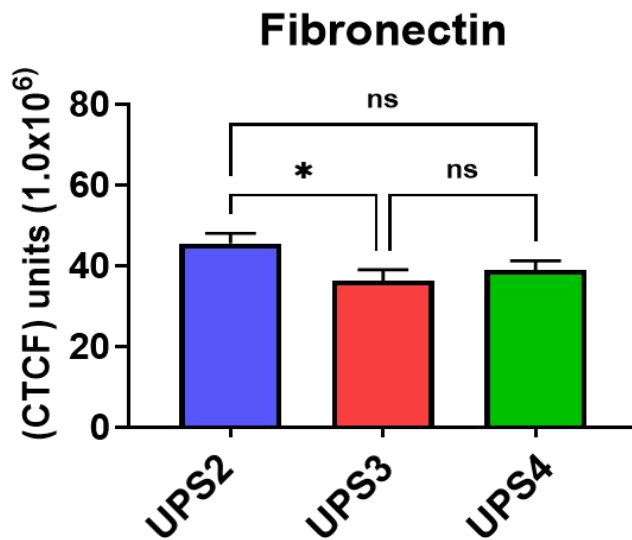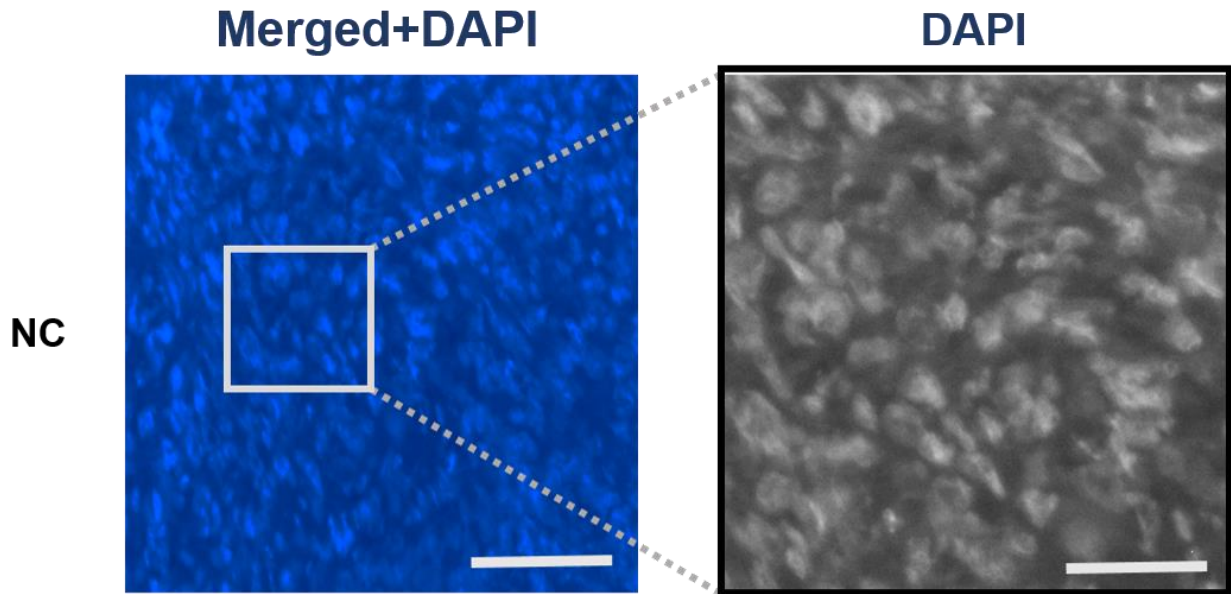
Figure 4. 13: IF staining for fibronectin in xenografts.

Fibronectin-stained xenografts at 20X magnification (scale bar=100 µm) and magnified images (scale bar = 20 µm). The nuclei are stained blue with DAPI and fibronectin is stained green. The nuclei are Negative control for fibronectin. Bar chart of fibronectin CTCF in xenografts. Key: *, P < 0.05; **, P < 0.01; ***, P < 0.001; ns, not significant. Error bars denote ± SEM.

4.3.6 FSP-1

FSP-1 or S100A is a cytoplasmic calcium-binding protein of the S100 family. It has been used as a fibroblast marker in different organs undergoing tissue remodelling or fibrosis. It plays an important role in cell adhesion, migration, angiogenesis, and invasion, promoting cancer progression in carcinomas (Sun et al., 2015). It is an intracellular protein located in the cytoplasm and nucleus. Positive FSP-1 staining was identified as a dark brown cytoplasmic and diffuse nuclear staining in all xenograft sections, which showed similar cellular staining patterns (Fig. 4.14). FSP-1 intensity was evaluated using Qupath software. FSP-1 intensity (%) means the percentage of transgelin positively stained cells in region of interest (in this case the whole tumour section. Quantification of staining of FSP-1 using IHC showed no significant differences in expression among the three xenografts (Fig.4.14D). The negative control was processed without adding the primary antibody (Fig.4.14C). Xenograft sections were also stained with FSP1 using an IF method. All xenograft sections showed positive patchy green cytoplasmic staining. Fluorescence intensity was measured using the ImageJ software and calculated as CTCF according to Section 2.6.1. Statistical analysis showed that FSP-1 levels did not differ significantly among the three xenografts (Fig. 4.15).

NC

C

D
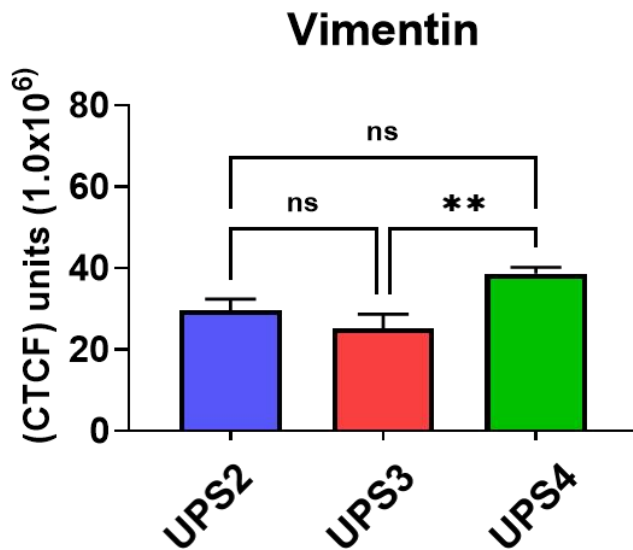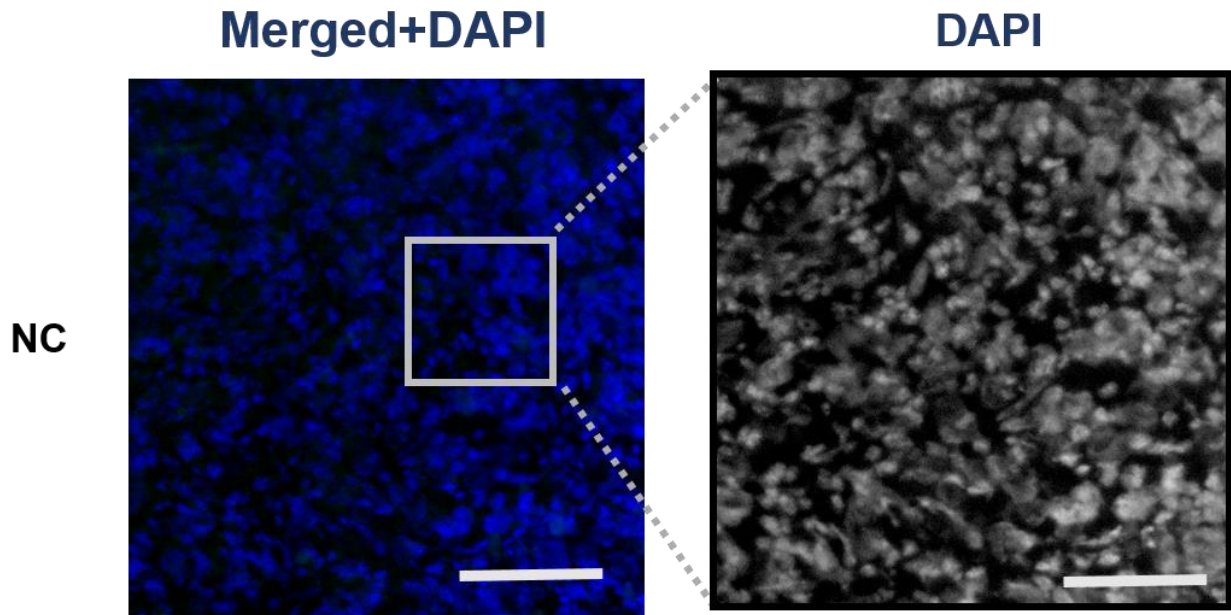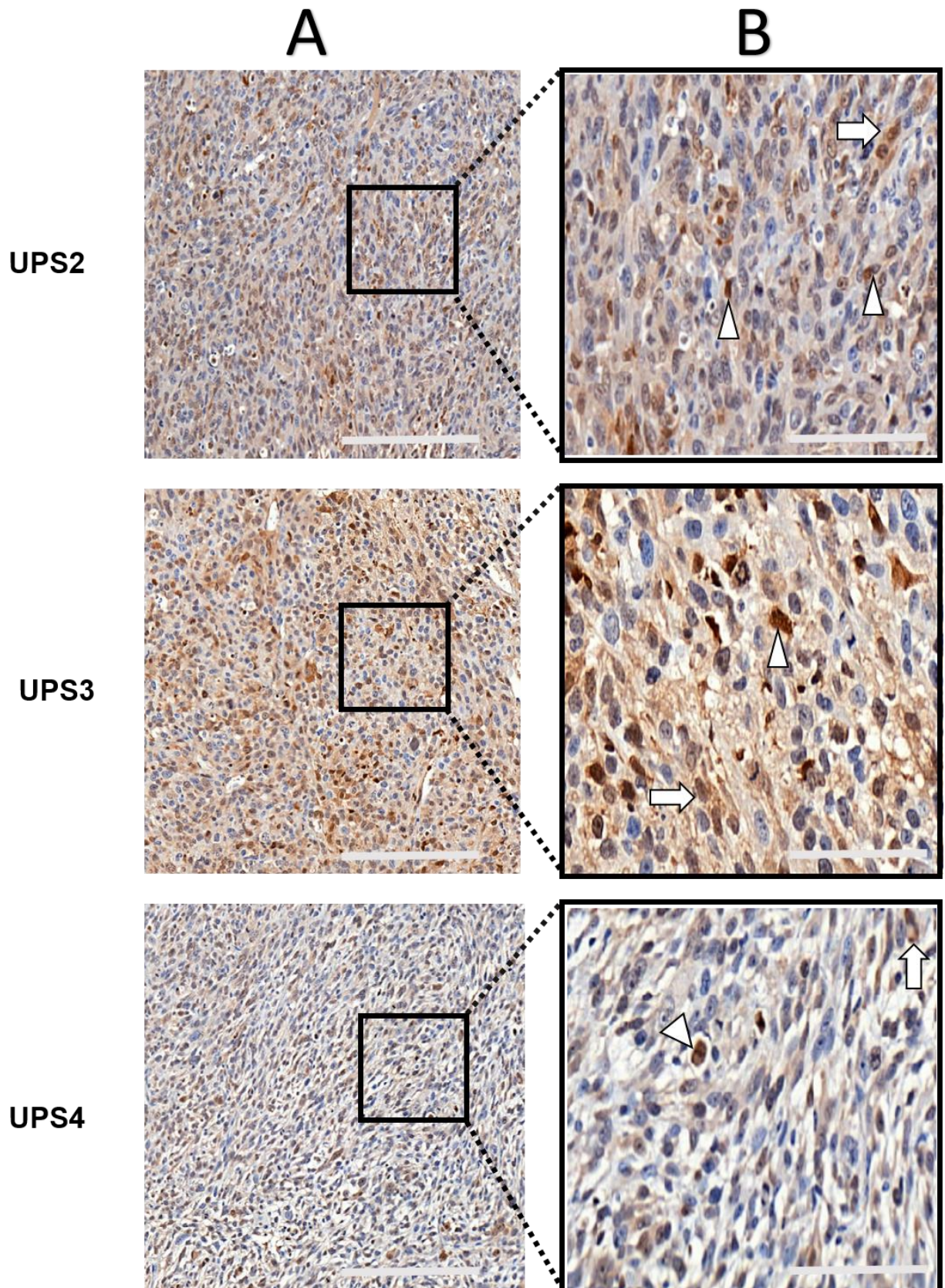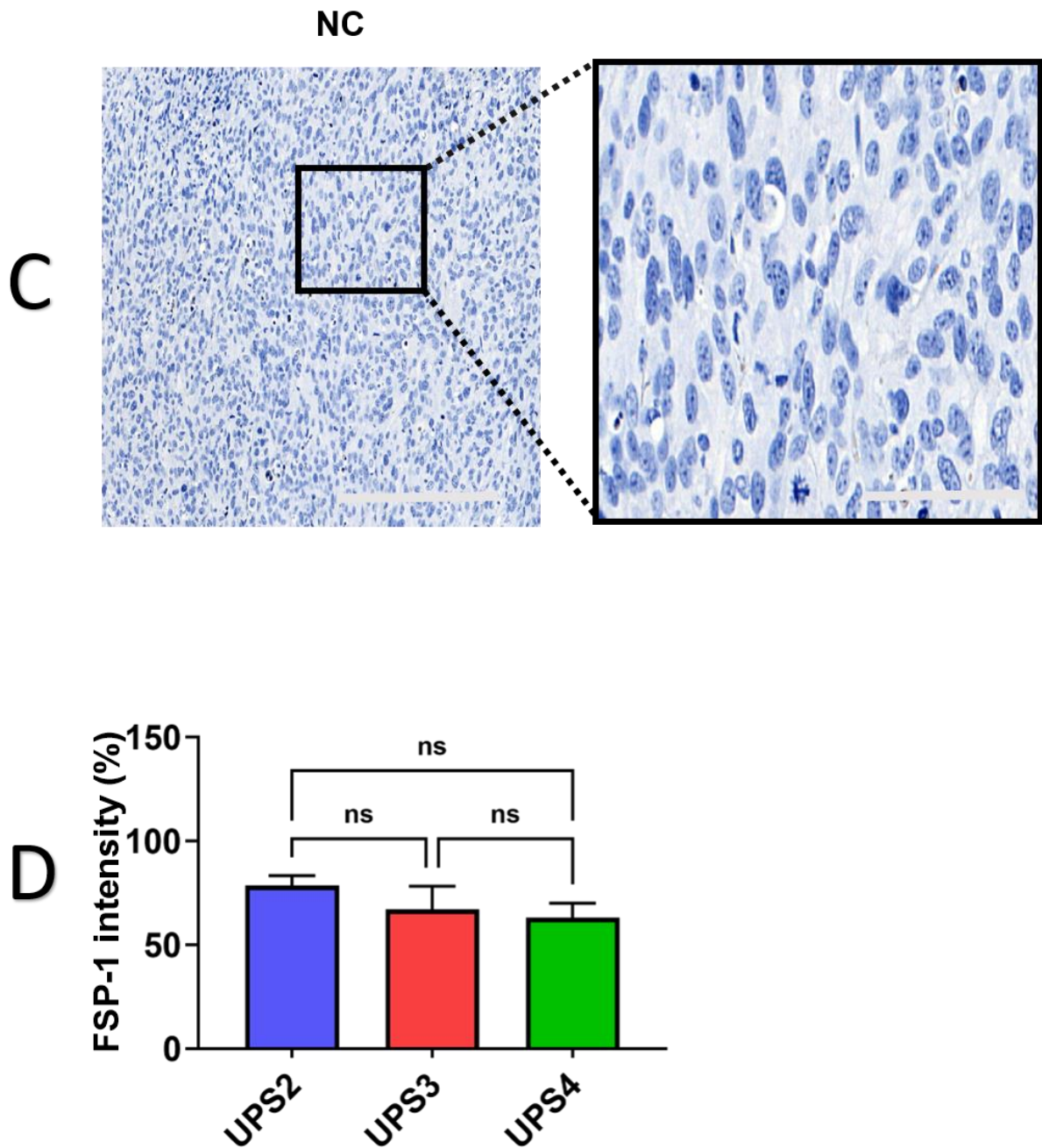
Figure 4. 14: IHC staining for FSP-1 in xenografts.

(A) FSP-1-stained xenografts at 20X magnification (scale bar = 100 µm). The nuclei are stained blue with haematoxylin and FSP-1 is stained brown. (B) Magnified images for respective xenografts (scale bar =20µm). Arrows indicate cytoplasmic staining and arrowheads indicate nuclear staining. (C) Negative control for FSP-1. (D) Bar chart for FSP-1 intensity in xenografts. Key: *, $P < 0.05$; **, $P < 0.01$; ***, $P < 0.001$; ns, not significant. Error bars denote ± SEM.

| **Merged+DAPI**	**FSP-1**

UPS2

UPS3

UPS4

Merged+DAPI

DAPI

NC
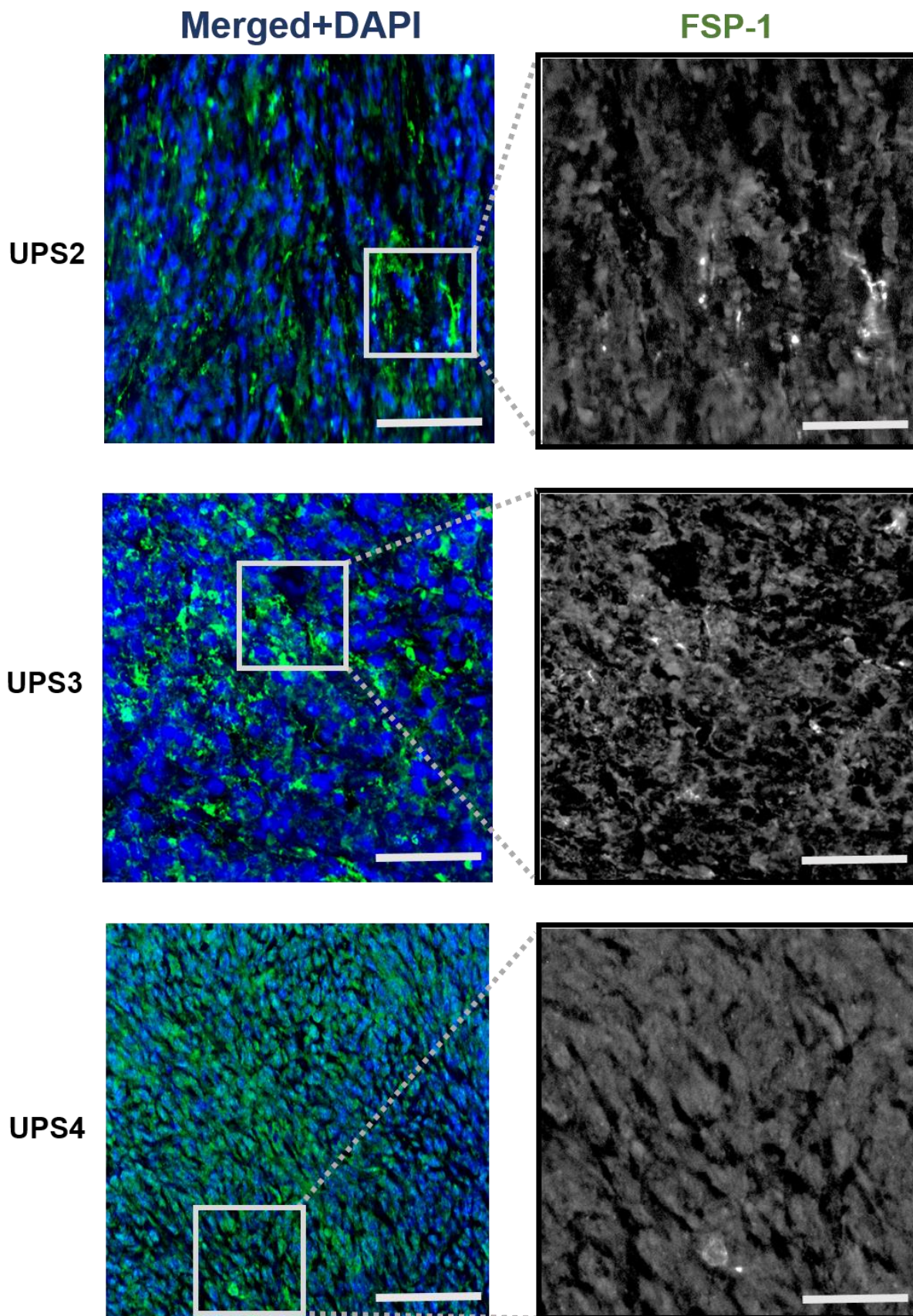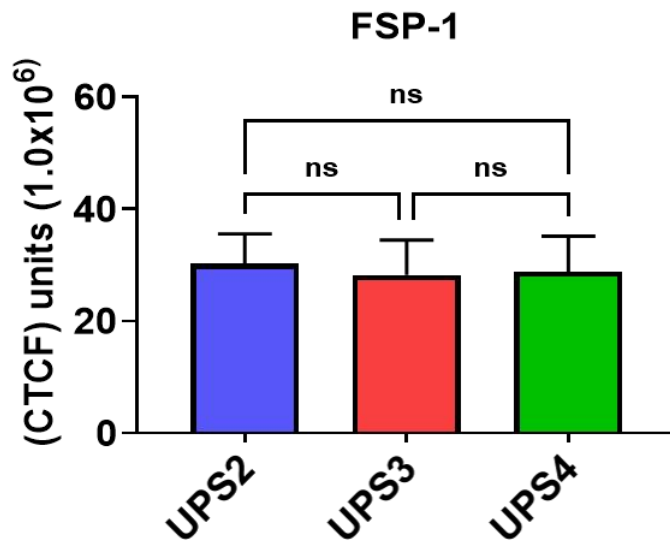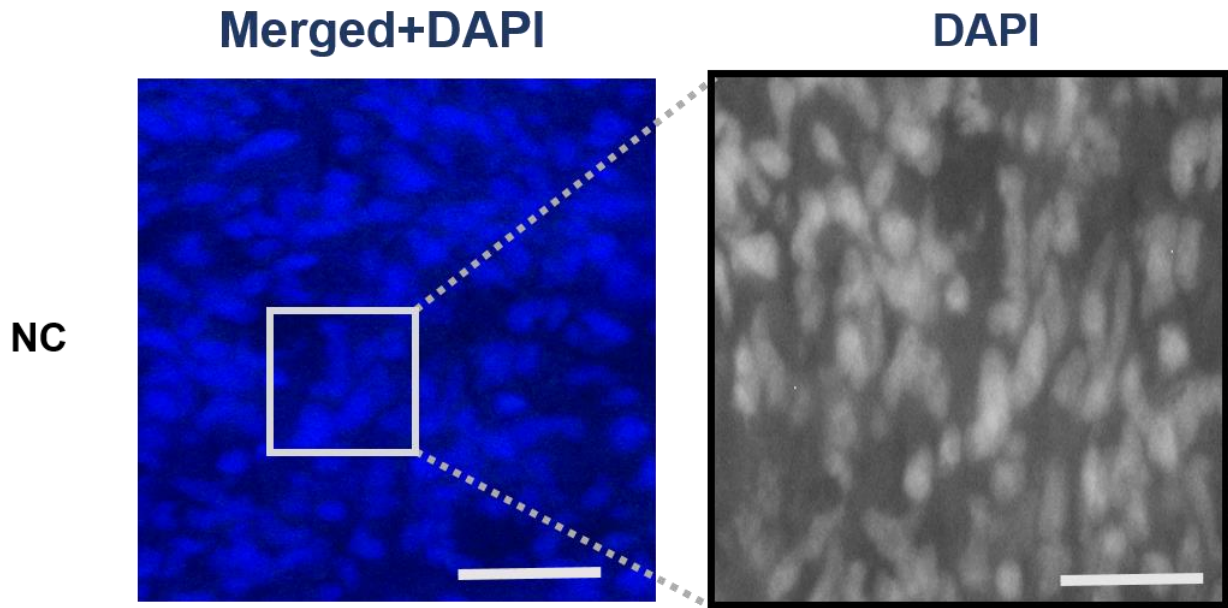
FSP-1

Figure 4. 15: IF staining for FSP-1 in xenografts.

FSP-1-stained xenografts at 20X magnification (scale bar=100 μm) and magnified images (scale bar = 20 μm). The nuclei are stained blue with DAPI and FSP-1 is stained green. The nuclei are Negative control for FSP-1. Bar chart of FSP-1 CTCF in xenografts. Key: *, $P < 0.05$; **, $P < 0.01$; ***, $P < 0.001$; ns, not significant. Error bars denote ± SEM.

4.3.3.7 FAPα

FAPα is an intracellular serine protease that plays a crucial role in tissue repair, wound healing, inflammation and fibrosis. It has been used as a CAF marker (Nurmik et al., 2020). FAPα has a vital function in cancer as it could promote tumorigenesis. High FAPα expression was associated with poor progression-free survival (PFS) in colon cancer (Henry, 2007). Positive FAPα was identified as dark brown cytoplasmic staining in all xenograft sections, which showed similar cellular staining patterns (Fig. 4.16). FAPα staining intensity was evaluated using Qupath software. FAPα intensity (%) means the percentage of transgelin positively stained cells in region of interest (in this case the whole tumour section.   Quantification of FAPα staining using IHC showed no significant differences in expression among the three xenografts (Fig.4.16D). The negative control was processed without adding the primary antibody (Fig.4.16C). Xenograft sections were also stained for FAPα using an IF method. All xenograft sections showed positive green cytoplasmic staining. Fluorescence intensity was measured using the ImageJ software and calculated as CTCF according to Section 2.6.1. Statistical analysis showed that FAPα levels did not differ significantly among the three xenografts (Fig. 4.17).
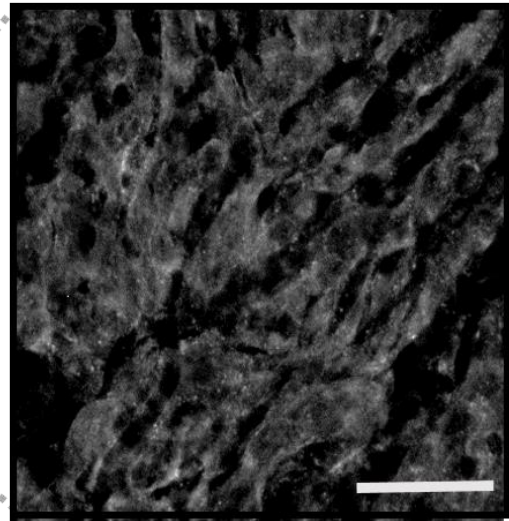
UPS2

UPS3

UPS4

A

B
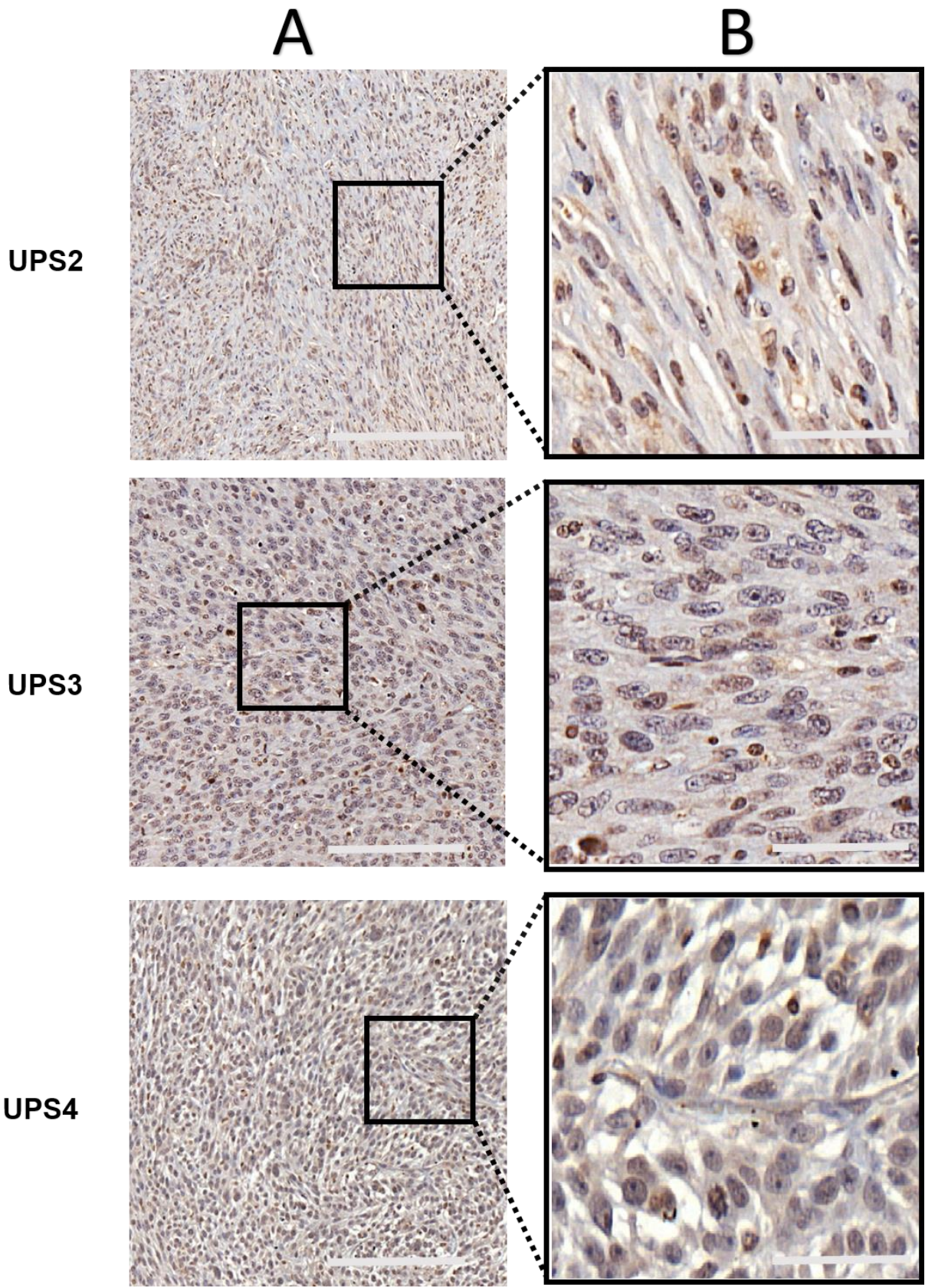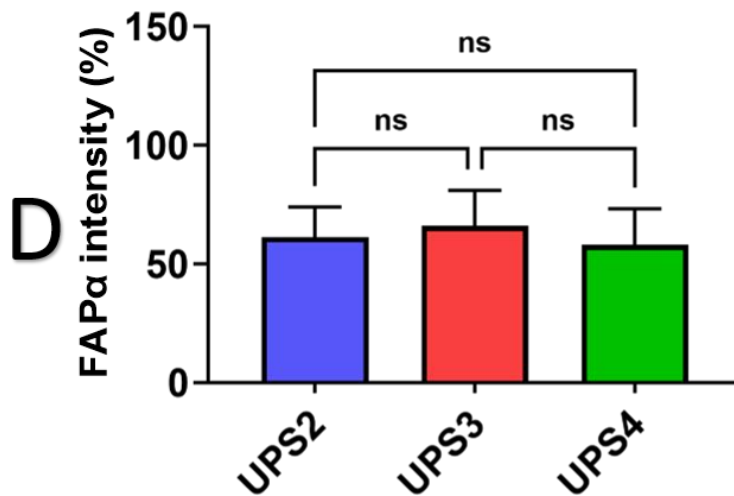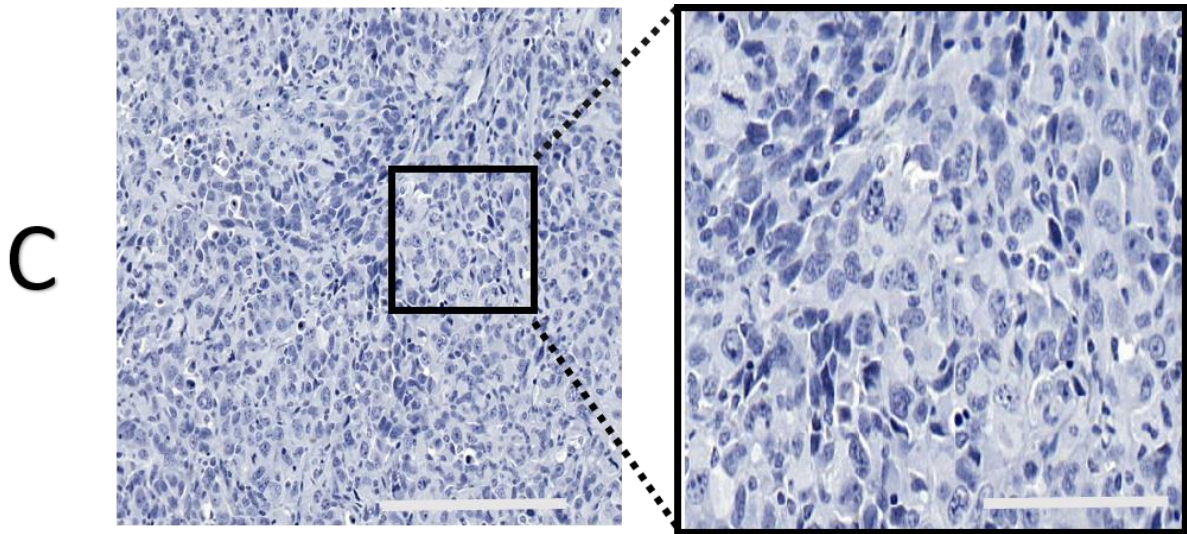
Figure 4. 16: IHC staining for FAPα in xenografts.

(A) FAPα -stained xenografts at 20X magnification (scale bar = 100 µm). The nuclei are stained blue with haematoxylin and FAPα is stained brown. (B) Magnified images for respective xenografts (scale bar =20µm). (C) Negative control for FAPα. (D) Bar chart for FAPα intensity in xenografts. Key: *, $P < 0.05$; **, $P < 0.01$; ***, $P < 0.001$; ns, not significant. Error bars denote ± SEM.

Merged+DAPI	**FAPα**

UPS2

UPS3

UPS4

Merged+DAPI **DAPI**

NC

FAP α
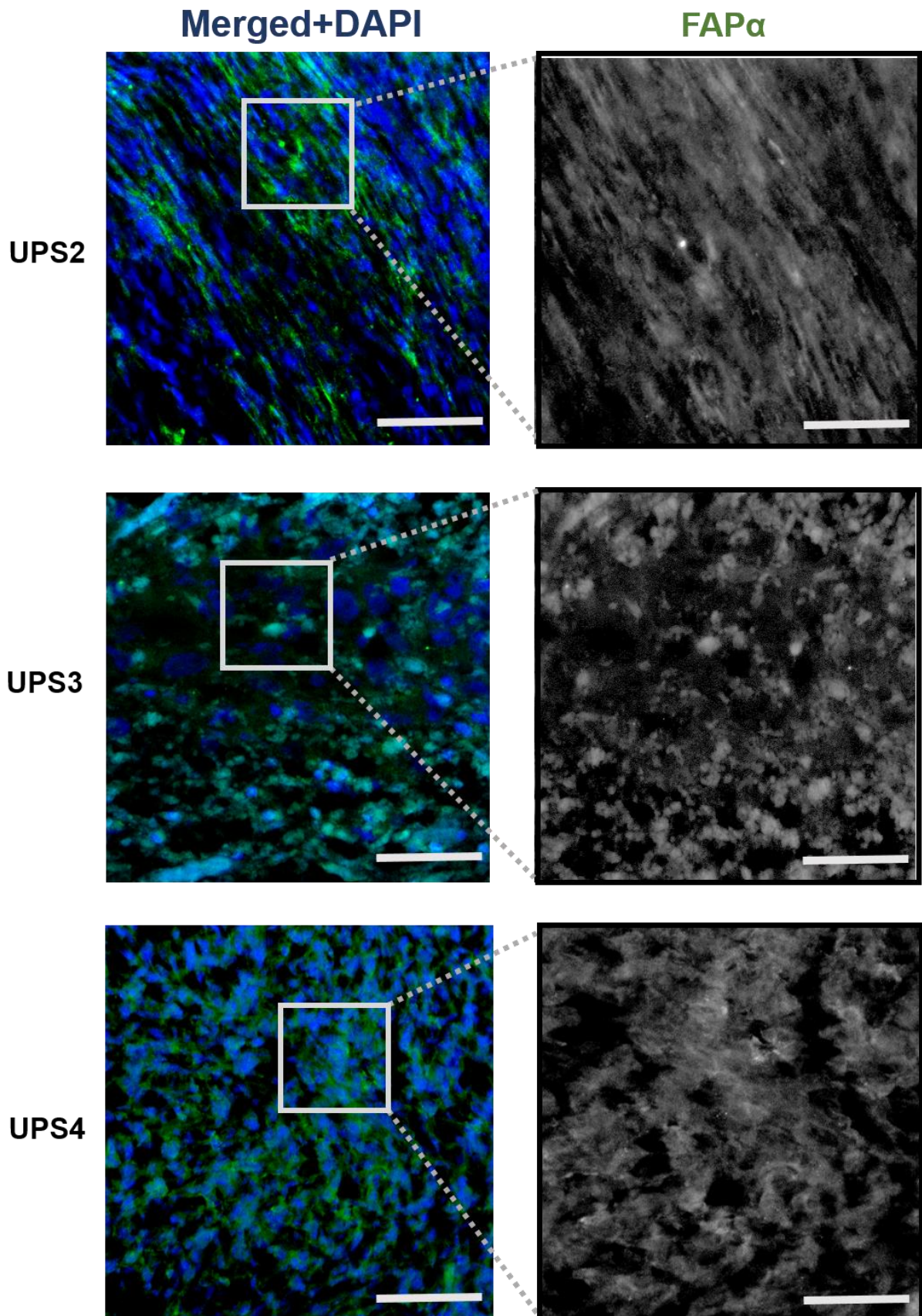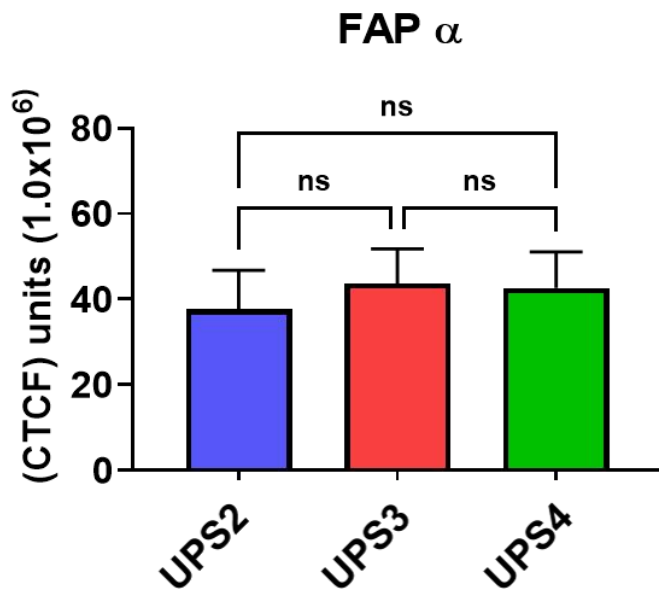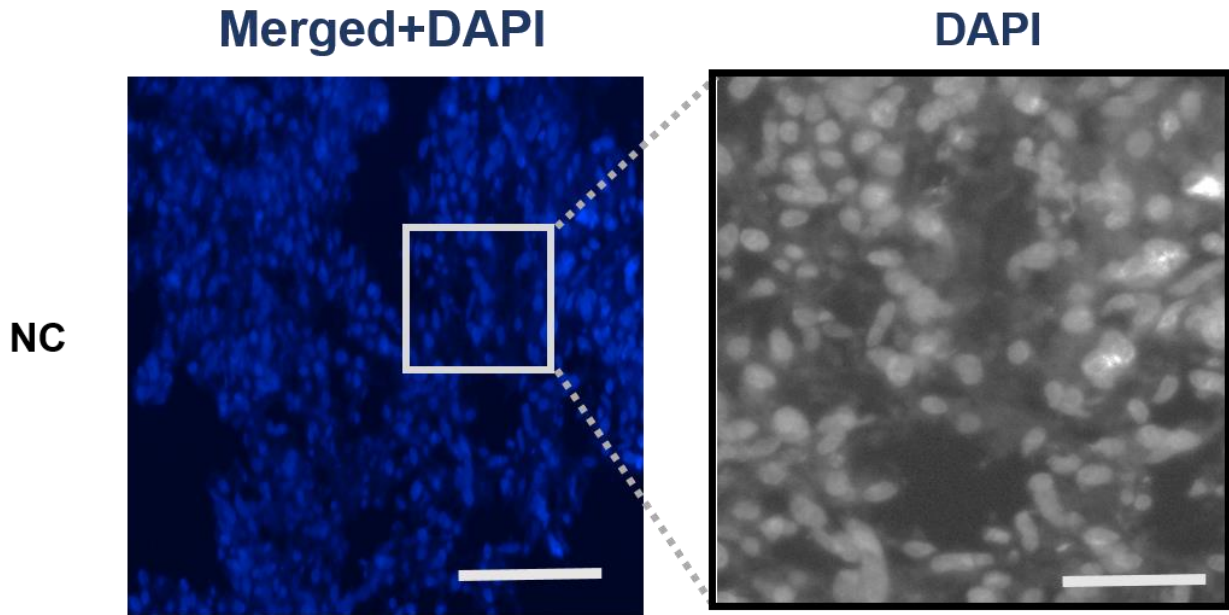
Figure 4. 17: IF staining for FAPα in xenografts.

FAPα -stained xenografts at 20X magnification (scale bar=100 μm) and magnified images (scale bar = 20 μm). The nuclei are stained blue with DAPI and FAPα is stained green. The nuclei are Negative control for FAPα. Bar chart of FAPα CTCF in xenografts. Key: *, $P < 0.05$; **, $P < 0.01$; ***, $P < 0.001$; ns, not significant. Error bars denote ± SEM.

4.3.3.8 SOX2

SOX2 is a transcription factor with a vital role in self-renewal, pluripotency and embryogenesis (Schaefer & Lengerke, 2020). SOX2 was associated with cellular proliferation in carcinomas, enhancing invasion, migration, and metastasis (Weina & Utikal, 2014). SOX2 is an intracellular protein located in the nucleoplasm. Positive SOX2 identified as a dark brown nuclear staining, in all xenograft sections, which showed similar staining intensities (Fig. 4.18). SOX2 staining intensity was evaluated using QuPath software. SOX2 intensity (%) means the percentage of transgelin positively stained cells in region of interest (in this case the whole tumour section. Quantification of staining of SOX2 using IHC showed no significant differences in expression among the three xenografts (Fig.4.18D). Negative control was processed without adding the primary antibody (Fig.4.18C). Xenograft sections were also stained for SOX2 using an IF method. All xenograft sections showed positive green nuclear/cytoplasmic staining with a variation in the staining pattern, as in UPS2 and UPS3 SOX2 staining was nuclear staining but in UPS1 Staining was both cytoplasmic and nuclear. Fluorescence intensity was measured using the ImageJ software and calculated as CTCF according to Section 2.6.1. Statistical analysis showed that SOX2 levels did not differ significantly among the three xenografts (Fig. 4.17).
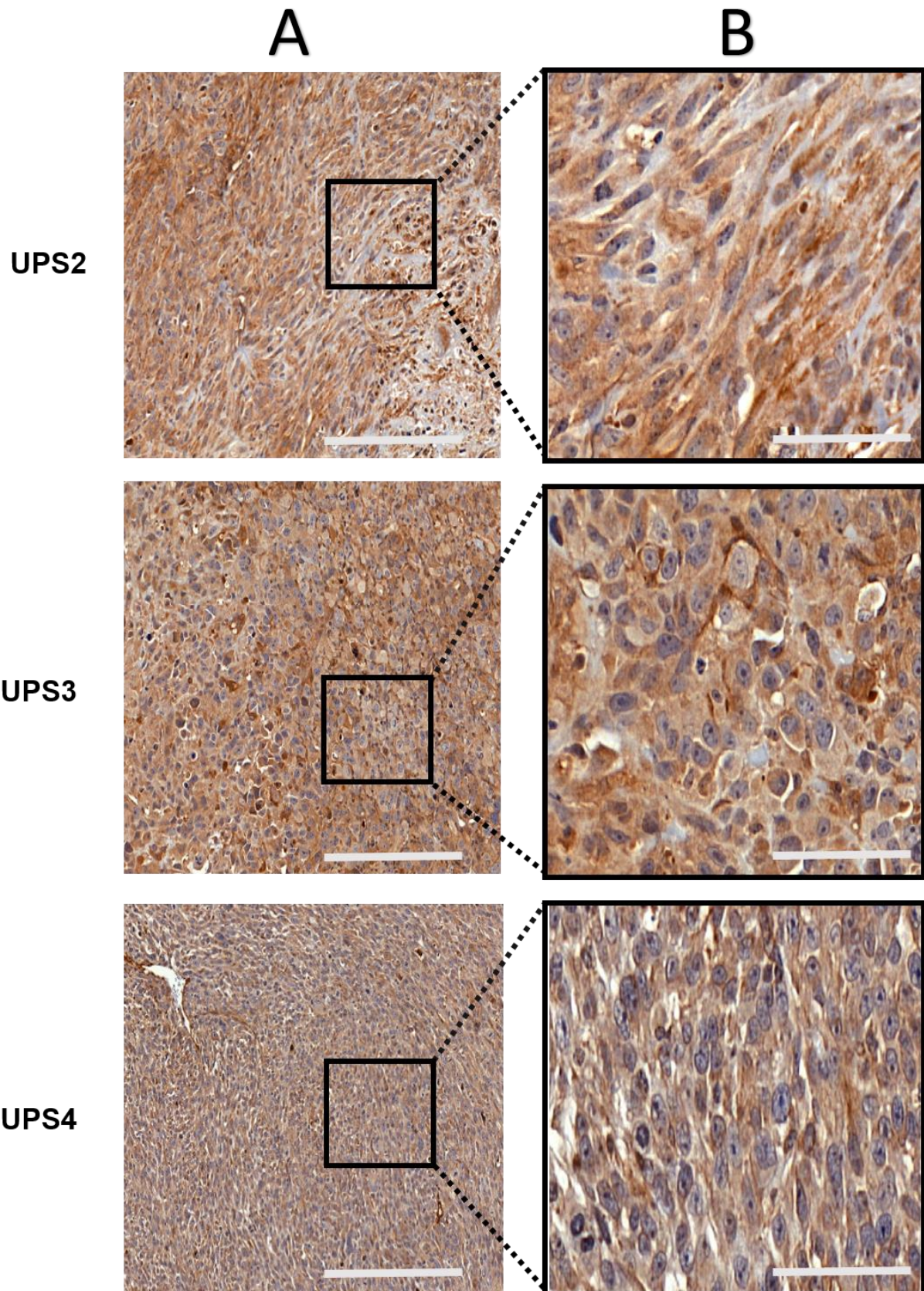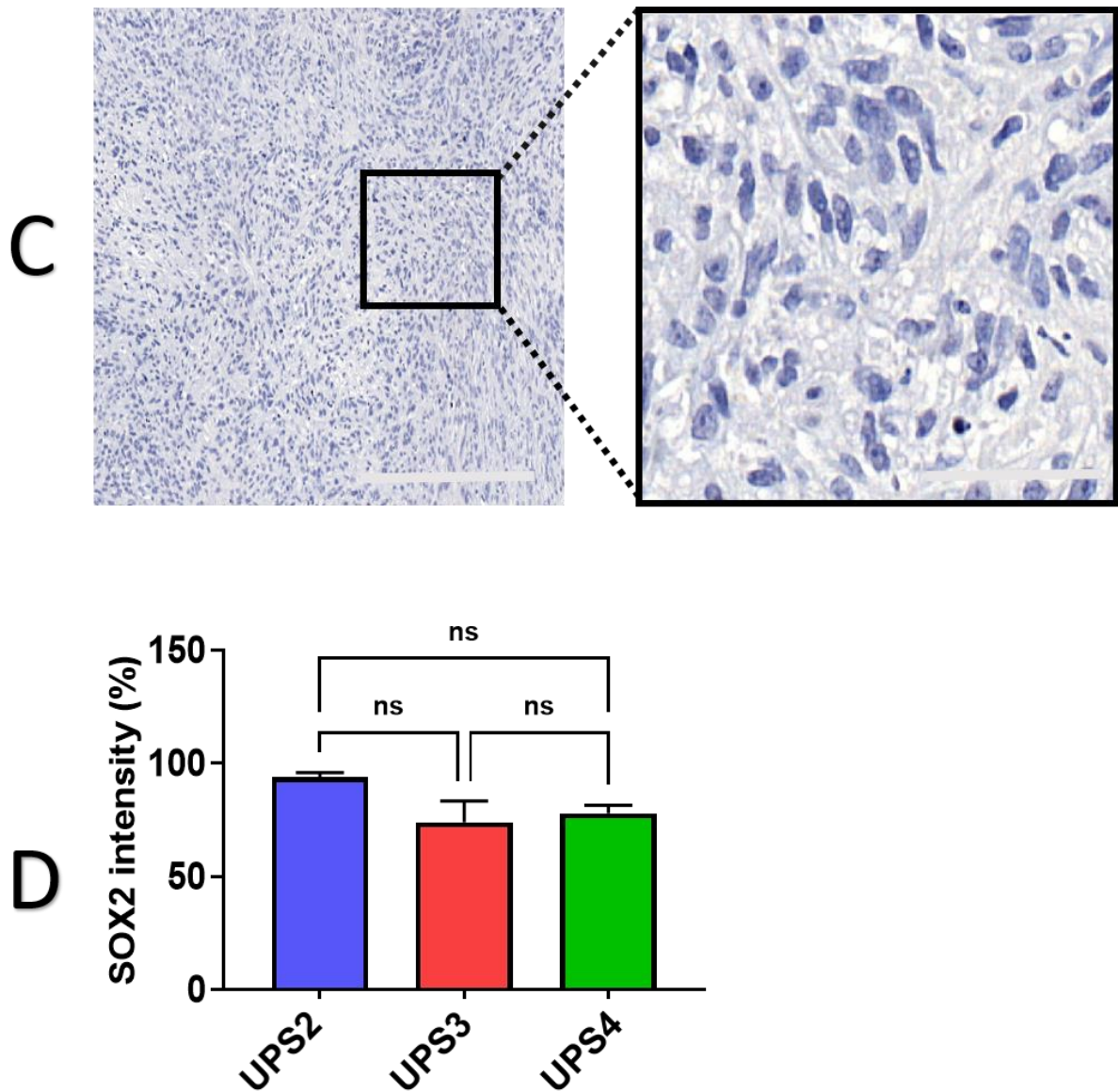
Figure 4. 18: IHC staining for SOX2 in xenografts.

(A) SOX2 -stained xenografts at 20X magnification (scale bar = 100 μm). The nuclei are stained blue with haematoxylin and SOX2 is stained brown. (B) Magnified images for respective xenografts (scale bar =20μm). (C) Negative control for SOX2. (D) Bar chart for SOX2 intensity in xenografts. Key: *, $P < 0.05$; **, $P < 0.01$; ***, $P < 0.001$; ns, not significant. Error bars denote ± SEM.
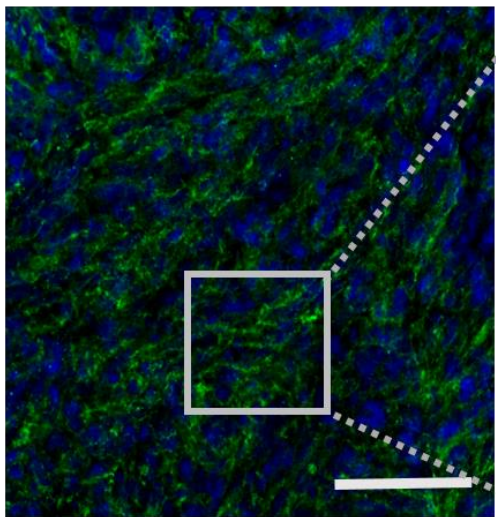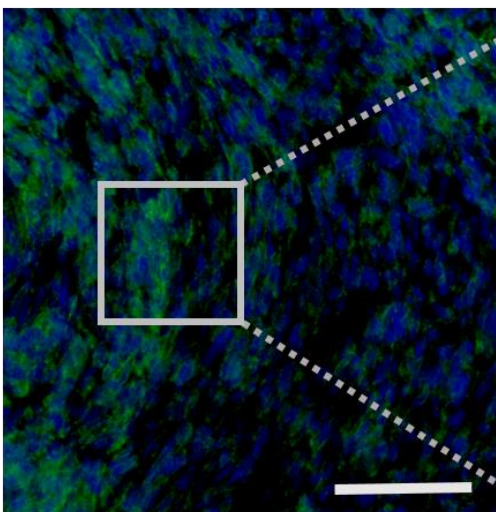
| Merged+DAPI | SOX2 |

UPS2

UPS3

UPS4
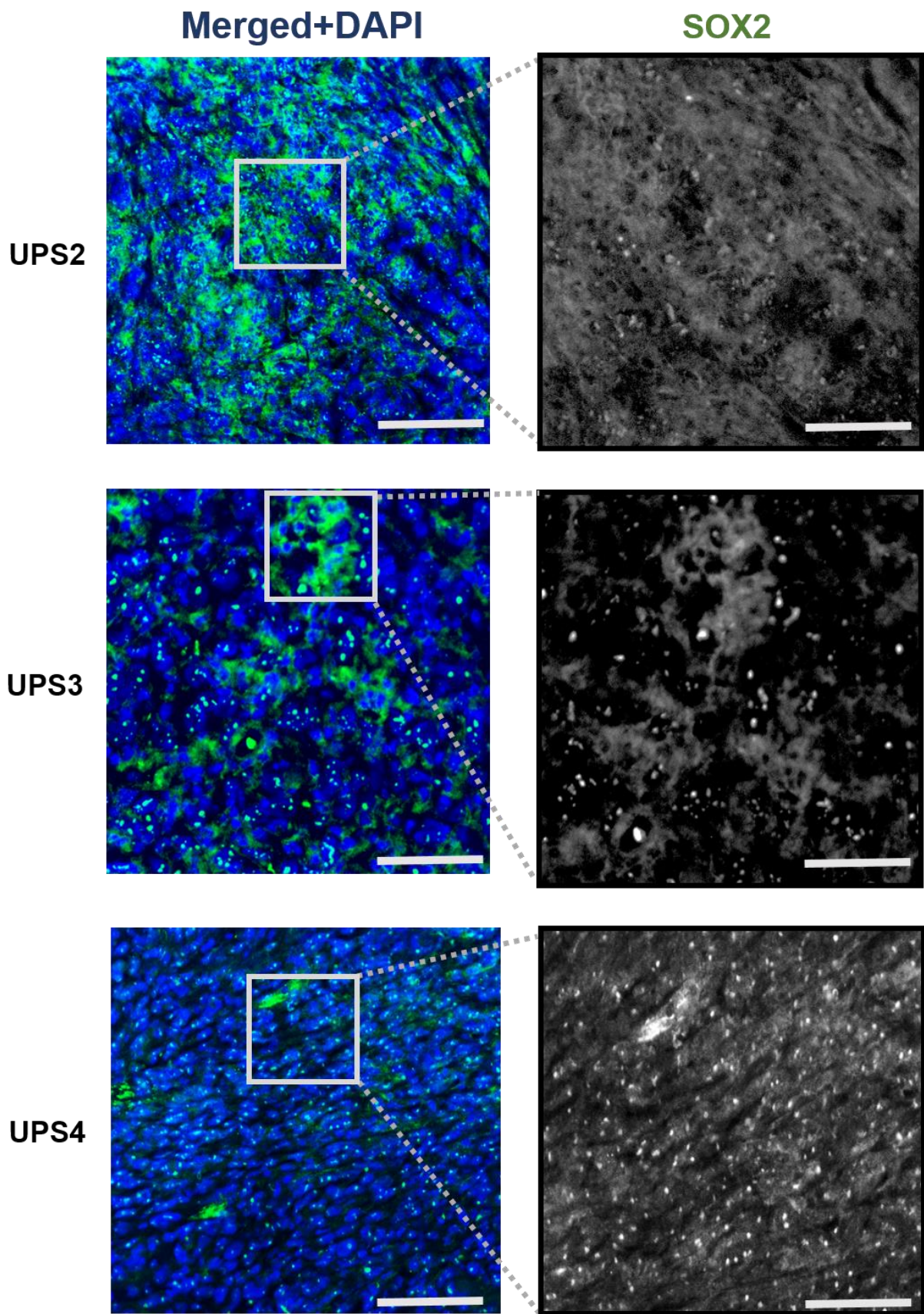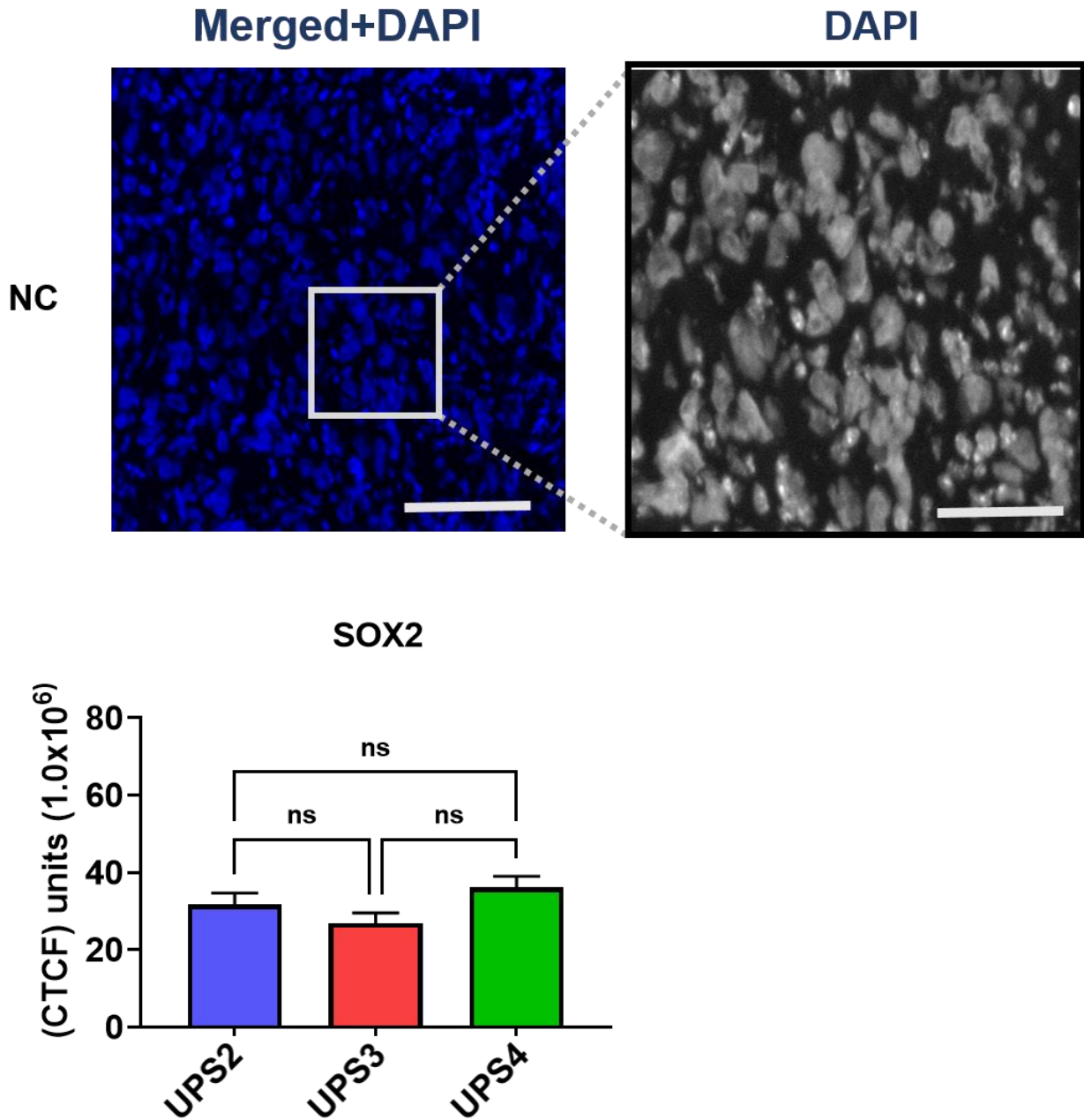
Figure 4. 19: IF staining for SOX2 in xenografts.

SOX2 -stained xenografts at 20X magnification (scale bar=100 μm) and magnified images (scale bar = 20 μm). The nuclei are stained blue with DAPI and SOX2 is stained green. The nuclei are Negative control for SOX2. Bar chart of SOX2 CTCF in xenografts. Key: *, $P < 0.05$; **, $P < 0.01$; ***, $P < 0.001$; ns, not significant. Error bars denote ± SEM.

4.4 Development of a method for differentiating human and mouse cells in UPS xenografts

It is essential to distinguish human (UPS cells) cells from mouse (stroma) cells in the xenografts. In this project, two mouse fibrosarcoma cell lines (T241 and FS188) were used to study cell morphology. The T241 cell line is a spontaneously occurring fibrosarcoma from C57BL/6J mice (Gutierrez et al., 2000). FS188 is a mouse fibrosarcoma cell line expressing only the vascular endothelial growth factor A (VEGFA)-188 isoform, isolated from *vegfa*$^{188/188}$ E13.5 embryonic fibroblasts transformed with simian virus 40 and Harvey rat sarcoma virus oncogene (English et al., 2017). These two cell lines were used since they are mouse pleomorphic tumours comparable to our STS cells rather than primary mouse fibroblasts. Xenograft tissues were co-stained with human-specific (MT-AB) and transgelin antibodies to count cancer (positive) versus tumour (negative) cells.

4.4.1 Characterisation of mouse cell line morphology and staining for human mitochondrial antibody (MT AB)
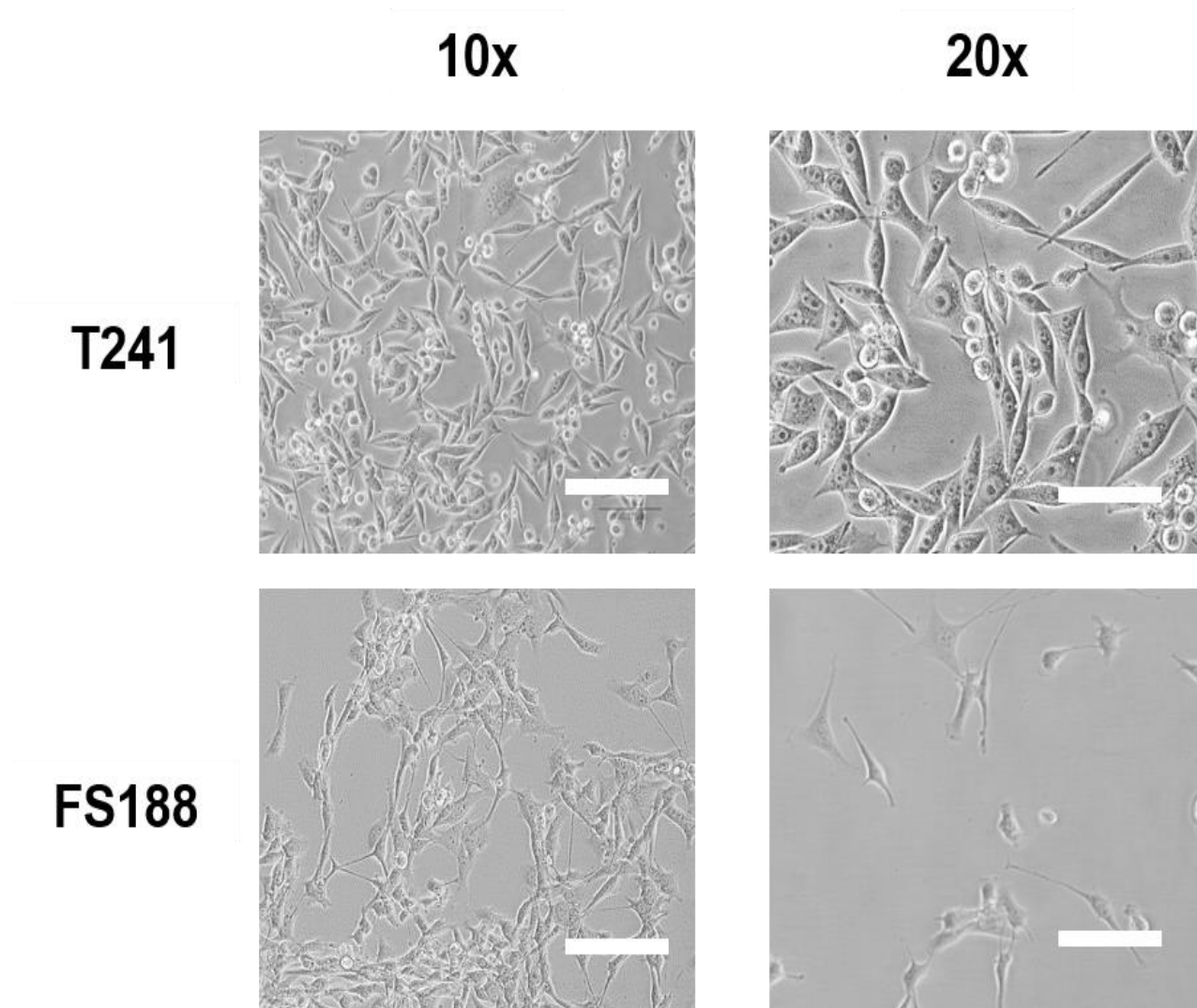
Figure 4. 20: Illustrative phase-contrast images of T241 and FS188 cells.

Scale bars denote 100 µm (10X magnification) and 50 µm (20X magnification).

4.4.2 Staining with the human mitochodrial antibody (Mt AB)

This project used two mouse cell lines to differentiate between human and mouse cells based on ICC and IF fluorescence staining. The two mouse fibrosarcoma cell lines, T241 and FS188, showed spindle-shaped morphology under a light microscope (Fig. 4.20).

The anti-human Mitochondrial antibody (Mt AB) was applied to all primary fibroblasts, human mesenchymal stem cells (hMSC) and mouse FS188 and T241 to distinguish between human (positive) and mouse (negative) cells, and to study their subcellular localisation using ICC. MT-AB is a human cell marker localised to the mitochondria, nucleus, and cytoplasm in all primary fibroblasts (Chang et al., 2020). MT AB staining was negative in FS188 & T241 (Fig. 4.21, & Table. 4.1). Moreover, xenograft sections co-stained for transgelin and MT-AB confirmed that MT AB could be used to distinguish human from mouse cells in xenografts. All UPS xenografts contained MT AB-positive cells (stained red; Fig. 4.22). MT AB staining was quantified, showing that UPS4 had fewer MT AB-positive cells than UPS2 and UPS3 (Fig.4.22B). The colocalisation of transgelin and MT-AB was assessed using Pearson's correlation coefficient (PCC) (r), as described in Section 3.6. The mean colocalisation coefficient was calculated for UPS2 ($r = 0.786$), UPS3 ($r = 0.750$), and UPS4 ($r = 0.730$; Fig. 4.22C.).

Mitochondrial AB	Subcellular localisation	NHDF	hMSC	HUF	HPF	FS188	T241
	Cytoplasmic	√	√	√	√	x	x
	Nucleus	x	x	x	x	x	x

Table 4. 1: Subcellular localisation of MT AB in human fibroblasts.

The table showing the subcellular localisation of mitochondrial antibody which shows cytoplasmic localisation in NHDF,hMSC, HUF & HPF. However, both FS188 & T241 don't express the antibody.
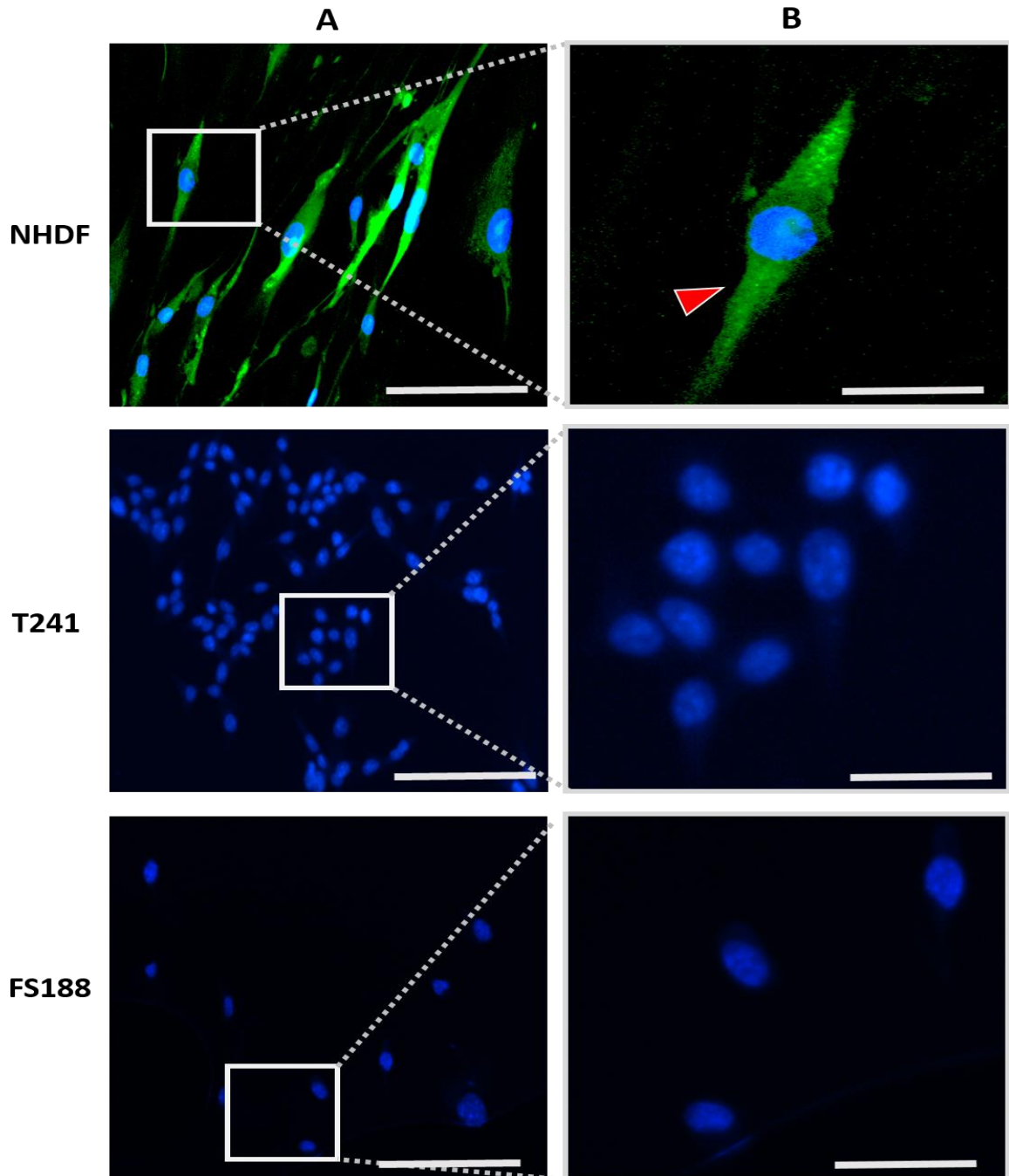
Figure 4. 21: Representative ICC images of human MT AB staining.

Mt AB localised to the cytoplasm (red arrows) in NHDF, while there is negative staining for MT AB in T241 and FS188. The nuclei are stained blue with DAPI and MT AB staining is green. **(A)** Scale bar = 100µm. **(B)** Scale bar = 50 µm. All images were taken at 20X magnification.

A | **Merged+DAPI** | **MT AB**

UPS2

UPS3

UPS4
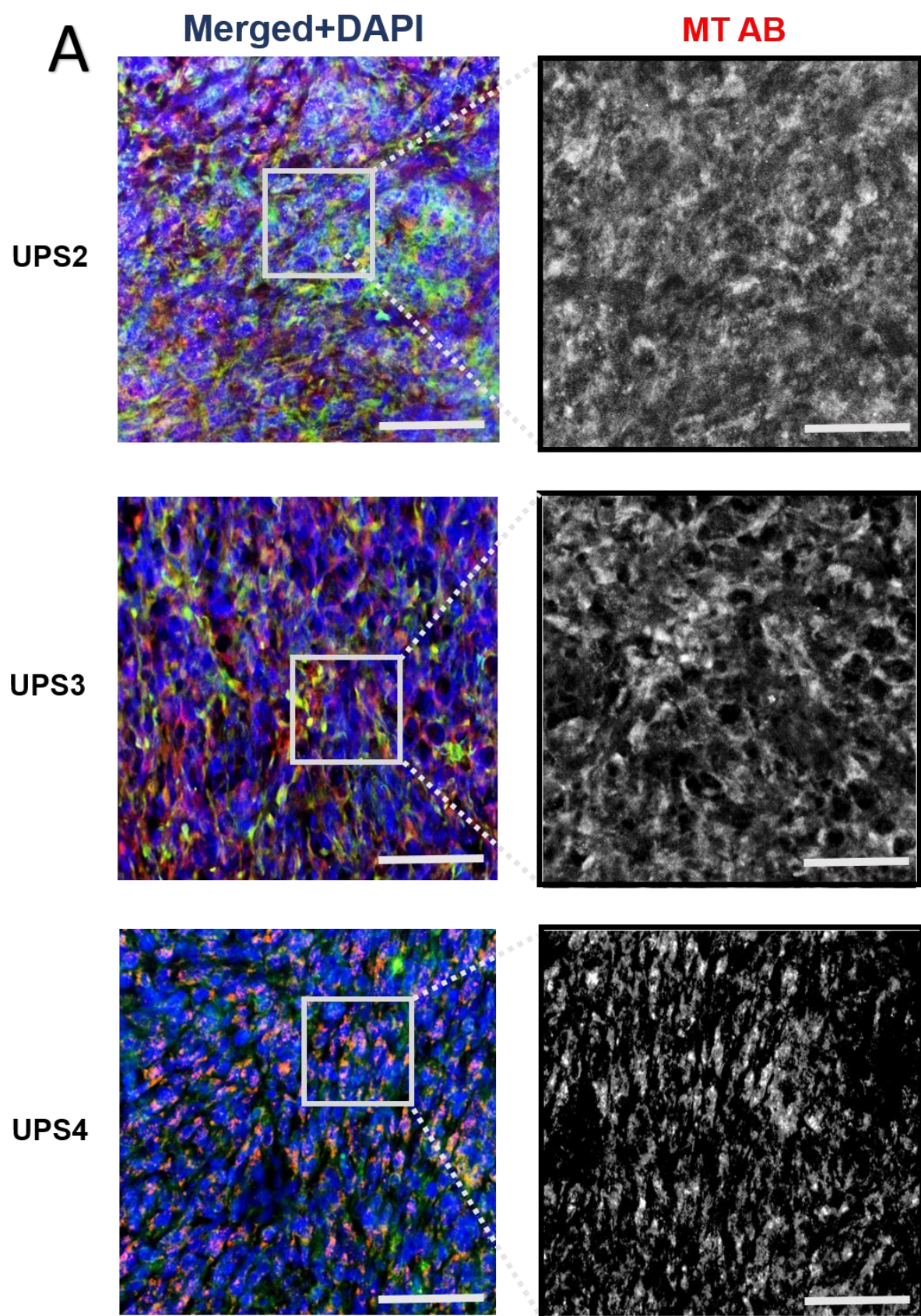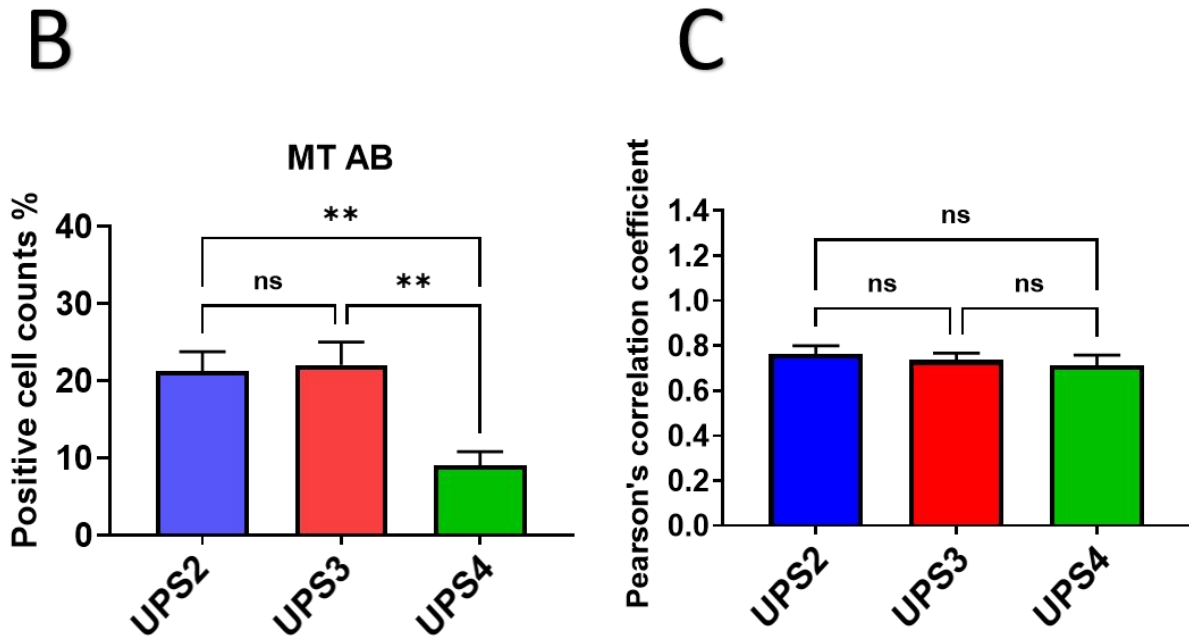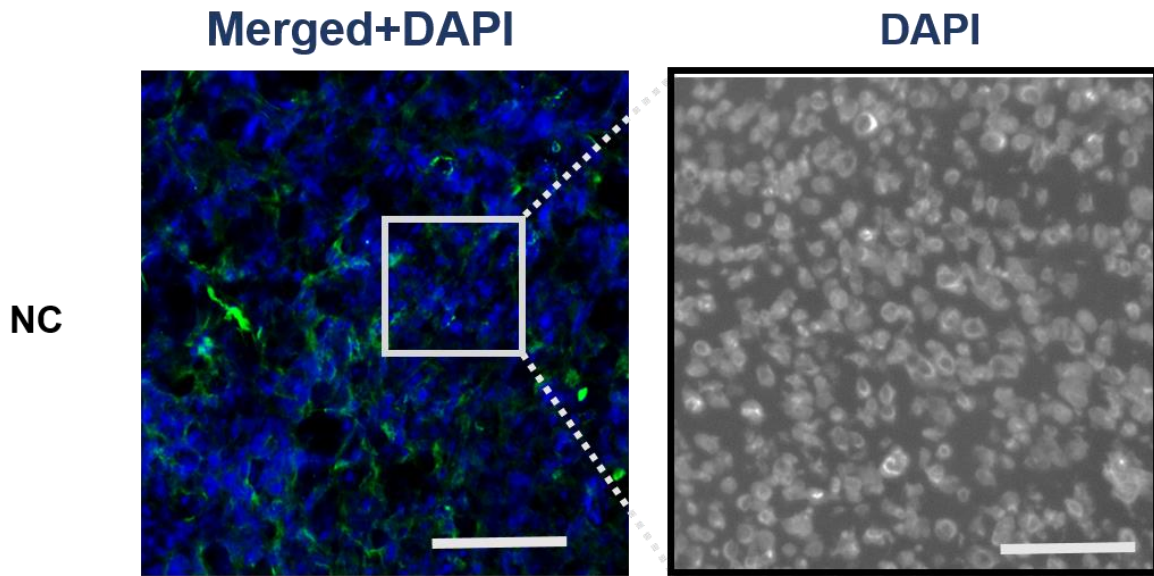
Figure 4. 22: IF co-staining of transgelin and MT AB in xenografts.

(A) Transgelin and Mt AB stained xenografts (scale bar=100μm) and magnified images for respective xenografts (scale bar 20μm). The nuclei are stained blue with DAPI, transgelin is stained green and MT AB is stained red. (B) Bar chart of MT AB positivity percentages. (C) Bar chart of colocalisation coefficients between transgelin and MT AB. Key: *, $P < 0.05$; **, $P < 0.01$; ***, $P < 0.001$; ns, not significant; NC, negative control. Error bars denote ± SEM.

4.4.3 Colocalisation of CD31 and αSMA for analysis of pericyte coverage

αSMA was co-stained with CD31 using IF to quantify pericyte coverage on vessels. Pericyte coverage is crucial for vasculature function, a strong indicator of tumour progression (Natarajan et al., 2022). Pericyte coverage is a factor in tumour angiogenesis. Abnormal pericyte coverage has been associated with various tumour outcomes. High pericyte coverage was associated with poor outcomes in melanoma and renal cancers (Gee et al., 2003). Low pericyte coverage was associated with enhanced metastasis (Cooke et al., 2012).

Tumour pericytes express various markers including αSMA, platelet-derived growth factor beta receptor (PDGFRβ), desmin and chondroitin sulfate proteoglycan 4 (CSPG4)/NG2(Ribeiro & Okamoto, 2015). In this experiment, αSMA was co-stained with CD31. Its colocalisation indicates a physical interaction between pericytes and endothelial cells (Natarajan et al., 2022).

αSMA and CD31 colocalisation was assessed using Pearson's correlation coefficient (r), as explained in Section 3.6. Their colocalisation was separately assessed in all three sections, UPS2 (r = 0.612), UPS3 (r = 0.788), and UPS4 (r = 0.598) sections. Colocalisation did not differ significantly among the xenografts (Fig. 4.23C). Moreover, the number of pericyte-positive vessels identified by CD31 staining did not differ significantly among the three xenografts (Fig. 4.23B).

Merged+DAPI   **CD31**

A

UPS2

UPS3

UPS4
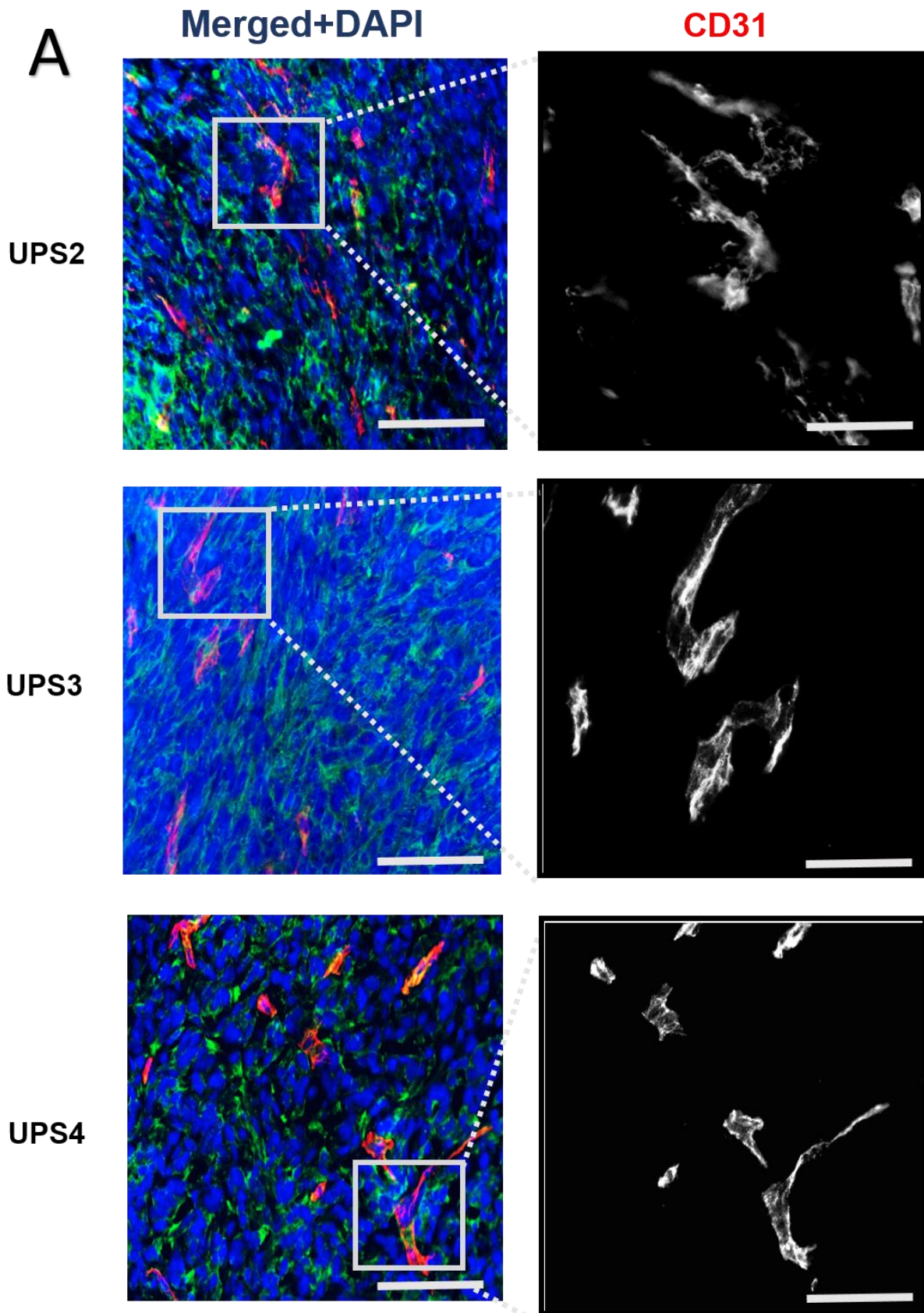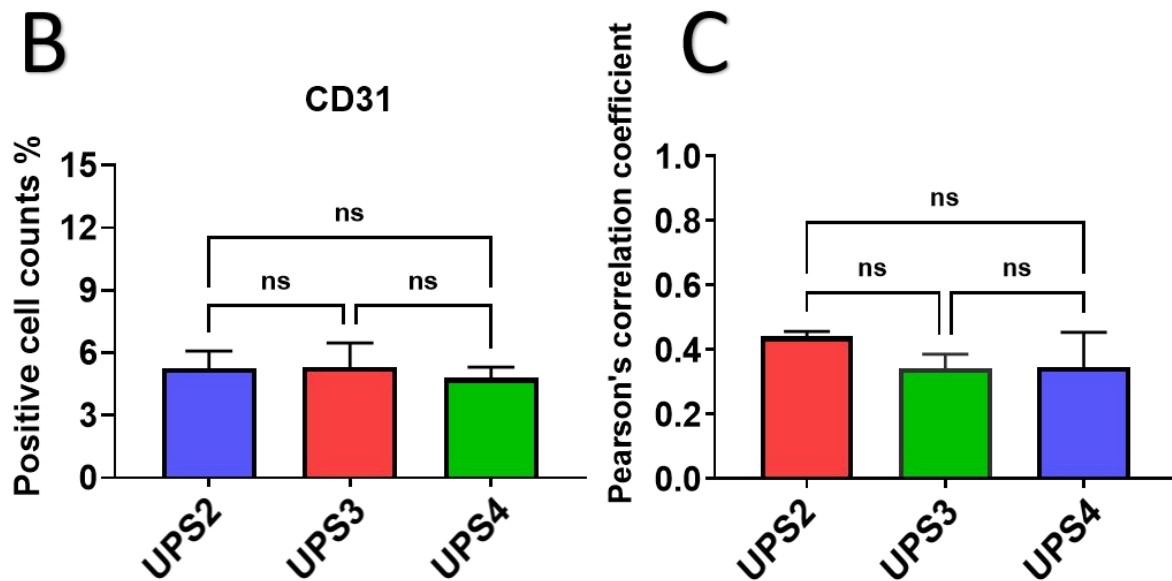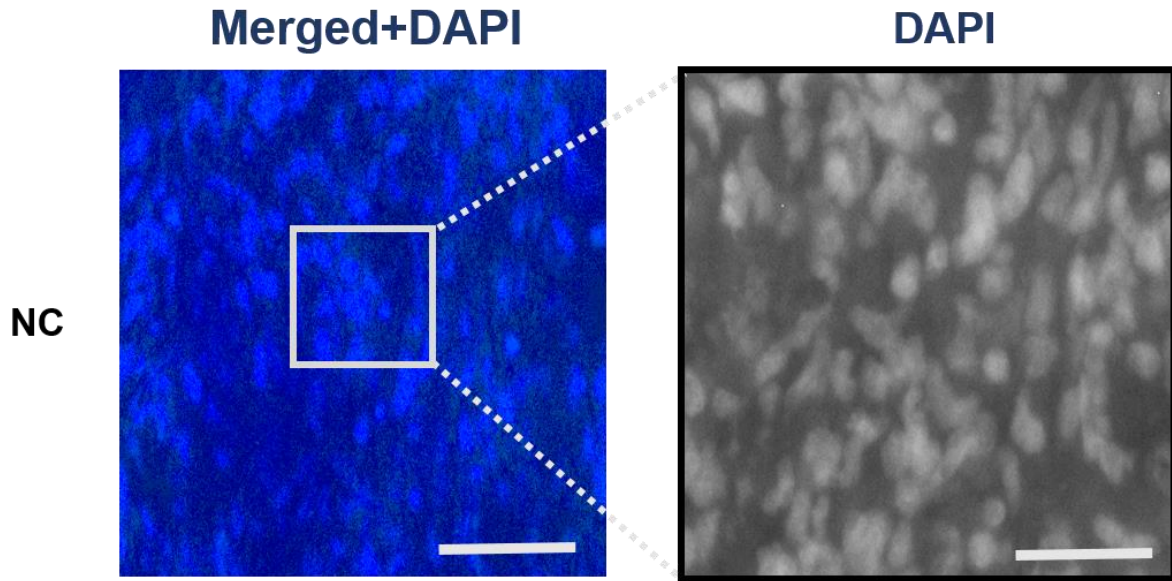
Figure 4. 23: IF co-staining of αSMA and CD31 in Xenografts.

(A) αSMA and CD31 co-staining in xenografts (scale bar =100μm) and magnified images for respective xenografts (scale bar =20μm). The nuclei are stained blue with DAPI, αSMA is stained green and CD31 is stained red. (B) Bar chart of pericyte positive vessels identified by CD31. (C) Bar chart of colocalisation coefficient between the xenografts. Key: *, $P < 0.05$; **, $P < 0.01$; ***, $P < 0.001$; ns, not significant; NC, negative control. Error bars denote ± SEM.

4.4.4 Colocalisation analysis of F4/80 with FSP-1 and FAPα

FSP-1 is a fibroblast marker also expressed by other cell types, including inflammatory macrophages found in cirrhosis and cancer. The F4/80 antigen has been widely used in mice as a specific macrophage marker (Österreicher et al., 2011). FAPα is used as a CAF marker but is also expressed by various other cells, including tumour-associated macrophages (TAMs) (Arnold et al., 2014; Muliaditan et al., 2018).

We first calculated the number of F4/80 positive cells in each xenograft. The number of F4/80-positive cells did not differ significantly among the three xenografts (Figs. 4.24B and 4.25B).

Next, FSP-1 and FAPα were co-stained with F4/80 to distinguish fibroblasts and mesenchymal cells from macrophages in tumour sections. The mean percentage of F4/80-positive cells that were FSP-1-positive was 47.6% with UPS2, 36.7% with UPS3, and 38% with UPS4. The mean percentage of F4/80-positive cells that were FAPα-positive was 53% with UPS2, 34.3% with UPS3, and 41% with UPS4 (Figs. 4.24C and 4.25C).

Merged+DAPI   **F4/80**

A

UPS2

UPS3

UPS4
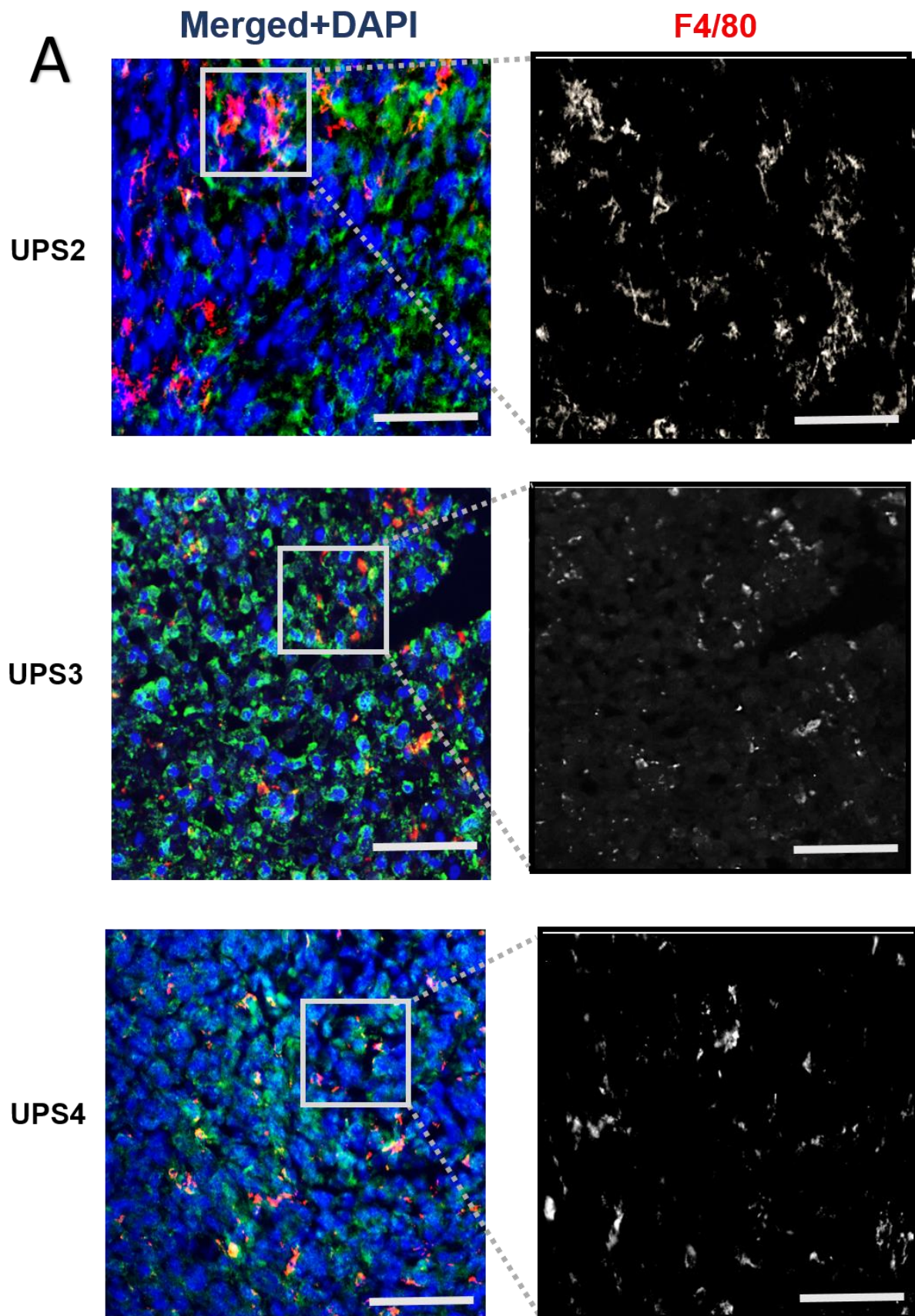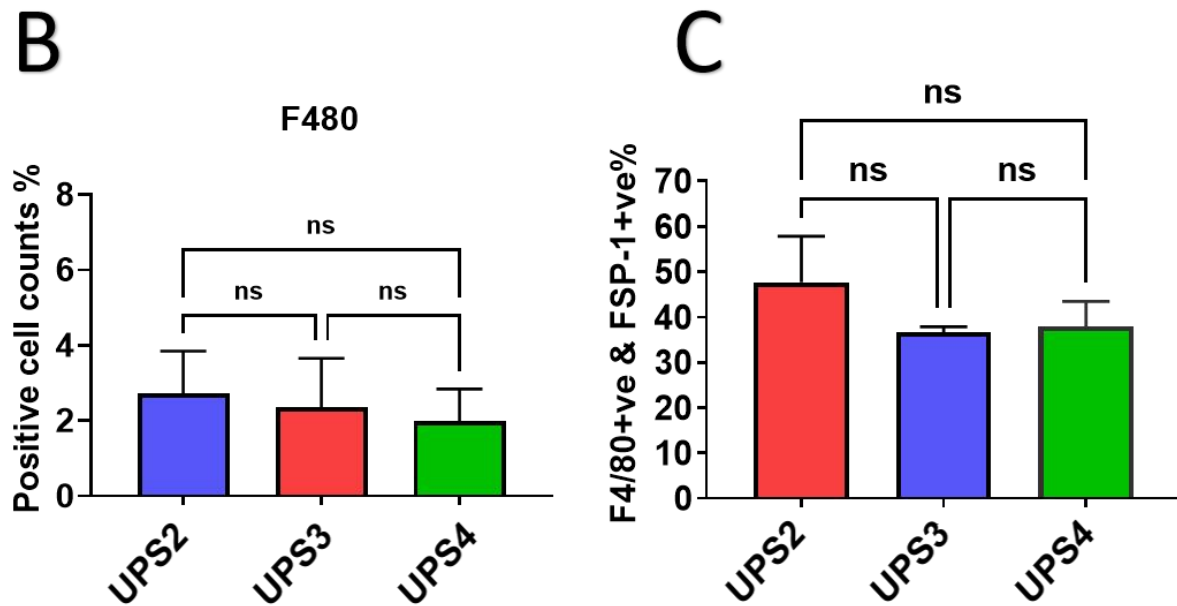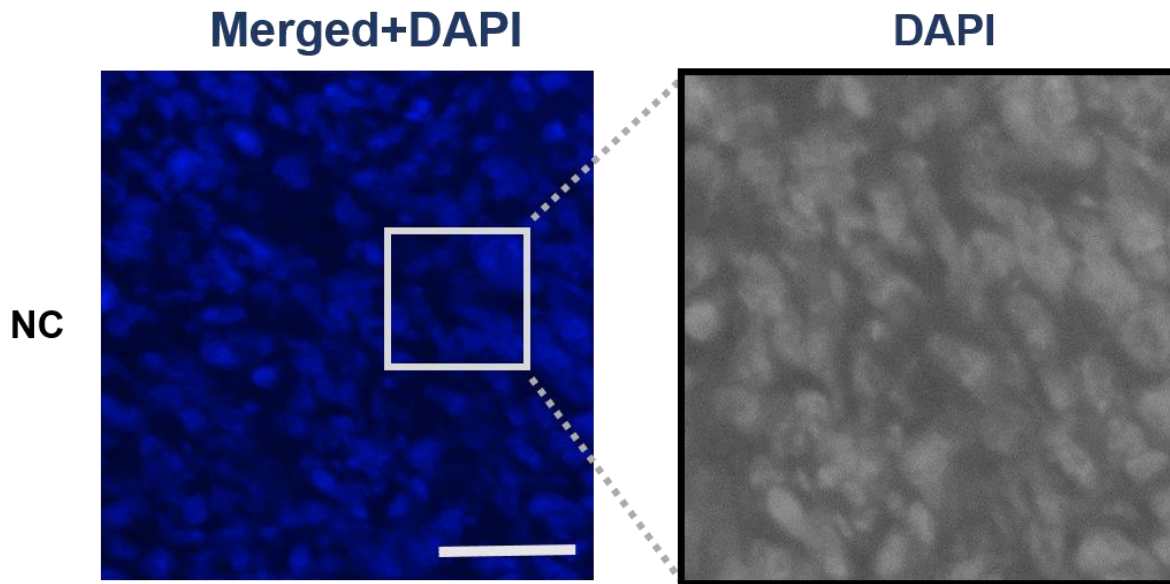
Figure 4. 24: IF co-staining of FSP-1 and F4/80 in xenografts.

(A) FSP-1 and F4/80 co-staining in xenografts (scale bar =100μm) and magnified images for respective xenografts (scale bar 20μm). The nuclei are stained blue with DAPI, FSP-1 is stained green and F4/80 is stained red. (B) Bar chart of F4/80 positive cells. (C) Bar chart of F4/80+ve FSP-1 +ve cells percentages. Key: *, $P < 0.05$; **, $P < 0.01$; ***, $P < 0.001$; ns, not significant; NC, negative control. Error bars denote ± SEM.

A   Merged+DAPI   F4/80

UPS2

UPS3

UPS4
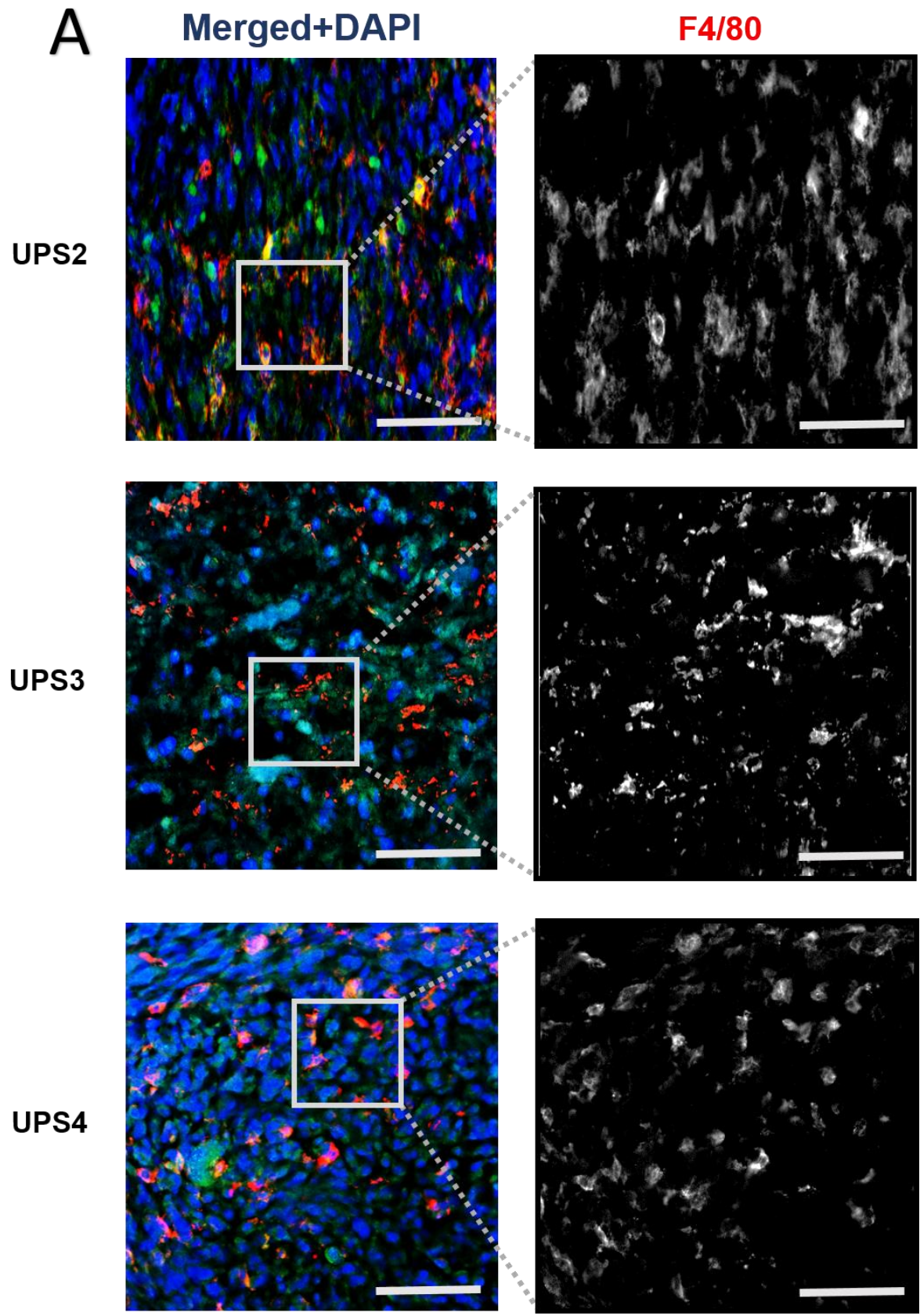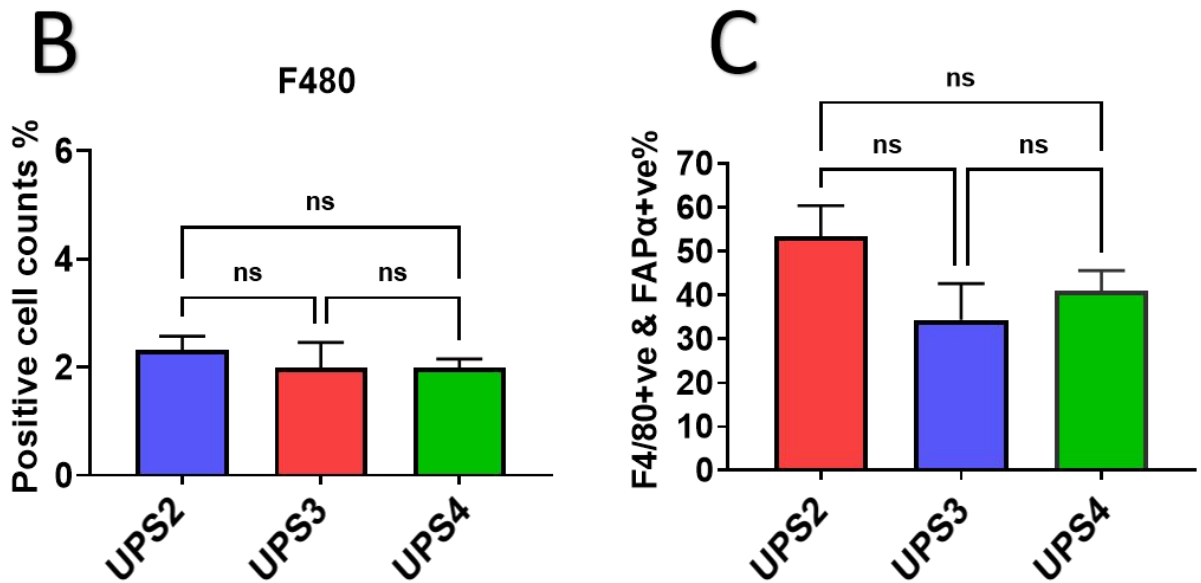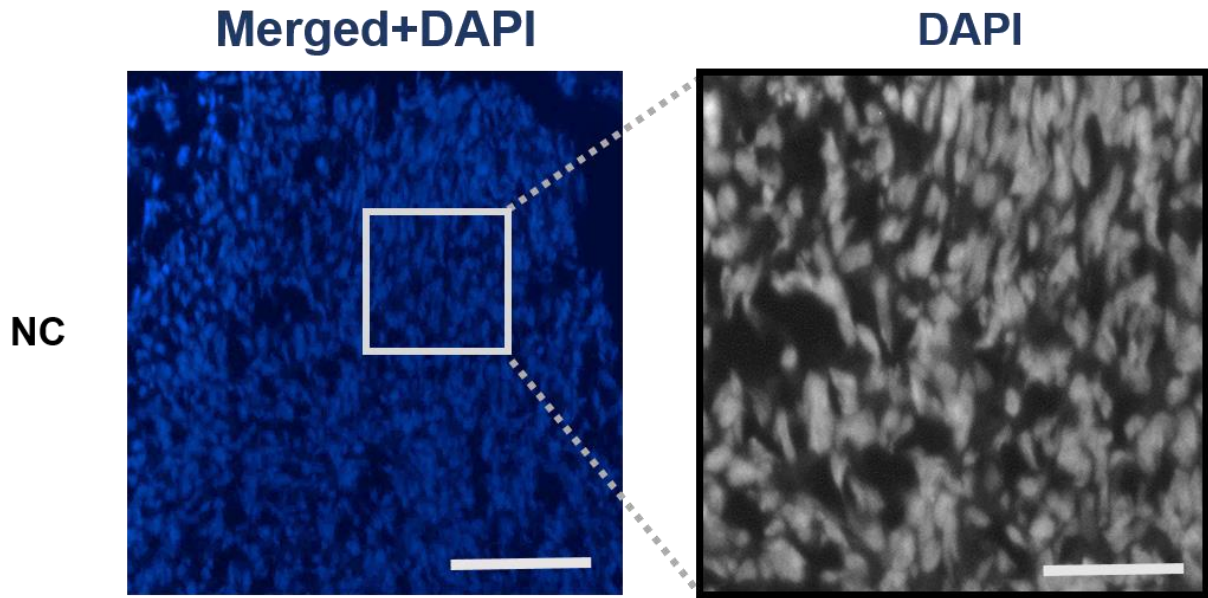
Figure 4. 25: IF co-staining of FAPα and F4/80 in Xenografts.

(A) FAPα and F4/80 co-staining in xenografts (scale bar = 100μm) and magnified images for respective xenografts (scale bar = 20μm). The nuclei are stained blue with DAPI, FAPα is stained green and F4/80 is stained red. (B) A bar chart of F4/80 positive cells. (C) A bar chart of F4/80+ve FAPα+ve cells percentages. Key: *, $P < 0.05$; **, $P < 0.01$; ***, $P < 0.001$; ns, not significant; NC, negative control. Error bars denote ± SEM.

4.4.5 Selection of UPS tumours for RNAseq

Out of the 16 xenografts created, we selected 12 for RNAseq, four from each cell line. Following the necrosis and MVD scoring, RNA was extracted from the frozen sections, as described in Section 2.4.2. RNA concentration and quality were determined using a NanoDrop spectrophotometer 1000 UV-Vis system, as described in Section 2.4.2.1. Moreover, the RNA integrity number (RIN) was obtained from an Agilent Bioanalyser. We aimed to select the least necrotic tissues with the lowest MVDs. However, since necrosis and MVD did not differ significantly across samples (Figs. 4.2 and 4.3), they were chosen based on their quality (RIN ≥9.1; 260/280 ≥1.97; 260/230 ≥2.0; Table.4.2).

Cell Lines	Necrosis	MVD	RNA(ng/µl)	260/280	260/230	RIN	Agilent(ng/µl)
UPS2	29%	5%	41.6	2.02	2.1	9.1	47
UPS2	13%	6%	172.8	2.1	1.88	9.3	246
UPS2	19%	6%	54.9	2.07	2.24	9.2	61
UPS2	34%	7%	71.5	2.2	2.15	9.3	67
UPS3	36%	5%	38.7	2.16	2.65	9.8	41
UPS3	47%	6%	37.2	2.08	1.94	9.4	63
UPS3	29%	5%	231.3	2.11	1.94	9.5	211
UPS3	42%	3.2%	159.9	2.11	2.19	9.2	155
UPS4	35%	2%	35.8	1.97	2.75	9.5	54
UPS4	32.40%	7%	57.1	2.09	1.82	9.8	58
UPS4	33%	5%	52.4	2.06	1.98	9.6	68
UPS4	37.40%	5%	22	1.96	2.19	9.3	33

Table 4. 2: UPS samples sent for RNAseq.

The table demonstrating necrosis, MVD percentages and RNA conentrations.

4.5 Conclusions

In this chapter, three UPS cell lines grew in mice, addressing one aim of this study. A pilot study was performed to investigate the growth of four UPS cell lines as xenografts in mice, of which three grew (UPS2, 3, and 4); UPS1 did not grow.

Following their western blot analysis in the previous chapter, a comparison of eight common mesenchymal protein levels was made between xenografts using IHC and IF methods. IHC was performed on FFPE sections, while IF was performed on frozen sections. Differentiating between cancer and stromal cells was impossible based on nuclear size and intensity using QuPath segmentation. Cancer cell nuclei are expected to be bigger than stromal cell nuclei (Salawu et al., 2016). However, the program may be limited in segmenting based on these parameters, with the similarity between tumour and stromal cell nuclei making it unable to differentiate them. Therefore, detecting differences in mesenchymal protein levels between STS and mouse stromal cells was impossible.

Nevertheless, IHC-based comparisons of global protein levels showed no significant differences in the tested proteins among xenografts. While IHC is an inexpensive method, comparisons in protein quantities between UPS and stromal cells were difficult to perform. While western blots in Chapter 3 showed that normal fibroblasts *in vitro* had higher transgelin and αSMA expression than STS cell lines *in vitro*, this could not be confirmed using IHC or IF. Therefore, we used RNAseq and the proper separation of human and mouse transcripts for analysis. Other methods, such as RNAscope or BASEscope, could be used to provide quantifications in different cells using mouse and human-specific transcript probes.

The quantities of eight common mesenchymal proteins were also compared among xenografts using IF. Again, no significant differences were observed for most proteins. However, vimentin showed higher levels in UPS4 than in UPS3 cells, and fibronectin showed higher levels in UPS2 than in UPS3 cells.

This project used two mouse cell lines, T241 and FS188 (see Section 2.1), to develop a method to distinguish human from mouse cells *in vitro* and xenografts. Using ICC, a human-specific antibody (MT-AB) was applied to mouse cell lines and human fibroblasts.

The results confirmed that MT-AB was human-specific since mouse cells were negative for staining. Then, the MT AB was co-stained with transgelin in UPS tumours using IF. UPS3 tumours contained fewer MT-AB-positive cells and had lower transgelin-MT AB colocalisation coefficients than UPS2 and UPS3. Therefore, UPS4 tumours have lower UPS cell line contents than UPS2 and UPS3 (Fig. 4.22B).

Pericyte coverage of blood vessel was determined by co-staining αSMA and CD31 using IF staining of UPS tumours. αSMA can be used as a tumour pericyte marker and CD31 as a blood vessel marker (Kim et al., 2020). CD31-positive vessel numbers did not differ significantly among UPS tumours. However, its colocalisation with αSMA tended to be weaker in UPS4 than in UPS2 and UPS3 tumours. Abnormal pericyte coverage of blood vessels impact tumour development. Higher pericyte coverage associated with poor outcome in renal cancer (Cao et al., 2013). Lower pericyte coverage was associated with lower overall survival and PFS in breast cancer patients (Cooke et al., 2012). As mentioned above, lower pericyte coverage in UPS4 tumours could reflect lower human UPS cell contents.

F4/80 is a cell surface glycoprotein and a known murine macrophage marker (Dos Anjos Cassado, 2017). The number of F4/80-positive cells did not differ significantly among UPS xenografts. However, F4/80 positivity was lower in UPS4 than in UPS2 and UPS3 tumours. Could that be an indication of lower macrophage content in UPS4 tumours? Further analyses will explore cell prediction in Chapter 5.

The numbers of F4/80-positive cells that were FSP1$^+$ or FAPα$^+$ were higher in UPS2 than in UPS3 and UPS4 tumours. So, higher macrophage abundance is expected in UPS2 tumours and will be further explored in Chapter 5. However, this indicates that many macrophages may be FAPα$^+$ or FSP$^+$1. Consequently, care must be taken when using these as markers for SAFs.

Finally, since UPS cells were feasible to grow and form tumours in mice, RNA from these tumours was isolated. The best samples were sent for RNAseq to identify mouse stromal mesenchymal gene transcripts by aligning RNAseq reads against the human and mouse reference genomes using the methods described in Bradford et al. (2013).

However, one limitation was that the UPS cell lines took a long time to grow, potentially due to subcutaneous injection. Could an orthotopic injection lead to faster growth?

Sixteen tumours were sectioned, and their RNA was extracted and subjected to quality assessment to select the best UPS tumours for RNAseq. IHC-based necrosis assessments and MVD scoring showed no significant differences between the three UPS tumours. Therefore, RNA was extracted from the frozen sections, and RNA quality was measured using a NanoDrop and Bioanalyser. After careful screening of four quality parameters, 12 UPS sections were sent for RNAseq (four sections from each tumour; Table 4.2).

Due to the limitations of IHC and IF methods, a more specific method was needed to characterise stromal genes in stromal and UPS cells. RNAseq is an evolving method that enables the quantification of genome-wide expression in xenografts.

Chapter 5

Characterisation of stromal gene expression identified by RNAseq.

5.1 Introduction

The tumour microenvironment (TME) is a complex environment composed of the tumour, stromal cells, immune cells, and non-cellular components, including the extracellular matrix (ECM) and secreted cytokines and growth factors (Hanahan & Weinberg, 2011). Cancer-associated fibroblasts (CAFs) are an abundant cell type found in the TME. They are activated fibroblasts with an elongated morphology that develop migratory characteristics and produce pro-tumorigenic cytokines and chemokines (Sahai et al., 2020). A number of mesenchymal proteins are used as CAF markers in different carcinomas, including αSMA, FSP-1, FAPα, PDGFRα/β, desmin, and vimentin (Kalluri, 2016b). However, less is known about specific markers in sarcoma for stromal mesenchymal cells, which we will refer to as sarcoma-associated fibroblasts (SAFs). Identifying specific markers for SAFs will help increase our understanding of the sarcoma TME.

Human tumour xenografts and cell line-derived xenografts (CDXs) are powerful methods of recapitulating the TME and represent an evolving area of research in cancer biology. Xenograft models were generated in our study by subcutaneously injecting UPS cell lines into immunodeficient mice. UPS cell lines were grown in mice, tumours were removed, and RNA was isolated from frozen tissues and underwent sequencing (Section 2.4.2).

RNA sequencing (RNAseq) is a high-throughput technique for transcriptomic analysis that facilitates the study of gene expression in xenografts. RNAseq was performed to identify stromal gene expression of mouse mesenchymal transcripts by aligning RNAseq reads against the human and mouse reference genomes using the methodology described by Bradford *et al.* (2013). Around 35 million reads were mapped separately to the human reference genome (GRC38/hg38) and mouse reference genome (GRCm38/mm10). Some reads will map to only human or mouse reference genome, however, some reads will map to both human and mouse reference genome. In order to distinguish human mRNA from mouse mRNA, we applied the species-specific mapping tool XenofilteR in R software to remove reads common to both transcriptomes (Kluin *et al.*, 2018). XenofilteR tool work by calculating the number of base pairs different between the sequences read and the reference genome which called "edit distance", then based on "edit distance"

XenofilteR will classify the sequence read as human or mouse (Kluin *et al.*, 2018). (Differential Expressed Genes (DEGs) tools in R were used to identify up/down-regulated genes in the xenografts and undifferentiated pleomorphic sarcoma (UPS)/ Myxofibrosarcoma (MFS) samples from the VorteX and The Cancer Genomic Atlas Sarcoma (TCGA-SARC) (Forker et al., 2017; Goldman et al., 2020).

5.1.1 Aim

- To grow STS cell lines as xenografts in mice to allow identification of stromal gene expression of mouse transcripts by aligning RNAseq reads against the human and mouse reference genomes.

- To identify STS and SAF specific gene expression profiles to improve our fundamental understanding of STS biology.

- To determine if expression of mesenchymal genes influence prognosis in UPS and MFS STS subtypes.

5.1.2 Experimental approach

- Pre-process the fastq files using Galaxy software, followed by aligning the reads to reference genomes and then gene expression analysis using R software.

- Survival analysis to study if expression of mesenchymal gene influence prognosis in clinical data.

5.2 Quality control and alignment of RNAseq data against universal, human and mouse reference genomes

RNAseq quality was assessed using FASTQ tools in Galaxy (Fig. S1). All samples were aligned against the "universal reference" which is human and mouse reference combined (hg38/mm10), the human (GRCh38/hg38) and the mouse (GRCm38/mm10) genomes. The pipeline is shown in Fig. 2.1, Section 2.12. The average of the count reads from each

sample was plotted, with an average of 35 million reads in all UPS xenografts, except for Sample 4, which had only 28 million reads (Fig. S2).

5.3 Global differences in gene expression between UPS xenografts after alignment against the universal reference genome

Unsupervised hierarchical clustering was performed using multi-dimensional scaling (MDS). MDS revealed greater variation in UPS4's replicates distribution compared with UPS2 and UPS3 (Fig. 5.1). Differential Expressed Genes (DEGs) analysis was performed using the Voom tool from the *Limma* packages in R software. Volcano plots showed the significant DEGs between UPS2 vs UPS4 and between UPS3 vs UPS4; however, no differences in DEGs were observed between UPS2 vs UPS3 (Fig.S 5.2 &Table 5.1). Venn diagram showed the overlap DEGs between xenografts (Fig. 5.3).
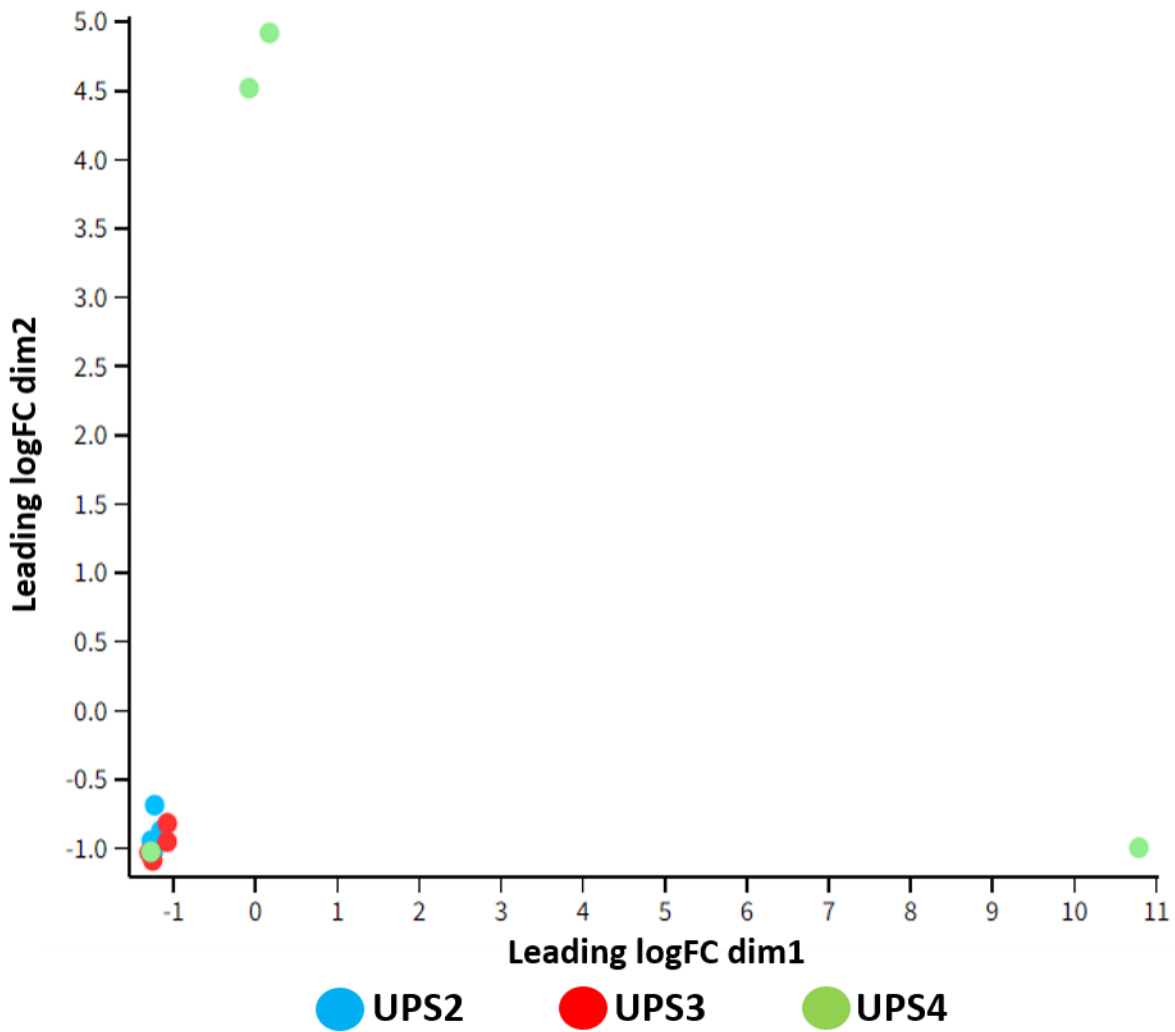
Figure 5. 1: MDS of the individual xenografts from each UPS cell line.

MDS plot is showing that UPS4 samples are clustered separately from UPS2 & UPS3 based on mRNA levels. **UPS2 is in blue**, **UPS3 is in red** and **UPS4 is in green**.

Table 5. 1: DEG between xenografts.

A table showing DEG between xenografts.
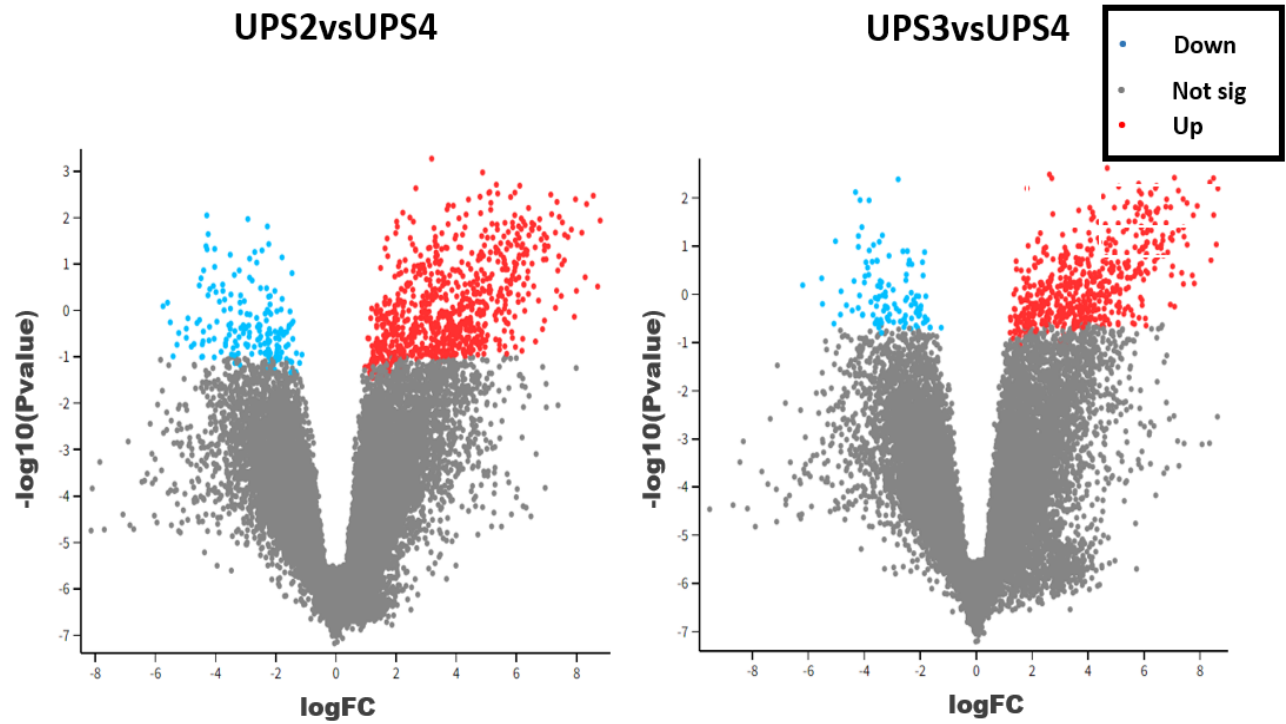
	UPS2vsUPS3	UPS2vsUPS4	UPS3vsUPS4
Down	1	1865	2432
Not sig	107534	103500	103131
Up	23	2193	1995

Figure 5. 2: Volcano plots for xenografts.

The logFC represents the change in gene expression between UPS2 and UPS4 or UPS3 and UPS4, while the p values indicates the level of significance of each gene. Each dot illustrates one gene. The cut-off criterion for DEG significance was FDR ≤ 0.05 and logFC of 1. **Blue dots represents down-regulated genes**, grey dots represents no significant differential expression genes **and red dots represents up-regulated genes.**

5.3.1 Biological process enriched in xenografts

Gene set enrichment analysis (GSEA) using the gene sets identified by the molecular signatures database (MsigDB), 15,906 genes were uploaded and GSEA identified the (4141) up- / (1832) downregulated genes in the xenograft transcriptomes. Only five of the most up/downregulated genes were mentioned in (Table S2). Moreover, it classified some biological processes as activated or suppressed. Examples of activated biological processes in both sets (UPS2 vs UPS4 and UPS3 vs UPS4) were cell morphogenesis, animal organ morphogenesis, neuron projection development, and plasma membrane region (Fig.5.4 & Fig.5.5). GSEA revealed that anatomical structure formation involved in morphogenesis was enriched in UPS2 vs UPS4 and UPS3 vs UPS4 sets. There were 1244 genes in this hallmark; 947 genes were upregulated, and 297 genes were downregulated. A study by Koh *et al.* (2022) revealed that genes enriched in the anatomical structure of morphogenesis were related to genes involved in angiogenesis, like *TEK* and *EFNA3*, which were enriched in UPS2 vs UPS4 (Koh *et al.*, 2022). Another four genes were enriched in UPS3 vs UPS4 that were linked to angiogenesis, such as *PIK3R3* and *EFNA3* (Koh et al., 2022). Genes associated with cerebellar Purkinje cell layer formation were suppressed in UPS2 vs UPS4. There were 14 genes in this hallmark; three (*AGTPBP1, TTLL1,* and *HERC1*) were enriched in UPS2 vs UPS4, while two (*FIAM2* and *TTC21B*) were downregulated. Genes associated with regulation of transforming growth factor beta (TGFβ) signalling were suppressed in UPS3 vs UPS4. There were 18 genes in this set; 12 were downregulated, including *CDKN2B* and *TGIF1*. TGFβ pathways are broadly associated with different biological processes, and suppressing the regulation of these pathways has been linked to tumorigenesis (Yang et al., 2021).
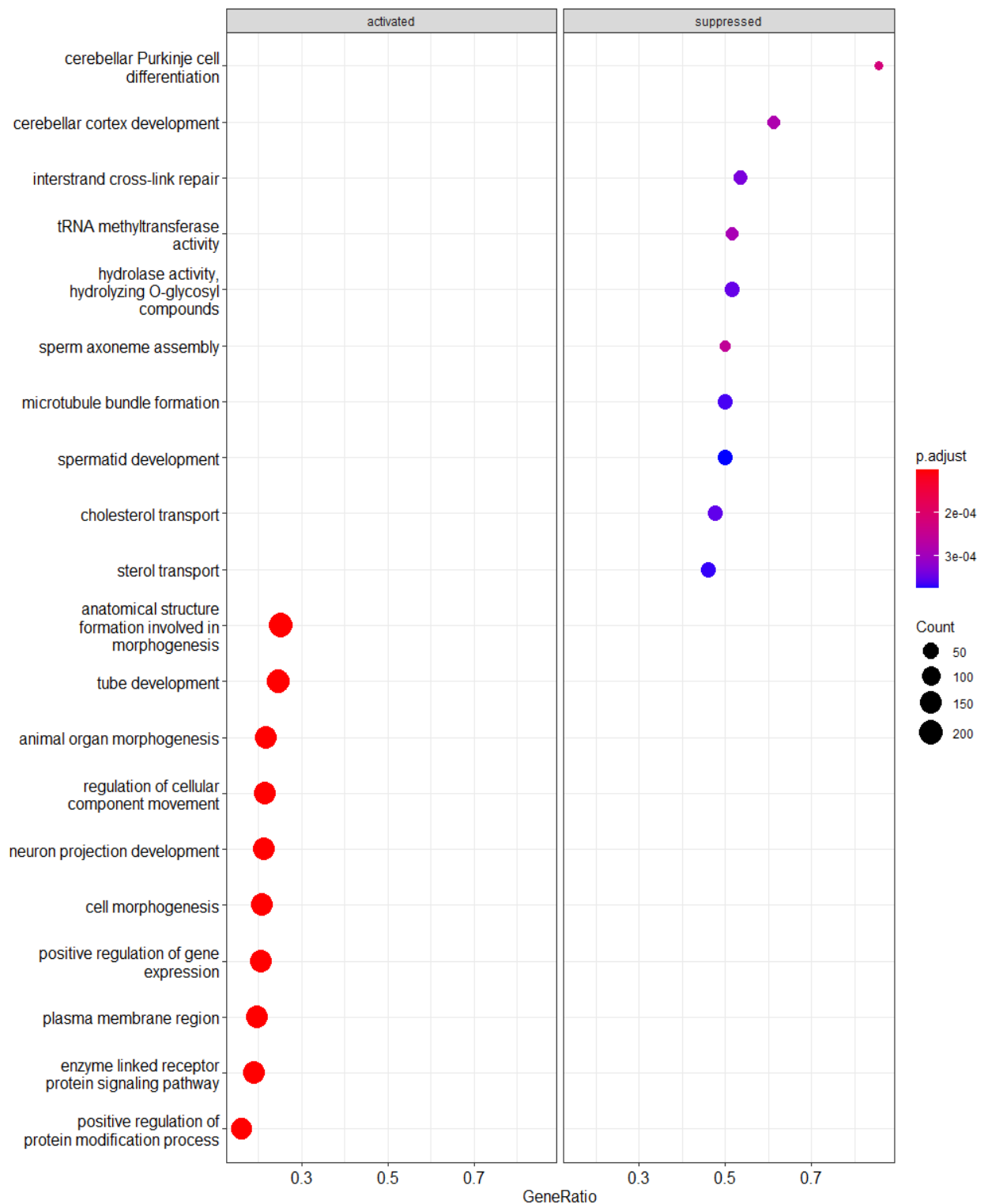
Figure 5. 3: Biological process enriched in UPS2 vs UPS4.

The hallmark gene sets (h.all.V7.1 MSigDB) shown above were significantly up/down-regulated in UPS2 samples .The cut-off criteria for significance was p-value ≤ 0.05.
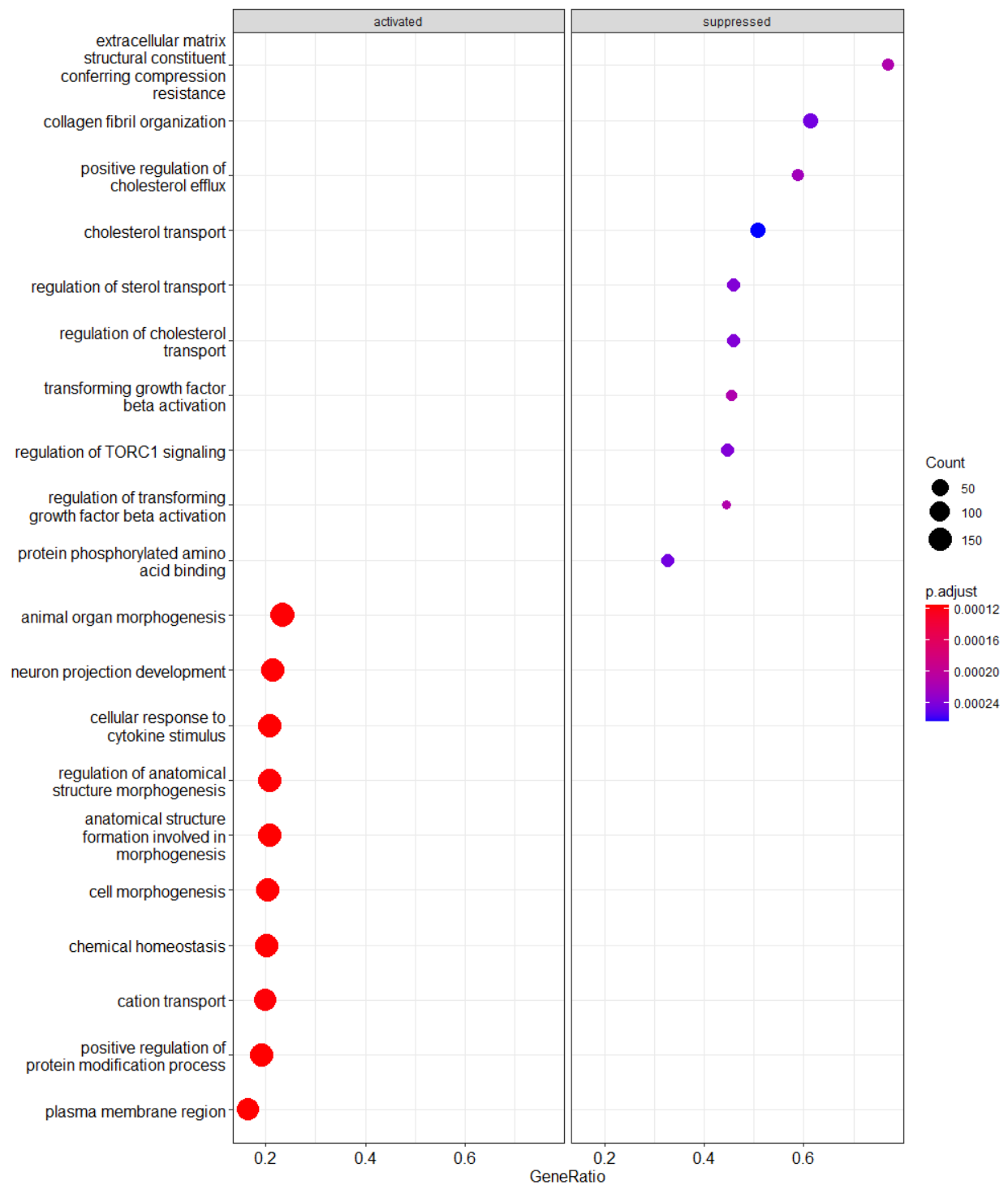
Figure 5. 4: Biological process enriched in UPS3 vs UPS4.

The hallmark gene sets (h.all.V7.1 MSigDB) shown above were significantly up/down-regulated in UPS3 samples. The cut-off criteria for significance was p-value ≤ 0.05.

5.3.2 Comparison of the transcriptome of UPS xenografts with clinical samples from VorteX and TCGA SARC

TCGA is a landmark collection of cancer genomic data (Thorsson et al., 2018). Genomic data have been widely used to study the TME in different cancer types (Thorsson et al, 2018). TCGA-SARC comprises soft tissue sarcomas, including: leiomyosarcoma (LMS), UPS, dedifferentiated liposarcomas (DDLP), myxofibrosarcoma (MFS), malignant peripheral nerve sheath tumour (MPNST), myofibroblastic sarcoma (MP) and synovial sarcoma (SS). The VorteX Biobank is a collection of clinical data and samples from the VorteX phase III trial in which adult extremity STS patients were randomised to groups that received different amounts of adjuvant radiotherapy to evaluate whether limb function could be increased by reducing the amount of adjuvant radiotherapy compared with administering adjuvant therapy to a wider area of tissue surrounding the tumour (standard care) (Forker et al, 2016). Our UPS xenograft RNAseq data were compared with clinical RNAseq data from TCGA-SARC and VorteX using MDS plots. As expected, the majority of UPS xenografts clustered with the clinical STS with complex karyotypes, including UPS and MFS, suggesting their transcriptomes are highly similar (Fig.5.6A & B).
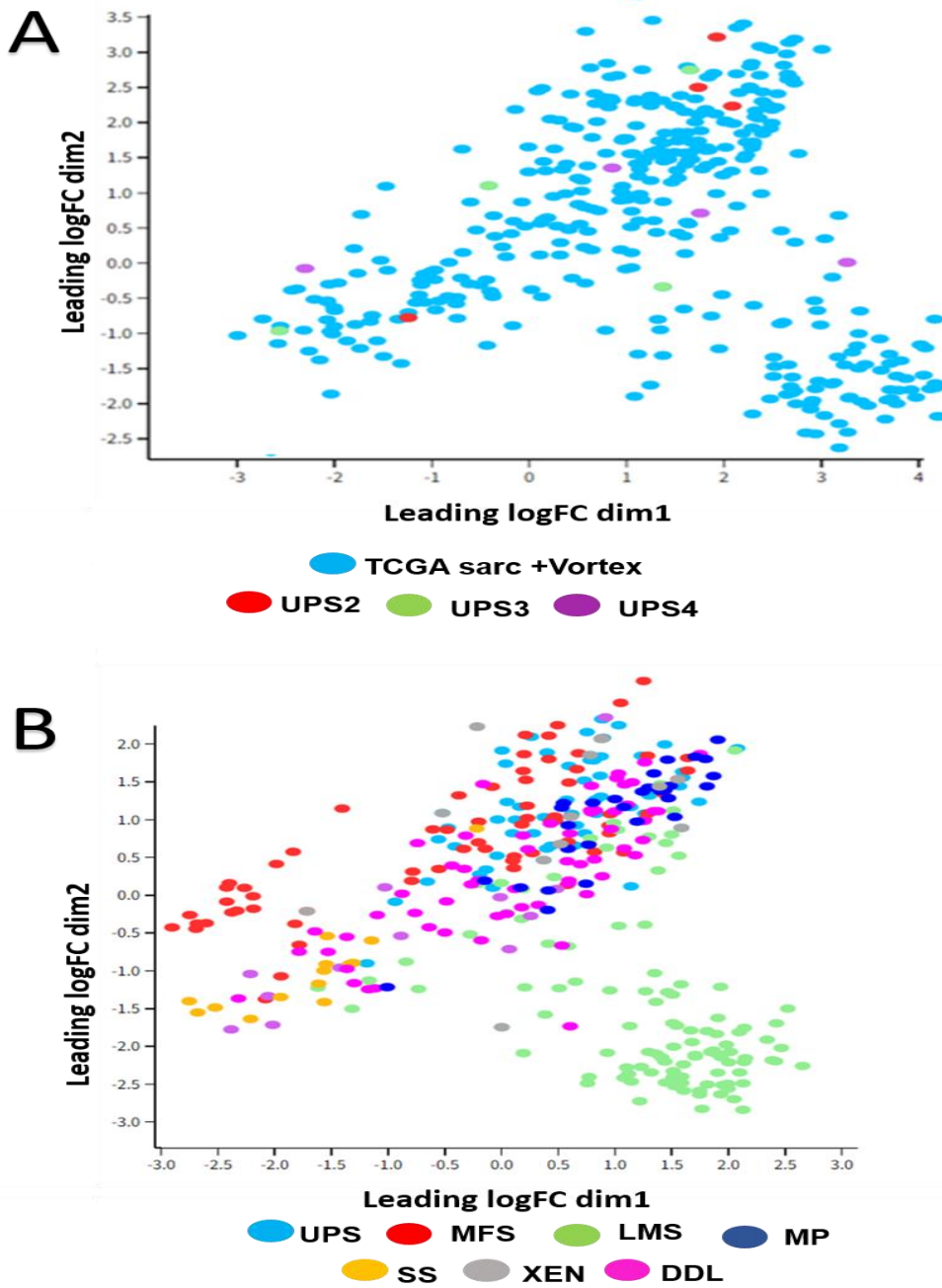
Figure 5. 5: MDS of the UPS human transcriptomes with TCGA and VorteX clinical transcriptomes.

(A) MDS plot is showing all clinical samples all in blue and UPS xenografts in red, green and purple. **(B)** MDS plot is showing the different clinical STS subtypes distributed across the plot with the xenografts (XEN) in grey. LMS, SS clustered separately from the UPS and MFS subtypes. UPS= undifferentiated pleomorphic sarcoma, MFS= myxofibrosarcoma, MS= leiomyosarcoma, MP= myofibroblastic sarcoma, SS= Synovial sarcoma, XEN= xenografts DDL=dedifferentiated Liposarcoma.

5.3.3 Differences in expression of mesenchymal genes commonly used to identify cancer associated fibroblasts in UPS xenografts

In this project's earlier chapters we studied eight CAFs markers and in this chapter we have expanded these studies to their expression in the transcriptome of our UPS xenografts including transgelin, αSMA, vimentin, N-cadherin, fibronectin,FSP-1, FAPα and SOX2. Statistical analysis showed no significant differences in gene expression between the three xenografts using the transcriptome generated from alignment with the universal reference genome (Fig.5.7).
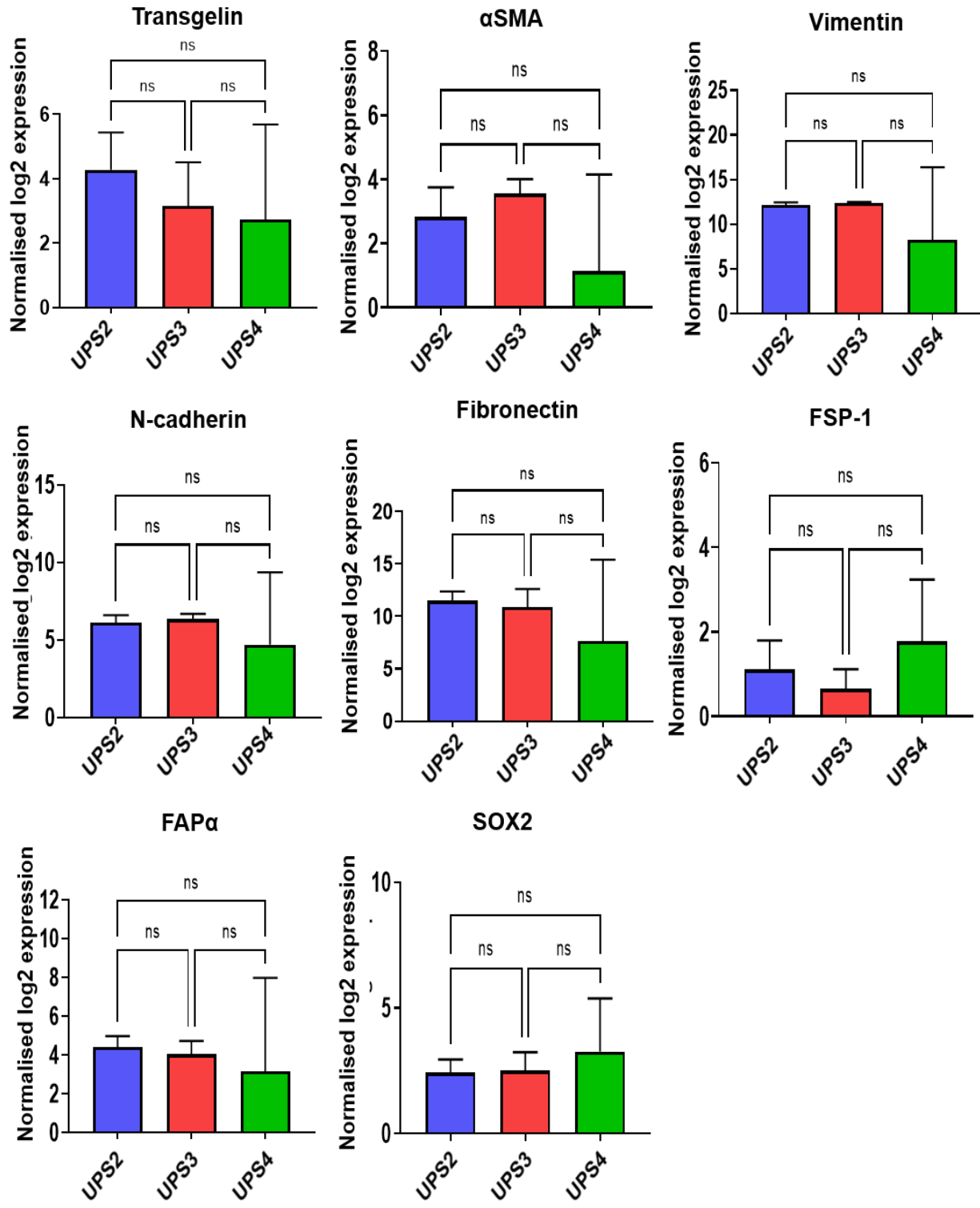
Figure 5. 6: Barchart analysis of the common mesenchymal gene expression in xenografts.

Statistical analysis shows no significant differences in gene expressions between the three xenografts. Error bars are ± SEM. *, P<0.05, **, P <0.01; ***, P < 0.001; NS, not significant.

There are more CAF markers that could be considered that were not in the initial eight examined in earlier chapters, and these were also studied in the transcriptome of the UPS xenografts. CAFs markers that are widely studied in the literature, like FAPα, αSMA, microfibril-associated protein (MFAP5), transgelin, collagen type XI alpha 1 chain (COL11A1), Tenascin-C (TN-C), podoplanin (PDPN), Integrin subunit alpha 11 (ITGA11), neuron glia antigen-2 (NG2) and desmin are highly expressed in CAFs in different carcinomas, while Platelet derived growth factor receptor alpha/beta (PDGFR α/β), vimentin, FSP-1, collagen type 1 alpha 1 and 2 (COL1A1, COL1A2) and periostin (POSTN) were also considered as fibroblasts markers (Nurmik et al., 2020). There were no significant differences in PDGFRα, PDGFRβ, MFAP5, NG2 and desmin gene expression between the three xenografts, however Tenascin-C showed lower expression in UPS4 when compared to UPS2 and UPS3 (Fig.5.8). TN-C is an extracellular matrix glycoprotein that plays an important role in cell proliferation, migration and higher expression of Tenascin-C was observed in inflammation, tissue repair and cancer (Midwood & Orend, 2009).
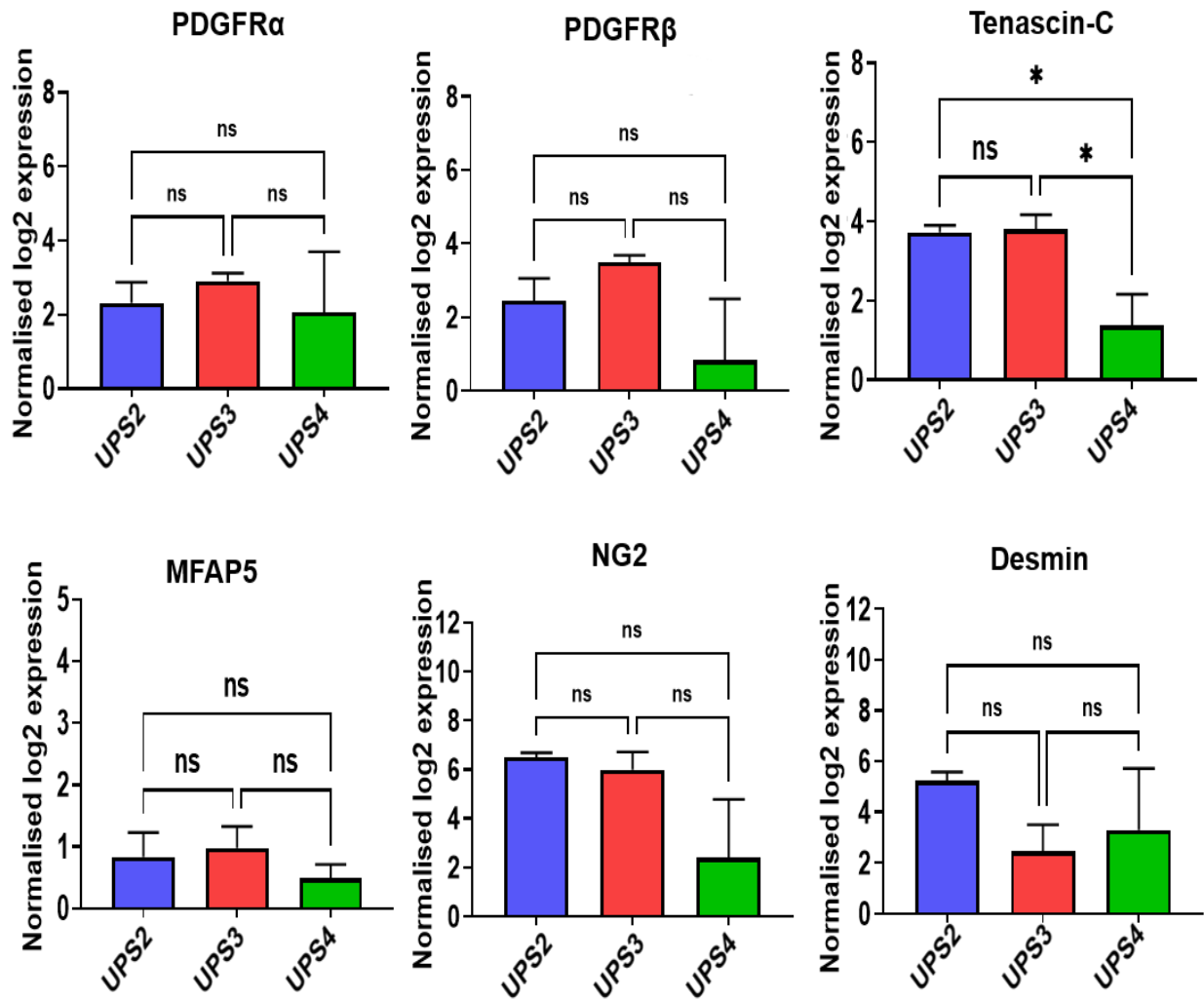
Figure 5. 7: Barchart analysis of the common CAFs gene expression in xenografts.

Statistical analysis shows no significant differences in gene expressions between the three xenografts. Error bars are ± SEM. *,P<0.05 , **,P <0.01; ***,P < 0.001 ;NS, not significant.

5.3.4 Cell population prediction in UPS xenografts using transcriptomic data derived from alignment against the universal reference genome.

As the TME is composed of different cell types, including immune and non-immune cells, cell population predictions were investigated to explore differences between the xenografts. We evaluated 16 immune and non-immune cell types using xCell software (Section 2.12.6). xCell uses GSEA results and linearises the enrichment score to identify the cells enriched in our samples. The cut-off was a cell score ≥0.001(Aran et al., 2017). Any score below this cut-off was considered an absence of the cells in our samples (Aran et al., 2017).The evaluation predicted UPS4 to be higher in pericytes, skeletal muscle, smooth muscle, lymphatic endothelial cells, and fibroblasts and significantly higher in haematopoietic stem cells (HSCs) (Fig. 5.9).

Furthermore, mesenchymal stem cells (MSCs) were predicted to be significantly lower in UPS4 compared with UPS2 and UPS3. However, this result was negligible as the cell score was <0.001. Although the difference was not statistically significant, UPS2 tended to have higher predicted levels of total macrophages and M1-polarised macrophages than UPS3 and UPS4 (Fig. 5.9).

In order to identify unique genes for each cell subset to understand why these cell subsets were predicted to be enriched, we used published gene set prediction for each cell type from single cell RNA sequencing (snRNA-seq) analysis because the list of genes in the xCell prediction algorithm, although proprietary, is based on these. Three pericyte genes were enriched in UPS2 vs UPS4 and UPS3 vs UPS4, including myosin heavy chain 11 (MYH11), which is a kidney pericyte-specific marker, platelet-derived growth factor receptor beta (PDGFRβ), which is a lung, heart, kidney, and bladder pericyte marker, and Purkinje cell protein 4-like protein 1 (PCP4L1), which is kidney- and bladder-specific marker (Baek et al., 2022). Two skeletal muscle cell genes were enriched in our xenografts; chemokine ligand 14 (CXCL14) and paired box protein (PAX7) (De Micheli et al., 2020). Four smooth muscle genes were enriched: desmin, MYH11, regulator of G protein signalling 5 (RGS5), and actin gamma 1 (ACTG1) (Lee et al., 2015). Three lymphatic endothelial cell genes were enriched: podoplanin (PDPN), Fms-related tyrosine kinase 4 (FLT-4), and mucosal vascular addressin cell adhesion molecule 1 (MADCAM-

1) (Fujimoto et al., 2020). Two HSC genes were enriched: protein C receptor (PROCR) and cathepsin F (CTSF) (Forsberg et al., 2010). Two endothelial cell genes were upregulated: C-X-C motif chemokine ligand 2 (CXCL2) and claudin 5 (CLDN) (De Micheli et al., 2020). One MSC gene was enriched: S100A4 (or FSP-1) (Weng et al., 2011). Three fibroblast genes were upregulated: microfibril-associated protein 5 (MFAP5), SPARC-like 1 (SPARCL1), and TGFβ (Dinh et al., 2021; Guerrero-Juarez et al., 2019). Two genes associated with M2-polarised macrophages were enriched: C-C motif chemokine ligand 8 (CCL8) and secreted phosphoprotein1 (SPP1) (Dinh et al., 2021). Two M1 macrophage genes were enriched: SPP1 (which is also a marker for M2) and dehydrogenase/reductase 3 (DHRS3) (Zhuang et al., 2020). Three total macrophage-associated genes were enriched: Fas cell-surface death receptor (FAS), apolipoprotein C1, and apolipoprotein L2 (Chai et al., 2018).
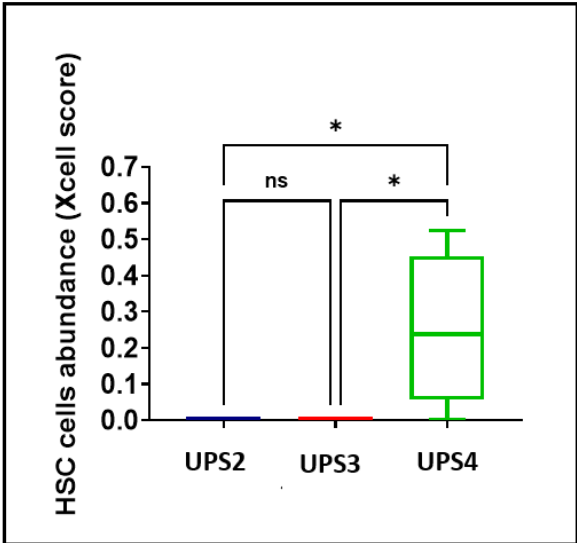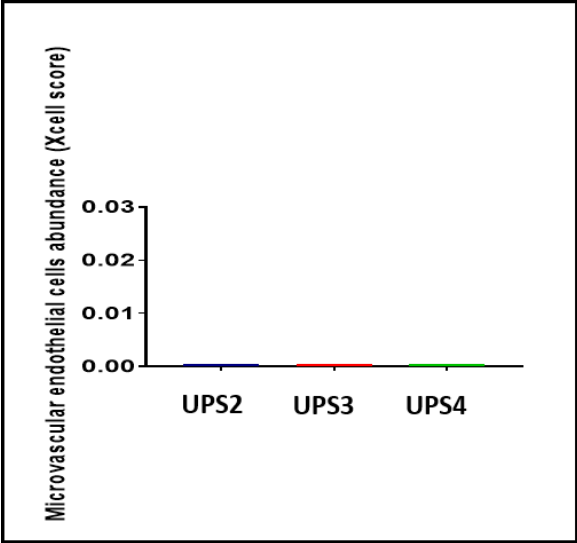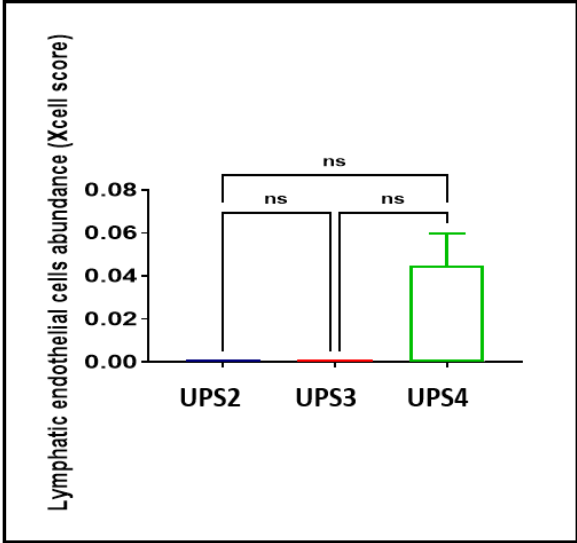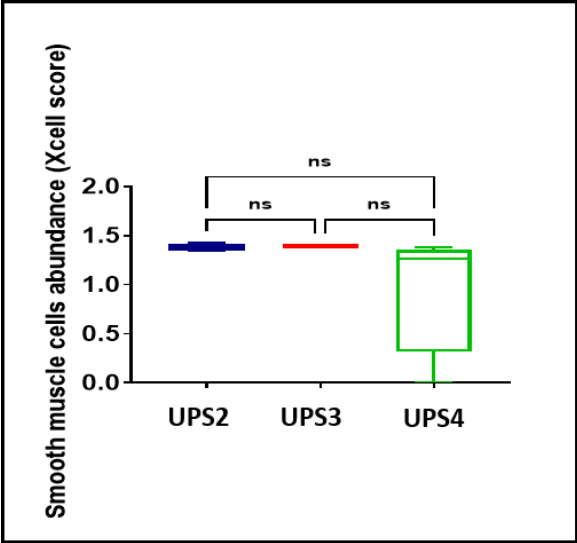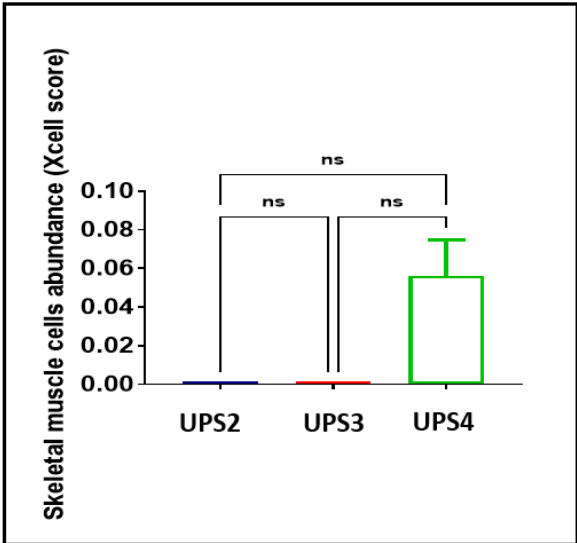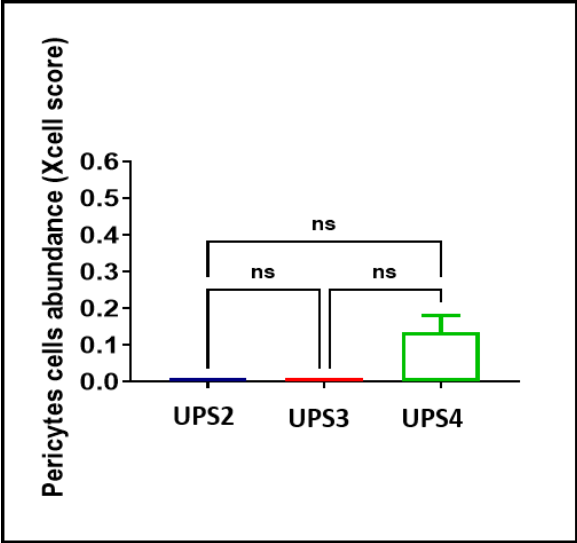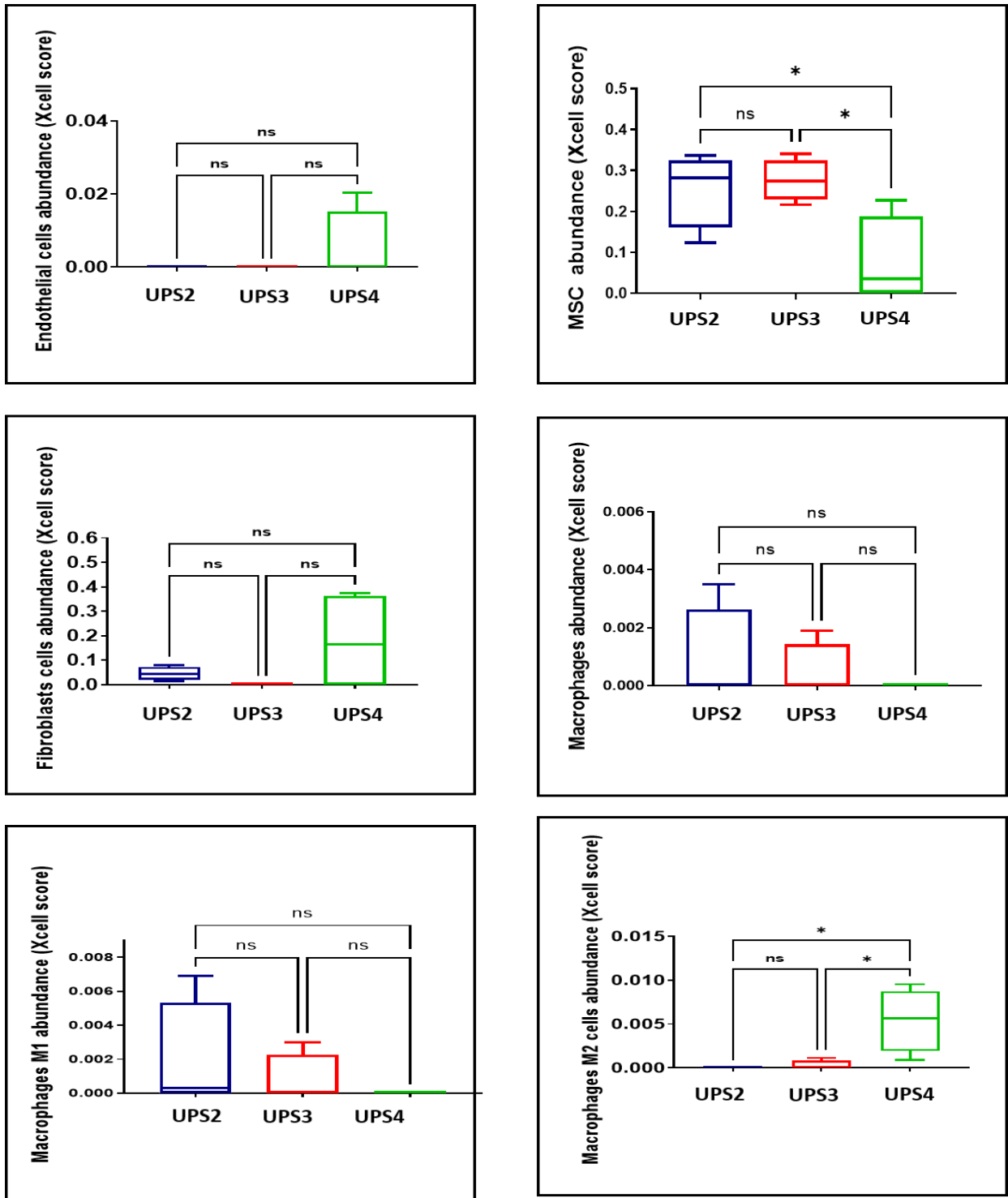
Figure 5. 8: Cell subset abundance in xenografts using universal transcriptome alignment.

XCell scores for different cells in xenografts. Box and Whiskers plots showing the differences. Multiple comparison analysis was done using Tukey's test. Error bars are ± SEM. *,P<0.05 , **,P <0.01; ***,P < 0.001 ;NS, not significant.

5.4 Analysis of the human transcriptome in UPS xenografts

To further understand the differences between xenografts of UPS2, 3 and 4 and to identify differences in expression of DEGs and mesenchymal genes in particular, we performed a separate alignment against the human reference genome (GRCh37/hg38) and used XenofilteR to quantify the abundance of human transcripts (XenofilteR tool (section 2.12.3). This will enable us to identify the transcriptome of the UPS cells within the xenograft separately from the murine stroma.

5.4.1 Differential gene expression between human transcriptome in UPS xenografts

A MDS plot shows that human transcriptome of UPS3 clustered separately from UPS1 and UPS2 (Fig.5.10). DEGs analysis was performed using the Voom tool from the *Limma* packages in R. For human transcripts, there were few significant DEGs between UPS2 and UPS3 (Fig. 5.11), however there were significant differences in DEGs between UPS4 and UPS2, and UPS4 and UPS3, similar to the pattern seen using the transcriptome generated after alignment against the universal reference genome. There were 917 and 1122 up-/downregulated genes between UPS2 and UPS4, respectively. Furthermore, 1102 genes were upregulated and 940 genes were downregulated between UPS2 and UPS3 (Fig. 5.11 & Table 5.2).
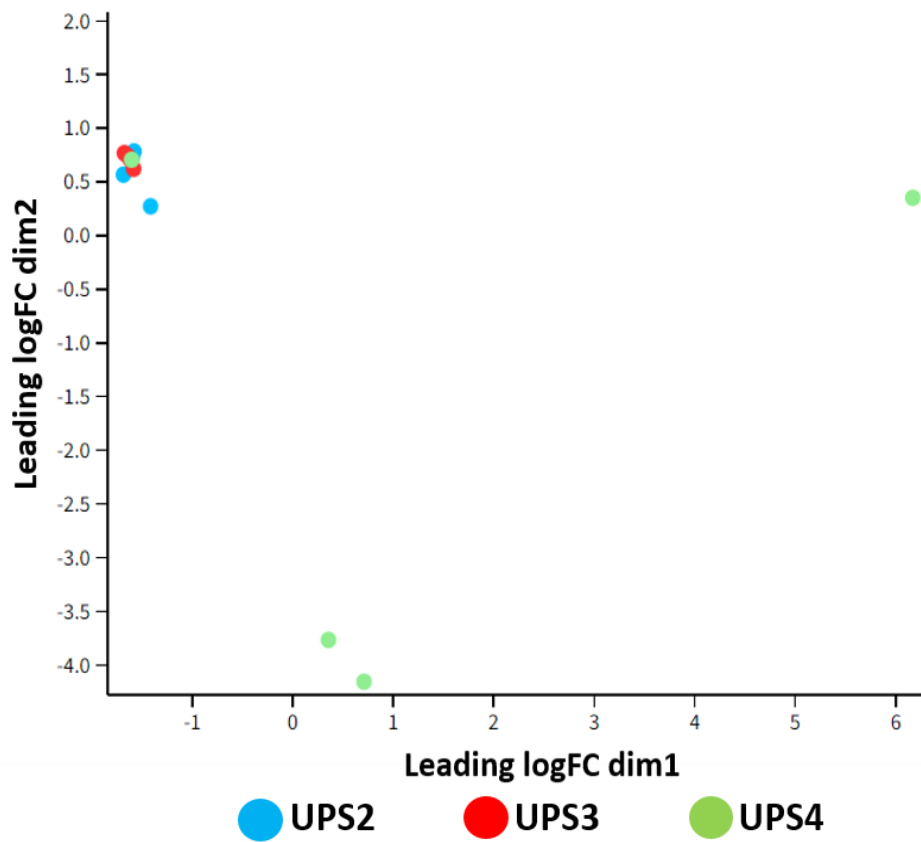
Figure 5. 9: MDS of human transcriptomes from UPS xenografts.

UPS2 in **blue, UPS3** in **red** and **UPS4** in **green. UPS4 clustered separately from UPS2 and UPS3.**
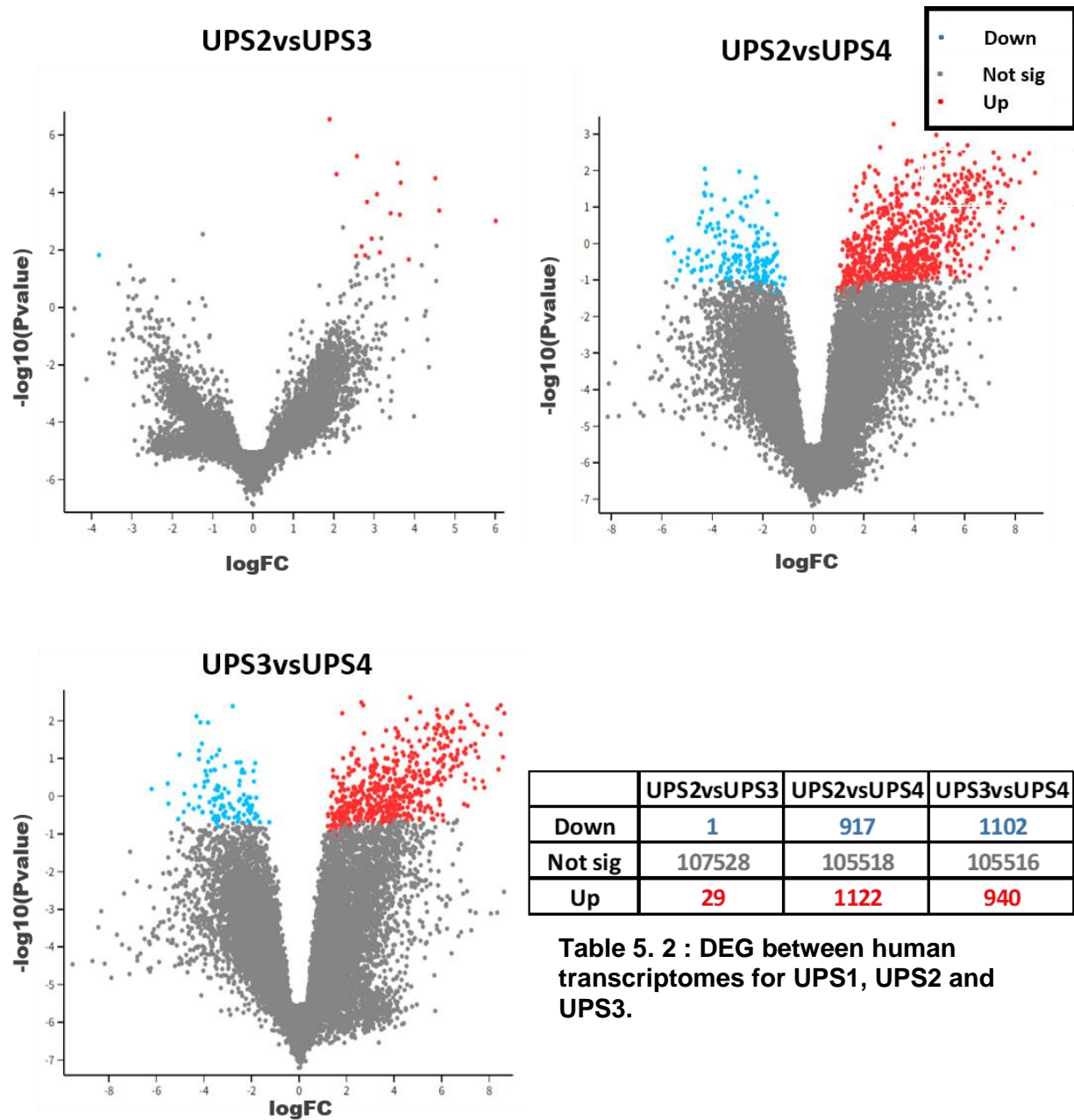
Figure 5. 10: Volcano plots for human transcriptomes.

The logFC represents the change in gene expression between UPS2 and UPS3, UPS2 and UPS4 or UPS3 and UPS4, while the p values indicates the level of significance of each gene. Each dot illustrates one gene**.** The cut-off criterion for DEG significance was FDR ≤ 0.05 and logFC of 1. **Blue dots represent down-regulated genes,** grey dots represent no significant differential expression genes **and** red dots represents up-regulated genes**.**

5.4.2 Biological process enriched in human transcriptomes

Gene Set Enrichment Analysis (GSEA) analysis using the gene sets presented by the molecular signatures database (MsigDB), 15,906 genes were uploaded and GSEA identified the (2326) up- / (1950) downregulated genes in the human transcriptomes. Only five of the most up/downregulated genes were mentioned in (Table S3). Moreover, many biological processes were activated in both sets (UPS2 vs UPS4 and UPS3 vs UPS4) and just one was suppressed in (UPS2 vs UPS4, multi cellular organismal water homeostasis). Activated biological process in both sets (UPS2 vs UPS4 and UPS3 vs UPS4) were: membrane bounded organelle. Membrane bounded organelle are organelle surrounded by biological membrane like nucleus, mitochondrial and lysosomes (Fig.5.12 & Fig.5.13). There are 128 genes in this membrane bounded organelle (Stroberg & Schnell, 2017). 89 genes were enriched and 39 genes were downregulated. Defensin Beta 1 (DEFB1), Lysosomal associated membrane protein-2 (LAMP2) and Mucin1 (MUC1) were enriched in both sets. Multi-cellular organismal water homeostasis is biological process in organelle or tissue that involves water, it was supressed in UPS3 vs UPS4 set, and there are 68 genes in this hallmark (Delpire & Gagnon, 2018) . 49 genes were downregulated and 19 up-regulated genes. CFTR and stathmin 1 (STMN1) were downregulated in UPS3 vs UPS4.
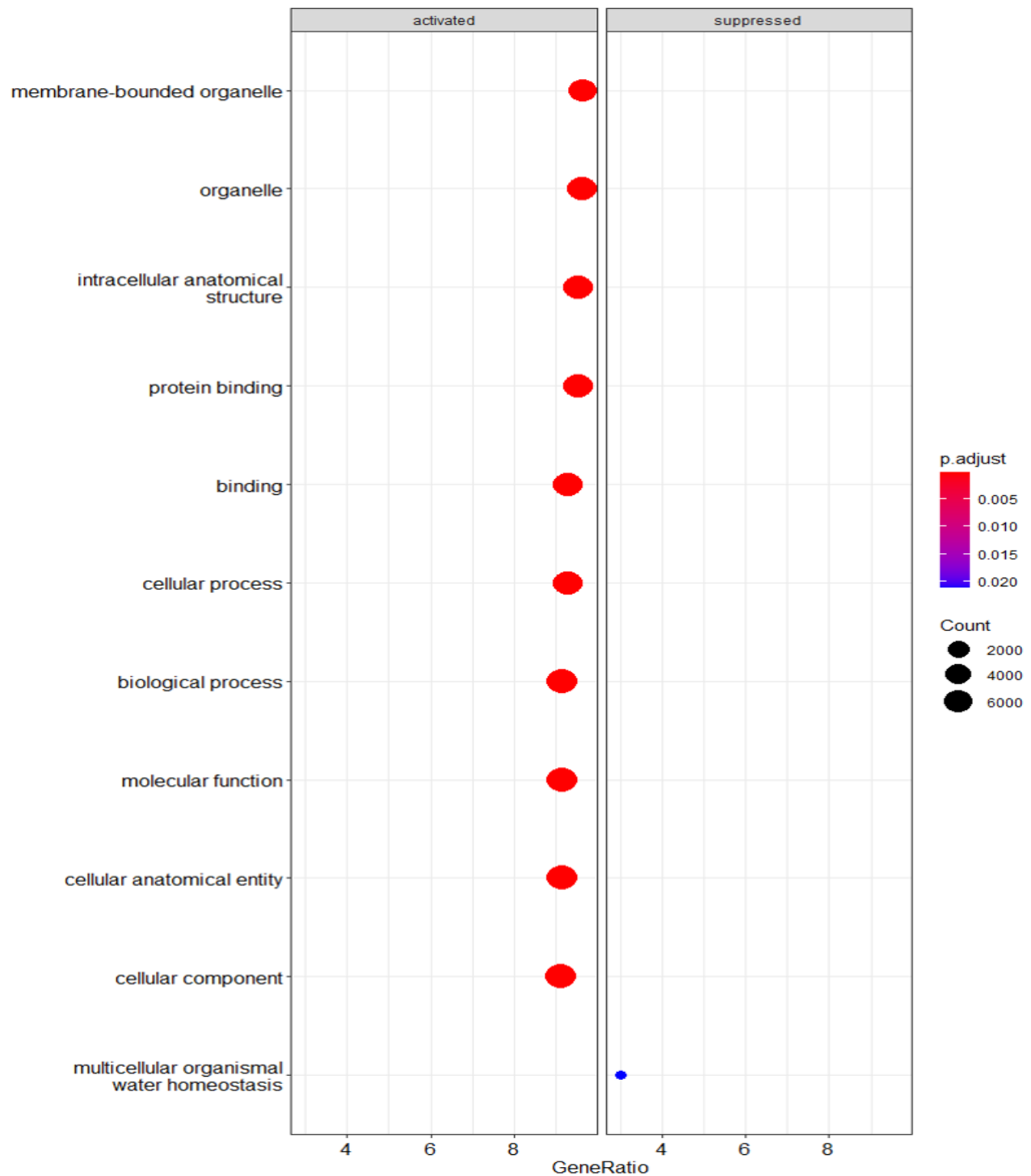
Figure 5. 11: Biological process enriched in UPS2 and UPS4 human transcriptomes.

The hallmark gene sets (h.all.V7.1 MSigDB) shown above were significantly up/down-regulated in UPS2.The cut-off criteria for significance was p-value ≤ 0.05.
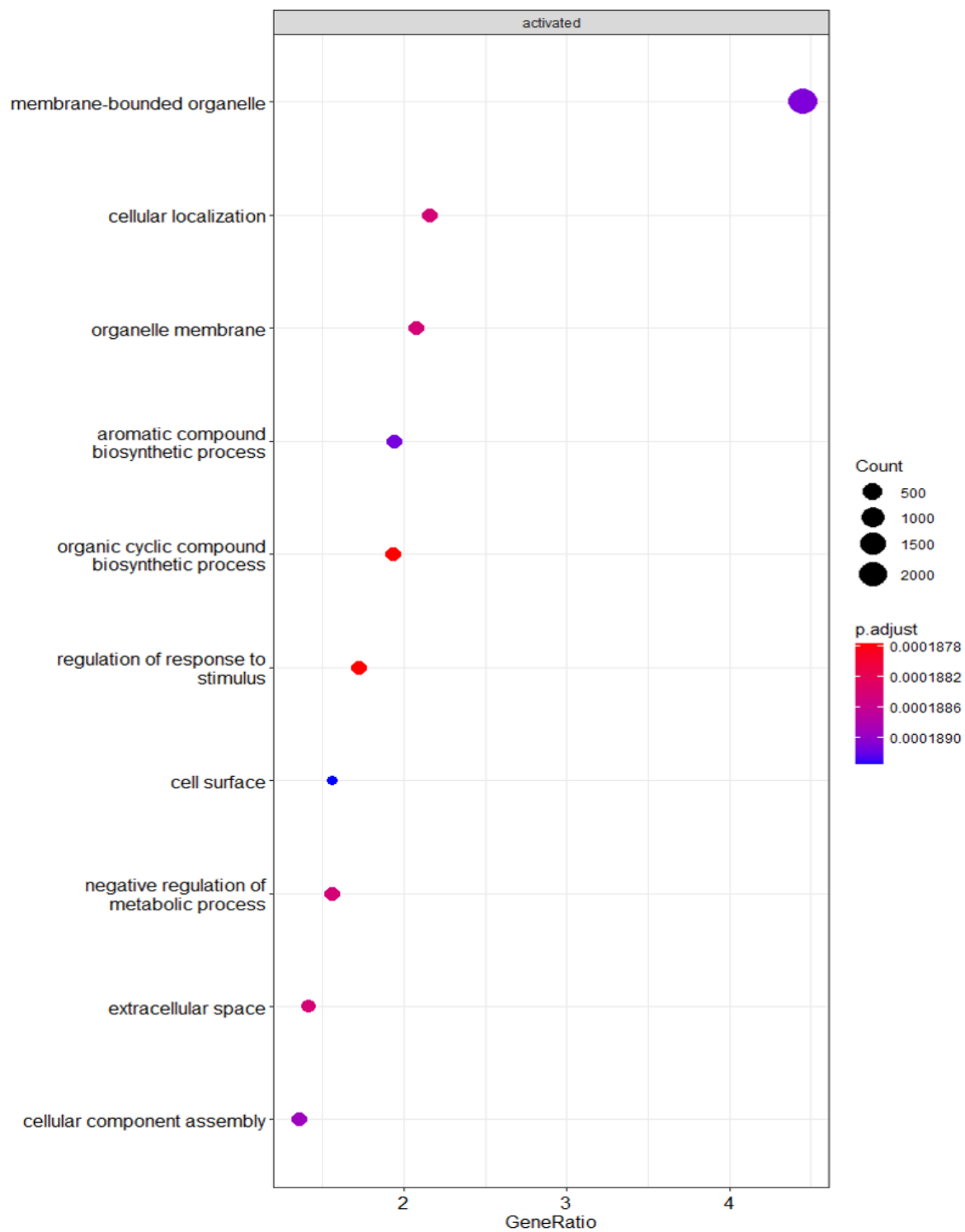
**Figure 5. 12: Biological process enriched in UPS3 and UPS4 human transcriptomes.**

The hallmark gene sets (h.all.V7.1 MSigDB) shown above were significantly upregulated in UPS3. The cut-off criteria for significance was p-value ≤ 0.05.

5.4.3 Differences in expression of mesenchymal genes commonly used to identify cancer associated fibroblasts between human transcriptomes of UPS xenografts

In this project's earlier chapters we studied eight CAFs markers and in this chapter we expanded these studies to their expression in the human transcriptome of our UPS xenografts including transgelin, αSMA, vimentin, N-cadherin, fibronectin, FSP-1, FAPα and SOX2. Statistical analysis showed no significant differences in gene expression between the three human transcriptomes except for transgelin which was decreased in UPS4 when compared with UPS2 and UPS3 (Fig. 5.14). Fibronectin expression was very low for all three UPS xenografts in the human transcriptome (Fig 5.14).
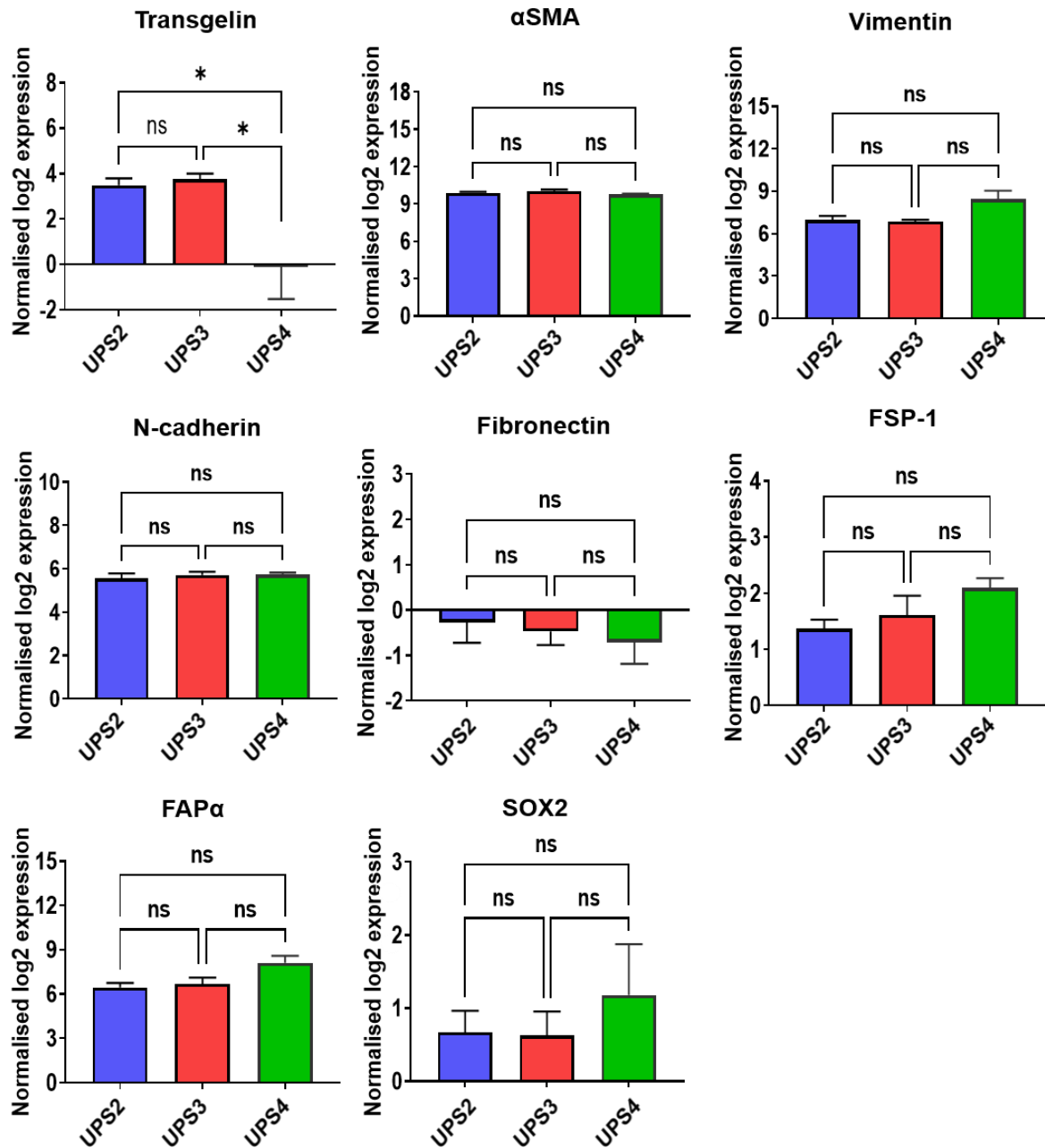
Figure 5. 13: Bar chart analysis of the common mesenchymal gene expressions in human transcriptomes.

Statistical analysis shows no significant difference in gene expression between the human transcripts except for transgelin. X-axis is the human transcripts samples. Y-axis is the normalised log 2 expression. Error bars are ± SEM. *, $P<0.05$, **, $P <0.01$; ***, $P < 0.001$; NS, not significant.

5.4.4 Differences in expression of additional mesenchymal genes used to identify cancer associated fibroblasts in the human transcriptome of UPS xenografts

As discussed in previous sections of this chapter, as in section 5.3.4, we also examined the differences in expression of additional mesenchymal genes associated with CAF. MFAP5 and NG2 expression were very low in the human transcriptome (Fig.5.15).
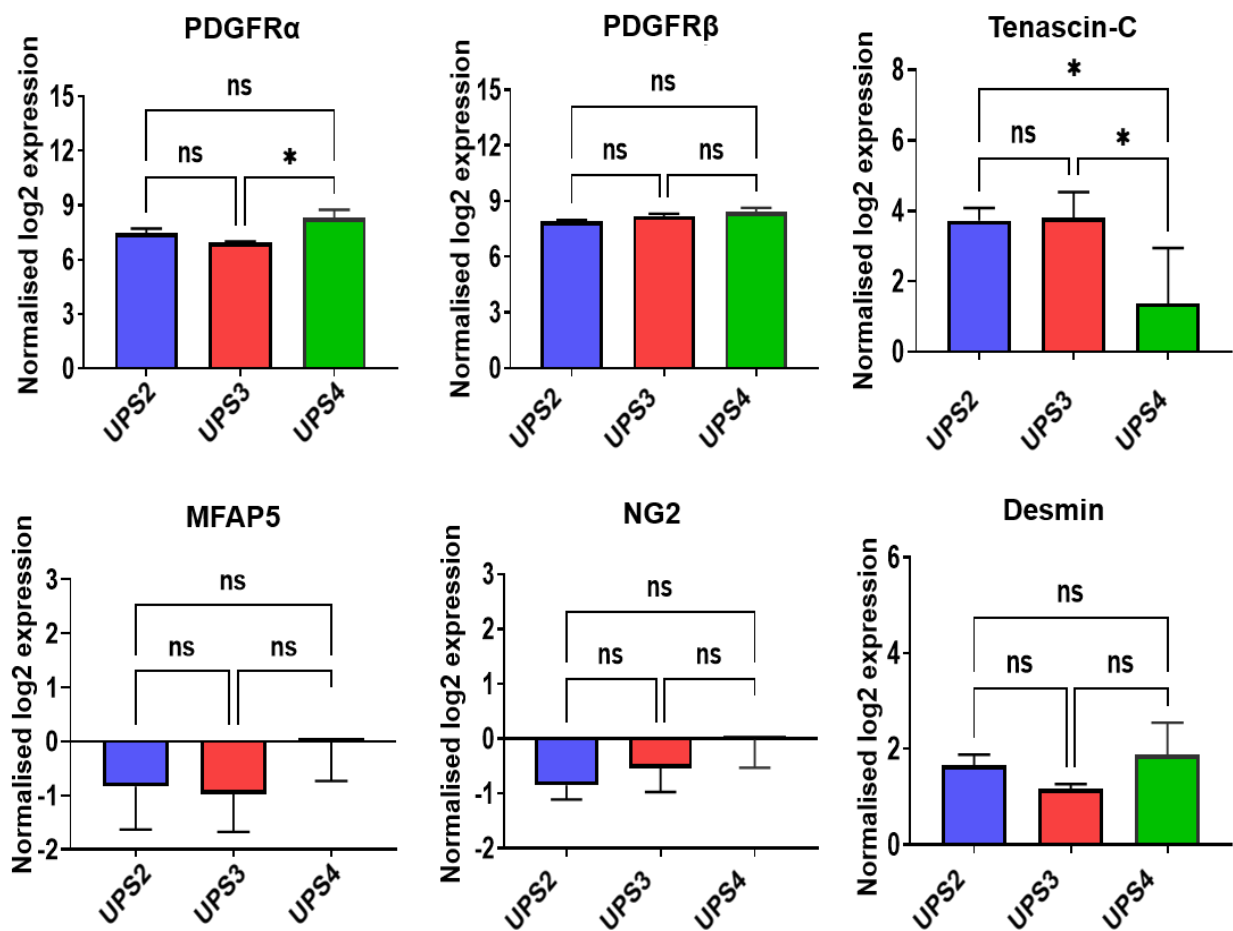
Figure 5. 14: Bar chart analysis of the common CAFs gene expression in human transcriptomes.

Statistical analysis shows no significant differences in gene expressions between the human transcriptomes except for PDGFRα and Tenascin c. Error bars are ± SEM. *,P<0.05 , **,P <0.01; ***,P < 0.001 ;NS, not significant.

5.4.5 Cell population prediction from the human transcriptome of UPS xenografts

As discussed in section 5.3.5 cell population analysis showed that UPS3 is predicted to be higher in pericytes, microvascular endothelial cells, lymphatic endothelial cells and fibrooblasts, and significanlty higher in M2 Macrophage and HSC linked genes when compared with UPS2 (Fig. 5.16). UPS1 was found to be higher in skeletal muscle, total macrophage and M1 macrophage genes (Fig.5.16). Mesechmyal Stem Cell (MSC) associated genes were also predicted to be significantly lower in UPS4 with respect to UPS2 & UPS3 (Fig.5.16).

As mentioned in section 5.3.5 about snRNA-seq, two pericyte genes were enriched in UPS2 vs UPS4 and UPS3 vs UPS4 are, CSPG4/NG2 and gunaylate cyclase 1 (GUCY1a3) (Table S3) (Baek et al., 2022). Four skeletal muscle cells genes were enriched in xenografts chemokine ligand 14 (CXCL14), Paired box protein (PAX7), Myogenic differentiation 1(MYOD1) and Myogenin (MYOG) (De Micheli et al., 2020). Two smooth muscle genes were enriched including desmin, and ACTA2 (Lee et al., 2015).Two lymphatic endothelial cell genes were enriched only in UPS3 vs UPS4, Mucosal vascular Addressin Cell Adhesion Moleulce 1 (MADCAM1) and annexin(ANXA2) (Fujimoto et al., 2020). Two HSC cells genes were enriched Protein C receptor (PROCR) and Cathepsin F(CTSF) (Forsberg,2010). Two endothelial cells genes were upregulated Interleukin-6 (IL-6) and Claudin 5 (CLDN) (De Micheli et al., 2020). One MSC gene was enriched which is 5'-Nucleotidase Ecto(NT5E) (Weng et al., 2011). Four fibroblast genes were upregulalted Decorin (Dcn), collagen type 1(Col1A1), ACTA2 and transforming growth factor-beta (TGFβ) (Dinh et al., 2021; Guerrero-Juarez et al., 2019) .Three genes M2 Macrophage genes were enriched Chemokine Ligand 18 (CCL18),Secreted Phosphoprotein1 (SPP1) and CD163 (Dinh et al., 2021). Two M1 macrophages genes were enriched including SPP1 and Dehydrogenase/Reductase 3 (DHRS3) (Zhuang et al., 2020).Three macrophage genes were enriched Protein Kinase AMP-activated catalytic subunit alpha1 (PRKAA1) and ATP binding Cassette Subfamily A member 1 (ABCA1) (Chai et al., 2018).
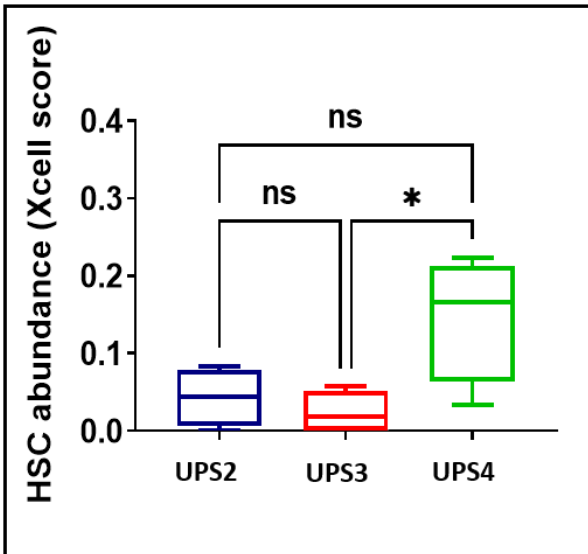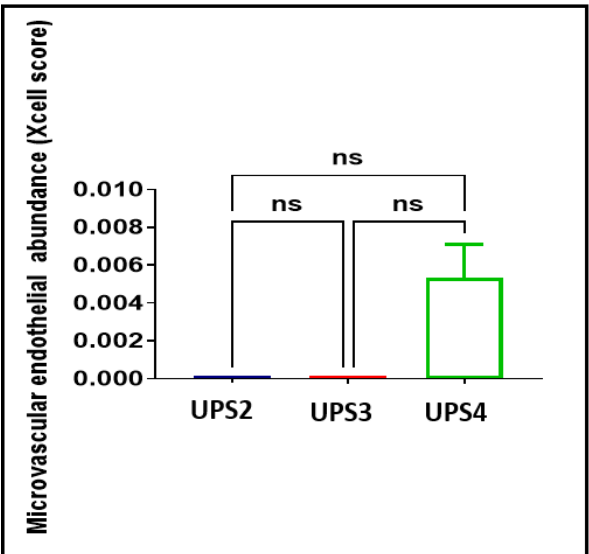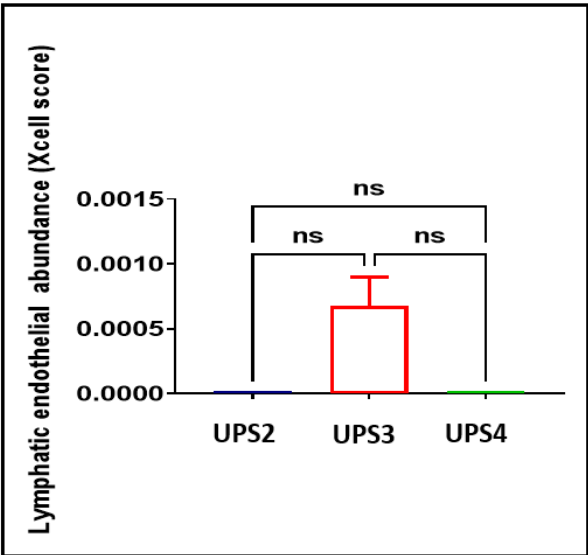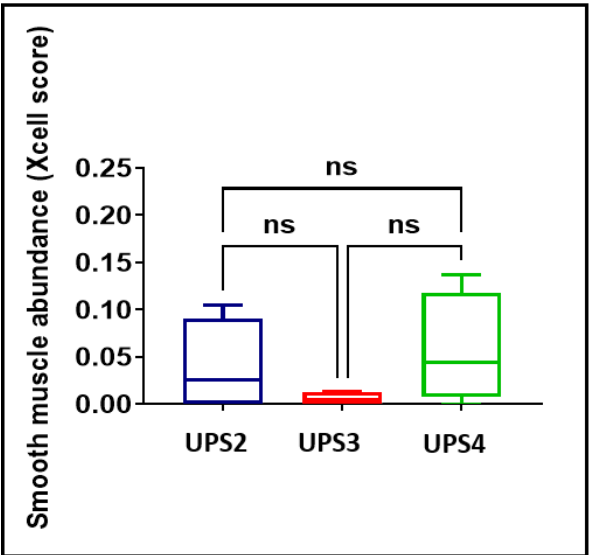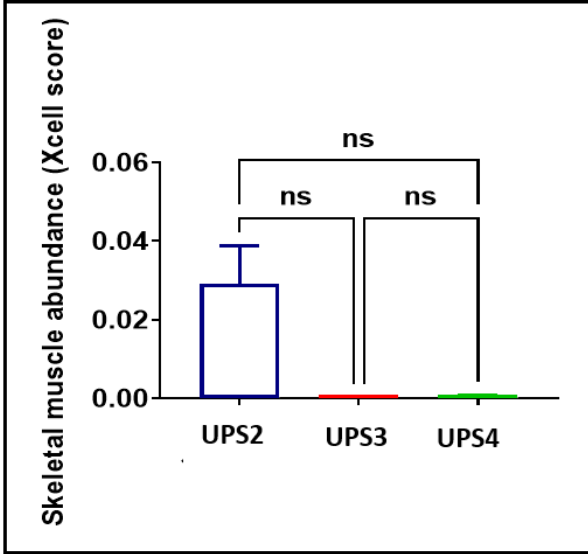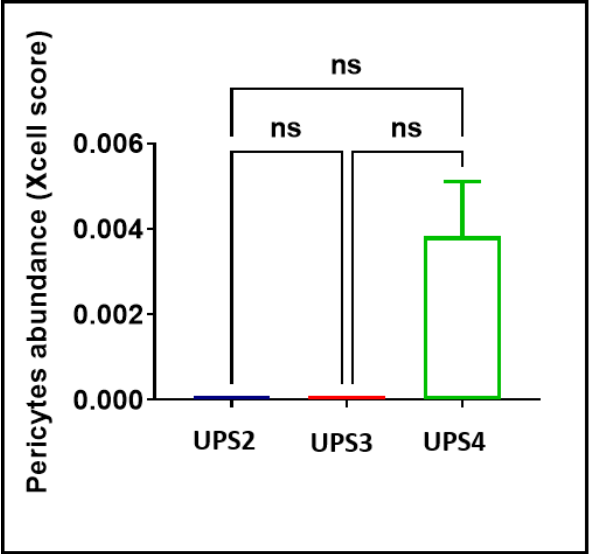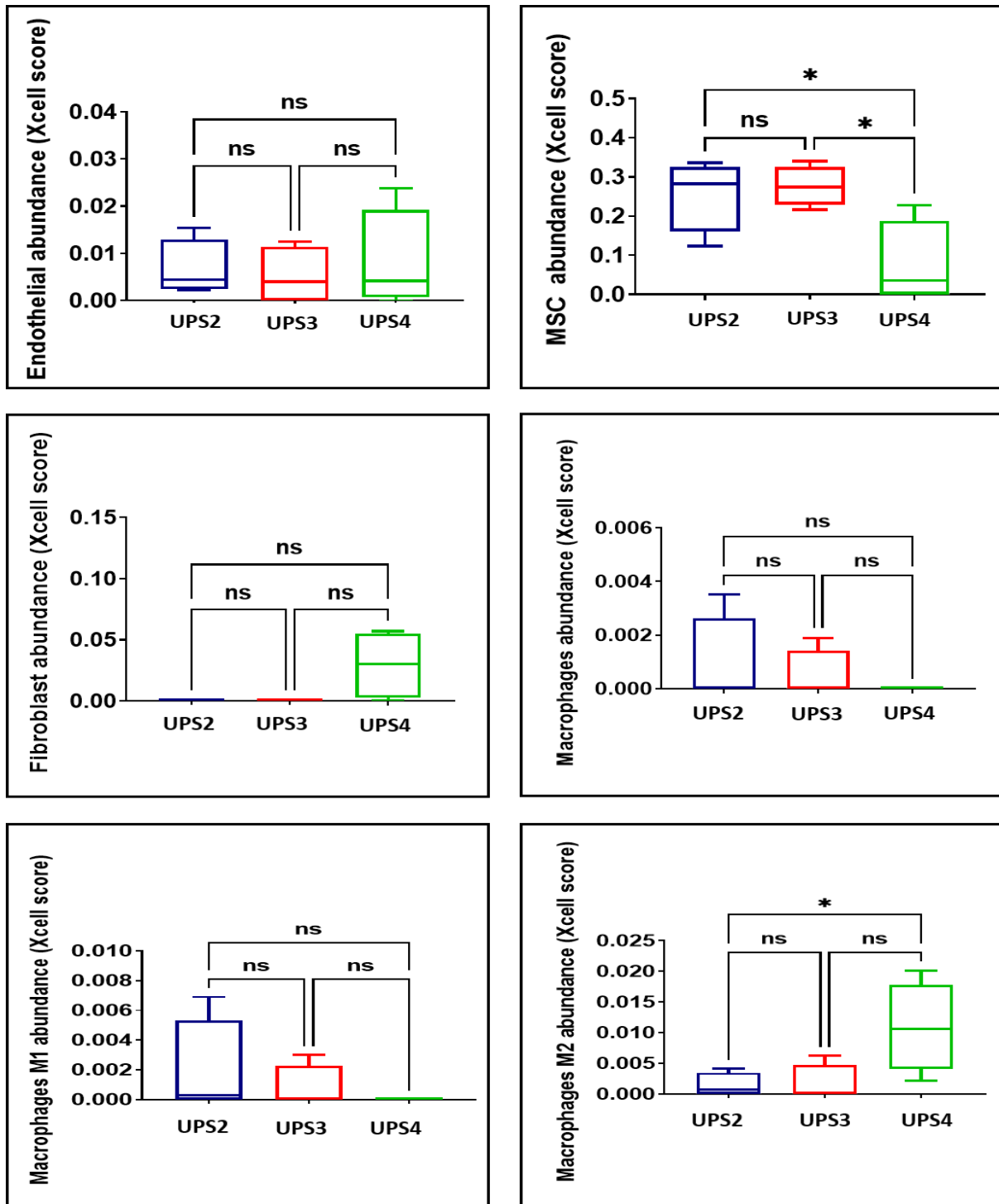
Figure 5. 15: Cell subset prediction in human transcriptomes of UPS xenografts.

xCell scores for different cells in xenografts. Box and Whiskers plots showing the differences. Multiple comparison analysis was done using Tukey's test. Error bars are ± SEM. *,P<0.05 , **,P <0.01; ***,P < 0.001 ;NS, not significant.

5.5 Analysis of the mouse transcriptomes

5.5.1 Differences in gene expression between mouse transcripts (Stroma) in UPS xenografts

In this section, we studied global differences in gene expression between mouse (host) transcriptomes in our xenografts. Unsupervised Hierarchical clustering was performed using Multi-Dimensional Scaling (MDS). MDS shows that most samples were distributed evenly except for three samples from UPS4, which clustered separately, although samples clustered together more closely than the human transcriptomes, suggesting they are more similar (Fig.5.17). Although, some UPS4 tumours clustered separately, DEGs analysis revealed there is no significant differences in gene expression between mouse transcriptomes for the three different cell line derived xenografts (Table 5.3 and Fig.5.18).
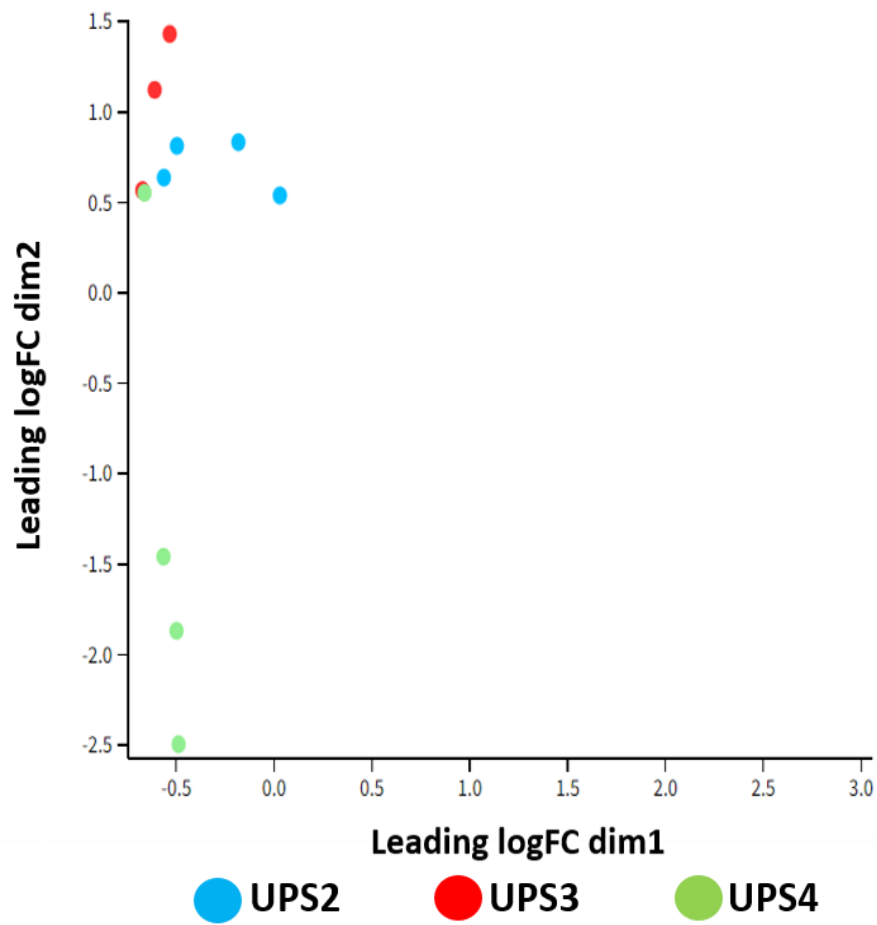
Figure 5. 16: MDS of the mouse transcriptomes from UPS xenografts.

UPS2 in blue, UPS3 in red and UPS4 in green. The plot is shows that three samples of UPS4 are clustered separately from the majority of the samples.
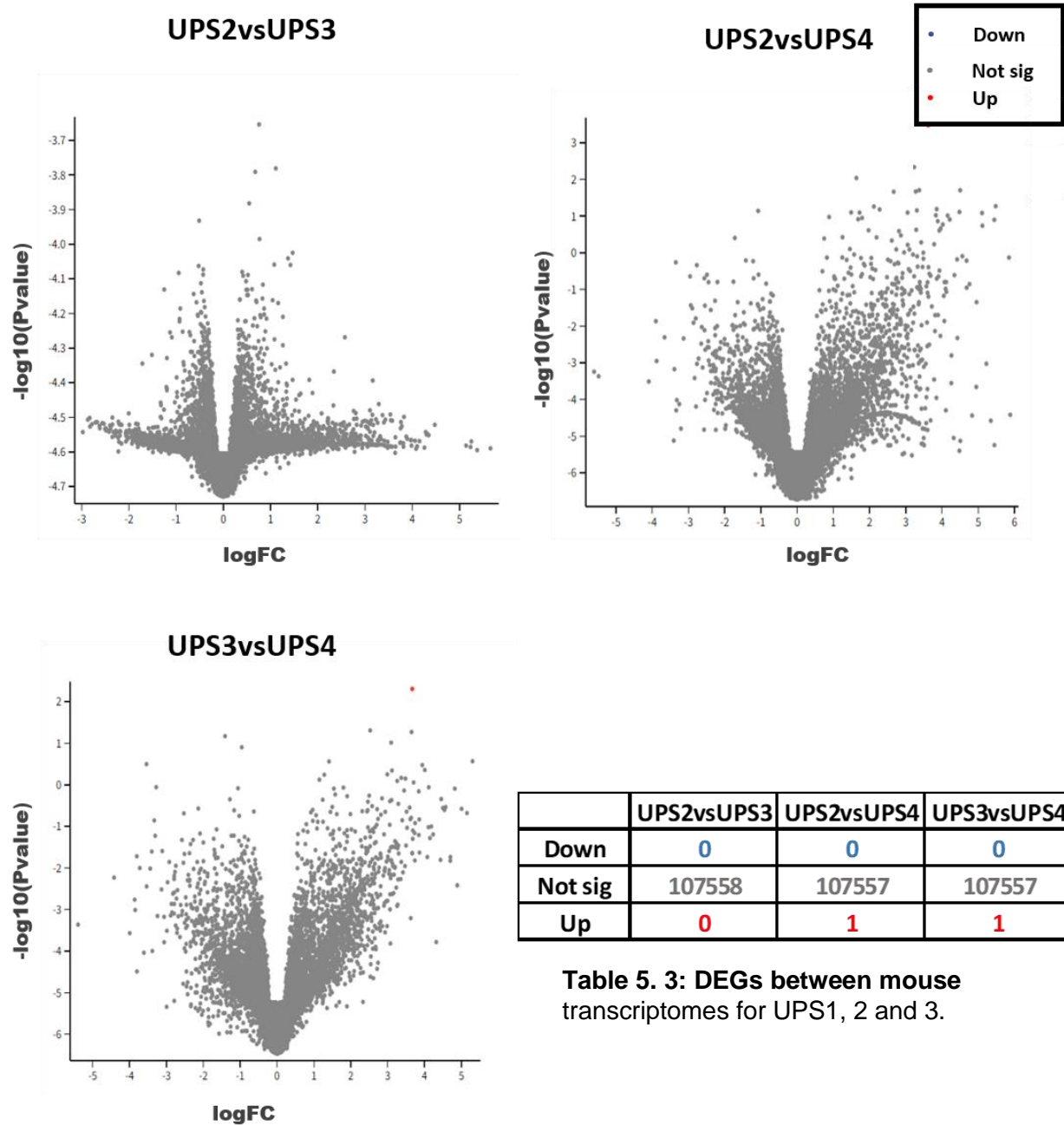
Figure 5. 17: Volcano plots for mouse transcriptomes from UPS xenografts.

The logFC represents the change in gene expression between UPS2 and UPS4,UPS2 and UPS4 or UPS3 and UPS4, while the pvalues indicates the level of significance of each gene. Each dot illustrates one gene. The cut-off criterion for DEG significance was FDR ≤ 0.05 and logFC of 1. **Blue dots represent down-regulated genes, grey dots represents no significant differential expression genes and red dots represents up-regulated genes.**

	UPS2vsUPS3	UPS2vsUPS4	UPS3vsUPS4
Down	0	0	0
Not sig	107558	107557	107557
Up	0	1	1

Table 5. 3: DEGs between mouse transcriptomes for UPS1, 2 and 3.

211

5.5.2 Biological process enriched in Mouse transcriptomes

Gene Set Enrichment Analysis (GSEA) analysis using the gene sets presented by the molecular signatures database (MsigDB), 15,906 genes were uploaded and GSEA identified the (3290) up- / (3307) downregulated genes in the mouse transcriptomes. Although there was no significant DEGs between mouse transcriptomes, some biological processes were enriched in both sets of comparisons (UPS2 vs UPS4 and UPS3 vs UPS4) (Fig.5.19 & Fig.5.20). Four biological processes were suppressed in UPS2 vs UPS4 and just one was suppressed in UPS3 vs UPS4. Regulation of cellular biosynthesis is the most activated biological process in both sets (UPS2 vs UPS4 and UPS3 vs UPS4). Regulation of cellular biosynthesis includes biological processes that stimulate or control the rate of any chemical reaction or pathways (Joly et al., 2021).There are 1984 genes in this hallmark, 1587 genes were enriched while, 397 were downregulated.

Some common genes were upregulated in both sets including Alanyl-TRNA synthetase 1 (AARS1), ATP binding Cassette Subfamily A member 7 (ABCA7), Mesenchyme homobox 2 (MEOX2) and Zona Pellucida Glycoprotein 3 (ZP 3).

The Toll-like receptor 4 signalling pathway was downregulated in the UPS2 vs UPS4 set. This pathway has crucial role in innate immune system (Kuzmich et al., 2017). There are 102 genes in this hallmark most of it (98) were downregulated in this set including, TGF-beta activated kinase 1 (TAB1), Mitogen-Activated protein kinase 8 (MAP3K8), Mitogen-Activated protein kinase 14 (MAPK14), Cathepsin K (CTSK) and C-X-C Motif chemokine Ligand 9 (CXCL9)

Negative regulation of the forebrain neuron differentiation hallmark was seen in the UPS3 vs UPS4 set. There are 18 genes in this hallmark, four of them were downregulated in this set including, Cannabinoid receptor 1 (CNR1), Potassium voltage gated channel subfamily A regulatory beta subunit1 (KCNAB1), Potassium two pore domain channel subfamily K member 2 (KCNK2) and Syntax in 3 (STX3).
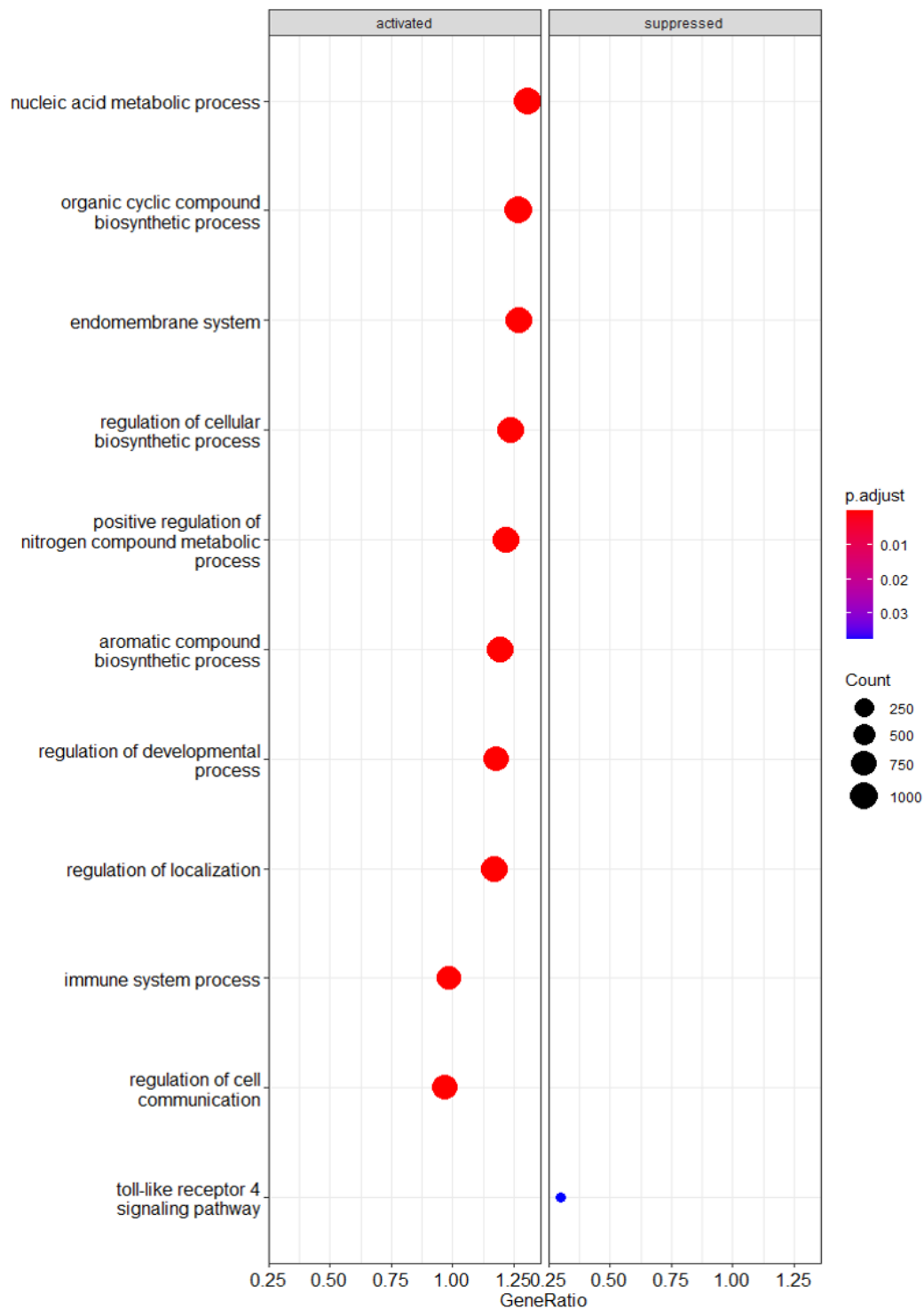
Figure 5. 18: Biological process enriched in UPS2 and UPS4 mouse transcripts.

The hallmark gene sets (h.all.V7.1 MSigDB) shown above were significantly up/down regulated in UPS2 samples .The cut-off criteria for significance was p-value ≤ 0.05.
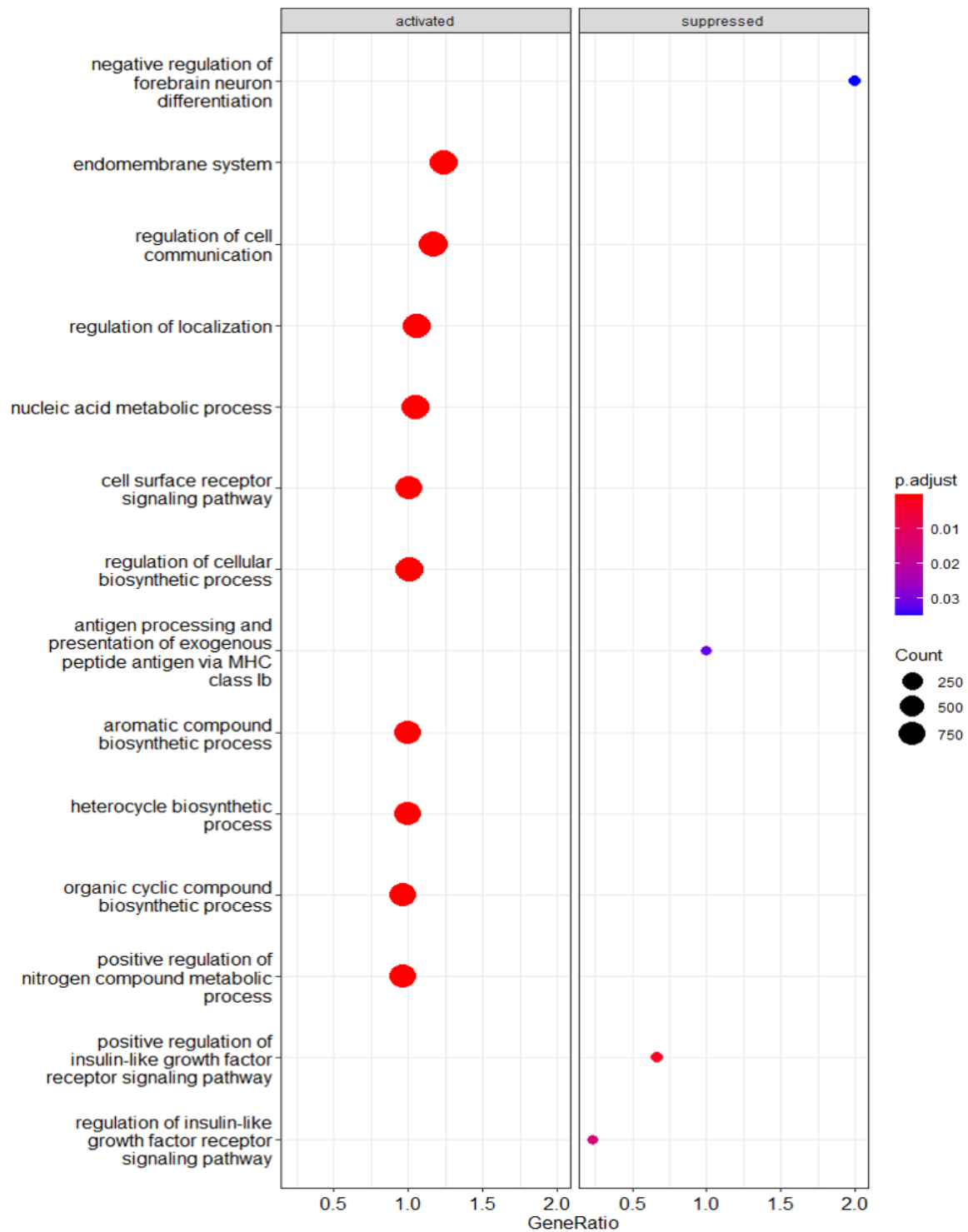
Figure 5. 19: Biological process enriched in UPS3 and UPS4 mouse transcripts.

The hallmark gene sets (h.all.V7.1 MSigDB) shown above were significantly up/down regulated in UPS3 .The cut-off criteria for significance was p-value ≤ 0.05.

5.5.3 Differences in expression of mesenchymal genes commonly used to identify cancer associated fibroblasts between the mouse transcriptomes of UPS xenografts.

In this project's earlier chapters we studied eight CAFs markers and in this chapter we expanded these studies to their expression in the human transcriptome of our UPS xenografts including transgelin, αSMA, vimentin, N-cadherin, fibronectin,FSP-1, FAPα and SOX2. Statistical analysis showed no significant differences in gene expressions between the three mouse transcriptomes except for FSP-1 which showed to be less in UPS4 when compared to UPS3 (Fig.5.21). Very low levels of N-Cadherin expression was seen within the mouse transcriptome.
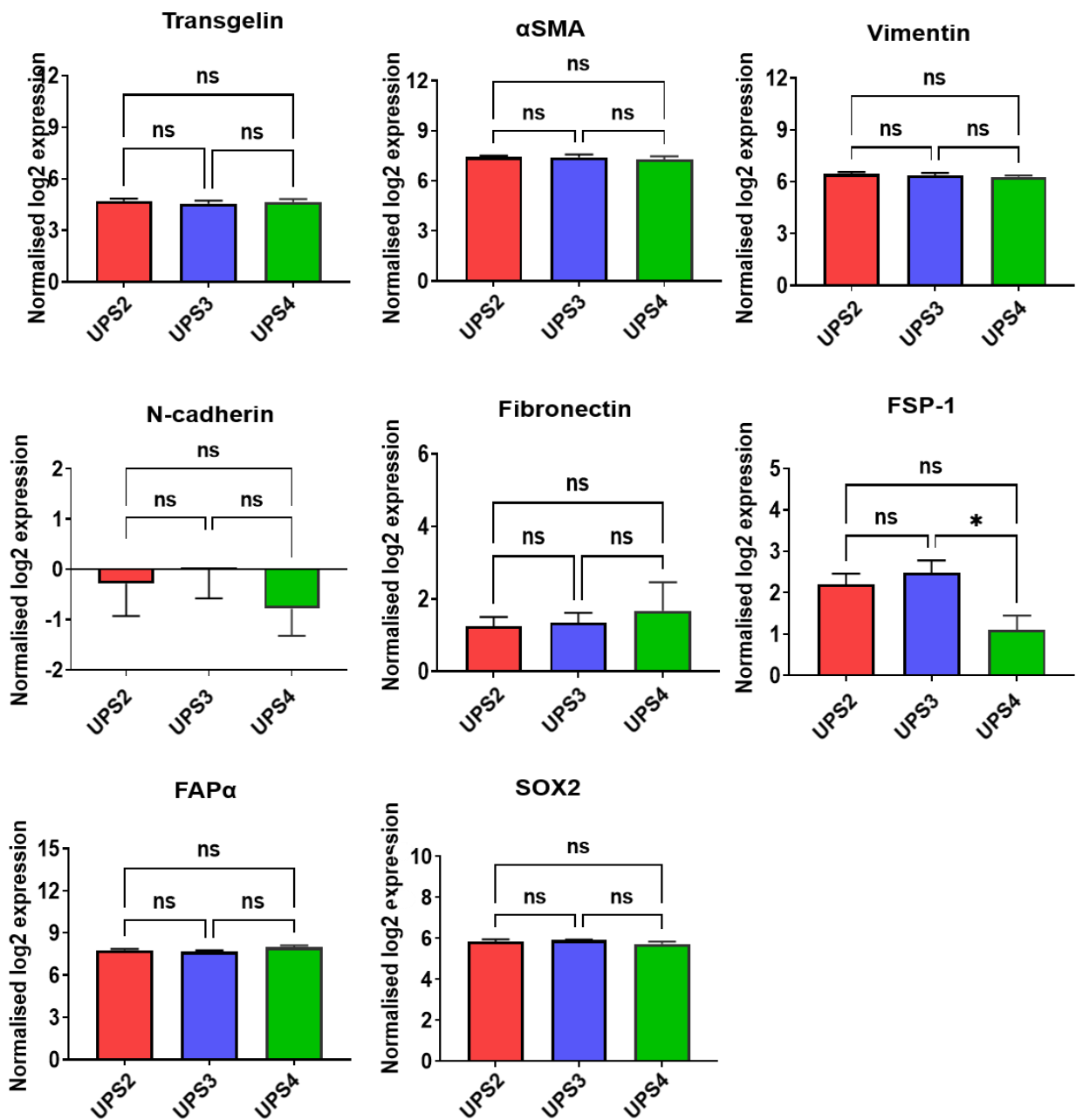
Figure 5. 20: Bar chart analysis of the common mesenchymal gene expressions in mouse transcriptomes.

Statistical analysis shows no significant differences in gene expression between the human transcripts except for FSP-1 in UPS3. X-axis is the UPS samples, Y-axis is the normalised log 2 expression. Error bars are ± SEM. *,P<0.05 , **,P <0.01; ***,P < 0.001 ;NS, not significant.

5.5.4 Differences in expression of additional mesenchymal genes used to identify cancer associated fibroblasts in the mouse transcriptome of UPS xenografts.

As in section 5.3.3, we also examined the differences in expression of additional mesenchymal genes associated with CAF. There were no significant differences in PDGFRα, PDGFRβ, Tenascin-C (TN-C), MFAP5, NG2 or desmin gene expression between the mouse transcriptomes (Fig.5.22). MFAP5 expression was low for all mouse transcriptomes.
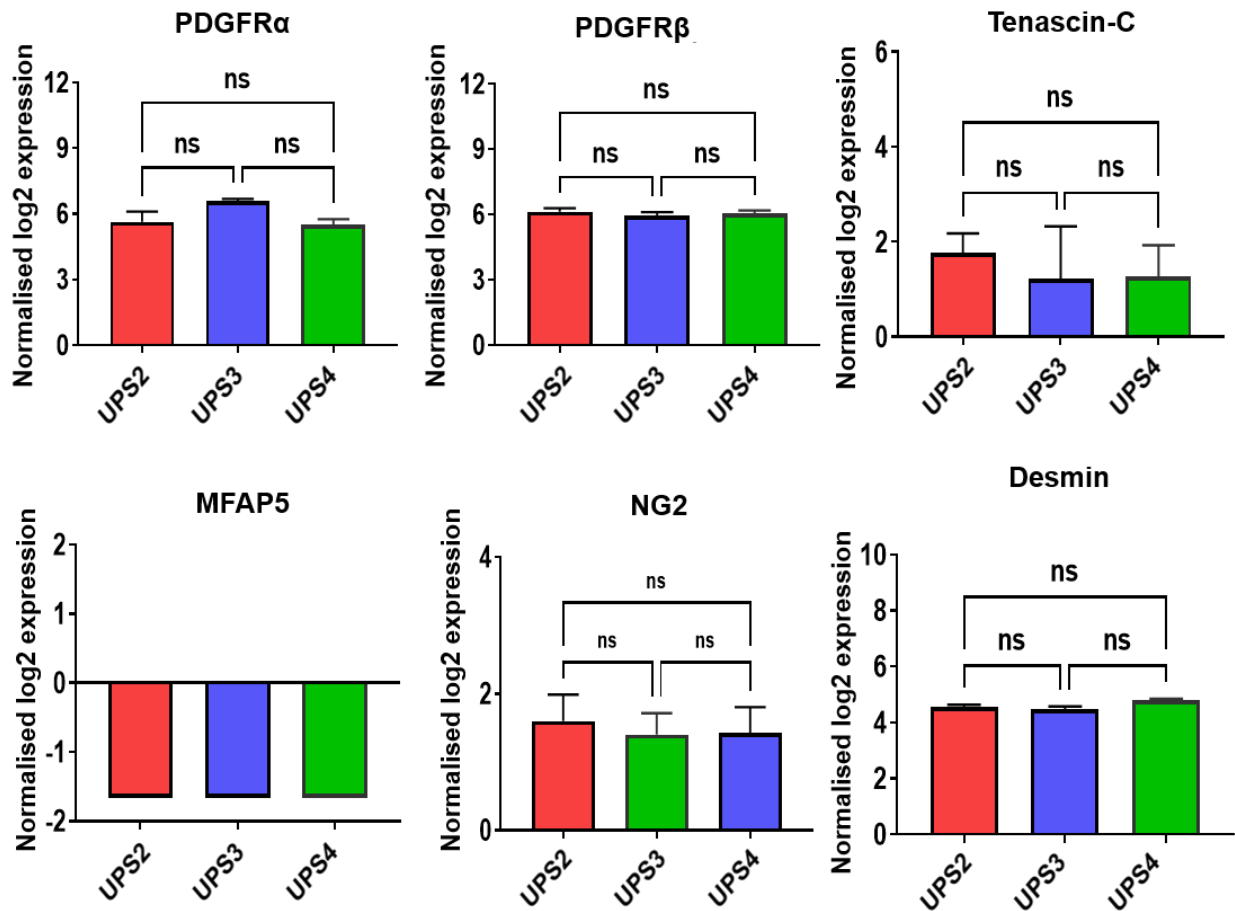
Figure 5. 21: Bar chart analysis of the common CAFs gene expression in mouse transcriptomes.

Statistical analysis shows no significant differences in gene expressions between the mouse transcriptomes. Error bars are ± SEM. *,P<0.05 , **,P <0.01; ***,P < 0.001 ;NS, not significant.

5.5.5 Cell subset prediction from the mouse transcriptome of UPS xenografts

As discussed in section 5.3.5 cell population analysis predicted that UPS4 stroma is higher in skeletal muscle, lymphatic endothelial and total macrophage, and significanlty higher in M1 Macrophage abundancy when compared with UPS2 and UPS3 (Fig. 5.23). UPS2 was predicted to be higher in MSCs, fibroblasts and M2 Macrophages (Fig.5.23).

As mentioned in section 5.3.5 using single cell RNA sequencing (snRNA-seq) analysis. Four pericytes genes were enriched in UPS2 vs UPS4 and UPS3 vs UPS4 including MYH11, pdgfb, CSPG4/NG2 and Regulator of G protein signalling 5 (RGS5) (Table S4) (Baek et al., 2022).Two skeletal muscle cells genes were enriched in the mouse transcriptomes; chemokine ligand 14 (CXCL14) and Myogenic differentiation 1 (MYOD1) (De Micheli et al., 2020). Two smooth muscles genes were enriched including desmin, and MYH11(Lee et al., 2015) . Two lymphatic endothelial cell genes were enriched only in UPS2 vs UP3, Mucosal vascular Addressin Cell Adhesion Moleulce 1 (MADCAM1) and Integrin alpha-llb/beta 3 (ITG2AB) (Fujimoto et al., 2020).Two HSC cells associated genes were enriched Protein C receptor (PROCR) and ANXA2 (Forsberg et al., 2010). Four endothelial cell associted genes were upregulated SOX11, Caveolin 1 (CAV1), Von willebrand factor (VWF) and Intercellular Adnesion Molecule 2 (ICAM2) (De Micheli et al., 2020).Three MSC genes were enriched; 5'-Nucleotidase Ecto (NT5E), S100A4 and FN1 (Weng et al., 2011). Three fibroblast associated genes were upregulalted Tagln, MFAP5 and ACTA2 (Dinh et al., 2021; Guerrero-Juarez et al., 2019). One M2 Macrophages associated gene was enriched Apolipoprotein E (APOE) (Dinh et al., 2021) . Two M1 macrophages genes were enriched including Secreted Phosphoprotein 1 (SPP1) and Dehydrogenase/Reductase 3 (DHRS3) (Zhuang et al., 2020). Five total macrophage genes were enriched Phospholipid transfer protein (PLTP), (APOC1), ATP binding Cassette Subfamily A member 1 (ABCA1), (APOE) and Cholesteryl Ester Transfer Protein (CETP)(Chai et al., 2018) (Table S4). The xCell score were lower than the cut-off in skeletal muscles, lymphatic endothelial, microvascular endothelial, endothelial, Macrophages , M1 macrophages and M2 macrophages; does this mean the prediction is any good?
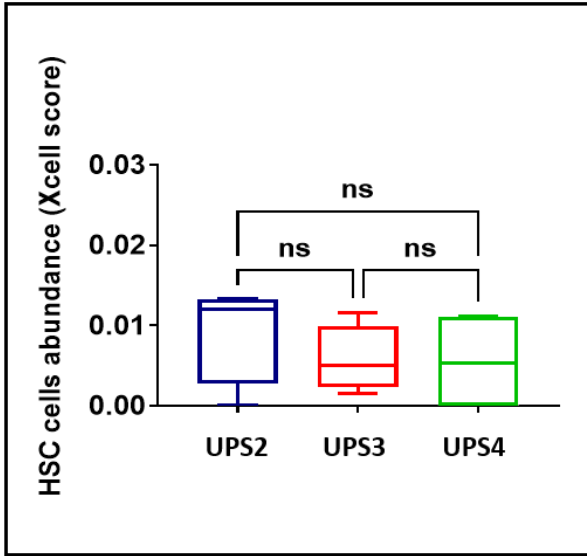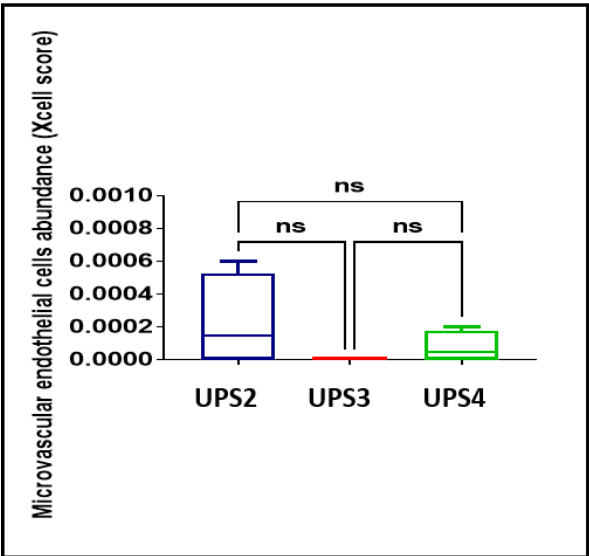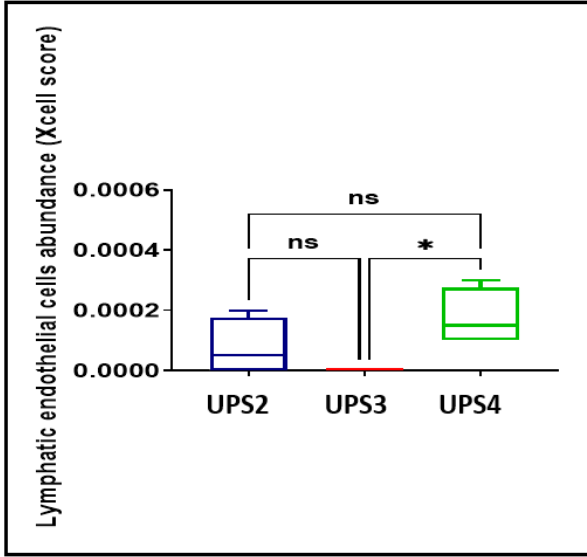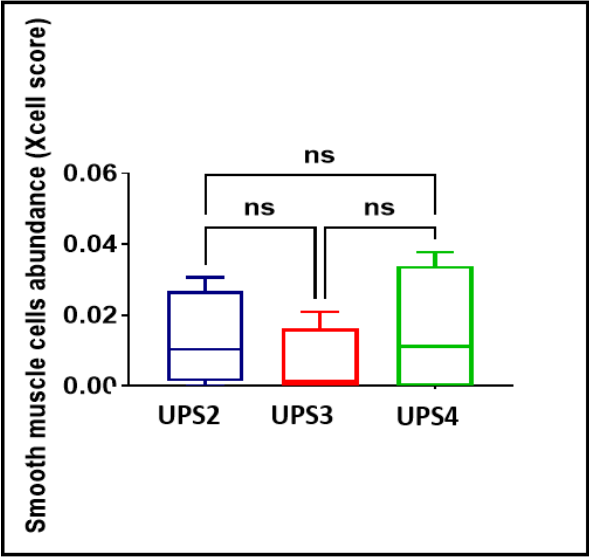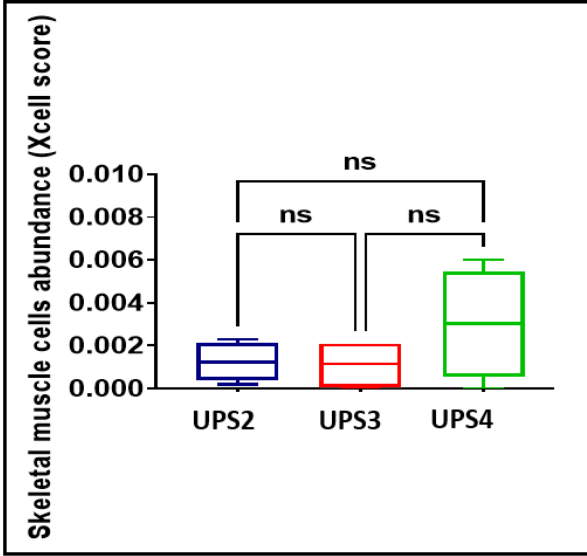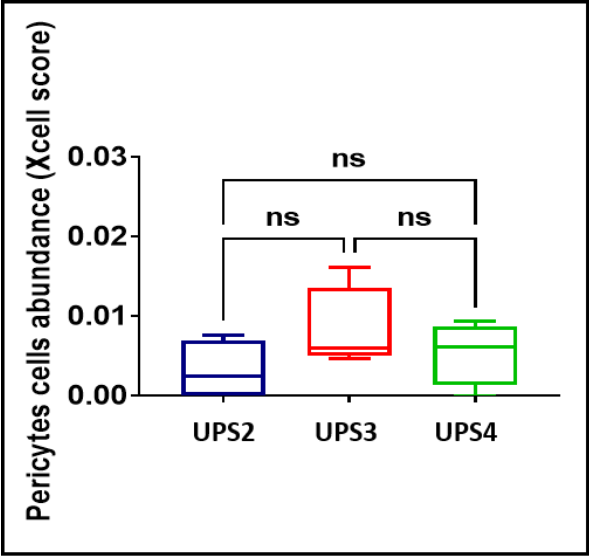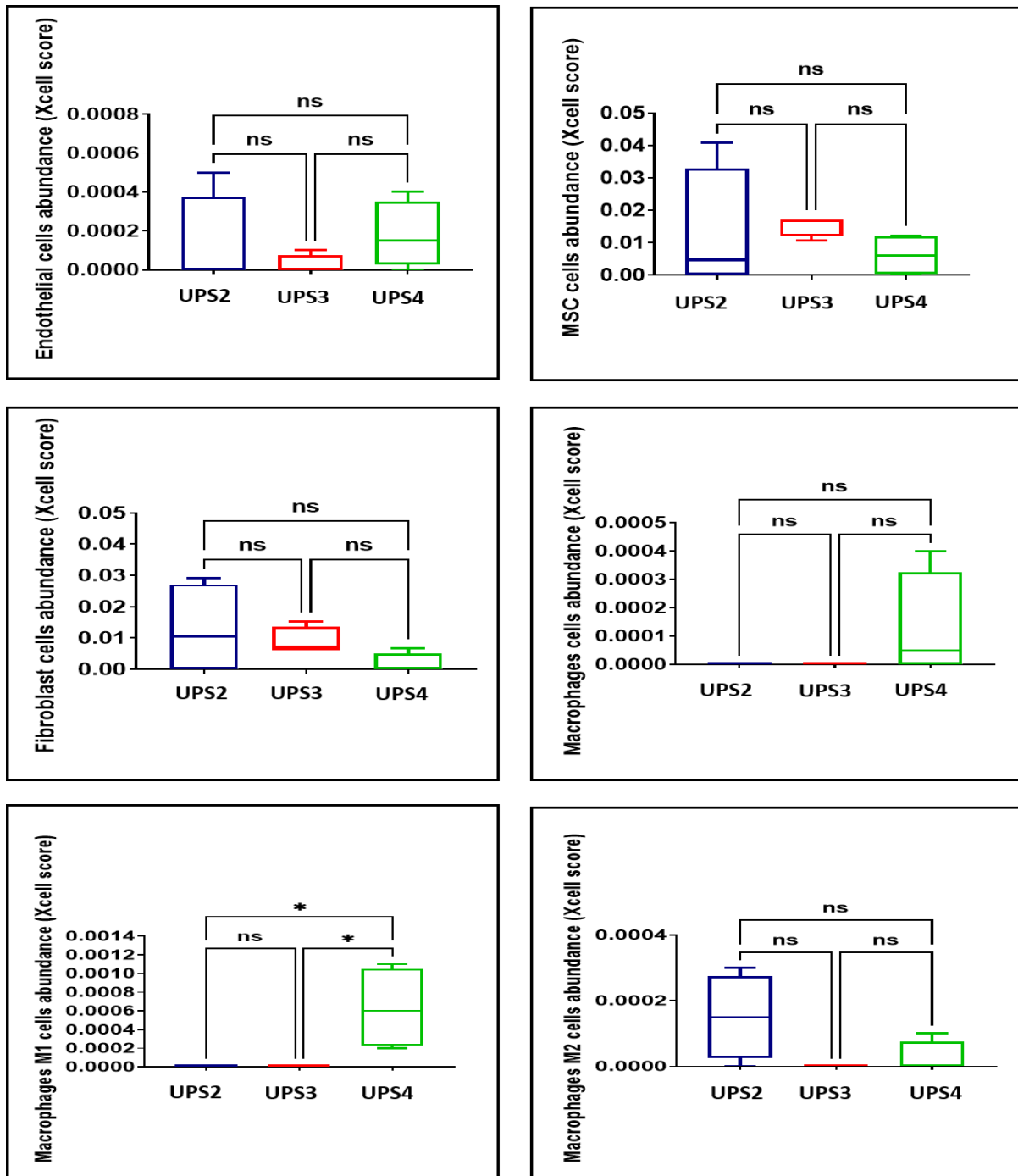
Figure 5. 22: Cell subset abundance in mouse transcriptomes.

xCell scores for different cells in mouse transcripts. Box and Whiskers plots showing the differences. Multiple comparison analysis was done using Tukey's test. Whiskers are min to max, the line is the median. *, P<0.05, **, P <0.01; ***, P < 0.001; NS, not significant.

5.6 Differences in gene expression between human UPS and mouse stromal transcriptomes of UPS xenografts

Studying differential gene expression between the UPS cell lines and the mouse stroma (Host) in order to identify specific SAFs marker to improve our knowledge and our understanding of sarcoma and its tumour microenvironment. In this section, unsupervised Hierarchical clustering was performed using Multi-Dimensional scaling (MDS), MDS shows that human samples distributed separately from mouse samples (Fig 5.24). Differential Expressed Genes (DEGs) analysis was performed using Voom tool from *Limma* packages in R. Volcano plots (MDplots) shows there are significant differences in DEG between human and mouse transcriptomes Fig (5.25 &Table 5.4).
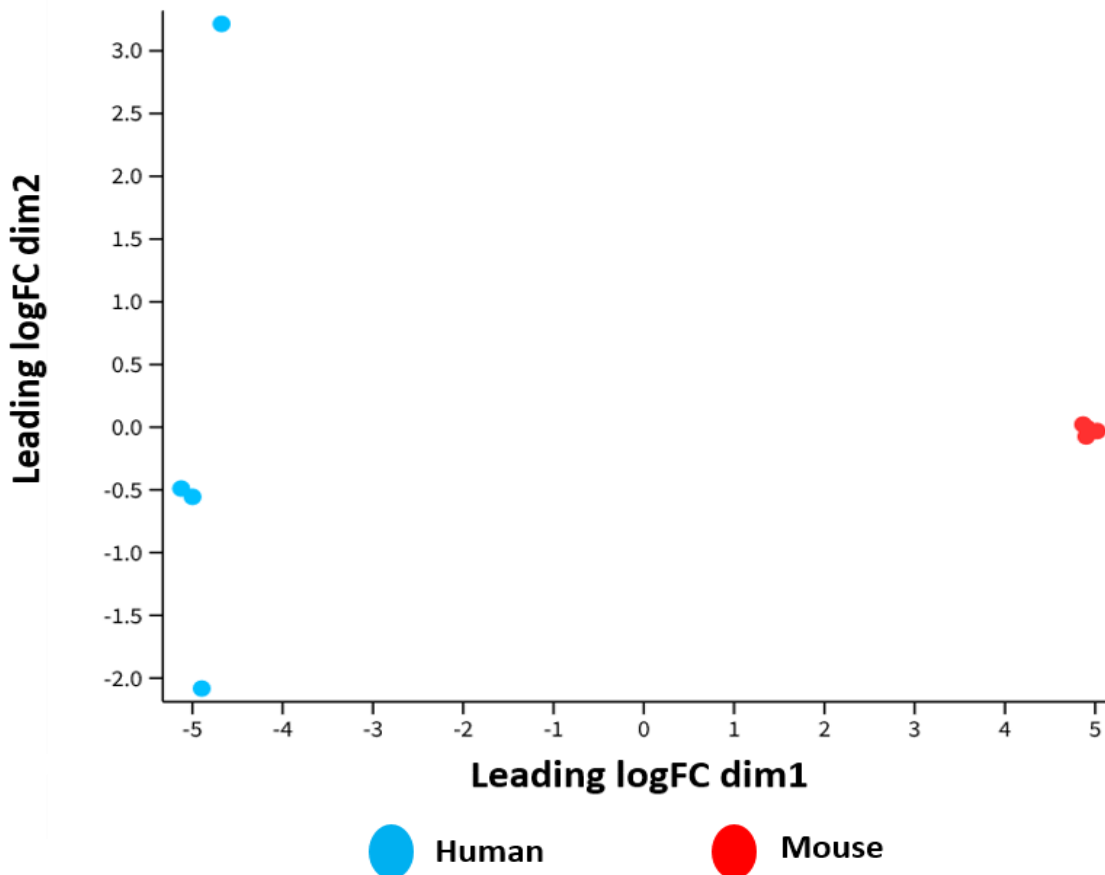
Figure 5. 23: MDS of human and mouse transcriptomes in xenografts.

Human in blue, and Mouse in red. The plot is shows that human (UPS) is clustered separately from the mouse samples (Host).

UPS2

UPS3

UPS4

	UPS2	UPS3	UPS4
Down	8800	7341	6642
Not sig	801	2829	3653
Up	2634	2065	1940

Table 5. 4: DEG between human and mouse transcriptomes.
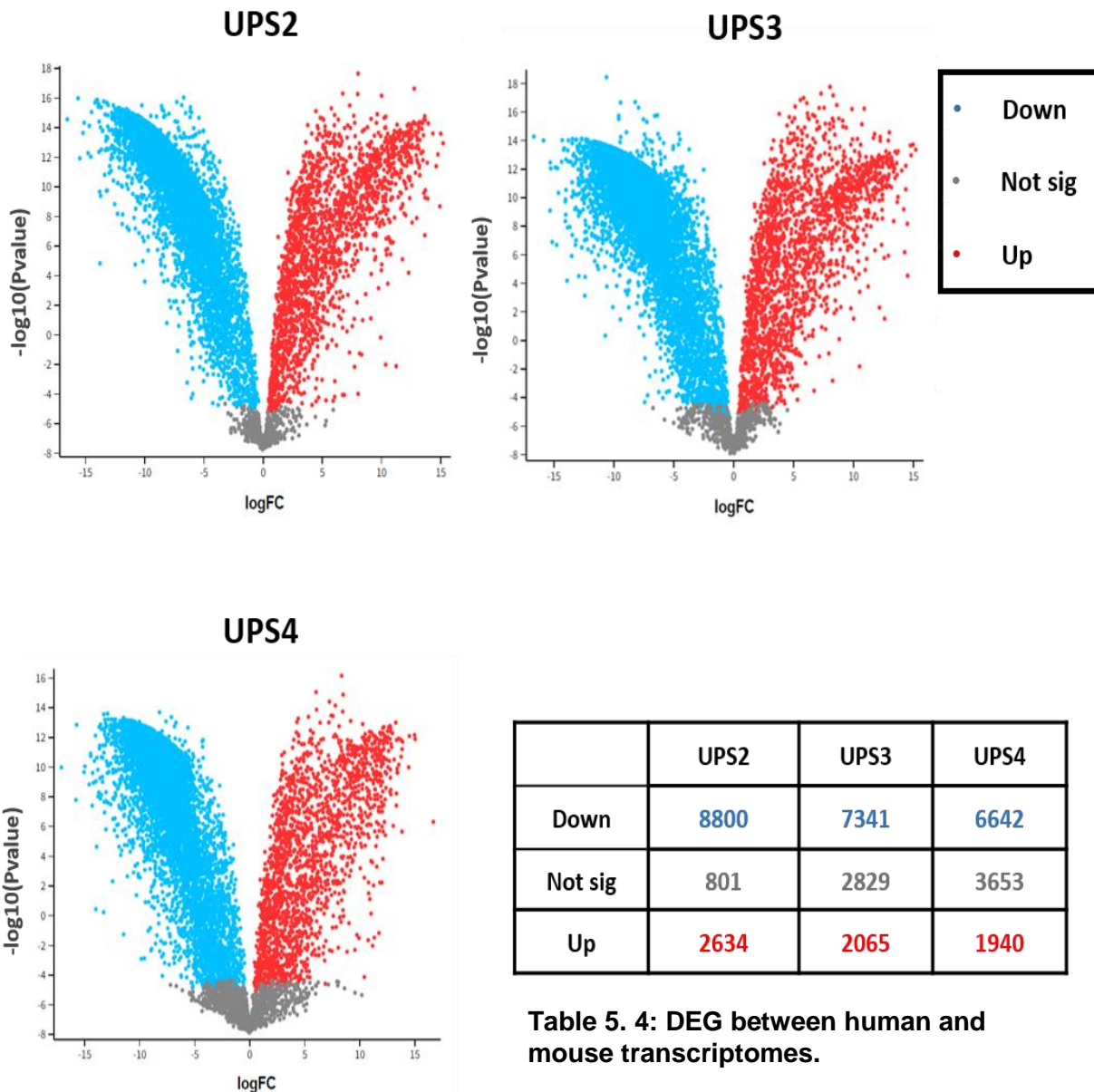
Figure 5. 24: Volcano plots for DEG between human and mouse transcriptomes.

The logFC represents the change in gene expression between human and mouse transcriptomes in UPS1, UPS2 & UPS3, while the p-values indicates the level of significance of each gene. Each dot illustrates one gene. The cut-off criterion for DEG significance was FDR ≤ 0.05 and logFC of 1. **Blue dots represent down-regulated genes**, grey dots represents no significant differential expression genes and **red dots represents up-regulated genes.**

5.6.2 Biological process enriched in human and mouse transcriptomes

Gene Set Enrichment Analysis (GSEA) analysis using the gene sets presented by the molecular signatures database (MsigDB), 15,906 genes were uploaded and GSEA identified the (4243) up- / (7993) downregulated genes between the human and mouse transcriptomes. Only five of the most up/downregulated genes were mentioned in (Table S4). Some biological processes were activated in all xenografts, in UPS2 human STS cells AP-1 adaptor complex was activated (Fig.5.26). Adaptor protein (AP)-1 is member of the AP family which play an important role in cell development, proliferation, migration and apoptosis (Shaulian & Karin, 2001). Another study emphasised on AP-1 proteins roles in cancer proliferation and tumourgenesis in breast cancer (Shen et al., 2008). There are 11 genes associated with this hallmark, only three of it were enriched in UPS2, Adaptor related protein complex 1 subunit sigma 2 and Sigma 3 (AP1S2 & AP1S3) and Solute Carrier Family 18 Member A3 (SLC18a3).

DNA double strand break processing is a hallmark that was enriched in UPS3 human STS cells (Fig.5.27). DNA double strand break (DSBs) is chromosomal aberration and DSBs repair includes many pathways and dysfunction of any pathways can lead to genomic mutations which subsequently can lead to various diseases and cancer (Scully et al., 2019). There are 20 genes in this hallmark, three of it were activated in UPS3, DNA replication helicase 2 (Dna2), RB binding protein 8 (RBBP8), and SPO11 inhibitor of meiotic double stranded breaks (SPO11).

In UPS4, gamma-tubulin complex hallmark was enriched (Fig.5.28). Gamma-tubulin protein involved in microtubule nucleation, regulating mitosis (Oakley et al., 2015). There are 38 genes in this hallmark, eight of them were enriched in UPS3 includes, Biogenesis of lysosomal organelle complex 1 subunit 2 (BLOC1S2), GIT ArdGAP 1 (GIT1), Centorsomal protein70 (CEP70), B9 domain containing 2 (B9D2), Rho guanine nucleotide exchange factor 7 (ARHGEF7), Tubulin Gamma Complex Associated protein 6 (TUBGCP6) and Fasciculation and elongation protein zeta-1(FEZ1).

Translation factor activity RNA binding was suppressed in UPS3 and UPS4. Translation factor activity RNA binding comprises of the translation activities for mRNA binding (Berset, 2003). There are 91 genes in this hallmark, most of the genes were

downregulated but Eukaryotic Elongation Factor 2 kinase (EEF2K) was upregulated in both UPS3 and UPS4.
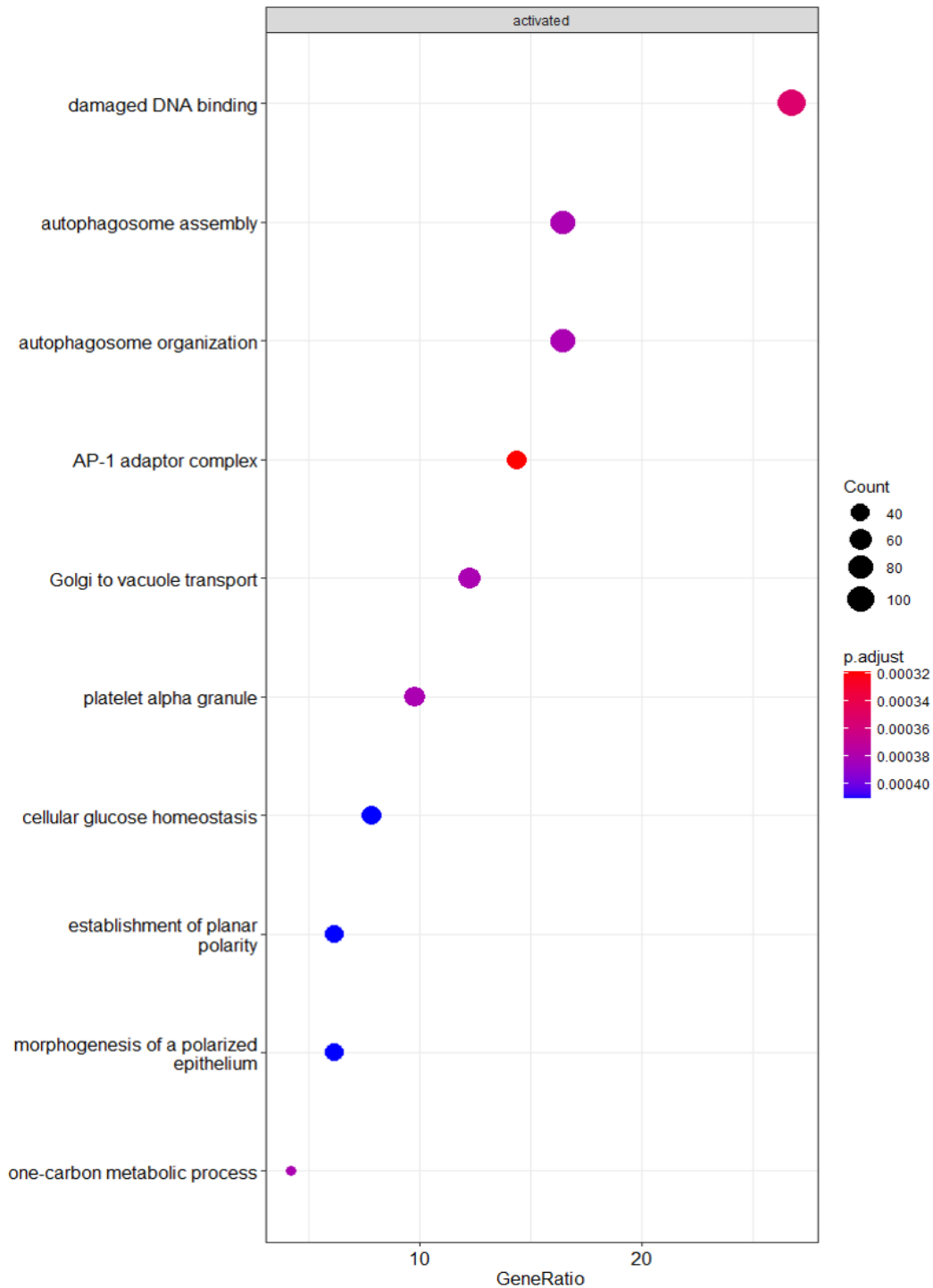
Figure 5. 25: Biological process enriched in human versus mouse samples from UPS2 xenografts.

The hallmark gene sets (h.all.V7.1 MSigDB) shown above were significantly up regulated in human STS cells .The cut-off criteria for significance was p-value ≤ 0.05.
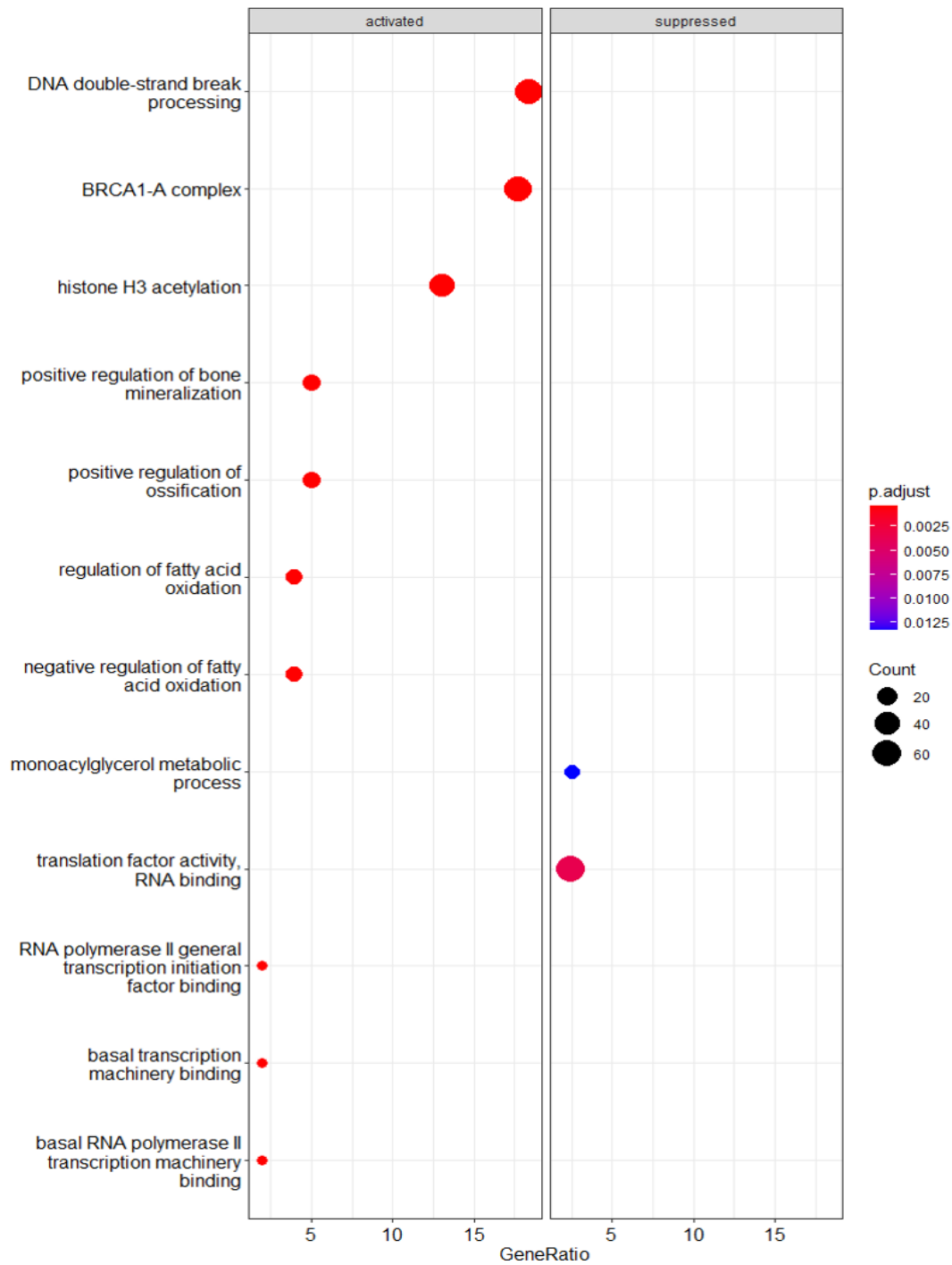
Figure 5. 26: Biological process enriched in human versus mouse samples from UPS3 xenografts.

The hallmark gene sets (h.all.V7.1 MSigDB) shown above were significantly up regulated in human STS cells .The cut-off criteria for significance was p-value ≤ 0.05.
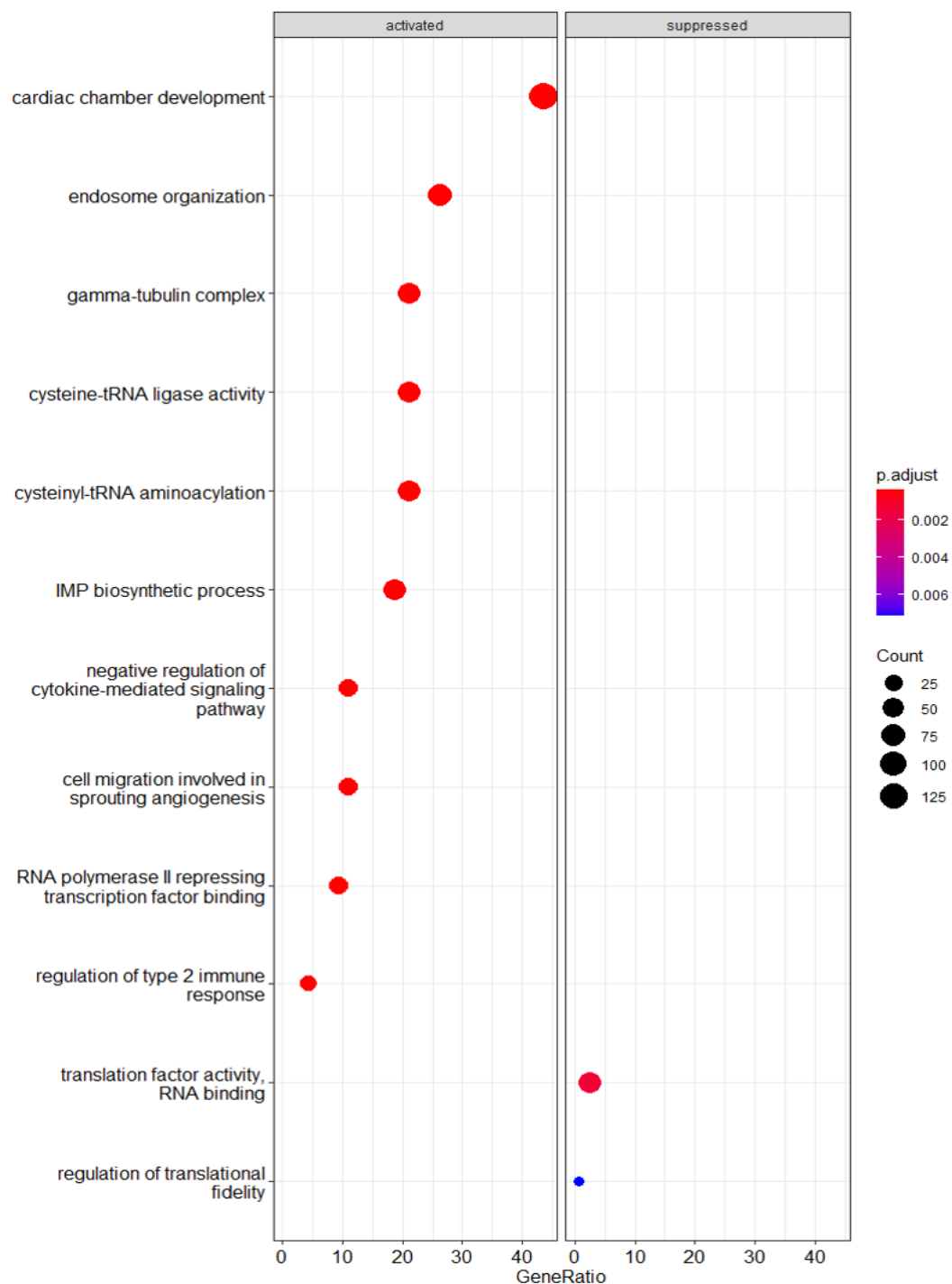
Figure 5. 27: Biological process enriched in human versus mouse samples from UPS4 xenografts.

The hallmark gene sets (h.all.V7.1 MSigDB) shown above were significantly up regulated in human STS cells.The cut-off criteria for significance was p-value ≤ 0.05.

5.6.3 Differences in expression of mesenchymal genes commonly used to identify cancer associated fibroblasts between the human and mouse transcriptomes in xenografts

In this project's earlier chapters we studied eight CAFs markers and in this chapter we expanded these studies to their expression between the human and mouse transcriptomes of our UPS xenografts including Transgelin, αSMA, Vimentin, N-cadherin, Fibronectin, FSP-1, FAPα and SOX2. Statistical analysis showed no significant differences in gene expressions between the human and mouse transcriptomes for fibronectin and N-cadherin. transgelin, αSMA, vimentin, FSP-1, FAPα and SOX2 were significantly higher in mouse transcriptomes when compared with the human transcriptomes (Fig.5.29).
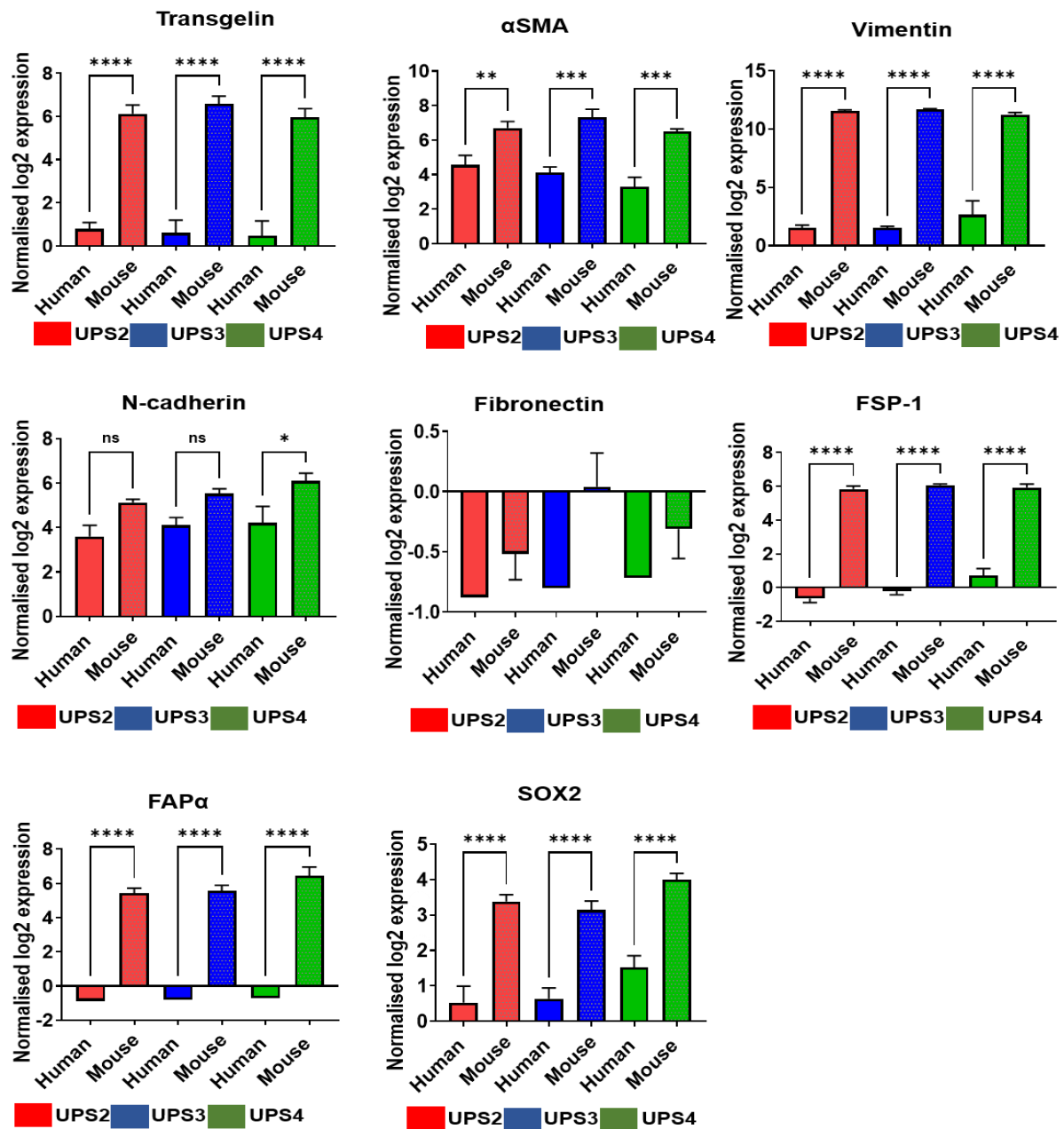
Figure 5. 28: Bar chart analysis of the common mesenchymal gene expressions in human vs mouse transcriptomes in UPS xenografts.

Statistical analysis shows no significant analysis in Fibronectin and N-cadherin gene expression between the xenografts. All the other genes expression shows significant differences between human and mouse transcriptomes. X-axis is the human transcripts samples, Y-axis is the normalised log 2 expression. Error bars are ± SEM. *,P<0.05 , **,P <0.01; ***,P < 0.001 ;NS, not significant.

5.6.4 Differences in expression of additional mesenchymal genes used to identify cancer associated fibroblasts in the mouse transcriptome of UPS xenografts.

As in section 5.3.4, we also examined the differences in expression of additional mesenchymal genes associated with CAF. MFAP5 showed significantly higher expression in the mouse transcriptome (stroma) when compared to human, PDGFRβ and desmin were higher in human transcriptomes when compared to mouse transcriptomes (Fig.5.30).
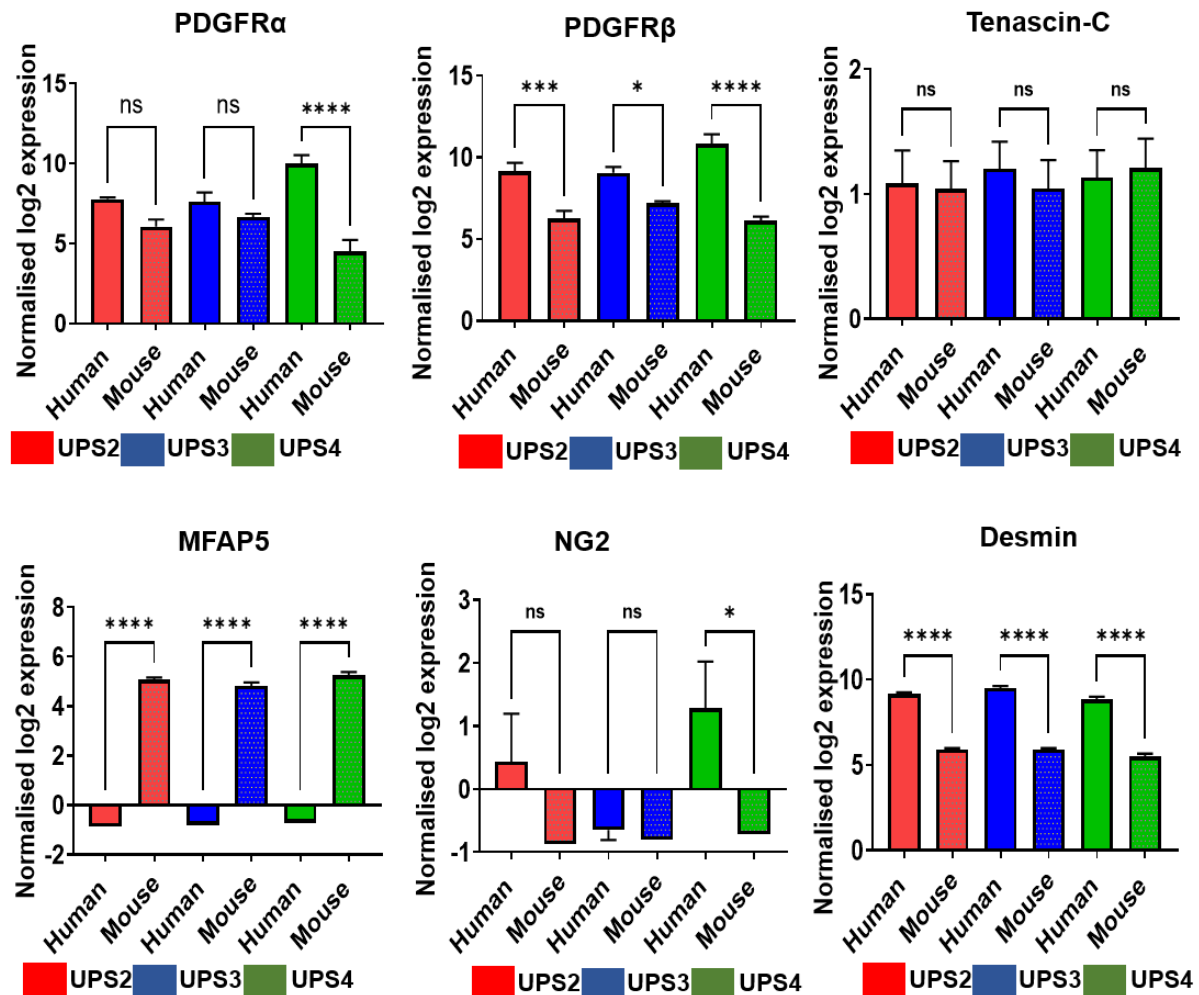
Figure 5. 29: Bar chart analysis of the common CAFs gene expression in human vs mouse transcriptomes in UPS xenografts.

Error bars are ± SEM. *,P<0.05 , **,P <0.01; ***,P < 0.001 ;NS, not significant.

Genes	UPS2		UPS3		UPS4	
	Stroma	UPS	Stroma	UPS	Stroma	UPS
Transgelin	****		****		****	
αSMA	**		***		***	
Vimentin	****		****		****	
N-cadherin	ns	ns	ns	ns	*	
Fibronectin	ns	ns	ns	ns	ns	ns
FSP-1	****		****		****	
FAPα	****		****		****	
SOX2	****		****		****	
PDGFRα	ns	ns	ns	ns		****
PDGFRβ		***		*		****
Desmin		****		****		****
NG2	ns	ns	ns	ns	ns	*
Tenascin C	ns	ns	ns	ns	ns	ns
MFAP5	****		****		****	

Table 5. 5: Differential expression gene of the most common mesenchymal gene between stroma and UPS cells in xenografts.

This table summarised the differences in gene expression of the most common mesenchymal genes between the stroma and UPS cell in each xenograft. (*) indicates higher expression of the gene. Stroma is the mouse cells. UPS cell is the STS cells engrafted in mouse.*,$P<0.05$, **,$P <0.01$; ***,$P < 0.001$;ns, not significant.

5.6.5 Cell subset prediction between human and in mouse transcripts

As discussed in section 5.3.4 Xcell analysis indicated that UPS cells have things in common with HSC and MSC that are not seen in the mouse stroma as in both cells showed higher abundadcny in UPS cells in UPS2 and UPS3 when compared with the mouse stroma (Fig.5.30). similarly Macrophages, M1 macrophages and M2 macrophages showed higher predicted levels in human UPS. As the human cells are not macrophages, but they must have a common transcript set. However, since the Xcell score <0.001, this will be negibligible.This suggests the cell subset predcition methods are not reliable in sarcoma models but do highlight common gene expression within sarcoma. Pericytes appears enriched in the stroma, as expected. Regulator of G protein signaling 5 (RGS5) is a perciyte marker that was enriched in the stroma but not UPS cells (Bondjers et al., 2003),could some of these be 'SAF' markers?

There are genes associated with mesenchymal lineage such GUCY1a1, VCAM1 RGS5, TAGLN, MYF5, IL6, COL1A1, SOX11, NT5E, PDFRAα/β, VIM, S100A4, FN1, ACTA2, CSPG4 and MFAP5. Moreover, there are genes at each end which are particularly enriched in mouse versus stroma (Fig.5.31).
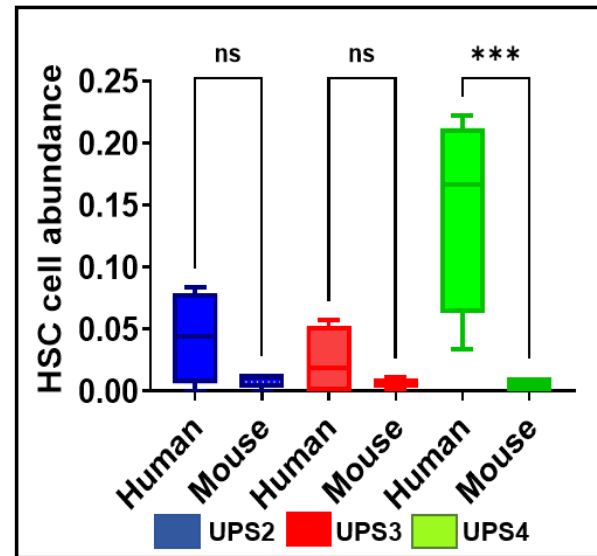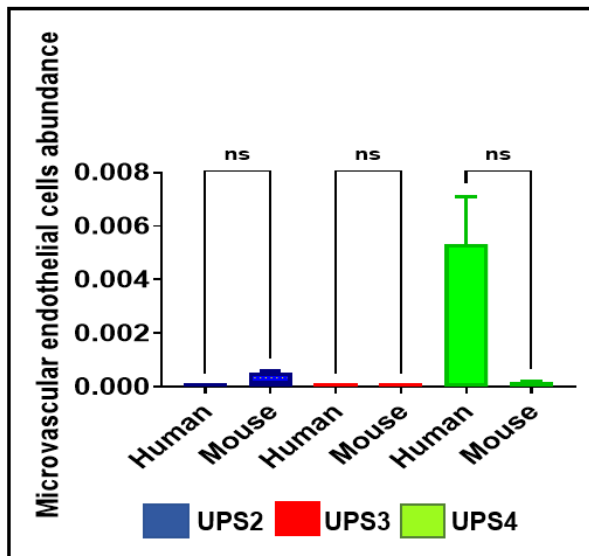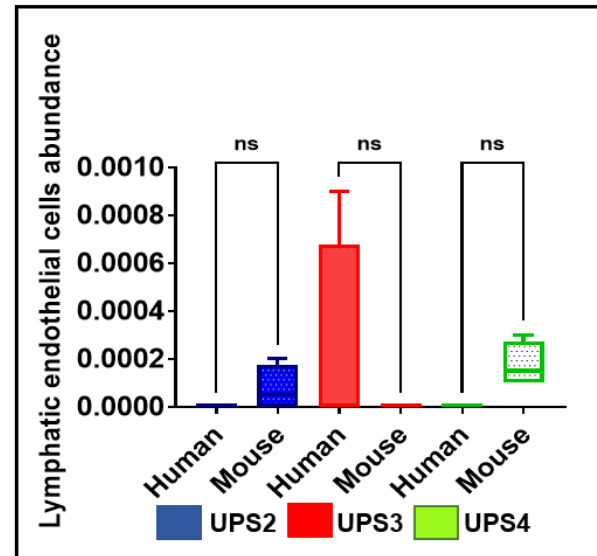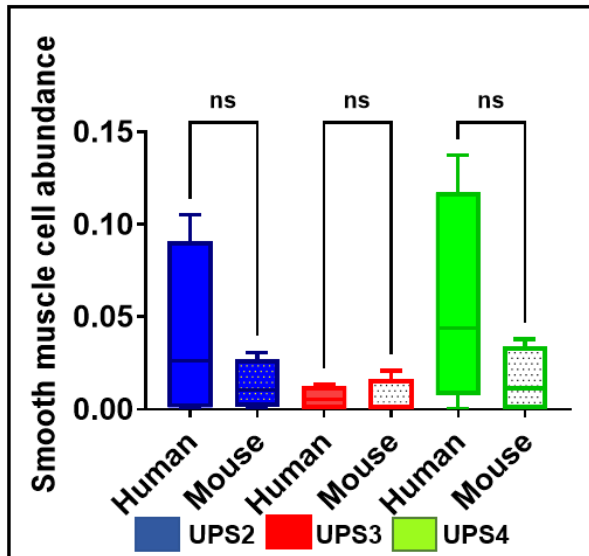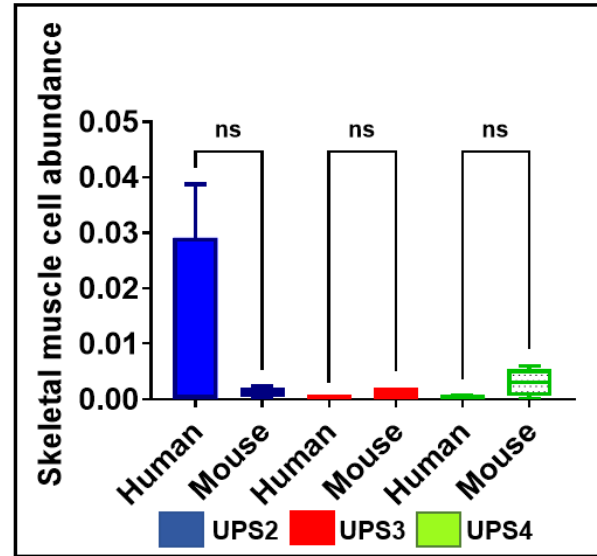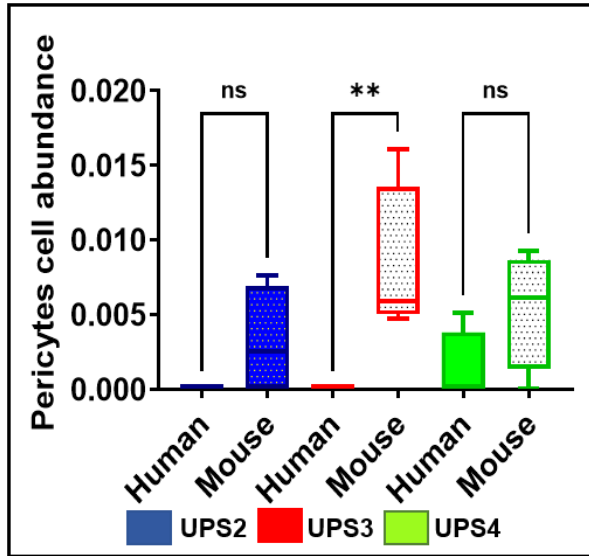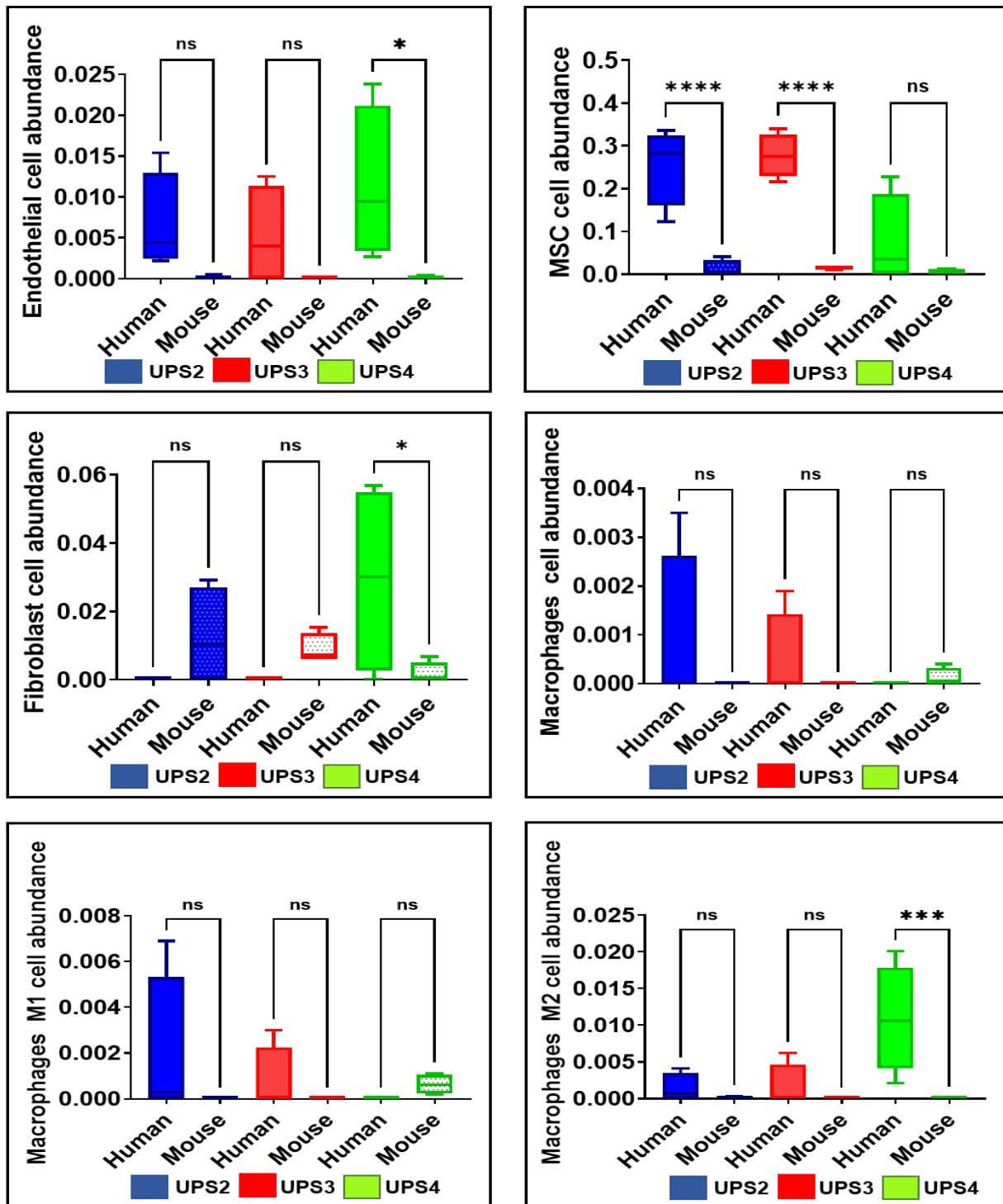
Figure 5. 30: Cell subset abundance between human and mouse.

XCell scores for different cells in mouse transcripts. Box and Whiskers plots showing the differences. Multiple comparison analysis was done using Tukey's test. UPS1 in blue, UPS2 in red & UPS3 in green. Whiskers are min to max, the line is the median. *,P<0.05 , **,P <0.01; ***,P < 0.001 ;NS, not significant.
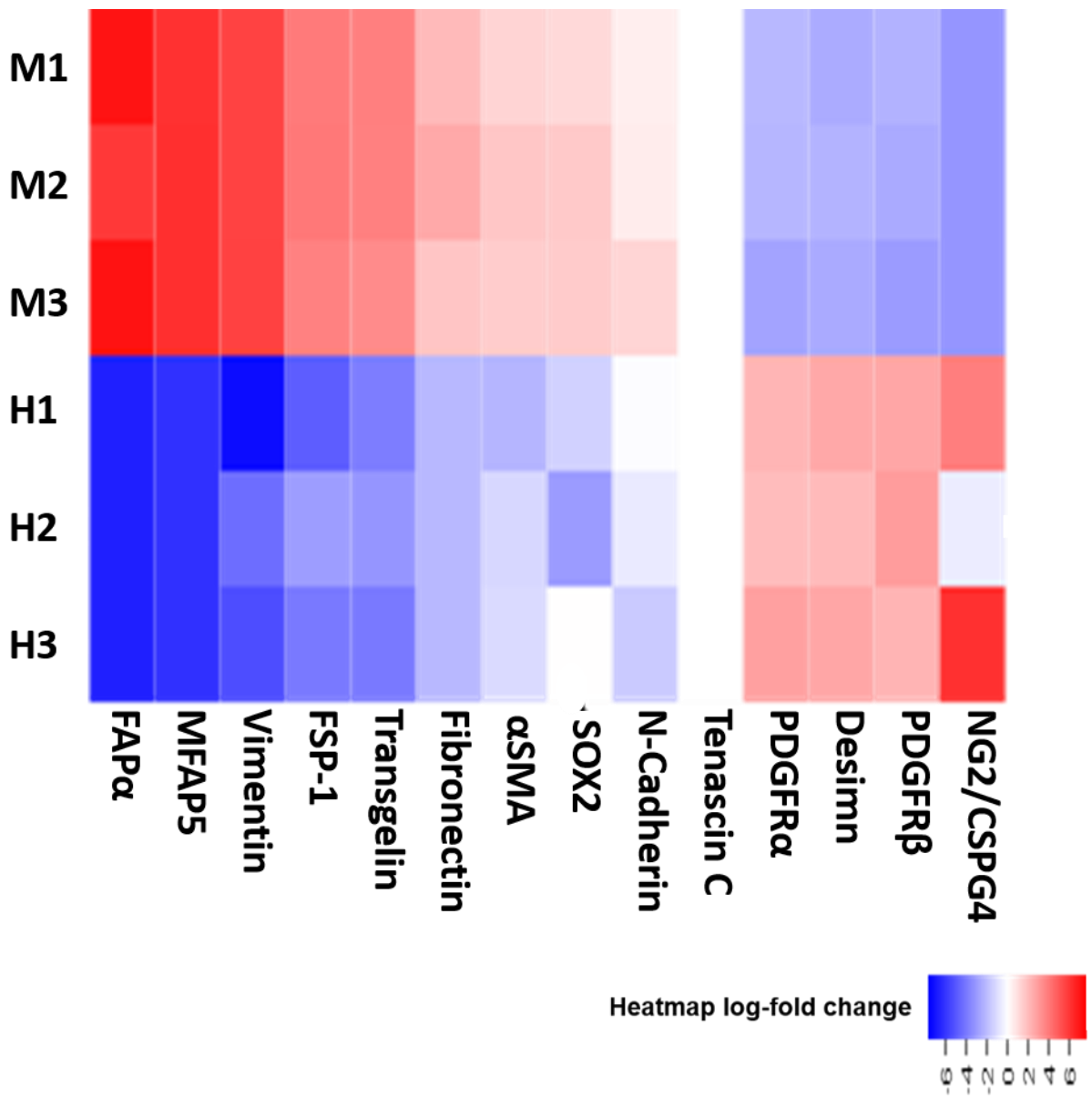
Figure 5. 31: Heatmap to visualize expression of common mesenchymal genes known as CAFs.

Mouse transcriptomes (M1, M2 & M3) Human transcriptomes (H1, H2 & H3).

5.7 Influence of mesenchymal gene expression on survival of patients with fibroblastic STS subtypes

TCGA and VorteX clinical data were used in this section to study the influence of mesenchymal gene expression on patient's survivals. Changes in overall survival (OS) analysis and progression-free survival (PFS) was analysed based on gene expression of (transgelin, αSMA, vimentin, N-Cadherin, fibronectin, FSP-1, FAPα & SOX2) in both TCGA and VorteX samples. OS and PFS was also estimated by combining some genes that might be "SAF markers" (transgelin, αSMA, vimentin and MFAP5) (Fig.5.34 and Fig.5.35).The TCGA-SARC group composed of poorly differentiated sarcomas, including MFS and UPS (25 and 52 samples, respectively), and the VorteX group composed of MFS and UPS (30 and 40, respectively). OS and PFS were estimated using Kaplan-Meier analysis along with the computed hazard ratio for each group. Kaplan-Meier analysis is a valuable method that may have an important role in generating evidence-based information on survival. It has been widely used because of its simplicity in analysis and the ability to add additional factors to studies (Goel et al., 2010).

The average age of the patients included in this study was 66.7 years and 60 years in TCGA and VorteX, respectively. The sex distribution was almost equal in both cohorts (Table 5.5). OS and PFS in TCGA-SARC and VorteX were not significantly different in all the survival plots between the **High** and **Low (**25th-75th quartiles**)** groups. The null hypothesis was evaluated using the log-rank test and Cox regression hazard test (HR). For the log-rank test, we calculated the expected number of events (survival) and compared them to the event times (years) between the two groups. Cox regression hazard was used as a risk of hazard could occur at any time in any group (Goel et al., 2010). OS and PFS were analysed for three different intervals: 2, 5, and 10 years. There were no significant differences in OS between high and low gene expression in all groups after 2 and 5 years; however, high N-cadherin expression was associated with lower OS and PFS at 10 years (Table 5.6). αSMA expression impacted PFS at 2 years but had no impact at 5 and 10 years. Increased expression of vimentin, fibronectin, and FAPα was

significantly associated with PFS at 2 and 5 years but not at 10 years (Fig. S34 & Table 5.6). There were no significant differences in OS and PFS for the combined 'SAF' group of genes (Fig. 5.35 and Fig. 5.36)
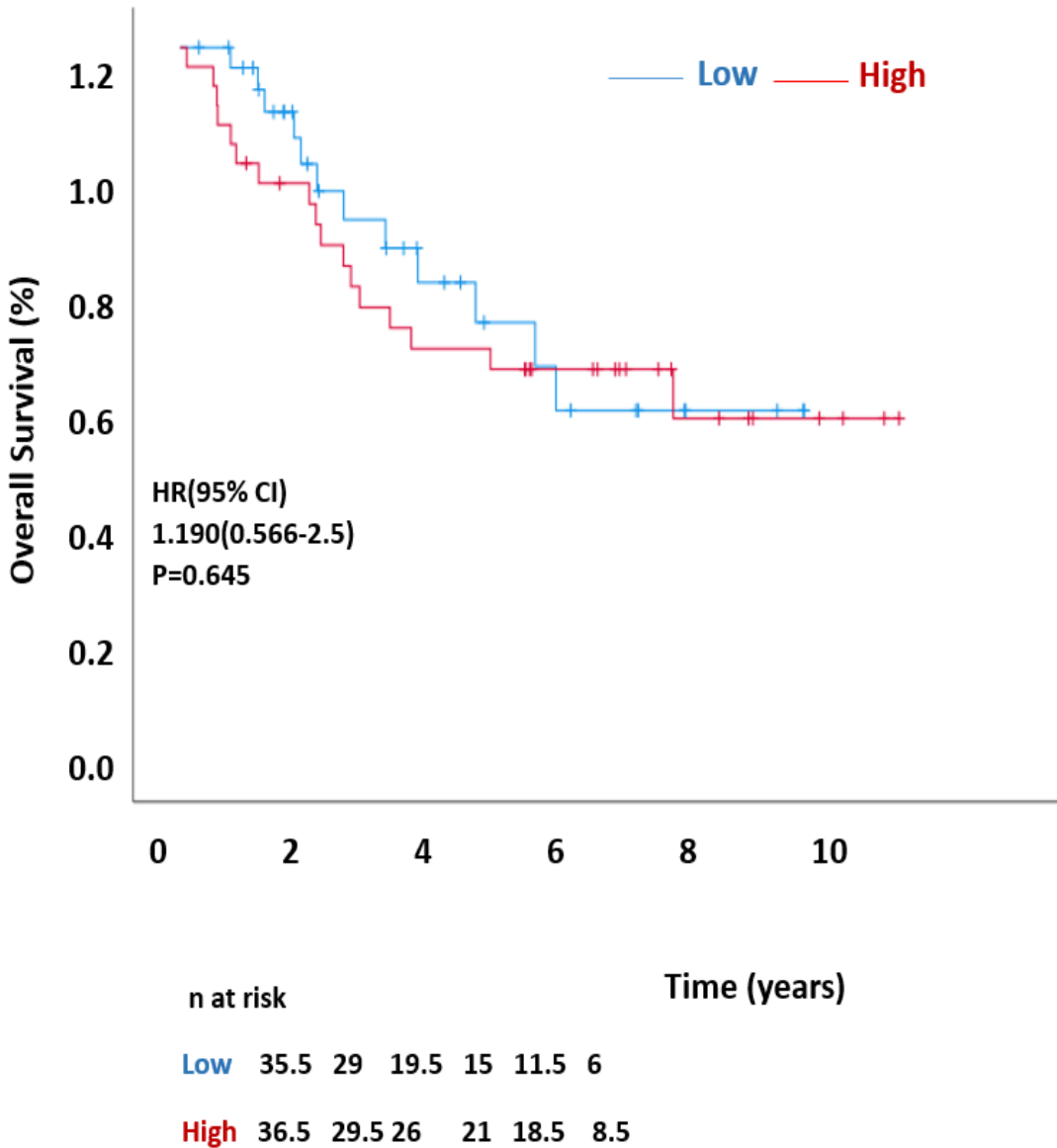
Figure 5. 32: Overall Survival Analysis of common SAF gene expression in the TCGA SARC and VorteX RNAseq dataset.
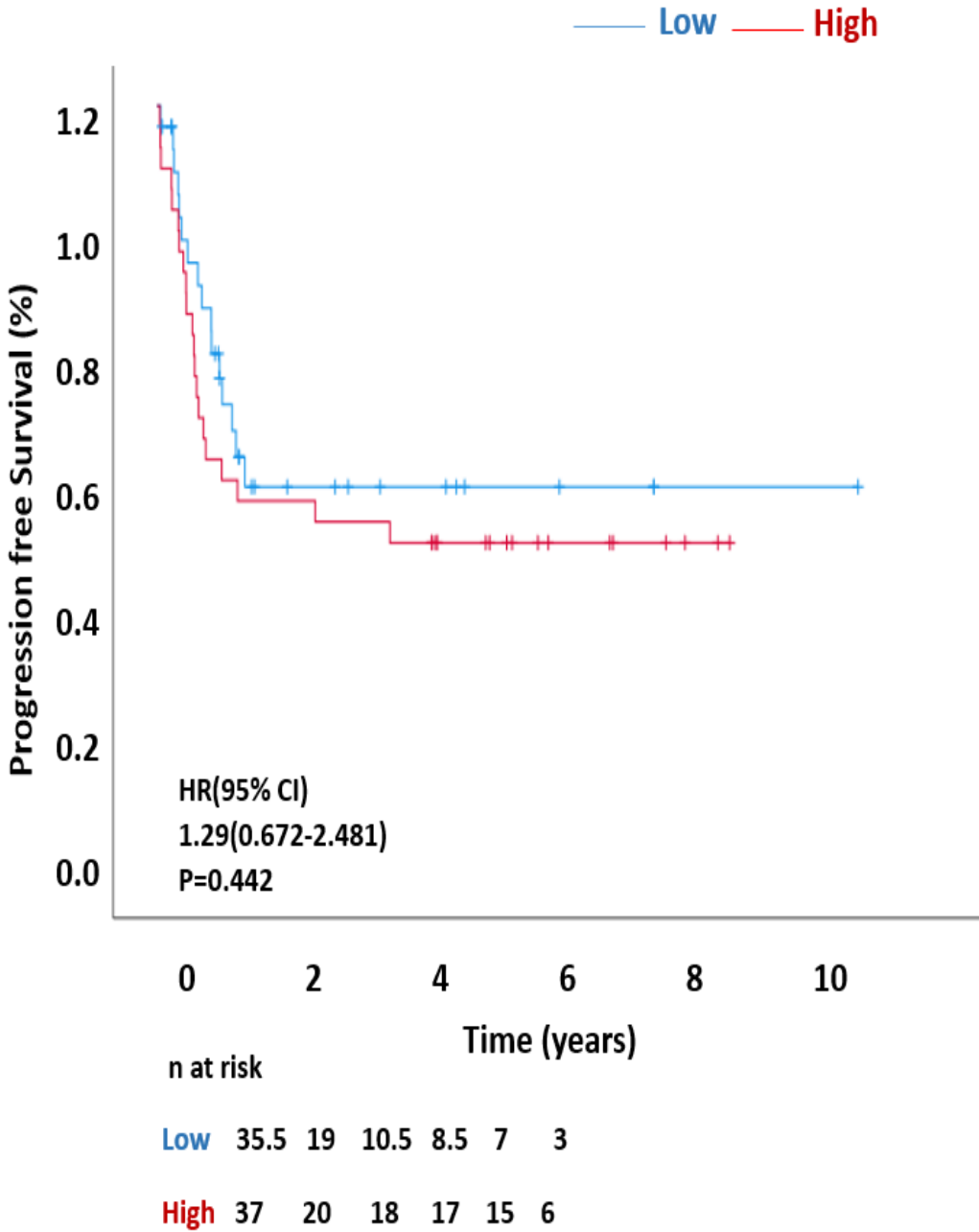
Figure 5. 33: progression free Survival Analysis of common SAF gene expression in the TCGA SARC and VorteX RNAseq dataset.

Genes	OS			PFS		
	2 years	5 years	10 years	2 years	5 years	10 years
Transgelin	HR(95%CI) 1(0.43-2.34) P=0.5	HR(95%CI) 0.992(0.46-2.17) P=0.984	HR(95%CI) 0.738(0.32-1.50) P=0.356	HR(95%CI) 0.307(0.57-1.77) P=0.079	HR(95%CI) 1.75(0.88-3.5) P=0.129	HR(95%CI) 0.341(0.64-2.42) P=0.529
αSMA	HR(95%CI) 2.3(1.84-2.15) P=0.077	HR(95%CI) 1.163(8.3-24) P=0.324	HR(95%CI) 0.745(0.31-1.77) P=0.504	**HR(95%CI) 1.95(0.99-3.83) P=0.049**	HR(95%CI) 0.485(0.38-2.24) P=0.324	HR(95%CI) 0.728(0.37-1.44) P=0.36
Vimentin	HR(95%CI) 1.42(0.86-2.23) P=0.073	HR(95%CI) 0.916(6.3-19.3) P=0.077	HR(95%CI) 1.410(0.65-3.05) P=0.381	**HR(95%CI) 4.27(1.95-9.36) P=<0.001**	**HR(95%CI) 2.619(1.2-5.72) P=0.012**	HR(95%CI) 1.668(0.83-3.34) P=0.145
N-cadherin	HR(95%CI) 1.181(11.9-16.9) P=0.466	HR(95%CI) 2.005(0.92-4.39) P=0.077	**HR(95%CI) 2.623(1.25-5.5) P=0.008**	HR(95%CI) 1.265(0.66-2.45) P=0.48	HR(95%CI) 1.771(0.93-3.37) P=0.077	**HR(95%CI) 137.4(0.23-8.5) P=0.008**
Fibronectin	HR(95%CI) 2.096(0.67-6.57) P=0.196	HR(95%CI) 2.038(0.89-4.68) P=0.087	HR(95%CI) 1.215(0.55-2.68) P=0.628	**HR(95%CI) 3.285(1.57-6.88) P=<0.01**	**HR(95%CI) 2.101(1.07-4.15) P=0.029**	HR(95%CI) 1.180(0.62-2.25) P=0.615
FSP-1	HR(95%CI) 2.07(0.84-5.10) P=0.108	HR(95%CI) 0.941(0.43-2.04) P=0.877	HR(95%CI) 0.638(0.30-1.36) P=0.242	HR(95%CI) 1.620(0.86-3.04) P=0.127	HR(95%CI) 0.852(0.45-1.62) P=0.625	HR(95%CI) 0.734(0.40-1.40) P=0.322
FAPα	HR(95%CI) 0.988(0.95-1.03) P=0.093	HR(95%CI) 1.97(1.12-3.46) P=0.051	HR(95%CI) 0.971(0.45-2.11) P=0.94	**HR(95%CI) 2.279(1.36-3.83) P=0.001**	**HR(95%CI) 2.445(1.22-4.89) P=0.009**	HR(95%CI) 1.053(0.54-2.04) P=0.878
SOX2	HR(95%CI) 1.48(0.60-3.66) P=0.388	HR(95%CI) 1.031(0.94-1.14) P=0.534	HR(95%CI) 1.561(0.61-4.02) P=0.351	HR(95%CI) 0.596(0.30-1.22) P=0.154	HR(95%CI) 0.953(0.86-1.05) P=0.5	HR(95%CI) 1.131(0.60-2.15) P=0.707

Table 5. 6: Overall and progression free survivals in 2, 5 and 10 years between high and low respective gene expression in TCGA and vortex clinical data.

The highlighted cells indicate poor survivals with high expressions of a specific gene (red cells) and low expression of the relative gene (yellow cells) with p<0.05.

5.8 Summary

Results from these studies indicate that growing human STS cell lines isolated from patients in mice is feasible; however, UPS1 did not grow. Because the UPS cells were subcutaneously injected into the mice, orthotopic injection might overcome this limitation. Subcutaneous injection is easier to perform as it does not require surgical intervention; however, orthotopic injection was shown to produce more successful tumour growth in breast cancer (Kocatürk & Versteeg, 2015).

Transcriptomic analysis of the human transcripts revealed that UPS3 clustered separately from both UPS2 and UPS3.

Data from TCGA-SARC, VorteX, and our UPS xenografts indicated that UPS and MFS samples were uniformly clustered throughout the MDS plot, although the UPS xenografts were more spatially distributed. This is a similar result to (Abeshouse et al., 2017) who placed UPS and MFS in the same genomic group.

Expression of 15 stromal genes was evaluated between the human transcripts: transgelin, αSMA, vimentin, N-cadherin, fibronectin, FSP-1, FAPα, SOX2, PDGFRα/β, NG2, desmin, tenascin C, and MFAP5. There were no significant differences in the expression of most genes, except for transgelin and tenascin C, which exhibited lower expression in UPS3 compared with UPS2 and UPS3.

There were no significant differences among DEGs between mouse transcripts. Although UPS3 clustered separately in the MDS plots, there were no significant differences in gene expression between the three samples.

The mouse samples (stroma) clustered distinctly from the human samples (STS cell lines), which is demonstrated by MDS plots. DEGs analysis showed that transgelin and αSMA were significantly higher in the stroma compared with the UPS cells, which confirmed our findings from Chapter 3 of this study. Vimentin, FSP-1, FAPα, SOX2, and MFAP5 were significantly higher in the stroma than in the UPS cells. Could any of these markers be SAFs? There were no significant differences in fibronectin and tenascin C expression between the stroma and the STS cells.

There were no significant differences in N-cadherin expression between UPS2 and UPS3; however, N-cadherin expression was higher in the UPS4 stroma. PDGFRα and NG2 expression was not significantly different between UPS1 and UPS2; however, expression of PDGFRα and NG2 was higher in UPS4. PDGFRβ and desmin exhibited higher expression in stroma cells among the three UPS compared with the stroma (Table 5.5). So, we could establish a possible "SAF panel" from our data: transgelin, αSMA, vimentin and MFAP5. To identify common genes in each cell subset, we analysed the genes commonly expressed in pericytes: NG2/CSPG4 and PDGFRβ (Baek et al., 2022). PDGFRβ expression was higher in STS cell lines in all three xenografts, and NG2 expression was higher in UPS4.

Different MSC tissue sources express different markers, except for OCT4, Nanog, and stage-specific embryonic antigen 4 (SSEA-4), which are expressed by all MSCs cells. SOX2 plays a key role in pluripotency and was highly expressed in the stroma (Fig. 5.30 & Table 5.5). PDGFRα expression was higher in STS cells in UPS3. PDGFRβ and desmin were higher in STS cell lines (Fig. 5.31). No significant differences in fibronectin expression between STS cells and the stroma were observed (Fig. 5.30).

Cell subset prediction analysis indicated how poor these algorithms are in STS models and that they may also be poor at predicting cell subsets in clinical data.

OS and PFS analysis was performed among all the common genes used previously in this project; however, there were no significant differences on survival based in the expression of the tested genes. This might be due to the low sample number in this study. High N-cadherin expression showed poor OS and PFS in 10 years (Table.5.6). In contrast, mesenchymal genes identified as potential SAF markers might not be prognostic, unlike for carcinomas.

In this study, we identified several mesenchyme-associated genes (summarised in Table 5.5) that were enriched in the mouse stroma compared with the human STS cell lines. With further validation, these genes could be used to identify SAFs in the future.

Chapter 6

General Discussion

6.1 The challenge of identifying SAFs

Soft tissue sarcomas (STSs) are uncommon heterogeneous mesenchymal tumours arising from the mesoderm. There are >70 STS histological subtypes. Undifferentiated pleomorphic sarcoma (UPS) is the most common STS in adults. STS arise mainly in the extremities and trunk. STS treatment includes surgical excision, chemotherapy, and/or radiotherapy (Genadry et al., 2018). Molecular targeted therapies have opened a new era in sarcoma treatment. If molecular targeted therapies are to continue to be successfully used to treat STS, studying gene expression and function is important to improve our understanding of STS biology and the available STS treatments.

The tumour microenvironment (TME) is an important regulator of cancer biology and therapy response composed of various cellular components, including cancer cells, non-transformed stromal cells such as immune, vascular cells and fibroblasts, and non-cellular components such as the extracellular matrix, growth factors, and cytokines. TME considered to play an important role in cancer progression (Kalluri;2016).

Cancer associated fibroblasts (CAFs) are the most important stromal cell in the TME. CAFs are distinguished from normal fibroblasts by their morphology and specific CAF markers, including α-smooth muscle actin (αSMA), fibroblast activation protein-α (FAPα), fibroblast-specific protein 1 (FSP-1), and desmin (DES). CAFs have been shown to promote progression and metastasis in several cancers (Goh et al., 2007; Grum-Schwensen et al., 2005; Kuperwasser et al., 2004; Orimo et al., 2005). The few studies performed to date have shown significant overlaps in mesenchymal marker gene expression (e.g. vimentin , αSMA, FSP-1, and FAPα) between STS cells, sarcoma-associated fibroblasts (SAFs), and other mesenchymal cell populations (Fisher, 2004; Heim-Hall & Yohe, 2008). Further investigations are needed to determine whether there are significant gene expression differences between SAF and STS cells and whether these vary among histotypes.

Over recent decades, many studies have explored the role of CAFs in cancer progression in carcinomas. However, little is known about the role of CAFs in sarcoma, referred to as SAFs, to clarify the discussion of potential differences between fibroblasts in the different cancer types. Studying SAFs is more challenging than CAFs for two reasons. Firstly, few STS cell lines are available that are matched to their original histotype, particularly for the most common adult STS forms. Commercial, well-established cell lines do not show the same level of heterogeneity as tumours. However, primary cell cultures or cell lines from STS tumours would be the best alternative to better understanding cancer, and these are the type of cell lines used in this project (Salawu et al., 2016). Secondly, since STS cells and SAFs are both mesenchymal, no selective markers have yet been identified to facilitate their study. In this project, we compared mesenchymal gene expression in human STS (UPS, myxofibrosarcoma [MFS], and leiomyosarcoma [LMS]) cell lines and normal human mesenchymal cells. Then, we investigated the growth of UPS cell lines as xenografts in mice to identify the stromal expression of mesenchymal transcripts by next-generation RNA sequencing (RNAseq) and to determine whether mesenchymal gene expression influences survival in complex karyotype STS (UPS and MFS).

This project's aims were met as follows. Firstly, common mesenchymal protein levels were characterised in human STS cell lines and normal human mesenchymal cells cultured *in vitro* in Chapter 3. Secondly, after investigating the growth of UPS cell lines as xenografts, mesenchymal protein expression was further characterised in UPS tumours in Chapter 4. Thirdly, in Chapter 5, RNAseq was used to identify gene expression differences between UPS and stromal cells to characterise further mesenchymal gene expression and create a SAF gene signature. Here, we also explored whether the expression of these specific genes influenced STS patient survival.

6.2 Investigating expression of common CAF protein expressions in STS

To address the first aim of this thesis, common mesenchymal proteins expressions, including transgelin (TAGLN), αSMA, vimentin, N-cadherin fibronectin FSP-1, FAPα, and SRY-box transcription factor 2 (SOX2), were compared between STS cell lines (UPS, MFS, and LMS) with respect to primary human mesenchymal cells (normal dermal fibroblasts, uterine fibroblasts, pulmonary fibroblasts, and mesenchymal stem cells) using western blots (WBs). These findings showed positive expression of all proteins in all cells, with transgelin and αSMA showing lower levels in UPS and MFS cells than in primary fibroblasts and LMS cells. Transgelin is a smooth muscle differentiation marker, and *αSMA* is expressed at higher levels in activated fibroblasts, possibly indicating that UPS and MFS are less differentiated. Consistent with our findings, Robin *et al.* (2012) used immunohistochemistry (IHC) to show that transgelin levels were higher in LMS than in UPS and MFS, suggesting that transgelin could be used as a diagnostic biomarker. Another study showed that transgelin could be used as a diagnostic marker to distinguish endometrial stromal sarcoma (ESS) from uterine smooth muscle tumours since ESS did not express transgelin (Tawfik et al., 2014). The importance of transgelin as a diagnostic STS marker was shown by another study that measured *transgelin* expression in LMS and ESS samples, also finding that transgelin was highly expressed in LMS but not in ESS (Alabiad et al., 2020). These studies are consistent with our WB findings indicating that transgelin might be a diagnostic marker to differentiate STS subtypes.

Subcellular localisation was then investigated in this thesis using immunocytochemistry (ICC). ICC is an immunostaining method for cultured cells and was used to determine the subcellular localisation of common mesenchymal proteins (transgelin, αSMA, vimentin, N-cadherin, fibronectin, FSP-1, and FAPα) and a transcription factor (SOX2). ICC allowed us to compare protein localisations among STS cell lines and primary fibroblasts. Most proteins tended to localise in the same areas in all cells with slight variations (Chapter 3). Cells were also stained with phalloidin to visualise filamentous (F)-actin. Colocalisation coefficients showed that all mesenchymal proteins tested co-localised with F-actin, supporting our previous findings that the subcellular localisation is very similar between

the proteins and this suggests their function may not vary between the cell types (Zhao et al., 2009).

IHC was then performed in formalin-fixed paraffin-embedded (FFPE) UPS tissues to expand upon the previous WB analyses. IHC is a semi-quantitative method for analysing common mesenchymal protein's expression. All proteins showed positive expression in UPS xenografts, supporting the WB analyses. Unfortunately, it was not feasible to distinguish STS from stromal cells based on nuclear size and morphology using Qupath, despite UPS cell nuclei typically being larger than stromal cell nuclei. This inability might reflect similarities between STS and stromal cell nuclei or QuPath's inability to identify nuclei that also varied in 3,3'-diaminobenzidine (DAB) staining positivity since it uses the haematoxylin blue stain to identify nuclei.

Immunofluorescence (IF) staining was also performed in frozen xenograft sections to quantify mesenchymal protein expression initially characterised by WB (i.e., transgelin, αSMA, vimentin, N-cadherin, fibronectin, FSP-1, FAPα, and SOX2). All proteins were positively expressed in all three UPS tissues. However, this result also did not expand upon our WB results since IF could not distinguish between UPS and stromal cells. Nevertheless, a specific human mitochondrial antibody (MT-AB) was used to co-stain our UPS sections with transgelin. Our results showed that this approach could distinguish positively-stained UPS cells from negatively-stained mouse cells. MT-AB levels were lower in UPS4 sections than in UPS2 and UPS3 sections, indicating fewer STS cells in UPS3. However, this does not match our RNAseq results in Chapter 5, where we had equal human and mouse read counts for each sample. This discrepancy might reflect limitations in cryo-sectioning or IF of frozen sections.

Ultimately, the identification of human versus mouse gene expression at the single-cell level in tumour sections could be improved by using alternative methods such RNAscope or its variant BASEScope. RNAscope is a more sensitive and reliable *in situ* hybridisation (ISH) method for detecting specific RNA expression in different cells using human- and mouse-specific transcript probes(Grabinski et al., 2015). The English group has successfully used human BASEscope probes to detect human vascular endothelial growth factor A (VEGFA) isoform transcripts in FFPE sections of human STS xenografts,

which appear restricted to STS cells. QuPath could perform single-cell segmentation after ISH since the haematoxylin-stained nuclei were more readily detectable than after DAB staining (Aguero and English, unpublished).

This project used two mouse fibrosarcoma cell lines (FS188 and T241) to develop a method to distinguish between human UPS cells and mouse stromal cells. This method stained the mouse cells and normal human fibroblasts with MT-AB using ICC, showing no staining of mouse cells but positive staining of human cells.

6.3 Growing UPS cell lines in mice as xenografts

An *in vivo* study was performed to investigate the growth of four UPS cell lines as xenografts in mice to identify stromal expression of mesenchymal transcripts using RNAseq. Three UPS cell lines grew in mice (UPS2, 3, and 4); While UPS1 did not grow. Xenograft models have been widely used in cancer research since they retain key TME characteristics (Jianlin Shi et al., 2020). Overall, mean tumour latency was 60, 80, and 50 days for UPS1, UPS2 and UPS3, respectively. The long latency also raises questions about the genetic similarity of the UPS cells in the xenografts compared to their original cells cultured *in vitro*; as it is possible a subclone has been selected *in vivo*. Both cell lines and xenografts were sent for low-pass whole genome sequencing (LP-WGS). Unfortunately, these analyses could not be completed before the submission of this thesis. Nevertheless, they will be completed for inclusion in a future publication, and key genetic changes will be compared to the array comparative genomic hybridisation data of the original clinical samples. Could the long latency be due to subcutaneous injection? Will an orthotopic injection into a limb muscle reduce tumour latency? These questions are now being answered by a new project funded by Sarcoma UK.

6.4 TME characterisation

IHC and IF methods were used to characterise the TME in our xenografts (Chapter 4). Necrosis and mean vascular density did not differ significantly among the three xenografts. Pericytes are important cells in developing and maintaining tissue vasculature. They are characterised by the expression of different markers, including *αSMA*, platelet-derived growth factor receptor beta (PDGFRβ), desmin and neuron-glial antigen 2 (NG2) (Ribeiro & Okamoto, 2015). Cluster of differentiation 31 (CD31) is an endothelial marker used to identify vascularisation(Lugano et al., 2020). αSMA was co-stained with CD31 to quantify the pericyte coverage of xenograft vessels. While UPS3 showed lower pericyte coverage than UPS2 and UPS3, differences among xenografts were not statistically significant (Chapter 4).

Additionally, IF-based immune cell staining was used to examine macrophages in our xenografts. Tumour-associated macrophages (TAMs) are known for their role in epithelial-to-mesenchymal transition remodelling, enhancing tumour progression and metastasis in lung (Zhang et al., 2017) and breast (Baghel et al., 2016) cancer. Since FSP-1 and FAPα were considered specific to CAFs and macrophages (Herrera et al., 2013), they were co-stained with F4/80 (a macrophage marker). The number of F4/80-positive cells did not differ significantly among the three xenografts. IF staining showed high numbers of cells positive for both F4/80 and FSP1 or FAPα, indicating that many macrophages may be FAPα$^+$ or FSP1$^+$. Consequently, care must be taken when using these as SAF markers.

6.5 Characterisation of stromal gene expression using RNAseq

Given the limitations of IHC and IF methods, a more precise method was needed to identify gene expression differences between UPS and stromal cells. Therefore, RNAseq was used. RNA was isolated from frozen xenografts and sent for RNAseq. Pre-processing of the raw RNAseq data is illustrated in Figure 2.1 (Chapter 2). Stromal transcript levels were studied using the RNAseq XenofilteR tool to deconvolute host and graft reads. Four differentially expressed gene (DEGs) comparisons were performed: between human and mouse transcripts aligned against a universal reference genome (GRCh38/hg38 and

GRCm38/mm10 combined) for the whole tumour transcriptome, between human UPS transcriptomes only (GRCh38/hg38), between mouse stromal transcriptomes only (GRCm38/mm10), and between human (graft) and mouse (host) transcriptomes for each tumour.

6.6 Combining our UPS data with clinical data from TCGA-SARC and VorteX

Our UPS xenograft samples were compared with clinical RNAseq data from The Cancer Genome Atlas Sarcoma (TCGA-SARC) and the VorteX biobank. TCGA-SARC is a collection of cancer genomic databases comprising six STS types, including 52 UPS and 25 MFS. VorteX is a randomised phase III trial conducted with STS patients to determine whether a reduced radiotherapy volume administrated to patients will improve limb function without compromising local control. There was no difference in overall survival (OS) or progression-free survival (PFS) between the two study arms (West and Forker, personal communication, submitted for publication). The VorteX biobank is a sample and data collection from the VorteX trial that includes 30 MFS and 40 UPS. Multidimensional scaling (MDS) plots showed that most UPS xenografts clustered with the clinical STS with complex karyotypes, including UPS and MFS, suggesting their transcriptomes are highly similar (Chapter 5).

6.7 Characterisation of stromal gene expression in xenografts using RNAseq

In the human transcriptomes, UPS4 clustered separately from UPS2 and USP3, with 2,039 DEGs between UPS2 and UPS4 and 2,042 DEGs between UPS3 and UPS4. These results showed that UPS2 and USP3 were highly similar, with less variation in their transcriptomes between biological replicates. In contrast, UPS4 was less similar to UPS2 and USP3 and also had greater variation between biological replicates. This result also necessitated checks to determine whether the tumour genomes were comparable to the cell lines and differed significantly among the individual biological replicates. Again, could

a subset of clones in the *in vitro* cell culture have been selected *in vivo*? As discussed earlier, LP-WGS will hopefully answer this question.

As expected, comparisons of mouse transcriptomes between UPS2, USP3 and USP4 tumours identified no DEGs. This finding suggests that stromal cell recruitment and TME development are largely independent of the UPS cell line.

DEGs analysis between the human (STS cell lines) and mouse (the stroma) identified 11434, 9406, and 8582 DEGs in UPS2, UPS3, and UPS4 tumours, respectively. Here, we included our eight common mesenchymal genes examined using WB, ICC, IHC and IF. Transgelin and αSMA expressions were significantly higher in stromal cells than in UPS cells, confirming the preliminary WB findings. However, vimentin and SOX2 expression was also higher in stromal cells than in UPS cells, contradicting our WB findings. We then included more known CAF markers (PDGFRα/β, tenascin-C, microfibril-associated protein 5 (MFAP5), NG2, and desmin) in our transcriptome analysis. MFAP5 expression was higher in stromal cells than in UPS cells. We could establish a possible SAF panel from our data: transgelin, αSMA, vimentin and MFAP5. Could any of these be SAF markers? FSP-1 and FAPα were expressed in stromal cells but not in UPS cells. However, our IF analysis showed quite a few UPS xenograft cells positive for F4/80, indicating some are macrophages and suggesting that they may not be reliable, independent SAF markers.

Further validation is required to confirm whether any of these could be SAF markers, using larger sample sizes and confirming their protein levels using alternative methods (e.g. fluorescence-activated cell sorting (FACS) or RNAscope). Moreover, investigating the expression of additional stromal genes identified in our transcriptome analysis using *in vitro* WB analysis would be useful. Single-cell RNA-seq (scRNA-seq) could also increase our understanding of which cell types express specific genes.

6.8 Reliability of cell subset prediction in STS

As discussed earlier, to confirm the abundances of macrophages and other cells in our xenografts, we used cell subset prediction in our xenograft transcriptomes using Xcell software. XCell results showed very low macrophage abundances in UPS2 and UPS3

and almost no detectable macrophages in UPS4 (Chapter 5). This might indicate that cell subset prediction algorithms are not the most suitable for STS analysis. ScRNA-seq could be an alternative method to predict the numbers of FSP-1- or FAPα-positive macrophages in clinical STS. ScRNA-seq is a high throughput method recently used in carcinoma studies to explore single-cell-specific transcriptomes. Many scRNA-seq analyses were performed to study various immune cell populations in the colorectal cancer (CRC) TME to discover novel biomarkers that may aid precision medicine (Tieng et al., 2022). Endothelial cells express some common genes, such as platelet endothelial cell adhesion molecule (PECAM-1), cadherin 5 (CDH5), vimentin, and tyrosine kinase with immunoglobulin-like (Tie1) (Feng et al., 2019). All of these markers exhibited higher expression in the stroma than in the STS cells in xenografts (Fig. S35). Furthermore, the expression of M2 macrophage markers, including arginase (ARG1), C-type lectin domain family 18 member A (CLEC18A), and C-C motif chemokine ligand 17 (CCL17) (Yu et al.,2019) was higher in the stroma than in the STS cells; however, this difference was not statistically significant (Fig. S35). These findings indicate that the cell subset predictions may be partially accurate; however, the gene lists may require editing or amending to be more suited for STS studies.

6.9 Studying the influence of mesenchymal gene expression on patient survival using TCGA-SARC and VorteX data

Analysis was done using TCGA SARC and VorteX data for mesenchymal genes characterised in Chapters 3–5 (transgelin, αSMA, vimentin, N-cadherin, fibronectin, FSP-1, FAPα and SOX2) and the new markers identified in Chapter 5 (PDGFRβ, desmin, and MFAP5) to obtain correlations with survival in clinical disease. Data was separated into low- and high- expression groups using the 25th and 75th quartiles of normalised expression values. We combined UPS and MFS samples from the TCGA-SARC and VorteX, since sample numbers were small and MDS plots showed their transcriptomes were highly similar.

OS and PFS between groups were examined using Kaplan–Meier univariate analyses at 2, 5, and 10 years. OS is the patient survival time after diagnosis, while PFS is the time from diagnosis to disease progression. OS was not significantly correlated with mesenchymal gene expression. However, a non-significant trend of decreasing survival with lower transgelin expression was observed. Ten-year OS and PFS were significantly higher in the low N-cadherin expression group than in the high N-cadherin expression group (Figure 5.3). Two-year PFS was significantly lower in the low αSMA expression group than in the high αSMA expression group. The low vimentin and fibronectin expression groups showed decreased PFS at 2 and 5 years compared to the high vimentin and fibronectin expression groups.

We combined all predicted SAF markers (transgelin, αSMA, vimentin, and MFAP5) into "possible SAF panel" and analysed OS and PFS. However, OS and PFS did not differ significantly between the high and low groups. This finding might reflect the small sample size due to sarcoma's rarity. Another possibility is that more SAF markers are needed to provide a more reliable prognostic panel. High transgelin expression was associated with poor OS in metastatic pancreatic cancer (Zhou et al., 2013), while low transgelin expression was associated with poor OS in osteosarcoma (Xi et al., 2022). Our data showed transgelin expression did not have any effect on patient survivals. Higher *αSMA* expression was associated with decreased PFS and OS in pancreatic cancer (Sinn et al., 2014). Our data showed low αSMA expression had worse 2 years PFS. Higher vimentin expression was associated with poor OS and PFS in CRC (Du et al., 2018) and poor OS in pancreatic ductal adenocarcinoma (Maehira et al., 2019). While Maehira *et al.* (2019) combined vimentin with αSMA*,* patient survival did not differ significantly between their defined groups. Our data showed low vimentin expression caused poor 2 and 5 years PFS. Higher MFAP5 expression was associated with poor OS in bladder cancer patients (Zhou et al., 2020). Our data showed MFAP5 expression did not have any effects on patient's survivals.

6.10 Future directions

Since MFS cell lines showed decreased transgelin and *αSMA* expression *in vitro* in this project, further validation is needed. MFS cell lines from Prof. Dominique Heymann will need to be assessed for growth *in vivo* since pilot studies performed with MFS cell lines from Salawu *et al.* (2016) did not form tumours in mice, although the number of mice was small (*n* = 3). Therefore, could these cells be orthotopically injected into mice to improve growth? Alternatively, performing 3D spheroids could overcome this problem. Salereno *et al.* (2013) found that injecting spheroids into mice resulted in more reproducible and rapid tumour growth, showing that spheroids are more tumorigenic and more closely resemble the original disease. They concluded that this method was reliable for preclinical sarcoma studies and better understanding of sarcoma biology (Salerno et al., 2013). This approach could further help characterise stromal gene expression and likely add more SAF markers to our list. In addition, our SAF panel must be tested in additional STS cell lines *in vitro* and *in vivo.*

The additional stromal genes identified by our RNAseq analyses must be confirmed in our STS and additional STS cell lines using different methods (e.g. FACS, RNAscope, and BASEscope). Further mesenchymal gene expression characterisation using WBs could be used to confirm the difficulty to identify SAFs in STS by including *PDGFRα/β*, *NG2*, and *d*esmin. *PDGFRα/β* are considered CAF markers (Shiga et al., 2015). Since transgelin showed promising results, further studies could confirm it as a new therapeutic target for STS and a SAF marker. The Kyoto Encyclopaedia of Genes and Genomes is a collection of databases on gene function and pathways that includes an additional drug development database. It can also provide information about protein-protein interactions (Chen et al., 2015). Whole exome sequencing interrogates the exonic parts of genomic DNA, providing a better understanding of genetic biomarkers and mutations to complement RNA-seq to facilitate understating and improve precision medicine for STS (Rusch et al., 2018).

6.11 Conclusions

In conclusion, our *in vitro* experiments showed that transgelin expression was lower in UPS and MFS than in LMS cell lines and normal human mesenchymal cells. Additionally, bioinformatics analysis of UPS transcriptomes confirmed this result and led to the identification of more "possible SAF" markers. Identifying SAFs will improve our understanding of sarcoma biology and therapeutic avenues. Growing UPS cells in mice was feasible, and we could use the method described by Bradford *et al.* (2013) to study DEGs between the graft (UPS cells) and the stroma (mouse cells). While IHC and IF methods confirmed common protein expression in our xenografts, it was not possible to distinguish between UPS and stromal cells, emphasising the importance and accuracy of RNAseq analyses. Deconvolution between UPS and stroma cells was an essential but challenging step. Challenges we encountered included performing all bioinformatics pre-processing steps during the COVID-19 lockdown, resulting in slower software and problem-solving since everything was working remotely. Additionally, since the *XenofilteR* tool had never been used by the University of Sheffield's Bioinformatics Core Facility, it took longer to install and run.

Clinical data such as TCGA-SARC and VorteX helped us to study the distribution of different STS, confirming that UPS and MFS transcriptomes were highly similar. Our "possible SAF panel" was used to investigate the influence of gene expression on OS and PFS. As discussed earlier, individual SAF marker expression has been reported to impact carcinoma patient survival. This effect was not observed in our TCGA-SARC and VorteX data, potentially because our panel needs more "SAF" markers, or in contrast to other solid tumour types SAF are of little prognostic importance.

Overall, we conclude there are differences in mesenchymal gene expression between poorly differentiated STS with complex karyotypes *in vitro* and in xenografts that could aid the identification of SAFs, or a subset of SAFs, in clinical samples and facilitate their study. Further research is needed to validate these as SAF markers in clinical samples and characterise the role of these cells in STS development, metastasis, and therapy response. Our data also shows the newly isolated UPS cell lines derived from the tumours

of STS patients at the University of Sheffield have transcriptomes that closely resemble clinical STS, making them highly suitable for future translation studies.

Appendix

Supplementary Data
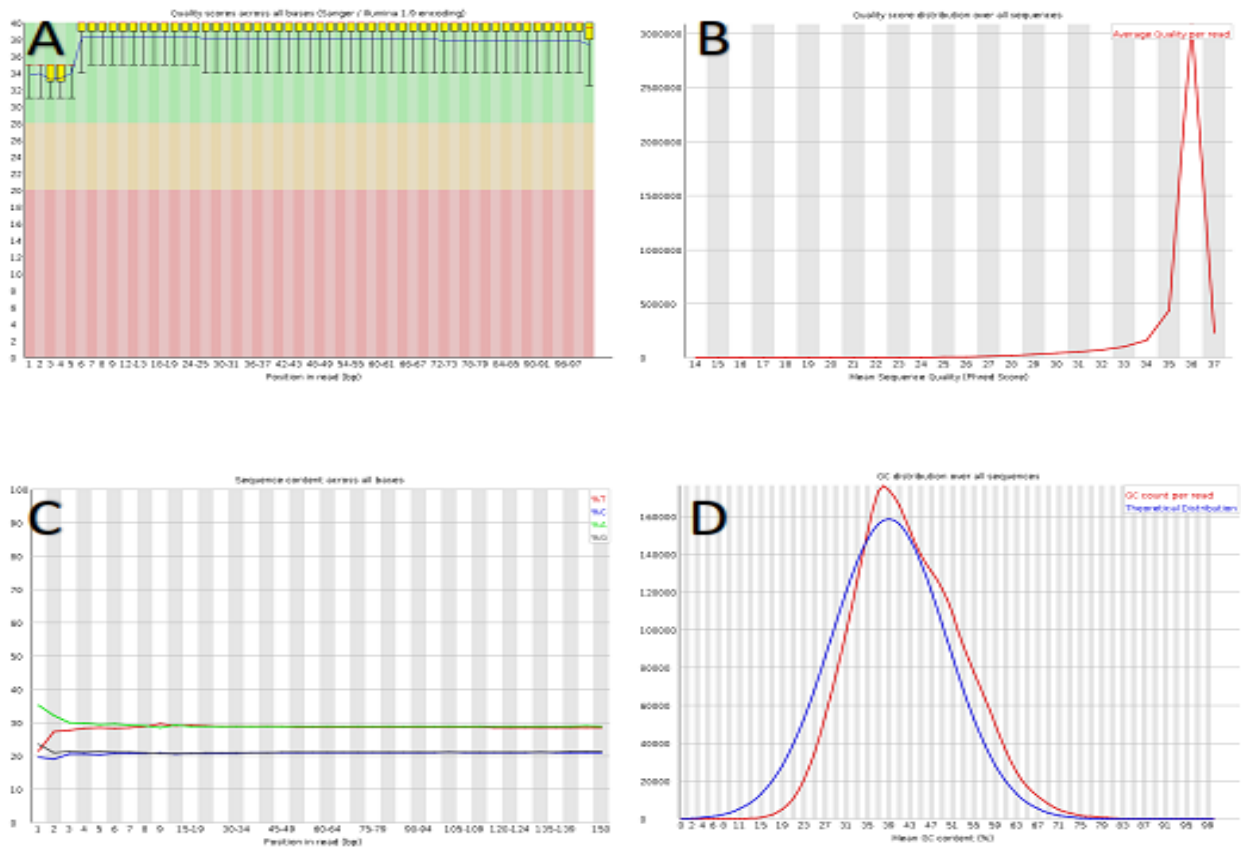
Figure S1: Representative quality report of RNAseq FASTQC.

(A) Box and Whisker plot shows the quality score across all bases. The blue line represents the mean value, the yellow boxes represent the inter-quartile (25-75%) of the range. Green are indicates good quality, orange area indicates reasonable quality and red indicates poor quality. (B) A plot of the average quality per read. (C) A plot of sequence content across all bases, it plots the percentage of each of the four nucleotides (T, C, G, A) at each position across all reads in the input sequence file. (D) GC distribution over all reads. This plot displays the number of reads vs. percentage of bases G and C per read.
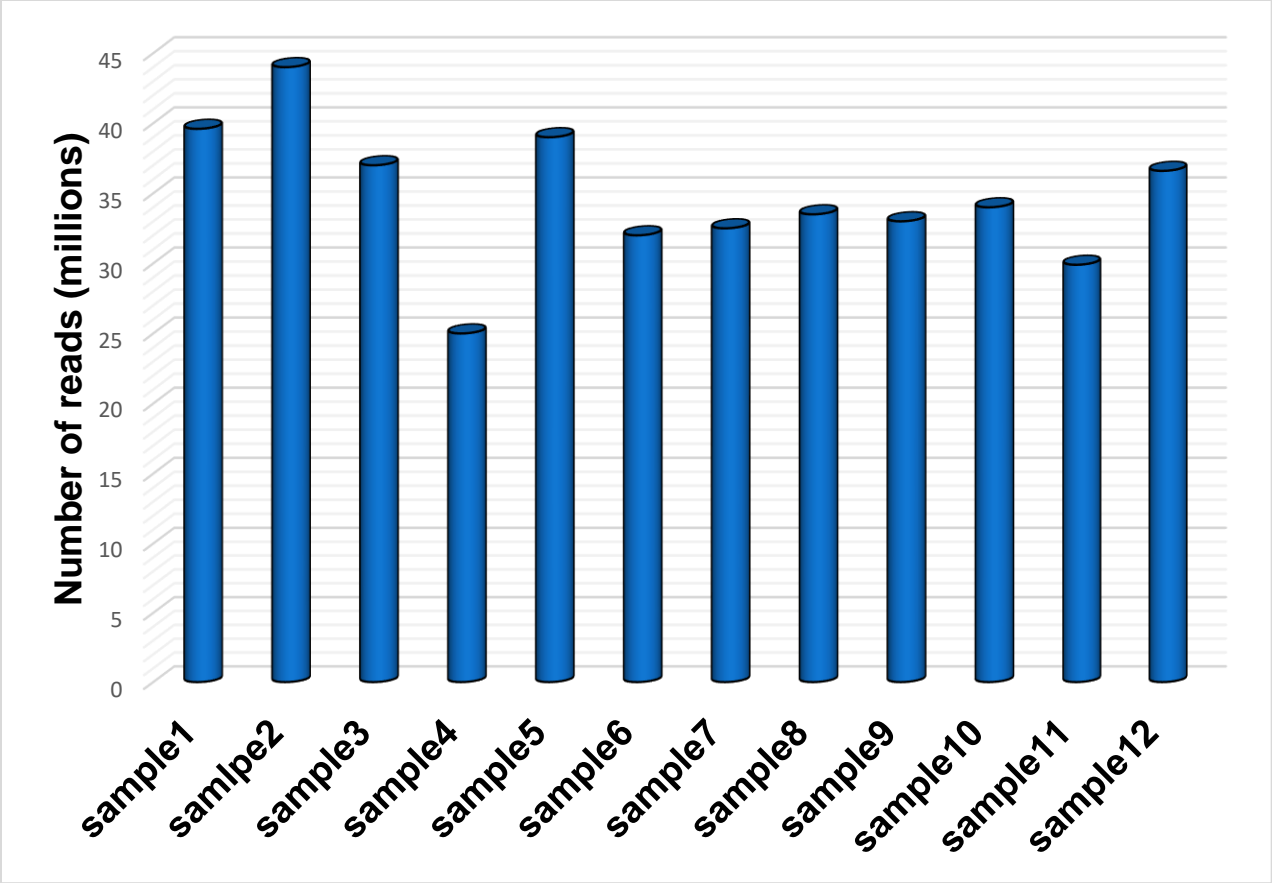
Figure S2: Number of counts reads of RNAseq data.

The average count read is 35 million reads. Sample4 shows the lowest count read of 28 million reads.
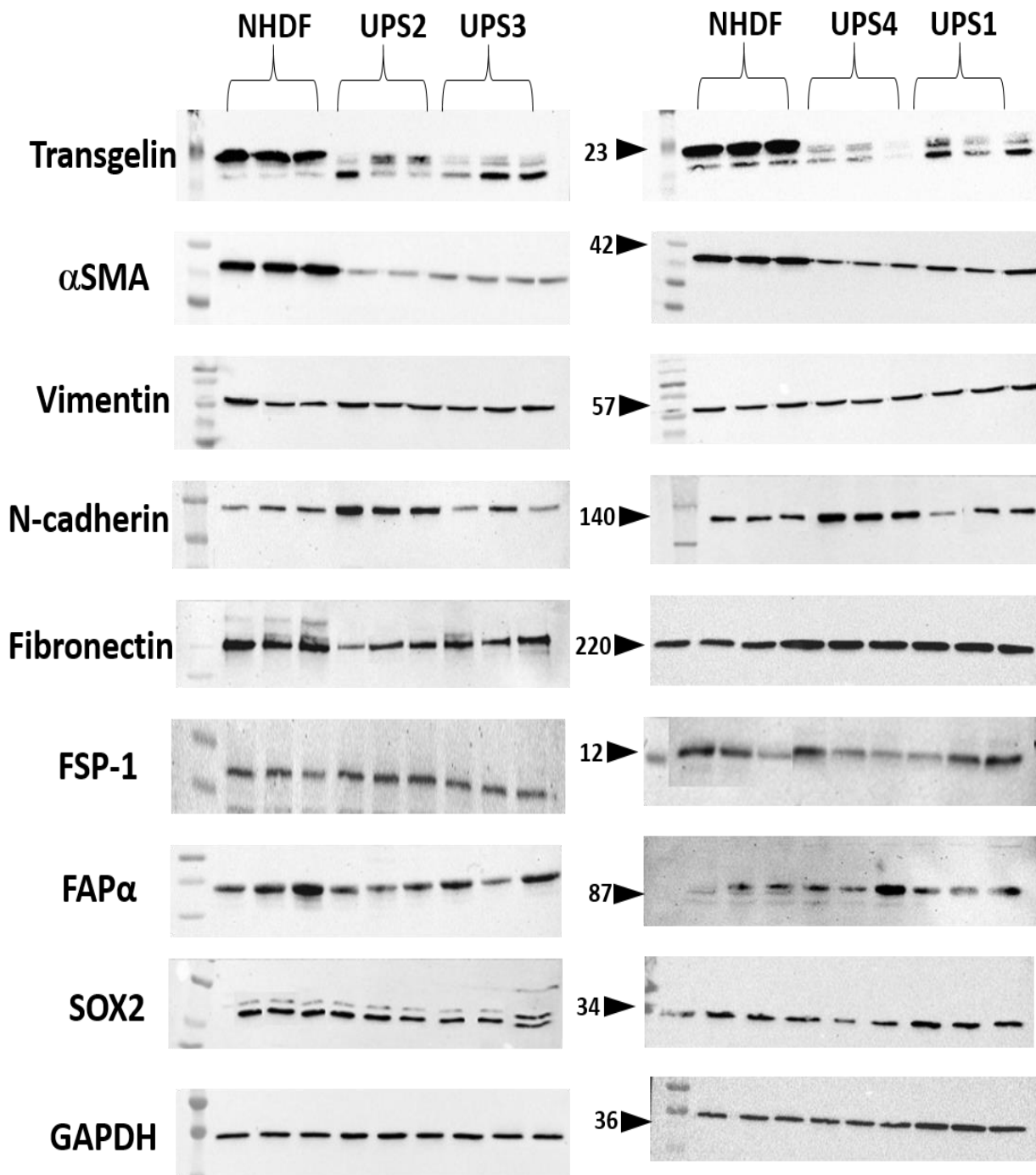
Figure S3: Western blot analysis of mesenchymal proteins in UPS cell lines.

GAPDH was used as loading control.

.
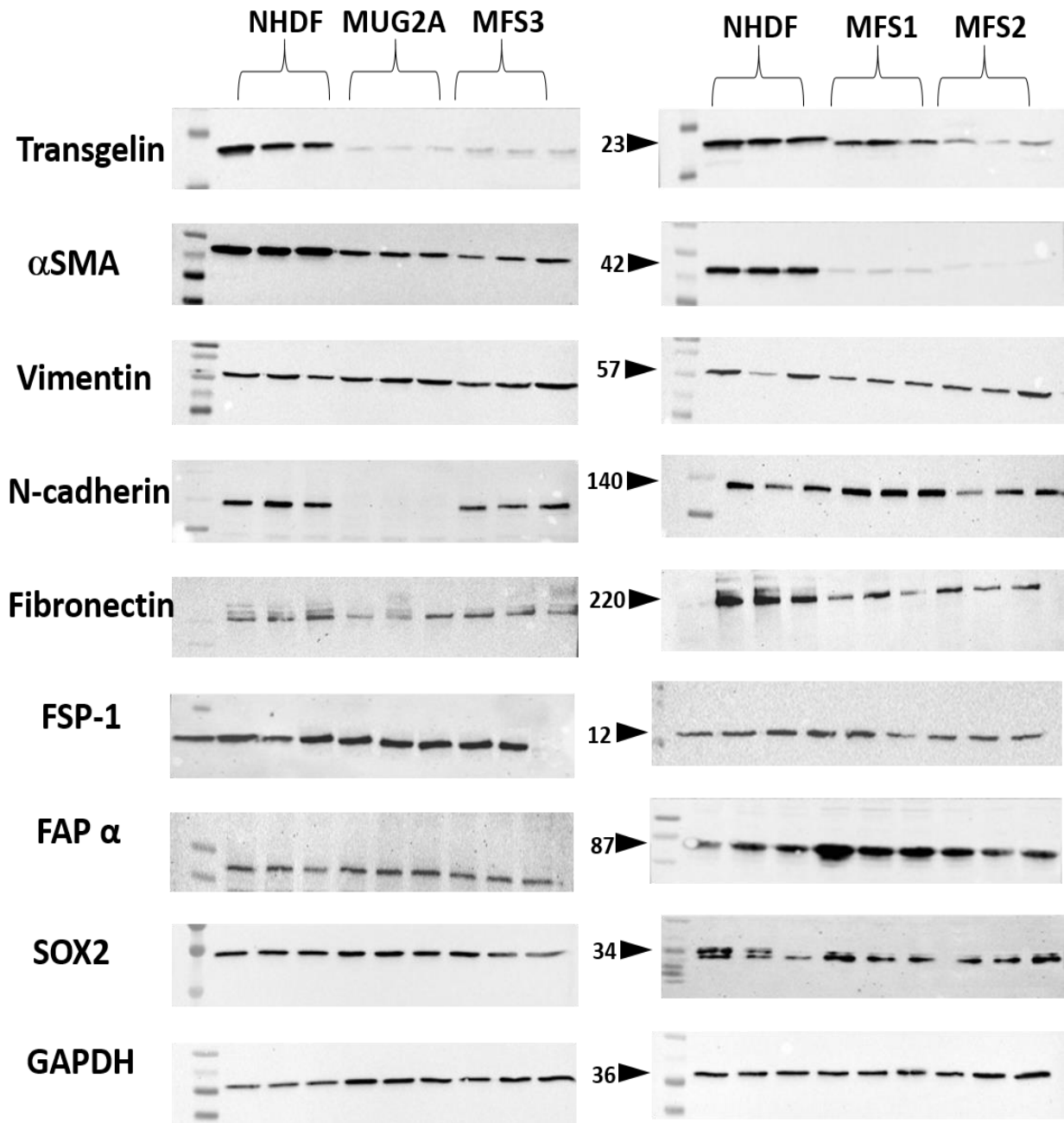
Figure S4: Western blot analysis of mesenchymal proteins in MFS cell lines.

GAPDH was used as loading control.
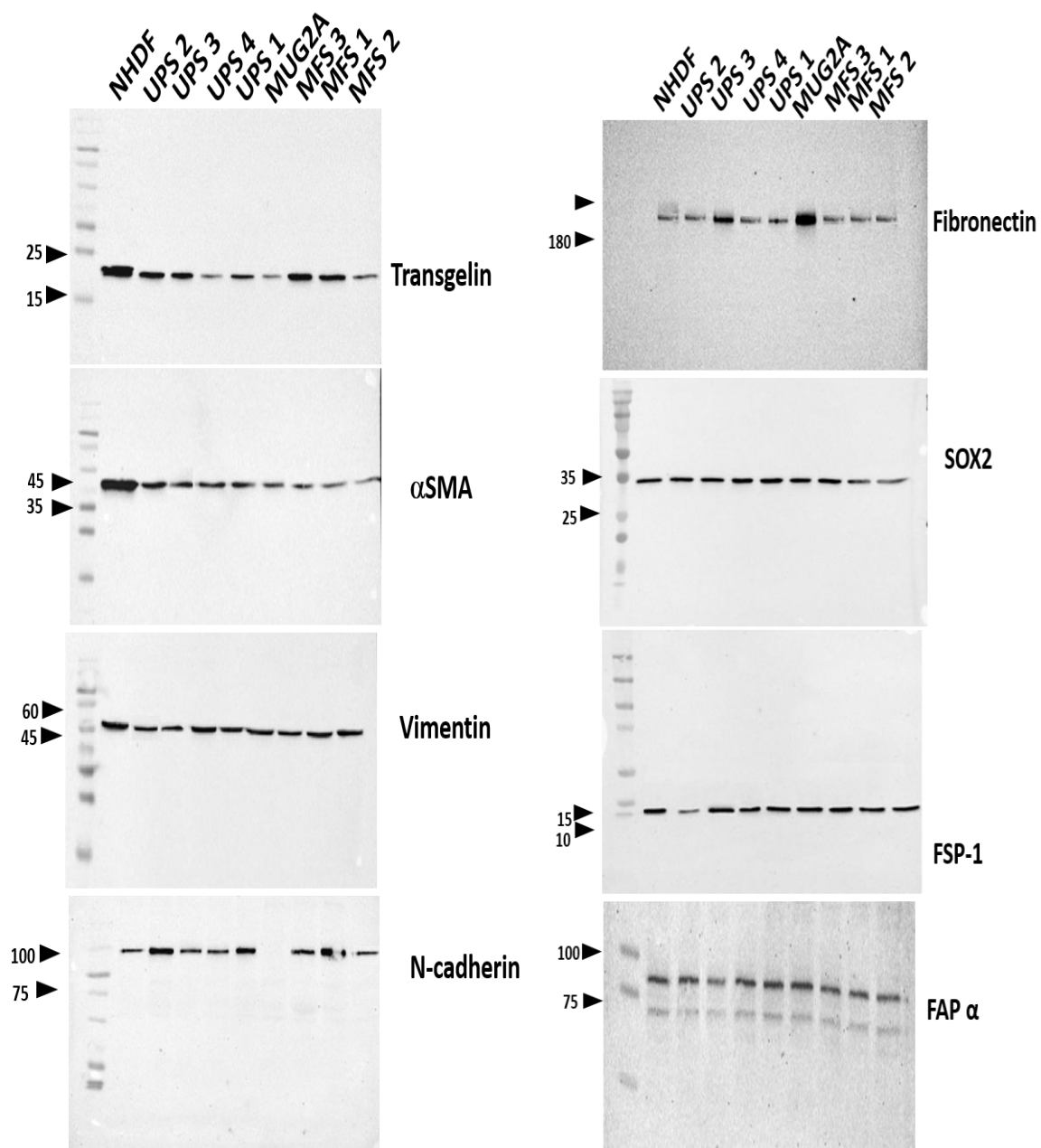
Figure S5: Western blot analysis of mesenchymal proteins in STS cell lines.

GAPDH was used as a loading control.
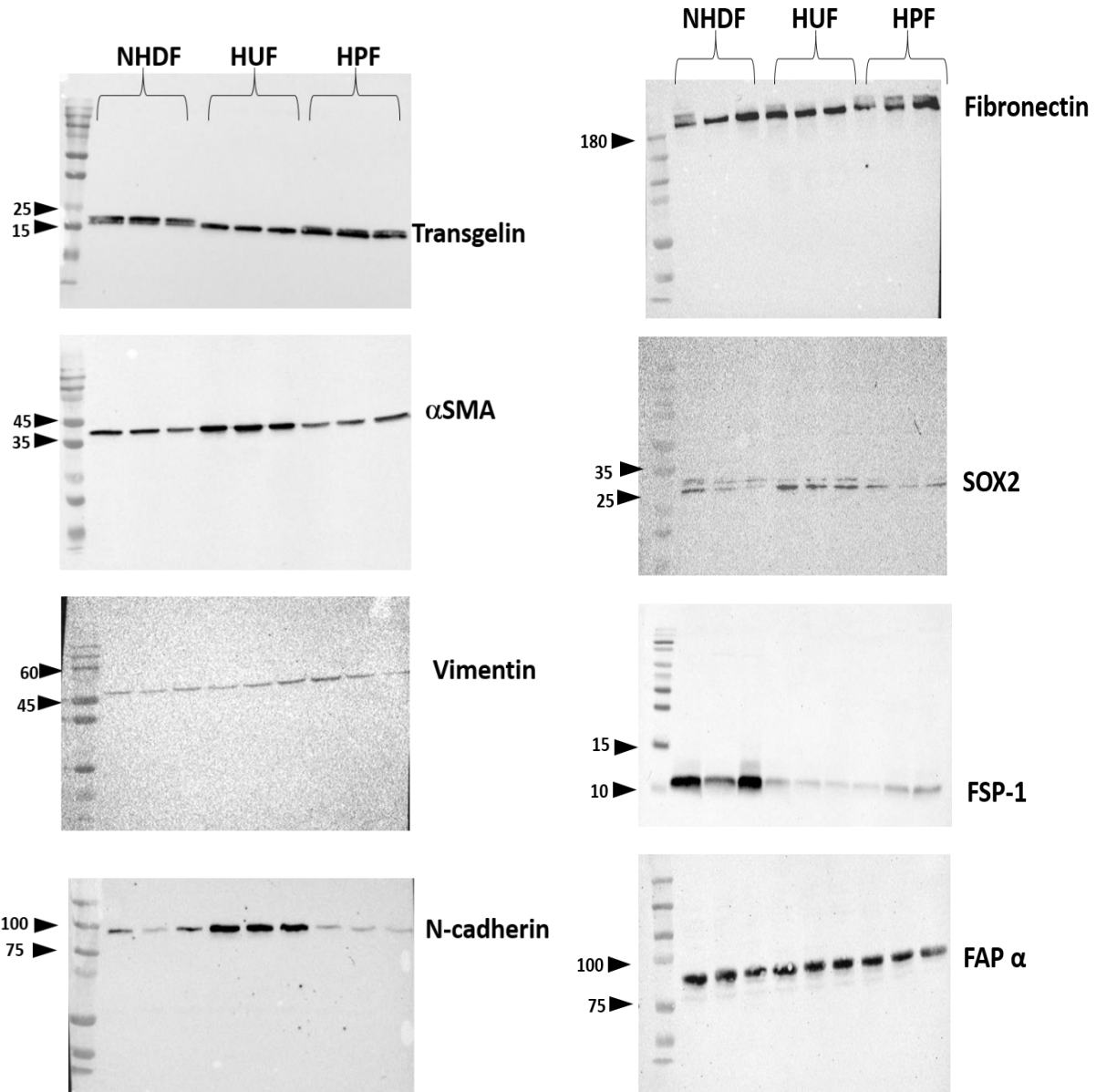
Figure S6: Western blot analysis of mesenchymal proteins in fibroblasts.

GAPDH was used as a loading control.
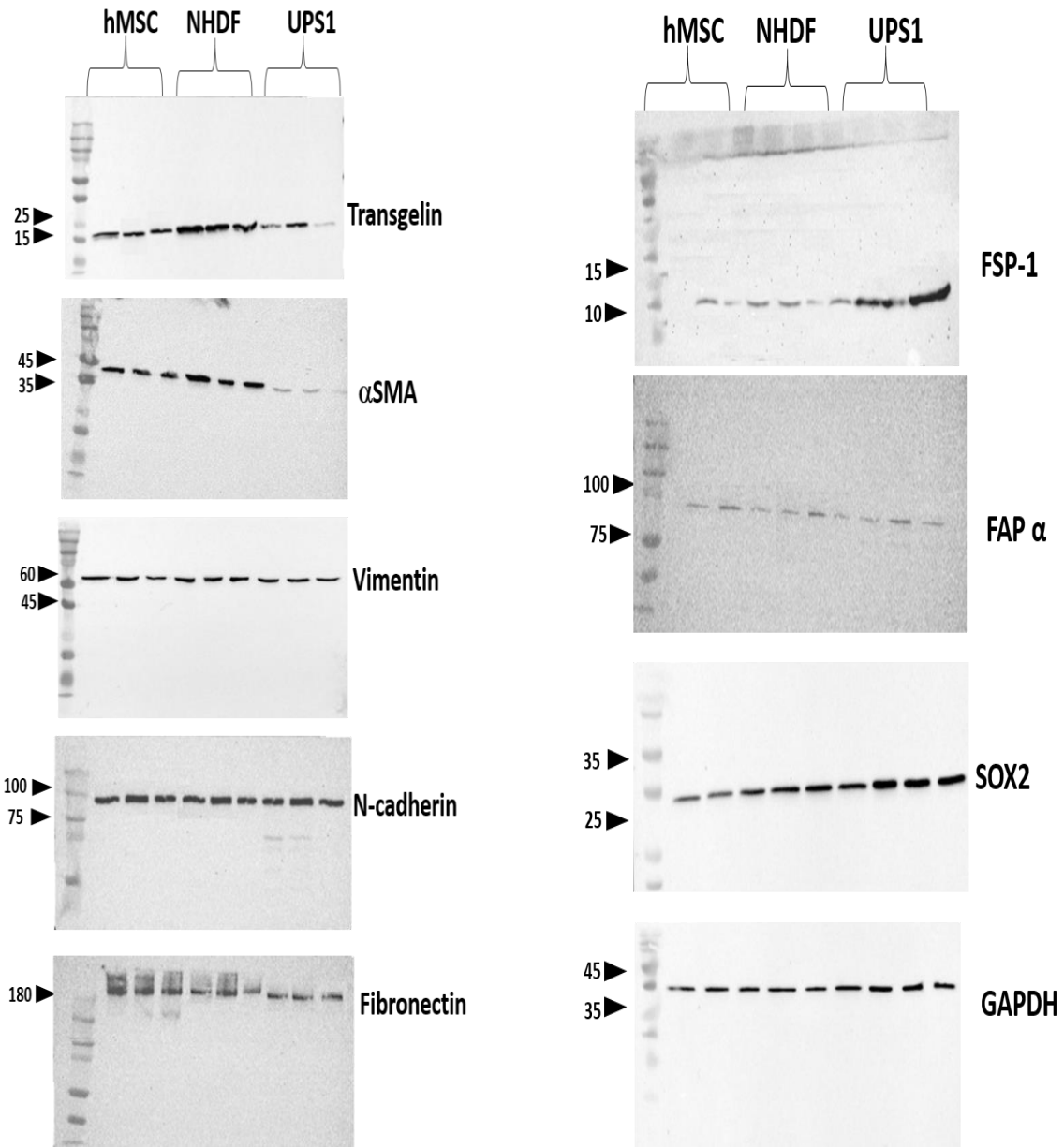
Figure S7: Western blots analysis of mesenchymal proteins in hMSC.

GAPDH was used as loading control.
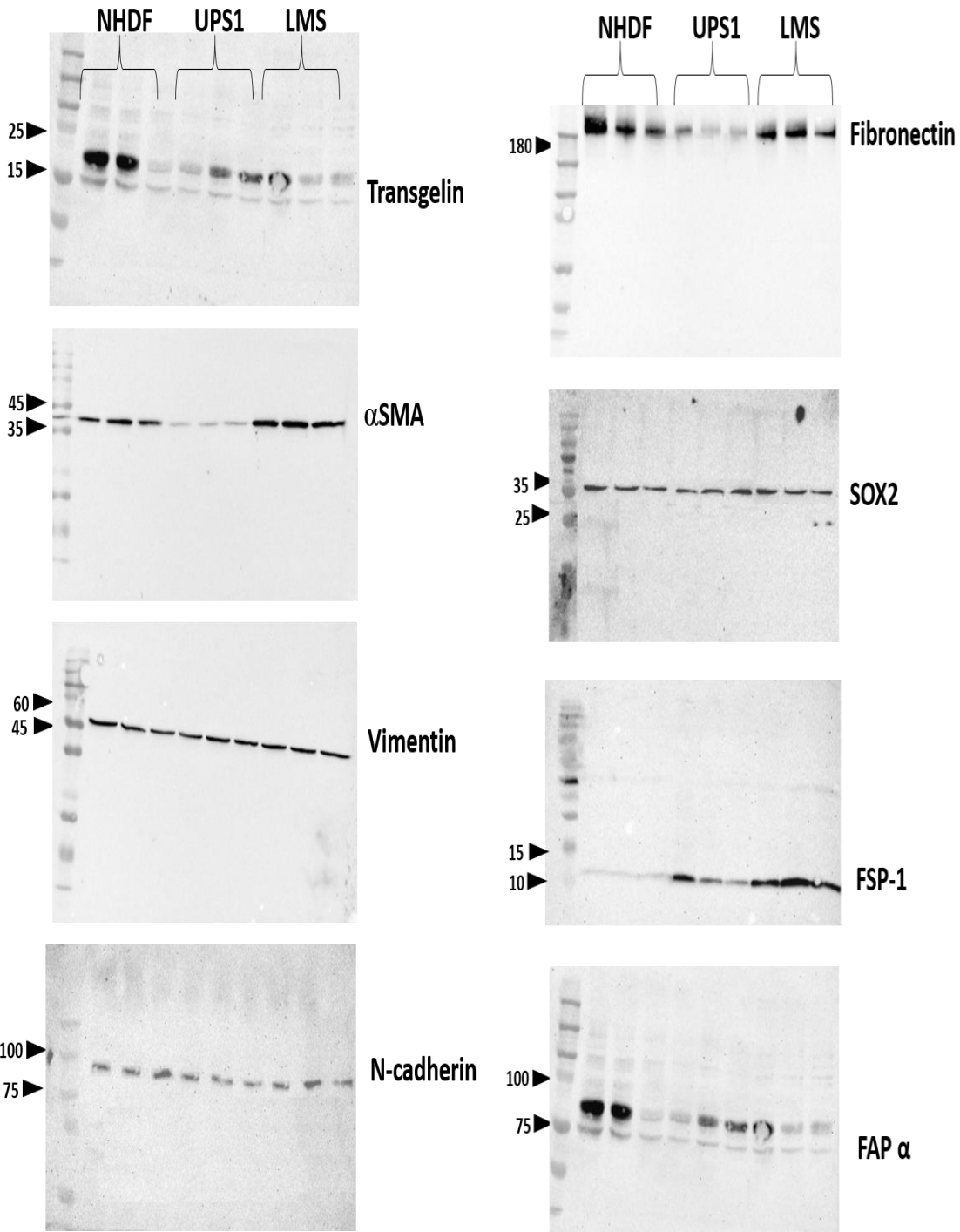
Figure S8: Western blot analysis of mesenchymal proteins in LMS cell lines
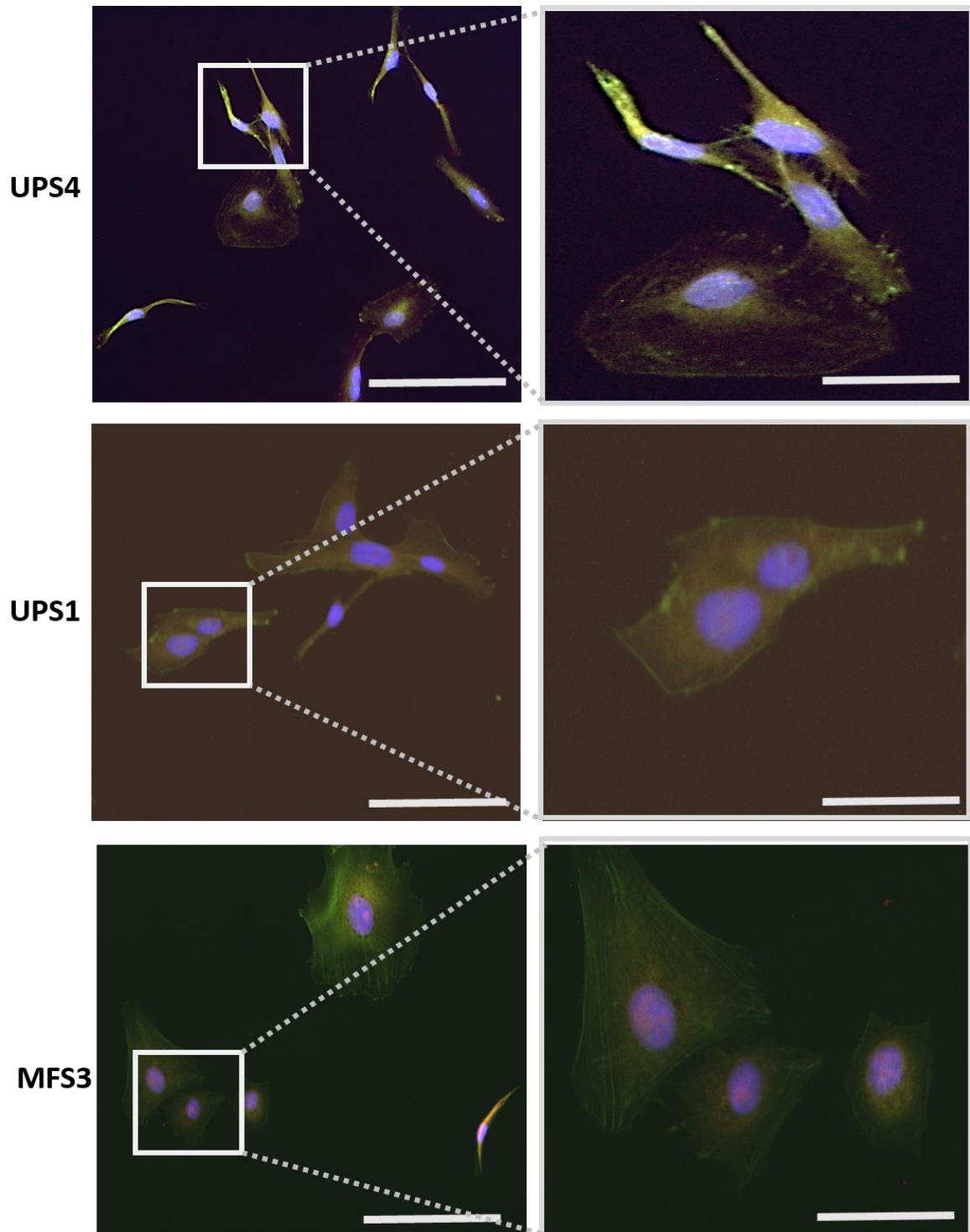
Figure S9: Immunocytochemistry images of Transgelin localisation in UPS4, UPS1 and MFS3 cell lines.
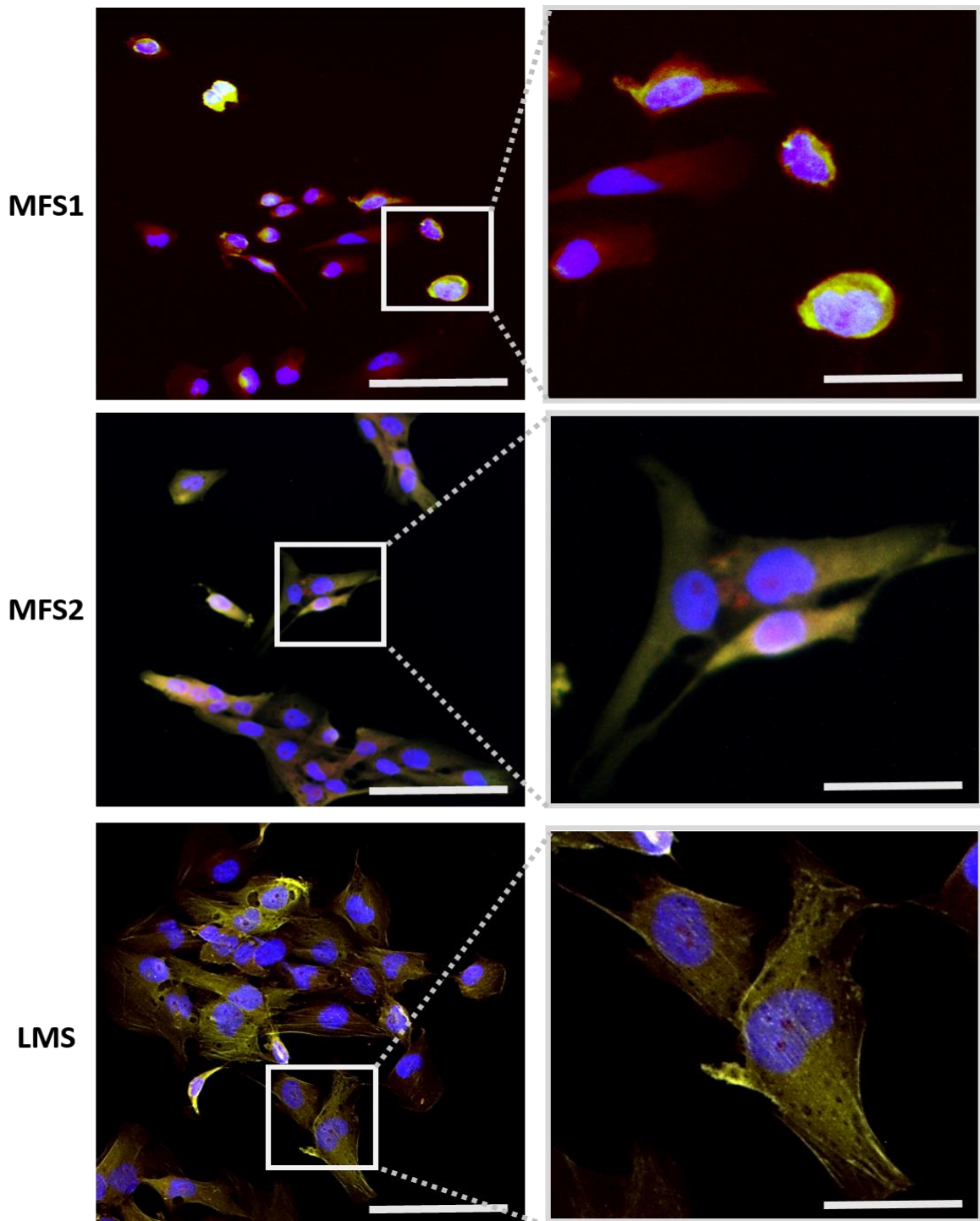
Figure S10: Immunocytochemistry images of Transgelin localisation in MFS1, MFS2 and LMS cell lines.
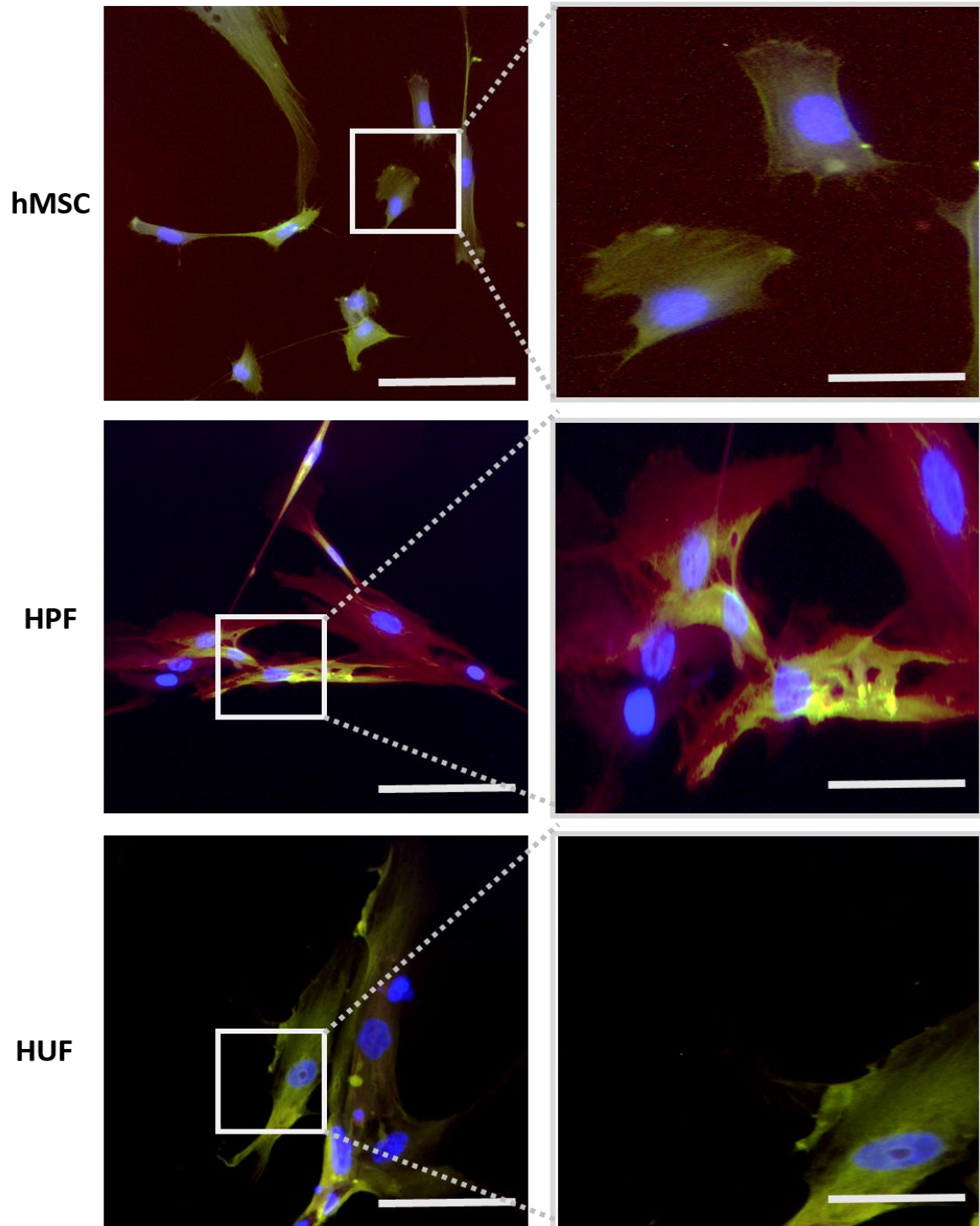
Figure S11: Immunocytochemistry images of Transgelin localisation in hMSC, HPF and HUF cell lines.
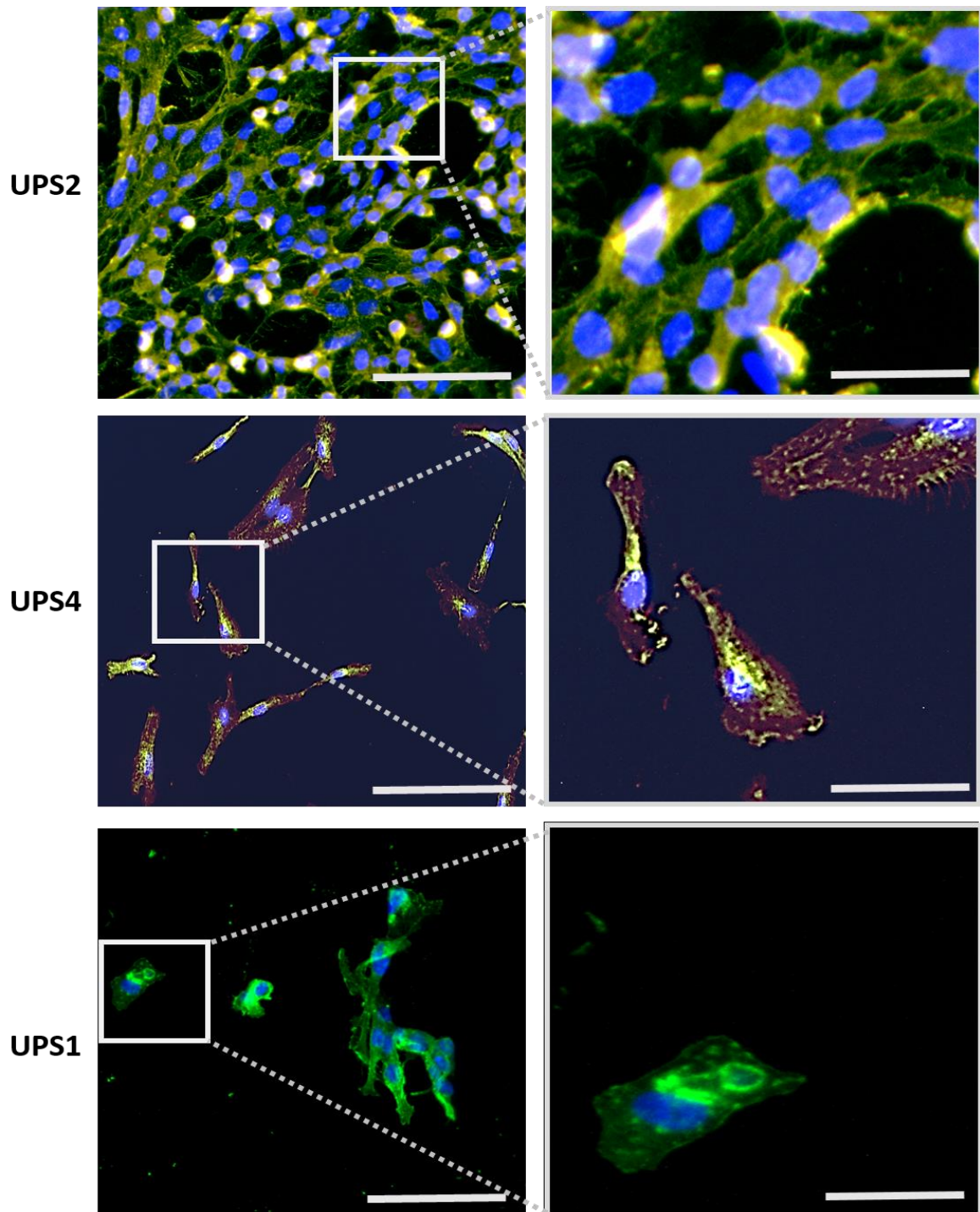
Figure S12: Immunocytochemistry images of αSMA localisation in UPS2, UPS4 and UPS1 cell lines.
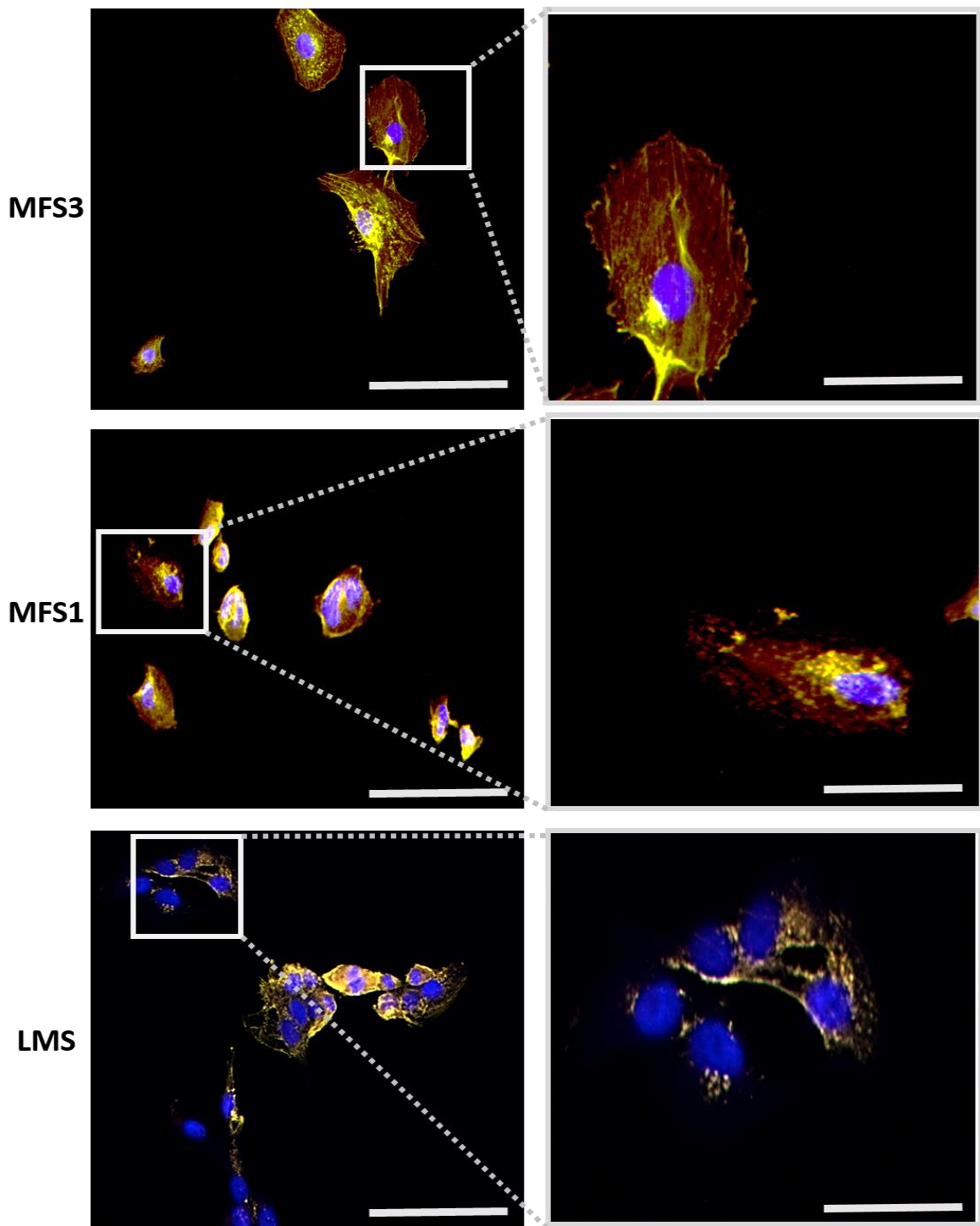
Figure S13: Immunocytochemistry images of αSMA localisation in MFS3, MFS1 and LMS cell lines.
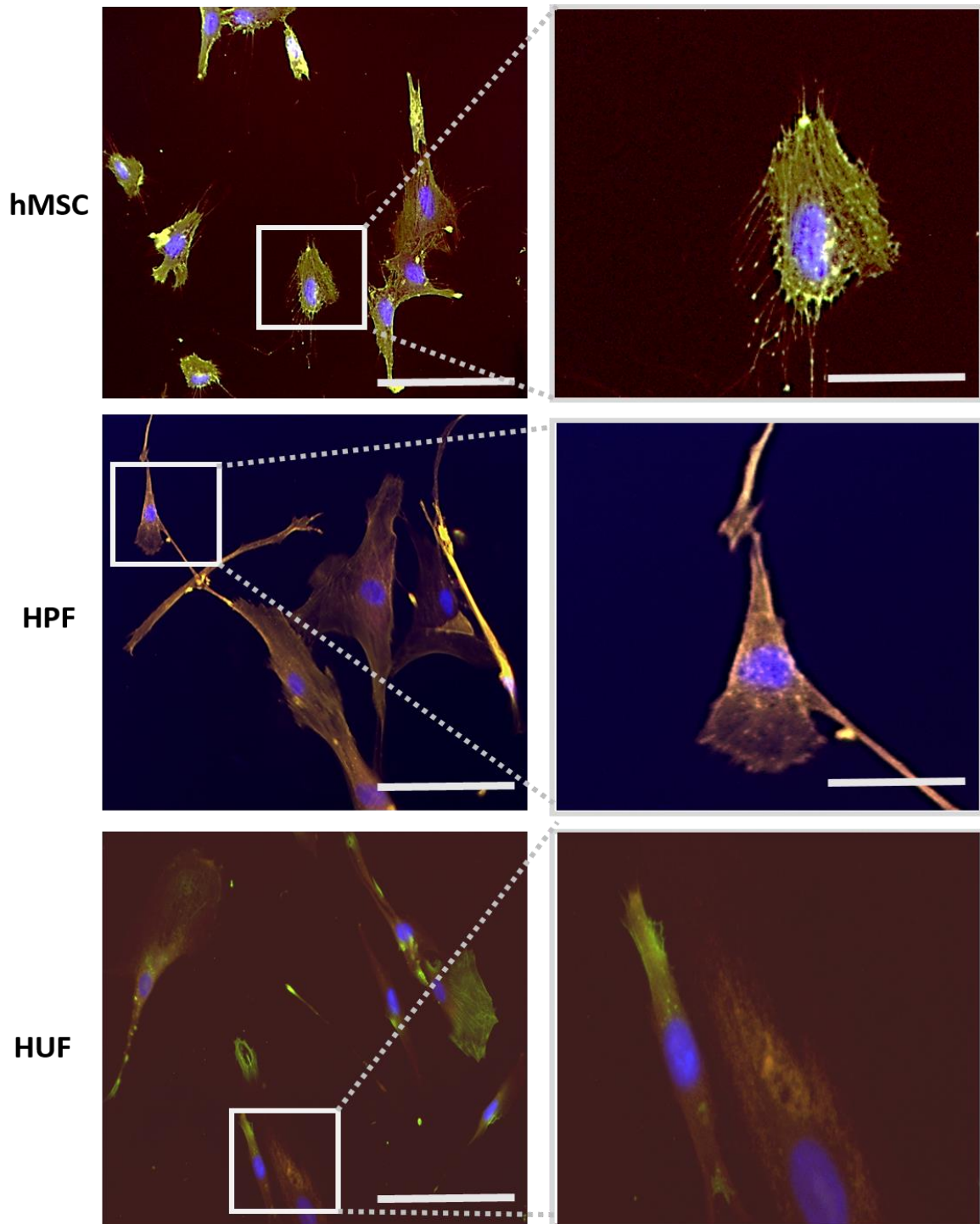
Figure S14: Immunocytochemistry images of αSMA localisation in hMSC, HPF and HUF cell lines.
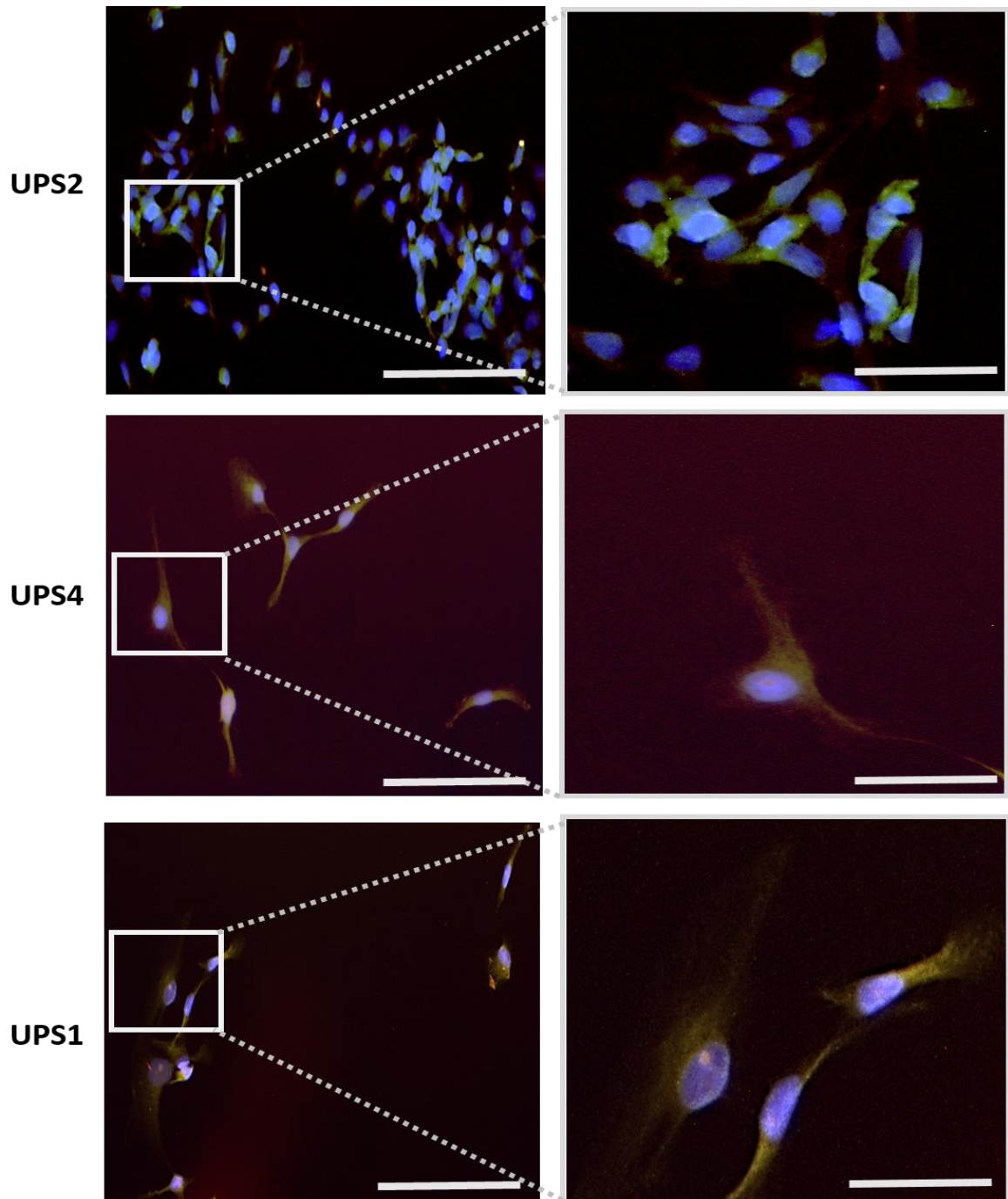
UPS2

UPS4

UPS1

Figure S15: Immunocytochemistry images of vimentin localisation in UPS2, UPS4 and UPS1 cell lines.
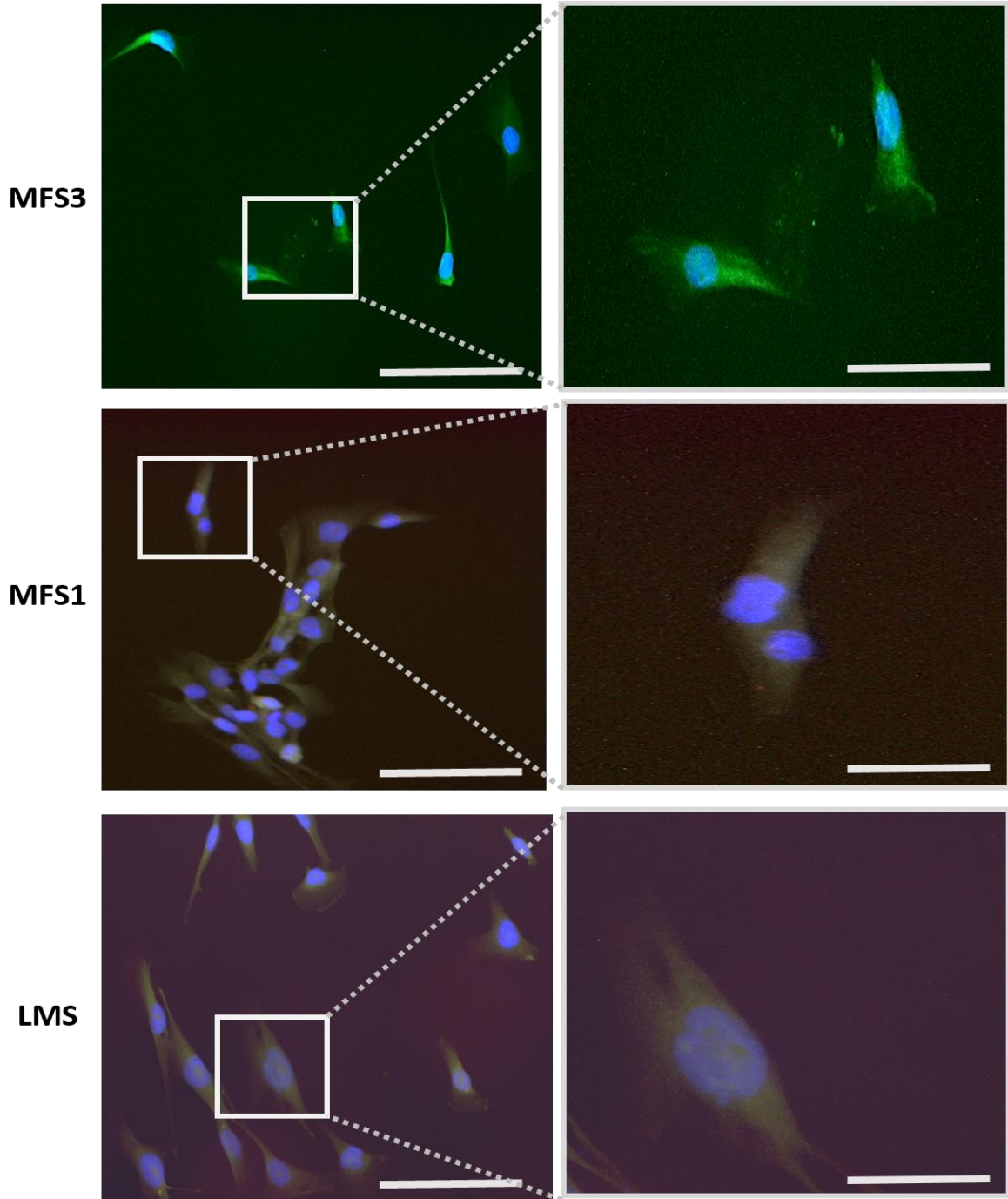
Figure S16: Immunocytochemistry images of vimentin localisation in MFS3, MFS1 and LMS cell lines.
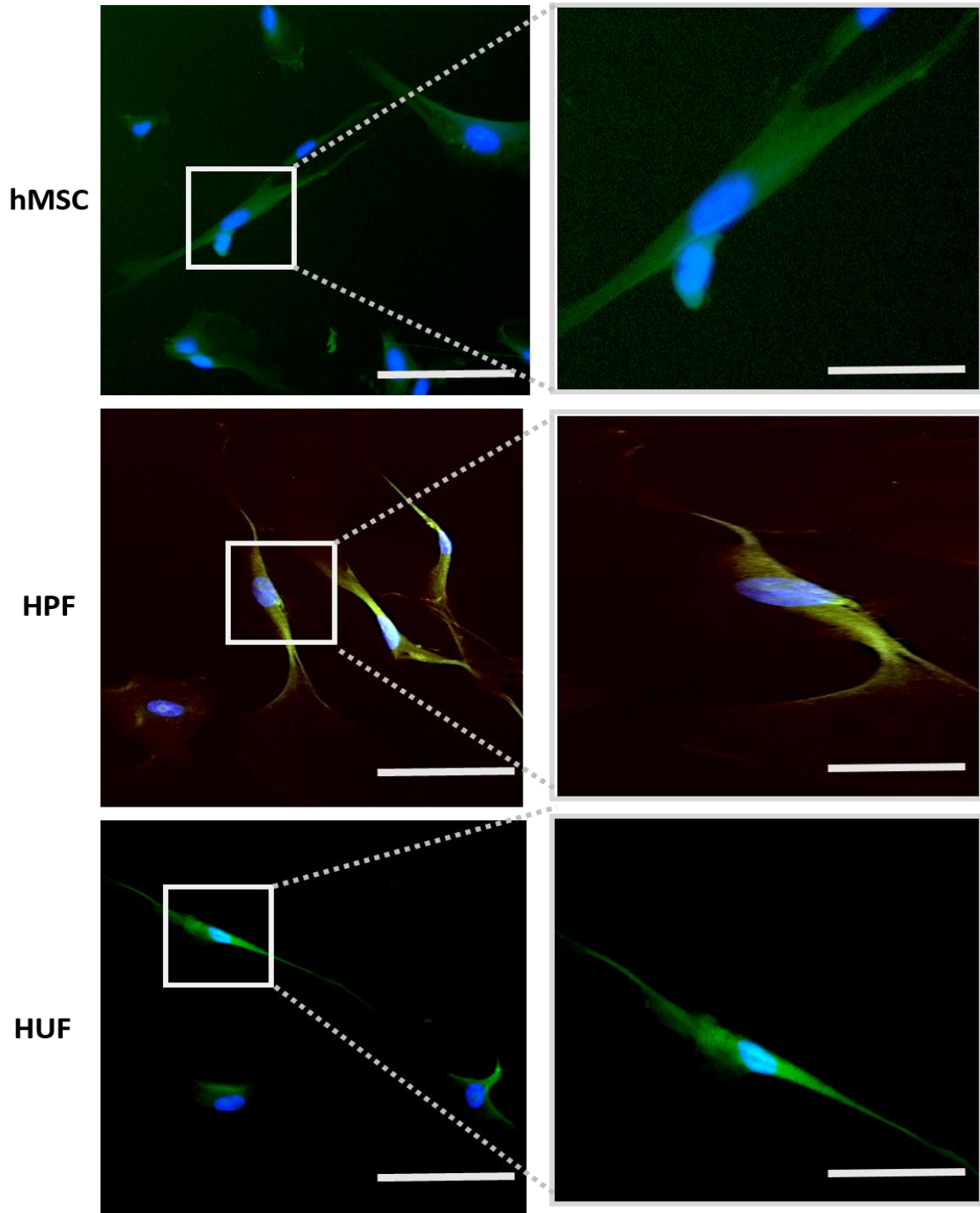
Figure S17: Immunocytochemistry images of vimentin localisation in hMSC, HPF and HUF cell lines.
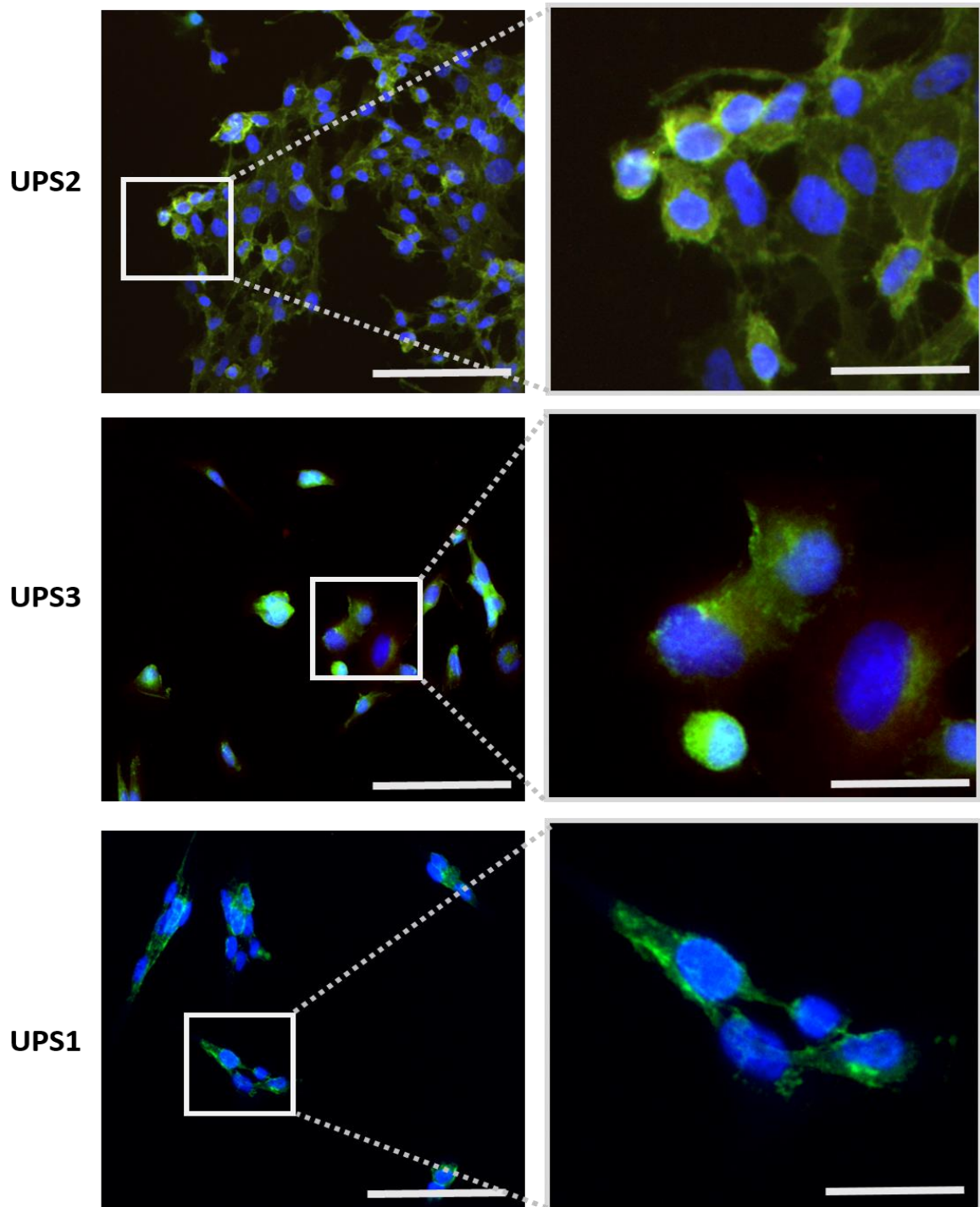
Figure S18: Immunocytochemistry images of N-cadherin localisation in UPS2, UPS3 and UPS1 cell lines.
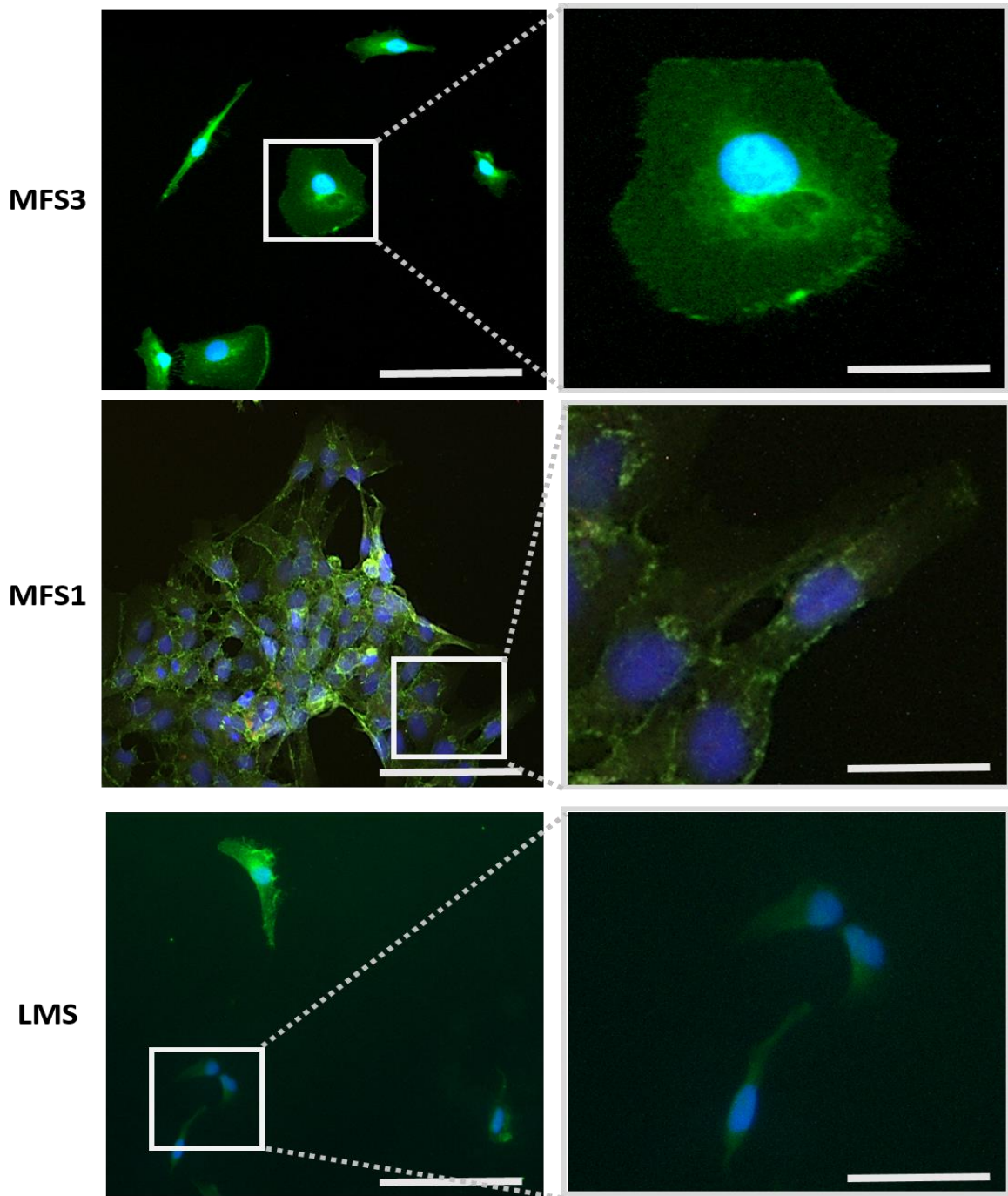
Figure S19: Immunocytochemistry images of N-cadherin localisation in MFS3, MFS1 and LMS cell lines.
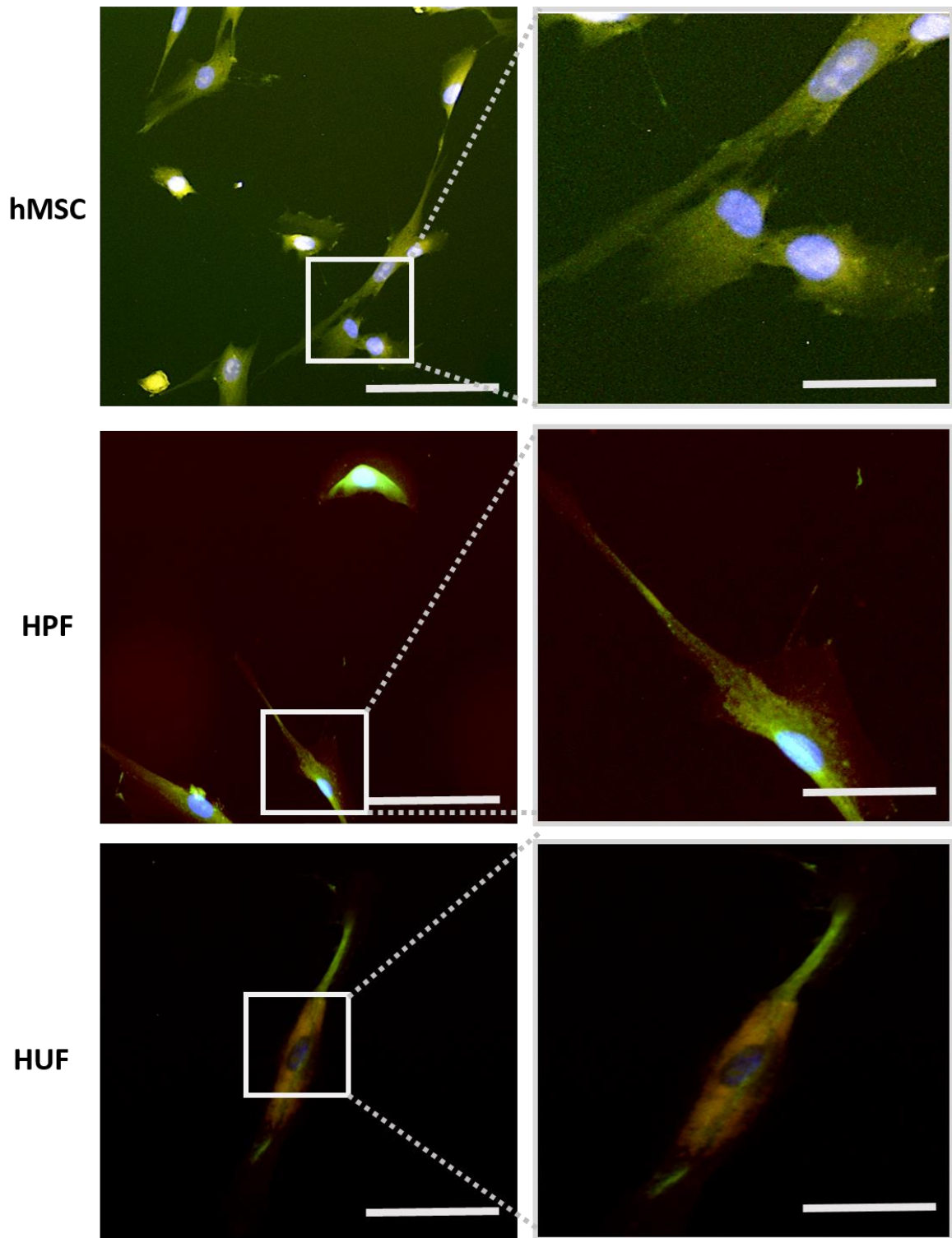
Figure S20: Immunocytochemistry images of N-cadherin localisation in hMSC, HPF and HUF cell lines.
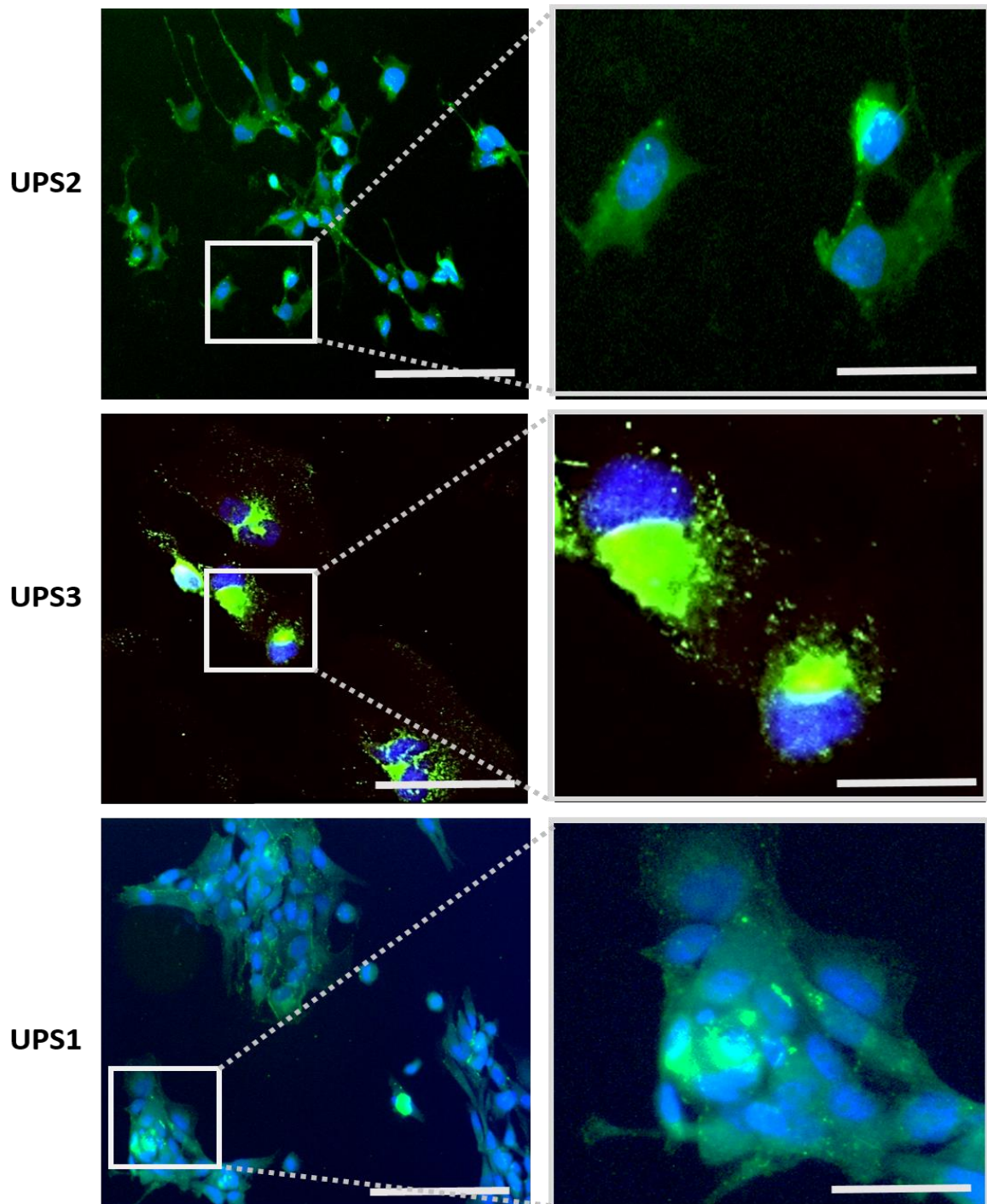
Figure S21: Immunocytochemistry images of fibronectin localisation in UPS2, UPS3 and UPS1 cell lines.
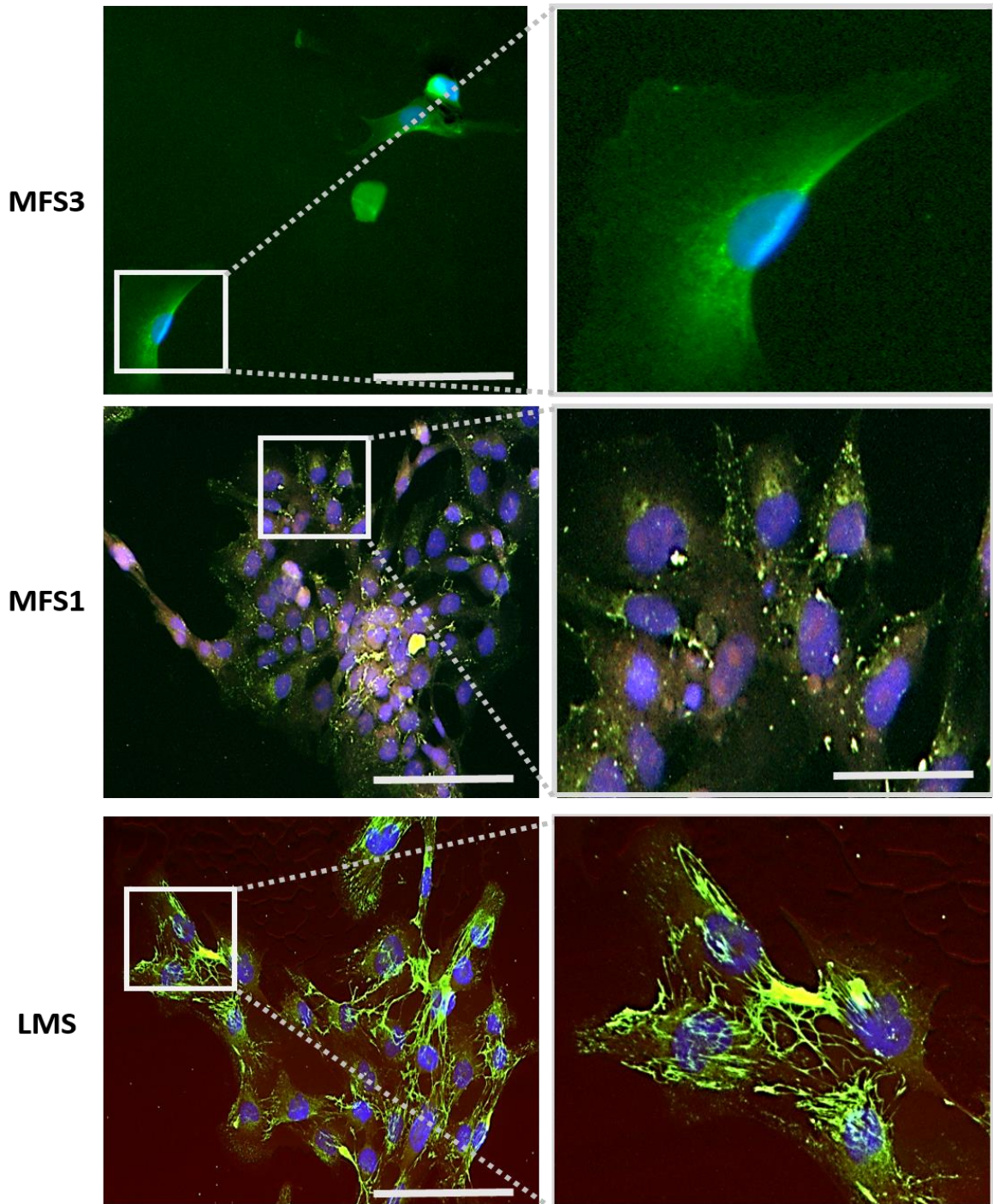
Figure S22: Immunocytochemistry images of fibronectin localisation in MFS3, MFS2 and LMS cell lines.
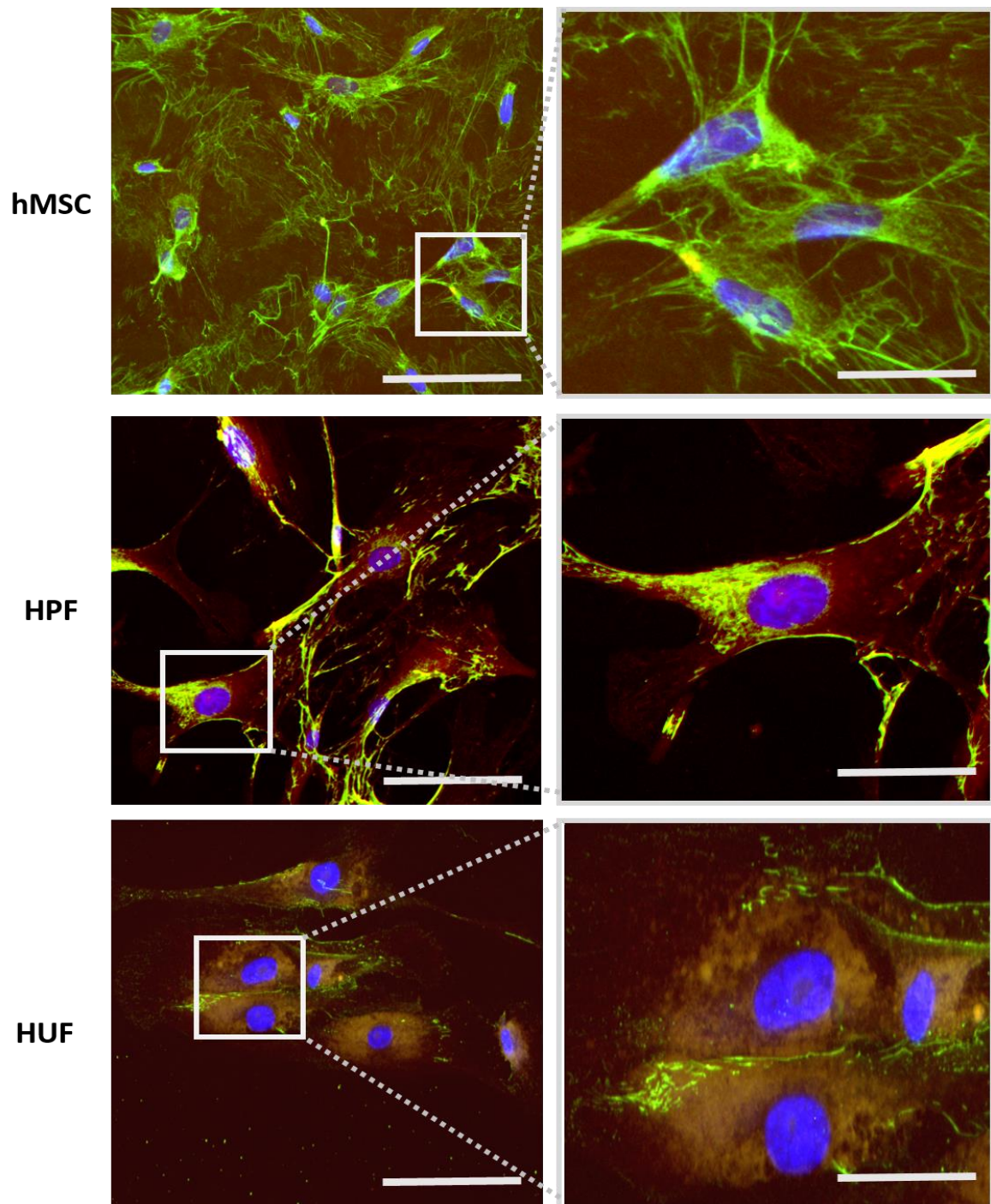
Figure S23: Immunocytochemistry images of fibronectin localisation in hMSC, HPF and HUF cell lines.
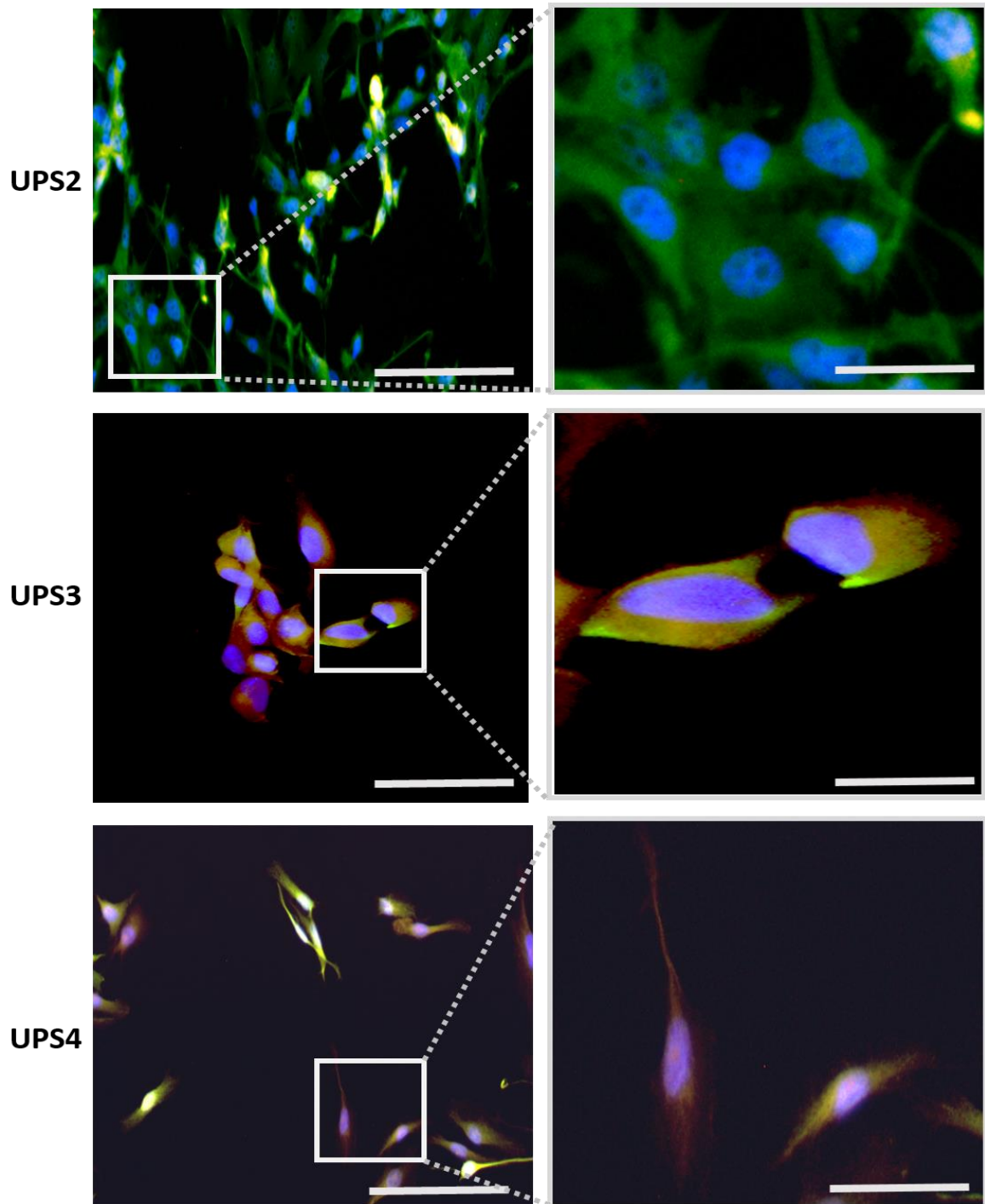
Figure S24: Immunocytochemistry images of FSP-1 localisation in UPS2, UPS3 and UPS4 cell lines.
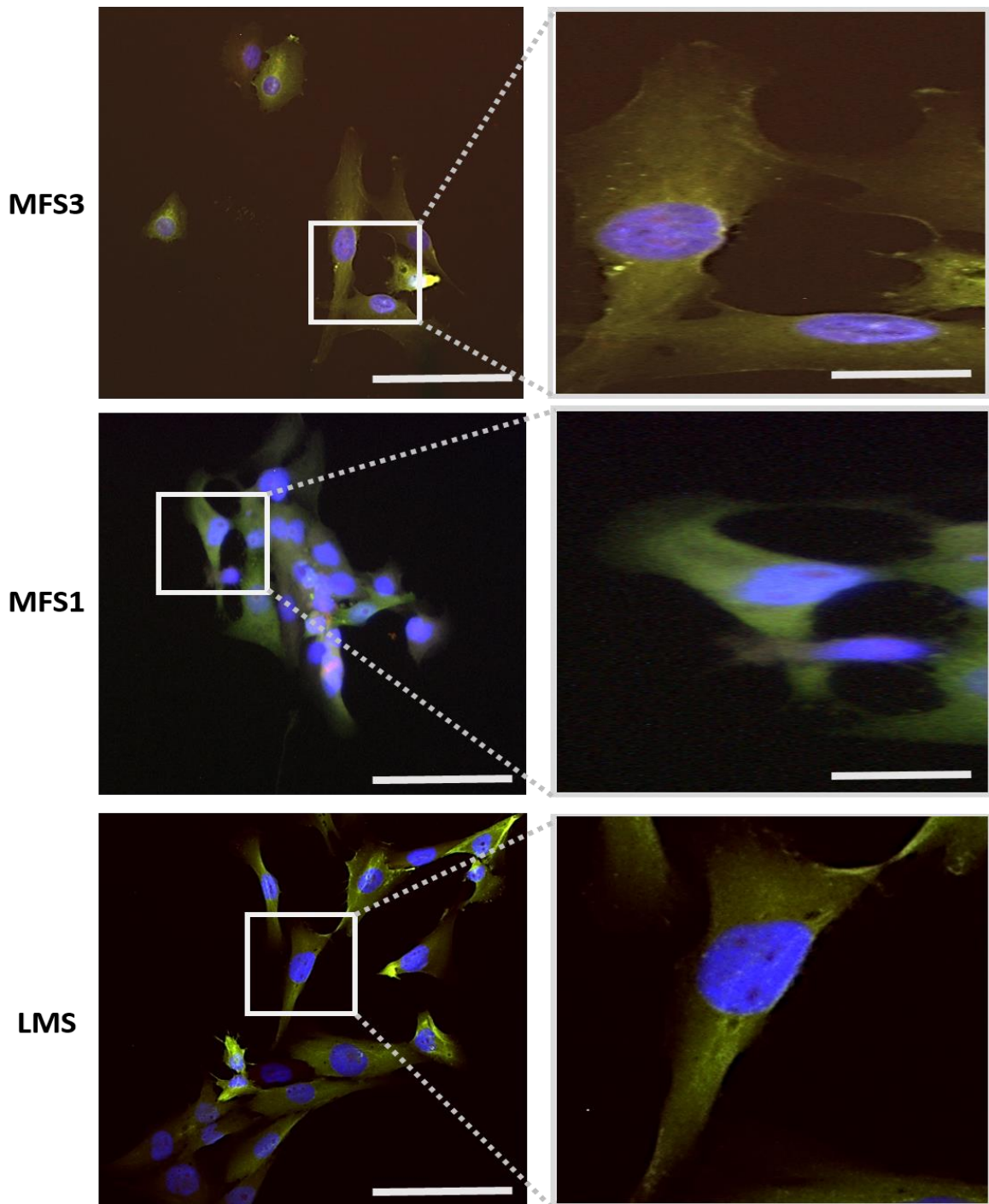
Figure S25: Immunocytochemistry images of FSP-1 localisation in MFS3, MFS1 and LMS cell lines.
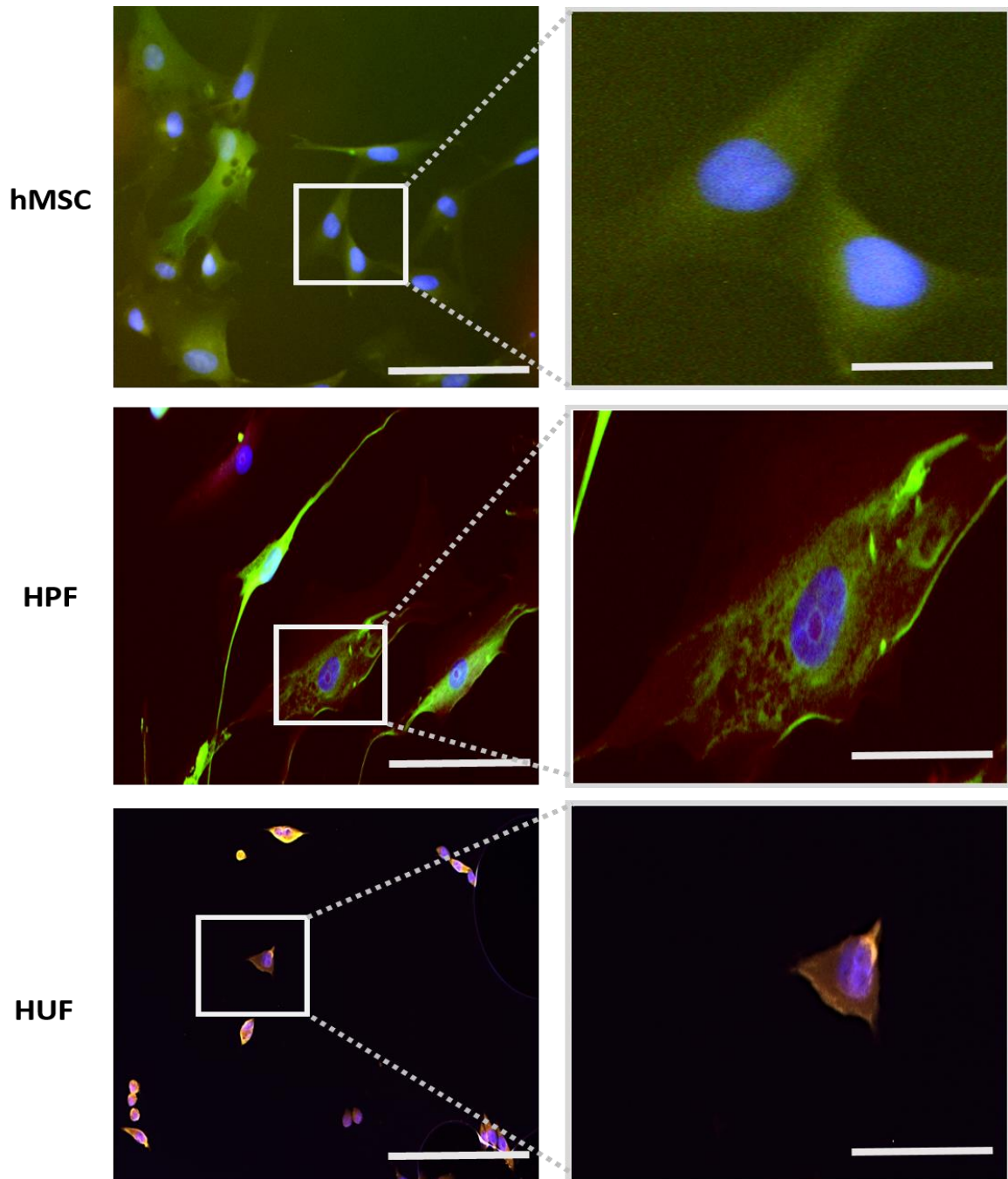
Figure S26: Immunocytochemistry images of FSP-1 localisation in hMSC, HPF and HUF cell lines.
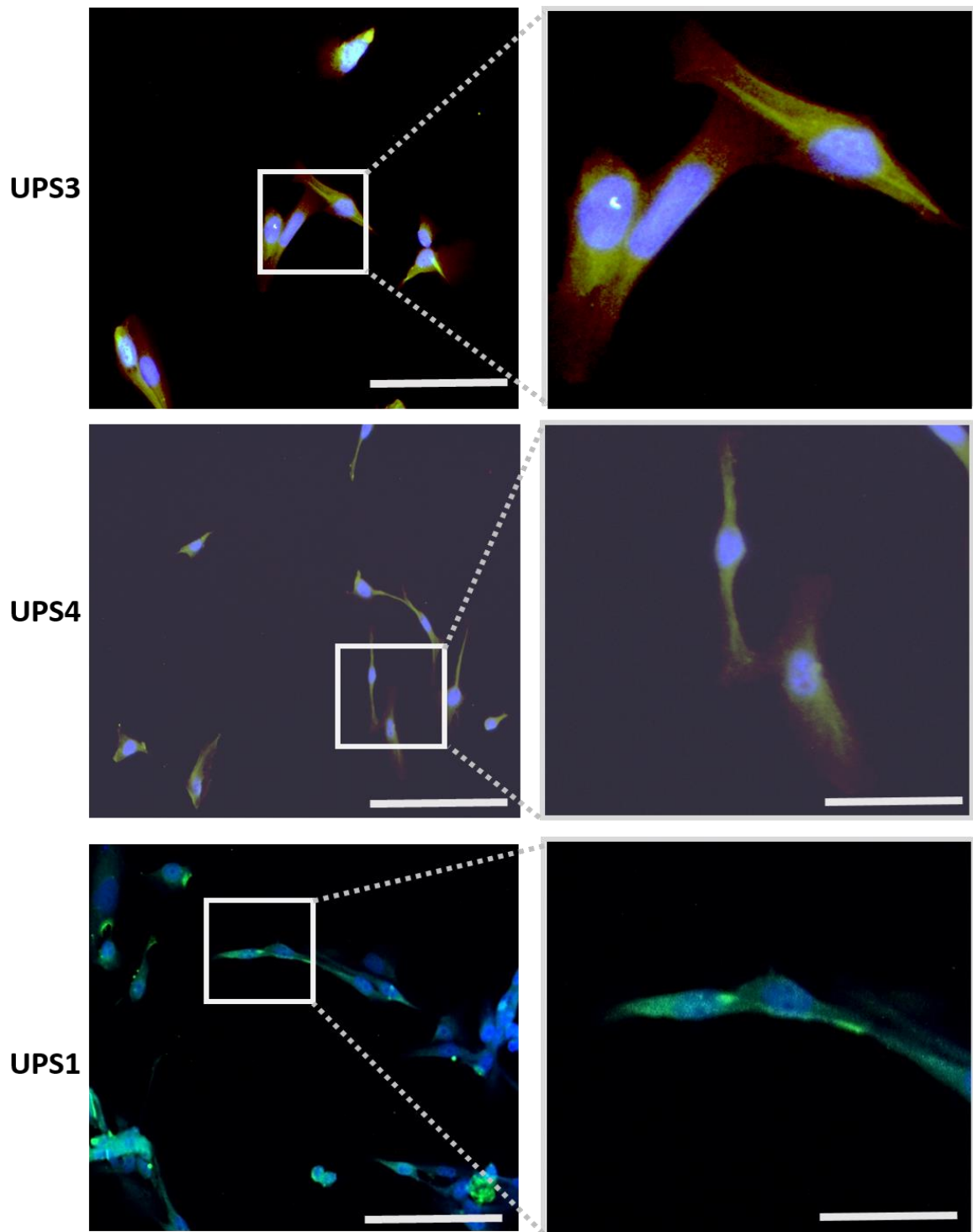
Figure S27: Immunocytochemistry images of FAPα localisation in UPS3, UPS4 and UPS1 cell lines.
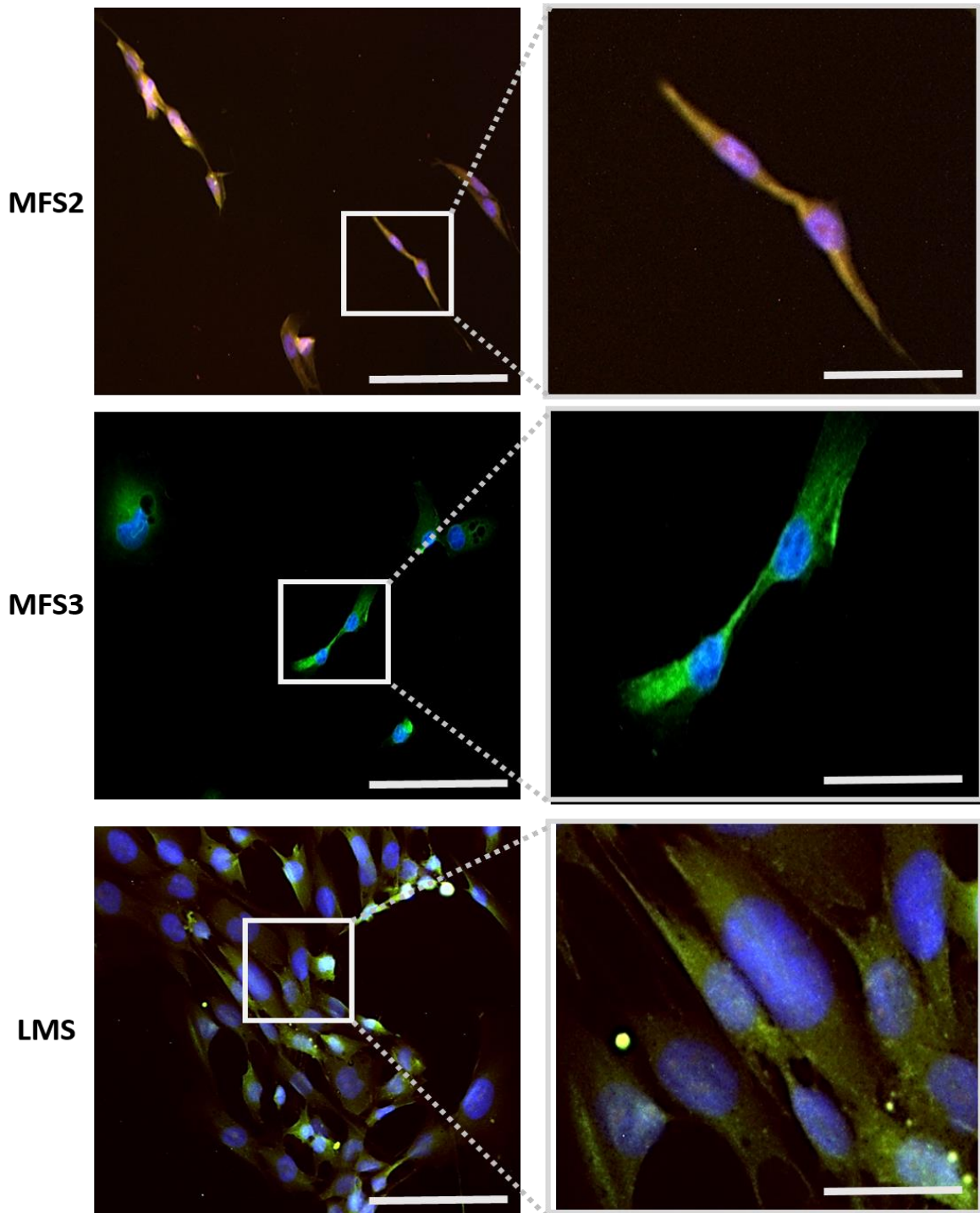
Figure S28: Immunocytochemistry images of FAPα localisation in MFS2, MFS3 and LMS cell lines.
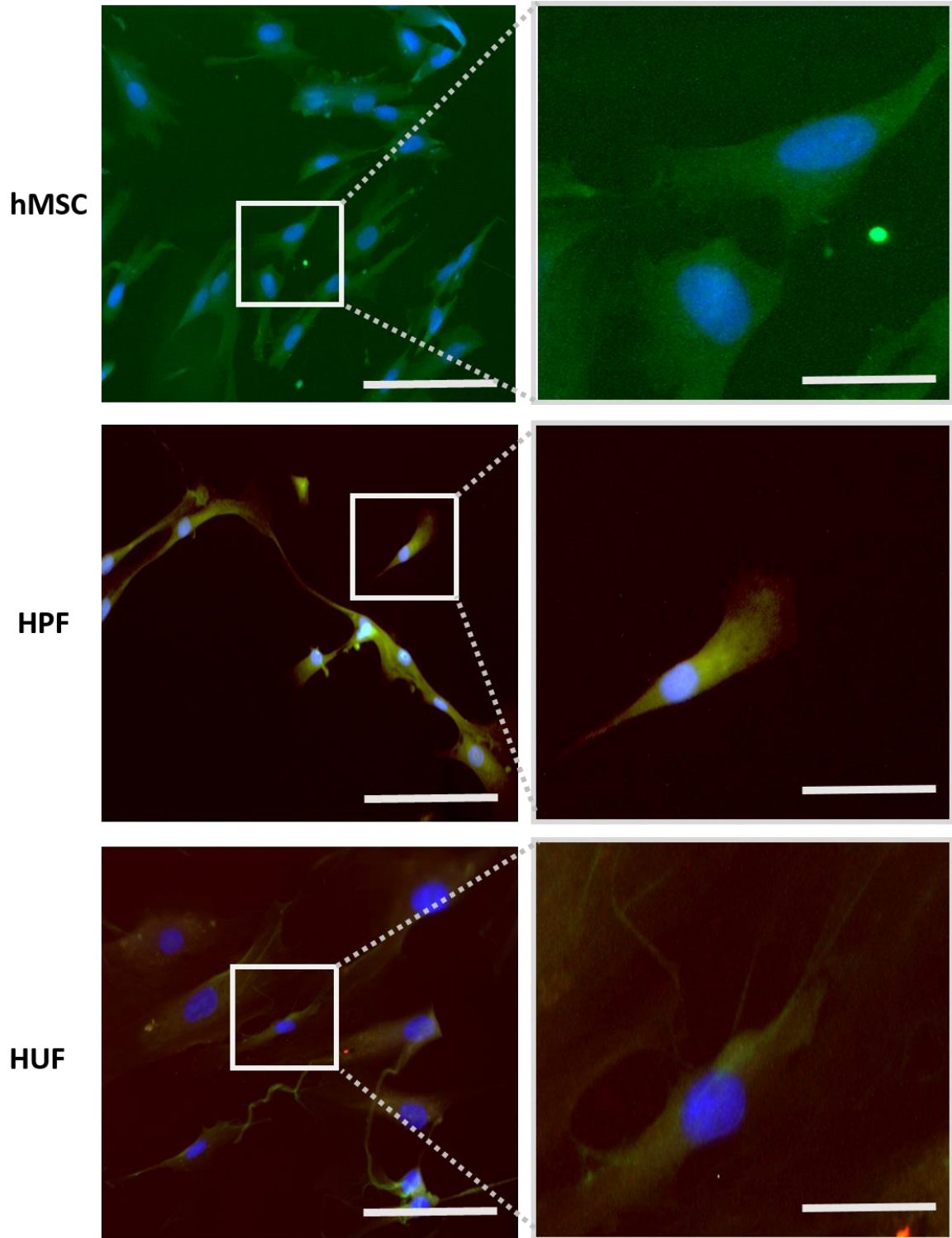
Figure S29: Immunocytochemistry images of FAPα localisation in hMSC, HPF and HUF cell lines.
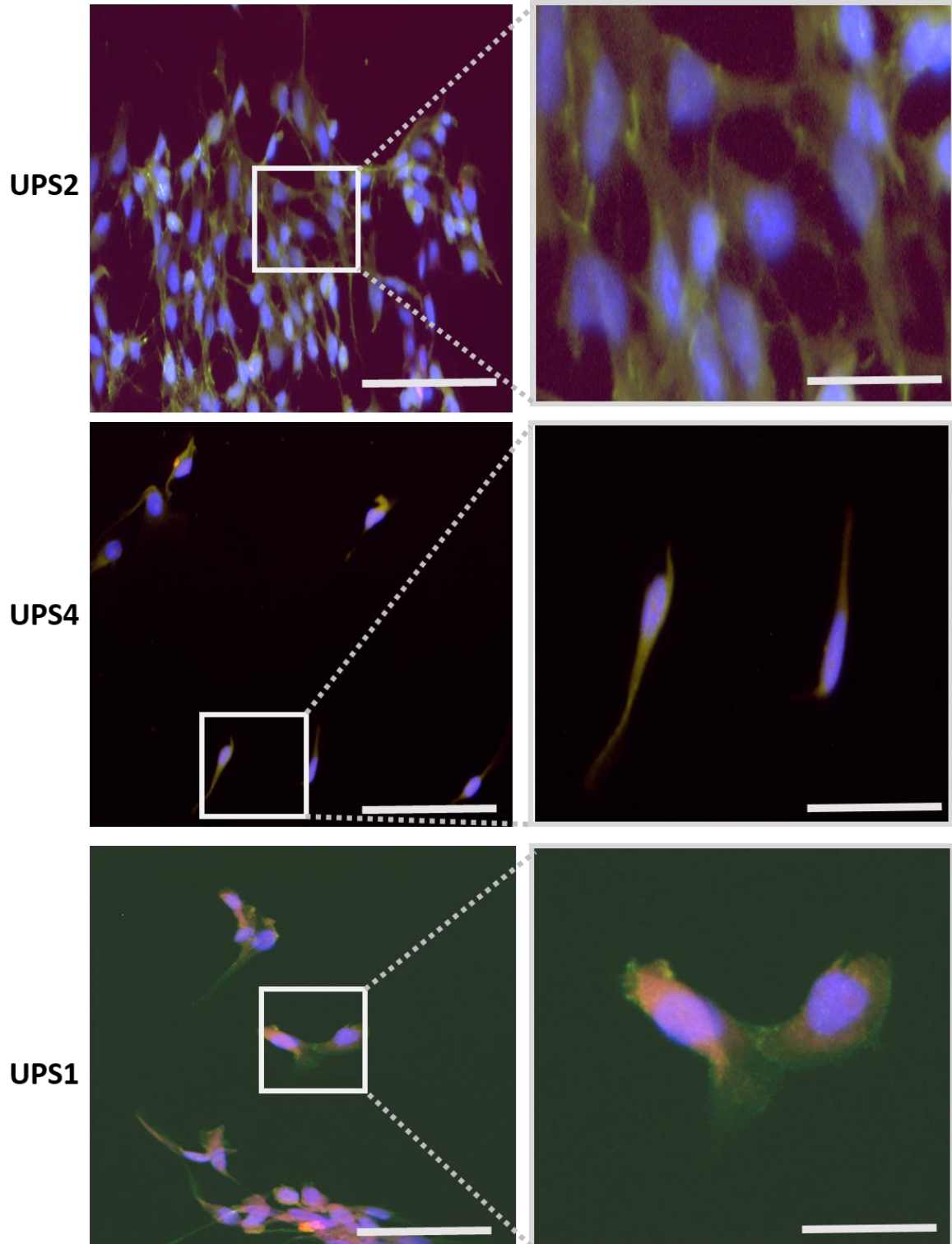
Figure S30: Immunocytochemistry images of SOX2 localisation in UPS2, UPS4 and UPS1 cell lines.
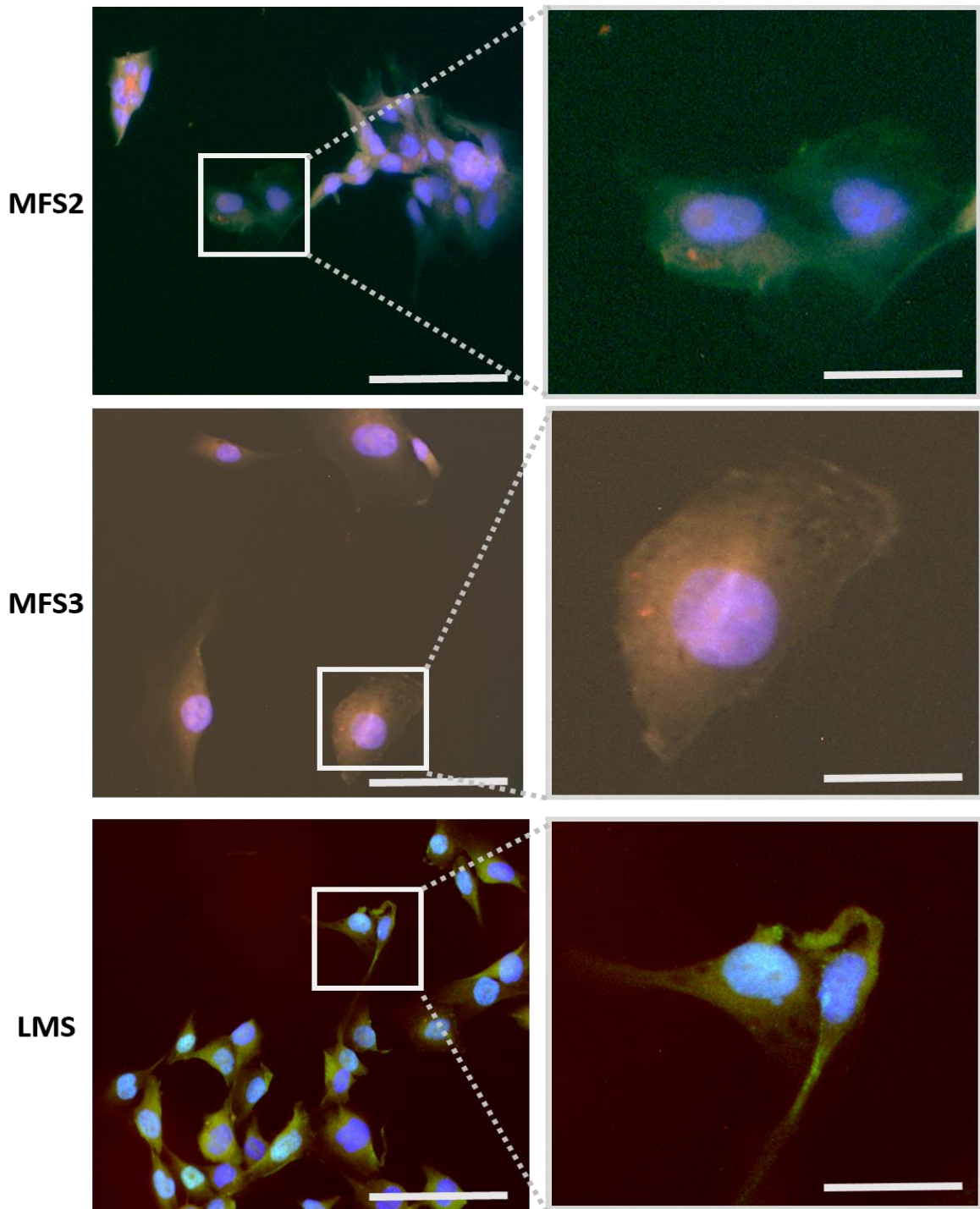
Figure S31: Immunocytochemistry images of SOX2 localisation in MFS2, MFS3 and LMS cell lines.
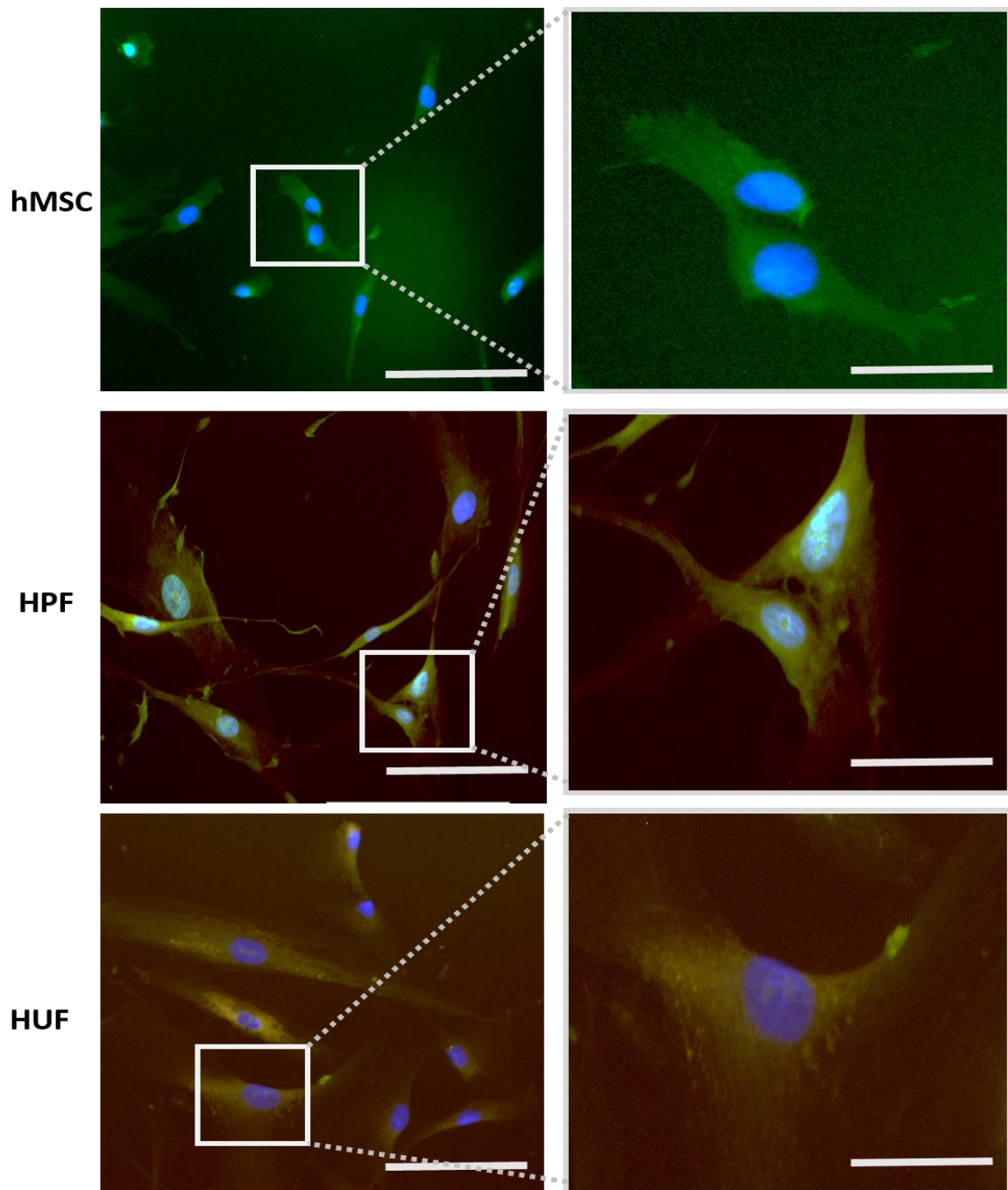
Figure S32: Immunocytochemistry images of SOX2 localisation in hMSC, HPF and HU
F cell lines.
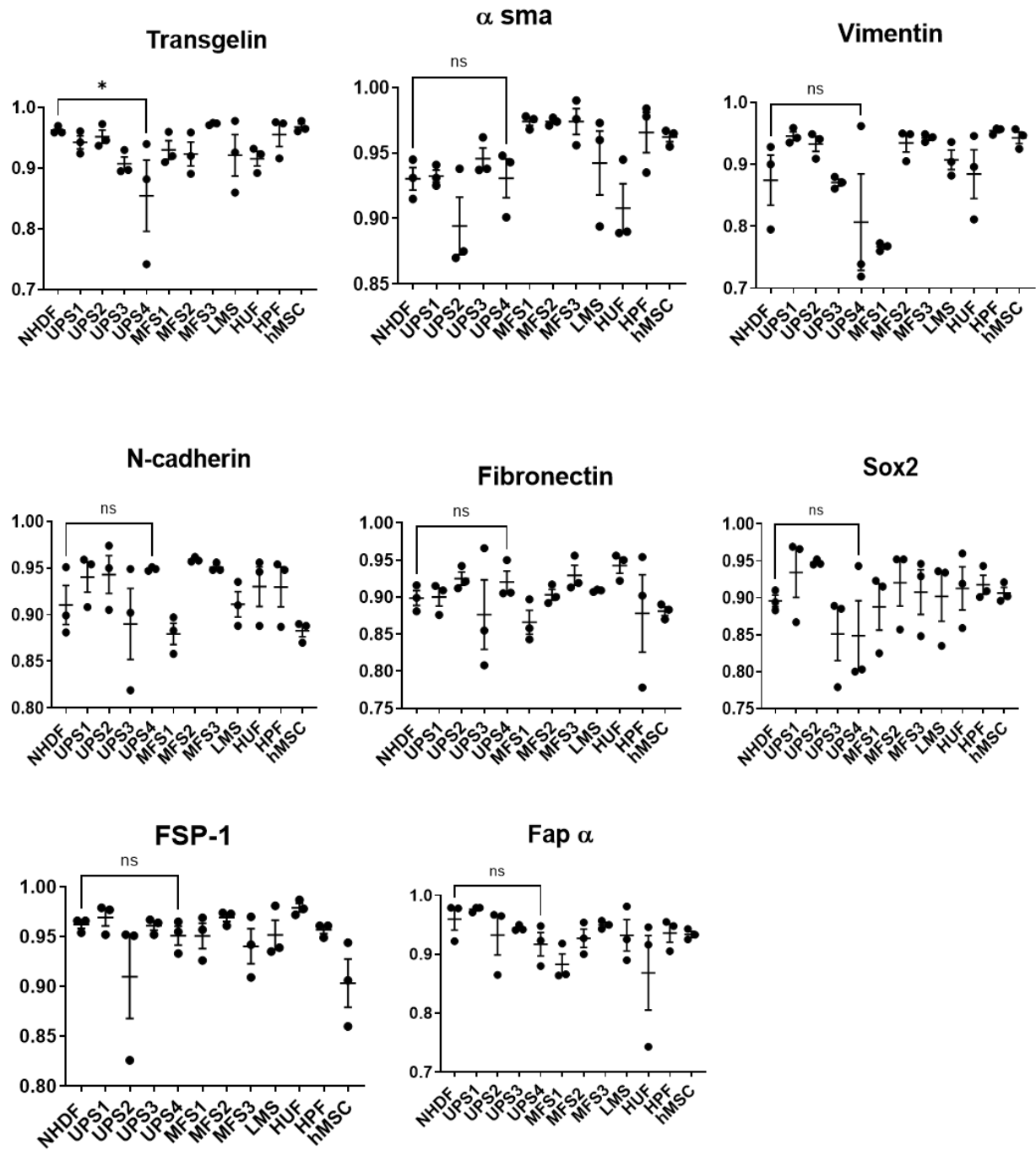
Figure S33: Semi-quantitative analysis of co-localisation between the protein and Phalloidin.

X-axis is cell lines and Y-axis is Pearson's correlation coefficient (PCC).

	Transgelin	αSMA	Vimentin	N-cadherin	Fibronectin	SOX2	FSP-1	FAPα
	R	R	R	R	R	R	R	R
NHDF	0.951	0.921	0.899	0.908	0.927	0.9	0.96	0.941
UPS2	0.931	0.926	0.954	0.968	0.886	0.966	0.953	0.979
UPS3	0.973	0.87	0.948	0.974	0.942	0.945	0.951	0.948
UPS4	0.897	0.923	0.879	0.811	0.804	0.885	0.964	0.941
UPS1	0.751	0.939	0.738	0.947	0.905	0.8	0.965	0.92
MFS3	0.899	0.976	0.761	0.843	0.864	0.923	0.957	0.864
MFS1	0.957	0.977	0.969	0.961	0.943	0.952	0.973	0.954
MFS2	0.971	0.956	0.786	0.953	0.897	0.798	0.915	0.939
LMS	0.977	0.9	0.786	0.909	0.967	0.933	0.981	0.981
HUF	0.891	0.844	0.835	0.946	0.876	0.959	0.976	0.915
HPF	0.974	0.983	0.957	0.948	0.938	0.941	0.961	0.903
hMSC	0.964	0.963	0.941	0.886	0.877	0.9	0.854	0.928

Table S1: Pearson's correlation coefficient (PCC) (R) for co-localisation of each protein with F-Actin in ICC experiment.

Xenografts					
UPS2 vs UPS3		**UPS2 vs UPS4**		**UPS3 vs UPS4**	
UP	**Down**	**UP**	**Down**	**UP**	**Down**
SCN5A	NFYB	IL2	MBP	IL2	LIRB4
NUP205		CCN1	PLAAT3	CCN1	AKT2
POT1		MAPK3	NFYB	EFNA3	CD01
MFSD4B		MYOL1A	CIQC	IPO5	UPOS
PTK6		IGLV3-19	LILRB4	TIMM8A	CD58

Table S2: UP/downregualted genes between the xenograft transcripts.

This table represent the five most upregulated genes (**UP**) and the five most downregulated genes (**Down**) in xenograft transcriptomes.

Human transcriptomes					
UPS2 vs UPS3		UPS2 vs UPS4		UPS3 vs UPS4	
UP	Down	UP	Down	UP	Down
MYOG	RBL1	MMP7	ZNF141	VAT1L	KRT79
SFRP5		VAT1L	MAGEC1	WNT7B	MAD1L1
HAPLN1		PPDPF	DCAF4L2	PPDPF	FGF16
TMEM47		LDOC1	KRT79	LDOC1	NDN
CA3		HOXD13	GALNT12	RPL3P2	DCAF4L2

Table S3: UP/downregualted genes between the human transcripts.

This table represent the five most upregulated genes (UP) and the five most downregulated genes (Down) in human transcriptomes.

UPS2		UPS3		UPS4	
UP	**Down**	**UP**	**Down**	**UP**	**Down**
CNTN2	BTG1	ABCB9	EEF1A1	TMEM87B	ARHGAP19
PRPF6	ITGB5	FBXO36	EIF2A1	MUL1	SERINC3
MRPS10	CCDC74B	COIL	VIM	BCAS1	PRKAA2
ODR4	SPARC	RPUSD4	ARF1	LRRC59	HOXA4
NUDT15	CHRNA5	HSPB11	BRAK	TMEM174	INTS3

Table S4: UP/downregualted genes between the human and mouse transcriptome.

This table represent the five most upregulated genes (UP) and the five most downregulated genes (Down) between human and mouse transcriptomes.

Overall Survival

Progression-free Survival

Transgelin

Overall Survival (%)

0.8
0.6
0.4
0.2
0.0

— Low — High

HR(95% CI)
0.738(0.32-1.494)
P=0.386

0   2   4   6   8   10
n at risk   Time (years)

Low   36.5 28 15 10.5 7 3
High   36.5 32.5 29.5 24 21 9.5

Progression free Survival (%)

0.8
0.6
0.4
0.2
0.0

— Low — High

HR(95% CI)
0.341(0.635-2.417)
P=0.529

0   2   4   6   8   10
n at risk   Time (years)

Low   36 21 11 8.5 6 2.5
High   37 24 21 18 16.5 7.5

αSMA

Overall Survival (%)

0.8
0.6
0.4
0.2
0.0

HR(95% CI)
0.745(0.312—1.774)
P=0.504

0   2   4   6   8   10
n at risk   Time (years)

Low   36 25.5 12.5 8.5 6 3
High   36.5 33 32 28 25 11

Progression free Survival (%)

0.8
0.6
0.4
0.2
0.0

HR(95% CI)
0.728(0.368-1.440)
P=0.360

0   2   4   6   8   10
n at risk   Time (years)

Low   31.5 14 8 6 3.5 1.5
High   37 27 24 22 19.5 8.5

Vimentin

Overall Survival (%)

0.8
0.6
0.4
0.2
0.0

HR(95% CI)
1.410(0.651-3.053)
P=0.394

0   2   4   6   8   10
n at risk   Time (years)

Low   35 27 16 11.5 7 4.5
High   36.5 31 27 20 17.5 7

Progression free Survival (%)

0.8
0.6
0.4
0.2
0.0

HR(95% CI)
1.668(0.832-3.344)
P=0.145

0   2   4   6   8   10
n at risk   Time (years)

Low   34.5 21 9.5 7 5 2.5
High   36   21 17 16 15 6.5

Overall Survival

Progression-free Survival

N-cadherin

Overall Survival (%)

Low — High

HR(95% CI)
2.623(1.249-5.506)
P=0.378

n at risk   Time (years)

Low   35.5 31.5 30 26.5 24 10.5
High   36.5 26.5 17.5 11 7 3

Progression free Survival (%)

Low — High

HR(95% CI)
137.4(0.23-812781)
P=0.008

n at risk   Time (years)

Low   36 21 11 8.5 6 2.5
High   37 24 21 18 16.5 7.5

Fibronectin

Overall Survival (%)

HR(95% CI)
1.215(0.552—2.674)
P=0.628

n at risk   Time (years)

Low   31 23.5 16.5 14 9 5
High   36.5 33 32 28 25 11

Progression free Survival (%)

HR(95% CI)
1.180(0.619-2.251)
P=0.615

n at risk   Time (years)

Low   38.5 21.5 13 10.5 8 4
High   37 23 21 20 17.5 8.5

FSP-1

Overall Survival (%)

HR(95% CI)
0.638(0.299-1.362)
P=0.386

n at risk   Time (years)

Low   33 24.5 15 10 5 2.5
High   35.5 29.5 26.5 20 18 8

Progression free Survival (%)

HR(95% CI)
0.734(0.397-1.357)
P=0.322

n at risk   Time (years)

Low   35 19 6.5 5 3 1.5
High   36 23 19 16.5 14 5.5

Figure S34: Overall and progression free Survival Analysis of common gene expression in the TCGA SARC and vortex RNAseq dataset.

NG2+PDGFRβ

Nanog

Oct4

SSEA-4

DCN

CDH11
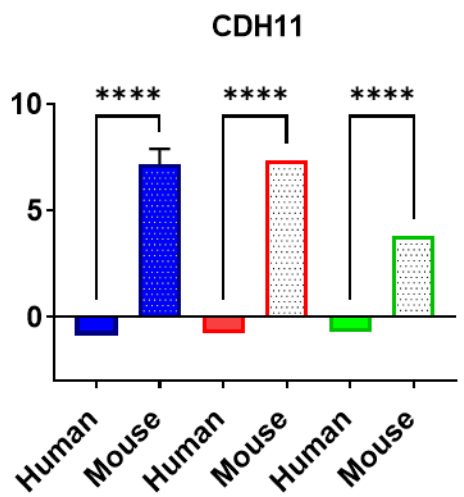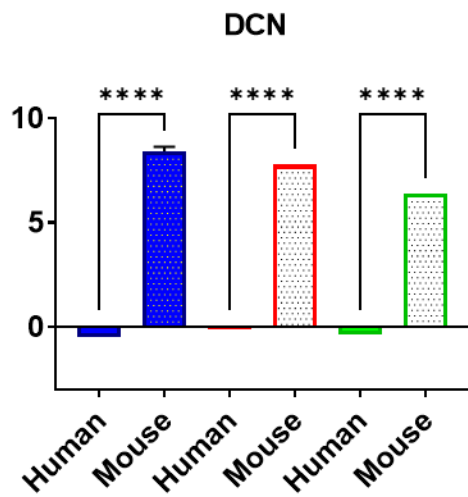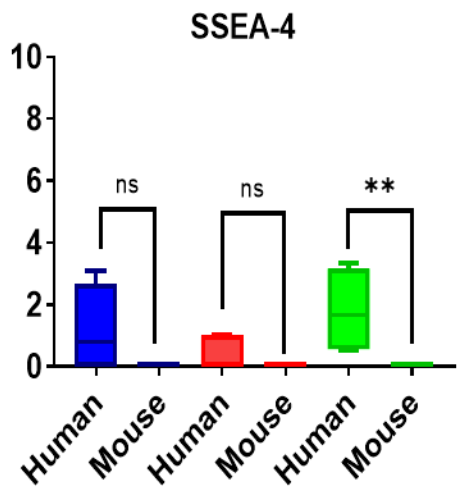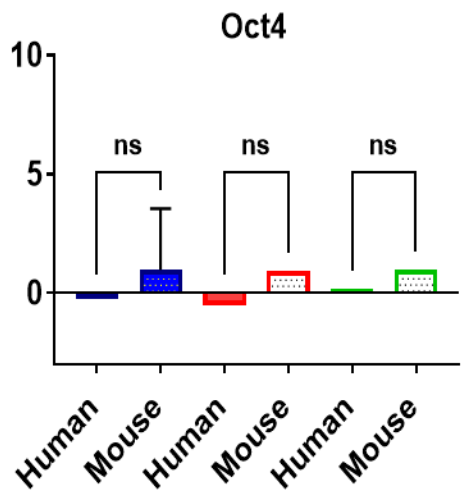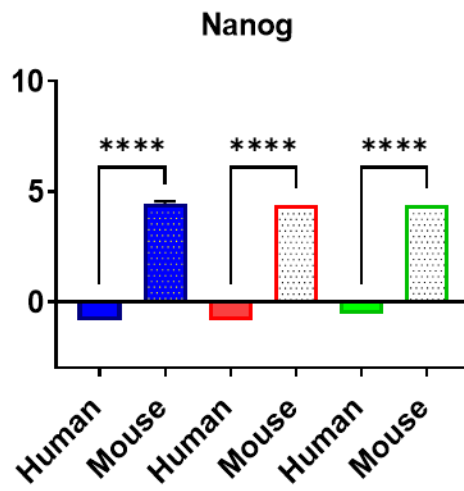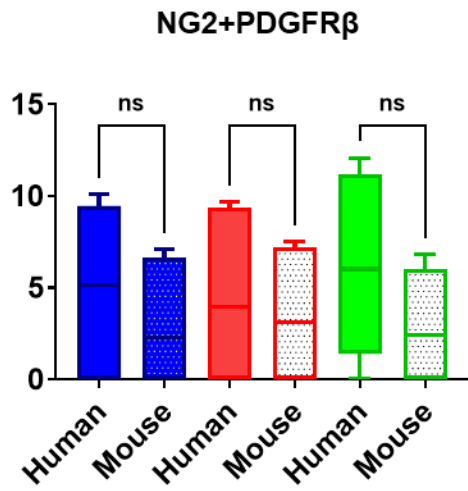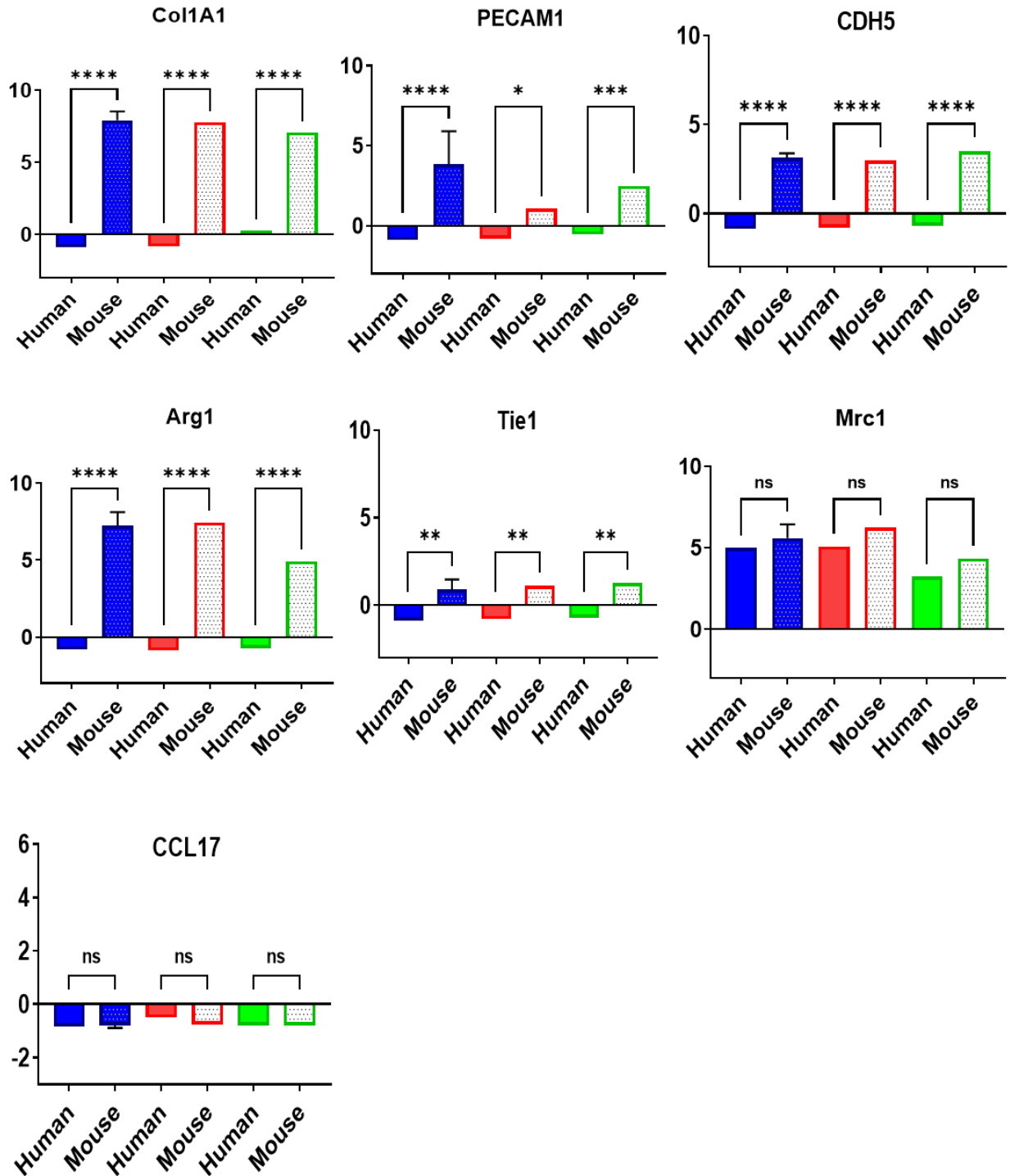
Figure S35: Box-plot analysis of the common CAFs gene expression in human vs mouse transcriptomes in UPS xenografts.

Error bars are ± SEM. *,P<0.05 , **,P <0.01; ***,P < 0.001 ;NS, not significant.

References:

Abeshouse, A., Adebamowo, C., Adebamowo, S. N., Akbani, R., Akeredolu, T., Ally, A., Anderson, M. L., Anur, P., Appelbaum, E. L., Armenia, J., Auman, J. T., Bailey, M. H., Baker, L., Balasundaram, M., Balu, S., Barthel, F. P., Bartlett, J., Baylin, S. B., Behera, M., . . . Wilson, R. K. (2017). Comprehensive and Integrated Genomic Characterization of Adult Soft Tissue Sarcomas. *Cell*, *171*(4), 950-965.e928. https://doi.org/10.1016/j.cell.2017.10.014

Adolfo, P. (2009). Regenerative medicine: a review Medicina regenerativa: uma revisão. *Revista Brasileira de Hematologia e Hemoterapia*, *31*(suppl 2), 63-66. https://doi.org/10.1590/S1516-84842009000800017

Alabiad, M. A., Harb, O. A., Abdelfattah, M. T., El-Shafaay, B. S., El-Taher, A. K., & El-Hendawy, E. I. (2020). The values of Transgelin, Stathmin, BCOR and Cyclin-D1 expression in differentiation between Uterine Leiomyosarcoma (ULMS) and Endometrial Stromal Sarcoma (ESS); diagnostic and prognostic implications. *Surgical and Experimental Pathology*, *3*(1), 13. https://doi.org/10.1186/s42047-020-00065-0

Anderberg, C., Li, H., Fredriksson, L., Andrae, J., Betsholtz, C., Li, X., Eriksson, U., & Pietras, K. (2009). Paracrine signaling by platelet-derived growth factor-CC promotes tumor growth by recruitment of cancer-associated fibroblasts. *Cancer Res*, *69*(1), 369-378. https://doi.org/10.1158/0008-5472.CAN-08-2724

Anderson, N. D., Babichev, Y., Fuligni, F., Comitani, F., Layeghifard, M., Venier, R. E., Dentro, S. C., Maheshwari, A., Guram, S., Wunker, C., Thompson, J. D., Yuki, K. E., Hou, H., Zatzman, M., Light, N., Bernardini, M. Q., Wunder, J. S., Andrulis, I. L., Ferguson, P., . . . Shlien, A. (2021). Lineage-defined leiomyosarcoma subtypes emerge years before diagnosis and determine patient survival. *Nat Commun*, *12*(1), 4496. https://doi.org/10.1038/s41467-021-24677-6

Anggorowati, N., Ratna Kurniasari, C., Damayanti, K., Cahyanti, T., Widodo, I., Ghozali, A., . . . Arfian, N. (2017). Histochemical and Immunohistochemical Study of α-SMA, Collagen, and PCNA in Epithelial Ovarian Neoplasm. *Asian Pac J Cancer Prev, 18*(3), 667-671. doi:10.22034/APJCP.2017.18.3.667

Antoine, E. K., Ajeeta, B. D., Annie, P. V., Andrew, S., Mary, W. B., George, W. B., Andrea, L. R., Kornelia, P., Ross, T., & Robert, A. W. (2007). Mesenchymal stem cells within tumour stroma promote breast cancer metastasis. *Nature*, *449*(7162), 557. https://doi.org/10.1038/nature06188

Aran, D., Hu, Z., & Butte, A. J. (2017). xCell: digitally portraying the tissue cellular heterogeneity landscape. *Genome Biol*, *18*(1), 220. https://doi.org/10.1186/s13059-017-1349-1

Arnold, S. A., Loomans, H. A., Ketova, T., Andl, C. D., Clark, P. E., & Zijlstra, A. (2016). Urinary oncofetal ED-A fibronectin correlates with poor prognosis in patients with bladder cancer. *Clin Exp Metastasis, 33*(1), 29-44. doi:10.1007/s10585-015-9754-x

Arnold, J. N., Magiera, L., Kraman, M., & Fearon, D. T. (2014). Tumoral immune suppression by macrophages expressing fibroblast activation protein-α and heme oxygenase-1. *Cancer Immunol Res*, *2*(2), 121-126. https://doi.org/10.1158/2326-6066.CIR-13-0150

Arvinius, C., Torrecilla, E., Beano-Collado, J., García-Coiradas, J., García-Maroto, R., Puerto-Vázquez, M., & Cebrián-Parra, J. L. (2017). A clinical review of 11 cases of large-sized well-differentiated liposarcomas. *European Journal of Orthopaedic Surgery & Traumatology*, *27*(6), 837-841. https://doi.org/10.1007/s00590-017-1968-y

Assinder, S. J., Stanton, J.-A. L., & Prasad, P. D. (2009). Transgelin: An actin- binding protein and tumour suppressor. *International Journal of Biochemistry and Cell Biology, 41*(3), 482-486. doi:10.1016/j.biocel.2008.02.011

Augsten, M. (2014). Cancer- associated fibroblasts as another polarized cell type of the tumor microenvironment. *Frontiers in Oncology*, *4*, 62-62. https://doi.org/10.3389/fonc.2014.00062

Bae, Y. K., Kim, A., Kim, M. K., Choi, J. E., Kang, S. H., & Lee, S. J. (2013). Fibronectin expression in carcinoma cells correlates with tumor aggressiveness and poor clinical outcome in patients with invasive breast cancer. *Hum Pathol*, *44*(10), 2028-2037. https://doi.org/10.1016/j.humpath.2013.03.006

Baek, S. H., Maiorino, E., Kim, H., Glass, K., Raby, B. A., & Yuan, K. (2022). Single Cell Transcriptomic Analysis Reveals Organ Specific Pericyte Markers and Identities. *Front Cardiovasc Med*, *9*, 876591. https://doi.org/10.3389/fcvm.2022.876591

Baghel, K. S., Tewari, B. N., Shrivastava, R., Malik, S. A., Lone, M. U. D., Jain, N. K., Tripathi, C., Kanchan, R. K., Dixit, S., Singh, K., Mitra, K., Negi, M. P. S., Srivastava, M., Misra, S., Bhatt, M. L. B., & Bhadauria, S. (2016). Macrophages promote matrix protrusive and invasive function of breast cancer cells via MIP-1β dependent upregulation of MYO3A gene in breast cancer cells. *Oncoimmunology*, *5*(7), e1196299. https://doi.org/10.1080/2162402X.2016.1196299

Balkwill, F., & Mantovani, A. (2001). Inflammation and cancer: back to Virchow? *The Lancet*, *357*(9255), 539-545. https://doi.org/10.1016/S0140-6736(00)04046-0

Balkwill, F. R., Capasso, M., & Hagemann, T. (2012). The tumor microenvironment at a glance. *Journal of cell science*, *125*(Pt 23), 5591-5596. https://doi.org/10.1242/jcs.116392

Barcellos-de-Souza, P., Gori, V., Bambi, F., & Chiarugi, P. (2013). Tumor microenvironment: Bone marrow- mesenchymal stem cells as key players. *BBA - Reviews on Cancer*, *1836*(2), 321-335. https://doi.org/10.1016/j.bbcan.2013.10.004

Basu-Roy, U., Seo, E., Ramanathapuram, L., Rapp, T. B., Perry, J. A., Orkin, S. H., . . . Basilico, C. (2012). Sox2 maintains self renewal of tumor-initiating cells in osteosarcomas. *Oncogene, 31*(18), 2270-2282. doi:10.1038/onc.2011.405

Benassi, M. S., Pazzaglia, L., Chiechi, A., Alberghini, M., Conti, A., Cattaruzza, S., Wassermann, B., Picci, P., & Perris, R. (2009). NG2 expression predicts the metastasis formation in soft-tissue sarcoma patients. *J Orthop Res*, *27*(1), 135-140. https://doi.org/10.1002/jor.20694

Benna, C., Simioni, A., Pasquali, S., De Boni, D., Rajendran, S., Spiro, G., Colombo, C., Virgone, C., DuBois, S. G., Gronchi, A., Rossi, C. R., & Mocellin, S. (2018). Genetic susceptibility to bone and soft tissue sarcomas: a field synopsis and meta-analysis. *Oncotarget*, *9*(26), 18607-18626. https://doi.org/10.18632/oncotarget.24719

Bennewith, K. L., Huang, X., Ham, C. M., Graves, E. E., Erler, J. T., Kambham, N., Feazell, J., Yang, G. P., Koong, A., & Giaccia, A. J. (2009). The role of tumor cell-derived connective tissue growth factor (CTGF/CCN2) in pancreatic tumor growth. *Cancer Res*, *69*(3), 775-784. https://doi.org/10.1158/0008-5472.CAN-08-0987

Betterle, C., & Zanchetta, R. (2012). The immunofluorescence techniques in the diagnosis of endocrine autoimmune diseases. *Auto Immun Highlights*, *3*(2), 67-78. https://doi.org/10.1007/s13317-012-0034-3

Bhowmick, N. A., Chytil, A., Plieth, D., Gorska, A. E., Dumont, N., Shappell, S., Washington, M. K., Neilson, E. G., & Moses, H. L. (2004). TGF-β Signaling in Fibroblasts Modulates the Oncogenic Potential of Adjacent Epithelia. *Science*, *303*(5659), 848-851. https://doi.org/10.1126/science.1090922

Blankenberg, D., Gordon, A., Von Kuster, G., Coraor, N., Taylor, J., Nekrutenko, A., & Team, G. (2010). Manipulation of FASTQ data with Galaxy. *Bioinformatics*, *26*(14), 1783-1785. https://doi.org/10.1093/bioinformatics/btq281

Bleloch, J. S., Ballim, R. D., Kimani, S., Parkes, J., Panieri, E., Willmer, T., & Prince, S. (2017). Managing sarcoma: where have we come from and where are we going? In (Vol. 9, pp. 637-659). London, England.

Bondjers, C., Kalén, M., Hellström, M., Scheidl, S. J., Abramsson, A., Renner, O., Lindahl, P., Cho, H., Kehrl, J., & Betsholtz, C. (2003). Transcription profiling of platelet-derived growth factor-B-deficient mouse embryos identifies RGS5 as a novel marker for pericytes and vascular smooth muscle cells. *Am J Pathol*, *162*(3), 721-729. https://doi.org/10.1016/S0002-9440(10)63868-0

Bonuccelli, G., Avnet, S., Grisendi, G., Salerno, M., Granchi, D., Dominici, M., Kusuzaki, K., & Baldini, N. (2014). Role of mesenchymal stem cells in osteosarcoma and metabolic reprogramming of tumor cells. *Oncotarget*, *5*(17), 7575-7588. https://doi.org/10.18632/oncotarget.2243

Bulbul, A., Fahy, B. N., Xiu, J., Rashad, S., Mustafa, A., Husain, H., & Hayes-Jordan, A. (2017). Desmoplastic Small Round Blue Cell Tumor: A Review of Treatment and Potential Therapeutic Genomic Alterations. *Sarcoma*, *2017*, 1278268. https://doi.org/10.1155/2017/1278268

Busek, P., Mateu, R., Zubal, M., Kotackova, L., & Sedo, A. (2018). Targeting fibroblast activation protein in cancer - Prospects and caveats. *Front Biosci (Landmark Ed), 23*(10), 1933-1968. doi:10.2741/4682

Butti, R., Nimma, R., Kundu, G., Bulbule, A., Kumar, T. V. S., Gunasekaran, V. P., Tomar, D., Kumar, D., Mane, A., Gill, S. S., Patil, T., Weber, G. F., & Kundu, G. C. (2021). Tumor-derived osteopontin drives the resident fibroblast to myofibroblast differentiation through Twist1 to promote breast cancer progression. Oncogene, 40(11), 2002-2017. https://doi.org/10.1038/s41388-021-01663-2

Cannon, A., Thompson, C., Hall, B. R., Jain, M., Kumar, S., & Batra, S. K. (2018). Desmoplasia in pancreatic ductal adenocarcinoma: insight into pathological function and therapeutic potential. *Genes & cancer*, *9*(3-4), 78-86. https://doi.org/10.18632/genesandcancer.171

Cao, Y., Zhang, Z. L., Zhou, M., Elson, P., Rini, B., Aydin, H., Feenstra, K., Tan, M. H., Berghuis, B., Tabbey, R., Resau, J. H., Zhou, F. J., Teh, B. T., & Qian, C. N. (2013). Pericyte coverage of differentiated vessels inside tumor vasculature is an independent unfavorable prognostic factor for patients with clear cell renal cell carcinoma. *Cancer*, *119*(2), 313-324. https://doi.org/10.1002/cncr.27746

Carneiro, A., Francis, P., Bendahl, P. O., Fernebro, J., Akerman, M., Fletcher, C., Rydholm, A., Borg, A., & Nilbert, M. (2009). Indistinguishable genomic profiles and shared prognostic markers in undifferentiated pleomorphic sarcoma and leiomyosarcoma: different sides of a single coin? Lab Invest, 89(6), 668-675. https://doi.org/10.1038/labinvest.2009.18

Cedric, G., Steven, H., Cristina, H.-C., Robert, G., John, F. M., Kevin, H., & Erik, S. (2007). Fibroblast- led collective invasion of carcinoma cells with differing roles for RhoGTPases in leading and following cells. Nature Cell Biology, 9(12), 1392. https://doi.org/10.1038/ncb1658

Chai, J. T., Ruparelia, N., Goel, A., Kyriakou, T., Biasiolli, L., Edgar, L., Handa, A., Farrall, M., Watkins, H., & Choudhury, R. P. (2018). Differential Gene Expression in Macrophages From Human Atherosclerotic Plaques Shows Convergence on Pathways Implicated by Genome-Wide Association Study Risk Variants. Arterioscler Thromb Vasc Biol, 38(11), 2718-2730. https://doi.org/10.1161/ATVBAHA.118.311209

Chang, T. H., Shanti, R. M., Liang, Y., Zeng, J., Shi, S., Alawi, F., Carrasco, L., Zhang, Q., & Le, A. D. (2020). LGR5. Cell Death Dis, 11(5), 338. https://doi.org/10.1038/s41419-020-2560-7

Charlotte, K., Tony, C., Min, W., Greg, M., Joe, W. G., Loucinda, C., Andrea, R., & Robert, A. W. (2004). Reconstruction of functionally normal and malignant human breast tissues in mice. *Proceedings of the National Academy of Sciences of the United States of America*, *101*(14), 4966. https://doi.org/10.1073/pnas.0401064101

Chaurasia, S. S., Kaur, H., de Medeiros, F. W., Smith, S. D., & Wilson, S. E. (2009). Dynamics of the expression of intermediate filaments vimentin and desmin during myofibroblast differentiation after corneal injury. *Experimental Eye Research*, *89*(2), 133-139. https://doi.org/10.1016/j.exer.2009.02.022

Chen, L., Chu, C., Lu, J., Kong, X., Huang, T., & Cai, Y. D. (2015). Gene Ontology and KEGG Pathway Enrichment Analysis of a Drug Target-Based Classification System. *PLoS One*, *10*(5), e0126492. https://doi.org/10.1371/journal.pone.0126492

Chen, Y., Shi, L., Zhang, L., Li, R., Liang, J., Yu, W., Sun, L., Yang, X., Wang, Y., Zhang, Y., & Shang, Y. (2008). The molecular mechanism governing the oncogenic potential of SOX2 in breast cancer. *J Biol Chem*, *283*(26), 17969-17978. https://doi.org/10.1074/jbc.M802917200

Christine, F., James, O. J., Matthew, K., Richard, J. B. W., Andrew, D., Derek, S. C., Claire, M. C., Edward, W. R., Qi, Z., Otavia, L. C., Sarah, A. T., Tobias, J., Duncan, I. J., David, A. T., & Douglas, T. F. (2013). Targeting CXCL12 from FAP- expressing carcinoma-associated fibroblasts synergizes with anti– PD- L1 immunotherapy in pancreatic cancer. Proceedings of the National Academy of Sciences, 110(50), 20212. https://doi.org/10.1073/pnas.1320318110

Cirri, P., & Chiarugi, P. (2011). Cancer associated fibroblasts: the dark side of the coin. *Am. J. Cancer Res.*, *1*(4), 482-497.

Cooke, V. G., LeBleu, V. S., Keskin, D., Khan, Z., O'Connell, J. T., Teng, Y., Duncan, M. B., Xie, L., Maeda, G., Vong, S., Sugimoto, H., Rocha, R. M., Damascena, A., Brentani, R. R., & Kalluri, R. (2012). Pericyte depletion results in hypoxia-associated epithelial-to-mesenchymal transition and metastasis mediated by met signaling pathway. *Cancer Cell*, *21*(1), 66-81. https://doi.org/10.1016/j.ccr.2011.11.024

Costa, M., Escaleira, R., Cataldo, A., Oliveira, F., & Mermelstein, C. S. (2004). Desmin: molecular interactions and putative functions of the muscle intermediate filament protein. *Brazilian J. Med. Biol. Res.*, *37*(12), 1819-1830.

Crawford, Y., Kasman, I., Yu, L., Zhong, C., Wu, X., Modrusan, Z., Kaminker, J., & Ferrara, N. (2009). PDGF- C Mediates the Angiogenic and Tumorigenic Properties of Fibroblasts Associated with Tumors Refractory to Anti- VEGF Treatment. *Cancer Cell*, *15*(1), 21-34. https://doi.org/10.1016/j.ccr.2008.12.004

Cushing, M. C., Mariner, P. D., Liao, J.-T., Sims, E. A., & Anseth, K. S. (2008). Fibroblast growth factor represses Smad- mediated myofibroblast activation in aortic valvular interstitial cells. *FASEB journal : official publication of the Federation of American Societies for Experimental Biology*, *22*(6), 1769-1777. https://doi.org/10.1096/fj.07-087627

D'Angelo, S. P., Shoushtari, A. N., Agaram, N. P., Kuk, D., Qin, L.-X., Carvajal, R. D., Dickson, M. A., Gounder, M., Keohan, M. L., Schwartz, G. K., & Tap, W. D. (2015). Prevalence of tumor-infiltrating lymphocytes and PD-L1 expression in the soft tissue sarcoma microenvironment. *Human Pathology*, *46*(3), 357-365. https://doi.org/https://doi.org/10.1016/j.humpath.2014.11.001

De Micheli, A. J., Laurilliard, E. J., Heinke, C. L., Ravichandran, H., Fraczek, P., Soueid-Baumgarten, S., De Vlaminck, I., Elemento, O., & Cosgrove, B. D. (2020). Single-Cell Analysis of the Muscle Stem Cell Hierarchy Identifies Heterotypic Communication Signals Involved in Skeletal Muscle Regeneration. *Cell Rep*, *30*(10), 3583-3595.e3585. https://doi.org/10.1016/j.celrep.2020.02.067

De Palma, M., & Lewis, C. E. (2013). Macrophage regulation of tumor responses to anticancer therapies. *Cancer Cell*, *23*(3), 277-286. https://doi.org/10.1016/j.ccr.2013.02.013

Declerck, Y. A. (2012). Desmoplasia: a response or a niche? *Cancer discovery*, *2*(9), 772-774. https://doi.org/10.1158/2159-8290.CD-12-0348

Delgado, J., Pereira, A., Villamor, N., López-Guillermo, A., & Rozman, C. (2014). Survival analysis in hematologic malignancies: recommendations for clinicians. *Haematologica*, *99*(9), 1410-1420. https://doi.org/10.3324/haematol.2013.100784

Delise, A. M., & Tuan, R. S. (2002). Analysis of N-cadherin function in limb mesenchymal chondrogenesis in vitro. *Dev Dyn, 225*(2), 195-204. doi:10.1002/dvdy.10151

Delpire, E., & Gagnon, K. B. E. (2018). Water Homeostasis and Cell Volume Maintenance and Regulation. *Current topics in membranes*, *81*, 3-52.

Denu, R. A., Nemcek, S., Bloom, D. D., Goodrich, A. D., Kim, J., Mosher, D. F., & Hematti, P. (2016). Fibroblasts and Mesenchymal Stromal/Stem Cells Are Phenotypically Indistinguishable. *Acta Haematol*, *136*(2), 85-97. https://doi.org/10.1159/000445096

Ding, W., Knox, T. R., Tschumper, R. C., Wu, W., Schwager, S. M., Boysen, J. C., Jelinek, D. F., & Kay, N. E. (2010). Platelet-derived growth factor (PDGF)-PDGF receptor interaction activates bone marrow-derived mesenchymal stromal cells derived from chronic lymphocytic leukemia: implications for an angiogenic switch. Blood, 116(16), 2984-2993. https://doi.org/10.1182/blood-2010-02-269894

Dinh, H. Q., Pan, F., Wang, G., Huang, Q. F., Olingy, C. E., Wu, Z. Y., Wang, S. H., Xu, X., Xu, X. E., He, J. Z., Yang, Q., Orsulic, S., Haro, M., Li, L. Y., Huang, G. W., Breunig, J. J., Koeffler, H. P., Hedrick, C. C., Xu, L. Y., . . . Li, E. M. (2021). Integrated single-cell transcriptome analysis reveals heterogeneity of esophageal squamous cell carcinoma microenvironment. *Nat Commun*, *12*(1), 7335. https://doi.org/10.1038/s41467-021-27599-5

Dinu, D., Dobre, M., Panaitescu, E., Bîrlă, R., Iosif, C., Hoara, P., Caragui, A., Boeriu, M., Constantinoiu, S., & Ardeleanu, C. (2014). Prognostic significance of KRAS gene mutations in colorectal cancer-- preliminary study. *J Med Life*, *7*(4), 581-587. https://www.ncbi.nlm.nih.gov/pubmed/25713627

Dohi, O., Ohtani, H., Hatori, M., Sato, E., Hosaka, M., Nagura, H., Itoi, E., & Kokubun, S. (2009). Histogenesis- specific expression of fibroblast activation protein and dipeptidylpeptidase- IV in human bone and soft tissue tumours. *Histopathology*, *55*(4), 432-440. https://doi.org/10.1111/j.1365-2559.2009.03399.x

Dos Anjos Cassado, A. (2017). F4/80 as a Major Macrophage Marker: The Case of the Peritoneum and Spleen. *Results Probl Cell Differ*, *62*, 161-179. https://doi.org/10.1007/978-3-319-54090-0_7

Doyle, L. A. (2014). Sarcoma classification: An update based on the 2013 World Health Organization Classification of Tumors of Soft Tissue and Bone. In (Vol. 120, pp. 1763-1774).

Du, L., Li, J., Lei, L., He, H., Chen, E., Dong, J., & Yang, J. (2018). High Vimentin Expression Predicts a Poor Prognosis and Progression in Colorectal Cancer: A Study with Meta-Analysis and TCGA Database. *Biomed Res Int*, *2018*, 6387810. https://doi.org/10.1155/2018/6387810

Duffy, M. J., Synnott, N. C., & Crown, J. (2018). Mutant p53 in breast cancer: potential as a therapeutic target and biomarker. *Breast Cancer Res Treat*, *170*(2), 213-219. https://doi.org/10.1007/s10549-018-4753-7

Ehlerding, E. B., Lacognata, S., Jiang, D., Ferreira, C. A., Goel, S., Hernandez, R., Jeffery, J. J., Theuer, C. P., & Cai, W. (2018). Targeting angiogenesis for radioimmunotherapy with a. *Eur J Nucl Med Mol Imaging*, *45*(1), 123-131. https://doi.org/10.1007/s00259-017-3793-2

Ehnman, M., & Larsson, O. (2015). Microenvironmental Targets in Sarcoma. *Front Oncol*, *5*, 248. https://doi.org/10.3389/fonc.2015.00248

Elsafadi, M., Manikandan, M., Almalki, S., Mahmood, A., Shinwari, T., Vishnubalaji, R., . . . Alajez, N. M. (2020). Transgelin is a poor prognostic factor associated with advanced colorectal cancer (CRC) stage promoting tumor growth and migration in a TGFβ-dependent manner. *Cell Death Dis, 11*(5), 341. doi:10.1038/s41419-020-2529-6

English, W. R., Lunt, S. J., Fisher, M., Lefley, D. V., Dhingra, M., Lee, Y. C., Bingham, K., Hurrell, J. E., Lyons, S. K., Kanthou, C., & Tozer, G. M. (2017). Differential Expression of VEGFA Isoforms Regulates Metastasis and Response to Anti-VEGFA Therapy in Sarcoma. Cancer Res, 77(10), 2633-2646. https://doi.org/10.1158/0008-5472.CAN-16-0255

Erdogan, B., Ao, M., White, L. M., Means, A. L., Brewer, B. M., Yang, L., . . . Webb, D. J. (2017). Cancer-associated fibroblasts promote directional cancer cell migration by aligning fibronectin. J Cell Biol, 216(11), 3799-3816. doi:10.1083/jcb.201704053

Erez, N., Truitt, M., Olson, P., & Hanahan, D. (2010). Cancer- Associated Fibroblasts Are Activated in Incipient Neoplasia to Orchestrate Tumor- Promoting Inflammation in an NF- κB- Dependent Manner. Cancer Cell, 17(2), 135-147. https://doi.org/10.1016/j.ccr.2009.12.041

Fan, H., & Chu, J.-Y. (2007). A Brief Review of Short Tandem Repeat Mutation. Genomics, Proteomics & Bioinformatics, 5(1), 7-14. doi:10.1016/S1672-0229(07)60009-6

Feng, W., Chen, L., Nguyen, P. K., Wu, S. M., & Li, G. (2019). Single Cell Analysis of Endothelial Cells Identified Organ-Specific Molecular Signatures and Heart-Specific Cell Populations and Molecular Features. Front Cardiovasc Med, 6, 165. https://doi.org/10.3389/fcvm.2019.00165

Festjens, N., Vanden Berghe, T., & Vandenabeele, P. (2006). Necrosis, a well-orchestrated form of cell demise: signalling cascades, important mediators and concomitant immune response. Biochim Biophys Acta, 1757(9-10), 1371-1387. https://doi.org/10.1016/j.bbabio.2006.06.014

Fischer, M., Quaas, M., Steiner, L., & Engeland, K. (2016). The p53-p21-DREAM-CDE/CHR pathway regulates G2/M cell cycle genes. Nucleic Acids Res, 44(1), 164-174. https://doi.org/10.1093/nar/gkv927

Fisher, C. (2004). Myofibrosarcoma. *Official Journal of the European Society of Pathology*, *445*(3), 215-223. https://doi.org/10.1007/s00428-004-1038-9

Fletcher, C. D. (2014). The evolving classification of soft tissue tumours - an update based on the new 2013 WHO classification. *Histopathology*, *64*(1), 2-11. https://doi.org/10.1111/his.12267

Fogh, B. S., Multhaupt, H. A., & Couchman, J. R. (2014). Protein kinase C, focal adhesions and the regulation of cell migration. *J Histochem Cytochem*, *62*(3), 172-184. https://doi.org/10.1369/0022155413517701

Forker, L., Gaunt, P., Sioletic, S., Shenjere, P., Potter, R., Roberts, D., Irlam, J., Valentine, H., Hughes, D., Hughes, A., Billingham, L., Grimer, R., Seddon, B., Choudhury, A., Robinson, M., & West, C. M. L. (2017). The hypoxia marker CAIX is prognostic in the UK phase III VorteX-Biobank cohort: an important resource for translational research in soft tissue sarcoma.

Forsberg, E. C., Passegué, E., Prohaska, S. S., Wagers, A. J., Koeva, M., Stuart, J. M., & Weissman, I. L. (2010). Molecular signatures of quiescent, mobilized and leukemia-initiating hematopoietic stem cells. *PLoS One*, *5*(1), e8785. https://doi.org/10.1371/journal.pone.0008785

Fujimoto, N., He, Y., D'Addio, M., Tacconi, C., Detmar, M., & Dieterich, L. C. (2020). Single-cell mapping reveals new markers and functions of lymphatic endothelial cells in lymph nodes. *PLoS Biol*, *18*(4), e3000704. https://doi.org/10.1371/journal.pbio.3000704

Gazdic, M., Volarevic, V., Arsenijevic, N., & Stojkovic, M. (2015). Mesenchymal Stem Cells: A Friend or Foe in Immune- Mediated Diseases. *Stem Cell Reviews and Reports*, *11*(2), 280-287. https://doi.org/10.1007/s12015-014-9583-3

Gee, M. S., Procopio, W. N., Makonnen, S., Feldman, M. D., Yeilding, N. M., & Lee, W. M. (2003). Tumor vessel development and maturation impose limits on the effectiveness of anti-vascular therapy. *Am J Pathol*, *162*(1), 183-193. https://doi.org/10.1016/S0002-9440(10)63809-6

Genadry, K. C., Pietrobono, S., Rota, R., & Linardic, C. M. (2018). Soft Tissue Sarcoma Cancer Stem Cells: An Overview. *Frontiers in Oncology*, *8*, 475-475. https://doi.org/10.3389/fonc.2018.00475

Genin, O., Rechavi, G., Nagler, A., Ben-Itzhak, O., Nazemi, K. J., & Pines, M. (2008). Myofibroblasts in Pulmonary and Brain Metastases of Alveolar Soft- Part Sarcoma: A Novel Target for Treatment? *Neoplasia*, *10*(9), 940-948. https://doi.org/10.1593/neo.08456

Goel, M. K., Khanna, P., & Kishore, J. (2010). Understanding survival analysis: Kaplan- Meier estimate. *International journal of Ayurveda research*, *1*(4), 274-278. https://doi.org/10.4103/0974-7788.76794

Goh, P., Sze, D., & Roufogalis, B. (2007). Molecular and Cellular Regulators of Cancer Angiogenesis. *Current Cancer Drug Targets*, *7*(8), 743-758. https://doi.org/10.2174/156800907783220462

Goldman, M. J., Craft, B., Hastie, M., Repečka, K., McDade, F., Kamath, A., Banerjee, A., Luo, Y., Rogers, D., Brooks, A. N., Zhu, J., & Haussler, D. (2020). Visualizing and interpreting cancer genomics data via the Xena platform. *Nat Biotechnol*, *38*(6), 675-678. https://doi.org/10.1038/s41587-020-0546-8

Grabinski, T. M., Kneynsberg, A., Manfredsson, F. P., & Kanaan, N. M. (2015). A method for combining RNAscope in situ hybridization with immunohistochemistry in thick free-floating brain sections and primary neuronal cultures. *PLoS One*, *10*(3), e0120120. https://doi.org/10.1371/journal.pone.0120120

Grum-Schwensen, B., Klingelhofer, J., Berg, C. H., El-Naaman, C., Grigorian, M., Lukanidin, E., & Ambartsumian, N. (2005). Suppression of tumor development and metastasis formation in mice lacking the S100A4(mts1) gene. *Cancer research*, *65*(9), 3772-3780. https://doi.org/10.1158/0008-5472.CAN-04-4510

Guerrero-Juarez, C. F., Dedhia, P. H., Jin, S., Ruiz-Vega, R., Ma, D., Liu, Y., Yamaga, K., Shestova, O., Gay, D. L., Yang, Z., Kessenbrock, K., Nie, Q., Pear, W. S., Cotsarelis, G., & Plikus, M. V. (2019). Single-cell analysis reveals fibroblast heterogeneity and myeloid-derived adipocyte progenitors in murine skin wounds. *Nat Commun*, *10*(1), 650. https://doi.org/10.1038/s41467-018-08247-x

Guled, M., Pazzaglia, L., Borze, I., Mosakhani, N., Novello, C., Benassi, M. S., & Knuutila, S. (2014). Differentiating soft tissue leiomyosarcoma and undifferentiated pleomorphic sarcoma: A miRNA analysis. *Genes Chromosomes Cancer*, *53*(8), 693-702. https://doi.org/10.1002/gcc.22179

Guo, X., Jo, V., Mills, A., Zhu, S., Lee, C.-H., Espinosa, I., Nucci, M., Varma, S., Forgo, E., Hastie, T., Anderson, S., Ganjoo, K., Beck, A., West, R., Fletcher, C., & van de Rijn, M. (2015). Clinically Relevant Molecular Subtypes in Leiomyosarcoma. *Clinical Cancer Research*, *21*(15), 3501-3511. https://doi.org/10.1158/1078-0432.CCR-14-3141

Gutierrez, L. S., Schulman, A., Brito-Robinson, T., Noria, F., Ploplis, V. A., & Castellino, F. J. (2000). Tumor development is retarded in mice lacking the gene for urokinase-type plasminogen activator or its inhibitor, plasminogen activator inhibitor-1. *Cancer Res*, *60*(20), 5839-5847. https://www.ncbi.nlm.nih.gov/pubmed/11059781

Ha, S. Y., Yeo, S. Y., Xuan, Y. H., & Kim, S. H. (2014). The prognostic significance of cancer-associated fibroblasts in esophageal squamous cell carcinoma. *PLoS One*, *9*(6), e99955. https://doi.org/10.1371/journal.pone.0099955

Habif, G., Crinier, A., André, P., Vivier, E., & Narni-Mancinelli, E. (2019). Targeting natural killer cells in solid tumors. *Cellular & Molecular Immunology*, *16*(5), 415-422. https://doi.org/10.1038/s41423-019-0224-2

Han, C., Liu, T., & Yin, R. (2020). Biomarkers for cancer-associated fibroblasts. *Biomark Res*, *8*(1), 64. https://doi.org/10.1186/s40364-020-00245-w

Han, S., Khuri, F., & Roman, J. (2006). Fibronectin Stimulates Non- Small Cell Lung Carcinoma Cell Growth through Activation of Akt/ Mammalian Target of Rapamycin/ S6 Kinase and Inactivation of LKB1/ AMP- Activated Protein Kinase Signal Pathways. *Cancer research*, *66*(1), 315-323.

Hanahan, D. (2022). Hallmarks of Cancer: New Dimensions. *Cancer Discov*, *12*(1), 31-46. https://doi.org/10.1158/2159-8290.CD-21-1059

Hanahan, D., & Weinberg, Robert a. (2011). Hallmarks of Cancer: The Next Generation. *Cell*, *144*(5), 646-674. https://doi.org/10.1016/j.cell.2011.02.013

Hashimoto, H., Daimaru, Y., & Enjoji, M. (1984). S- 100 protein distribution in liposarcoma An immunoperoxidase study with special reference to the distinction of liposarcoma from myxoid malignant fibrous histiocytoma. Pathological Anatomy and Histopathology, 405(1), 1-10. https://doi.org/10.1007/BF00694921

Hazan, R. B., Qiao, R., Keren, R., Badano, I., & Suyama, K. (2004). Cadherin switch in tumor progression. *Ann N Y Acad Sci*, *1014*, 155-163. https://doi.org/10.1196/annals.1294.016

Heim-Hall, J., & Yohe, S. (2008). Application of immunohistochemistry to soft tissue neoplasms. *Arch. Pathol. Lab. Med.*, *132*(3), 476-489. https://doi.org/10.1043/1543-2165(2008)132[476:AOITST]2.0.CO;2

Herrera, M., Herrera, A., Domínguez, G., Silva, J., García, V., García, J. M., Gómez, I., Soldevilla, B., Muñoz, C., Provencio, M., Campos-Martin, Y., García de Herreros, A., Casal, I., Bonilla, F., & Peña, C. (2013). Cancer-associated fibroblast and M2 macrophage markers together predict outcome in colorectal cancer patients. *Cancer Sci*, *104*(4), 437-444. https://doi.org/10.1111/cas.12096

Hinz, B., Celetta, G., Tomasek, J. J., Gabbiani, G., & Chaponnier, C. (2001). Alpha-smooth muscle actin expression upregulates fibroblast contractile activity. *Mol Biol Cell*, *12*(9), 2730-2741. https://doi.org/10.1091/mbc.12.9.2730

Hoefkens, F., Dehandschutter, C., Somville, J., Meijnders, P., & Van Gestel, D. (2016). Soft tissue sarcoma of the extremities: pending questions on surgery and radiotherapy. *Radiat Oncol*, *11*(1), 136. https://doi.org/10.1186/s13014-016-0668-9

Homsi, J., & Daud, A. I. (2007). Spectrum of activity and mechanism of action of VEGF/PDGF inhibitors. *Cancer Control*, *14*(3), 285-294. https://doi.org/10.1177/107327480701400312

Hwang, K. T., Kim, B. H., Oh, S., Park, S. Y., Jung, J., Kim, J., Choi, I. S., Jeon, S. Y., & Kim, W. Y. (2019). Prognostic Role of. *J Breast Cancer*, *22*(4), 548-561. https://doi.org/10.4048/jbc.2019.22.e55

Isakson, M., de Blacam, C., Whelan, D., McArdle, A., & Clover, A. J. P. (2015). Mesenchymal Stem Cells and Cutaneous Wound Healing: Current Evidence and Future Potential. *Stem cells international*, *2015*(2015), 831095-831095. https://doi.org/10.1155/2015/831095

Ivaska, J., Pallari, H. M., Nevo, J., & Eriksson, J. E. (2007). Novel functions of vimentin in cell adhesion, migration, and signaling. *Exp Cell Res*, *313*(10), 2050-2062. https://doi.org/10.1016/j.yexcr.2007.03.040

Jain, S., Xu, R., Prieto, V. G., & Lee, P. (2010). Molecular classification of soft tissue sarcomas and its clinical applications. *International journal of clinical and experimental pathology*, *3*(4), 416-428.

Järveläinen, H., Sainio, A., Koulu, M., Wight, T. N., & Penttinen, R. (2009). Extracellular matrix molecules: potential targets in pharmacotherapy. *Pharmacol Rev*, *61*(2), 198-223. https://doi.org/10.1124/pr.109.001289

Jennbacken, K., Tesan, T., Wang, W., Gustavsson, H., Damber, J. E., & Welén, K. (2010). N-cadherin increases after androgen deprivation and is associated with metastasis in prostate cancer. *Endocr Relat Cancer*, *17*(2), 469-479. https://doi.org/10.1677/ERC-10-0015

Jo, V. Y., & Fletcher, C. D. M. (2014). WHO classification of soft tissue tumours: An update based on the 2013 (4th) edition. *Pathology*, *46*(2), 95-104. https://doi.org/10.1097/PAT.0000000000000050

Johanna, A. J., & Jeffrey, W. P. (2008). Microenvironmental regulation of metastasis. *Nature Reviews Cancer*, *9*(4), 239. https://doi.org/10.1038/nrc2618

Joly, J. H., Chew, B. T. L., & Graham, N. A. (2021). The landscape of metabolic pathway dependencies in cancer cell lines. *PLoS Comput Biol*, *17*(4), e1008942. https://doi.org/10.1371/journal.pcbi.1008942

Jones, R. L., Ravi, V., Brohl, A. S., Chawla, S., Ganjoo, K. N., Italiano, A., Attia, S., Burgess, M. A., Thornton, K., Cranmer, L. D., Cheang, M. C. U., Liu, L., Robertson, L., Adams, B., Theuer, C., & Maki, R. G. (2022). Efficacy and Safety of TRC105 Plus Pazopanib vs Pazopanib Alone for Treatment of Patients With Advanced Angiosarcoma: A Randomized Clinical Trial. *JAMA Oncol*, *8*(5), 740-747. https://doi.org/10.1001/jamaoncol.2021.3547

Joyce, J. A., & Pollard, J. W. (2009). Microenvironmental regulation of metastasis. *Nat Rev Cancer*, *9*(4), 239-252. https://doi.org/10.1038/nrc2618

Kalluri, R., & Zeisberg, M. (2006). Fibroblasts in cancer. *Nature Reviews Cancer*, *6*(5), 392-401. https://doi.org/10.1038/nrc1877

Kalluri, R. (2016). The biology and function of fibroblasts in cancer. *Nature reviews. Cancer*, *16*(9), 582-598. https://doi.org/10.1038/nrc.2016.73

Keung, E. Z., Burgess, M., Salazar, R., Parra, E. R., Rodrigues-Canales, J., Bolejack, V., Van Tine, B. A., Schuetze, S. M., Attia, S., Riedel, R. F., Hu, J., Okuno, S. H., Priebat, D. A., Movva, S., Davis, L. E., Reed, D. R., Reuben, A., Roland, C. L., Reinke, D., . . . Tawbi, H. A. (2020). Correlative Analyses of the SARC028 Trial Reveal an Association Between Sarcoma-Associated Immune Infiltrate and Response to Pembrolizumab. *Clin Cancer Res*, *26*(6), 1258-1266. https://doi.org/10.1158/1078-0432.CCR-19-1824

Kidd, S., Spaeth, E., Watson, K., Burks, J., Lu, H., Klopp, A., Andreeff, M., & Marini, F. (2012). Origins of the Tumor Microenvironment: Quantitative Assessment of Adipose- Derived and Bone Marrow–Derived Stroma. *PLoS One*, *7*(2), e30563. https://doi.org/10.1371/journal.pone.0030563

Kim, S. A., Cho, E. J., Lee, S., Cho, Y. Y., Kim, B., Yoon, J.-H., & Park, T. (2020). Changes in serum fibronectin levels predict tumor recurrence in patients with early hepatocellular carcinoma after curative treatment. *Scientific reports*, *10*(1), 21313. https://doi.org/10.1038/s41598-020-78440-w

Kisiel, J. B., Yab, T. C., Taylor, W. R., Chari, S. T., Petersen, G. M., Mahoney, D. W., & Ahlquist, D. A. (2012). Stool DNA testing for the detection of pancreatic cancer: assessment of methylation marker candidates. *Cancer*, *118*(10), 2623-2631. https://doi.org/10.1002/cncr.26558

Kitadai, Y., Sasaki, T., Kuwai, T., Nakamura, T., Bucana, C. D., & Fidler, I. J. (2006). Targeting the expression of platelet-derived growth factor receptor by reactive stroma inhibits growth and metastasis of human colon carcinoma. *Am J Pathol*, *169*(6), 2054-2065. https://doi.org/10.2353/ajpath.2006.060653

Kluin, R. J. C., Kemper, K., Kuilman, T., de Ruiter, J. R., Iyer, V., Forment, J. V., Cornelissen-Steijger, P., de Rink, I., Ter Brugge, P., Song, J. Y., Klarenbeek, S., McDermott, U., Jonkers, J., Velds, A., Adams, D. J., Peeper, D. S., & Krijgsman, O. (2018). XenofilteR: computational deconvolution of mouse and human reads in tumor xenograft sequence data. *BMC Bioinformatics*, *19*(1), 366. https://doi.org/10.1186/s12859-018-2353-5

Kocatürk, B., & Versteeg, H. H. (2015). Orthotopic injection of breast cancer cells into the mammary fat pad of mice to study tumor growth. *J Vis Exp*(96). https://doi.org/10.3791/51967

Koga, K., Nabeshima, K., Aoki, M., Kawakami, T., Hamasaki, M., Toole, B. P., Nakayama, J., & Iwasaki, H. (2007). Emmprin in epithelioid sarcoma: Expression in tumor cell membrane and stimulation of MMP- 2 production in tumor- associated fibroblasts. International Journal of Cancer, 120(4), 761-768. https://doi.org/10.1002/ijc.22412

Koh, Y. E., Choi, E. H., Kim, J. W., & Kim, K. P. (2022). The Kleisin Subunits of Cohesin are Involved in the Fate Determination of Embryonic Stem Cells. *Mol Cells*. https://doi.org/10.14348/molcells.2022.2042

Kojima, Y., Acar, A., Eaton, E. N., Mellody, K. T., Scheel, C., Ben-Porath, I., Onder, T. T., Wang, Z. C., Richardson, A. L., Weinberg, R. A., & Orimo, A. (2010). Autocrine TGF-beta and stromal cell-derived factor-1 (SDF-1) signaling drives the evolution of tumor-promoting mammary stromal

myofibroblasts. *Proc Natl Acad Sci U S A*, *107*(46), 20009-20014. https://doi.org/10.1073/pnas.1013805107

Krieg, T. (2008). Fibroblast – matrix interactions in tissue repair and fibrosis. *Experimental Dermatology*, *17*(10), 877-879. https://doi.org/10.1111/j.1600-0625.2008.00789_3.x

Krizbai, I. A., Gasparics, Á., Nagyőszi, P., Fazakas, C., Molnár, J., Wilhelm, I., Bencs, R., Rosivall, L., & Sebe, A. (2015). Endothelial-mesenchymal transition of brain endothelial cells: possible role during metastatic extravasation. *PLoS One*, *10*(3), e0119655. https://doi.org/10.1371/journal.pone.0119655

Kujawa, K. A., Zembala-Nożyńska, E., Cortez, A. J., Kujawa, T., Kupryjańczyk, J., & Lisowska, K. M. (2020). Fibronectin and Periostin as Prognostic Markers in Ovarian Cancer. *Cells*, *9*(1). https://doi.org/10.3390/cells9010149

Kuperwasser, C., Chavarria, T., Wu, M., Magrane, G., Gray, J. W., Carey, L., Richardson, A., & Weinberg, R. A. (2004). Reconstruction of functionally normal and malignant human breast tissues in mice. *Proc Natl Acad Sci U S A*, *101*(14), 4966-4971. https://doi.org/10.1073/pnas.0401064101

Kuzmich, N. N., Sivak, K. V., Chubarev, V. N., Porozov, Y. B., Savateeva-Lyubimova, T. N., & Peri, F. (2017). TLR4 Signaling Pathway Modulators as Potential Therapeutics in Inflammation and Sepsis. *Vaccines (Basel)*, *5*(4). https://doi.org/10.3390/vaccines5040034

Lagacé, R., Schürch, W., & Seemayer, T. A. (1980). Myofibroblasts in soft tissue sarcomas. *Virchows Archiv A Pathological Anatomy and Histology*, *389*(1), 1-11. https://doi.org/10.1007/BF00428664

Lai, D., Ma, L., & Wang, F. (2012). Fibroblast activation protein regulates tumor- associated fibroblasts and epithelial ovarian cancer cells. *International Journal of Oncology*, *41*(2), 541-550. https://doi.org/10.3892/ijo.2012.1475

Langmead, B., & Salzberg, S. L. (2012). Fast gapped-read alignment with Bowtie 2. *Nat Methods*, *9*(4), 357-359. https://doi.org/10.1038/nmeth.1923

Lee, M. Y., Park, C., Berent, R. M., Park, P. J., Fuchs, R., Syn, H., Chin, A., Townsend, J., Benson, C. C., Redelman, D., Shen, T. W., Park, J. K., Miano, J. M., Sanders, K. M., & Ro, S. (2015). Smooth Muscle Cell Genome Browser: Enabling the Identification of Novel Serum Response Factor Target Genes. *PLoS One*, *10*(8), e0133751. https://doi.org/10.1371/journal.pone.0133751

Lei, X., Lei, Y., Li, J. K., Du, W. X., Li, R. G., Yang, J., Li, J., Li, F., & Tan, H. B. (2020). Immune cells within the tumor microenvironment: Biological functions and roles in cancer immunotherapy. Cancer Lett, 470, 126-133. https://doi.org/10.1016/j.canlet.2019.11.009

Li, H., Fan, X., & Houghton, J. (2007). Tumor microenvironment: The role of the tumor stroma in cancer. *Journal of Cellular Biochemistry*, *101*(4), 805-815. https://doi.org/10.1002/jcb.21159

Li, H., Handsaker, B., Wysoker, A., Fennell, T., Ruan, J., Homer, N., Marth, G., Abecasis, G., Durbin, R., & Subgroup, G. P. D. P. (2009). The Sequence Alignment/Map format and SAMtools. *Bioinformatics*, *25*(16), 2078-2079. https://doi.org/10.1093/bioinformatics/btp352

Li, Z., Li, Y., Liu, S., & Qin, Z. (2020). Extracellular S100A4 as a key player in fibrotic diseases. *J Cell Mol Med*, *24*(11), 5973-5983. https://doi.org/10.1111/jcmm.15259

Li, Z. H., Dulyaninova, N. G., House, R. P., Almo, S. C., & Bresnick, A. R. (2010). S100A4 regulates macrophage chemotaxis. *Mol Biol Cell*, *21*(15), 2598-2610. https://doi.org/10.1091/mbc.e09-07-0609

Liberzon, A., Birger, C., Thorvaldsdóttir, H., Ghandi, M., Mesirov, J. P., & Tamayo, P. (2015). The Molecular Signatures Database (MSigDB) hallmark gene set collection. *Cell Syst*, *1*(6), 417-425. https://doi.org/10.1016/j.cels.2015.12.004

Libura, J., Drukala, J., Majka, M., Tomescu, O., Navenot, J. M., Kucia, M., Marquez, L., Peiper, S. C., Barr, F. G., Janowska-Wieczorek, A., & Ratajczak, M. Z. (2002). CXCR4- SDF- 1 signaling is active in

rhabdomyosarcoma cells and regulates locomotion, chemotaxis, and adhesion. *Blood*, *100*(7), 2597-2606. https://doi.org/10.1182/blood-2002-01-0031

Liska, D., Xiang, S., Karagkounis, G., Signs, S., Kalady, M., & Huang, E. (2017). 1020 - Cancer Associated Fibroblasts Mediate Resistance to Radiotherapy in Rectal Cancer Cells. *Gastroenterology*, *152*(5), S1234-S1234. https://doi.org/10.1016/S0016-5085(17)34109-4

Liu, R., Hossain, M. M., & Jin, J. P. (2017). The Expression and Degradation of SM22- Alpha/ Transgelin are Regulated by Mechanical Tension in the Cytoskeleton. *Biophysical Journal*, *112*(3), 435a-435a. https://doi.org/10.1016/j.bpj.2016.11.2325

Liu, X., Jakubowski, M., & Hunt, J. L. (2011). KRAS gene mutation in colorectal cancer is correlated with increased proliferation and spontaneous apoptosis. *Am J Clin Pathol*, *135*(2), 245-252. https://doi.org/10.1309/AJCP7FO2VAXIVSTP

Loeffler, M., Krüger, J. A., Niethammer, A. G., & Reisfeld, R. A. (2006). Targeting tumor- associated fibroblasts improves cancer chemotherapy by increasing intratumoral drug uptake. *The Journal of clinical investigation*, *116*(7), 1955-1962. https://doi.org/10.1172/JCI26532

Lowy, C. M., & Oskarsson, T. (2015). Tenascin C in metastasis: A view from the invasive front. *Cell Adh Migr*, *9*(1-2), 112-124. https://doi.org/10.1080/19336918.2015.1008331

Lu, P., Weaver, V. M., & Werb, Z. (2012). The extracellular matrix: a dynamic niche in cancer progression. *The Journal of cell biology*, *196*(4), 395-406. https://doi.org/10.1083/jcb.201102147

Lugano, R., Ramachandran, M., & Dimberg, A. (2020). Tumor angiogenesis: causes, consequences, challenges and opportunities. *Cell Mol Life Sci*, *77*(9), 1745-1770. https://doi.org/10.1007/s00018-019-03351-7

Maehira, H., Miyake, T., Iida, H., Tokuda, A., Mori, H., Yasukawa, D., Mukaisho, K.-i., Shimizu, T., & Tani, M. (2019). Vimentin Expression in Tumor Microenvironment Predicts Survival in Pancreatic Ductal Adenocarcinoma: Heterogeneity in Fibroblast Population. *Annals of Surgical Oncology*, *26*(13), 4791-4804. https://doi.org/10.1245/s10434-019-07891-x

Mahmood, T., & Yang, P.-C. (2012). Western blot: technique, theory, and trouble shooting. *North American journal of medical sciences*, *4*(9), 429-434. https://doi.org/10.4103/1947-2714.100998

Marion, N. W., & Mao, J. J. (2006). Mesenchymal Stem Cells and Tissue Engineering. *Methods in Enzymology*, *420*, 339-361. https://doi.org/10.1016/S0076-6879(06)20016-8

Marsh, D., Suchak, K., Moutasim, K. A., Vallath, S., Hopper, C., Jerjes, W., Upile, T., Kalavrezos, N., Violette, S. M., Weinreb, P. H., Chester, K. A., Chana, J. S., Marshall, J. F., Hart, I. R., Hackshaw, A. K., Piper, K., & Thomas, G. J. (2011). Stromal features are predictive of disease mortality in oral cancer patients. *J Pathol*, *223*(4), 470-481. https://doi.org/10.1002/path.2830

Matushansky, I., Charytonowicz, E., Mills, J., Siddiqi, S., Hricik, T., & Cordon-Cardo, C. (2009). MFH classification: differentiating undifferentiated pleomorphic sarcoma in the 21st Century. *Expert Rev Anticancer Ther*, *9*(8), 1135-1144. https://doi.org/10.1586/era.09.76

Matsuyama, M., Tanaka, H., Inoko, A., Goto, H., Yonemura, S., Kobori, K., Hayashi, Y., Kondo, E., Itohara, S., Izawa, I., & Inagaki, M. (2013). Defect of mitotic vimentin phosphorylation causes microophthalmia and cataract via aneuploidy and senescence in lens epithelial cells. *J Biol Chem*, *288*(50), 35626-35635. https://doi.org/10.1074/jbc.M113.514737

Mendez, M. G., Kojima, S.-I., & Goldman, R. D. (2010). Vimentin induces changes in cell shape, motility, and adhesion during the epithelial to mesenchymal transition. *FASEB journal : official publication of the Federation of American Societies for Experimental Biology*, *24*(6), 1838-1851. https://doi.org/10.1096/fj.09-151639

Menendez, S. T., Rey, V., Martinez-Cruzado, L., Gonzalez, M. V., Morales-Molina, A., Santos, L., Blanco, V., Alvarez, C., Estupiñan, O., Allonca, E., Rodrigo, J. P., García-Castro, J., Garcia-Pedrero, J. M., & Rodriguez, R. (2020). SOX2 Expression and Transcriptional Activity Identifies a Subpopulation of

Cancer Stem Cells in Sarcoma with Prognostic Implications. *Cancers (Basel)*, *12*(4). https://doi.org/10.3390/cancers12040964

Mhawech, P., Dulguerov, P., Assaly, M., Ares, C., & Allal, A. S. (2005). EB-D fibronectin expression in squamous cell carcinoma of the head and neck. *Oral Oncol*, *41*(1), 82-88. https://doi.org/10.1016/j.oraloncology.2004.07.003

Midwood, K. S., & Orend, G. (2009). The role of tenascin-C in tissue injury and tumorigenesis. *J Cell Commun Signal*, *3*(3-4), 287-310. https://doi.org/10.1007/s12079-009-0075-1

Miller, M. S., & Miller, L. D. (2011). RAS Mutations and Oncogenesis: Not all RAS Mutations are Created Equally. *Front Genet*, *2*, 100. https://doi.org/10.3389/fgene.2011.00100

Miyazaki, Y., Oda, T., Mori, N., & Kida, Y. S. (2020). Adipose-derived mesenchymal stem cells differentiate into pancreatic cancer-associated fibroblasts in vitro. *FEBS Open Bio*, *10*(11), 2268-2281. https://doi.org/https://doi.org/10.1002/2211-5463.12976

Monika, E., & Olle, E. (2015). Microenvironmental targets in sarcoma. *Frontiers in Oncology*, *5*. https://doi.org/10.3389/fonc.2015.00248

Mrozik, K. M., Blaschuk, O. W., Cheong, C. M., Zannettino, A. C. W., & Vandyke, K. (2018). N-cadherin in cancer metastasis, its emerging role in haematological malignancies and potential as a therapeutic target in cancer. *BMC Cancer*, *18*(1), 939. https://doi.org/10.1186/s12885-018-4845-0

Morozov, A., Downey, R. J., Healey, J., Moreira, A. L., Lou, E., Franceschino, A., Dogan, Y., Leung, R., Edgar, M., Laquaglia, M., Maki, R. G., & Moore, M. A. S. (2010). Benign mesenchymal stromal cells in human sarcomas. *Clinical cancer research : an official journal of the American Association for Cancer Research*, *16*(23), 5630-5640. https://doi.org/10.1158/1078-0432.CCR-09-2886

Muchlińska, A., Nagel, A., Popęda, M., Szade, J., Niemira, M., Zieliński, J., Skokowski, J., Bednarz-Knoll, N., & Żaczek, A. J. (2022). Alpha-smooth muscle actin-positive cancer-associated fibroblasts secreting osteopontin promote growth of luminal breast cancer. *Cell Mol Biol Lett*, *27*(1), 45. https://doi.org/10.1186/s11658-022-00351-7

Muliaditan, T., Caron, J., Okesola, M., Opzoomer, J. W., Kosti, P., Georgouli, M., Gordon, P., Lall, S., Kuzeva, D. M., Pedro, L., Shields, J. D., Gillett, C. E., Diebold, S. S., Sanz-Moreno, V., Ng, T., Hoste, E., & Arnold, J. N. (2018). Macrophages are exploited from an innate wound healing response to facilitate cancer metastasis. *Nat Commun*, *9*(1), 2951. https://doi.org/10.1038/s41467-018-05346-7

Nieminen, M., Henttinen, T., Merinen, M., Marttila-Ichihara, F., Eriksson, J. E., & Jalkanen, S. (2006). Vimentin function in lymphocyte adhesion and transcellular migration. *Nat Cell Biol*, *8*(2), 156-162. https://doi.org/10.1038/ncb1355

Nims, R., Sykes, G., Cottrill, K., Ikonomi, P., & Elmore, E. (2010). Short tandem repeat profiling: part of an overall strategy for reducing the frequency of cell misidentification. *In Vitro Cellular & Developmental Biology - Animal*, *46*(10), 811-819. https://doi.org/10.1007/s11626-010-9352-9

Nishitani, Y., Iwano, M., Yamaguchi, Y., Harada, K., Nakatani, K., Akai, Y., Nishino, T., Shiiki, H., Kanauchi, M., Saito, Y., & Neilson, E. G. (2005). Fibroblast-specific protein 1 is a specific prognostic marker for renal survival in patients with IgAN. *Kidney Int*, *68*(3), 1078-1085. https://doi.org/10.1111/j.1523-1755.2005.00500.x

Noma, K., Smalley, K. S. M., Lioni, M., Naomoto, Y., Tanaka, N., El–Deiry, W., King, A. J., Nakagawa, H., & Herlyn, M. (2008). The Essential Role of Fibroblasts in Esophageal Squamous Cell Carcinoma–Induced Angiogenesis. *Gastroenterology*, *134*(7), 1981-1993. https://doi.org/10.1053/j.gastro.2008.02.061

Natarajan, V., Ha, S., Delgado, A., Jacobson, R., Alhalhooly, L., Choi, Y., & Kim, J. (2022). Acquired αSMA Expression in Pericytes Coincides with Aberrant Vascular Structure and Function in Pancreatic Ductal Adenocarcinoma. *Cancers (Basel)*, *14*(10). https://doi.org/10.3390/cancers14102448

Nurmik, M., Ullmann, P., Rodriguez, F., Haan, S., & Letellier, E. (2020). In search of definitions: Cancer-associated fibroblasts and their markers. *Int J Cancer*, *146*(4), 895-905. https://doi.org/10.1002/ijc.32193

Oakley, B. R., Paolillo, V., & Zheng, Y. (2015). γ-Tubulin complexes in microtubule nucleation and beyond. *Mol Biol Cell*, *26*(17), 2957-2962. https://doi.org/10.1091/mbc.E14-11-1514

Orimo, A., Gupta, P. B., Sgroi, D. C., Arenzana-Seisdedos, F., Delaunay, T., Naeem, R., Carey, V. J., Richardson, A. L., & Weinberg, R. A. (2005). Stromal fibroblasts present in invasive human breast carcinomas promote tumor growth and angiogenesis through elevated SDF-1/CXCL12 secretion. *Cell*, *121*(3), 335-348. https://doi.org/10.1016/j.cell.2005.02.034

Orth, M. F., Buecklein, V. L., Kampmann, E., Subklewe, M., Noessner, E., Cidre-Aranaz, F., Romero-Pérez, L., Wehweck, F. S., Lindner, L., Issels, R., Kirchner, T., Altendorf-Hofmann, A., Grünewald, T. G. P., & Knösel, T. (2020). A comparative view on the expression patterns of PD-L1 and PD-1 in soft tissue sarcomas. *Cancer Immunology, Immunotherapy*, *69*(7), 1353-1362. https://doi.org/10.1007/s00262-020-02552-5

Österreicher, C. H., Penz-Österreicher, M., Grivennikov, S. I., Guma, M., Koltsova, E. K., Datz, C., Sasik, R., Hardiman, G., Karin, M., & Brenner, D. A. (2011). Fibroblast-specific protein 1 identifies an inflammatory subpopulation of macrophages in the liver. *Proc Natl Acad Sci U S A*, *108*(1), 308-313. https://doi.org/10.1073/pnas.1017547108

Paciorek, T., Sauer, M., Balla, J., Wiśniewska, J., & Friml, J. (2006). Immunocytochemical technique for protein localization in sections of plant tissues. *Nat Protoc*, *1*(1), 104-107. https://doi.org/10.1038/nprot.2006.16

Painter, J. T., Clayton, N. P., & Herbert, R. A. (2010). Useful Immunohistochemical Markers of Tumor Differentiation. *Toxicologic Pathology*, *38*(1), 131-141. https://doi.org/10.1177/0192623309356449

Pankova, V., Thway, K., Jones, R. L., & Huang, P. H. (2021). The Extracellular Matrix in Soft Tissue Sarcomas: Pathobiology and Cellular Signalling. *Front Cell Dev Biol*, *9*, 763640. https://doi.org/10.3389/fcell.2021.763640

Paraiso, K. H. T., & Smalley, K. S. M. (2013). Fibroblast- mediated drug resistance in cancer. *Biochemical Pharmacology*, *85*(8), 1033-1041. https://doi.org/10.1016/j.bcp.2013.01.018

Park, S. B., Seo, K. W., So, A. Y., Seo, M. S., Yu, K. R., Kang, S. K., & Kang, K. S. (2012). SOX2 has a crucial role in the lineage determination and proliferation of mesenchymal stem cells through Dickkopf-1 and c-MYC. *Cell Death Differ*, *19*(3), 534-545. https://doi.org/10.1038/cdd.2011.137

Pickup, M. W., Mouw, J. K., & Weaver, V. M. (2014). The extracellular matrix modulates the hallmarks of cancer. In (Vol. 15, pp. 1243-1253).

Piersma, B., Hayward, M. K., & Weaver, V. M. (2020). Fibrosis and cancer: A strained relationship. *Biochim Biophys Acta Rev Cancer*, *1873*(2), 188356. https://doi.org/10.1016/j.bbcan.2020.188356

Potenta, S., Zeisberg, E., & Kalluri, R. (2008). The role of endothelial-to- mesenchymal transition in cancer progression. *British journal of cancer*, *99*(9), 1375-1379. https://doi.org/10.1038/sj.bjc.6604662

Povýšil, C., Tomanova, R., & Matějovsky, Z. (1997). Muscle- specific actin expression in chondroblastomas. *Human Pathology*, *28*(3), 316-320. https://doi.org/10.1016/S0046-8177(97)90130-1

Puré, E., & Blomberg, R. (2018). Pro-tumorigenic roles of fibroblast activation protein in cancer: back to the basics. *Oncogene*, *37*(32), 4343-4357. https://doi.org/10.1038/s41388-018-0275-3

Quante, M., Tu, S. P., Tomita, H., Gonda, T., Wang, S. S. W., Takashi, S., Baik, G. H., Shibata, W., Diprete, B., Betz, K. S., Friedman, R., Varro, A., Tycko, B., & Wang, T. C. (2011). Bone Marrow- Derived

Myofibroblasts Contribute to the Mesenchymal Stem Cell Niche and Promote Tumor Growth. *Cancer Cell*, *19*(2), 257-272. https://doi.org/10.1016/j.ccr.2011.01.020

Raitz, R., Martins, M. D., & Araújo, V. C. (2003). A study of the extracellular matrix in salivary gland tumors. *J Oral Pathol Med*, *32*(5), 290-296. https://doi.org/10.1034/j.1600-0714.2003.00019.x

Rastegar, F., Shenaq, D., Huang, J., Zhang, W., Zhang, B.-Q., He, B.-C., Chen, L., Zuo, G.-W., Luo, Q., Shi, Q., Wagner, E. R., Huang, E., Gao, Y., Gao, J.-L., Kim, S. H., Zhou, J.-Z., Bi, Y., Su, Y., Zhu, G., . . . He, T.-C. (2010). Mesenchymal stem cells: Molecular characteristics and clinical applications. *World journal of stem cells*, *2*(4), 67-80. https://doi.org/10.4252/wjsc.v2.i4.67

Reardon, D. A., Akabani, G., Coleman, R. E., Friedman, A. H., Friedman, H. S., II, J. E. H., McLendon, R. E., Pegram, C. N., Provenzale, J. M., Quinn, J. A., Rich, J. N., Vredenburgh, J. J., Desjardins, A., Guruangan, S., Badruddoja, M., Dowell, J. M., Wong, T. Z., Zhao, X.-G., Zalutsky, M. R., & Bigner, D. D. (2006). Salvage Radioimmunotherapy With Murine Iodine-131–Labeled Antitenascin Monoclonal Antibody 81C6 for Patients With Recurrent Primary and Metastatic Malignant Brain Tumors: Phase II Study Results. *Journal of Clinical Oncology*, *24*(1), 115-122. https://doi.org/10.1200/jco.2005.03.4082

Ribatti, D., Mangialardi, G., & Vacca, A. (2006). Stephen Paget and the ' seed and soil' theory of metastatic dissemination. *Clinical and Experimental Medicine*, *6*(4), 145-149. https://doi.org/10.1007/s10238-006-0117-4

Ribeiro, A. L., & Okamoto, O. K. (2015). Combined effects of pericytes in the tumor microenvironment. Stem Cells Int, 2015, 868475. https://doi.org/10.1155/2015/868475

Ridge, S. M., Sullivan, F. J., & Glynn, S. A. (2017). Mesenchymal stem cells: key players in cancer progression. Molecular cancer, 16(1), 31-31. https://doi.org/10.1186/s12943-017-0597-8

Robin, Y. M., Penel, N., Pérot, G., Neuville, A., Vélasco, V., Ranchère-Vince, D., Terrier, P., & Coindre, J. M. (2013). Transgelin is a novel marker of smooth muscle differentiation that improves diagnostic accuracy of leiomyosarcomas: a comparative immunohistochemical reappraisal of myogenic markers in 900 soft tissue tumors. Mod Pathol, 26(4), 502-510. https://doi.org/10.1038/modpathol.2012.192

Robles-Tenorio, A., & Solis-Ledesma, G. (2022). Undifferentiated Pleomorphic Sarcoma. In StatPearls. StatPearls Publishing Copyright © 2022, StatPearls Publishing LLC.

Ruiz-Zapata, A. M., Heinz, A., Kerkhof, M. H., van de Westerlo-van Rijt, C., Schmelzer, C. E. H., Stoop, R., Kluivers, K. B., & Oosterwijk, E. (2020). Extracellular Matrix Stiffness and Composition Regulate the Myofibroblast Differentiation of Vaginal Fibroblasts. Int J Mol Sci, 21(13). https://doi.org/10.3390/ijms21134762

Rusch, M., Nakitandwe, J., Shurtleff, S., Newman, S., Zhang, Z., Edmonson, M. N., Parker, M., Jiao, Y., Ma, X., Liu, Y., Gu, J., Walsh, M. F., Becksfort, J., Thrasher, A., Li, Y., McMurry, J., Hedlund, E., Patel, A., Easton, J., . . . Zhang, J. (2018). Clinical cancer genomic profiling by three-platform sequencing of whole genome, whole exome and transcriptome. Nature Communications, 9(1), 3962. https://doi.org/10.1038/s41467-018-06485-7

Saggioro, M., D'Angelo, E., Bisogno, G., Agostini, M., & Pozzobon, M. (2020). Carcinoma and Sarcoma Microenvironment at a Glance: Where We Are. Front Oncol, 10, 76. https://doi.org/10.3389/fonc.2020.00076

Sahai, E., Astsaturov, I., Cukierman, E., DeNardo, D. G., Egeblad, M., Evans, R. M., Fearon, D., Greten, F. R., Hingorani, S. R., Hunter, T., Hynes, R. O., Jain, R. K., Janowitz, T., Jorgensen, C., Kimmelman, A. C., Kolonin, M. G., Maki, R. G., Powers, R. S., Puré, E., . . . Werb, Z. (2020). A framework for advancing our understanding of cancer-associated fibroblasts. *Nat Rev Cancer*, *20*(3), 174-186. https://doi.org/10.1038/s41568-019-0238-1

Saito, K., Kobayashi, E., Yoshida, A., Araki, Y., Kubota, D., Tanzawa, Y., Kawai, A., Yanagawa, T., Takagishi, K., & Chuman, H. (2017). Angiomatoid fibrous histiocytoma: a series of seven cases including

genetically confirmed aggressive cases and a literature review. BMC Musculoskelet Disord, 18(1), 31. https://doi.org/10.1186/s12891-017-1390-y

Salawu, A., Fernando, M., Hughes, D., Reed, M. W. R., Woll, P., Greaves, C., Day, C., Alhajimohammed, M., & Sisley, K. (2016). Establishment and molecular characterisation of seven novel soft-tissue sarcoma cell lines. *British journal of cancer*, *115*(9), 1058-1068. https://doi.org/10.1038/bjc.2016.259

Salawu, A., Wright, K., Al-Kathiri, A., Wyld, L., Reed, M., & Sisley, K. (2018). Sister Chromatid Exchange and Genomic Instability in Soft Tissue Sarcomas: Potential Implications for Response to DNA-Damaging Treatments. *Sarcoma*, *2018*, 3082526. https://doi.org/10.1155/2018/3082526

Salerno, M., Avnet, S., Bonuccelli, G., Eramo, A., De Maria, R., Gambarotti, M., Gamberi, G., & Baldini, N. (2013). Sphere- forming cell subsets with cancer stem cell properties in human musculoskeletal sarcomas. *International Journal of Oncology*, *43*(1), 95-102. https://doi.org/10.3892/ijo.2013.1927

Salvatore, V., Focaroli, S., Teti, G., Mazzotti, A., & Falconi, M. (2015). Changes in the gene expression of co- cultured human fibroblast cells and osteosarcoma cells: the role of microenvironment. Oncotarget, 6(30), 28988-28998. https://doi.org/10.18632/oncotarget.4902

Salvatore, V., Teti, G., Bolzani, S., Focaroli, S., Durante, S., Mazzotti, M., & Falconi, M. (2014). Simulating tumor microenvironment: changes in protein expression in an in vitro co- culture system. *Cancer Cell International*, *14*(1). https://doi.org/10.1186/1475-2867-14-40

Sannino, G., Marchetto, A., Ranft, A., Jabar, S., Zacherl, C., Alba-Rubio, R., Stein, S., Wehweck, F. S., Kiran, M. M., Hölting, T. L. B., Musa, J., Romero-Pérez, L., Cidre-Aranaz, F., Knott, M. M. L., Li, J., Jürgens, H., Sastre, A., Alonso, J., Da Silveira, W., . . . Grünewald, T. G. P. (2019). Gene expression and immunohistochemical analyses identify SOX2 as major risk factor for overall survival and relapse in Ewing sarcoma patients. *EBioMedicine*, *47*, 156-162. https://doi.org/10.1016/j.ebiom.2019.08.002

Satelli, A., & Li, S. (2011). Vimentin in cancer and its potential as a molecular target for cancer therapy. Cellular and Molecular Life Sciences, 68(18), 3033-3046. https://doi.org/10.1007/s00018-011-0735-1

Savvidou, O., Papakonstantinou, O., Lakiotaki, E., Zafeiris, I., Melissaridou, D., Korkolopoulou, P., & Papagelopoulos, P. J. (2021). Surface bone sarcomas: an update on current clinicopathological diagnosis and treatment. *EFORT Open Rev*, *6*(10), 905-917. https://doi.org/10.1302/2058-5241.6.210064

Sbaraglia, M., Bellan, E., & Dei Tos, A. P. (2021). The 2020 WHO Classification of Soft Tissue Tumours: news and perspectives. *Pathologica*, *113*(2), 70-84. https://doi.org/10.32074/1591-951X-213

Schaefer, T., & Lengerke, C. (2020). SOX2 protein biochemistry in stemness, reprogramming, and cancer: the PI3K/AKT/SOX2 axis and beyond. *Oncogene*, *39*(2), 278-292. https://doi.org/10.1038/s41388-019-0997-x

Scully, R., Panday, A., Elango, R., & Willis, N. A. (2019). DNA double-strand break repair-pathway choice in somatic mammalian cells. *Nat Rev Mol Cell Biol*, *20*(11), 698-714. https://doi.org/10.1038/s41580-019-0152-0

Schürch, W., Skalli, O., Seemayer, T. A., & Gabbiani, G. (1987). Intermediate filament proteins and actin isoforms as markers for soft tissue tumor differentiation and origin. I. Smooth muscle tumors. The American journal of pathology, 128(1), 91-103.

Scott. (2003). A phase I dose-escalastion study of sibrtuzumab in patients with advanced or metastatic fibroblast activation protein-positive cancer. *Clin Cancer Res*, 1639-1647.

Shaulian, E., & Karin, M. (2001). AP-1 in cell proliferation and survival. *Oncogene*, *20*(19), 2390-2400. https://doi.org/10.1038/sj.onc.1204383

Shen, Q., Uray, I. P., Li, Y., Krisko, T. I., Strecker, T. E., Kim, H. T., & Brown, P. H. (2008). The AP-1 transcription factor regulates breast cancer cell growth via cyclins and E2F factors. *Oncogene*, *27*(3), 366-377. https://doi.org/10.1038/sj.onc.1210643

Shen, Z., Qin, X., Yan, M., Li, R., Chen, G., Zhang, J., & Chen, W. (2017). Cancer- associated fibroblasts promote cancer cell growth through a miR- 7- RASSF2- PAR- 4 axis in the tumor microenvironment. *Oncotarget*, *8*(1), 1290-1303. https://doi.org/10.18632/oncotarget.13609

Shi, J., Li, Y., Jia, R., & Fan, X. (2020). The fidelity of cancer cells in PDX models: Characteristics, mechanism and clinical significance. Int J Cancer, 146(8), 2078-2088. https://doi.org/10.1002/ijc.32662

Shi, J., Hou, Z., Yan, J., Qiu, W., Liang, L., Meng, M., Li, L., Wang, X., Xie, Y., Jiang, L., & Wang, W. (2020). The prognostic significance of fibroblast activation protein-α in human lung adenocarcinoma. *Annals of Translational Medicine*, *8*(5), 224. https://atm.amegroups.com/article/view/37401

Shiga, K., Hara, M., Nagasaki, T., Sato, T., Takahashi, H., & Takeyama, H. (2015). Cancer- Associated Fibroblasts: Their Characteristics and Their Roles in Tumor Growth. *Cancers*, *7*(4), 2443-2458. https://doi.org/10.3390/cancers7040902

Sholl, L. M., Long, K. B., & Hornick, J. L. (2010). Sox2 expression in pulmonary non-small cell and neuroendocrine carcinomas. *Appl Immunohistochem Mol Morphol*, *18*(1), 55-61. https://doi.org/10.1097/PAI.0b013e3181b16b88

Sie, M., de Bont, E. S., Scherpen, F. J., Hoving, E. W., & den Dunnen, W. F. (2010). Tumour vasculature and angiogenic profile of paediatric pilocytic astrocytoma; is it much different from glioblastoma? *Neuropathol Appl Neurobiol*, *36*(7), 636-647. https://doi.org/10.1111/j.1365-2990.2010.01113.x

Simian, M., Hirai, Y., Navre, M., Werb, Z., Lochter, A., & Bissell, M. J. (2001). The interplay of matrix metalloproteinases, morphogens and growth factors is necessary for branching of mammary epithelial cells. Development (Cambridge, England), 128(16), 3117-3131.

Sinn, M., Denkert, C., Striefler, J. K., Pelzer, U., Stieler, J. M., Bahra, M., Lohneis, P., Dörken, B., Oettle, H., Riess, H., & Sinn, B. V. (2014). α-Smooth muscle actin expression and desmoplastic stromal reaction in pancreatic cancer: results from the CONKO-001 study. *Br J Cancer*, *111*(10), 1917-1923. https://doi.org/10.1038/bjc.2014.495

Skoda, J., Nunukova, A., Loja, T., Zambo, I., Neradil, J., Mudry, P., Zitterbart, K., Hermanova, M., Hampl, A., Sterba, J., & Veselska, R. (2016). Cancer stem cell markers in pediatric sarcomas: Sox2 is associated with tumorigenicity in immunodeficient mice. Tumour Biol, 37(7), 9535-9548. https://doi.org/10.1007/s13277-016-4837-0

Snel, B., Lehmann, G., Bork, P., & Huynen, M. A. (2000). STRING: a web-server to retrieve and display the repeatedly occurring neighbourhood of a gene. Nucleic Acids Res, 28(18), 3442-3444. https://doi.org/10.1093/nar/28.18.3442

Song, S., Ewald, A. J., Stallcup, W., Werb, Z., & Bergers, G. (2005). PDGFRbeta+ perivascular progenitor cells in tumours regulate pericyte differentiation and vascular survival. *Nat Cell Biol*, *7*(9), 870-879. https://doi.org/10.1038/ncb1288

Spaeth, E., Dembinski, J., Sasser, A., Watson, K., Klopp, A., Hall, B., Andreeff, M., & Marini, F. (2009). Mesenchymal Stem Cell Transition to Tumor- Associated Fibroblasts Contributes to Fibrovascular Network Expansion and Tumor Progression. *PLoS One*, *4*(4), e4992. https://doi.org/10.1371/journal.pone.0004992

Stahl, D., Gentles, A. J., Thiele, R., & Gütgemann, I. (2019). Prognostic profiling of the immune cell microenvironment in Ewing´s Sarcoma Family of Tumors. *Oncoimmunology*, *8*(12), e1674113. https://doi.org/10.1080/2162402X.2019.1674113

Strahm, B., Durbin, A., Sexsmith, E., & Malkin, D. (2008). The CXCR4-SDF1α axis is a critical mediator of rhabdomyosarcoma metastatic signaling induced by bone marrow stroma. *Official Journal of the Metastasis Research Society*, *25*(1), 1-10. https://doi.org/10.1007/s10585-007-9094-6

Stroberg, W., & Schnell, S. (2017). On the origin of non-membrane-bound organelles, and their physiological function. *J Theor Biol*, *434*, 42-49. https://doi.org/10.1016/j.jtbi.2017.04.006

Sun, L., Sun, C., Liang, Z., Li, H., Chen, L., Luo, H., Zhang, H., Ding, P., Sun, X., Qin, Z., & Zhao, Y. (2015). FSP1(+) fibroblast subpopulation is essential for the maintenance and regeneration of medullary thymic epithelial cells. *Sci Rep*, *5*, 14871. https://doi.org/10.1038/srep14871

Svendsen, A., Verhoeff, J. J., Immervoll, H., Brøgger, J. C., Kmiecik, J., Poli, A., Netland, I. A., Prestegarden, L., Planagumà, J., Torsvik, A., Kjersem, A. B., Sakariassen, P., Heggdal, J. I., Van Furth, W. R., Bjerkvig, R., Lund-Johansen, M., Enger, P., Felsberg, J., Brons, N. H., . . . Chekenya, M. (2011). Expression of the progenitor marker NG2/CSPG4 predicts poor survival and resistance to ionising radiation in glioblastoma. *Acta Neuropathol*, *122*(4), 495-510. https://doi.org/10.1007/s00401-011-0867-2

Tanabe, S. (2014). Role of mesenchymal stem cells in cell life and their signaling. *World journal of stem cells*, *6*(1), 24-32. https://doi.org/10.4252/wjsc.v6.i1.24

Tang, P. A., & Moore, M. J. (2013). Aflibercept in the treatment of patients with metastatic colorectal cancer: latest findings and interpretations. *Therap Adv Gastroenterol*, *6*(6), 459-473. https://doi.org/10.1177/1756283X13502637

Tao, L., Huang, G., Wang, R., Pan, Y., He, Z., Chu, X., Song, H., & Chen, L. (2016). Cancer- associated fibroblasts treated with cisplatin facilitates chemoresistance of lung adenocarcinoma through IL-11/ IL- 11R/ STAT3 signaling pathway. *Scientific reports*, *6*(1), 38408-38408. https://doi.org/10.1038/srep38408

Tap, W. D., Jones, R. L., Van Tine, B. A., Chmielowski, B., Elias, A. D., Adkins, D., Agulnik, M., Cooney, M. M., Livingston, M. B., Pennock, G., Hameed, M. R., Shah, G. D., Qin, A., Shahir, A., Cronier, D. M., Ilaria, R., Conti, I., Cosaert, J., & Schwartz, G. K. (2016). Olaratumab and doxorubicin versus doxorubicin alone for treatment of soft- tissue sarcoma: an open- label phase 1b and randomised phase 2 trial. *The Lancet*, *388*(10043), 488-497. https://doi.org/10.1016/S0140-6736(16)30587-6

Tawfik, O., Rao, D., Nothnick, W. B., Graham, A., Mau, B., & Fan, F. (2014). Transgelin, a Novel Marker of Smooth Muscle Differentiation, Effectively Distinguishes Endometrial Stromal Tumors from Uterine Smooth Muscle Tumors. *Int J Gynecol Obstet Reprod Med Res*, *1*(1), 26-31. https://www.ncbi.nlm.nih.gov/pubmed/26023684

Tawfik, O., Rao, D., Nothnick, W. B., Graham, A., Mau, B., & Fan, F. (2014). Transgelin, a Novel Marker of Smooth Muscle Differentiation, Effectively Distinguishes Endometrial Stromal Tumors from Uterine Smooth Muscle Tumors. *Int J Gynecol Obstet Reprod Med Res*, *1*(1), 26-31. https://www.ncbi.nlm.nih.gov/pubmed/26023684

Thway, K., Nicholson, A. G., Lawson, K., Gonzalez, D., Rice, A., Balzer, B., Swansbury, J., Min, T., Thompson, L., Adu-Poku, K., Campbell, A., & Fisher, C. (2011). Primary pulmonary myxoid sarcoma with EWSR1-CREB1 fusion: a new tumor entity. *Am J Surg Pathol*, *35*(11), 1722-1732. https://doi.org/10.1097/PAS.0b013e318227e4d2

Thorsson, V., Gibbs, D. L., Brown, S. D., Wolf, D., Bortone, D. S., Ou Yang, T.-H., Porta-Pardo, E., Gao, G. F., Plaisier, C. L., Eddy, J. A., Ziv, E., Culhane, A. C., Paull, E. O., Sivakumar, I. K. A., Gentles, A. J., Malhotra, R., Farshidfar, F., Colaprico, A., Parker, J. S., . . . Shmulevich, L. (2018). The Immune Landscape of Cancer. *Immunity*, *48*(4), 812-830.e814. https://doi.org/10.1016/j.immuni.2018.03.023

Thoenen, E., Curl, A., & Iwakuma, T. (2019). TP53 in bone and soft tissue sarcomas. *Pharmacol Ther*, *202*, 149-164. https://doi.org/10.1016/j.pharmthera.2019.06.010

Tieng, F. Y. F., Lee, L. H., & Ab Mutalib, N. S. (2022). Deciphering colorectal cancer immune microenvironment transcriptional landscape on single cell resolution - A role for immunotherapy. *Front Immunol*, *13*, 959705. https://doi.org/10.3389/fimmu.2022.959705

To, W., & Midwood, K. (2011). Plasma and cellular fibronectin: distinct and independent functions during tissue repair. *Fibrogenesis & Tissue Repair*, *4*(1), 21. https://doi.org/10.1186/1755-1536-4-21

Togo, S., Polanska, U., Horimoto, Y., & Orimo, A. (2013). Carcinoma- Associated Fibroblasts Are a Promising Therapeutic Target. *Cancers*, *5*(1), 149-169. https://doi.org/10.3390/cancers5010149

Tracy, L. E., Minasian, R. A., & Caterson, E. J. (2016). Extracellular Matrix and Dermal Fibroblast Function in the Healing Wound. *Adv Wound Care (New Rochelle)*, *5*(3), 119-136. https://doi.org/10.1089/wound.2014.0561

Tsujino, T., Seshimo, I., Yamamoto, H., Ngan, C. Y., Ezumi, K., Takemasa, I., Ikeda, M., Sekimoto, M., Matsuura, N., & Monden, M. (2007). Stromal myofibroblasts predict disease recurrence for colorectal cancer. *Clin Cancer Res*, *13*(7), 2082-2090. https://doi.org/10.1158/1078-0432.CCR-06-2191

Tuhkanen, H., Anttila, M., Kosma, V. M., Ylä-Herttuala, S., Heinonen, S., Kuronen, A., Juhola, M., Tammi, R., Tammi, M., & Mannermaa, A. (2004). Genetic alterations in the peritumoral stromal cells of malignant and borderline epithelial ovarian tumors as indicated by allelic imbalance on chromosome 3p. *International Journal of Cancer*, *109*(2), 247-252. https://doi.org/10.1002/ijc.11733

Vodanovich, D. A., & M Choong, P. F. (2018). Soft- tissue Sarcomas. *Indian journal of orthopaedics*, *52*(1), 35-44. https://doi.org/10.4103/ortho.IJOrtho_220_17

Wang, D., Stockard, C. R., Harkins, L., Lott, P., Salih, C., Yuan, K., Buchsbaum, D., Hashim, A., Zayzafoon, M., Hardy, R. W., Hameed, O., Grizzle, W., & Siegal, G. P. (2008). Immunohistochemistry in the evaluation of neovascularization in tumor xenografts. *Biotech Histochem*, *83*(3-4), 179-189. https://doi.org/10.1080/10520290802451085

Wang, J., Li, R., Li, M., & Wang, C. (2021). Fibronectin and colorectal cancer: signaling pathways and clinical implications. *J Recept Signal Transduct Res*, *41*(4), 313-320. https://doi.org/10.1080/10799893.2020.1817074

Wang, L., Luo, R., Xiong, Z., Xu, J., & Fang, D. (2018). Pleomorphic liposarcoma: An analysis of 6 case reports and literature review. *Medicine (Baltimore)*, *97*(8), e9986. https://doi.org/10.1097/MD.0000000000009986

Wang, M., Ren, D., Guo, W., Huang, S., Wang, Z., Li, Q., Du, H., Song, L., & Peng, X. (2016). N-cadherin promotes epithelial-mesenchymal transition and cancer stem cell-like traits via ErbB signaling in prostate cancer cells. *Int J Oncol*, *48*(2), 595-606. https://doi.org/10.3892/ijo.2015.3270

Wang, Z., Han, B., Zhang, Z., Pan, J., & Xia, H. (2010). Expression of angiopoietin-like 4 and tenascin C but not cathepsin C mRNA predicts prognosis of oral tongue squamous cell carcinoma. *Biomarkers*, *15*(1), 39-46. https://doi.org/10.3109/13547500903261362

Weina, K., & Utikal, J. (2014). SOX2 and cancer: current research and its implications in the clinic. *Clin Transl Med*, *3*, 19. https://doi.org/10.1186/2001-1326-3-19

Weitz, J., Antonescu, C. R., & Brennan, M. F. (2003). Localized extremity soft tissue sarcoma: improved knowledge with unchanged survival over time. *Journal of clinical oncology : official journal of the American Society of Clinical Oncology*, *21*(14), 2719-2725. https://doi.org/10.1200/JCO.2003.02.026

Weng, S. L., Chang, S. J., Cheng, Y. C., Wang, H. Y., Wang, T. Y., Chang, M. D., & Wang, H. W. (2011). Comparative transcriptome analysis reveals a fetal origin for mesenchymal stem cells and novel

fetal surface antigens for noninvasive prenatal diagnosis. *Taiwan J Obstet Gynecol*, *50*(4), 447-457. https://doi.org/10.1016/j.tjog.2011.10.009

Widemann, B. C., & Italiano, A. (2018). Biology and Management of Undifferentiated Pleomorphic Sarcoma, Myxofibrosarcoma, and Malignant Peripheral Nerve Sheath Tumors: State of the Art and Perspectives. *J Clin Oncol*, *36*(2), 160-167. https://doi.org/10.1200/JCO.2017.75.3467

Wintzell, M., Hjerpe, E., Åvall Lundqvist, E., & Shoshan, M. (2012). Protein markers of cancer- associated fibroblasts and tumor- initiating cells reveal subpopulations in freshly isolated ovarian cancer ascites. *BMC Cancer*, *12*(359), 359-359. https://doi.org/10.1186/1471-2407-12-359

Wu, Y., Wu, P., Zhang, Q., Chen, W., Liu, X., & Zheng, W. (2019). MFAP5 promotes basal-like breast cancer progression by activating the EMT program. *Cell Biosci*, *9*, 24. https://doi.org/10.1186/s13578-019-0284-0

Wuebben, E. L., & Rizzino, A. (2017). The dark side of SOX2: cancer - a comprehensive overview. *Oncotarget*, *8*(27), 44917-44943. https://doi.org/10.18632/oncotarget.16570

Xi, Y., Liu, J., & Shen, G. (2022). Low expression of IGFBP4 and TAGLN accelerate the poor overall survival of osteosarcoma. *Scientific reports*, *12*(1), 9298. https://doi.org/10.1038/s41598-022-13163-8

Xiao, W., Mohseny, A. B., Hogendoorn, P. C. W., & Cleton-Jansen, A.-M. (2013). Mesenchymal stem cell transformation and sarcoma genesis. *Clinical sarcoma research*, *3*(1), 10-10. https://doi.org/10.1186/2045-3329-3-10

Xin, Z., Qirui, W., Xiuqing, G., Jinfeng, L., & Yujie, a. M. (2021). Osteosarcoma: a review of current and future therapeutic approaches. In (Vol. 20). BioMed Eng OnLine.

Xing. (2011). Cancer associated fibroblasts (CAFs) in tumor microenviroment. *Front Biosci*, 166-179.

Xing, F., Saidou, J., & Watabe, K. (2010). Cancer associated fibroblasts (CAFs) in tumor microenvironment. *Frontiers in Bioscience-Landmark*, *15*, 166-179. https://doi.org/10.2741/3613

Yao, Y., & Dai, W. (2014). Genomic Instability and Cancer. *J Carcinog Mutagen*, *5*. https://doi.org/10.4172/2157-2518.1000165

Yamashita, M., Ogawa, T., Zhang, X., Hanamura, N., Kashikura, Y., Takamura, M., Yoneda, M., & Shiraishi, T. (2012). Role of stromal myofibroblasts in invasive breast cancer: stromal expression of alpha-smooth muscle actin correlates with worse clinical outcome. *Breast Cancer*, *19*(2), 170-176. https://doi.org/10.1007/s12282-010-0234-5

Yang, Y., Ye, W. L., Zhang, R. N., He, X. S., Wang, J. R., Liu, Y. X., Wang, Y., Yang, X. M., Zhang, Y. J., & Gan, W. J. (2021). The Role of TGF-. *Evid Based Complement Alternat Med*, *2021*, 6675208. https://doi.org/10.1155/2021/6675208

Yu, L., Guo, W., Zhao, S., Wang, F., & Xu, Y. (2011). Fusion between cancer cells and myofibroblasts is involved in osteosarcoma. Oncology letters, 2(6), 1083-1087. https://doi.org/10.3892/ol.2011.363

Zhang, J., Chang, D. Y., Mercado-Uribe, I., & Liu, J. (2012). Sex-determining region Y-box 2 expression predicts poor prognosis in human ovarian carcinoma. *Hum Pathol*, *43*(9), 1405-1412. https://doi.org/10.1016/j.humpath.2011.10.016

Zhang, S., Che, D., Yang, F., Chi, C., Meng, H., Shen, J., Qi, L., Liu, F., Lv, L., Li, Y., Meng, Q., Liu, J., Shang, L., & Yu, Y. (2017). Tumor-associated macrophages promote tumor metastasis via the TGF-β/SOX9 axis in non-small cell lung cancer. *Oncotarget*, *8*(59), 99801-99815. https://doi.org/10.18632/oncotarget.21068

Zhang, S., Xiong, X., & Sun, Y. (2020). Functional characterization of SOX2 as an anticancer target. *Signal Transduct Target Ther*, *5*(1), 135. https://doi.org/10.1038/s41392-020-00242-3

Zhang, W., & Liu, H. T. (2002). MAPK signal pathways in the regulation of cell proliferation in mammalian cells. *Cell Res*, *12*(1), 9-18. https://doi.org/10.1038/sj.cr.7290105

Zhao, L., Wang, H., Deng, Y.-J., Wang, S., Liu, C., Jin, H., & Ding, Y.-Q. (2009). Transgelin as a suppressor is associated with poor prognosis in colorectal carcinoma patients. Modern Pathology, 22(6), 786-796. https://doi.org/10.1038/modpathol.2009.29

Zhou, H.-M., Fang, Y.-Y., Weinberger, P. M., Ding, L.-L., Cowell, J. K., Hudson, F. Z., Ren, M., Lee, J. R., Chen, Q.-K., Su, H., Dynan, W. S., & Lin, Y. (2016). Transgelin increases metastatic potential of colorectal cancer cells in vivo and alters expression of genes involved in cell motility. *BMC Cancer*, *16*(59), 55-55. https://doi.org/10.1186/s12885-016-2105-8

Zhou, L., Zhang, R., Zhang, L., Sun, Y., Yao, W., Zhao, A., Li, J., & Yuan, Y. (2013). Upregulation of transgelin is an independent factor predictive of poor prognosis in patients with advanced pancreatic cancer. *Cancer Sci*, *104*(4), 423-430. https://doi.org/10.1111/cas.12107

Zhou, Z., Cui, D., Sun, M. H., Huang, J. L., Deng, Z., Han, B. M., Sun, X. W., Xia, S. J., Sun, F., & Shi, F. (2020). CAFs-derived MFAP5 promotes bladder cancer malignant behavior through NOTCH2/HEY1 signaling. *FASEB J*, *34*(6), 7970-7988. https://doi.org/10.1096/fj.201902659R

Zhuang, G., Zeng, Y., Tang, Q., He, Q., & Luo, G. (2020). Identifying M1 Macrophage-Related Genes Through a Co-expression Network to Construct a Four-Gene Risk-Scoring Model for Predicting Thyroid Cancer Prognosis. *Front Genet*, *11*, 591079. https://doi.org/10.3389/fgene.2020.591079

Zinchuk, V., & Zinchuk, O. (2008). Quantitative colocalization analysis of confocal fluorescence microscopy images. Curr Protoc Cell Biol, Chapter 4, Unit 4.19. https://doi.org/10.1002/0471143030.cb0419s39

Abeshouse, A., Adebamowo, C., Adebamowo, S. N., Akbani, R., Akeredolu, T., Ally, A., Anderson, M. L., Anur, P., Appelbaum, E. L., Armenia, J., Auman, J. T., Bailey, M. H., Baker, L., Balasundaram, M., Balu, S., Barthel, F. P., Bartlett, J., Baylin, S. B., Behera, M., . . . Wilson, R. K. (2017). Comprehensive and Integrated Genomic Characterization of Adult Soft Tissue Sarcomas. *Cell*, *171*(4), 950-965.e928. https://doi.org/10.1016/j.cell.2017.10.014

Adolfo, P. (2009). Regenerative medicine: a review Medicina regenerativa: uma revisão. *Revista Brasileira de Hematologia e Hemoterapia*, *31*(suppl 2), 63-66. https://doi.org/10.1590/S1516-84842009000800017

Alabiad, M. A., Harb, O. A., Abdelfattah, M. T., El-Shafaay, B. S., El-Taher, A. K., & El-Hendawy, E. I. (2020). The values of Transgelin, Stathmin, BCOR and Cyclin-D1 expression in differentiation between Uterine Leiomyosarcoma (ULMS) and Endometrial Stromal Sarcoma (ESS); diagnostic and prognostic implications. *Surgical and Experimental Pathology*, *3*(1), 13. https://doi.org/10.1186/s42047-020-00065-0

Anderberg, C., Li, H., Fredriksson, L., Andrae, J., Betsholtz, C., Li, X., Eriksson, U., & Pietras, K. (2009). Paracrine signaling by platelet-derived growth factor-CC promotes tumor growth by recruitment of cancer-associated fibroblasts. *Cancer Res*, *69*(1), 369-378. https://doi.org/10.1158/0008-5472.CAN-08-2724

Anderson, N. D., Babichev, Y., Fuligni, F., Comitani, F., Layeghifard, M., Venier, R. E., Dentro, S. C., Maheshwari, A., Guram, S., Wunker, C., Thompson, J. D., Yuki, K. E., Hou, H., Zatzman, M., Light, N., Bernardini, M. Q., Wunder, J. S., Andrulis, I. L., Ferguson, P., . . . Shlien, A. (2021). Lineage-defined leiomyosarcoma subtypes emerge years before diagnosis and determine patient survival. *Nat Commun*, *12*(1), 4496. https://doi.org/10.1038/s41467-021-24677-6

Andrade, C. R., Takahama Junior, A., Nishimoto, I. N., Kowalski, L. P., & Lopes, M. A. (2010). Rhabdomyosarcoma of the head and neck: a clinicopathological and immunohistochemical

analysis of 29 cases. *Braz Dent J*, *21*(1), 68-73. https://doi.org/10.1590/s0103-64402010000100011

Anggorowati, N., Ratna Kurniasari, C., Damayanti, K., Cahyanti, T., Widodo, I., Ghozali, A., Romi, M. M., Sari, D. C., & Arfian, N. (2017). Histochemical and Immunohistochemical Study of α-SMA, Collagen, and PCNA in Epithelial Ovarian Neoplasm. *Asian Pac J Cancer Prev*, *18*(3), 667-671. https://doi.org/10.22034/APJCP.2017.18.3.667

Antoine, E. K., Ajeeta, B. D., Annie, P. V., Andrew, S., Mary, W. B., George, W. B., Andrea, L. R., Kornelia, P., Ross, T., & Robert, A. W. (2007). Mesenchymal stem cells within tumour stroma promote breast cancer metastasis. *Nature*, *449*(7162), 557. https://doi.org/10.1038/nature06188

Aran, D., Hu, Z., & Butte, A. J. (2017). xCell: digitally portraying the tissue cellular heterogeneity landscape. *Genome Biol*, *18*(1), 220. https://doi.org/10.1186/s13059-017-1349-1

Arnold, J. N., Magiera, L., Kraman, M., & Fearon, D. T. (2014). Tumoral immune suppression by macrophages expressing fibroblast activation protein-α and heme oxygenase-1. *Cancer Immunol Res*, *2*(2), 121-126. https://doi.org/10.1158/2326-6066.CIR-13-0150

Arnold, S. A., Loomans, H. A., Ketova, T., Andl, C. D., Clark, P. E., & Zijlstra, A. (2016). Urinary oncofetal ED-A fibronectin correlates with poor prognosis in patients with bladder cancer. *Clin Exp Metastasis*, *33*(1), 29-44. https://doi.org/10.1007/s10585-015-9754-x

Arvinius, C., Torrecilla, E., Beano-Collado, J., García-Coiradas, J., García-Maroto, R., Puerto-Vázquez, M., & Cebrián-Parra, J. L. (2017). A clinical review of 11 cases of large-sized well-differentiated liposarcomas. *European Journal of Orthopaedic Surgery & Traumatology*, *27*(6), 837-841. https://doi.org/10.1007/s00590-017-1968-y

Assinder, S. J., Stanton, J.-A. L., & Prasad, P. D. (2009). Transgelin: An actin- binding protein and tumour suppressor. *International Journal of Biochemistry and Cell Biology*, *41*(3), 482-486. https://doi.org/10.1016/j.biocel.2008.02.011

Augsten, M. (2014). Cancer- associated fibroblasts as another polarized cell type of the tumor microenvironment. *Frontiers in Oncology*, *4*, 62-62. https://doi.org/10.3389/fonc.2014.00062

Bae, Y. K., Kim, A., Kim, M. K., Choi, J. E., Kang, S. H., & Lee, S. J. (2013). Fibronectin expression in carcinoma cells correlates with tumor aggressiveness and poor clinical outcome in patients with invasive breast cancer. *Hum Pathol*, *44*(10), 2028-2037. https://doi.org/10.1016/j.humpath.2013.03.006

Baek, S. H., Maiorino, E., Kim, H., Glass, K., Raby, B. A., & Yuan, K. (2022). Single Cell Transcriptomic Analysis Reveals Organ Specific Pericyte Markers and Identities. *Front Cardiovasc Med*, *9*, 876591. https://doi.org/10.3389/fcvm.2022.876591

Baghel, K. S., Tewari, B. N., Shrivastava, R., Malik, S. A., Lone, M. U. D., Jain, N. K., Tripathi, C., Kanchan, R. K., Dixit, S., Singh, K., Mitra, K., Negi, M. P. S., Srivastava, M., Misra, S., Bhatt, M. L. B., & Bhadauria, S. (2016). Macrophages promote matrix protrusive and invasive function of breast cancer cells via MIP-1β dependent upregulation of MYO3A gene in breast cancer cells. *Oncoimmunology*, *5*(7), e1196299. https://doi.org/10.1080/2162402X.2016.1196299

Baird, S. K., Allan, L., Renner, C., Scott, F. E., & Scott, A. M. (2015). Fibroblast activation protein increases metastatic potential of fibrosarcoma line HT1080 through upregulation of integrin-mediated signaling pathways. *Clin Exp Metastasis*, *32*(5), 507-516. https://doi.org/10.1007/s10585-015-9723-4

Balkwill, F., & Mantovani, A. (2001). Inflammation and cancer: back to Virchow? *The Lancet*, *357*(9255), 539-545. https://doi.org/10.1016/S0140-6736(00)04046-0

Balkwill, F. R., Capasso, M., & Hagemann, T. (2012). The tumor microenvironment at a glance. *Journal of cell science*, *125*(Pt 23), 5591-5596. https://doi.org/10.1242/jcs.116392

Barcellos-de-Souza, P., Gori, V., Bambi, F., & Chiarugi, P. (2013). Tumor microenvironment: Bone marrow- mesenchymal stem cells as key players. *BBA - Reviews on Cancer*, *1836*(2), 321-335. https://doi.org/10.1016/j.bbcan.2013.10.004

Basu-Roy, U., Seo, E., Ramanathapuram, L., Rapp, T. B., Perry, J. A., Orkin, S. H., Mansukhani, A., & Basilico, C. (2012). Sox2 maintains self renewal of tumor-initiating cells in osteosarcomas. *Oncogene*, *31*(18), 2270-2282. https://doi.org/10.1038/onc.2011.405

Benassi, M. S., Pazzaglia, L., Chiechi, A., Alberghini, M., Conti, A., Cattaruzza, S., Wassermann, B., Picci, P., & Perris, R. (2009). NG2 expression predicts the metastasis formation in soft-tissue sarcoma patients. *J Orthop Res*, *27*(1), 135-140. https://doi.org/10.1002/jor.20694

Benna, C., Simioni, A., Pasquali, S., De Boni, D., Rajendran, S., Spiro, G., Colombo, C., Virgone, C., DuBois, S. G., Gronchi, A., Rossi, C. R., & Mocellin, S. (2018). Genetic susceptibility to bone and soft tissue sarcomas: a field synopsis and meta-analysis. *Oncotarget*, *9*(26), 18607-18626. https://doi.org/10.18632/oncotarget.24719

Betterle, C., & Zanchetta, R. (2012). The immunofluorescence techniques in the diagnosis of endocrine autoimmune diseases. *Auto Immun Highlights*, *3*(2), 67-78. https://doi.org/10.1007/s13317-012-0034-3

Bhowmick, N. A., Chytil, A., Plieth, D., Gorska, A. E., Dumont, N., Shappell, S., Washington, M. K., Neilson, E. G., & Moses, H. L. (2004). TGF-β Signaling in Fibroblasts Modulates the Oncogenic Potential of Adjacent Epithelia. *Science*, *303*(5659), 848-851. https://doi.org/10.1126/science.1090922

Blankenberg, D., Gordon, A., Von Kuster, G., Coraor, N., Taylor, J., Nekrutenko, A., & Team, G. (2010). Manipulation of FASTQ data with Galaxy. *Bioinformatics*, *26*(14), 1783-1785. https://doi.org/10.1093/bioinformatics/btq281

Bleloch, J. S., Ballim, R. D., Kimani, S., Parkes, J., Panieri, E., Willmer, T., & Prince, S. (2017). Managing sarcoma: where have we come from and where are we going? In (Vol. 9, pp. 637-659). London, England.

Bondjers, C., Kalén, M., Hellström, M., Scheidl, S. J., Abramsson, A., Renner, O., Lindahl, P., Cho, H., Kehrl, J., & Betsholtz, C. (2003). Transcription profiling of platelet-derived growth factor-B-deficient mouse embryos identifies RGS5 as a novel marker for pericytes and vascular smooth muscle cells. *Am J Pathol*, *162*(3), 721-729. https://doi.org/10.1016/S0002-9440(10)63868-0

Bonuccelli, G., Avnet, S., Grisendi, G., Salerno, M., Granchi, D., Dominici, M., Kusuzaki, K., & Baldini, N. (2014). Role of mesenchymal stem cells in osteosarcoma and metabolic reprogramming of tumor cells. *Oncotarget*, *5*(17), 7575-7588. https://doi.org/10.18632/oncotarget.2243

Boudin, L., de Nonneville, A., Finetti, P., Mescam, L., Le Cesne, A., Italiano, A., Blay, J.-Y., Birnbaum, D., Mamessier, E., & Bertucci, F. (2022). CSPG4 expression in soft tissue sarcomas is associated with poor prognosis and low cytotoxic immune response. *Journal of Translational Medicine*, *20*(1), 464. https://doi.org/10.1186/s12967-022-03679-y

Brahmi, M., Lesluyes, T., Dufresne, A., Toulmonde, M., Italiano, A., Mir, O., Le Cesne, A., Valentin, T., Chevreau, C., Bonvalot, S., Penel, N., Coindre, J. M., Le Guellec, S., Le Loarer, F., Karanian, M., Blay, J. Y., & Chibon, F. (2021). Expression and prognostic significance of PDGF ligands and receptors across soft tissue sarcomas. *ESMO Open*, *6*(1), 100037. https://doi.org/10.1016/j.esmoop.2020.100037

Bulbul, A., Fahy, B. N., Xiu, J., Rashad, S., Mustafa, A., Husain, H., & Hayes-Jordan, A. (2017). Desmoplastic Small Round Blue Cell Tumor: A Review of Treatment and Potential Therapeutic Genomic Alterations. *Sarcoma*, *2017*, 1278268. https://doi.org/10.1155/2017/1278268

Busek, P., Mateu, R., Zubal, M., Kotackova, L., & Sedo, A. (2018). Targeting fibroblast activation protein in cancer - Prospects and caveats. *Front Biosci (Landmark Ed)*, *23*(10), 1933-1968. https://doi.org/10.2741/4682

Butti, R., Nimma, R., Kundu, G., Bulbule, A., Kumar, T. V. S., Gunasekaran, V. P., Tomar, D., Kumar, D., Mane, A., Gill, S. S., Patil, T., Weber, G. F., & Kundu, G. C. (2021). Tumor-derived osteopontin drives the resident fibroblast to myofibroblast differentiation through Twist1 to promote breast cancer progression. *Oncogene*, *40*(11), 2002-2017. https://doi.org/10.1038/s41388-021-01663-2

Cannon, A., Thompson, C., Hall, B. R., Jain, M., Kumar, S., & Batra, S. K. (2018). Desmoplasia in pancreatic ductal adenocarcinoma: insight into pathological function and therapeutic potential. *Genes & cancer*, *9*(3-4), 78-86. https://doi.org/10.18632/genesandcancer.171

Cao, Y., Zhang, Z. L., Zhou, M., Elson, P., Rini, B., Aydin, H., Feenstra, K., Tan, M. H., Berghuis, B., Tabbey, R., Resau, J. H., Zhou, F. J., Teh, B. T., & Qian, C. N. (2013). Pericyte coverage of differentiated vessels inside tumor vasculature is an independent unfavorable prognostic factor for patients with clear cell renal cell carcinoma. *Cancer*, *119*(2), 313-324. https://doi.org/10.1002/cncr.27746

Carneiro, A., Francis, P., Bendahl, P. O., Fernebro, J., Akerman, M., Fletcher, C., Rydholm, A., Borg, A., & Nilbert, M. (2009). Indistinguishable genomic profiles and shared prognostic markers in undifferentiated pleomorphic sarcoma and leiomyosarcoma: different sides of a single coin? *Lab Invest*, *89*(6), 668-675. https://doi.org/10.1038/labinvest.2009.18

Cedric, G., Steven, H., Cristina, H.-C., Robert, G., John, F. M., Kevin, H., & Erik, S. (2007). Fibroblast- led collective invasion of carcinoma cells with differing roles for RhoGTPases in leading and following cells. *Nature Cell Biology*, *9*(12), 1392. https://doi.org/10.1038/ncb1658

Chai, J. T., Ruparelia, N., Goel, A., Kyriakou, T., Biasiolli, L., Edgar, L., Handa, A., Farrall, M., Watkins, H., & Choudhury, R. P. (2018). Differential Gene Expression in Macrophages From Human Atherosclerotic Plaques Shows Convergence on Pathways Implicated by Genome-Wide Association Study Risk Variants. *Arterioscler Thromb Vasc Biol*, *38*(11), 2718-2730. https://doi.org/10.1161/ATVBAHA.118.311209

Chang, T. H., Shanti, R. M., Liang, Y., Zeng, J., Shi, S., Alawi, F., Carrasco, L., Zhang, Q., & Le, A. D. (2020). LGR5. *Cell Death Dis*, *11*(5), 338. https://doi.org/10.1038/s41419-020-2560-7

Charlotte, K., Tony, C., Min, W., Greg, M., Joe, W. G., Loucinda, C., Andrea, R., & Robert, A. W. (2004). Reconstruction of functionally normal and malignant human breast tissues in mice. *Proceedings of the National Academy of Sciences of the United States of America*, *101*(14), 4966. https://doi.org/10.1073/pnas.0401064101

Chaurasia, S. S., Kaur, H., de Medeiros, F. W., Smith, S. D., & Wilson, S. E. (2009). Dynamics of the expression of intermediate filaments vimentin and desmin during myofibroblast differentiation after corneal injury. *Experimental Eye Research*, *89*(2), 133-139. https://doi.org/10.1016/j.exer.2009.02.022

Chen, L., Chu, C., Lu, J., Kong, X., Huang, T., & Cai, Y. D. (2015). Gene Ontology and KEGG Pathway Enrichment Analysis of a Drug Target-Based Classification System. *PLoS One*, *10*(5), e0126492. https://doi.org/10.1371/journal.pone.0126492

Chen, Y., Shi, L., Zhang, L., Li, R., Liang, J., Yu, W., Sun, L., Yang, X., Wang, Y., Zhang, Y., & Shang, Y. (2008). The molecular mechanism governing the oncogenic potential of SOX2 in breast cancer. *J Biol Chem*, *283*(26), 17969-17978. https://doi.org/10.1074/jbc.M802917200

Chen, Z., Yan, X., Li, K., Ling, Y., & Kang, H. (2020). Stromal fibroblast-derived MFAP5 promotes the invasion and migration of breast cancer cells via Notch1/slug signaling. *Clin Transl Oncol*, *22*(4), 522-531. https://doi.org/10.1007/s12094-019-02156-1

Christine, F., James, O. J., Matthew, K., Richard, J. B. W., Andrew, D., Derek, S. C., Claire, M. C., Edward, W. R., Qi, Z., Otavia, L. C., Sarah, A. T., Tobias, J., Duncan, I. J., David, A. T., & Douglas, T. F. (2013). Targeting CXCL12 from FAP- expressing carcinoma-associated fibroblasts synergizes with anti– PD- L1 immunotherapy in pancreatic cancer. *Proceedings of the National Academy of Sciences*, *110*(50), 20212. https://doi.org/10.1073/pnas.1320318110

Cirri, P., & Chiarugi, P. (2011). Cancer associated fibroblasts: the dark side of the coin. *Am. J. Cancer Res.*, *1*(4), 482-497.

Cooke, V. G., LeBleu, V. S., Keskin, D., Khan, Z., O'Connell, J. T., Teng, Y., Duncan, M. B., Xie, L., Maeda, G., Vong, S., Sugimoto, H., Rocha, R. M., Damascena, A., Brentani, R. R., & Kalluri, R. (2012). Pericyte depletion results in hypoxia-associated epithelial-to-mesenchymal transition and metastasis mediated by met signaling pathway. *Cancer Cell*, *21*(1), 66-81. https://doi.org/10.1016/j.ccr.2011.11.024

Costa, M., Escaleira, R., Cataldo, A., Oliveira, F., & Mermelstein, C. S. (2004). Desmin: molecular interactions and putative functions of the muscle intermediate filament protein. *Brazilian J. Med. Biol. Res.*, *37*(12), 1819-1830.

Crawford, Y., Kasman, I., Yu, L., Zhong, C., Wu, X., Modrusan, Z., Kaminker, J., & Ferrara, N. (2009). PDGF-C Mediates the Angiogenic and Tumorigenic Properties of Fibroblasts Associated with Tumors Refractory to Anti- VEGF Treatment. *Cancer Cell*, *15*(1), 21-34. https://doi.org/10.1016/j.ccr.2008.12.004

Cushing, M. C., Mariner, P. D., Liao, J.-T., Sims, E. A., & Anseth, K. S. (2008). Fibroblast growth factor represses Smad- mediated myofibroblast activation in aortic valvular interstitial cells. *FASEB journal : official publication of the Federation of American Societies for Experimental Biology*, *22*(6), 1769-1777. https://doi.org/10.1096/fj.07-087627

D'Angelo, S. P., Shoushtari, A. N., Agaram, N. P., Kuk, D., Qin, L.-X., Carvajal, R. D., Dickson, M. A., Gounder, M., Keohan, M. L., Schwartz, G. K., & Tap, W. D. (2015). Prevalence of tumor-infiltrating lymphocytes and PD-L1 expression in the soft tissue sarcoma microenvironment. *Human Pathology*, *46*(3), 357-365. https://doi.org/https://doi.org/10.1016/j.humpath.2014.11.001

Davidson, S., Efremova, M., Riedel, A., Mahata, B., Pramanik, J., Huuhtanen, J., Kar, G., Vento-Tormo, R., Hagai, T., Chen, X., Haniffa, M. A., Shields, J. D., & Teichmann, S. A. (2020). Single-Cell RNA Sequencing Reveals a Dynamic Stromal Niche That Supports Tumor Growth. *Cell Rep*, *31*(7), 107628. https://doi.org/10.1016/j.celrep.2020.107628

De Micheli, A. J., Laurilliard, E. J., Heinke, C. L., Ravichandran, H., Fraczek, P., Soueid-Baumgarten, S., De Vlaminck, I., Elemento, O., & Cosgrove, B. D. (2020). Single-Cell Analysis of the Muscle Stem Cell Hierarchy Identifies Heterotypic Communication Signals Involved in Skeletal Muscle Regeneration. *Cell Rep*, *30*(10), 3583-3595.e3585. https://doi.org/10.1016/j.celrep.2020.02.067

De Palma, M., & Lewis, C. E. (2013). Macrophage regulation of tumor responses to anticancer therapies. *Cancer Cell*, *23*(3), 277-286. https://doi.org/10.1016/j.ccr.2013.02.013

Declerck, Y. A. (2012). Desmoplasia: a response or a niche? *Cancer discovery*, *2*(9), 772-774. https://doi.org/10.1158/2159-8290.CD-12-0348

Delgado, J., Pereira, A., Villamor, N., López-Guillermo, A., & Rozman, C. (2014). Survival analysis in hematologic malignancies: recommendations for clinicians. *Haematologica*, *99*(9), 1410-1420. https://doi.org/10.3324/haematol.2013.100784

Delpire, E., & Gagnon, K. B. E. (2018). Water Homeostasis and Cell Volume Maintenance and Regulation. *Current topics in membranes*, *81*, 3-52.

Denu, R. A., Nemcek, S., Bloom, D. D., Goodrich, A. D., Kim, J., Mosher, D. F., & Hematti, P. (2016). Fibroblasts and Mesenchymal Stromal/Stem Cells Are Phenotypically Indistinguishable. *Acta Haematol*, *136*(2), 85-97. https://doi.org/10.1159/000445096

Ding, W., Knox, T. R., Tschumper, R. C., Wu, W., Schwager, S. M., Boysen, J. C., Jelinek, D. F., & Kay, N. E. (2010). Platelet-derived growth factor (PDGF)-PDGF receptor interaction activates bone marrow-derived mesenchymal stromal cells derived from chronic lymphocytic leukemia: implications for an angiogenic switch. *Blood*, *116*(16), 2984-2993. https://doi.org/10.1182/blood-2010-02-269894

Dinh, H. Q., Pan, F., Wang, G., Huang, Q. F., Olingy, C. E., Wu, Z. Y., Wang, S. H., Xu, X., Xu, X. E., He, J. Z., Yang, Q., Orsulic, S., Haro, M., Li, L. Y., Huang, G. W., Breunig, J. J., Koeffler, H. P., Hedrick, C. C., Xu, L. Y., . . . Li, E. M. (2021). Integrated single-cell transcriptome analysis reveals heterogeneity of esophageal squamous cell carcinoma microenvironment. *Nat Commun*, *12*(1), 7335. https://doi.org/10.1038/s41467-021-27599-5

Dinu, D., Dobre, M., Panaitescu, E., Bîrlă, R., Iosif, C., Hoara, P., Caragui, A., Boeriu, M., Constantinoiu, S., & Ardeleanu, C. (2014). Prognostic significance of KRAS gene mutations in colorectal cancer--preliminary study. *J Med Life*, *7*(4), 581-587. https://www.ncbi.nlm.nih.gov/pubmed/25713627

Dohi, O., Ohtani, H., Hatori, M., Sato, E., Hosaka, M., Nagura, H., Itoi, E., & Kokubun, S. (2009). Histogenesis- specific expression of fibroblast activation protein and dipeptidylpeptidase- IV in human bone and soft tissue tumours. *Histopathology*, *55*(4), 432-440. https://doi.org/10.1111/j.1365-2559.2009.03399.x

Dos Anjos Cassado, A. (2017). F4/80 as a Major Macrophage Marker: The Case of the Peritoneum and Spleen. *Results Probl Cell Differ*, *62*, 161-179. https://doi.org/10.1007/978-3-319-54090-0_7

Doyle, L. A. (2014). Sarcoma classification: An update based on the 2013 World Health Organization Classification of Tumors of Soft Tissue and Bone. In (Vol. 120, pp. 1763-1774).

Du, L., Li, J., Lei, L., He, H., Chen, E., Dong, J., & Yang, J. (2018). High Vimentin Expression Predicts a Poor Prognosis and Progression in Colorectal Cancer: A Study with Meta-Analysis and TCGA Database. *Biomed Res Int*, *2018*, 6387810. https://doi.org/10.1155/2018/6387810

Duffy, M. J., Synnott, N. C., & Crown, J. (2018). Mutant p53 in breast cancer: potential as a therapeutic target and biomarker. *Breast Cancer Res Treat*, *170*(2), 213-219. https://doi.org/10.1007/s10549-018-4753-7

Ehlerding, E. B., Lacognata, S., Jiang, D., Ferreira, C. A., Goel, S., Hernandez, R., Jeffery, J. J., Theuer, C. P., & Cai, W. (2018). Targeting angiogenesis for radioimmunotherapy with a. *Eur J Nucl Med Mol Imaging*, *45*(1), 123-131. https://doi.org/10.1007/s00259-017-3793-2

Ehnman, M., & Larsson, O. (2015). Microenvironmental Targets in Sarcoma. *Front Oncol*, *5*, 248. https://doi.org/10.3389/fonc.2015.00248

Elsafadi, M., Manikandan, M., Almalki, S., Mahmood, A., Shinwari, T., Vishnubalaji, R., Mobarak, M., Alfayez, M., Aldahmash, A., Kassem, M., & Alajez, N. M. (2020). Transgelin is a poor prognostic factor associated with advanced colorectal cancer (CRC) stage promoting tumor growth and migration in a TGFβ-dependent manner. *Cell Death Dis*, *11*(5), 341. https://doi.org/10.1038/s41419-020-2529-6

English, W. R., Lunt, S. J., Fisher, M., Lefley, D. V., Dhingra, M., Lee, Y. C., Bingham, K., Hurrell, J. E., Lyons, S. K., Kanthou, C., & Tozer, G. M. (2017). Differential Expression of VEGFA Isoforms Regulates Metastasis and Response to Anti-VEGFA Therapy in Sarcoma. *Cancer Res*, *77*(10), 2633-2646. https://doi.org/10.1158/0008-5472.CAN-16-0255

Erez, N., Truitt, M., Olson, P., & Hanahan, D. (2010). Cancer- Associated Fibroblasts Are Activated in Incipient Neoplasia to Orchestrate Tumor- Promoting Inflammation in an NF- κB- Dependent Manner. *Cancer Cell*, *17*(2), 135-147. https://doi.org/10.1016/j.ccr.2009.12.041

Fan, H., & Chu, J.-Y. (2007). A Brief Review of Short Tandem Repeat Mutation. *Genomics, Proteomics & Bioinformatics*, *5*(1), 7-14. https://doi.org/10.1016/S1672-0229(07)60009-6

Feng, W., Chen, L., Nguyen, P. K., Wu, S. M., & Li, G. (2019). Single Cell Analysis of Endothelial Cells Identified Organ-Specific Molecular Signatures and Heart-Specific Cell Populations and Molecular Features. *Front Cardiovasc Med*, *6*, 165. https://doi.org/10.3389/fcvm.2019.00165

Festjens, N., Vanden Berghe, T., & Vandenabeele, P. (2006). Necrosis, a well-orchestrated form of cell demise: signalling cascades, important mediators and concomitant immune response. *Biochim Biophys Acta*, *1757*(9-10), 1371-1387. https://doi.org/10.1016/j.bbabio.2006.06.014

Fischer, M., Quaas, M., Steiner, L., & Engeland, K. (2016). The p53-p21-DREAM-CDE/CHR pathway regulates G2/M cell cycle genes. *Nucleic Acids Res*, *44*(1), 164-174. https://doi.org/10.1093/nar/gkv927

Fisher, C. (2004). Myofibrosarcoma. *Official Journal of the European Society of Pathology*, *445*(3), 215-223. https://doi.org/10.1007/s00428-004-1038-9

Fletcher, C. D. (2014). The evolving classification of soft tissue tumours - an update based on the new 2013 WHO classification. *Histopathology*, *64*(1), 2-11. https://doi.org/10.1111/his.12267

Folpe, A. L., & Deyrup, A. T. (2006). Alveolar soft-part sarcoma: a review and update. *J Clin Pathol*, *59*(11), 1127-1132. https://doi.org/10.1136/jcp.2005.031120

Forker, L., Gaunt, P., Sioletic, S., Shenjere, P., Potter, R., Roberts, D., Irlam, J., Valentine, H., Hughes, D., Hughes, A., Billingham, L., Grimer, R., Seddon, B., Choudhury, A., Robinson, M., & West, C. M. L. (2017). The hypoxia marker CAIX is prognostic in the UK phase III VorteX-Biobank cohort: an important resource for translational research in soft tissue sarcoma.

Forsberg, E. C., Passegué, E., Prohaska, S. S., Wagers, A. J., Koeva, M., Stuart, J. M., & Weissman, I. L. (2010). Molecular signatures of quiescent, mobilized and leukemia-initiating hematopoietic stem cells. *PLoS One*, *5*(1), e8785. https://doi.org/10.1371/journal.pone.0008785

Fujimoto, N., He, Y., D'Addio, M., Tacconi, C., Detmar, M., & Dieterich, L. C. (2020). Single-cell mapping reveals new markers and functions of lymphatic endothelial cells in lymph nodes. *PLoS Biol*, *18*(4), e3000704. https://doi.org/10.1371/journal.pbio.3000704

Gazdic, M., Volarevic, V., Arsenijevic, N., & Stojkovic, M. (2015). Mesenchymal Stem Cells: A Friend or Foe in Immune- Mediated Diseases. *Stem Cell Reviews and Reports*, *11*(2), 280-287. https://doi.org/10.1007/s12015-014-9583-3

Gee, M. S., Procopio, W. N., Makonnen, S., Feldman, M. D., Yeilding, N. M., & Lee, W. M. (2003). Tumor vessel development and maturation impose limits on the effectiveness of anti-vascular therapy. *Am J Pathol*, *162*(1), 183-193. https://doi.org/10.1016/S0002-9440(10)63809-6

Genadry, K. C., Pietrobono, S., Rota, R., & Linardic, C. M. (2018). Soft Tissue Sarcoma Cancer Stem Cells: An Overview. *Frontiers in Oncology*, *8*, 475-475. https://doi.org/10.3389/fonc.2018.00475

Genin, O., Rechavi, G., Nagler, A., Ben-Itzhak, O., Nazemi, K. J., & Pines, M. (2008). Myofibroblasts in Pulmonary and Brain Metastases of Alveolar Soft- Part Sarcoma: A Novel Target for Treatment? *Neoplasia*, *10*(9), 940-948. https://doi.org/10.1593/neo.08456

Goel, M. K., Khanna, P., & Kishore, J. (2010). Understanding survival analysis: Kaplan- Meier estimate. *International journal of Ayurveda research*, *1*(4), 274-278. https://doi.org/10.4103/0974-7788.76794

Goh, P., Sze, D., & Roufogalis, B. (2007). Molecular and Cellular Regulators of Cancer Angiogenesis. *Current Cancer Drug Targets*, *7*(8), 743-758. https://doi.org/10.2174/156800907783220462

Goldman, M. J., Craft, B., Hastie, M., Repečka, K., McDade, F., Kamath, A., Banerjee, A., Luo, Y., Rogers, D., Brooks, A. N., Zhu, J., & Haussler, D. (2020). Visualizing and interpreting cancer genomics data via the Xena platform. *Nat Biotechnol*, *38*(6), 675-678. https://doi.org/10.1038/s41587-020-0546-8

Grabinski, T. M., Kneynsberg, A., Manfredsson, F. P., & Kanaan, N. M. (2015). A method for combining RNAscope in situ hybridization with immunohistochemistry in thick free-floating brain sections and primary neuronal cultures. *PLoS One*, *10*(3), e0120120. https://doi.org/10.1371/journal.pone.0120120

Grum-Schwensen, B., Klingelhofer, J., Berg, C. H., El-Naaman, C., Grigorian, M., Lukanidin, E., & Ambartsumian, N. (2005). Suppression of tumor development and metastasis formation in mice lacking the S100A4(mts1) gene. *Cancer research*, *65*(9), 3772-3780. https://doi.org/10.1158/0008-5472.CAN-04-4510

Guerrero-Juarez, C. F., Dedhia, P. H., Jin, S., Ruiz-Vega, R., Ma, D., Liu, Y., Yamaga, K., Shestova, O., Gay, D. L., Yang, Z., Kessenbrock, K., Nie, Q., Pear, W. S., Cotsarelis, G., & Plikus, M. V. (2019). Single-cell analysis reveals fibroblast heterogeneity and myeloid-derived adipocyte progenitors in murine skin wounds. *Nat Commun*, *10*(1), 650. https://doi.org/10.1038/s41467-018-08247-x

Guled, M., Pazzaglia, L., Borze, I., Mosakhani, N., Novello, C., Benassi, M. S., & Knuutila, S. (2014). Differentiating soft tissue leiomyosarcoma and undifferentiated pleomorphic sarcoma: A miRNA analysis. *Genes Chromosomes Cancer*, *53*(8), 693-702. https://doi.org/10.1002/gcc.22179

Guo, X., Jo, V., Mills, A., Zhu, S., Lee, C.-H., Espinosa, I., Nucci, M., Varma, S., Forgo, E., Hastie, T., Anderson, S., Ganjoo, K., Beck, A., West, R., Fletcher, C., & van de Rijn, M. (2015). Clinically Relevant Molecular Subtypes in Leiomyosarcoma. *Clinical Cancer Research*, *21*(15), 3501-3511. https://doi.org/10.1158/1078-0432.CCR-14-3141

Gutierrez, L. S., Schulman, A., Brito-Robinson, T., Noria, F., Ploplis, V. A., & Castellino, F. J. (2000). Tumor development is retarded in mice lacking the gene for urokinase-type plasminogen activator or its inhibitor, plasminogen activator inhibitor-1. *Cancer Res*, *60*(20), 5839-5847. https://www.ncbi.nlm.nih.gov/pubmed/11059781

Ha, S. Y., Yeo, S. Y., Xuan, Y. H., & Kim, S. H. (2014). The prognostic significance of cancer-associated fibroblasts in esophageal squamous cell carcinoma. *PLoS One*, *9*(6), e99955. https://doi.org/10.1371/journal.pone.0099955

Habif, G., Crinier, A., André, P., Vivier, E., & Narni-Mancinelli, E. (2019). Targeting natural killer cells in solid tumors. *Cellular & Molecular Immunology*, *16*(5), 415-422. https://doi.org/10.1038/s41423-019-0224-2

Han, C., Liu, T., & Yin, R. (2020). Biomarkers for cancer-associated fibroblasts. *Biomark Res*, *8*(1), 64. https://doi.org/10.1186/s40364-020-00245-w

Han, S., Khuri, F., & Roman, J. (2006). Fibronectin Stimulates Non- Small Cell Lung Carcinoma Cell Growth through Activation of Akt/ Mammalian Target of Rapamycin/ S6 Kinase and Inactivation of LKB1/ AMP- Activated Protein Kinase Signal Pathways. *Cancer research*, *66*(1), 315-323.

Hanahan, D. (2022). Hallmarks of Cancer: New Dimensions. *Cancer Discov*, *12*(1), 31-46. https://doi.org/10.1158/2159-8290.CD-21-1059

Hanahan, D., & Weinberg, Robert a. (2011). Hallmarks of Cancer: The Next Generation. *Cell*, *144*(5), 646-674. https://doi.org/10.1016/j.cell.2011.02.013

Hashimoto, H., Daimaru, Y., & Enjoji, M. (1984). S- 100 protein distribution in liposarcoma An immunoperoxidase study with special reference to the distinction of liposarcoma from myxoid malignant fibrous histiocytoma. *Pathological Anatomy and Histopathology*, *405*(1), 1-10. https://doi.org/10.1007/BF00694921

Hashimoto, M., Uesugi, N., Osakabe, M., Yanagawa, N., Otsuka, K., Kajiwara, Y., Ueno, H., Sasaki, A., & Sugai, T. (2021). Expression Patterns of Microenvironmental Factors and Tenascin-C at the Invasive Front of Stage II and III Colorectal Cancer: Novel Tumor Prognostic Markers. *Front Oncol*, *11*, 690816. https://doi.org/10.3389/fonc.2021.690816

Hawkins, A. G., Basrur, V., da Veiga Leprevost, F., Pedersen, E., Sperring, C., Nesvizhskii, A. I., & Lawlor, E. R. (2018). The Ewing Sarcoma Secretome and Its Response to Activation of Wnt/beta-catenin Signaling. *Mol Cell Proteomics*, *17*(5), 901-912. https://doi.org/10.1074/mcp.RA118.000596

Hawkins, A. G., Julian, C. M., Konzen, S., Treichel, S., Lawlor, E. R., & Bailey, K. M. (2019). Microenvironmental Factors Drive Tenascin C and Src Cooperation to Promote Invadopodia Formation in Ewing Sarcoma. *Neoplasia*, *21*(10), 1063-1072. https://doi.org/10.1016/j.neo.2019.08.007

Hazan, R. B., Qiao, R., Keren, R., Badano, I., & Suyama, K. (2004). Cadherin switch in tumor progression. *Ann N Y Acad Sci*, *1014*, 155-163. https://doi.org/10.1196/annals.1294.016

Heim-Hall, J., & Yohe, S. (2008). Application of immunohistochemistry to soft tissue neoplasms. *Arch. Pathol. Lab. Med.*, *132*(3), 476-489. https://doi.org/10.1043/1543-2165(2008)132[476:AOITST]2.0.CO;2

Herrera, M., Herrera, A., Domínguez, G., Silva, J., García, V., García, J. M., Gómez, I., Soldevilla, B., Muñoz, C., Provencio, M., Campos-Martin, Y., García de Herreros, A., Casal, I., Bonilla, F., & Peña, C. (2013). Cancer-associated fibroblast and M2 macrophage markers together predict outcome in colorectal cancer patients. *Cancer Sci*, *104*(4), 437-444. https://doi.org/10.1111/cas.12096

Hinz, B., Celetta, G., Tomasek, J. J., Gabbiani, G., & Chaponnier, C. (2001). Alpha-smooth muscle actin expression upregulates fibroblast contractile activity. *Mol Biol Cell*, *12*(9), 2730-2741. https://doi.org/10.1091/mbc.12.9.2730

Hinz, B., Pittet, P., Smith-Clerc, J., Chaponnier, C., & Meister, J. J. (2004). Myofibroblast development is characterized by specific cell-cell adherens junctions. *Mol Biol Cell*, *15*(9), 4310-4320. https://doi.org/10.1091/mbc.e04-05-0386

Hoefkens, F., Dehandschutter, C., Somville, J., Meijnders, P., & Van Gestel, D. (2016). Soft tissue sarcoma of the extremities: pending questions on surgery and radiotherapy. *Radiat Oncol*, *11*(1), 136. https://doi.org/10.1186/s13014-016-0668-9

Homsi, J., & Daud, A. I. (2007). Spectrum of activity and mechanism of action of VEGF/PDGF inhibitors. *Cancer Control*, *14*(3), 285-294. https://doi.org/10.1177/107327480701400312

Hwang, K. T., Kim, B. H., Oh, S., Park, S. Y., Jung, J., Kim, J., Choi, I. S., Jeon, S. Y., & Kim, W. Y. (2019). Prognostic Role of. *J Breast Cancer*, *22*(4), 548-561. https://doi.org/10.4048/jbc.2019.22.e55

Isakson, M., de Blacam, C., Whelan, D., McArdle, A., & Clover, A. J. P. (2015). Mesenchymal Stem Cells and Cutaneous Wound Healing: Current Evidence and Future Potential. *Stem cells international*, *2015*(2015), 831095-831095. https://doi.org/10.1155/2015/831095

Ivaska, J., Pallari, H. M., Nevo, J., & Eriksson, J. E. (2007). Novel functions of vimentin in cell adhesion, migration, and signaling. *Exp Cell Res*, *313*(10), 2050-2062. https://doi.org/10.1016/j.yexcr.2007.03.040

Jain, S., Xu, R., Prieto, V. G., & Lee, P. (2010). Molecular classification of soft tissue sarcomas and its clinical applications. *International journal of clinical and experimental pathology*, *3*(4), 416-428.

Järveläinen, H., Sainio, A., Koulu, M., Wight, T. N., & Penttinen, R. (2009). Extracellular matrix molecules: potential targets in pharmacotherapy. *Pharmacol Rev*, *61*(2), 198-223. https://doi.org/10.1124/pr.109.001289

Jennbacken, K., Tesan, T., Wang, W., Gustavsson, H., Damber, J. E., & Welén, K. (2010). N-cadherin increases after androgen deprivation and is associated with metastasis in prostate cancer. *Endocr Relat Cancer*, *17*(2), 469-479. https://doi.org/10.1677/ERC-10-0015

Jo, V. Y., & Fletcher, C. D. M. (2014). WHO classification of soft tissue tumours: An update based on the 2013 (4th) edition. *Pathology*, *46*(2), 95-104. https://doi.org/10.1097/PAT.0000000000000050

Johanna, A. J., & Jeffrey, W. P. (2008). Microenvironmental regulation of metastasis. *Nature Reviews Cancer*, *9*(4), 239. https://doi.org/10.1038/nrc2618

Joly, J. H., Chew, B. T. L., & Graham, N. A. (2021). The landscape of metabolic pathway dependencies in cancer cell lines. *PLoS Comput Biol*, *17*(4), e1008942. https://doi.org/10.1371/journal.pcbi.1008942

Jones, R. L., Ravi, V., Brohl, A. S., Chawla, S., Ganjoo, K. N., Italiano, A., Attia, S., Burgess, M. A., Thornton, K., Cranmer, L. D., Cheang, M. C. U., Liu, L., Robertson, L., Adams, B., Theuer, C., & Maki, R. G. (2022). Efficacy and Safety of TRC105 Plus Pazopanib vs Pazopanib Alone for Treatment of Patients With Advanced Angiosarcoma: A Randomized Clinical Trial. *JAMA Oncol*, *8*(5), 740-747. https://doi.org/10.1001/jamaoncol.2021.3547

Joyce, J. A., & Pollard, J. W. (2009). Microenvironmental regulation of metastasis. *Nat Rev Cancer*, *9*(4), 239-252. https://doi.org/10.1038/nrc2618

Kalluri, R. (2016a). The biology and function of fibroblasts in cancer. *Nature Reviews Cancer*, *16*(9), 582-598. https://doi.org/10.1038/nrc.2016.73

Kalluri, R. (2016b). The biology and function of fibroblasts in cancer. *Nature reviews. Cancer*, *16*(9), 582-598. https://doi.org/10.1038/nrc.2016.73

Kalluri, R., & Zeisberg, M. (2006). Fibroblasts in cancer. *Nature Reviews Cancer*, *6*(5), 392-401. https://doi.org/10.1038/nrc1877

Ke, Y., You, L., Xu, Y., Wu, D., Lin, Q., & Wu, Z. (2022). DPP6 and MFAP5 are associated with immune infiltration as diagnostic biomarkers in distinguishing uterine leiomyosarcoma from leiomyoma. *Front Oncol*, *12*, 1084192. https://doi.org/10.3389/fonc.2022.1084192

Keung, E. Z., Burgess, M., Salazar, R., Parra, E. R., Rodrigues-Canales, J., Bolejack, V., Van Tine, B. A., Schuetze, S. M., Attia, S., Riedel, R. F., Hu, J., Okuno, S. H., Priebat, D. A., Movva, S., Davis, L. E., Reed, D. R., Reuben, A., Roland, C. L., Reinke, D., . . . Tawbi, H. A. (2020). Correlative Analyses of the SARC028 Trial Reveal an Association Between Sarcoma-Associated Immune Infiltrate and Response to Pembrolizumab. *Clin Cancer Res*, *26*(6), 1258-1266. https://doi.org/10.1158/1078-0432.CCR-19-1824

Kidd, S., Spaeth, E., Watson, K., Burks, J., Lu, H., Klopp, A., Andreeff, M., & Marini, F. (2012). Origins of the Tumor Microenvironment: Quantitative Assessment of Adipose- Derived and Bone Marrow–Derived Stroma. *PLoS One*, *7*(2), e30563. https://doi.org/10.1371/journal.pone.0030563

Kim, S. A., Cho, E. J., Lee, S., Cho, Y. Y., Kim, B., Yoon, J.-H., & Park, T. (2020). Changes in serum fibronectin levels predict tumor recurrence in patients with early hepatocellular carcinoma after curative treatment. *Scientific reports*, *10*(1), 21313. https://doi.org/10.1038/s41598-020-78440-w

Kisiel, J. B., Yab, T. C., Taylor, W. R., Chari, S. T., Petersen, G. M., Mahoney, D. W., & Ahlquist, D. A. (2012). Stool DNA testing for the detection of pancreatic cancer: assessment of methylation marker candidates. *Cancer*, *118*(10), 2623-2631. https://doi.org/10.1002/cncr.26558

Kitadai, Y., Sasaki, T., Kuwai, T., Nakamura, T., Bucana, C. D., & Fidler, I. J. (2006). Targeting the expression of platelet-derived growth factor receptor by reactive stroma inhibits growth and metastasis of human colon carcinoma. *Am J Pathol*, *169*(6), 2054-2065. https://doi.org/10.2353/ajpath.2006.060653

Kluin, R. J. C., Kemper, K., Kuilman, T., de Ruiter, J. R., Iyer, V., Forment, J. V., Cornelissen-Steijger, P., de Rink, I., Ter Brugge, P., Song, J. Y., Klarenbeek, S., McDermott, U., Jonkers, J., Velds, A., Adams, D. J., Peeper, D. S., & Krijgsman, O. (2018). XenofilteR: computational deconvolution of mouse and human reads in tumor xenograft sequence data. *BMC Bioinformatics*, *19*(1), 366. https://doi.org/10.1186/s12859-018-2353-5

Kocatürk, B., & Versteeg, H. H. (2015). Orthotopic injection of breast cancer cells into the mammary fat pad of mice to study tumor growth. *J Vis Exp*(96). https://doi.org/10.3791/51967

Koga, K., Nabeshima, K., Aoki, M., Kawakami, T., Hamasaki, M., Toole, B. P., Nakayama, J., & Iwasaki, H. (2007). Emmprin in epithelioid sarcoma: Expression in tumor cell membrane and stimulation of MMP- 2 production in tumor- associated fibroblasts. *International Journal of Cancer*, *120*(4), 761-768. https://doi.org/10.1002/ijc.22412

Koh, Y. E., Choi, E. H., Kim, J. W., & Kim, K. P. (2022). The Kleisin Subunits of Cohesin are Involved in the Fate Determination of Embryonic Stem Cells. *Mol Cells*. https://doi.org/10.14348/molcells.2022.2042

Kojima, Y., Acar, A., Eaton, E. N., Mellody, K. T., Scheel, C., Ben-Porath, I., Onder, T. T., Wang, Z. C., Richardson, A. L., Weinberg, R. A., & Orimo, A. (2010). Autocrine TGF-beta and stromal cell-derived factor-1 (SDF-1) signaling drives the evolution of tumor-promoting mammary stromal

myofibroblasts. *Proc Natl Acad Sci U S A*, *107*(46), 20009-20014. https://doi.org/10.1073/pnas.1013805107

Krieg, T. (2008). Fibroblast – matrix interactions in tissue repair and fibrosis. *Experimental Dermatology*, *17*(10), 877-879. https://doi.org/10.1111/j.1600-0625.2008.00789_3.x

Krizbai, I. A., Gasparics, Á., Nagyőszi, P., Fazakas, C., Molnár, J., Wilhelm, I., Bencs, R., Rosivall, L., & Sebe, A. (2015). Endothelial-mesenchymal transition of brain endothelial cells: possible role during metastatic extravasation. *PLoS One*, *10*(3), e0119655. https://doi.org/10.1371/journal.pone.0119655

Kujawa, K. A., Zembala-Nożyńska, E., Cortez, A. J., Kujawa, T., Kupryjańczyk, J., & Lisowska, K. M. (2020). Fibronectin and Periostin as Prognostic Markers in Ovarian Cancer. *Cells*, *9*(1). https://doi.org/10.3390/cells9010149

Kuperwasser, C., Chavarria, T., Wu, M., Magrane, G., Gray, J. W., Carey, L., Richardson, A., & Weinberg, R. A. (2004). Reconstruction of functionally normal and malignant human breast tissues in mice. *Proc Natl Acad Sci U S A*, *101*(14), 4966-4971. https://doi.org/10.1073/pnas.0401064101

Kuzmich, N. N., Sivak, K. V., Chubarev, V. N., Porozov, Y. B., Savateeva-Lyubimova, T. N., & Peri, F. (2017). TLR4 Signaling Pathway Modulators as Potential Therapeutics in Inflammation and Sepsis. *Vaccines (Basel)*, *5*(4). https://doi.org/10.3390/vaccines5040034

Lagacé, R., Schürch, W., & Seemayer, T. A. (1980). Myofibroblasts in soft tissue sarcomas. *Virchows Archiv A Pathological Anatomy and Histology*, *389*(1), 1-11. https://doi.org/10.1007/BF00428664

Lai, D., Ma, L., & Wang, F. (2012). Fibroblast activation protein regulates tumor- associated fibroblasts and epithelial ovarian cancer cells. *International Journal of Oncology*, *41*(2), 541-550. https://doi.org/10.3892/ijo.2012.1475

Langmead, B., & Salzberg, S. L. (2012). Fast gapped-read alignment with Bowtie 2. *Nat Methods*, *9*(4), 357-359. https://doi.org/10.1038/nmeth.1923

Lee, M. Y., Park, C., Berent, R. M., Park, P. J., Fuchs, R., Syn, H., Chin, A., Townsend, J., Benson, C. C., Redelman, D., Shen, T. W., Park, J. K., Miano, J. M., Sanders, K. M., & Ro, S. (2015). Smooth Muscle Cell Genome Browser: Enabling the Identification of Novel Serum Response Factor Target Genes. *PLoS One*, *10*(8), e0133751. https://doi.org/10.1371/journal.pone.0133751

Lei, X., Lei, Y., Li, J. K., Du, W. X., Li, R. G., Yang, J., Li, J., Li, F., & Tan, H. B. (2020). Immune cells within the tumor microenvironment: Biological functions and roles in cancer immunotherapy. *Cancer Lett*, *470*, 126-133. https://doi.org/10.1016/j.canlet.2019.11.009

Li, H., Fan, X., & Houghton, J. (2007). Tumor microenvironment: The role of the tumor stroma in cancer. *Journal of Cellular Biochemistry*, *101*(4), 805-815. https://doi.org/10.1002/jcb.21159

Li, H., Handsaker, B., Wysoker, A., Fennell, T., Ruan, J., Homer, N., Marth, G., Abecasis, G., Durbin, R., & Subgroup, G. P. D. P. (2009). The Sequence Alignment/Map format and SAMtools. *Bioinformatics*, *25*(16), 2078-2079. https://doi.org/10.1093/bioinformatics/btp352

Li, Z., Li, Y., Liu, S., & Qin, Z. (2020). Extracellular S100A4 as a key player in fibrotic diseases. *J Cell Mol Med*, *24*(11), 5973-5983. https://doi.org/10.1111/jcmm.15259

Li, Z. H., Dulyaninova, N. G., House, R. P., Almo, S. C., & Bresnick, A. R. (2010). S100A4 regulates macrophage chemotaxis. *Mol Biol Cell*, *21*(15), 2598-2610. https://doi.org/10.1091/mbc.e09-07-0609

Liberzon, A., Birger, C., Thorvaldsdóttir, H., Ghandi, M., Mesirov, J. P., & Tamayo, P. (2015). The Molecular Signatures Database (MSigDB) hallmark gene set collection. *Cell Syst*, *1*(6), 417-425. https://doi.org/10.1016/j.cels.2015.12.004

Libura, J., Drukala, J., Majka, M., Tomescu, O., Navenot, J. M., Kucia, M., Marquez, L., Peiper, S. C., Barr, F. G., Janowska-Wieczorek, A., & Ratajczak, M. Z. (2002). CXCR4- SDF- 1 signaling is active in

rhabdomyosarcoma cells and regulates locomotion, chemotaxis, and adhesion. *Blood*, *100*(7), 2597-2606. https://doi.org/10.1182/blood-2002-01-0031

Liska, D., Xiang, S., Karagkounis, G., Signs, S., Kalady, M., & Huang, E. (2017). 1020 - Cancer Associated Fibroblasts Mediate Resistance to Radiotherapy in Rectal Cancer Cells. *Gastroenterology*, *152*(5), S1234-S1234. https://doi.org/10.1016/S0016-5085(17)34109-4

Liu, R., Hossain, M. M., & Jin, J. P. (2017). The Expression and Degradation of SM22- Alpha/ Transgelin are Regulated by Mechanical Tension in the Cytoskeleton. *Biophysical Journal*, *112*(3), 435a-435a. https://doi.org/10.1016/j.bpj.2016.11.2325

Liu, X., Jakubowski, M., & Hunt, J. L. (2011). KRAS gene mutation in colorectal cancer is correlated with increased proliferation and spontaneous apoptosis. *Am J Clin Pathol*, *135*(2), 245-252. https://doi.org/10.1309/AJCP7FO2VAXIVSTP

Loeffler, M., Krüger, J. A., Niethammer, A. G., & Reisfeld, R. A. (2006). Targeting tumor- associated fibroblasts improves cancer chemotherapy by increasing intratumoral drug uptake. *The Journal of clinical investigation*, *116*(7), 1955-1962. https://doi.org/10.1172/JCI26532

Lowy, C. M., & Oskarsson, T. (2015). Tenascin C in metastasis: A view from the invasive front. *Cell Adh Migr*, *9*(1-2), 112-124. https://doi.org/10.1080/19336918.2015.1008331

Lu, P., Weaver, V. M., & Werb, Z. (2012). The extracellular matrix: a dynamic niche in cancer progression. *The Journal of cell biology*, *196*(4), 395-406. https://doi.org/10.1083/jcb.201102147

Lugano, R., Ramachandran, M., & Dimberg, A. (2020). Tumor angiogenesis: causes, consequences, challenges and opportunities. *Cell Mol Life Sci*, *77*(9), 1745-1770. https://doi.org/10.1007/s00018-019-03351-7

Maehira, H., Miyake, T., Iida, H., Tokuda, A., Mori, H., Yasukawa, D., Mukaisho, K.-i., Shimizu, T., & Tani, M. (2019). Vimentin Expression in Tumor Microenvironment Predicts Survival in Pancreatic Ductal Adenocarcinoma: Heterogeneity in Fibroblast Population. *Annals of Surgical Oncology*, *26*(13), 4791-4804. https://doi.org/10.1245/s10434-019-07891-x

Mahmood, T., & Yang, P.-C. (2012). Western blot: technique, theory, and trouble shooting. *North American journal of medical sciences*, *4*(9), 429-434. https://doi.org/10.4103/1947-2714.100998

Marion, N. W., & Mao, J. J. (2006). Mesenchymal Stem Cells and Tissue Engineering. *Methods in Enzymology*, *420*, 339-361. https://doi.org/10.1016/S0076-6879(06)20016-8

Marsh, D., Suchak, K., Moutasim, K. A., Vallath, S., Hopper, C., Jerjes, W., Upile, T., Kalavrezos, N., Violette, S. M., Weinreb, P. H., Chester, K. A., Chana, J. S., Marshall, J. F., Hart, I. R., Hackshaw, A. K., Piper, K., & Thomas, G. J. (2011). Stromal features are predictive of disease mortality in oral cancer patients. *J Pathol*, *223*(4), 470-481. https://doi.org/10.1002/path.2830

Matsuyama, M., Tanaka, H., Inoko, A., Goto, H., Yonemura, S., Kobori, K., Hayashi, Y., Kondo, E., Itohara, S., Izawa, I., & Inagaki, M. (2013). Defect of mitotic vimentin phosphorylation causes microophthalmia and cataract via aneuploidy and senescence in lens epithelial cells. *J Biol Chem*, *288*(50), 35626-35635. https://doi.org/10.1074/jbc.M113.514737

Matushansky, I., Charytonowicz, E., Mills, J., Siddiqi, S., Hricik, T., & Cordon-Cardo, C. (2009). MFH classification: differentiating undifferentiated pleomorphic sarcoma in the 21st Century. *Expert Rev Anticancer Ther*, *9*(8), 1135-1144. https://doi.org/10.1586/era.09.76

Mendez, M. G., Kojima, S.-I., & Goldman, R. D. (2010). Vimentin induces changes in cell shape, motility, and adhesion during the epithelial to mesenchymal transition. *FASEB journal : official publication of the Federation of American Societies for Experimental Biology*, *24*(6), 1838-1851. https://doi.org/10.1096/fj.09-151639

Menendez, S. T., Rey, V., Martinez-Cruzado, L., Gonzalez, M. V., Morales-Molina, A., Santos, L., Blanco, V., Alvarez, C., Estupiñan, O., Allonca, E., Rodrigo, J. P., García-Castro, J., Garcia-Pedrero, J. M., & Rodriguez, R. (2020). SOX2 Expression and Transcriptional Activity Identifies a Subpopulation of

Cancer Stem Cells in Sarcoma with Prognostic Implications. *Cancers (Basel)*, *12*(4). https://doi.org/10.3390/cancers12040964

Mhawech, P., Dulguerov, P., Assaly, M., Ares, C., & Allal, A. S. (2005). EB-D fibronectin expression in squamous cell carcinoma of the head and neck. *Oral Oncol*, *41*(1), 82-88. https://doi.org/10.1016/j.oraloncology.2004.07.003

Midwood, K. S., & Orend, G. (2009). The role of tenascin-C in tissue injury and tumorigenesis. *J Cell Commun Signal*, *3*(3-4), 287-310. https://doi.org/10.1007/s12079-009-0075-1

Miettinen, M. (2014). Immunohistochemistry of soft tissue tumours - review with emphasis on 10 markers. *Histopathology*, *64*(1), 101-118. https://doi.org/10.1111/his.12298

Miller, M. S., & Miller, L. D. (2011). RAS Mutations and Oncogenesis: Not all RAS Mutations are Created Equally. *Front Genet*, *2*, 100. https://doi.org/10.3389/fgene.2011.00100

Miyazaki, Y., Oda, T., Mori, N., & Kida, Y. S. (2020). Adipose-derived mesenchymal stem cells differentiate into pancreatic cancer-associated fibroblasts in vitro. *FEBS Open Bio*, *10*(11), 2268-2281. https://doi.org/https://doi.org/10.1002/2211-5463.12976

Monika, E., & Olle, E. (2015). Microenvironmental targets in sarcoma. *Frontiers in Oncology*, *5*. https://doi.org/10.3389/fonc.2015.00248

Morozov, A., Downey, R. J., Healey, J., Moreira, A. L., Lou, E., Franceschino, A., Dogan, Y., Leung, R., Edgar, M., Laquaglia, M., Maki, R. G., & Moore, M. A. S. (2010). Benign mesenchymal stromal cells in human sarcomas. *Clinical cancer research : an official journal of the American Association for Cancer Research*, *16*(23), 5630-5640. https://doi.org/10.1158/1078-0432.CCR-09-2886

Mrozik, K. M., Blaschuk, O. W., Cheong, C. M., Zannettino, A. C. W., & Vandyke, K. (2018). N-cadherin in cancer metastasis, its emerging role in haematological malignancies and potential as a therapeutic target in cancer. *BMC Cancer*, *18*(1), 939. https://doi.org/10.1186/s12885-018-4845-0

Muchlińska, A., Nagel, A., Popęda, M., Szade, J., Niemira, M., Zieliński, J., Skokowski, J., Bednarz-Knoll, N., & Żaczek, A. J. (2022). Alpha-smooth muscle actin-positive cancer-associated fibroblasts secreting osteopontin promote growth of luminal breast cancer. *Cell Mol Biol Lett*, *27*(1), 45. https://doi.org/10.1186/s11658-022-00351-7

Muliaditan, T., Caron, J., Okesola, M., Opzoomer, J. W., Kosti, P., Georgouli, M., Gordon, P., Lall, S., Kuzeva, D. M., Pedro, L., Shields, J. D., Gillett, C. E., Diebold, S. S., Sanz-Moreno, V., Ng, T., Hoste, E., & Arnold, J. N. (2018). Macrophages are exploited from an innate wound healing response to facilitate cancer metastasis. *Nat Commun*, *9*(1), 2951. https://doi.org/10.1038/s41467-018-05346-7

Natarajan, V., Ha, S., Delgado, A., Jacobson, R., Alhalhooly, L., Choi, Y., & Kim, J. (2022). Acquired αSMA Expression in Pericytes Coincides with Aberrant Vascular Structure and Function in Pancreatic Ductal Adenocarcinoma. *Cancers (Basel)*, *14*(10). https://doi.org/10.3390/cancers14102448

Nieminen, M., Henttinen, T., Merinen, M., Marttila-Ichihara, F., Eriksson, J. E., & Jalkanen, S. (2006). Vimentin function in lymphocyte adhesion and transcellular migration. *Nat Cell Biol*, *8*(2), 156-162. https://doi.org/10.1038/ncb1355

Nims, R., Sykes, G., Cottrill, K., Ikonomi, P., & Elmore, E. (2010). Short tandem repeat profiling: part of an overall strategy for reducing the frequency of cell misidentification. *In Vitro Cellular & Developmental Biology - Animal*, *46*(10), 811-819. https://doi.org/10.1007/s11626-010-9352-9

Nishitani, Y., Iwano, M., Yamaguchi, Y., Harada, K., Nakatani, K., Akai, Y., Nishino, T., Shiiki, H., Kanauchi, M., Saito, Y., & Neilson, E. G. (2005). Fibroblast-specific protein 1 is a specific prognostic marker for renal survival in patients with IgAN. *Kidney Int*, *68*(3), 1078-1085. https://doi.org/10.1111/j.1523-1755.2005.00500.x

Noma, K., Smalley, K. S. M., Lioni, M., Naomoto, Y., Tanaka, N., El–Deiry, W., King, A. J., Nakagawa, H., & Herlyn, M. (2008). The Essential Role of Fibroblasts in Esophageal Squamous Cell Carcinoma–

Induced Angiogenesis. *Gastroenterology*, *134*(7), 1981-1993. https://doi.org/10.1053/j.gastro.2008.02.061

Nurmik, M., Ullmann, P., Rodriguez, F., Haan, S., & Letellier, E. (2020). In search of definitions: Cancer-associated fibroblasts and their markers. *Int J Cancer*, *146*(4), 895-905. https://doi.org/10.1002/ijc.32193

Oakley, B. R., Paolillo, V., & Zheng, Y. (2015). γ-Tubulin complexes in microtubule nucleation and beyond. *Mol Biol Cell*, *26*(17), 2957-2962. https://doi.org/10.1091/mbc.E14-11-1514

Orimo, A., Gupta, P. B., Sgroi, D. C., Arenzana-Seisdedos, F., Delaunay, T., Naeem, R., Carey, V. J., Richardson, A. L., & Weinberg, R. A. (2005). Stromal fibroblasts present in invasive human breast carcinomas promote tumor growth and angiogenesis through elevated SDF-1/CXCL12 secretion. *Cell*, *121*(3), 335-348. https://doi.org/10.1016/j.cell.2005.02.034

Orth, M. F., Buecklein, V. L., Kampmann, E., Subklewe, M., Noessner, E., Cidre-Aranaz, F., Romero-Pérez, L., Wehweck, F. S., Lindner, L., Issels, R., Kirchner, T., Altendorf-Hofmann, A., Grünewald, T. G. P., & Knösel, T. (2020). A comparative view on the expression patterns of PD-L1 and PD-1 in soft tissue sarcomas. *Cancer Immunology, Immunotherapy*, *69*(7), 1353-1362. https://doi.org/10.1007/s00262-020-02552-5

Österreicher, C. H., Penz-Österreicher, M., Grivennikov, S. I., Guma, M., Koltsova, E. K., Datz, C., Sasik, R., Hardiman, G., Karin, M., & Brenner, D. A. (2011). Fibroblast-specific protein 1 identifies an inflammatory subpopulation of macrophages in the liver. *Proc Natl Acad Sci U S A*, *108*(1), 308-313. https://doi.org/10.1073/pnas.1017547108

Paciorek, T., Sauer, M., Balla, J., Wiśniewska, J., & Friml, J. (2006). Immunocytochemical technique for protein localization in sections of plant tissues. *Nat Protoc*, *1*(1), 104-107. https://doi.org/10.1038/nprot.2006.16

Painter, J. T., Clayton, N. P., & Herbert, R. A. (2010). Useful Immunohistochemical Markers of Tumor Differentiation. *Toxicologic Pathology*, *38*(1), 131-141. https://doi.org/10.1177/0192623309356449

Pankova, V., Thway, K., Jones, R. L., & Huang, P. H. (2021). The Extracellular Matrix in Soft Tissue Sarcomas: Pathobiology and Cellular Signalling. *Front Cell Dev Biol*, *9*, 763640. https://doi.org/10.3389/fcell.2021.763640

Paraiso, K. H. T., & Smalley, K. S. M. (2013). Fibroblast- mediated drug resistance in cancer. *Biochemical Pharmacology*, *85*(8), 1033-1041. https://doi.org/10.1016/j.bcp.2013.01.018

Park, S. B., Seo, K. W., So, A. Y., Seo, M. S., Yu, K. R., Kang, S. K., & Kang, K. S. (2012). SOX2 has a crucial role in the lineage determination and proliferation of mesenchymal stem cells through Dickkopf-1 and c-MYC. *Cell Death Differ*, *19*(3), 534-545. https://doi.org/10.1038/cdd.2011.137

Pickup, M. W., Mouw, J. K., & Weaver, V. M. (2014). The extracellular matrix modulates the hallmarks of cancer. In (Vol. 15, pp. 1243-1253).

Piersma, B., Hayward, M. K., & Weaver, V. M. (2020). Fibrosis and cancer: A strained relationship. *Biochim Biophys Acta Rev Cancer*, *1873*(2), 188356. https://doi.org/10.1016/j.bbcan.2020.188356

Potenta, S., Zeisberg, E., & Kalluri, R. (2008). The role of endothelial-to- mesenchymal transition in cancer progression. *British journal of cancer*, *99*(9), 1375-1379. https://doi.org/10.1038/sj.bjc.6604662

Povýšil, C., Tomanova, R., & Matějovsky, Z. (1997). Muscle- specific actin expression in chondroblastomas. *Human Pathology*, *28*(3), 316-320. https://doi.org/10.1016/S0046-8177(97)90130-1

Puré, E., & Blomberg, R. (2018). Pro-tumorigenic roles of fibroblast activation protein in cancer: back to the basics. *Oncogene*, *37*(32), 4343-4357. https://doi.org/10.1038/s41388-018-0275-3

Quante, M., Tu, S. P., Tomita, H., Gonda, T., Wang, S. S. W., Takashi, S., Baik, G. H., Shibata, W., Diprete, B., Betz, K. S., Friedman, R., Varro, A., Tycko, B., & Wang, T. C. (2011). Bone Marrow- Derived Myofibroblasts Contribute to the Mesenchymal Stem Cell Niche and Promote Tumor Growth. *Cancer Cell*, *19*(2), 257-272. https://doi.org/10.1016/j.ccr.2011.01.020

Raitz, R., Martins, M. D., & Araújo, V. C. (2003). A study of the extracellular matrix in salivary gland tumors. *J Oral Pathol Med*, *32*(5), 290-296. https://doi.org/10.1034/j.1600-0714.2003.00019.x

Rastegar, F., Shenaq, D., Huang, J., Zhang, W., Zhang, B.-Q., He, B.-C., Chen, L., Zuo, G.-W., Luo, Q., Shi, Q., Wagner, E. R., Huang, E., Gao, Y., Gao, J.-L., Kim, S. H., Zhou, J.-Z., Bi, Y., Su, Y., Zhu, G., . . . He, T.-C. (2010). Mesenchymal stem cells: Molecular characteristics and clinical applications. *World journal of stem cells*, *2*(4), 67-80. https://doi.org/10.4252/wjsc.v2.i4.67

Reardon, D. A., Akabani, G., Coleman, R. E., Friedman, A. H., Friedman, H. S., II, J. E. H., McLendon, R. E., Pegram, C. N., Provenzale, J. M., Quinn, J. A., Rich, J. N., Vredenburgh, J. J., Desjardins, A., Guruangan, S., Badruddoja, M., Dowell, J. M., Wong, T. Z., Zhao, X.-G., Zalutsky, M. R., & Bigner, D. D. (2006). Salvage Radioimmunotherapy With Murine Iodine-131–Labeled Antitenascin Monoclonal Antibody 81C6 for Patients With Recurrent Primary and Metastatic Malignant Brain Tumors: Phase II Study Results. *Journal of Clinical Oncology*, *24*(1), 115-122. https://doi.org/10.1200/jco.2005.03.4082

Ribatti, D., Mangialardi, G., & Vacca, A. (2006). Stephen Paget and the ' seed and soil' theory of metastatic dissemination. *Clinical and Experimental Medicine*, *6*(4), 145-149. https://doi.org/10.1007/s10238-006-0117-4

Ribeiro, A. L., & Okamoto, O. K. (2015). Combined effects of pericytes in the tumor microenvironment. *Stem Cells Int*, *2015*, 868475. https://doi.org/10.1155/2015/868475

Ridge, S. M., Sullivan, F. J., & Glynn, S. A. (2017). Mesenchymal stem cells: key players in cancer progression. *Molecular cancer*, *16*(1), 31-31. https://doi.org/10.1186/s12943-017-0597-8

Robin, Y. M., Penel, N., Pérot, G., Neuville, A., Vélasco, V., Ranchère-Vince, D., Terrier, P., & Coindre, J. M. (2013). Transgelin is a novel marker of smooth muscle differentiation that improves diagnostic accuracy of leiomyosarcomas: a comparative immunohistochemical reappraisal of myogenic markers in 900 soft tissue tumors. *Mod Pathol*, *26*(4), 502-510. https://doi.org/10.1038/modpathol.2012.192

Robles-Tenorio, A., & Solis-Ledesma, G. (2022). Undifferentiated Pleomorphic Sarcoma. In *StatPearls*. StatPearls Publishing

Copyright © 2022, StatPearls Publishing LLC.

Ruiz-Zapata, A. M., Heinz, A., Kerkhof, M. H., van de Westerlo-van Rijt, C., Schmelzer, C. E. H., Stoop, R., Kluivers, K. B., & Oosterwijk, E. (2020). Extracellular Matrix Stiffness and Composition Regulate the Myofibroblast Differentiation of Vaginal Fibroblasts. *Int J Mol Sci*, *21*(13). https://doi.org/10.3390/ijms21134762

Rusch, M., Nakitandwe, J., Shurtleff, S., Newman, S., Zhang, Z., Edmonson, M. N., Parker, M., Jiao, Y., Ma, X., Liu, Y., Gu, J., Walsh, M. F., Becksfort, J., Thrasher, A., Li, Y., McMurry, J., Hedlund, E., Patel, A., Easton, J., . . . Zhang, J. (2018). Clinical cancer genomic profiling by three-platform sequencing of whole genome, whole exome and transcriptome. *Nature Communications*, *9*(1), 3962. https://doi.org/10.1038/s41467-018-06485-7

Saggioro, M., D'Angelo, E., Bisogno, G., Agostini, M., & Pozzobon, M. (2020). Carcinoma and Sarcoma Microenvironment at a Glance: Where We Are. *Front Oncol*, *10*, 76. https://doi.org/10.3389/fonc.2020.00076

Sahai, E., Astsaturov, I., Cukierman, E., DeNardo, D. G., Egeblad, M., Evans, R. M., Fearon, D., Greten, F. R., Hingorani, S. R., Hunter, T., Hynes, R. O., Jain, R. K., Janowitz, T., Jorgensen, C., Kimmelman, A. C., Kolonin, M. G., Maki, R. G., Powers, R. S., Puré, E., . . . Werb, Z. (2020). A framework for

advancing our understanding of cancer-associated fibroblasts. *Nat Rev Cancer*, *20*(3), 174-186. https://doi.org/10.1038/s41568-019-0238-1

Saito, K., Kobayashi, E., Yoshida, A., Araki, Y., Kubota, D., Tanzawa, Y., Kawai, A., Yanagawa, T., Takagishi, K., & Chuman, H. (2017). Angiomatoid fibrous histiocytoma: a series of seven cases including genetically confirmed aggressive cases and a literature review. *BMC Musculoskelet Disord*, *18*(1), 31. https://doi.org/10.1186/s12891-017-1390-y

Salawu, A., Fernando, M., Hughes, D., Reed, M. W. R., Woll, P., Greaves, C., Day, C., Alhajimohammed, M., & Sisley, K. (2016). Establishment and molecular characterisation of seven novel soft-tissue sarcoma cell lines. *British journal of cancer*, *115*(9), 1058-1068. https://doi.org/10.1038/bjc.2016.259

Salawu, A., Wright, K., Al-Kathiri, A., Wyld, L., Reed, M., & Sisley, K. (2018). Sister Chromatid Exchange and Genomic Instability in Soft Tissue Sarcomas: Potential Implications for Response to DNA-Damaging Treatments. *Sarcoma*, *2018*, 3082526. https://doi.org/10.1155/2018/3082526

Salerno, M., Avnet, S., Bonuccelli, G., Eramo, A., De Maria, R., Gambarotti, M., Gamberi, G., & Baldini, N. (2013). Sphere- forming cell subsets with cancer stem cell properties in human musculoskeletal sarcomas. *International Journal of Oncology*, *43*(1), 95-102. https://doi.org/10.3892/ijo.2013.1927

Salvatore, V., Focaroli, S., Teti, G., Mazzotti, A., & Falconi, M. (2015). Changes in the gene expression of co- cultured human fibroblast cells and osteosarcoma cells: the role of microenvironment. *Oncotarget*, *6*(30), 28988-28998. https://doi.org/10.18632/oncotarget.4902

Salvatore, V., Teti, G., Bolzani, S., Focaroli, S., Durante, S., Mazzotti, M., & Falconi, M. (2014). Simulating tumor microenvironment: changes in protein expression in an in vitro co- culture system. *Cancer Cell International*, *14*(1). https://doi.org/10.1186/1475-2867-14-40

Sannino, G., Marchetto, A., Ranft, A., Jabar, S., Zacherl, C., Alba-Rubio, R., Stein, S., Wehweck, F. S., Kiran, M. M., Hölting, T. L. B., Musa, J., Romero-Pérez, L., Cidre-Aranaz, F., Knott, M. M. L., Li, J., Jürgens, H., Sastre, A., Alonso, J., Da Silveira, W., . . . Grünewald, T. G. P. (2019). Gene expression and immunohistochemical analyses identify SOX2 as major risk factor for overall survival and relapse in Ewing sarcoma patients. *EBioMedicine*, *47*, 156-162. https://doi.org/10.1016/j.ebiom.2019.08.002

Satelli, A., & Li, S. (2011). Vimentin in cancer and its potential as a molecular target for cancer therapy. *Cellular and Molecular Life Sciences*, *68*(18), 3033-3046. https://doi.org/10.1007/s00018-011-0735-1

Savvidou, O., Papakonstantinou, O., Lakiotaki, E., Zafeiris, I., Melissaridou, D., Korkolopoulou, P., & Papagelopoulos, P. J. (2021). Surface bone sarcomas: an update on current clinicopathological diagnosis and treatment. *EFORT Open Rev*, *6*(10), 905-917. https://doi.org/10.1302/2058-5241.6.210064

Sbaraglia, M., Bellan, E., & Dei Tos, A. P. (2021). The 2020 WHO Classification of Soft Tissue Tumours: news and perspectives. *Pathologica*, *113*(2), 70-84. https://doi.org/10.32074/1591-951X-213

Schaefer, T., & Lengerke, C. (2020). SOX2 protein biochemistry in stemness, reprogramming, and cancer: the PI3K/AKT/SOX2 axis and beyond. *Oncogene*, *39*(2), 278-292. https://doi.org/10.1038/s41388-019-0997-x

Schürch, W., Skalli, O., Seemayer, T. A., & Gabbiani, G. (1987). Intermediate filament proteins and actin isoforms as markers for soft tissue tumor differentiation and origin. I. Smooth muscle tumors. *The American journal of pathology*, *128*(1), 91-103.

Scott. (2003). A phase I dose-escalastion study of sibrtuzumab in patients with advanced or metastatic fibroblast activation protein-positive cancer. *Clin Cancer Res*, 1639-1647.

Scully, R., Panday, A., Elango, R., & Willis, N. A. (2019). DNA double-strand break repair-pathway choice in somatic mammalian cells. *Nat Rev Mol Cell Biol*, *20*(11), 698-714. https://doi.org/10.1038/s41580-019-0152-0

Shaulian, E., & Karin, M. (2001). AP-1 in cell proliferation and survival. *Oncogene*, *20*(19), 2390-2400. https://doi.org/10.1038/sj.onc.1204383

Shen, Q., Uray, I. P., Li, Y., Krisko, T. I., Strecker, T. E., Kim, H. T., & Brown, P. H. (2008). The AP-1 transcription factor regulates breast cancer cell growth via cyclins and E2F factors. *Oncogene*, *27*(3), 366-377. https://doi.org/10.1038/sj.onc.1210643

Shen, Z., Qin, X., Yan, M., Li, R., Chen, G., Zhang, J., & Chen, W. (2017). Cancer- associated fibroblasts promote cancer cell growth through a miR- 7- RASSF2- PAR- 4 axis in the tumor microenvironment. *Oncotarget*, *8*(1), 1290-1303. https://doi.org/10.18632/oncotarget.13609

Shi, J., Hou, Z., Yan, J., Qiu, W., Liang, L., Meng, M., Li, L., Wang, X., Xie, Y., Jiang, L., & Wang, W. (2020). The prognostic significance of fibroblast activation protein-α in human lung adenocarcinoma. *Annals of Translational Medicine*, *8*(5), 224. https://atm.amegroups.com/article/view/37401

Shi, J., Li, Y., Jia, R., & Fan, X. (2020). The fidelity of cancer cells in PDX models: Characteristics, mechanism and clinical significance. *Int J Cancer*, *146*(8), 2078-2088. https://doi.org/10.1002/ijc.32662

Shiga, K., Hara, M., Nagasaki, T., Sato, T., Takahashi, H., & Takeyama, H. (2015). Cancer- Associated Fibroblasts: Their Characteristics and Their Roles in Tumor Growth. *Cancers*, *7*(4), 2443-2458. https://doi.org/10.3390/cancers7040902

Sholl, L. M., Long, K. B., & Hornick, J. L. (2010). Sox2 expression in pulmonary non-small cell and neuroendocrine carcinomas. *Appl Immunohistochem Mol Morphol*, *18*(1), 55-61. https://doi.org/10.1097/PAI.0b013e3181b16b88

Sie, M., de Bont, E. S., Scherpen, F. J., Hoving, E. W., & den Dunnen, W. F. (2010). Tumour vasculature and angiogenic profile of paediatric pilocytic astrocytoma; is it much different from glioblastoma? *Neuropathol Appl Neurobiol*, *36*(7), 636-647. https://doi.org/10.1111/j.1365-2990.2010.01113.x

Simian, M., Hirai, Y., Navre, M., Werb, Z., Lochter, A., & Bissell, M. J. (2001). The interplay of matrix metalloproteinases, morphogens and growth factors is necessary for branching of mammary epithelial cells. *Development (Cambridge, England)*, *128*(16), 3117-3131.

Sinn, M., Denkert, C., Striefler, J. K., Pelzer, U., Stieler, J. M., Bahra, M., Lohneis, P., Dörken, B., Oettle, H., Riess, H., & Sinn, B. V. (2014). α-Smooth muscle actin expression and desmoplastic stromal reaction in pancreatic cancer: results from the CONKO-001 study. *Br J Cancer*, *111*(10), 1917-1923. https://doi.org/10.1038/bjc.2014.495

Skoda, J., Nunukova, A., Loja, T., Zambo, I., Neradil, J., Mudry, P., Zitterbart, K., Hermanova, M., Hampl, A., Sterba, J., & Veselska, R. (2016). Cancer stem cell markers in pediatric sarcomas: Sox2 is associated with tumorigenicity in immunodeficient mice. *Tumour Biol*, *37*(7), 9535-9548. https://doi.org/10.1007/s13277-016-4837-0

Song, S., Ewald, A. J., Stallcup, W., Werb, Z., & Bergers, G. (2005). PDGFRbeta+ perivascular progenitor cells in tumours regulate pericyte differentiation and vascular survival. *Nat Cell Biol*, *7*(9), 870-879. https://doi.org/10.1038/ncb1288

Spaeth, E., Dembinski, J., Sasser, A., Watson, K., Klopp, A., Hall, B., Andreeff, M., & Marini, F. (2009). Mesenchymal Stem Cell Transition to Tumor- Associated Fibroblasts Contributes to Fibrovascular Network Expansion and Tumor Progression. *PLoS One*, *4*(4), e4992. https://doi.org/10.1371/journal.pone.0004992

Stahl, D., Gentles, A. J., Thiele, R., & Gütgemann, I. (2019). Prognostic profiling of the immune cell microenvironment in Ewing´s Sarcoma Family of Tumors. *Oncoimmunology*, *8*(12), e1674113. https://doi.org/10.1080/2162402X.2019.1674113

Strahm, B., Durbin, A., Sexsmith, E., & Malkin, D. (2008). The CXCR4-SDF1α axis is a critical mediator of rhabdomyosarcoma metastatic signaling induced by bone marrow stroma. *Official Journal of the Metastasis Research Society*, *25*(1), 1-10. https://doi.org/10.1007/s10585-007-9094-6

Stroberg, W., & Schnell, S. (2017). On the origin of non-membrane-bound organelles, and their physiological function. *J Theor Biol*, *434*, 42-49. https://doi.org/10.1016/j.jtbi.2017.04.006

Sun, L., Sun, C., Liang, Z., Li, H., Chen, L., Luo, H., Zhang, H., Ding, P., Sun, X., Qin, Z., & Zhao, Y. (2015). FSP1(+) fibroblast subpopulation is essential for the maintenance and regeneration of medullary thymic epithelial cells. *Sci Rep*, *5*, 14871. https://doi.org/10.1038/srep14871

Svendsen, A., Verhoeff, J. J., Immervoll, H., Brøgger, J. C., Kmiecik, J., Poli, A., Netland, I. A., Prestegarden, L., Planagumà, J., Torsvik, A., Kjersem, A. B., Sakariassen, P., Heggdal, J. I., Van Furth, W. R., Bjerkvig, R., Lund-Johansen, M., Enger, P., Felsberg, J., Brons, N. H., . . . Chekenya, M. (2011). Expression of the progenitor marker NG2/CSPG4 predicts poor survival and resistance to ionising radiation in glioblastoma. *Acta Neuropathol*, *122*(4), 495-510. https://doi.org/10.1007/s00401-011-0867-2

Tanabe, S. (2014). Role of mesenchymal stem cells in cell life and their signaling. *World journal of stem cells*, *6*(1), 24-32. https://doi.org/10.4252/wjsc.v6.i1.24

Tang, P. A., & Moore, M. J. (2013). Aflibercept in the treatment of patients with metastatic colorectal cancer: latest findings and interpretations. *Therap Adv Gastroenterol*, *6*(6), 459-473. https://doi.org/10.1177/1756283X13502637

Tao, L., Huang, G., Wang, R., Pan, Y., He, Z., Chu, X., Song, H., & Chen, L. (2016). Cancer- associated fibroblasts treated with cisplatin facilitates chemoresistance of lung adenocarcinoma through IL-11/ IL- 11R/ STAT3 signaling pathway. *Scientific reports*, *6*(1), 38408-38408. https://doi.org/10.1038/srep38408

Tap, W. D., Jones, R. L., Van Tine, B. A., Chmielowski, B., Elias, A. D., Adkins, D., Agulnik, M., Cooney, M. M., Livingston, M. B., Pennock, G., Hameed, M. R., Shah, G. D., Qin, A., Shahir, A., Cronier, D. M., Ilaria, R., Conti, I., Cosaert, J., & Schwartz, G. K. (2016). Olaratumab and doxorubicin versus doxorubicin alone for treatment of soft- tissue sarcoma: an open- label phase 1b and randomised phase 2 trial. *The Lancet*, *388*(10043), 488-497. https://doi.org/10.1016/S0140-6736(16)30587-6

Tawfik, O., Rao, D., Nothnick, W. B., Graham, A., Mau, B., & Fan, F. (2014). Transgelin, a Novel Marker of Smooth Muscle Differentiation, Effectively Distinguishes Endometrial Stromal Tumors from Uterine Smooth Muscle Tumors. *Int J Gynecol Obstet Reprod Med Res*, *1*(1), 26-31. https://www.ncbi.nlm.nih.gov/pubmed/26023684

Thoenen, E., Curl, A., & Iwakuma, T. (2019). TP53 in bone and soft tissue sarcomas. *Pharmacol Ther*, *202*, 149-164. https://doi.org/10.1016/j.pharmthera.2019.06.010

Thorsson, V., Gibbs, D. L., Brown, S. D., Wolf, D., Bortone, D. S., Ou Yang, T.-H., Porta-Pardo, E., Gao, G. F., Plaisier, C. L., Eddy, J. A., Ziv, E., Culhane, A. C., Paull, E. O., Sivakumar, I. K. A., Gentles, A. J., Malhotra, R., Farshidfar, F., Colaprico, A., Parker, J. S., . . . Shmulevich, L. (2018). The Immune Landscape of Cancer. *Immunity*, *48*(4), 812-830.e814. https://doi.org/10.1016/j.immuni.2018.03.023

Thway, K., Nicholson, A. G., Lawson, K., Gonzalez, D., Rice, A., Balzer, B., Swansbury, J., Min, T., Thompson, L., Adu-Poku, K., Campbell, A., & Fisher, C. (2011). Primary pulmonary myxoid sarcoma with EWSR1-CREB1 fusion: a new tumor entity. *Am J Surg Pathol*, *35*(11), 1722-1732. https://doi.org/10.1097/PAS.0b013e318227e4d2

Tieng, F. Y. F., Lee, L. H., & Ab Mutalib, N. S. (2022). Deciphering colorectal cancer immune microenvironment transcriptional landscape on single cell resolution - A role for immunotherapy. *Front Immunol*, *13*, 959705. https://doi.org/10.3389/fimmu.2022.959705

To, W., & Midwood, K. (2011). Plasma and cellular fibronectin: distinct and independent functions during tissue repair. *Fibrogenesis & Tissue Repair*, *4*(1), 21. https://doi.org/10.1186/1755-1536-4-21

Togo, S., Polanska, U., Horimoto, Y., & Orimo, A. (2013). Carcinoma- Associated Fibroblasts Are a Promising Therapeutic Target. *Cancers*, *5*(1), 149-169. https://doi.org/10.3390/cancers5010149

Tracy, L. E., Minasian, R. A., & Caterson, E. J. (2016). Extracellular Matrix and Dermal Fibroblast Function in the Healing Wound. *Advances in Wound Care*, *5*(3), 119-136. https://doi.org/10.1089/wound.2014.0561

Tracy, L. E., Minasian, R. A., & Caterson, E. J. (2016). Extracellular Matrix and Dermal Fibroblast Function in the Healing Wound. *Adv Wound Care (New Rochelle)*, *5*(3), 119-136. https://doi.org/10.1089/wound.2014.0561

Tsujino, T., Seshimo, I., Yamamoto, H., Ngan, C. Y., Ezumi, K., Takemasa, I., Ikeda, M., Sekimoto, M., Matsuura, N., & Monden, M. (2007). Stromal myofibroblasts predict disease recurrence for colorectal cancer. *Clin Cancer Res*, *13*(7), 2082-2090. https://doi.org/10.1158/1078-0432.CCR-06-2191

Tuhkanen, H., Anttila, M., Kosma, V. M., Ylä-Herttuala, S., Heinonen, S., Kuronen, A., Juhola, M., Tammi, R., Tammi, M., & Mannermaa, A. (2004). Genetic alterations in the peritumoral stromal cells of malignant and borderline epithelial ovarian tumors as indicated by allelic imbalance on chromosome 3p. *International Journal of Cancer*, *109*(2), 247-252. https://doi.org/10.1002/ijc.11733

Vodanovich, D. A., & M Choong, P. F. (2018). Soft- tissue Sarcomas. *Indian journal of orthopaedics*, *52*(1), 35-44. https://doi.org/10.4103/ortho.IJOrtho_220_17

Wang, D., Stockard, C. R., Harkins, L., Lott, P., Salih, C., Yuan, K., Buchsbaum, D., Hashim, A., Zayzafoon, M., Hardy, R. W., Hameed, O., Grizzle, W., & Siegal, G. P. (2008). Immunohistochemistry in the evaluation of neovascularization in tumor xenografts. *Biotech Histochem*, *83*(3-4), 179-189. https://doi.org/10.1080/10520290802451085

Wang, J., Li, R., Li, M., & Wang, C. (2021). Fibronectin and colorectal cancer: signaling pathways and clinical implications. *J Recept Signal Transduct Res*, *41*(4), 313-320. https://doi.org/10.1080/10799893.2020.1817074

Wang, L., Luo, R., Xiong, Z., Xu, J., & Fang, D. (2018). Pleomorphic liposarcoma: An analysis of 6 case reports and literature review. *Medicine (Baltimore)*, *97*(8), e9986. https://doi.org/10.1097/MD.0000000000009986

Wang, M., Ren, D., Guo, W., Huang, S., Wang, Z., Li, Q., Du, H., Song, L., & Peng, X. (2016). N-cadherin promotes epithelial-mesenchymal transition and cancer stem cell-like traits via ErbB signaling in prostate cancer cells. *Int J Oncol*, *48*(2), 595-606. https://doi.org/10.3892/ijo.2015.3270

Wang, Z., Han, B., Zhang, Z., Pan, J., & Xia, H. (2010). Expression of angiopoietin-like 4 and tenascin C but not cathepsin C mRNA predicts prognosis of oral tongue squamous cell carcinoma. *Biomarkers*, *15*(1), 39-46. https://doi.org/10.3109/13547500903261362

Weina, K., & Utikal, J. (2014). SOX2 and cancer: current research and its implications in the clinic. *Clin Transl Med*, *3*, 19. https://doi.org/10.1186/2001-1326-3-19

Weitz, J., Antonescu, C. R., & Brennan, M. F. (2003). Localized extremity soft tissue sarcoma: improved knowledge with unchanged survival over time. *Journal of clinical oncology : official journal of the American Society of Clinical Oncology*, *21*(14), 2719-2725. https://doi.org/10.1200/JCO.2003.02.026

Weng, S. L., Chang, S. J., Cheng, Y. C., Wang, H. Y., Wang, T. Y., Chang, M. D., & Wang, H. W. (2011). Comparative transcriptome analysis reveals a fetal origin for mesenchymal stem cells and novel fetal surface antigens for noninvasive prenatal diagnosis. *Taiwan J Obstet Gynecol*, *50*(4), 447-457. https://doi.org/10.1016/j.tjog.2011.10.009

Widemann, B. C., & Italiano, A. (2018). Biology and Management of Undifferentiated Pleomorphic Sarcoma, Myxofibrosarcoma, and Malignant Peripheral Nerve Sheath Tumors: State of the Art and Perspectives. *J Clin Oncol*, *36*(2), 160-167. https://doi.org/10.1200/JCO.2017.75.3467

Wintzell, M., Hjerpe, E., Åvall Lundqvist, E., & Shoshan, M. (2012). Protein markers of cancer- associated fibroblasts and tumor- initiating cells reveal subpopulations in freshly isolated ovarian cancer ascites. *BMC Cancer*, *12*(359), 359-359. https://doi.org/10.1186/1471-2407-12-359

Wu, Y., Wu, P., Zhang, Q., Chen, W., Liu, X., & Zheng, W. (2019). MFAP5 promotes basal-like breast cancer progression by activating the EMT program. *Cell Biosci*, *9*, 24. https://doi.org/10.1186/s13578-019-0284-0

Wuebben, E. L., & Rizzino, A. (2017). The dark side of SOX2: cancer - a comprehensive overview. *Oncotarget*, *8*(27), 44917-44943. https://doi.org/10.18632/oncotarget.16570

Xi, Y., Liu, J., & Shen, G. (2022). Low expression of IGFBP4 and TAGLN accelerate the poor overall survival of osteosarcoma. *Scientific reports*, *12*(1), 9298. https://doi.org/10.1038/s41598-022-13163-8

Xiao, W., Mohseny, A. B., Hogendoorn, P. C. W., & Cleton-Jansen, A.-M. (2013). Mesenchymal stem cell transformation and sarcoma genesis. *Clinical sarcoma research*, *3*(1), 10-10. https://doi.org/10.1186/2045-3329-3-10

Xin, L., Gao, J., Zheng, Z., Chen, Y., Lv, S., Zhao, Z., Yu, C., Yang, X., & Zhang, R. (2021). Fibroblast Activation Protein-α as a Target in the Bench-to-Bedside Diagnosis and Treatment of Tumors: A Narrative Review. *Front Oncol*, *11*, 648187. https://doi.org/10.3389/fonc.2021.648187

Xin, Z., Qirui, W., Xiuqing, G., Jinfeng, L., & Yujie, a. M. (2021). Osteosarcoma: a review of current and future therapeutic approaches. In (Vol. 20). BioMed Eng OnLine.

Xing. (2011). Cancer associated fibroblasts (CAFs) in tumor microenviroment. *Front Biosci*, 166-179.

Xing, F., Saidou, J., & Watabe, K. (2010). Cancer associated fibroblasts (CAFs) in tumor microenvironment. *Frontiers in Bioscience-Landmark*, *15*, 166-179. https://doi.org/10.2741/3613

Yamashita, M., Ogawa, T., Zhang, X., Hanamura, N., Kashikura, Y., Takamura, M., Yoneda, M., & Shiraishi, T. (2012). Role of stromal myofibroblasts in invasive breast cancer: stromal expression of alpha-smooth muscle actin correlates with worse clinical outcome. *Breast Cancer*, *19*(2), 170-176. https://doi.org/10.1007/s12282-010-0234-5

Yang, Y., Ye, W. L., Zhang, R. N., He, X. S., Wang, J. R., Liu, Y. X., Wang, Y., Yang, X. M., Zhang, Y. J., & Gan, W. J. (2021). The Role of TGF-. *Evid Based Complement Alternat Med*, *2021*, 6675208. https://doi.org/10.1155/2021/6675208

Yao, Y., & Dai, W. (2014). Genomic Instability and Cancer. *J Carcinog Mutagen*, *5*. https://doi.org/10.4172/2157-2518.1000165

Yu, L., Guo, W., Zhao, S., Wang, F., & Xu, Y. (2011). Fusion between cancer cells and myofibroblasts is involved in osteosarcoma. *Oncology letters*, *2*(6), 1083-1087. https://doi.org/10.3892/ol.2011.363

Yuan, Z., Hu, H., Zhu, Y., Zhang, W., Fang, Q., Qiao, T., Ma, T., Wang, M., Huang, R., Tang, Q., Gao, F., Zou, C., Gao, X., Wang, G., & Wang, X. (2021). Colorectal cancer cell intrinsic fibroblast activation protein alpha binds to Enolase1 and activates NF-κB pathway to promote metastasis. *Cell Death & Disease*, *12*(6), 543. https://doi.org/10.1038/s41419-021-03823-4

Zayed, H., & Petersen, I. (2018). Stem cell transcription factor SOX2 in synovial sarcoma and other soft tissue tumors. *Pathol Res Pract*, *214*(7), 1000-1007. https://doi.org/10.1016/j.prp.2018.05.004

Zhang, J., Chang, D. Y., Mercado-Uribe, I., & Liu, J. (2012). Sex-determining region Y-box 2 expression predicts poor prognosis in human ovarian carcinoma. *Hum Pathol*, *43*(9), 1405-1412. https://doi.org/10.1016/j.humpath.2011.10.016

Zhang, S., Che, D., Yang, F., Chi, C., Meng, H., Shen, J., Qi, L., Liu, F., Lv, L., Li, Y., Meng, Q., Liu, J., Shang, L., & Yu, Y. (2017). Tumor-associated macrophages promote tumor metastasis via the TGF-

β/SOX9 axis in non-small cell lung cancer. *Oncotarget*, *8*(59), 99801-99815. https://doi.org/10.18632/oncotarget.21068

Zhang, S., Xiong, X., & Sun, Y. (2020). Functional characterization of SOX2 as an anticancer target. *Signal Transduct Target Ther*, *5*(1), 135. https://doi.org/10.1038/s41392-020-00242-3

Zhao, L., Wang, H., Deng, Y.-J., Wang, S., Liu, C., Jin, H., & Ding, Y.-Q. (2009). Transgelin as a suppressor is associated with poor prognosis in colorectal carcinoma patients. *Modern Pathology*, *22*(6), 786-796. https://doi.org/10.1038/modpathol.2009.29

Zhou, H.-M., Fang, Y.-Y., Weinberger, P. M., Ding, L.-L., Cowell, J. K., Hudson, F. Z., Ren, M., Lee, J. R., Chen, Q.-K., Su, H., Dynan, W. S., & Lin, Y. (2016). Transgelin increases metastatic potential of colorectal cancer cells in vivo and alters expression of genes involved in cell motility. *BMC Cancer*, *16*(59), 55-55. https://doi.org/10.1186/s12885-016-2105-8

Zhou, L., Zhang, R., Zhang, L., Sun, Y., Yao, W., Zhao, A., Li, J., & Yuan, Y. (2013). Upregulation of transgelin is an independent factor predictive of poor prognosis in patients with advanced pancreatic cancer. *Cancer Sci*, *104*(4), 423-430. https://doi.org/10.1111/cas.12107

Zhou, Z., Cui, D., Sun, M. H., Huang, J. L., Deng, Z., Han, B. M., Sun, X. W., Xia, S. J., Sun, F., & Shi, F. (2020). CAFs-derived MFAP5 promotes bladder cancer malignant behavior through NOTCH2/HEY1 signaling. *FASEB J*, *34*(6), 7970-7988. https://doi.org/10.1096/fj.201902659R

Zhuang, G., Zeng, Y., Tang, Q., He, Q., & Luo, G. (2020). Identifying M1 Macrophage-Related Genes Through a Co-expression Network to Construct a Four-Gene Risk-Scoring Model for Predicting Thyroid Cancer Prognosis. *Front Genet*, *11*, 591079. https://doi.org/10.3389/fgene.2020.591079

Zinchuk, V., & Zinchuk, O. (2008). Quantitative colocalization analysis of confocal fluorescence microscopy images. *Curr Protoc Cell Biol*, *Chapter 4*, Unit 4.19. https://doi.org/10.1002/0471143030.cb0419s39